Editors: Mato Uljarević, Sabid Zekan, Sabrina Salković, Dženan Ibrahimović

ReSyLAB

Proceedings of the 4th Regional Symposium on

LANDSLIDES

in the Adriatic - Balkan Region
23-25 October 2019, Sarajevo, Bosnia and Herzegovina

ICL

ABN ADRIATIC-BALKAN NETWORK

DGT BiH

Editors: Mato Uljarević, Sabid Zekan, Sabrina Salković, Dženan Ibrahimović

ReSyLAB

Proceedings of the 4th Regional Symposium on

LANDSLIDES

in the Adriatic - Balkan Region
23-25 October 2019, Sarajevo, Bosnia and Herzegovina

GOLD SPONSORS OF THE RESYLAB 2019

МЈЕШОВИТИ ХОЛДИНГ
"ЕЛЕКТРОПРИВРЕДА РЕПУБЛИКЕ СРПСКЕ"
Матично предузеће, акционарско друштво Требиње

MIXED HOLDING
"POWER UTILITY OF THE REPUBLIC OF SRPSKA"
Parent Joint-stock Company Trebinje

GEOINVEST
geotehnička rješenja

Geotechnical Society of Bosnia and Herzegovina
October, 2019

Proceedings of the 4th Regional Symposium on Landslides in the Adriatic - Balkan Region
23-25 October 2019, Sarajevo, Bosnia and Herzegovina

Editors

Mato Uljarević, University of Banja Luka, Faculty of Architecture, Civil Engineering and Geodesy
Sabid Zekan, University of Tuzla, Faculty of mining, geology and civil engineering
Sabrina Salković, Geotechnical Society of Bosnia and Herzegovina
Dženan Ibrahimović, Geotechnical Society of Bosnia and Herzegovina

Scientific Programme Committee

Organizing Committee

Citation

The publication should be cited in the bibliography using doi number as follows:
Uljarević M., Zekan S., Ibrahimović Dž. (eds.): Proceedings of the 4th Regional Symposium on Landslides in the Adriatic Balkan Region, 23-25 October 2019, Sarajevo, Bosnia and Herzegovina. Geotechnical Society of Bosnia and Herzegovina, 2019.
doi: **https://doi.org/ 10.35123/ReSyLAB_2019**

In cooperation with: Federal Institute for Geology, Bosnia and Herzegovina
Geological Survey of the Republic of Srpska, Bosnia and Herzegovina
ICL ABN - International Consortium on Landslides Adriatic-Balkan Network

Published by: Geotechnical Society of Bosnia and Herzegovina

Graphic Design: Dženan Ibrahimović

Web page: http://geotehnika.ba/ReSyLAB_&_GEO-EXPO_2019.html

Printed by: Mit-Alex d.o.o. Tuzla

Print run: 140

CIP - Katalogizacija u publikaciji
Nacionalna i univerzitetska biblioteka Bosne i Hercegovine, Sarajevo
624.131.53(497)(063)(082)

REGIONAL Symposium on Landslides in the Adriatic - Balkan Region (4 ; 2019 ; Sarajevo)
Proceedings of the 4th Regional Symposium on Landslides in the Adriatic - Balkan Region / editors Mato Uljarević, Sabid Zekan, Dženan Ibrahimović. - Sarajevo : Geotechnical Society of Bosnia and Herzegovina = Društvo za geotehniku u Bosni i Hercegovini, 2019. - 242 str. : ilustr. ; 30 cm

ISBN 978-9926-8400-0-6
COBISS.BH-ID 28158214

Preface

The Geotechnical Society of Bosnia and Herzegovina hosts the ReSyLAB & GEO-EXPO 2019 symposium consisting of the 4th Regional Symposium on Landslides in the Adriatic-Balkan Region „ReSyLAB“ and the 9th Scientific and Expert conference "GEO-EXPO", on 23-25 October, 2019 in Sarajevo. This year symposium is also the first regional gathering of geotechnical societies from Balkan and the fourth gathering of the ICL ABN members.

ABN group (Adriatic-Balkan Network) consists of institutions from the region that are full members of the International Consortium on Landslides (ICL). The ABN group members are: Geotechnical Society of Bosnia and Herzegovina, Faculty of Civil Engineering - University of Rijeka, Faculty of Mining, Geology and Petroleum - University of Zagreb and City of Zagreb, Faculty of Civil Engineering and Geodesy and Faculty of Natural Sciences and Engineering - University in Ljubljana and Geological Survey of Slovenia, Faculty of Mining and Geology - University of Belgrade and Geological Survey of Albania.

Organizational assistance has been provided by the Geological Survey of the Republic of Srpska and Federal Institute for Geology of Bosnia and Herzegovina, the Faculty of Mining, Geology and Civil Engineering – University of Tuzla and numerous sponsors. MH „Power Utility of the Republic of Srpska“ Parent Joint-Stock Company from Trebinje and Geoinvest from Sarajevo are the ReSyLAB & GEO-EXPO 2019 symposium gold sponsors.

Inviting lectures will be delivered by Professor Charles Wang Wai Ng, President of ISSMGE, Professor Norikazu Shimizu, Professor Alessandro Corsini, Professor Željko Arbanas and Professor Martina Vivoda-Prodan. The topics of this year's ReSyLAB & GEO-EXPO 2019 symposium are: landslides, mapping, geotechnical investigation and monitoring, landslides hazards and risks. As in previous years, the conference provides an opportunity to share experiences, analyze methodologies, discuss on landslide stabilization measures among interested parties. During the conference, a lot of local and regional experts will present their scientific papers. Several companies will present themselves through their products, equipment, software and consulting.

By organizing this conference, Bosnia and Herzegovina contributes the advancement of the ISDR-ICL Sendai Partnerships 2015-2025 for the Global Promotion of Understanding and Reducing Landslide Disaster Risk and the 2017 Ljubljana Declaration on Landslide Risk Reduction. The ReSyLAB 2019 Symposium promotes contribution to the Kyoto 2020 Commitment (KC2020). After heavy rainfall in May 2014, thousands of landslides were triggered across the country. We are thankful to UNDP and the Government of Japan for their substantial financial support in the landslide remediation.

We would like to thank the authors and landslide experts for writing scientific papers and attending the conference in Sarajevo. Special thanks to the Honorable Member of our Society, Professor Emeritus Hideaki Marui from Niigata University, who has been visiting Bosnia and Herzegovina for the fifth time with a purpose to contribute to the investigation of landslides. This symposium will be of great benefit to the regional government's institutions, municipalities, universities, companies and engineers who are involved in issues of landslides. We organize a roundtable on the harmonization of relations between state and the scientific sector in order to reduce the cost of investigation, stabilization and landslide risk. At the end of the conference, we shall visit three characteristic landslides in an aim to introduce the participants with the methods of landslides' remediation in Bosnia and Herzegovina.

Especially, we would like to thank ICL Secretary General, Professor Emeritus Kyoji Sassa and ICL President, Professor Peter Bobrowsky, heading of the ICL organization.

We invite you to visit the Fifth World Landslide Forum, November 2 - 6, 2020, in Kyoto, Japan, GEO-EXPO 2020 and the following ReSyLAB 2021.

President
of the Geotechnical Society of Bosnia and Herzegovina
Professor Mato Uljarević

Content

doi.org/ 10.35123/ReSyLAB_2019_1

Landslide monitoring using satellite technology and collaborative researches with Balkan countries

Norikazu Shimizu[(1)]

1) Yamaguchi University, Department of Civil and Environmental Engineering, Ube 755-8611, Japan

Abstract Monitoring is important for assessing the stability of the ground and for confirming the validity of the design during the construction and operation of structures. The ideal monitoring system for projects in Rock and Geotechnical Engineering would be able to monitor the behavior of small to extensive areas continuously and automatically with high accuracy. In addition, the costs would be low and the system would be easy to handle. Satellite technology has the potential to realize the above monitoring system by combining it with conventional geotechnical instruments. In this paper, satellite technology for displacement monitoring, i.e., GPS and SAR, is firstly outlined and then the concept of spatio-temporal continuous displacement monitoring is introduced. The use of both satellite technology and geotechnical instruments is effective for geotechnical monitoring. Practical applications of GPS for landslide monitoring and collaborative researches using DInSAR with Balkan countries are described.

Keywords displacement monitoring, satellite technology, GPS, DInSAR, landslide, mass movement, subsidence

Introduction

Monitoring is important for assessing the stability of the ground and for confirming the validity of the design during the construction and operation of structures. Monitoring is also useful for predicting risks, for managing safe operations, and for reducing project costs.

The ideal monitoring system for projects in Rock and Geotechnical Engineering should be able to continuously and automatically monitor the behavior of small to extensive areas with high accuracy. In addition, the costs should be low and the system should be easy to handle.

There are various types of instruments for taking field measurements in Rock and Geotechnical Engineering, such as extensometers, inclinometers, etc. Although they are useful, these instruments may not be adequate for monitoring large slopes or extensive areas because they can only be applied to limited areas.

On the other hand, satellite technology, GPS (Global Positioning System) and DInSAR (Differential Interferometric Synthetic Aperture Radar), is capable of overcoming the above problems, since it can be applied to monitor the displacements of the ground and the surfaces of structures over large areas.

Satellite technology can make the invisible behavior of the ground visible, and it can provide new information, i.e., three-dimensional continuous displacements and the distribution of displacements over a huge area, for assessing the stability of the ground and structures and for predicting their future behavior.

This paper firstly provides outlines of GPS and DInSAR for displacement monitoring. Then, a new concept, "spatio-temporal continuous displacement monitoring", is described. It uses satellite technology and geotechnical instruments together. Finally, practical applications of GPS for monitoring an unstable steep slope, landslide and mass movement, and collaborative researches with Balkan countries, using DInSAR to monitor the subsidence and a landslide, are illustrated.

Outline of satellite technology -GPS and DInSAR- for displacement monitoring

Displacement monitoring by GPS

GPS is a satellite-based positioning system that was developed in the USA. It was established as a method for navigation and long baseline surveys (e.g., Hoffmann-Wellenhof et al. 2001; Misra and Enge 2006). The advantage of GPS is that it can easily provide three-dimensional displacements with mm accuracy over extensive areas.

A GPS displacement monitoring system using an L1 signal was developed by the author and his colleagues, as illustrated in Figure 1 (Iwasaki et al. 2003; Masunari et al. 2003; Shimizu and Matsuda 2002, 2003). In this system, sensors are set on measurement points and a reference point, respectively. They are connected to a control box into which a computer, data memory, and a network device are installed. The data from the satellites are received at each sensor and then transferred to the control box through cables. The server computer, which is located in an office away from the measurement area, automatically controls the entire system to acquire and analyze the data. Then, three-dimensional displacements are obtained for all the monitoring points. The monitoring results are provided to users through the Internet in real time. A user only needs to access the home page to see the monitoring results.

The most important issue in the practical use of GPS is how to improve the measurement accuracy. The author and his colleagues have proposed methods for removing errors and for estimating the real values of the

measurements. Those methods have succeeded in providing measurement results that are a few times higher (i.e., mm) in accuracy than the standard GPS (Shimizu et al. 2011; Shimizu and Nakashima 2017). The procedure has been approved as "the ISRM suggested method for monitoring rock displacements using the Global Positioning System" (Shimizu et al. 2014).

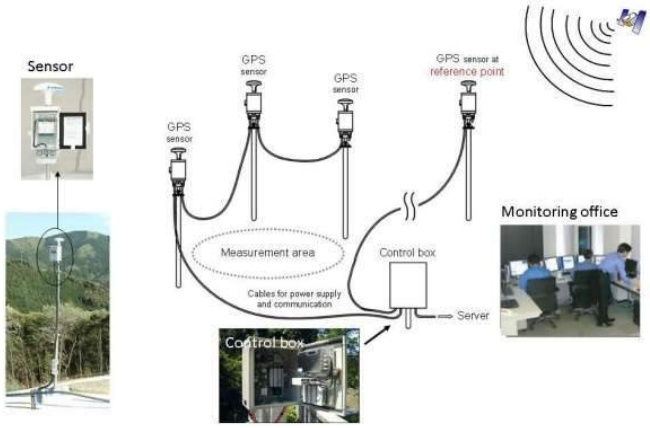

Figure 1 GPS fully automatic continuous displacement monitoring system (Iwasaki et al. 2003; Masunari et al. 2003; Shimizu and Matsuda 2002, 2003)

Displacement monitoring by DInSAR

SAR is a radar device mounted on an aircraft or artificial satellite that generates high resolution remote sensing imagery all day and all night (Hanssen 2002). Interferometric SAR (InSAR) is a method for taking the signal phase difference (interference) from two SAR data images, which are observed in the same area at different periods by a satellite on the same orbit (see Figure 2).

Differential Interferometric SAR (DInSAR) is the commonly used term for the production of interferograms from which the topographic influence has been removed (Ferretti et al. 2007). The advantage of DInSAR is that it can provide centimeter-scale displacements of the surface of the Earth over vast areas, i.e., thousands of square kilometers, with a spatial resolution of 3-30 m (Ferretti 2014). The observed displacements are one-dimensional along the Line of Sight (LOS: the direction from the satellite to the observed Earth's surface (see Figure 3(b)). When continuous displacement monitoring is conducted by DInSAR, SBAS (Small Baseline Subset) DInSAR (Berardino et al. 2002) could be a useful tool for this analysis.

Comparison of GPS and DInSAR

The features of GPS and DInSAR are compared in Table 1 and Figure 3. GPS can continuously monitor three-dimensional displacements at certain points 24 hours a day with mm accuracy, whereas DInSAR can take one-dimensional displacement measurements of much greater areas usually once every few days/weeks with cm accuracy in spatial resolution areas of 3-30 m. DInSAR does not require any sensors on the ground, while GPS requires a sensor at each monitoring point. Therefore, GPS and DInSAR are complementary to each other.

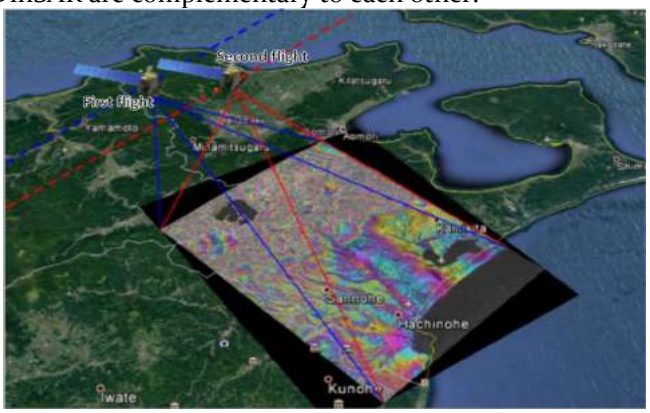

Figure 2 DInSAR for measuring the displacement of the Earth's surface (background : Google Earth)

Table 1 Features of GPS and DInSAR

	GPS	DInSAR
Required devices for user	Receivers	**Not necessary**
Observable displacements	Point(s)	**Entire areas** (3-30 m spatial resolution)
Continuous monitoring	**Every hour or shorter periods; available 24 hours a day**	Periodic: every few days/weeks
Dimension of measurements	**3-dimensional**	1-dimensional
Accuracy	**mm level**	cm level

Boldface: advantages

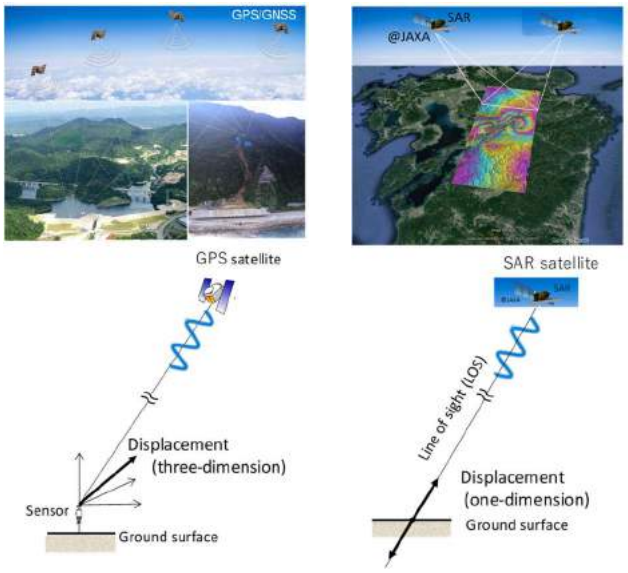

(a) GPS (b) DInSAR

Figure 3 GPS and DInSAR, and their monitored displacements

Spatio-temporal continuous displacement monitoring using satellite technology

Figure 4(a) shows a schematic diagram of the relationship between the measurement accuracy and the size of a monitoring area expressed by the representative

length. The applicable ranges of geotechnical instruments and conventional surveying methods are illustrated in this figure. It can be seen that there is a gap in accuracy between the two methods. GPS could cover this gap. In addition, DInSAR is able to expand the validity of displacement monitoring to huge areas.

Looking at the relative accuracies of the two methods, they are almost the same, in the order of about 10-5 - 10-6, i.e., 0.1 mm (accuracy)/100 m (baseline length) for geotechnical instruments, a few mm/1 km for GPS, and a few cm/10 km for DInSAR. This means that displacements could be measured with almost the same accuracy as 10-5 - 10-6 over small to large areas by applying both geotechnical instruments and satellite technology (GPS and DInSAR). Spatially continuous (spatio-continuous) monitoring can be realized.

On the other hand, Figure 4(b) shows a diagram of the relationship between the measurement interval (period) and the size of a monitoring area. Geotechnical instruments can measure displacements at any interval. In the case of GPS, the interval of the measurements is usually an hour when the baseline length is within one kilometer. Recently, however, the measurement interval can be a few minutes or even a second if accuracy of several mm is acceptable.

In the case of DInSAR, the interval of the measurements depends on the satellite regression cycle. It is usually several days or a few weeks or more. Although there may be a limitation in the measurement interval for extensive areas at present, temporally continuous monitoring can be done. Therefore, spatio-temporal continuous displacement monitoring can be realized by combining the two types of satellite technology with geotechnical instruments.

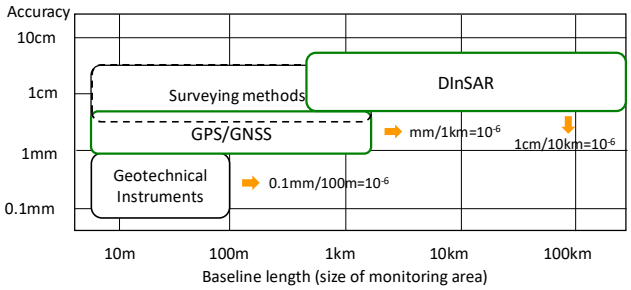

(a) Measurement accuracy and baseline length

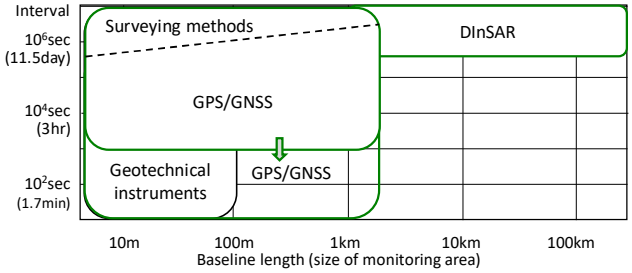

(b) Measurement interval and baseline length

Figure 4 Spatio-temporal continuous monitoring using geotechnical instruments and satellite technology

Monitoring using GPS

Unstable steep slope along traffic road

The GPS displacement monitoring system (see Figure 1) was applied to monitor the displacements of an unstable steep slope along a road. Since local slope failures have occurred several times over the last 20 years, displacement monitoring has been conducted by borehole inclinometers and surface extensometers. Some of the instruments, however, have occasionally not worked well due to large displacements, and it has been difficult to perform the monitoring continuously. In order to overcome such trouble, the GPS monitoring system has been employed for continuous monitoring (Furuyama et al. 2014; Kien 2019).

(a) Slope and monitoring area

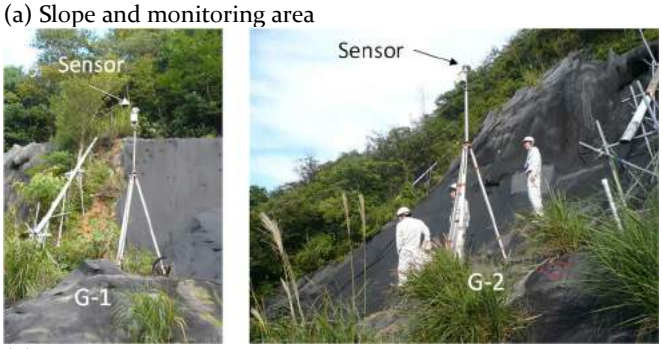

(b) GPS sensors at G-1 and G-2

Figure 5 Monitoring site and slope beside road

Monitoring site

Figure 5(a) presents photographs of a slope and the monitoring area. The slope is composed primarily of rhyolite and granite which formed in the Cretaceous period of the Mesozoic era, and its surface is partially covered with a colluvial deposit. The left side of the slope, as seen in the photograph in Figure 5(a), has been gradually failing over the last 20 years, and a concrete rock-shed tunnel has been constructed to cover the road and to protect it.

Two antennas were set at the top of the slope to monitor displacements, and another antenna was set at a fixed point in a stable area as a reference point, denoted by K-1, beneath the slope. The monitoring points, denoted as G-1 and G-2, were set on the left and right sides of the slope, respectively (see Figure 5(b)).

The distance between monitoring point G-1 and reference point K-1 was 221 m, while that between monitoring point

G-2 and the reference point was 258 m. The differences in height between the two points and the reference point were 103 m and 112 m, respectively.

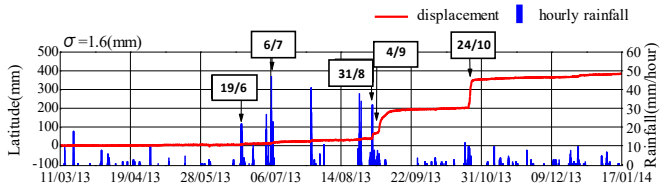

(a) Displacement in the direction of latitude

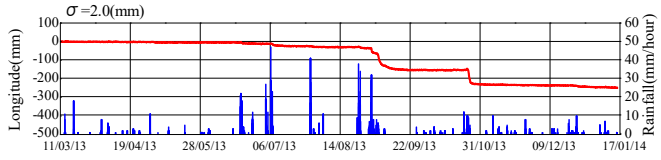

(b) Displacement in the direction of longitude

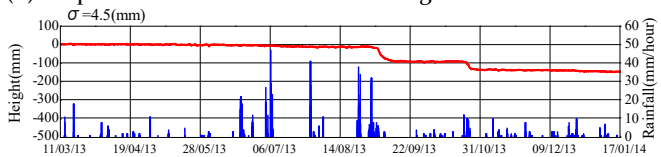

(c) Vertical displacement

Figure 6 Temporal transition of three-dimensional displacements at G-1 (Furuyama et al. 2014)

Monitoring results

Three-dimensional displacements were continuously measured every hour. The monitoring results at G-1 are shown in Figure 6 along with the hourly amount of rainfall. Small displacements of less than 2-3 mm/month were generated at G-1 during the low rainfall period from March to early June. Whenever heavy rain fell from July to October, the displacement gradually increased.

By the end of October, it had reached 355 mm in the north direction and 234 mm in the west direction, and the settlement had reached 137 mm. However, the displacements at G-1 gradually converged and became stable after this rainfall period.

On the other hand, no remarkable displacements were measured at G-2 in this period. This means that the right-hand side of the slope was more stable than the left-hand side.

Figure 7(a) shows the displacement vectors in the plan view of the slope, while Figures 7(b) and 7(c) show the vertical sections including G-1 and G-2, respectively. The directions of the vectors for G-1 and G-2 are seen to almost coincide with the steepest direction of the slope in the plan view. The direction of the displacement at G-1 was toward the front of the slope in the vertical section until the middle of August. After heavy rainfall at the end of August and early September, the direction changed to be parallel to the slip plane of the slope, and it was toward the front of the slope again after the last large displacement on October 24. On the other hand, the direction of the displacement at G-2 was parallel to the slip plane at the top of the slope in the vertical section.

Regulations (criteria) for traffic safety along this road are given in Table 2. It is seen that when the displacement velocity (mm/day) goes beyond 10 mm/day and the total amount of continuous rainfall exceeds 100 mm, one lane of the roadway is temporarily closed. And when the displacement velocity goes over 20 mm/day and the total amount of continuous rainfall exceeds 200 mm, both lanes of the road are temporarily closed.

Figure 8 shows the displacement velocity obtained from the monitored displacement as shown in Figure 6. During this period, the road was closed a few times.

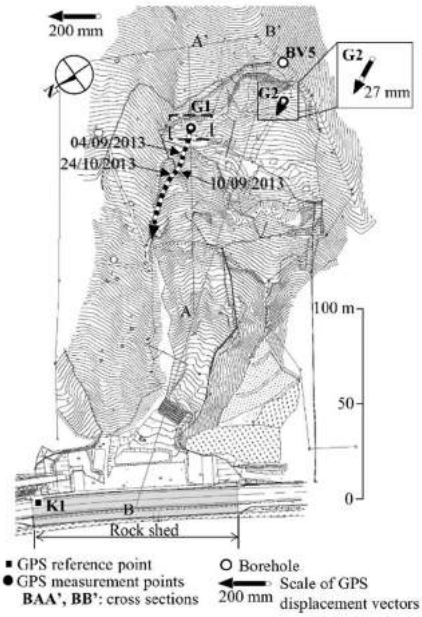

(a) Plan view

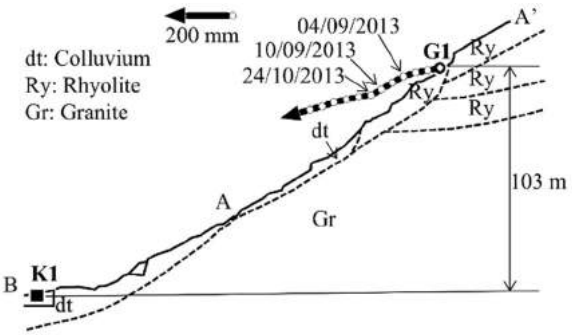

(b) Section A-A'

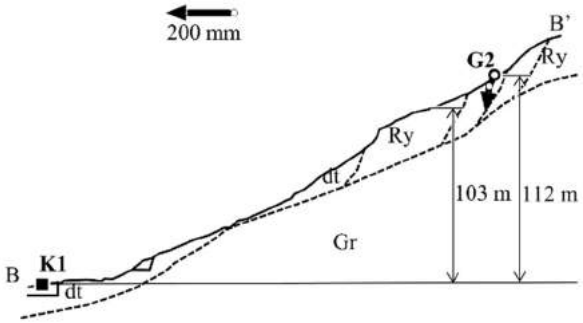

(c) Section B-B'

Figure 7 Transitions of displacement vectors (Kien 2019)

Table 2 Criteria for assessing the stability

	Criteria	Safety measure
Level 1	Displacement velocity > 10 mm/day	One lane of the road is closed
Level 2	Displacement velocity > 20 mm/day	Both lanes of the road are closed

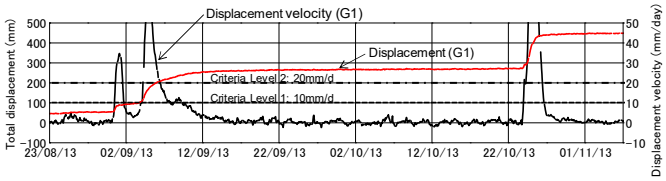

Figure 8 Total displacement (red line) and its velocity (black line) at G-1

Landslide caused by heavy rain

A large-scale slope failure occurred in a mountainous area of Western Japan due to a heavy rainfall brought about by a typhoon. The huge volume of colluvial deposit blocked a river channel and created a landslide dam (see Figure 9). Then, a debris flow occurred due to the erosion of part of the deposit. In order to prevent the collapse of the landslide dam and the occurrence of further debris flows, disaster recovery works were carried out. The GPS monitoring system was applied to monitor the behavior of the unstable colluvial deposit (Sato et al. 2014).

Figure 9 Landslide dam and unstable colluvial deposit (Sato et al. 2014)

Monitoring site

The slope failure occurred over an area that was 650 m long, 410 m wide, and 60 m deep (Figure 9). The volume of the colluvial deposit was estimated to be 4.1 million m3. The slope was formed by alternating beds of sandstone and mudstone.

GPS sensors were set at 11 measurement points on the slope of the colluvial deposit (denoted by the bullets; G-1, G-2, ..., and G-8) and at a reference point outside of the area (se Figure 10) in order to perform the safety management of disaster recovery works. The distance between the measurement points and the reference point was about 100 m – 700 m. Electric power was supplied to the monitoring system by means of a solar panel, and the measurement data were transmitted via a cellular phone to a computer at the control office. Extensometers, denoted by S-1 to S-4, were also set in the upper area of the unstable slope (see Figure 10).

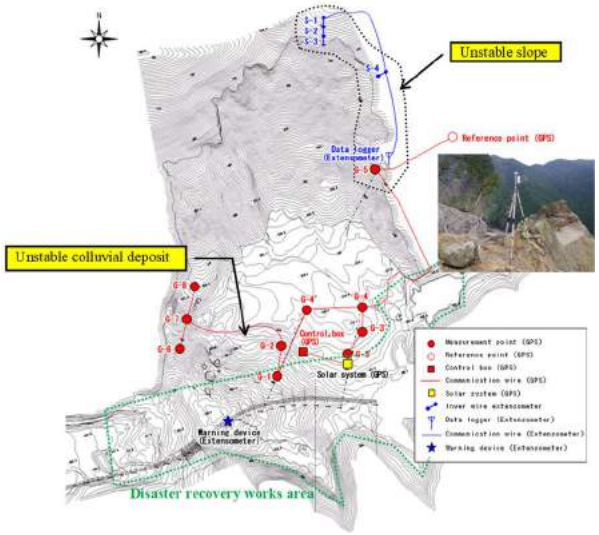

Figure 10 Plan view of monitoring site and location of GPS sensors (Sato et al. 2014)

Monitoring results

The temporal displacement monitoring results of G-5 over three years are presented in Figure 11(a), and the displacement vectors are given on the plan view in Figure 11(b). The displacement vectors show that the total displacements in the lower area of the slope (G-1 to G-8, except for G-5 in Figure 11(b)) were not large and ranged from a few mm to 34 mm.

On the other hand, the displacements in the upper area of the unstable slope (G-5, and S-1 to S-4 in Figure 11(b)) increased up to 540 mm and to 3353 mm. The displacements often exceeded the criteria (see Table 3) for the suspension of disaster recovery work (see Figure 12). At those times, the monitoring center issued a warning for unstable slope conditions to the engineers and workers at the site and the work was suspended. Over the three-year period, people in that vicinity were evacuated to a safe area several times.

GPS monitoring is useful for the safety management of disaster recovery works.

Table 3 Criteria for assessing the stability

Warning criteria	Precipitation	Seismic intensity	GPS	Extensometer
Caution	5 mm/hour	-	Displacement velocity >10 mm/day	-
Warning (Halt work)	10 mm/hour	Scale 4	Displacement velocity >25 mm/day	4 mm/hour

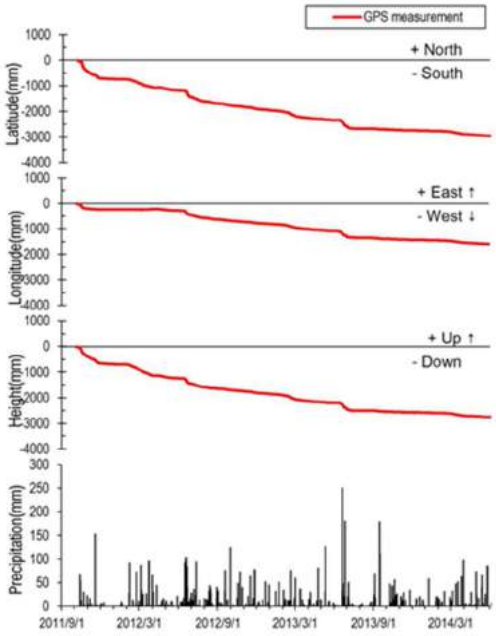

(a) Monitoring displacements and rainfall at G-5

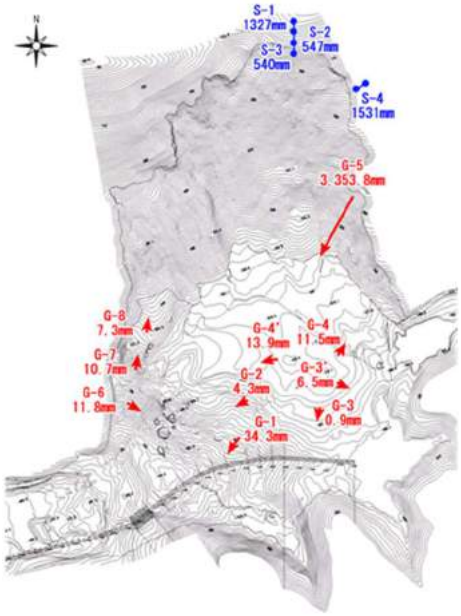

(b) Displacement vectors in plan view

Figure 11 Monitoring results (Sato et al. 2014)

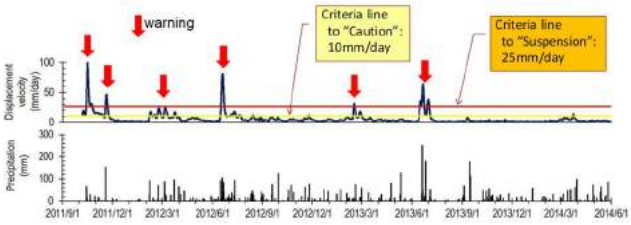

Figure 12 Displacement velocity at G-5 and criteria (Sato et al. 2014)

Mass movement with a high velocity

A landslide occurred in a portion of a hill covered with snow located in the northwest part of Japan a few days after the temperature had suddenly increased. The mass was 500 m in length, 150 m in width, and 20 m in depth, and moved down with a high velocity, namely, a maxi-mum value of 20 m per day, to an alluvial fan with a village (see Figure 13). The GPS displacement monitoring system was applied to continuously monitor the movement in order to issue an evacuation advisory or to give orders to the local residents (Tosa et al. 2014).

Figure 13 Landslide with a high velocity (Tosa et al. 2014)

Monitoring site

The upper and lower areas of the hill are composed of mainly unconsolidated conglomerate and massive mudstone, respectively. The mass of the slope moved down along the ground surface (alluvial fan) with an inclination of only 2 degrees (see Figure 13).

The landslide occurred on March 7, 2012. In order to monitor such a mass movement, the total station was used immediately after the movement began at the points denoted by T1 and T4 in Figure 14. A drainage system using surface drains and boring was applied to drain water from the landslide area after March 11 together with countermeasures consisting of concrete blocks to resist the movements.

However, the velocity of the movement was still large; and thus, some other system, available for continuous monitoring 24 hours a day, was required for obtaining displacements in real time to protect the local area and its residents from damage and injury. For this purpose, the GPS displacement monitoring system was installed on March 14 and 15, one week after the occurrence of the movement.

The four monitoring points, G-1 to G-4, were set on the inside of the landslide area (see Figure 14) and the other points were set on the outside of the area. A reference point was fixed 200 m north of the landslide area.

Monitoring results

The trace of the horizontal displacements at T-1 and T-4 by the total station and at G-1, G-2, G-3, and G-4 by GPS are presented in Figure 14. The displacement velocity of the upper area of the slope rose to the maximum between March 9 and 13, and it reached 20 m/day between March 11 and 12. The toe of the lower area of the slope moved down 100 m during the 15-hour period from 16:00 on March 8 to 7:00 on March 9.

Figure 15 shows the monitoring results at G-4 by GPS. It is found that the landslide movement became slow after March 20 and had almost converged by March 23. Although the total amount of the movement of the toe of the slope reached about 250 m and the landslide crushed several houses, there were no injuries to the residents themselves due to the evacuation advisory issued by referring to the monitoring results.

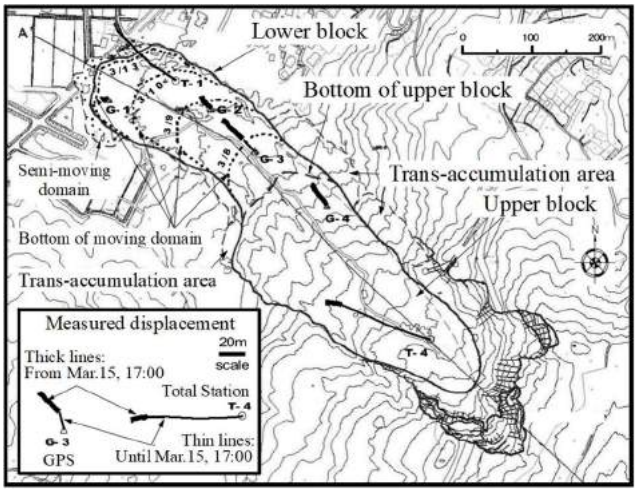

Figure 14 Plan view of landslide area and trace of displacements at monitoring points (Tosa et al. 2014)

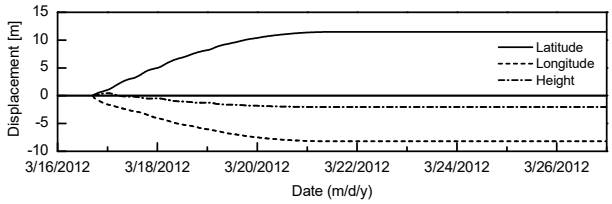

Figure 15 Displacement monitoring results at G-4

Monitoring using DInSAR - collaborations with Balkan countries

Subsidence induced by underground salt mining in Tuzla, Bosnia and Herzegovina

The subsidence in Tuzla has been creating a large hazard for a long period, mainly since the 1950s. It was reported that the main factor of this subsidence is caused by the salt mining activities (Mancini et al. 2009a).

The subsidence was measured by traditional topographic surveys from 1956 to 2003. The GPS surveys produced subsidence information in three periods, namely, 2004 to 2005, 2005 to 2006, and 2006 to 2007 (Mancini et al. 2009b). DInSAR was applied to know the present situation of the subsidence. In order to update the subsidence data, SBAS-DInSAR has been applied (Parwata et al. 2018, 2019).

Monitoring site

The Tuzla salt deposit is located beneath Tuzla City in an area of approximately 2 km2 (see Figure 16(a)). It consists of five separated salt series embedded in syncline with one of the wings close to the surface of the city's center. The maximum thickness of the salt formation is 600 meters (see Figure 16(b)). The lithological composition is halite, gypsum, anhydrite, laminated and thin-layered marls, tuff, poriferous limestone, etc.

The total amount of subsidence during the period of 1956 to 2003 was up to 12 m, while it was more than 1 m in the area of about 2 km2 of the city (Mancini et al. 2009a). The official date of termination of the salt deposit exploitation was in May 2007. However, subsidence still continued at a rate of 10-20 cm/year from 2004 to 2007 according to GPS surveys using the static method (Mancini et al. 2009b).

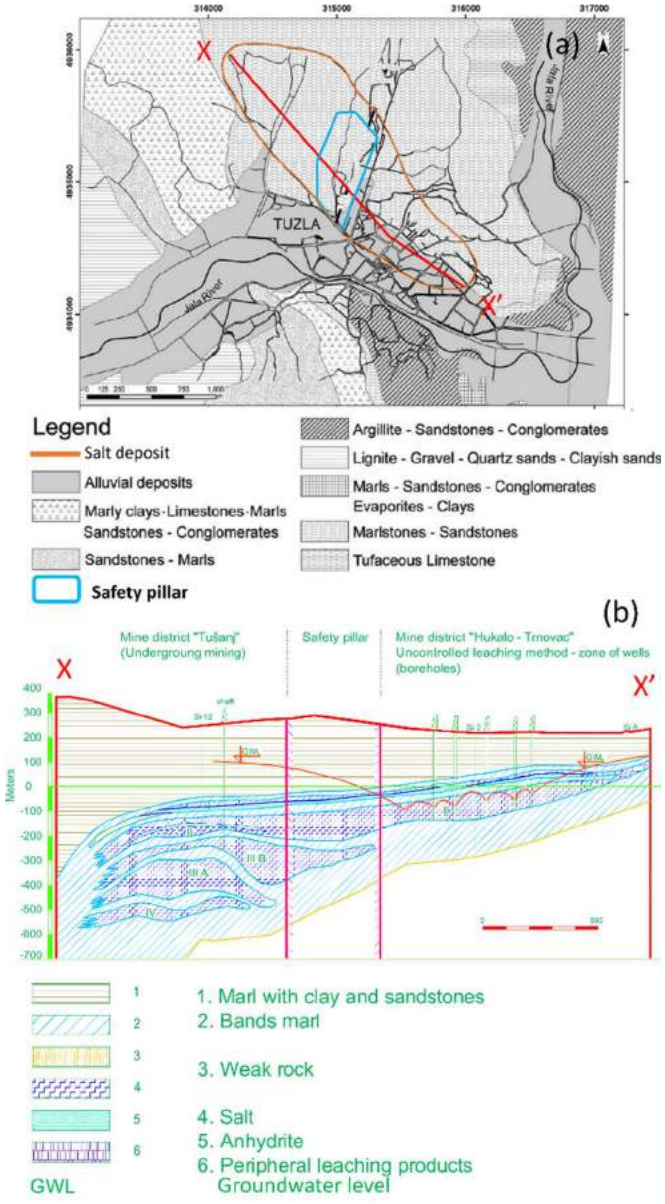

Figure 16 Geological condition of Tuzla: (a) Plan view (modified from Mancini et al. (2009a)) and (b) Vertical X-X' cross section (Parwata et al. 2019)

Monitoring results

This study used the 145 SAR data images observed every 6-12 days by Sentinel-1A/B satellites (ESA) from October 2014 to July 2018 in the descending orbit.

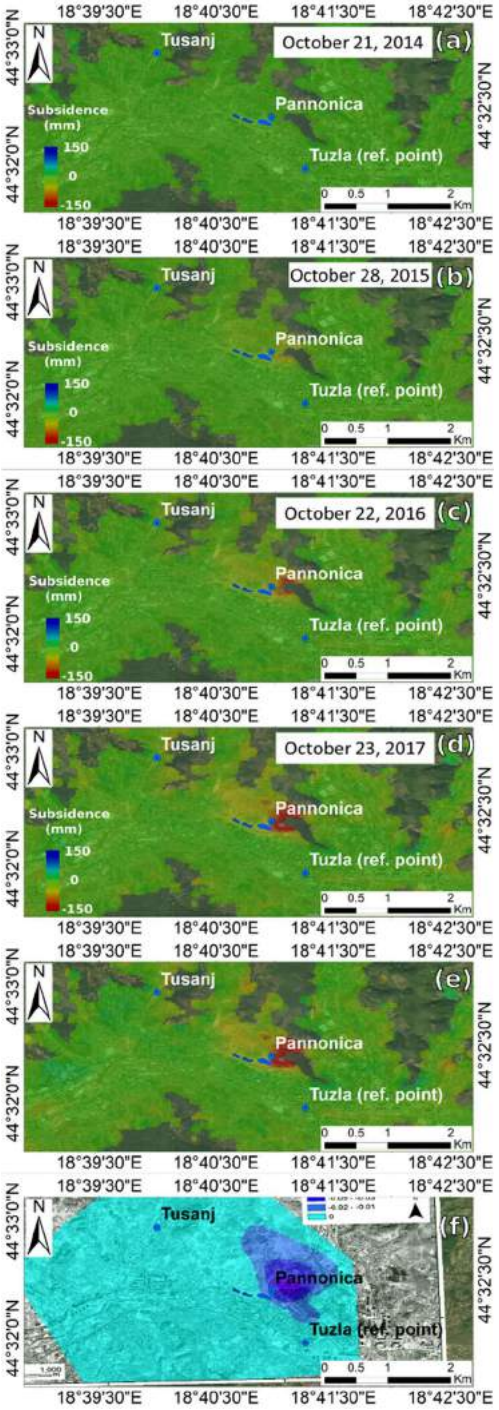

Figure 17 Subsidence distribution obtained by SBAS-DInSAR on several dates: (a) Oct. 21, 2014, (b) Oct. 28, 2015, (c) Oct. 22, 2016, (d) Oct. 23, 2017, (e) July 2, 2018, and (f) GPS results (2006 to 2007) (Parwata et al. 2019)

Figures 17(a)-(e) show the distribution of subsidence obtained by SBAS-DInSAR. The maps show that the incremental subsidence started on October 9, 2014. The subsidence area is indicated by yellow and red colors (negative values). The location of large subsidence is almost the same as that obtained by GPS (see Figure 17(f)).

Comparisons of the displacements measured by DInSAR and GPS using the kinematic method in the direction of LOS are shown in Figure 18. The temporal transition and the total amount of LOS displacement by DInSAR almost coincide with the results by GPS at "Pannonica" point (see Figure 17(f)) for 3.7 years.

At "Tusanj" point, the effective results of GPS were quite limited because the GPS monitoring results were rather scattered. Nevertheless, DInSAR could continuously obtain the LOS displacements, and the results agreed well too.

In addition, the DInSAR results show that the "Tuzla" point was very stable. The total amount of LOS displacement was only a few mm for 3.7 years. This result is reasonable, because this is the reference point (fixed point) of the GPS monitoring system.

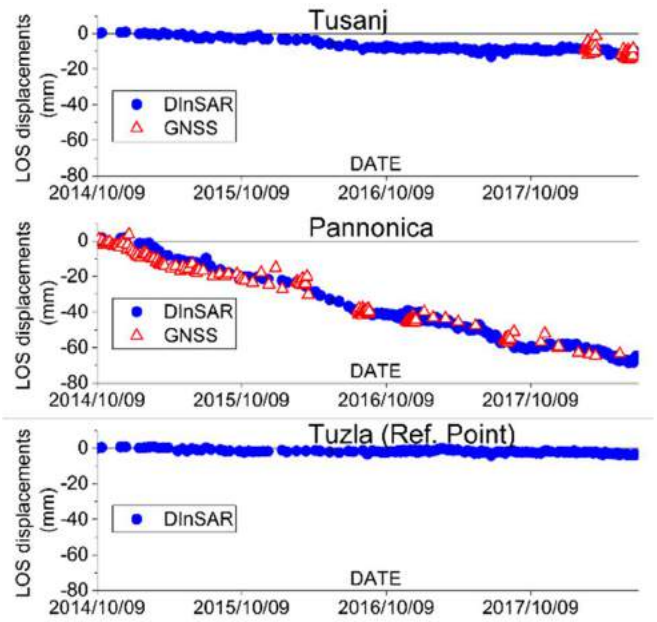

Figure 18 Comparison between DInSAR and GPS results (Parwata et al. 2019)

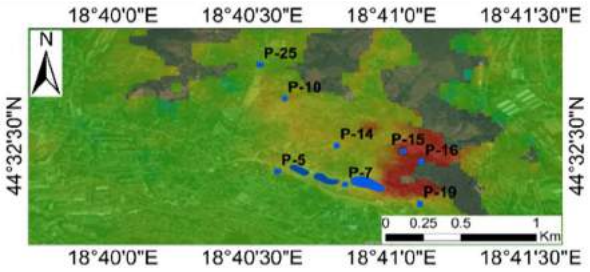

(a) Location of points

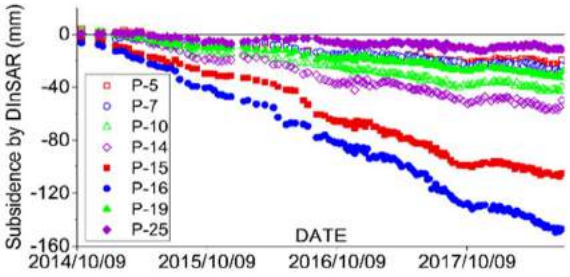

(b) Subsidence in temporal evolution for each point

Figure 19 Subsidence at several points (Parwata et al. 2019)

The temporal evolution of subsidence at several points, P-5, P-7, ..., P-25 (see Figure 19(a)), from 2014 to 2018 are shown in Figure 19(b). Among these points, the highest subsidence rate was detected at P-16, about -40 mm/year, while the lowest one was found at P-25, about -3 mm/year. There is still a possibility that subsidence will continue into the future.

SBAS-DInSAR is a useful tool for monitoring long-term land subsidence due to groundwater extraction (Yastika et al. 2019).

Landslides in the Vipava River Valley, Slovenia

The Vipava River Valley, located in the southwest part of Slovenia, is well known as a landslide-prone area (see Figure 20). There are four remarkable landslides in this area (Bizjak and Zupančič 2009; Jemec Auflič et al. 2017; Verbovšek et al. 2018), namely, Rebrnice, Stogovce, Slano blato, and Selo. The area extends 40 km in length and several km in width. The landslides are characterized by the various volumes and velocities of their movement. The occurrence of debris flows and landslides sometimes causes damage to residences, infrastructures, farmland, etc.

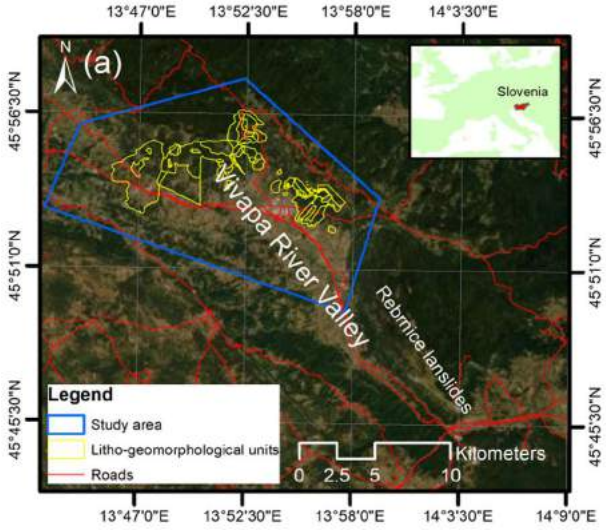

Figure 20 Vipava River Valley and study area

It is vital that the current situation of these landslides be known and that better mitigation plans be designed by monitoring the landslide behavior and conducting geological and geotechnical studies. An effective monitoring method that is capable of covering extensive areas is needed. The SBAS-DInSAR has been applied to this area (Yastika et al. 2019).

Monitoring site

Complex landslides, which have been occurring from Pleistocene to recent times, are related to the geological structure - Mesozoic carbonates have been thrust over folded and tectonically fractured Tertiary siliciclastic flysch (Jemec Auflič et al. 2017). Such overthrusting has caused steep slopes and the fracturing of rocks, producing intensely weathered carbonates and large amounts of carbonate scree deposits. The differences in elevation here are significant and range from 100 m at the valley bottom to over 1200 m on the high karstic plateau. The combination of unfavorable geological conditions and periods of intense short or prolonged rainfall has led to the formation of different types of complex landslides. The blue color polygon in Figure 20 shows the study area.

Monitoring results

This study used 134 and 139 SAR data images in the ascending and descending passes, respectively, observed from September 2016 to January 2019 by Sentinel-1A/B satellites. Figures 21(a) and (b) show the LOS displacement distributions in the ascending and descending passes, respectively. The magenta color on the maps represents areas of geometrical distortion in the SAR data, such as radar layover or shadowing. Although there were some areas that had no results (no color) due to low temporal coherence, it was clearly found that the distribution of displacements could be detected in this area.

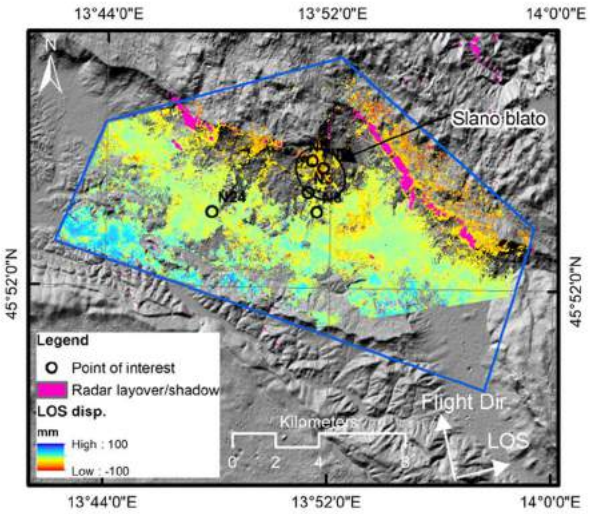

(a) Results in ascending pass

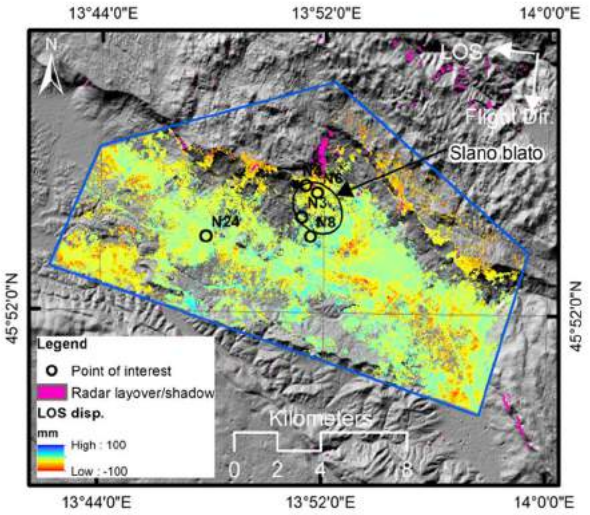

(b) Results in descending pass

Figure 21 LOS displacement distribution maps in Vipava River Valley (2016 to 2019) (Yastika et al. 2019)

The "Slano blato landslide area" is taken to see the detailed transition of the LOS displacements from Figure 26. Figure 27 shows the LOS displacement distribution maps and the temporal transition at several points in the Slano blato landslide area. The spatial distribution of the surface displacements is clearly visible. Several deep wells were constructed in the top of the slope as a countermeasure to the landslide. The locations of the wells are marked by black circles and labeled as W1 to W11 on the maps.

In Figures 22(a) and (b), the temporal transition of the LOS displacements at well points W1, W6, W11, UW1, and WD1 are shown. Figure 23 illustrates the geometrical relationship between the actual three-dimensional displacement vector and the LOS (ascending and descending) displacements.

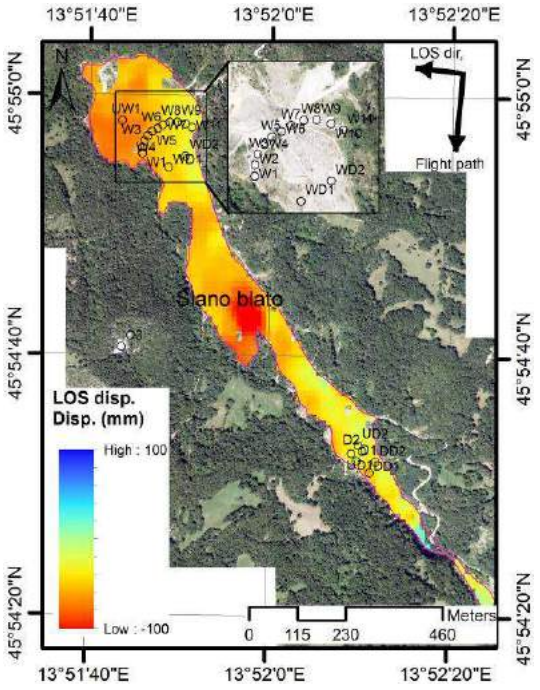

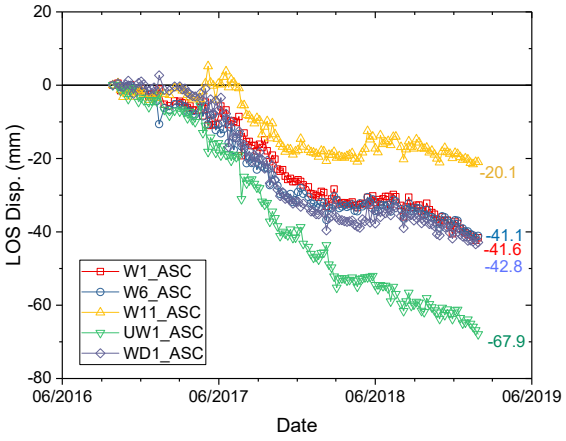

(a) Results in ascending pass

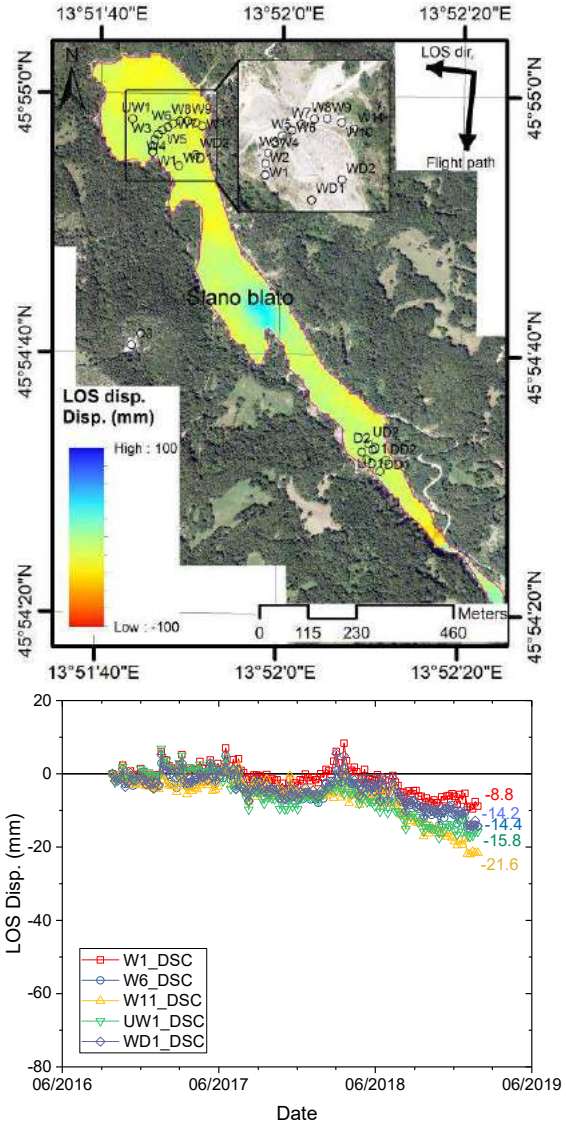

(b) Results in descending pass

Figure 22 LOS displacement distribution map and temporal transition at several points in Slano blato landslide area (Yastika et al. 2019)

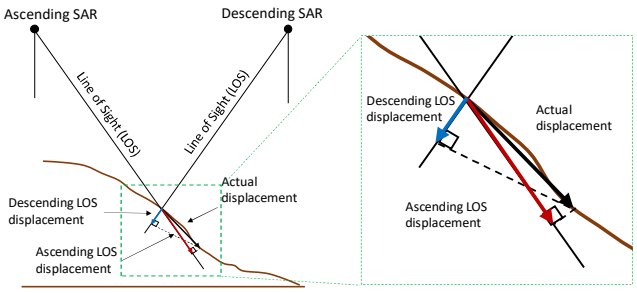

Figure 23 Geometrical relationship between actual displacement vector and LOS (ascending and descending) displacements.

Since the LOS displacements are projections of the actual displacement vectors with the LOS direction, it is natural that the ascending LOS displacements are different from the descending ones (see Figure 23). The results in Figure 22 indicate that the displacement at the top of the Slano blato landslide area seems to be moving down toward the toe of the slope at a rate of at least 10-30 mm/year.

Other cases

Collaborations with Balkan countries have been extended to landslides in Hrvatska Kostajnica, Croatia (Podolszki et al. 2019), in Kranevo, Bulgaria, etc. More fruitful results are highly anticipated.

Conclusions

Satellite technology, namely, GPS and DInSAR, comprises important engineering tools for monitoring ground displacements. The concluding remarks are as follows:

- Methods of displacement monitoring using GPS can provide the three-dimensional displacements of the ground automatically and continuously with high accuracy (i.e., mm level).
- "The ISRM suggested method for monitoring rock displacements using the Global Positioning System" has been published, and this technology has become a standard tool for displacement monitoring.
- DInSAR is an attractive tool for monitoring the displacement of extensive areas without the necessity for any devices by the users.
- Case studies of applications of GPS and DInSAR to practical problems were demonstrated in this paper. All cases indicated that both methods were very effective for displacement monitoring over extensive areas.
- Satellite technology can make invisible ground behavior visible over an extensive area.
- Collaborations with Balkan countries have been conducted to monitoring the subsidence of the ground and landslides. Fruitful results have already been reported.

Acknowledgments

This research has been partially supported by JSPS KAKENHI (Grant-in-Aid for Scientific Research, Japan Society for the Promotion of Science) Grant Numbers 25350506, and 16H03153. The author wishes to express his appreciation to his colleagues and students for the contributions they made to the field work and the analysis of the data.

All the Sentinel-1A/B SAR data used in this research were provided by the European Space Agency (ESA) and are downloadable from the Alaska Satellite Facility (ASF).

The author also thanks Ms. H. Griswold for proofreading this paper.

References

Berardino P, Fornaro G, Lanari R, Sansosti E (2002) A new algorithm for surface deformation monitoring based on small baseline differential SAR interferograms. IEEE Trans Geosci Remote Sens, 40:2375–2383.

Bizjak K F, Zupančič A (2009) Site and laboratory investigation of the Slano blato landslide. Eng Geology, 105:171-185.

Ferretti A (2014) Satellite InSAR data: reservoir monitoring from space. EAGE Publication, The Netherlands.

Ferretti A, Monti-Guarnieri A, Prati C, Rocca F (2007) InSAR Principles: Guidelines for SAR interferometry processing and interpretation. Netherlands: ESA Publications.

Furuyama Y, Nakashima S, Shimizu N (2014) Displacement monitoring using GPS for assessing stability of unstable steep slope by means of ISRM suggested method. Proceedings of the ISRM International Symposium - 8th Asian Rock Mechanics Symposium (ARMS8), Sapporo, Japan, 1897-1904.

Hanssen R F (2002) Radar Interferometry. New York: Kluwer Academic Publisher.

Hoffman-Wellenhof, B., Lichtengger, H. & Collins, J. (2001) GPS – Theory and Practice. 5th revised edition, Springer.

Iwasaki T, Takechi K, Takeishi A, Masunari T, Takechi Y, Shimizu N (2003) Web-based displacement monitoring system using GPS for the maintenance of roadside slopes. Proceedings of 6th International Symposium on Field Measurements in Geomechanics, Oslo, Norway, 137-143.

Jemec Auflič M, Jež J, Popit T, Košir A, Maček M, Logar J, Petkovšek A, Mikoš M, Calligaris C, Boccali C, Zini L, Reitner J, Verbovšek T (2017) The variety of landslide forms in Slovenia and its immediate NW surroundings. Landslides, 14(4):1537-1546.

Kien G T (2019) Continuous displacement monitoring by using GPS and its application to a large-scale steep slope. Doctoral Dissertation, Yamaguchi University.

Mancini F, Stecchi F, Gabbianelli G (2009a) GIS-based assessment of risk due to salt mining activities at Tuzla (Bosnia and Herzegovina). Engineering Geology, 109:170–182.

Mancini F, Stecchi F, Zanni M, Gabbianelli G (2009b) Monitoring ground subsidence induced by salt mining in the city of Tuzla (Bosnia and Herzegovina). Environmental Geology, 58:381–389.

Masunari T, Tanaka K, Okubo N, Oikawa H, Takechi K, Iwasaki T, Shimizu N (2003) GPS-based continuous displacement monitoring system. Proceedings of 6th International Symposium on Field Measurements in Geomechanics, Oslo, Norway, 537-543.

Misra P, Enge P (2006) Global Positioning System - signals, measurements, and performance. 2nd Ed, Ganga-Jamuna Press.

Parwata I N S, Shimizu N, Zekan S, Grujić B, Vrkljan I (2018) Application of DInSAR for monitoring the subsidence induced by salt mining in Tuzla, Bosnia and Herzegovina. Proceedings of ISRM

International Symposium -10th Asian Rock Mechanics Symposium, Singapore, G2, 8p.

Parwata I N S, Shimizu N, Grujić B, Zekan S, Čeliković R, Vrkljan I. (2019) Validity of SBAS-DInSAR monitoring of subsidence induced by salt mining in Tuzla. Proceedings of ISRM Specialized Conference on Geotechnical Challenges in Karst, Omiš, Croatia, 311-316.

Podolszki L, Parwata I N S, Shimizu N, Pollak D, Vrkljan I (2019) Landslide in Hrvatska Kostajnica – collected data and analysis in progress. Proceedings of ISRM Specialized Conference on Geotechnical Challenges in Karst, Omiš, Croatia, 323-328.

Satoh W, Iwasaki T, Sakurai W, Fujii A, Shimizu N (2014) Monitoring the stability of a large-scale colluvium deposited by slope failures due to heavy rainfall using a GPS automatic monitoring system, Proceedings of the ISRM International Symposium - 8th Asian Rock Mechanics Symposium (ARMS8), Sapporo, Japan, 1778-1783.

Shimizu N, Masunari T, Iwasaki T (2011) GPS displacement monitoring system for the precise measuring of rock movements. Proceedings of 12th International Congress on Rock Mechanics, Beijing, China, 1117-1120.

Shimizu N, Matsuda H (2002) Practical applications of the Global Positioning System for the assessment of slope stability based on the Displacement Monitoring Approach. Proceedings of the 3rd Korea-Japan Joint Symposium on Rock Engineering, ISRM Regional Symposium, Seoul, Korea, 57-70.

Shimizu N, Matsuda H (2003) Displacement monitoring using GPS and its interpretation method for the assessment of slope stability. Proceedings of 6th International Symposium on Field Measurements in Geomechanics, Oslo, Norway, 657-664.

Shimizu N. Nakashima S (2017) Review of GPS displacement monitoring in rock engineering. Rock Mechanics and Engineering, Volume 4, ed. Xia-Ting Feng, CRC Press, Chapter 19:593-626.

Shimizu N, Nakashima S, Masunari T (2014) ISRM suggested method for monitoring rock displacements using the Global Positioning System. Rock Mech Rock Eng, 47:313-328.

Tosa S, Yamasaki T, Ito K, Suganuma T, Oikawa N, Takeishi A, Shimizu N (2014) Case studies on landslide monitoring using the GPS Displacement Monitoring System. Proceedings of the ISRM International Symposium - 8th Asian Rock Mechanics Symposium (ARMS8), Sapporo, Japan, 1887-1896.

Verbovšek T, Popit T (2018) GIS-assisted classification of litho-geomorphological units using Maximum Likelihood Classification, Vipava Valley, SW Slovenia. Landslides, 15(7): 1415-1424.

Yastika P E, Shimizu N, Abidin H Z (2019) Monitoring of long-term land subsidence from 2003 to 2017 in coastal area of Semarang, Indonesia by SBAS DInSAR analyses using Envisat-ASAR, ALOS-PALSAR, and Sentinel-1A SAR data. Advances in Space Research, 63:1719–1736.

Yastika P E, Shimizu N, Verbovšek T (2019) A case study on landslide displacement monitoring by SBAS-DInSAR in the Vipava River Valley, Slovenia. ISRM Specialized Conference on 5th ISRM Young Scholars' Symposium on Rock Mechanics and International Symposium on Rock Engineering for Innovative Future, Okinawa, Japan. (in press)

doi.org/ 10.35123/ReSyLAB_2019_2

Unusual becoming Usual: recent persistent-rainstorm events and their implications for debris flow risk management in the northern Apennines of Italy

Alessandro Corsini [1], Giuseppe Ciccarese [1], Giovanni Truffelli [2]

1) University of Modena and Reggio Emilia – Department of Chemical and Geological Sciences, via Giuseppe Campi 103, 41125 Modena, Italy

2) Emilia-Romagna Region – Regional Agency for Civil Protection and Territorial Security, Strada Giuseppe Garibaldi 75, 43121 Parma, Italy

Abstract The alluvial events of Parma (13 October 2014) and Piacenza (13-14 September 2015) in the northern Apennines of Italy have had significant effects in terms of flooding and morphological changes along the main and secondary rivers of the affected areas. The paper presents a summary of the characteristics of the rainstorm events, as well as of the triggered debris flows and their consequences on infrastructures. In the perspective of an extremization of rainfall regimes as a consequence of ongoing climate changes, these phenomena might become quite usual in the future and should be further studied in order to define regional-specific triggering thresholds, analyse precursors from weather radar datasets and assess susceptibility on a regional scale basis.

Keywords Debris Flows, rainstorms, northern Apennines.

Introduction

The alluvial events of Parma (13 October 2014) and Piacenza (13-14 September 2015) have had significant effects in terms of flooding and morphological changes along the main and secondary rivers in upper Val Parma, Val Baganza Val d'Aveto, Val Nure, Val Trebbia (AIPO, 2014; ARPAE-SGSS, 2016). These events have been caused by severe rainstorms characterized by hourly rainfall peaks higher than 80 mm and rainfall duration between 6 hours (Piacenza) and 9 hours (Parma). Along the slopes and the streams, these rainstorm events have triggered several debris flows, causing damages to hydraulic works and road infrastructure networks.

Debris flows are quite common in the Alps (Arattano & Moia, 1998; Berti et al., 1999; Cavalli & Grisotto, 2005; Marchi & D'Agostino, 2004; Pavlova et. al., 2014) but are considered unusual in the Emilia-Romagna Apennines. However, debris flows have occurred in Emilia Romagna Region also in the past, for instance during the alluvial events of Piacenza (Val Trebbia) in September 1953 and Modena, Reggio Emilia e Parma provinces in September 1972 and September 1973 (Moratti & Pellegrini, 1977; Papani & Sgavetti, 1977; Rossetti & Tagliavini, 1977).

This short note, which derives from the summary of the works of Corsini et al. (2015) e Ciccarese et al. (2016), presents the rainfall data recorded during the alluvial events of 2014 and 2015, the distribution and characteristics of debris flows triggered during the events and the damages caused to the infrastructure.

Rainstorm events

Parma province event of 13 October 2014

During the alluvial event of 13 October 2014, debris flows have occurred in Val Parma and Val Baganza, along the slopes of Monte Cervellino-Monte Vitello (municipalities of Corniglio, Berceto and Calestano) (Fig.1a).

The rain-gauge of Marra, part of ARPAE (Regional Agency for Prevention, Environment and Energy) monitoring network located in the area affected by debris flows, has recorded, between 12th and 13th October 2014, a rainfall of 308.6 mm in 24 hours (Fig.1b). The hourly rainfall data show higher rainfall intensity values between 7.00 and 15.00 of 13th October 2014. The maximum hourly rainfall peak recorded has been of 81.8 mm/h. These rainfall intensity values are associated to return period exceeding 100 years and are above almost any of debris flow triggering rainfall thresholds presented in scientific literature (Caine, 1980; Ceriani et al., 1992; Cannon & Gartner, 2005; Crosta & Frattini, 2001; Innes, 1983; Marchi et al., 2002; Paronuzzi et al., 1998; Wieczorek, 1987) (Fig.1c).

Piacenza province event of 12-13 September 2015

During the alluvial event of 13th and 14th September 2015 several debris flows have occurred in Val d'Aveto, Val Nure and Val Trebbia (particularly affected were the municipalities of Ferriere, Cerignale and Ottone) (Fig.2a).

The rainstorm event has occurred between 22.00 of 13th and 03.00 of 14th September and the rainfall data have been recorded by ARPAE rain-gauges in the mountain basins of Trebbia and Nure rivers.

All stations have recorded rainfall values higher than 200 mm in 24 hours. The Salsominore rain-gauge, located in the area mostly affected by debris flow, has recorded rainfall values of 329 mm in 24 hours (maximum value recorded in the area) and hourly rainfall intensity peak (at

01.30 o'clock) of 107.6 mm (Fig.2b). The highest hourly precipitation peaks have been recorded by rain-gauges located at higher altitudes: the rain-gauge of Cabanne has recorded a hourly rainfall peak of 123.6 mm.

The rainfall values recorded by all rain-gauges are above the thresholds presented in scientific literature (Caine, 1980; Ceriani et al., 1992; Cannon & Gartner, 2005; Crosta & Frattini, 2001; Innes, 1983; Marchi et al., 2002; Paronuzzi et al.,1998; Wieczorek, 1987) (Fig.2c).

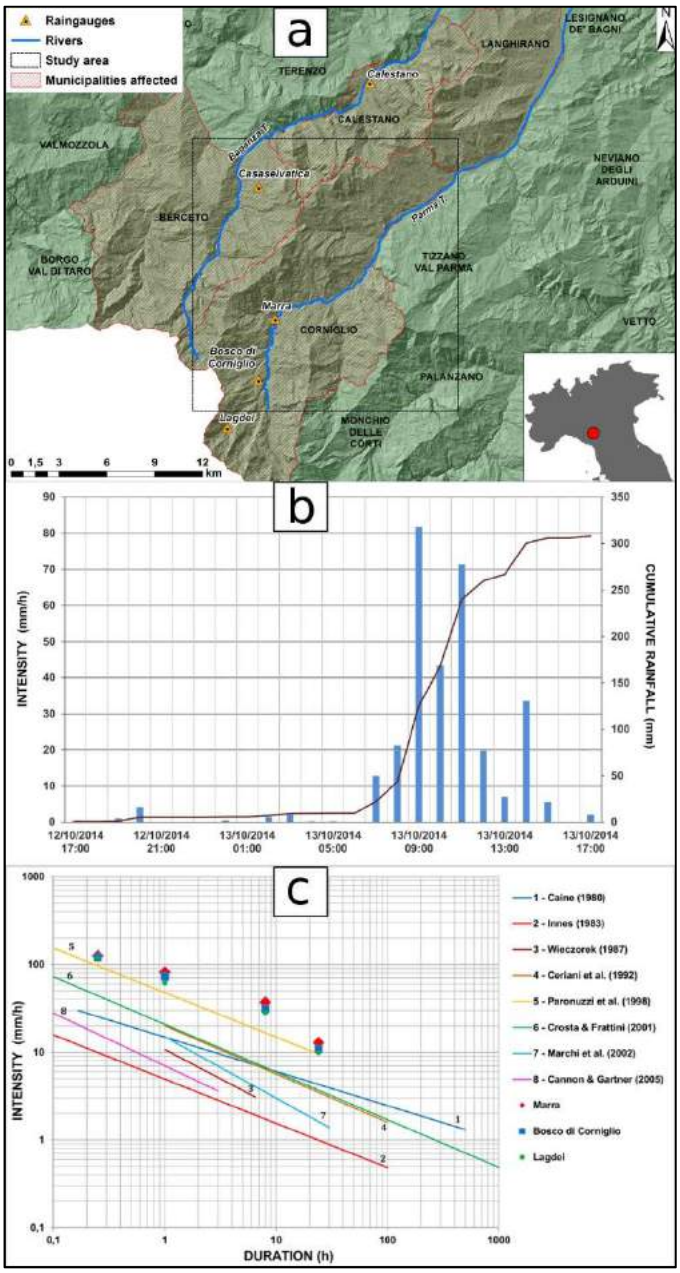

Figure 1 a) Area affected by debris flows during the Parma province alluvial event of 2014; b) rainfall data recorded by ARPAE raingauge of Marra during the alluvial event; c) comparison between rainfall data recorded by 3 raingauges and some rainfall thresholds triggering debris-flow proposed in scientific literature.

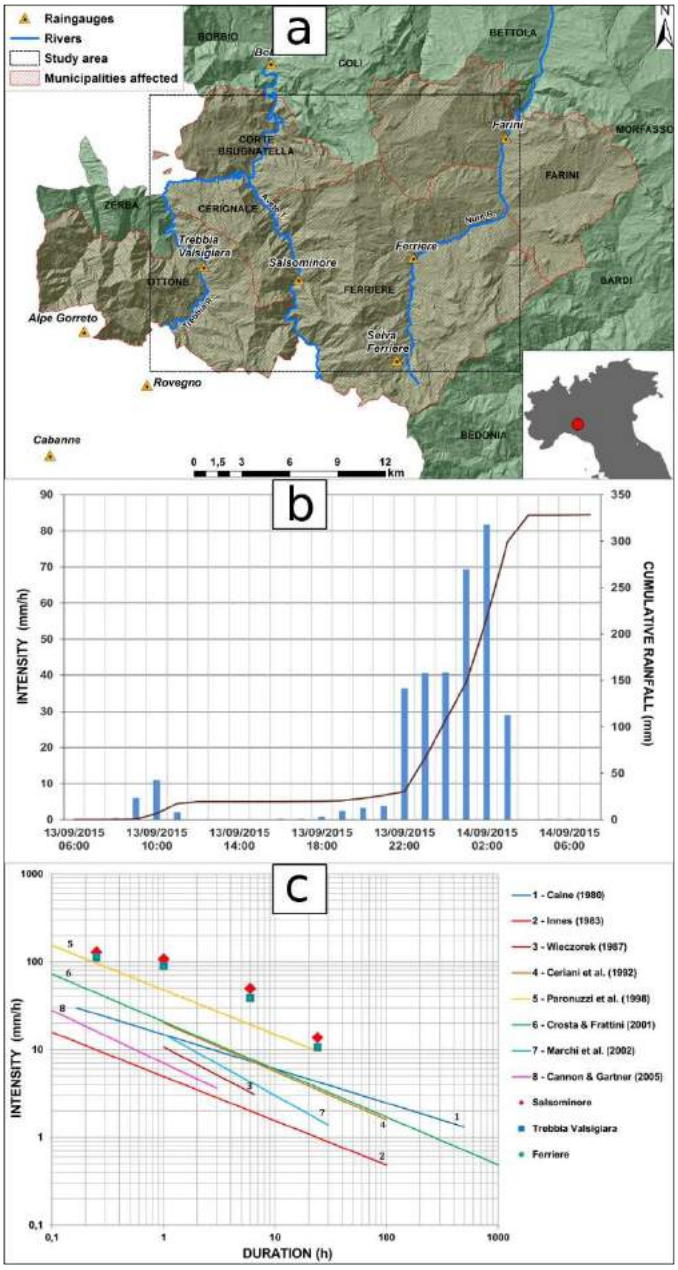

Figure 2 a) Area affected by debris flows during the Piacenza province alluvial event of 2015; b) rainfall data recorded by ARPAE raingauge of Salsominore during the alluvial event; c) comparison between rainfall data recorded by 3 raingauges and some rainfall thresholds triggering debris-flow proposed in scientific literature.

Debris flows occurrence

Parma province event of 13 October 2014

During the field surveys performed a few days after the event in Val Parma and Val Baganza, 26 debris flows have been identified along the torrents (Fig.3a). The length of the torrent tracks affected by debris flows ranges from 1000 m to 3000 m. The altitude difference between the triggering zone and the final accumulation ranges from 600 m to 150 m.

Bedrock lithology is flysch with sandstone or limestone components prevailing on pelitic component and mono-polygenic breccia. The triggering zones

correspond, in many cases, to areas of marked changes in slope gradient where coarse debris deposits has affected by rotational- translational slides. In the case of Rio Vestana more than 10.000 m³ of coarse debris have been mobilized (Fig.3b).

Along the channels, streambed scouring and debris deposits have been documented. Furthermore, the debris levees shows the typical inverse gradation of debris flow deposits (Fig.3c).

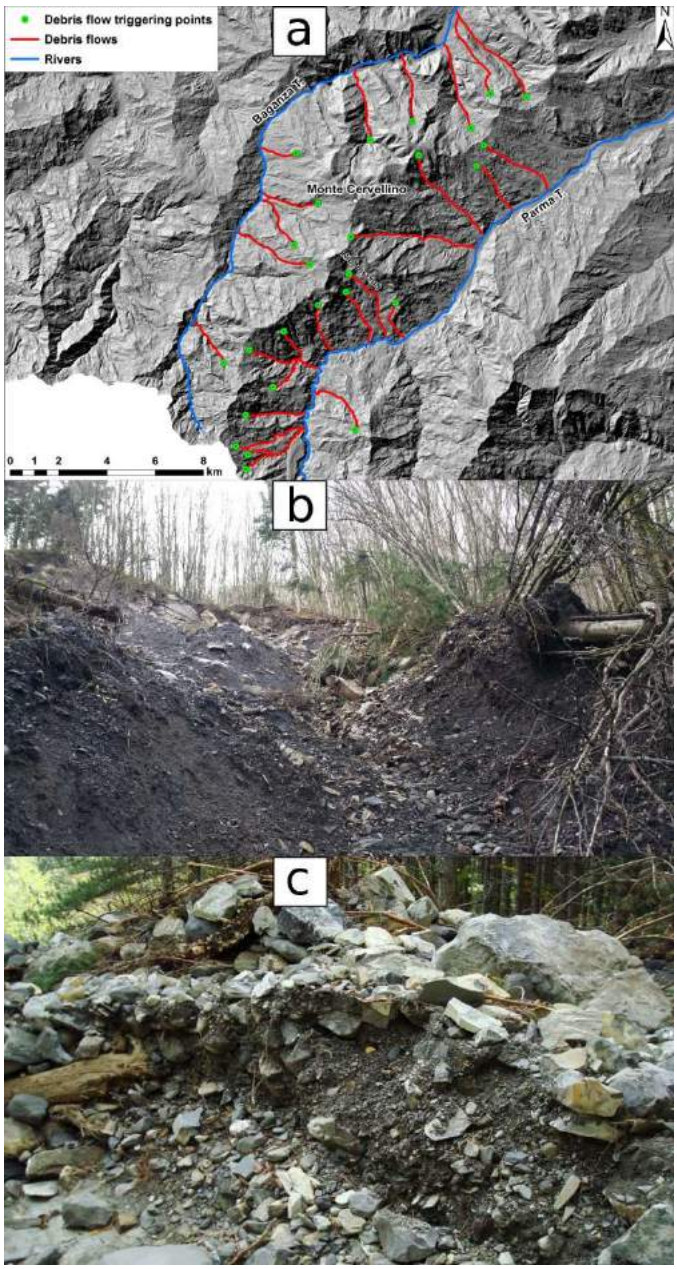

Figure 3 a) Map of debris flows distribution during the event of September 2014 in Parma province: torrents affected and triggering points; b) example of debris flow triggering zone documented in Parma province; c) debris flow deposit documented along Rio Vestana: levees with inverse gradation of debris flow deposits in Rio Vestana.

Piacenza province event of 12-13 September 2015

The field surveys and the analysis of post-event satellite and aerial images have concerned an area of around 350 km² comprising various sub-basins of Trebbia River, Nure Torrent and Aveto Torrent. Slope instability phenomena have been surveyed and mapped, including 113 debris flows (Fig.4a), 89 debris slides, 4 mud flows and 29 erosion on the banks. Furthermore, 110 debris flows triggering zones have been identified and mapped in form point: 57% of the phenomena surveyed has affected the sub-basins of the Aveto Torrent, 24% the sub-basins of the Nure Torrent and 19% those of the Trebbia River.

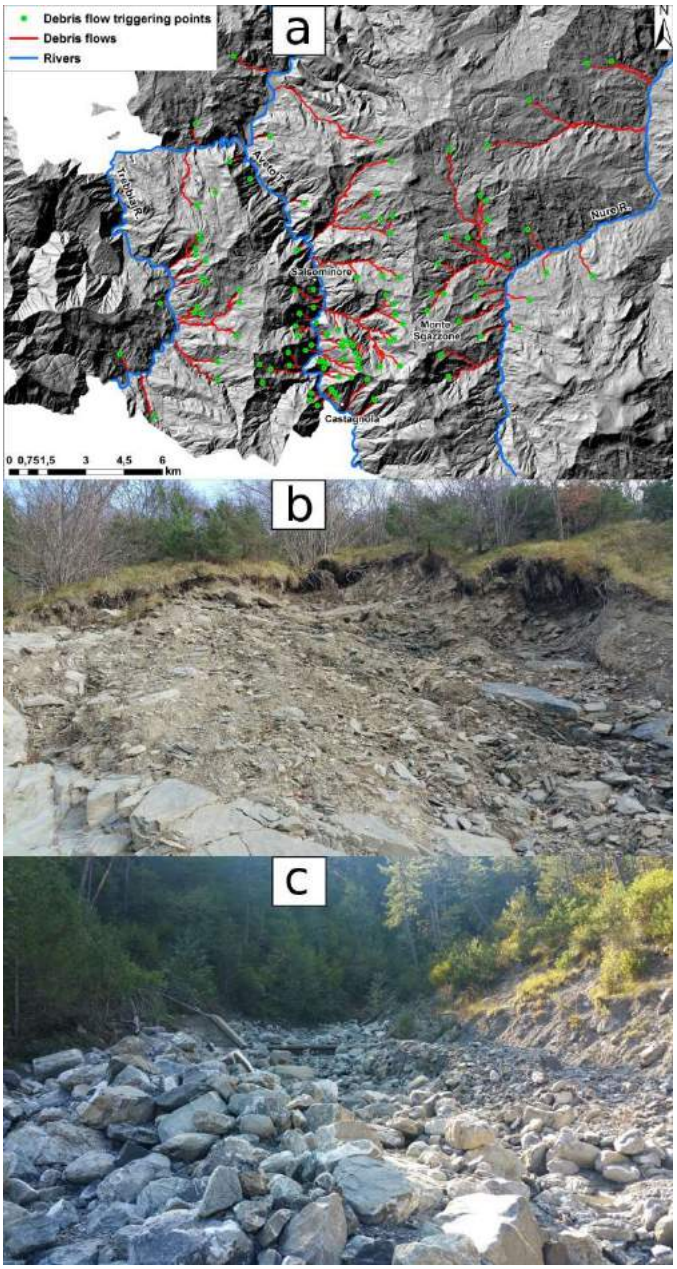

Figure 4 a) Map of debris flows distribution during the event of October 2015: torrents affected and triggering points; b) example of debris flow triggering zone documented in Piacenza province; c) debris flow deposit zone documented in Piacenza province along a torrent affected by debris flow: channel overrun by debris.

The sites of Salsominore and Castagnola, in Ferriere municipality (Val d'Aveto), along the slopes of Monte Sgazzone, are the areas mostly affected by debris flows during the rainstorm event.

The triggering zones correspond to areas in the upper part of the sub-basins where slope debris has been remobilized by rotational and translational slides and subsequently transported along the track channel (Fig.4b).

In 71% of the triggering zones identified, bedrock lithology is Flysch with an arenite or sandstone component prevailing over the pelite component and in in 29% is chaotic melangés with a dominant pelite component.

In most cases, the thickness of debris remobilized from the triggering zones is 5-7 m. The thickness reached by debris flows in the track channel is higher than 4-5 m (Fig.4c). Furthermore, in many torrents, the erosive action of debris flows has caused failures along the sides of the channel.

Effects on infrastructures

During the Parma province alluvial event, several check dams along the torrents affected by debris flows were destroyed or buried by debris (Fig. 5a). Consequently, large amounts of debris previously trapped upstream of the check-dams, have been mobilized along the channel. Severe damages have affected many local roads crossing the debris flow tracks (Fig.5b), mostly where the torrents have been previously channeled into 1 m diameter pipes under the roads. In these cases, the flow-pipes have been rapidly obstructed by the debris flows, causing the overflow of debris and the erosion and cut-through of the road track (Fig. 5c).

Similarly, during the Piacenza province alluvial event, the most relevant damages have suffered by the roads in the points of intersection with the channels affected by debris flows. In some cases, the same road has been crossed by debris flows in several sections (Fig.6a).The accumulations of debris reached thicknesses up to 2 m (Fig.6b).

In the fan-shaped accumulation zones at the confluence of the torrents into the main rivers large amounts of debris have overflowed the roads and, in the case of Rio Ruffinati, a hydropower plant (Fig.6c).

Conclusions

As demonstrated by the events of Parma 2014 and Piacenza 2015, as well as by the "historical" events ì Reggio Emilia-Modena in 1972 or Piacenza 1953, the occurrence of debris flows in Emilia Romagna Apennines is not to be considered so unusual as previously thought. Moreover, in the perspective of an extremization of rainfall regimes as a consequence of ongoing climate changes, these phenomena might become quite usual in the future.

Figure 5 Example of effects on infrastructures in Parma province: a) check-dams cut-through by debris flows; b) road overrun by debris; c) erosion and cut-through of the road track.

Their implications for debris flow risk management in the northern Apennines of Italy attain to the following problems: (i) definition of alert thresholds, which take into account the rainfall regimes of the different portions of the territory, to overcome the limits consequent to the use of a single threshold value (as indicated in DGR n°962/2018); (ii) analysis of the correlation between radar weather data, lightning and debris flows occurrence (Ciccarese et al., 2017 e Corsini et al., 2017); (iii) susceptibility and hazard mapping in order to take into account the predisposing hydro-morphometric and geological characteristics and the probability of exceeding the triggering rainfall threshold values. Research on these topics has been started and, while ongoing, has already provided some

significant results that allow raising the level of attention on this type of phenomena.

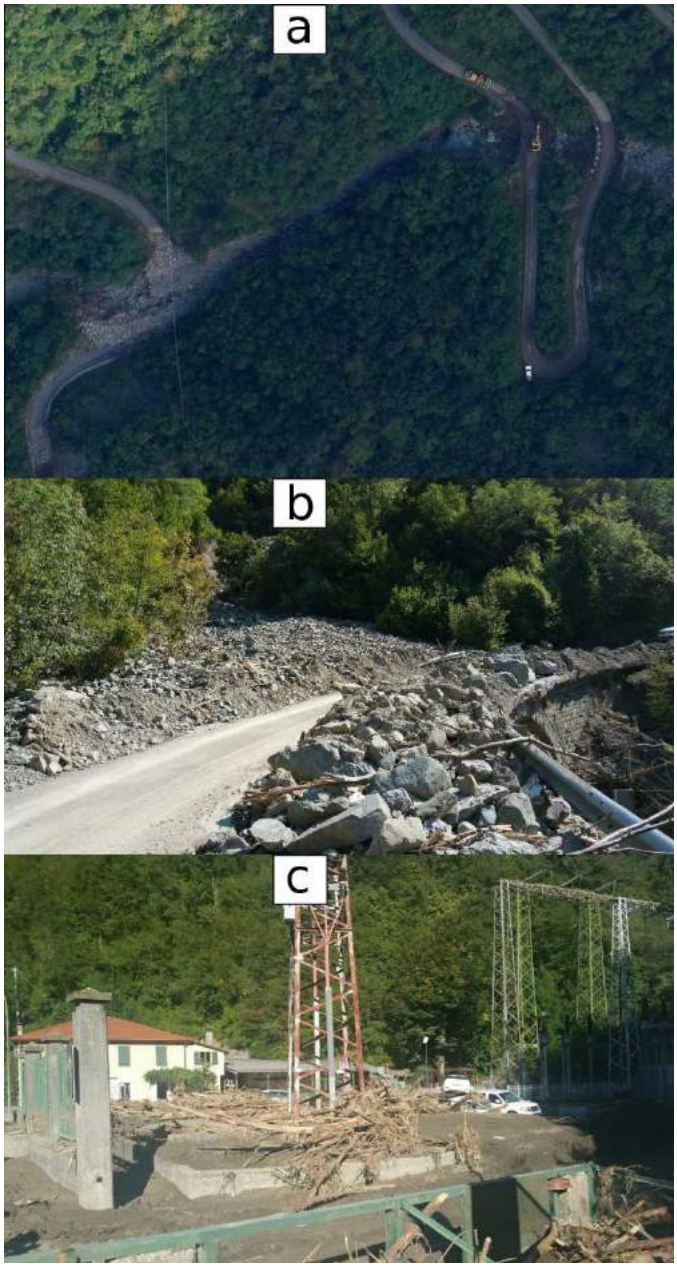

Figure 6 Example of effects on infrastructures in Piacenza province: a) aerial photo of a local road that crosses the debris flow in many sections; b) debris flow deposit along the local road; c) hydropower plant of Ruffinati overrun by debris.

Acknowledgments

This work was supported by the Emilia-Romagna Region - Agency for Civil Protection and Territorial Security, under the framework of the partnership agreement for "Research, technical, scientific and informative activities on support to the forecast, prevention and management of hydrogeological risk - 2016–2021" (responsible A. Corsini).

References

AIPO (Agenzia Interregionale per il Fiume Po) (2014). Relazione preliminare sugli eventi di Parma e Baganza del 13-14 ottobre 2014. www.agenziapo.it/file/1361/download?token=CPOwCZgp

Arattano M. & Moia F. (1998). Monitoring the propagation of a debris flow along a torrent - Hydrological Sciences Journal, 44 (5), pp. 811–823.

ARPAE-SGSS (ARPAE Servizio Idro Meteo Clima, Servizio Geologico Sismico e dei Suoli) (2016). Rapporto sull'evento alluvionale del 14 settembre 2015. http://ambiente.regione.emilia-romagna.it/geologia/notizie/notizie-2016/rapporto-sullevento-alluvionale-del-14-settembre-2015

Berti M., Genevois R., Simoni A., Tecca P.R. (1999). Field observations of a debris flow event in the Dolomites. Geomorphology 29, 265-274.

Caine N. (1980) - The rainfall intensity duration control of shallow landslides and debris flow. Geografiska Annaler, 62 (1-2), 659-675.

Cannon S.H. & Gartner, J.E. (2005). Wildfire-related debris flow from a hazards perspective. In Debris-flow hazards and related phenomena (pp. 363-385). Springer Berlin Heidelberg.

Cavalli M. & Grisotto S. (2005). GIS-based identification of debris flow dominated channels: application to the upper Avisio Basin (Trento). Servizio Sistemazione Montana della Provincia Autonoma di Trento, Interreg III Project Alpine Space, Work Package 7, Innovative Tools for Information Collection.

Ceriani M., Lauzi, S., Padovan N. (1992). Rainfalls and landslides in the alpine area of Lombardia region, central Alps, Italy. In Proc. Int. Symp. Interpraevent (pp. 9-20).

Ciccarese G., Corsini A., Pizziolo M., Truffelli G. (2016). Debris Flows in Val Nure and Val Trebbia (northern Apennines) during the September 2015 alluvial event In Piacenza Province (Italy). Rendiconti Online della Società Geologica Italiana, 41, 127-130

Ciccarese G., Corsini A., Alberoni P.P., Celano M., Fornasiero A. (2017). Using Weather Radar Data (Rainfall and Lightning Flashes) for the analysis of Debris Flows occurrence in Emilia-Romagna Apennines (Italy). Advancing Culture of Living with Landslides. Springer International Publishing, 4, 437 -448.

Corsini A., Ciccarese G., Diena M., Truffelli G., Alberoni, P.P., Amorati R. (2017). Debris flows in Val Parma and Val Baganza (northern Apennines) during the 12-13th October 2014 alluvial event in Parma province (Italy) - Italian Journal of Engineering Geology and Environment, Special Issue 2017, 29-38.

Corsini A., Ciccarese G., Berti M., Diena M., Truffelli G. (2015). Debris flows in Val Parma and Val Baganza (northern Apennines) during the October 2014 alluvial event in Parma Province (Italy) - Rendiconti Online della Società Geologica Italiana, 35, 85-88.

Crosta G. & Frattini P. (2001). Rainfall thresholds for the triggering of soil slips and debris flows. In Mediterranean Storms 2000 (pp. 463-488).

Genevois R., Tecca P.R., Berti M., Simoni A. (2000) - Debris flow in the Dolomites: experimental data from a monitoring system – G. Wieczorek, N. Naeser (Eds.), Proceedings, Second International Conference on Debris-flow Hazard Mitigation: Mechanics, Prediction, and Assessment, A.A. Balkema, Rotterdam, pp. 283–291.

Innes J.L. (1983). Debris flows. Progress in physical geography, 7(4), 469-501.

Marchi L., Arattano M., Deganutti A.M. (2002). Ten years of debris-flow monitoring in the Moscardo Torrent (Italian Alps). Geomorphology, 46(1), 1-17.

Marchi L. & D'Agostino V. (2004). Estimation of the debris-flow magnitude in the Eastern Italian Alps Earth Surface Processes and Landforms, 29, pp. 207–220.

Moratti L. & Pellegrini M. (1977). Alluvioni e dissesti verificatisi nel settembre 1972 e 1973 nei bacini dei fiumi Secchia e Panaro (Province di Modena e Reggio Emilia). Bollettino della Associazione Mineraria Subalpina, Anno XIV, n.2, pp. 323-374.

Papani G. & Sgavetti M. (1977) - Aspetti geomorfologici del bacino del T. Ghiara (Salsomaggiore Terme, PR) susseguenti all'evento del 18-09-1973. Bollettino dell'Associazione Mineraria Subalpina, 14, n. 3-4, 610-628.

Paronuzzi P., Coccolo A., Garlatti G. (1998). Eventi meteorici critici e debris flows nei bacini montani del Friuli. L'Acqua, Sezione I/Memorie, 6, 39-50.

Pavlova I., Jomelli V., Brunstein D., Grancher D., Martin E., Déqué M. (2014) - Debris flow activity related to recent climate conditions in the French Alps: A regional investigation. Geomorphology. 219, 248-259.

Rossetti G. & Tagliavini S. (1977) - L'alluvione ed i dissesti provocati nel bacino del Torrente Enza dagli eventi meteorologici del settembre 1972 (Province di Parma e Reggio Emilia). Bollettino dell'Associazione Mineraria Subalpina, 14, n. 3-4, 561-603.

Wieczorek G.F. (1987). Effect of rainfall intensity and duration on debris flows in central Santa Cruz Mountains, California. Reviews in Engineering Geology, 7, 93-104.

doi.org/ 10.35123/ReSyLAB_2019_3

The influence of weathering process on geotechnical and mineralogical properties of fine grained lithological flysch components along the northern Adriatic coast of Croatia

Martina Vivoda Prodan[(1)]

1) University of Rijeka, Faculty of Civil Engineering, Radmile Matejčić № 3, 51 000 Rijeka, Croatia

Abstract Investigation results of the influence of weathering process on the geotechnical and mineralogical properties of fine grained lithological flysch components, such as siltstones, in the area of north Istria, Rječina river valley and Vinodol valley are presented in this paper. Physical and mechanical so as mineralogical properties of incompetent, fine grained flysch lithological members significantly change due to weathering. Landslide occurrences in flysch deposits are frequent and slip surface is formed at the contact of surficial deposits and flysch rock mass or inside the weathered flysch rock mass. Weathering effect on the residual shear strength values of fine grained lithological flysch components are investigated by laboratory tests on samples of different weathering grades in direct shear and ring shear apparatus. Uniaxial compressive strength and durability of fine grained lithological flysch rock mass samples with different weathering grades are also investigated. Mineralogical composition of the same fine grained lithological flysch components of different weathering grades is determined. Numerical simulations of the Valići landslide reactivation in the Rječina river valley are conducted with residual strength parameters of different weathering grades of fine grained lithological flysch components obtained in laboratory tests.

Keywords flysch, weathering, durability, landslide, residual shear strength, mineralogy, numerical modelling

Introduction

Determination of processes and parameters that have a great influence on many landslide activation and reactivation in flysch rock formations along the northern Adriatic coast of Croatia is of big importance. Weathering process cause significant changes in the engineering properties of flysch rock mass especially in their incompetent fine grained lithological components such as siltstones. The flysch rock mass is characterized by high erodibility and low durability of its incompetent members, and it is almost completely covered by weathered surficial material that is susceptible to sliding. Determining changes in the residual shear strength due to weathering is highly useful, because many dormant landslides in the study area are reactivated due to the degradation of flysch rock mass. Slake durability tests, point load tests, ring shear tests, direct shear tests and mineralogical analysis to determine durability, uniaxial compressive strength, residual shear strength and mineralogical composition respectively of siltstones with different weathering grades were performed. The aim of this paper is to describe changes in the geotechnical and mineralogical properties of fine grained lithological flysch components, such as siltstones, due to long-term weathering processes. Implementation of performed laboratory results in the numerical analysis made in the LS-Rapid software to verify influence of residual shear strength on the landslide reactivation is also discussed.

Study area and flysch rock mass

The study area extends along the northern Adriatic coast of Croatia and includes the north part of the Istrian peninsula, the Rječina river valley and Vinodol valley regions. The area is composed of Paleogene flysch, Cretaceous and Jurassic limestone, and alluvial deposits (Velić and Vlahović 2009) and it is shown on Figure 1.

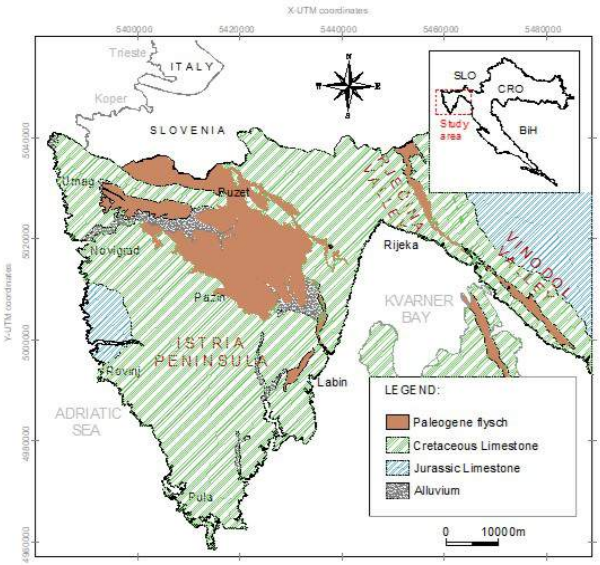

Figure 1 Simplified geological map of the study area (based on Velić and Vlahović 2009)

Flysch rock mass is characterized by rhythmic alternations of sandstone and fine-grained layers such as siltstones, silty shales and clayey shales, and may also contain breccias, conglomerates and limestone beds

(Marinos and Hoek 2001). Flysch rock mass belongs to soft rocks that can have undesirable behaviours, such as low strength, disaggregation, crumbling, high plasticity, slaking, fast weathering, and many other characteristics (Kanji 2014). The focus of this investigation was on siltstones, which are the flysch complex component most susceptible to weathering, and therefore their mechanical behaviour has the greatest influence on the behaviour of the overall flysch complex. Numerous instabilities and erosion processes (Figure 2) occur in the study area, and are most often related to the weathering of the flysch rock mass. Intense erosion is observed in flysch deposits in the Istrian peninsula (Gulam 2012) and Vinodol valley areas (Jurak et al. 2005), whereas no significant signs of erosion are present in the Rječina river valley. Numerous landslides have occurred in the flysch deposits in the Istrian peninsula, Rječina river valley and Vinodol valley regions (Dugonjić Jovančević 2013, Arbanas et al. 2014, Vivoda et al. 2012, Bernat et al. 2014). These geomorphological events are significantly influenced by weathering processes in the flysch deposits, especially in their fine grained, siltstone component. Weathering reduces the residual shear strength in these deposits, resulting in landslide reactivation.

Figure 2 Landslides in the study area a) the translational landslide Brus, b) a debris flow Krbavčići, c) the rotational landslide Marinci, d) erosion at Lesišćina in the Istrian peninsula, e) the Grohovo landslide, f) reactivated landslide Valići, g) landslide on the Grohovo road in the Rječina river valley, h) intense erosion at Slani Potok, i) dormant landslide in the Vinodol Valley

Weathering processes in flysch rock masses

Weathering is the process of alteration and breakdown of rock and soil materials at or near the earth's surface by physical, chemical and biotic processes. The weathering of rocks produces changes in their mineralogical composition, affecting colour, texture, composition, firmness and form. These changes result in a reduction in the mechanical properties of the rock (Selby 1993). During these processes, fresh rock is gradually transformed into granular soils, generally called residual soils, which differ from their parent rocks in mineralogical composition and structure (Eberhardt et al. 2005, Brown 1981). Flysch rock mass can have very diverse physical and mechanical properties, depending on its lithological composition and weathering state (Chandler 1969, Reiβmüller 1997). Incompetent members such as claystones, shales and siltstones are particularly affected by weathering processes. In contrast, sandstones, limestone and brecciocongloмerates are competent members and are considerably more resistant to the influence of exogenetic forces (Mihljević and Prelogović 1992). Figure 3 shows high degradation of a flysch rock mass due to weathering in flysch pillars that were exposed to atmospheric conditions for seven years. These processes gradually transformed the fresh rock mass to residual soils and caused changes in its mineralogical composition and reductions in its strength.

Figure 3 View of a landslide body and lateral scarp from the crown of the landslide in (a) August 2005 and (b) January 2013 (Vivoda Prodan 2016)

The evaluation of the weathering profile for the study area is based on a qualitative description of colours and discoloration, discontinues states, the presence or absence of the original rock texture and the uniaxial compressive strength (UCS) of the intact rock, σ_{ci}, based on the Schmidt hammer test (Ündül and Tuğrul 2012). Six

different standard grades of siltstone were investigated in a flysch weathering profile (Figure 4): Fresh rock mass (FR); Slightly Weathered (SW), Moderately Weathered (MW), Highly Weathered (HW) and Completely Weathered (CW) rock masses; and Residual Soil (RS). Progressive and gradual weakening and decomposition takes place from the ground surface downward to fresh rock, and thus the weathering of the flysch rock material decreases from RS to CW, HW, MW, SW and FR.

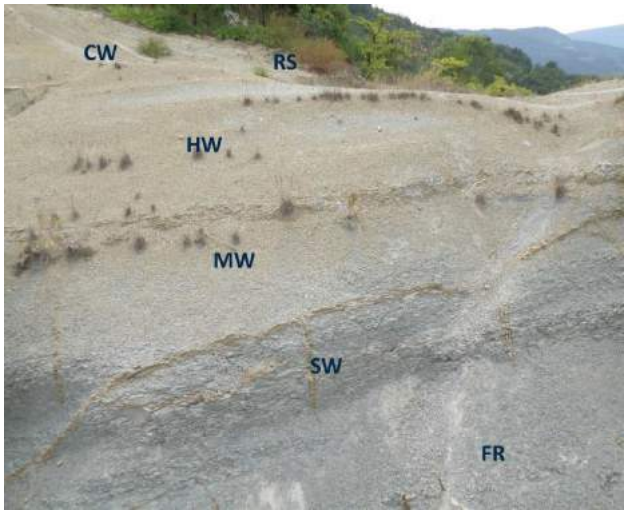

Figure 4 Examples of the weathering profile for the flysch rock mass in the Istria peninsula (Vivoda Prodan 2016)

Impact of weathering on uniaxial compressive strength and durability characteristics of siltstones

Uniaxial compressive strength and durability of fine grained lithological flysch rock mass samples with different weathering grades were investigated. Uniaxial Compressive Strength (UCS) was determined with a Schmidt hammer and the Point Load Test (PLT) while the slake durability test was performed in accordance with the ASTM standard procedure in five drying-wetting cycles. Tests were conducted on irregular block siltstone samples of FR and MW weathering grades from the outcrops in Istria peninsula immediately after sampling to avoid further weathering.

Determination of durability of siltstones using only standardized tests is not sufficient because fragmented samples of flysch rock mass acquire high slake durability index but are highly degraded (Miščević and Vlastelica 2011, Cano and Tomás 2015, Erguler and Shakoor 2009, Cano and Tomas 2016). Figure 5 shows the sample retained in the drum that was extremely fragmented and appeared highly degraded. However, the fragments were larger than 2 mm, which led to the high Id2 values. However, high Id2 values do not correlate with this highly degraded state. Therefore, the fragment size distribution of the fragmented siltstone that was retained in the drum after each cycle of the slake durability test was quantified. Beside standardized slake durability index in the second cycle (I_{d2}), calculation of additional parameters, such as disintegration ratio (D_{R2}) and modified disintegration ratio (D_{RP2}), are needed to indicate not only the durability but also the manner of disintegration of siltstones of different weathering grades (Erguler and Shakoor 2009, Cano and Tomas 2016).

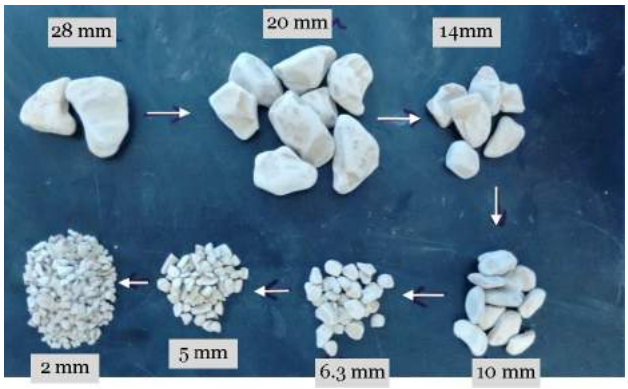

Figure 5 Fragments of FR siltstone sample taken from Istrian peninsula with various sizes retained in the drum after five cycles in the slake durability test (Vivoda Prodan 2016)

Results of point load test and slake durability test after second cycle for siltstones of different weathering grades from the Istrian peninsula are shown in Table 1. The uniaxial compressive strength (UCS) decreases with increasing weathering grade. The fresh siltstone sample was more durable and less susceptible to degradation than the moderately weathered siltstone sample. Fresh samples disintegrated less than moderately weathered samples; therefore, fewer drying-wetting cycles are required to reach the maximum possible degradation. According to the classification based on the slake durability index the siltstone samples with different weathering grades are classified in the higher durability class than in classification based on the fragmentation during the slake durability test. However, a significant portion of the disintegration occurred in subsequent drying–wetting cycles, indicating the need for a greater number of cycles in durability testing procedures.

Table 1 Point load test and slake durability test results; including the slake durability index (I_d), disintegration ratio (D_R) and modified disintegration ratio (D_{RP}) after the second cycle, for siltstones of different weathering grades from the Istrian peninsula (Vivoda Prodan 2016)

Sample	UCS [MPa]	I_{d2} [%]	D_{R2}	D_{RP2}
FR	53	97.03	0.81	0.19
MW	21	95.39	0.79	0.21

Impact of weathering on the residual shear strength of siltstones

Landslide occurrences in flysch deposits are frequent and slip surface is formed at the contact of surficial deposits and flysch rock mass or inside the weathered flysch rock mass. Rock mass defragmentation at the slip surface occurs due to sliding and shear strength decreases from peak to residual values through

occurred displacements. These residual strength values of the slip surface material are relevant to predict the dormant landslide reactivation along the same slip surface. Weathering effect on the residual shear strength values of siltstones were investigated by laboratory tests on samples of different weathering grades in direct shear and ring shear apparatus. The samples were disturbed and remolded to the engineering soil grade. The state of these siltstone samples matches the material state at the slip surface, where natural disintegration of the siltstone occurs due to stresses and strains that are caused by sliding.

Siltstone samples were tested in a standard direct shear device with 60 x 60 mm shear box dimensions. Slurry samples were consolidated under different levels of effective stresses, and then sheared under a constant shear speed of 0.15 mm/min.

The ICL-1 ring shear apparatus, developed in 2010 can maintain an undrained condition in a sample up to 1 MPa of pore water pressure and load normal stress up to 1 MPa (Sassa et al. 2004, Oštrić et al. 2014, Vivoda et al. 2013), Figure 6. Siltstone samples with different weathering grades were fully saturated with deaired distilled water and tested in the ring shear device. After checking the sample saturation and normal consolidation at different stress levels, shearing with pore pressure control or shear speed control was conducted. In natural slopes, pore pressure gradually increases due to rising groundwater level during rainfall. The pore pressure control tests, which simulate natural groundwater conditions, were conducted under a constant pore pressure speed of 0.50 kPa/min on prepared siltstone samples with different weathering grades. Water pressure supplied to the shear box was gradually increased, and water was free to drain up through the sample. After the stress path reached the failure line, shear stress suddenly dropped to a much lower value. Thereafter, the shear resistance recovered slightly to a certain value. The speed control tests were conducted under a constant shear speed of 0.01 cm/s in undrained conditions. In both types of shearing, basic parameters (peak and residual friction angles and cohesion) and the steady-state normal and shear stresses were determined. Figure 7 shows an example of a normal-shear stress diagram for the Istrian peninsula and Valići lake siltstone samples from the Rječina river valley with different weathering grades based on the ring shear test.

Test results, shown in Table 2, pointed to a decrease in overall residual shear strength with increasing weathering grade. The residual friction angle increased while the residual cohesion decreased with increasing of weathering grade. Significant differences were found between results obtained by the direct shear and ring shear devices. The ring shear device is more precise and better suited for residual strength investigation than the direct shear device, for the following reasons: (1) the ring shear device enables large (practically unlimited) shear deformations along the shear surface compared to the direct shear device (only some cm), which influences the final value of shear strength; (2) sample shearing in the ring shear device is developed under constant shear surface, whereas the shear surface changes (decreasing) during shearing in the direct shear device; and (3) the strength envelope in the direct shear device is based on three specific individual results, whereas the ring shear device enables plotting of the full strength envelope. Other identification test indicated that liquid limits and plasticity indexes increased with increasing weathering grade.

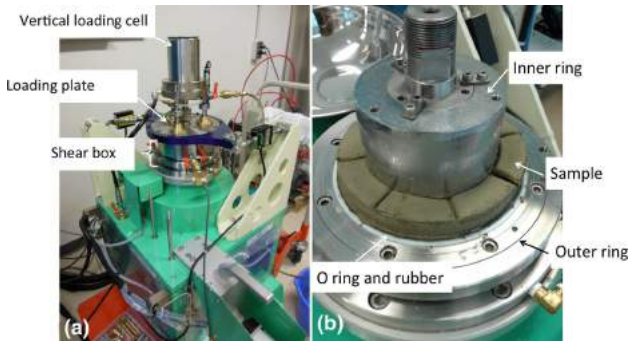

Figure 6 Siltstone sample in the ring shear device a) during and b) after testing

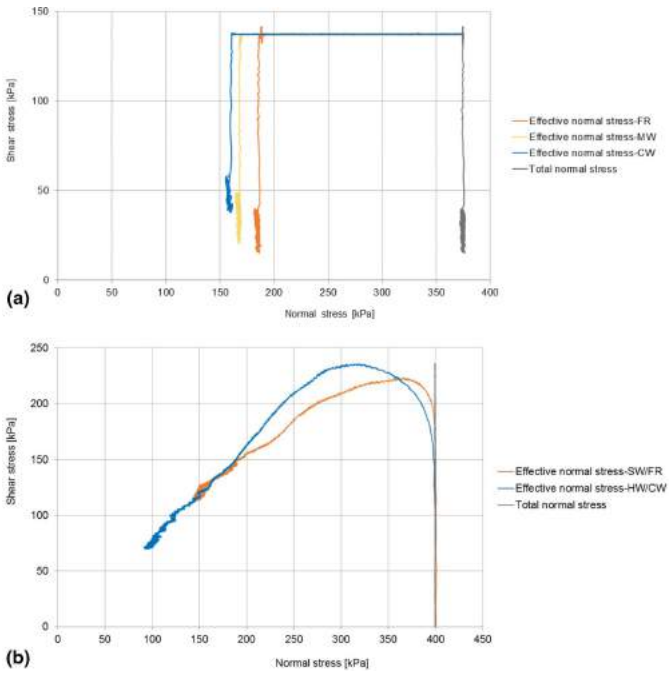

Figure 7 Normal stress–shear stress diagram based on the ring shear test for siltstone samples with different weathering grades: a) Istrian peninsula samples sheared in the pore pressure control test b) Valiči lake samples sheared in the speed control test under undrained conditions (Vivoda Prodan et al. 2016)

Weathering effect on the mineralogical composition of siltstones

The results of mineralogical analyses from previous studies in the study area (Arbanas et al. 2006, Benac et al.

2014, Jurak et al. 2005), shown on Figures 8 a, b, c ,indicate that the mineralogical composition of flysch samples differ based on weathering grade across the entire study area (Istrian peninsula, Rječina river valley and Vinodol valley), with clay mineral (phyllosilicate) content increasing and calcite content decreasing as weathering grade increases.

Results of previous studies were compared with the results of new mineralogical analyses investigated by Vivoda Prodan et al. (2016) where mineralogical composition of the fine grained lithological flysch components of different weathering grades from Istria peninsula was determined using X-ray diffraction. Cation exchange capacity (CEC) values were also determined. Calcite, quartz and phyllosilicates constituted 93–97 % of the mineralogical composition, and phyllosilicates were the prevalent minerals. The major clay minerals were illite and chlorite, with trace amounts of kaolinite and mixed-layer minerals. Mineralogical content of siltstones in the Istria peninsula differed according to weathering grade. Clay mineral content increased and calcite content decreased with increasing weathering grade (Figure 8d). The proportions of particular clay minerals such as chlorite and illite also increased with increasing weathering grade (Figure 8e). In addition, the cation exchange capacity (CEC) and water adsorption increased with increasing weathering grade.

Table 2 Identification test results, ring shear and direct shear test results; including plasticity index (PI), residual friction angle (ϕ_r) and residual cohesion (c_r), steady state shear resistance at sliding surface (τ_{ss}) for siltstones of different weathering grades from the Istrian peninsula, Valići lake in the Rječina river valley, and Vindol valley (Vivoda Prodan 2016)

Sample weathering grade	Location	PI [%]	Direct shear test		Ring shear test		
			ϕ_r [°]	c_r [kPa]	ϕ_r [°]	c_r [kPa]	τ_{ss} [kPa]
FR	Istrian peninsula	9	23	15	23	56	38
MW		12	22	14	27	51	44
CW		18	20	14	31	42	42
SW/FR	Valići lake	NP	28	28	30	32	55
HW/CW		NP	31	19	35	11	55
SW/FR	Vinodol valley	20	18	12	-	-	
HW/CW		25	18	11	-	-	

Impact of weathering on possible landslide reactivation

Influence of the weathering process on the fine grained lithological flysch components and a new long term rainy period on the Valići landslide reactivation in the Rječina river valley was analysed. Deterministic 3D stability analyses of Valići landslide reactivation using landslide simulation model software LS-Rapid were conducted using residual shear strength parameters of different weathering grades of siltstones obtained from laboratory ring shear and direct shear tests.

Numerous authors have investigated the stability of slopes in soft rocks subjected to weathering processes associated with changes in material strength (Eberhardt et al. 2005, Vlastelica 2015), while Sassa et al. (2010), Dugonjić et al. (2014), Sassa et al. (2014), Vivoda et al. (2014), Arbanas et al. (2017) performed numerical models of different landslides using LS-Rapid software.

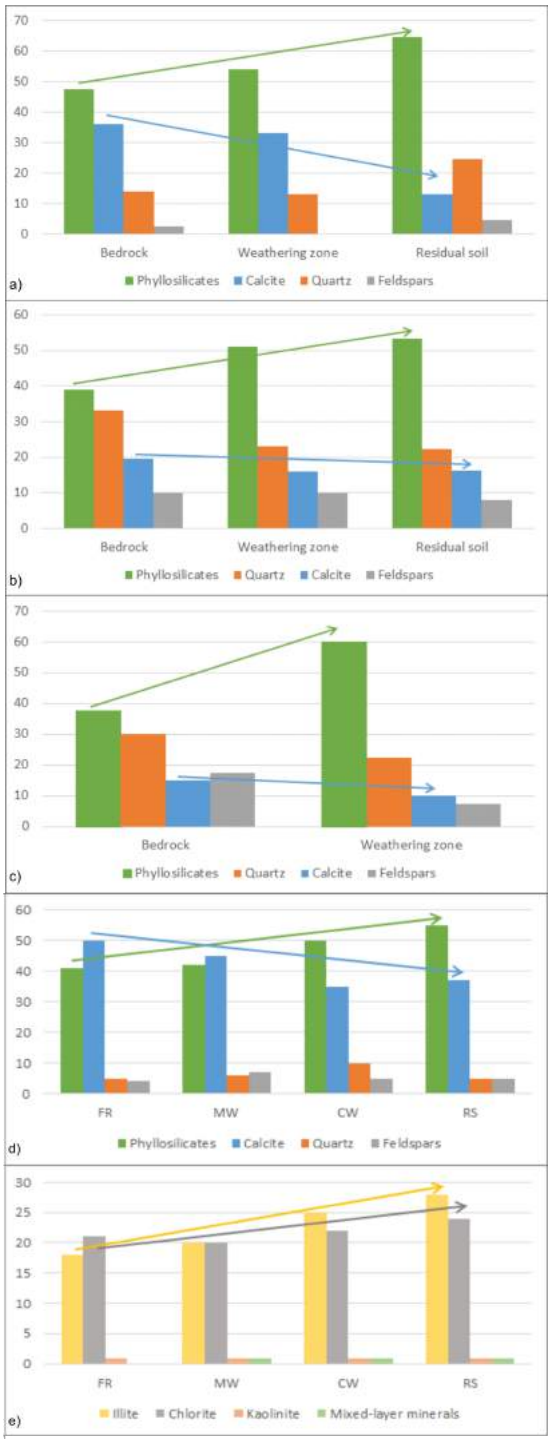

Figure 8 Mineralogical content of flysch samples from a) the Krbavčići landslide in northern Istria (Arbanas et al. 2006), b) the Grohovo landslide in the Rječina river valley (Benac et al. 2014), and c) the Mala Dubračina catchment in Vinodol valley (Jurak 1980), d) mineralogical content and e) content of different clay minerals in siltstone samples with different

weathering grades from the Istrian peninsula (Vivoda Prodan et al 2016)

The LS-Rapid software aims to integrate the initiation process (stability analysis) by pore pressure increase (rainfall) and seismic loading (earthquake), and the moving process (dynamic analysis) including the process of volume enlargement by entraining unstable deposits within the traveling course (Sassa et al. 2010). In the simulation, the friction angle and cohesion are reduced from their peak values to normal motion time values within the source area in the determined distribution of the unstable mass.

The results of the conducted deterministic 3D slope stability analyses using LS-Rapid software (Vivoda Prodan and Arbanas 2017) clearly show the critical areas for possible landslide reactivation in unfavourable hydrogeological conditions. Slopes built in flysch rock mass near the Rječina river valley are exposed to instabilities during raising of ground water level at different weathering grades of flysch rock mass. Landslide reactivation and filling of the Rječina river channel occurs during raising of ground water level to the ground surface. Comparison of the initial slope surface and numerical analysis results for the sliding surface in SW/FR and HW/CW weathering grade of flysch rock mass respectively is shown on Figure 9. Landslide in the slope built of more weathered flysch rock mass includes greater volume of initiated and deposited landslide mass (Figure 9c) than the slopes built in fresh or slightly weathered flysch rock mass (Figure 9b).

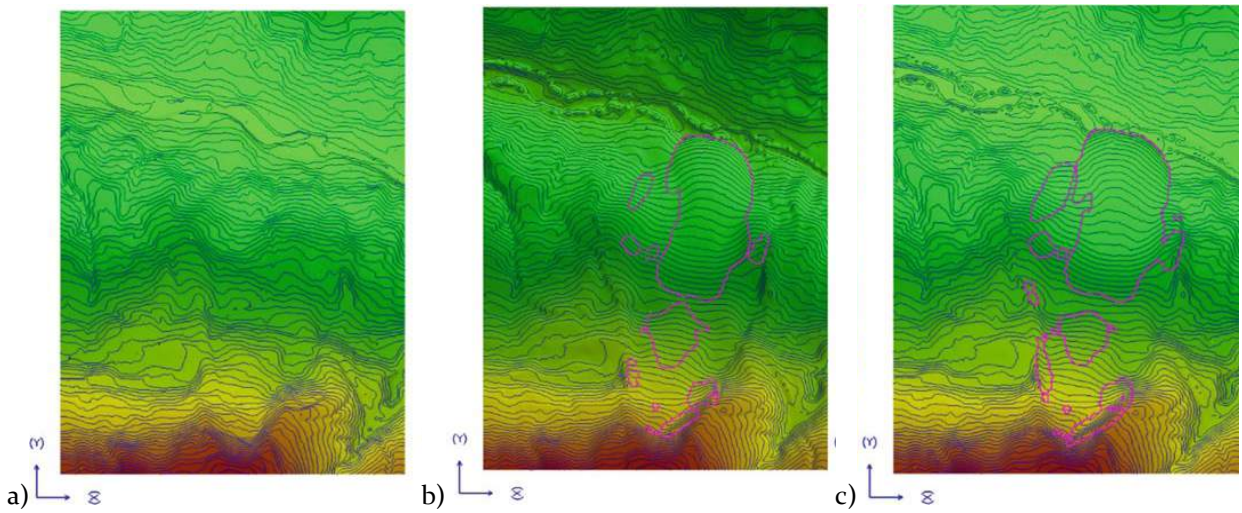

Figure 9 Top view of the terrain surface a) in the initial condition, at the end of the movement with sliding surface in b) SW/FR and c) HW/CW weathering grade of flysch rock mass (purple line shows the area of deposited landslide mass at the end of the movement) (Vivoda Prodan and Arbanas 2017)

Conclusions

The effects of weathering on flysch rock masses, especially on incompetent members such as siltstones, play a significant role in flysch rock mass behaviour and processes on slopes.

Weathering process has an influence on the plasticity of siltstones where the liquid limit and plasticity index values of silty material increase with increasing weathering grade. Weathering also has a significant influence on residual shear strength decrease, mobilized friction angle increase whereas mobilized cohesion decrease with increasing weathering grade. The uniaxial compressive strengths also decreases with increasing weathering grade. The use of the slake durability index does not adequately explain the slaking behaviour of siltstones because the fragmented samples are highly degraded by the slake durability test. Therefore, additional parameters, such as the disintegration ratio and the modified disintegration ratio, need to be calculated to indicate not only the durability but also the manner of disintegration of siltstones of different weathering grades. The siltstone sample of weathering grade FR are more durable and less susceptible to degradation than the siltstone sample of weathering grade MW. Fresh samples disintegrated less than moderately weathered samples; therefore, fewer drying-wetting cycles are required to reach the maximum possible degradation. The standard slake durability index increases the slaking resistance of the tested siltstone samples by at least one class.

Weathering process has a great influence on the residual shear strength decrease of the flysch rock mass and consequently on possible reactivation of the Valići landslide and other slope movement processes within the study area. Landslide mass volume, reached sliding length and sliding mass geometry after landslide stabilization are affected by weathering process.

Finally, with the obtained laboratory results it is proven that weathering process has a significant influence on the plasticity, residual shear strength, uniaxial compressive strength and durability characteristics of fine grained lithological flysch components from flysch rock masses and thus affecting

on landslide and erosion occurrences in the study area that is also proven by 3D numerical slope analysis.

References

Arbanas Ž, Benac Č, Jurak V (2006) Causes of debris flow formation in flysch area of North Istria, Croatia. In E. DE Lorenzini G, Brebbia CA (Ed.), Monitoring, Simulation, Prevention and Remediation of Dense and Debris Flows. WIT Transaction on Ecology and the Environment. pp. 283–292.

Arbanas Ž, Mihalić Arbanas S, Vivoda M, Peranić J, Dugonjić Jovančević S, Jagodnik V (2014) Identification, monitoring and simulation of landslides in the Rječina River Valley, Croatia. Proceedings of SATREP Workshop on Landslides, Hanoi, Vietnam. pp. 200–213.

Arbanas Ž, Vivoda M, Mihalić Arbanas S, Peranić J, Sečanj M, Bernat S, Krkač M (2017) Analysis of a reservoir water level impact on landslide reactivation. Proceedings of the 2nd Regional Symposium on Landslides in the Adriatic-Balkan Region. Belgrade, Serbia. pp. C1-C6

ASTM (2004) Standard test method for slake durability of shales and similar weak rocks (D4644-87). Philadelphia.

Benac Č, Oštrić M, Dugonjić Jovančević S (2014) Geotehnical properties in relation to grain-size and mineral composition: The Grohovo landslide case study (Croatia). Geologia Croatica, 67(2). pp. 127–136.

Bernat S, Đomlija P, Mihalić Arbanas S (2014) Slope movements and erosion phenomena in the Dubračina River basin: A geomorphological approach. Proceedings of 1st Regional Symposium on Landslides in the Adriatic-Balkan Region "Landslide and Flood Hazard Assessment". Zagreb, Croatia. pp. 79–84.

Brown E T (1981) Rock characterization, testing & monitoring: ISRM suggested methods. Published for the Commission on Testing Methods, International Society for Rock Mechanics by Pergamon Press.

Cano M, Tomás R (2015) An approach for characterising the weathering behaviour of Flysch slopes applied to the carbonatic Flysch of Alicante (Spain). Bulletin of Engineering Geology and the Environment, 74(2). pp. 443–463.

Cano M, Tomas R (2016) Proposal of a New Parameter for the Weathering Characterization of Carbonate Flysch-Like Rock Masses: The Potential Degradation Index (PDI). Rock Mechanics and Rock Engineering. pp. 1–18.

Chandler R J (1969) The effects of weathering on the shear strength properties of Keupler marl. Geotehnique, 19(3). pp. 321–334.

Dugonjić Jovančević S, Arbanas Ž (2012) Recent landslides on the Istrian Peninsula, Croatia. Natural Hazards, 62(3). pp. 1323–1338.

Dugonjić Jovančević S (2013) Landslide hazard assessment on flysch slopes. Doctoral thesis, University of Rijeka (in Croatian)

Dugonjić Jovančević S, Nagai O, Sassa K, Arbanas Ž (2014) Deterministic landslide susceptibility analyses using LS Rapid software. Proceedings of 1st Regional Symposium on Landslides in the Adriatic-Balkan Region "Landslide and Flood Hazard Assessment". Zagreb, Croatia. pp. 73-77

Eberhardt E, Thuro K, Luginbuehl M (2005) Slope instability mechanisms in dipping interbedded conglomerates and weathered marls—the 1999 Rufi landslide, Switzerland. Engineering Geology, 77(1-2). pp. 35–56.

Erguler Z A, Shakoor A (2009) Quantification of Fragment Size Distribution of Clay-Bearing Rocks after Slake Durability Testing. Environmental & Engineering Geoscience, 15. pp. 81–89.

Gulam V (2012) The erosion of flysch badlands in the Central Istria. Dissertation, University of Zagreb (in Croatian)

Jurak V, Slovenec D, Mileusnić M (2005) Excessive Flysch Erosion - Slani Potok. Excursion Guide book of the 3rd Croatian Geological Congress, Opatija, Croatia. pp. 51–55.

Kanji M A (2014) Critical issues in soft rocks. Journal of Rock Mechanics and Geotechnical Engineering, 6(3). pp. 186–195.

Marinos P, Hoek E (2001) Estimating the geotechnical properties of heterogeneous rock masses such as flysch. Bulletin of Engineering Geology and the Environment, 60(2), pp. 85–92.

Mihljević D, Prelogović E (1992) Structural - geomorphological characteristic of the mountain ranges Učka & Ćićarija. Proceedings of the International symposium Geomorphology and sea and The meeting of the geomorphological commission of the Carpatho-Balkan countries, Mali Lošinj, Croatia. pp. 13–24.

Miščević P, Vlastelica G (2011) Durability Characterization of Marls from the Region of Dalmatia, Croatia. Geotechnical and Geological Engineering, 29(5). pp. 771–781.

Oštrić M, Sassa K, Ljutić K, Vivoda M, He B, Takara K (2014) Manual of transportable ring shear apparatus, ICL- 1. Proceedings of 1st Regional Symposium on Landslides in the Adriatic-Balkan Region "Landslide and Flood Hazard Assessment". Zagreb, Croatia. pp. 1–4.

Reißmüller M (1997) Geotechnische Eigenschaften verwitterter Kfssener Mergel. Diploma Thesis, Technical University of Munich, Munich (in German)

Sassa K, Fukuoka H, Wang G, Ishikawa N (2004) Undrained dynamic-loading ring-shear apparatus and its application to landslide dynamics. Landslides, 1(1). pp. 7–19.

Sassa K, Nagai O, Solidum R, Yamazaki Y, Ohta H (2010) An integrated model simulating the initiation and motion of earthquake and rain induced rapid landslides and its application to the 2006 Leyte landslide. Landslides 7(3). pp: 219–236.

Sassa K, DangK., He B, Takara K, Inoue K, Nagai O (2014) A new high-stress undrained ring-shear apparatus and its application to the 1792 Unzen–Mayuyama megaslide in Japan. Landslides, 11(5). pp. 827–842.

Selby M J (1993) Hillslope materials and processes. Oxford University Press, Oxford

Ündül O, Tuğrul A (2012) The Influence of Weathering on the Engineering Properties of Dunites. Rock Mechanics and Rock Engineering, 45. pp. 225–239.

Velić I, Vlahović I (2009) Geologic map of Republic of Croatia 1:300.000. Croatian Geological Survey, Zagreb.

Vivoda M, Benac Č, Žic E, Đomlija P, Dugonjić Jovančević S (2012). Geohazards in the Rječina valley in the past and present. Croatian Waters: Journal for the Water Economy, 20(81). pp. 105–116.

Vivoda M, Sassa K, Arbanas Ž, Dugonjić Jovančević S, Jagodnik V, Peranić J (2013) Shear strength properties of soil materials from the Grohovo Landslide. Book of abstracts of the 4th Workshop of the Japanese-Croatian Project on "Risk Identification and Land-Use Planning for Disaster Mitigation of Landslides and Floods in Croatia". Split, Croatia. pp. 22-22

Vivoda M, Dugonjić Jovančević S, Arbanas Ž (2014) Landslide Occurrence Prediction in the Rječina River Valley as a Base for an Early Warning System. Proceedings of 1st Regional Symposium on Landslides in the Adriatic-Balkan Region "Landslide and Flood Hazard Assessment". Zagreb, Croatia. pp. 85–90.

Vivoda Prodan M (2016) The influence of weathering process on residual shear strength of fine grained lithological flysch components. Dissertation, Faculty of Civil Engineering, University of Rijeka (in Croatian)

Vivoda Prodan M, Arbanas Ž (2016) Weathering Influence on Properties of Siltstones from Istria, Croatia. Advances in Materials Science and Engineering. 2016 (2016), 3073202. pp.1-15.

Vivoda Prodan M, Mileusnić M, Mihalić Arbanas S, Arbanas Ž (2017) Influence of weathering processes on the shear strength of siltstones from a flysch rock mass along the northern Adriatic coast of Croatia. Bulletin of engineering geology and the environment. 76 (2017), 2. pp. 695-711.

Vivoda Prodan M, Arbanas Ž (2017) Parametric Analysis of Weathering Effect on Possible Reactivation of the Valići Landslide, Croatia. Advancing culture of living with landslides, Vol 2. Advances in Landslide Science. Cham: Springer. pp. 621-631

Vlastelica G (2015) The Influence of Weathering on Durability of Cuts in Soft Rock Mass. Dissertation, University of Split (in Croatian)

doi.org/ 10.35123/ReSyLAB_2019_4

Geochemical Interpretation of groundwaters in the Kostanjek landslide in the western part of Zagreb, Croatia

Naoki Watanabe [1], Satoshi Yamamoto [2], Gen Furuya [3] , Martin Krkač [4], Snježana Mihalić Arbanas [4], Hideaki Marui [1]

1) Niigata University, Research Institute for Natural Hazards and Disaster Recovery, Niigata, 950-2181, Japan

2) Accutech Inc., Japan

3) Toyama Prefectural University, Japan

4) University of Zagreb, Croatia

Abstract Geochemical characteristics of groundwaters provide important key signatures to better understand the origin and behaviour of ground waters in landsides. Therefore, we investigated groundwaters from the Kostanjek landslide in the western part of Zagreb, Croatia. Most of groundwaters are characterized by Ca-HCO_3 type because aquifer lithologies mainly consist of calcareous strata such as limestone and several types of marls. We subdivided waters into four types by cluster analysis as follows; (1) Type-A is typical Ca-HCO_3 type water, (2) Type-B is weaker water in Ca-HCO_3 component than type-A, (3) Type-C is Mg-rich Ca-HCO_3 type water, (4) Type-D is Mg-Ca-HCO_3 type water. Both type-A and type-B waters are widely distributed over the landslide area and type-C waters limitedly appeared around the eastern margin of the landslide mass. Type-D waters are discharged from fissures in the dolomitic rocks in the inner part of the mining tunnel and are more enriched in Mg^{2+} and depleted in Sr^{2+} than type-C waters. For this reason, it is most likely that the dolomitic rock is a main source of Mg^{2+} in waters. In addition, the enviromental isotopic compositions of type-D waters are depleted in $\delta^{18}O$ and $\delta^{2}H$ comparing with others. Such isotopic depletions suggest that type-D waters are recharged in the higher area of Mt. Medvednica as a dolomitic mass and migrate through the deep dolomitic aquifer beneath the landslide mass. Type-C waters are formed by the mixing of type-A or type-B waters with type-D waters ascending from the deep dolomitic aquifer based on graphical plots of Mg/Ca vs. Sr/Ca ratios of waters. Continuous injection of artesian type-D waters from the deep dolomitic aquifer has an impact upon the groundwater behaviour in the landslide mass and is also one of the key factors related to the landslide susceptibility.

Keywords ground water, hydrochemistry, stable isotope, artesian aquifer, landslide susceptibility

Introduction

Landslides generally occur due to slope instability which is caused by lowering shear resistance. For example, increasing of pore water pressure particularly makes lower shear resistance of sliding surface and consequently plays key role to destabilize hillslopes. Therefore, in many cases, ground water behaviour is an important key factor for the occurrence and repetitive activity of landslides. Hydrochemical characteristics of groundwaters reflect compositional properties of solid phases of the parent rocks through which ground water flows and also provide signatures as natural tracers to better understand ground water migration and dynamics. Accordingly, it is significant to investigate the hydrochemical characteristics of groundwaters in landslide-prone areas. This hydrochemical study of groundwaters was carried out in the Kostanjek landslide in the western part of Zagreb, Croatia. Final goals of our research are to assess susceptibility and risk of the landslide and to find the optimum way to mitigate landslide disasters from geochemical and hydrogeological approaches. In this paper, we report hydrochemical and stable isotopic characteristics of groundwaters and their spatial distribution in the landslide, and propose a model of hydro geological and hydrochemical formation and behaviour of groundwaters.

Outline of research area

The Kostanjek landslideis located in the western part of Zagreb City (Figure 1), and approximately 10 kilometres

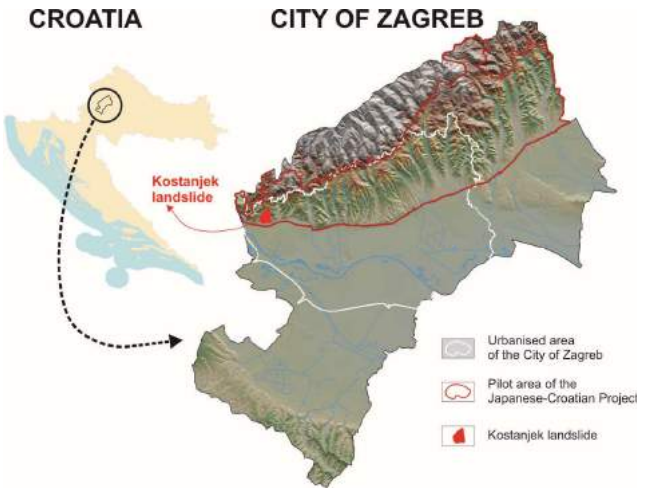

Figure 1 The Kostanjek landslide is located in the western part of the City of Zagreb and in residential area at the foot of the southwestern slope of Mt. Medvednica.

west away from the centre of city. The landslide involves an urbanized area of approximately 100 ha with a maximum length of 1250 m and a maximum width of 950 m. A volume of sliding mass is estimated approximately 32×10^6 m^3 with a maximum depth of 90 m. The more detail information about the landslide is described in Stanic and Nonveiller (1996). Bedrock geology of the landslide is Miocene marly strata mainly composed of alternation of calcareous sandstone, calcareous siltstone and limestone layers. In the head to middle part of landslide, the dip of strata is 10-15 degree to south direction but the strata are inclined to North direction with 10-30 degree in the foot of the landslide. The details of geological information is described in Vrsaljko (1999), Vrsaljko et al. (2005; 2006), etc. Hydrochemical investigation was also carried out in this area (e.g., Watanabe et al., 2012).

Samples

Water samples

One sample of spring water, seven samples of stream water, 11 samples from the mining tunnel (entrance of the tunnel and inner part of tunnel) and 74 ground water samples from private wells in the Kostajek area were collected for hydrochemical and isotope analyses during ground water surveys in September 2011 and in June 2012. Figure 2 shows the localities of water samples and respective water types that will be described later.

Rock samples

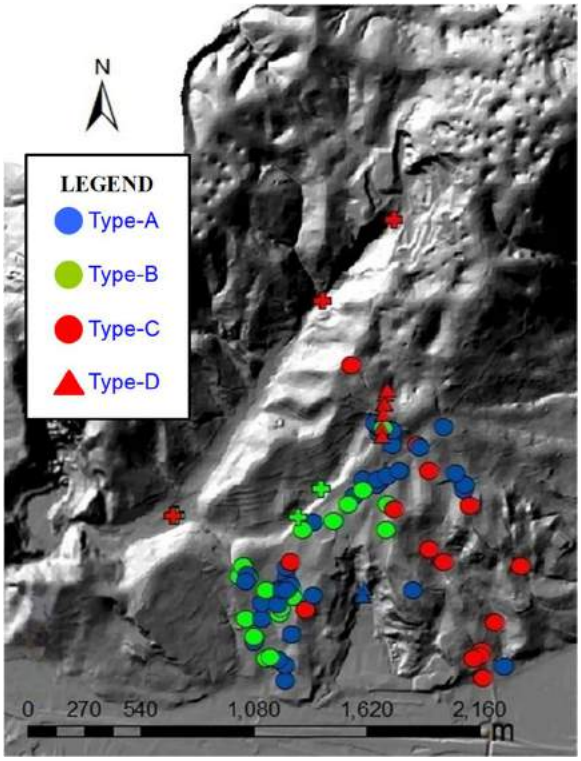

Figure 2 Sample localities of waters and spatial distribution of respective water types.

76 rock samples of soil layer and Miocene marl strata were collected from the drill core of the B-1 borehole. Three samples of Badenian limestone and two samples of Triassic dolomite were collected from outcrops for major elements analysis.

Analytical methods

Hydrochemistry

The pH, EC and water temperature of all samples were determined at the water sampling, while Na, NH_4, K, Mg, Ca, Sr, Cl, NO_3 and SO_4 were analysed by Ion chromatography systems and HCO_3 and CO_3 as alkalinity were measured by the titration with 0.02N-H_2SO_4 in the laboratory of the Research Institute for Natural Hazards and Disaster Recovery, Niigata University.

Stable isotope analysis

Oxygen and hydrogen isotope ratios for water samples have been measured on an isotope-ratio mass spectrometer (IRMS) in the laboratory of the Research Institute for Natural Hazards and Disaster Recovery, Niigata University by carbon dioxide equilibration and hydrogen with platinum catalysis equilibration techniques, respectively. Isotope ratios are expressed as δ (‰) values which are defined by the following equation.

$$\delta\ (‰) = 1000\{(R_X/R_S) - 1\}$$

where R_X and R_S represent isotope ratios of a sample and the standard as SMOW (Standard Mean Ocean Water), respectively.

Major elements analysis

Major elements as SiO_2, TiO_2, Al_2O_3, MnO, MgO, CaO, Na_2O, K_2O and P_2O_5 with trace elements (V, Cr, Ni, Rb, Sr, Ba, Y, Zr, Nb) are measured by X-ray fluorescence spectrometer (XRF) in the laboratory of the Faculty of Science, Niigata University.

Results

Hydrochemistry

Hydrochemistry of ground waters from shallow aquifers in the landslide are classified into four types by cluster analysis as follows; (1) Type-A is typical Ca-HCO_3 type water, (2) Type-B is weaker water in Ca-HCO_3 component than type-A, (3) Type-C is Mg-rich Ca-HCO_3 type water, (4) Type-D is Mg-Ca-HCO_3 type water (Figure 3). The spatial distribution of each hydrochemical

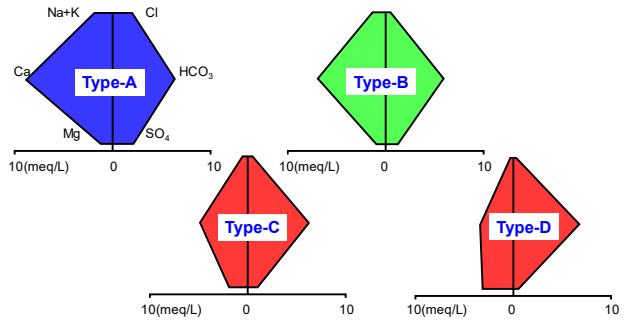

Figure 3 Classification of water types based on multivariate statistics (principal component analysis and clustering).

water type is also shown in Figure 2. Both type-A and type-B waters are predominately distributed over the research area and are closely related to the shallow aquifer lithology composed of Sarmatian-Panonian marly strata. Type-A waters are derived Ca and HCO_3 from marl aquifers. Type-B waters are formed by the mixing of Type-A water with dilute subsurface water from soil zones where soluble solids were almost removed during chemical weathering processes. Type-C waters are limitedly distributed around the eastern margin of the Kostanjek landslide and Type-D waters gush out from fissures in the dolomite outcrop in the inner part of the tunnel. In particular, Type-D waters are more enriched in Mg and depleted in Sr than type-C waters. It means that the dolomite is a major source of Mg in waters from this area as a later mention.

Stable isotopic composition

Isotopic compositions of waters range from -6.64 to -10.11‰ in δ18O and from -46.2 to -70.0‰ in δ2H, respectively. All waters are meteoric water (rain and snow) in origin even if type-D waters are depleted in δ18O and δ2H comparing with others (Figure 4).

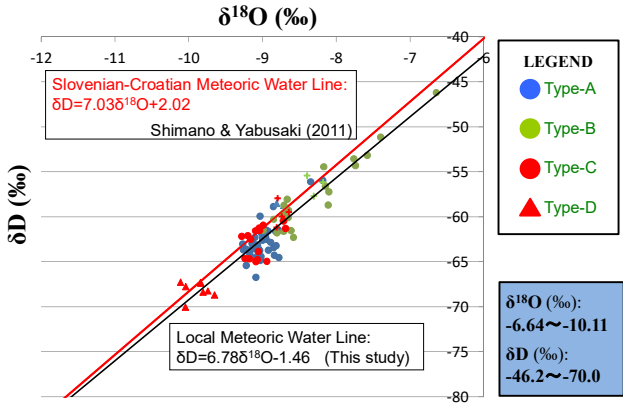

Figure 4 Isotopic composition of respective water types.

The depleted type-D waters in isotope compositions suggest that these are recharged in the higher area of the northern mountain, western part of Mt. Medvednica, and migrate through dolomite aquifer to the depths of the landslide mass. Type-C waters from shallow aquifers in the landslide also include Mg to some extent even though there is no dolomite layer in the landslide mass.

The massive dolomite is distributed in more than 1,000 m north away from this area and also underlies in more than 200 m depth beneath the landslide mass. Then type-C waters show a tendency to be slightly depleted in $\delta^{18}O$ and $\delta^{2}H$ comparing with type-A and type-B waters (Figure 4). It seems that type-C water is influenced by isotopically depleted type-D water from the dolomite aquifer.

Chemical composition of rock samples

Graphical plots of Mg/Ca vs. Sr/Mg ratios of rock samples from soil layer, Sarmatian-Panonian marly strata, Badenian limestone and Triassic dolomite are shown in Figure 5. The relationship between Mg/Ca and Sr/Mg from soil layer and Sarmatian-Panonian marly strata shows a systematic trend which means an array of weathering because Ca and Sr are more soluble than Mg during chemical weathering processes. In contrast, Badenian limestone and Triassic dolomite are extrmely different composition from Soil layer and Sarmatian-Panonian marly strata.

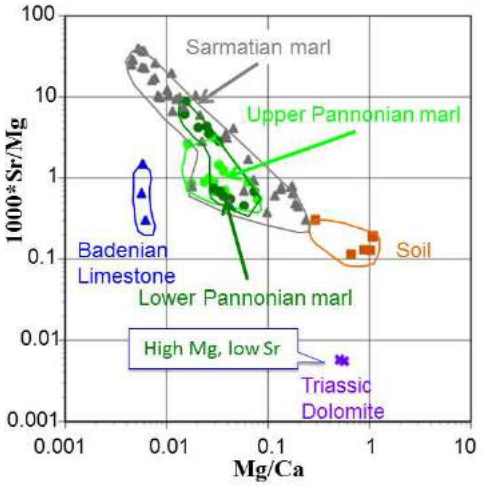

Figure 5 Mg-Ca-Sr systematics for rock samples.

Geochemical interpretation of groundwater behaviour

Ortolan (1996) and Ortolan et al. (2008) suggested that artesian aquifers related to Badenian limestone and Triassic dolomite underlay Sarmatian-Panonian marly strata and the Kostanjek landslide mass. Here we focus on the hydrochemical formation of Mg-rich type-C waters. According to graphical plots of Mg/Ca vs. Sr/Ma ratios of waters (Figure 6), it is clear that type-C waters are originally formed by mixing of common type-A or type-B waters with type-D waters ascending from the deep dolomite aquifer. On the other hand, in applied

isotope hydrology, the altitude effect on $\delta^{18}O$ of precipitations (meteoric water) is used to estimate the altitude of ground water recharge areas. This effect on $\delta^{18}O$ in mid latitudes ranges between -0.15 and -0.30‰ for each 100 m of altitude gained (Clark and Fritz, 1997). Depleted $\delta^{18}O$ values of type-D waters suggest that these are recharged around 650-800 m higher area than the Kostanjek landslide area, assuming that the altitude effect is -0.25‰/100m and average $\delta^{18}O$ value of precipitation is likely -8.0‰ in this area. Therefore, it is

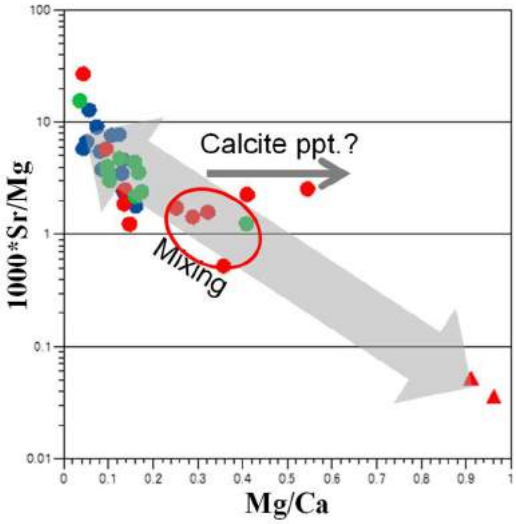

Figure 6 Formation of Type-C waters. Mg-rich Type-C waters are influenced by Type-D waters in deep artesian dolomite aquifer. Legends are the same as Figures 2 and 4.

most likely that type-D waters from the deep artesian aquifer constituted of dolomite continuously inject into shallow aquifers around the eastern margin of the Kostanjek landslide. Such injection of deep artesian waters has an impact upon the groundwater behaviour, e.g. excess pore water pressure, in the landslide mass and is also one of the key factors controlling the landslide susceptibility. In planning the counter-measures by ground water drainages for the effective reduction of pore water pressure in the Kostanjek landslide, it is useful to identify the source of groundwaters based on hydrochemical characteristics, especially Mg-rich waters from the deep artesian aquifer.

Conclusions

Depleted isotopic compositions of type-D waters, dolomite type waters, suggest that these are recharged in higher areas of the northern mountain (Mt. Medvednica) and migrate through dolomite aquifers to the depths of the landslide mass.

This study has paid attention to the formation of Mg-rich type-C waters distributed in the eastern margin of the Kostanjek landslide because there is no source of Mg in this area and the massive dolomite formation is distributed in more than 1,000 m north away from this area and also underlies in more than 200m depth beneath the landslide mass.

Mg rich Type-C waters show a tendency to be slightly depleted in $\delta^{18}O$ and $\delta^{2}H$ comparing with type-A and type-B waters. It is suggested that type-C waters are influenced by isotopically depleted type-D waters.

This result and graphical plots of Mg/Ca vs. Sr/Ca ratios of waters indicate that type-C waters are formed by the mixing of type-A and type-B waters with type-D waters ascending through fault fractures in the eastern margin of the landslide from the deep dolomite aquifer.

Continuous injection of artesian type-D waters from the deep aquifers has an impact upon the groundwater behavior in the landslide mass and is also one of the key factors controlling the landslide susceptibility.

References

Clark, I., Fritz, P., 1997. Environmental Isotopes in Hydrogeology, Lewis.

Ortolan, Z., 1996. The creation of a spatial engineering-geological model of deep multi-layered landslide (on an example of the Podsused landslide in Zagreb), Unpubl. PhD Thesis, University of Zagreb, 245 p. (in Croatian with an English abstract)

Ortolan, Z., Jurak, V., Ivšić, T., Herak, M., Vukelić, I., 2008. Geotechnical circumstances - Boundary condition for sustainable development of the "Sljeme foothills urbanized zone", Proc. of the Conference 'Development of the Zagreb', Zagreb (Croatia), 273-284. (in Croatian with an English abstract)

Shimano, Y., Yabusaki, S., 2005. Visit to valuable water springs (95) Waters in Slovenia and Croatia, Journal of Groundwater Hydrology, Vol.53, 411–427. (in Japanese with English abstract)

Stanic, B., Nonveiller, E., 1996. The Kostanjek landslide in Zagreb, Engineering Geology, Vol.42, 269–283.

Vrsaljko, D., 1999. The Pannonian Palaeoecology and biostratigraphy of molluscs from Kostanjek – Medvednica Mt., Croatia, Geol. Croat., Vol.52/1, 9–27.

Vrsaljko, D., Pavelić, D., Bajraktarević, Z., 2005. Stratigraphy and palaeogeography of Miocene deposits from the marginal area of Zumberak Mt. and the Samoborsko Gorje Mts. (Northwestern Croatia), Geol. Croat., Vol.58/2, 133–150.

Vrsaljko, D., Pavelić, D., Miknić, M., Brkić, M., Kovacic, M., Hecimovic, I., Hajek-Tadesse, V., Avanic, R., Kurtanjek, N., 2006. Middle Miocene (upper Badenian/Sarmatian) palaeoecology and evolution of the environments in the area of Medvednica Mt. (North Croatia), Geol. Croat., Vol.59/1, 51–63.

Watanabe, N., Krkač, M., Furuya, G., Wang, C., Mihalić Arbanas, S., 2012. Hydrochemical characteristics of groundwaters from the Kostanjek landslide in Croatia, Proc. of 2nd Project Workshop on Risk Identification and Land-Use Planning for Disaster Mitigation of Landslides and Floods, Rijeka (Croatia), 2011, 14–16.

doi.org/ 10.35123/ReSyLAB_2019_5

Monitoring of a retaining wall with innovative multi-parameter tools

Andrea Segalini[(1)], Alessandro Valletta[(1)], Andrea Carri[(2)], Edoardo Cavalca[(1)]

1) DIA – University of Parma, Parco Area delle Scienze 181/a, 43124 Parma (Italy) andrea.segalini@unipr.it +39 0521 905952

2) ASE – Advanced Slope Engineering S.r.l., Parco Area delle Scienze 181/a, 43124 Parma (Italy)

Abstract Retaining walls are geotechnical structures that frequently interacts with roads, railway lines and motorways, playing a key role in the safety of transport networks in mountain areas. For this reason, monitoring activities aimed to assess the stability condition of these works are extremely important to guarantee the practicability of communication lines, especially during adverse meteorological conditions. In particular, the integration of automatic devices and advanced deep learning algorithms permits to implement early warning measures characterized by high accuracy and the reduction of uncertainties due to a statistical approach to the measure, which significantly improve the system performances. Finally, the remote control of physical entities through a web based platform permits to apply an all new Internet of Natural Hazards (IoNH) approach, which is to be intended as the implementation of IoT (Internet of Things) in the geo-related Hazard field.

This paper presents a case study where a reinforced soil retaining wall was instrumented with innovative monitoring tools based on Modular Underground Monitoring System (MUMS) technology in order to control the displacements of the geotechnical structure together with the pore pressure and the temperature, applying Early Warning Procedures at the overcoming of predefined thresholds. In particular, two 15-meter long automatic inclinometers were installed on-site 3 meters apart, each of them composed of 15 multi-parametric tilt sensors spaced 1 meter along the vertical direction and one piezometer at a predefined depth.

Among the several features presented by the innovative system selected for this case study, one of the most relevant was the synergic integration of two tilt sensors featuring different resolution and sensitivity, thus obtaining a redundant system, which has been fundamental in the correct evaluation of the results. Should this IoNH approach become diffusely applied, the costs of its implementation would reduce significantly and its valuable support would be beneficial for the whole geotechnical field.

Keywords Monitoring, Displacement, Retaining Wall, Automatic Inclinometer, Early Warning System

Introduction

The major importance of maintenance and monitoring activities concerning retaining walls derives from their critical role as protection structures. In fact, retaining wall failures can lead to losses of human lives and significant damages to involved infrastructures and buildings, with consequent issues related also to following repair works (Lienhart et al. 2018). As reported by Koerner and Koerner (2011), it is possible to find a wide range of different approaches to retaining walls monitoring, ranging from deformation surveys with remote tools and slope indicators to pore pressure and water level measurements with piezometers.

For these reasons, scientific literature reports several case studies with different devices used to assess the structure conditions. Applied techniques include photogrammetric surveys of the wall face (Stirling et al. 1992), extensometers for vertical settlements (Benjamim et al. 2007), and strain gauges installed on reinforcing elements (Carrubba et al. 1999). The introduction of innovative technologies allowed also the application of a near-real time approach to monitoring activities, involving the integration of automatic inclinometers (Baily et al. 2014) and devices to measure the dynamic response of the structure under different conditions (Rainieri et al. 2010).

This paper describes the design and application of a multi-parametric system to monitor the condition of a reinforced earth retaining wall, with the main objective to identify potential instabilities and deformations involving the structure.

Materials and Methods

Case study description

The case study presented in this paper deals with the monitoring activity of a geogrids reinforced earth retaining wall 12-metres high. The structure was located on the French Alps at more than 1200 metres above sea level, protecting a road that gave access to a tunnel nearby.

Since its construction, the wall showed signs of instability phenomena and unexpected deformations, which prompted a first series of survey to assess the displacements entity. In particular, two inclinometer boreholes were realized near the wall and used to measure the structure displacement with a manual probe. Additionally, the wall was monitored with a series of topographic surveys involving the measurement of a total of 47 targets located on the wall face.

Results coming from both approaches were in good agreement and confirmed that the retaining wall was subject to relevant instabilities in different sections, with deformations up to several centimetres and noticeable fractures.

Monitoring system installed

Following these outcomes, it was decided to undertake reinforcement works and to improve the existing monitoring system by integrating innovative and automatized devices, more suited for early warning purposes. In particular, two automatic and remotely controlled inclinometers arrays featuring MUMS (Modular Underground Monitoring System) technologies were installed on-site.

MUMS is an innovative monitoring system developed and patented by ASE S.r.l. (IT), composed of a series of epoxy resin nodes, named Links, connected by an aramid fibre cable and a single quadrupole electrical cable to form an arbitrarily long array of sensors (Segalini and Carini 2013; Segalini et al. 2014). MUMS tools are customizable with respect to sensors number, distance and typology, with the possibility to integrate 3D MEMS (Micro Electro-Mechanical Systems), electrolytic tilt cells, piezometers, barometers and high-resolution thermometers. The result is a multi-parametric device able to measure displacements, pore pressure and temperatures at different depths according to the case.

A dedicated data logger reads the instrumentation at a specified frequency, which can be customized according to the monitoring requirements. The control unit stores locally the data in a SD card and sends them through an Internet connection to the elaboration centre. Here, raw data are processed by a proprietary software to obtain the physical monitored quantities. Both raw and elaborated data are stored in two separate sections of a dynamic MySQL database with a multilevel backup system. The system features also an automatic procedure to check the overcoming of predefined thresholds, sending alert messages (e.g. SMS and e-mail) when a warning level is reached. Finally, a web-based platform represents the monitoring results by means of interactive graphs and tools, allowing also to export images or spreadsheets files format. The innovative approach proposed by MUMS instrumentation exploits IoT (Internet of Things) principles to provide an integrated system with fully automated processes for data acquisition, elaboration and representation. The final result is the so-called Internet of Natural Hazards (IoNH) approach, representing the integration of IoT-based technologies into the geotechnical field.

For the case study presented in this paper, two 15-metre long Vertical Arrays (Tab.1) were installed on the retaining wall 3 metres apart along the maximum slope direction (Fig. 1). In particular, both tools were equipped with 15 Tilt Link HR 3D V nodes, designed for displacement monitoring, and composed of a MEMS sensor and an electrolytic tilt sensor. In the described case study, the interspace between nodes was 1 metre. Moreover, each of the Arrays included a piezometer (Piezo Link) located at 13 metres depth. Additionally, the first Array (DT0080) featured a barometer installed inside the data logger case while the second one (DT0081) integrated a high resolution thermometer (Therm Link) 1 metre below the top margin of the wall in order to measure the external structure temperature.

Additionally, a site-specific displacement threshold was imposed on inclinometers data for the activation of Early Warning procedures. In particular, the alert level was based on the overcoming of a daily displacement value of 1 mm/d consecutively for a whole week. According to this choice, an alarm message would have been issued to authorities responsible of the monitoring activity if the daily threshold was reached for 7 days in a row.

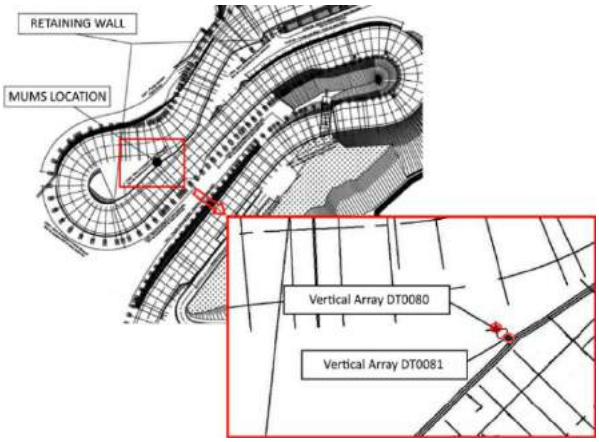

Figure 1 Planar view of the retaining wall and position of the two Vertical Arrays.

The on-site installation of both Arrays took place on 29 August 2017 and required less than one hour. The zero-reference date for data elaboration was set on 30 August 2017, and the data loggers were configured to read each sensor every 12 hours, sending data to the elaboration centre once a day. Monitoring activities lasted for a total of 17 months until January 2019, when the retaining wall was demolished for safety reasons.

Table 1 Information related to MUMS tools installed on the retaining wall.

Array ID	Array Typology	Length [m]	Sensor Number and Typology	Installation Date [dd/mm/yyyy]	Reference Date [dd/mm/yyyy]	End of Monitoring [dd/mm/yyyy]
DT0080	Vertical Array	15.00	15 Tilt Link HR 3D V 1 Piezo Link 1 Baro Link	29/08/2017	30/08/2017	08/01/2019
DT0081	Vertical Array	15.00	15 Tilt Link HR 3D V 1 Piezo Link 1 Therm Link	29/08/2017	30/08/2017	08/01/2019

Results and Discussion

DT0080

DT0080 Vertical Array refers to the inclinometer located in the upper part of the monitored site, as in Fig.1, and it started to record data the day after its installation. Fig. 2 shows the local displacements starting from the reference date, while Fig. 3 reports the cumulative ones. From these trends, it is possible to identify a sliding surface at a depth of 5 metres, displaying a local displacement value of 13.7 mm and a cumulative displacement of 35.3 mm. Furthermore, cumulated data referring to the top of the wall reports a total displacement of 49.1 mm.

Fig. 4 and Fig. 5 show the local and cumulative displacements over time, respectively. It is possible to observe the major displacement that started on December 2017 and peaked on May 2018, reaching 56 mm of cumulative displacement at the top of the inclinometer. The following relaxation process, probably caused by thermal variations of the structure, lasted until November 2018, when another event started to develop until the end of the monitoring activity. As a consequence of this phenomenon, the final displacement is lower than the value recoded at the end of the May 2018 event.

While these data confirmed the critical condition of the retaining wall, the alert threshold was never overcome for 7 days consecutively, hence no alarm message related to these events was issued during the monitoring period. This could depend of the threshold nature, which was focused on a continuous displacement variation, while the event recorded by DT0080 displayed a rapid evolution in the initial phase and continued with several oscillations for the rest of its duration.

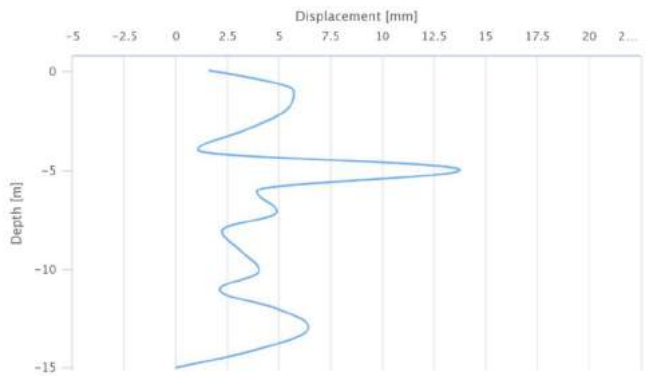

Figure 2 Local displacement recorded by DT0080 MEMS at the end of the monitoring activity (January 8th, 2019).

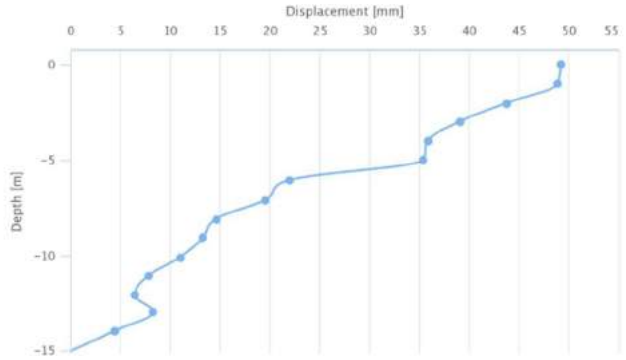

Figure 3 Cumulative displacement recorded by DT0080 MEMS at the end of the monitoring activity (January 8th, 2019).

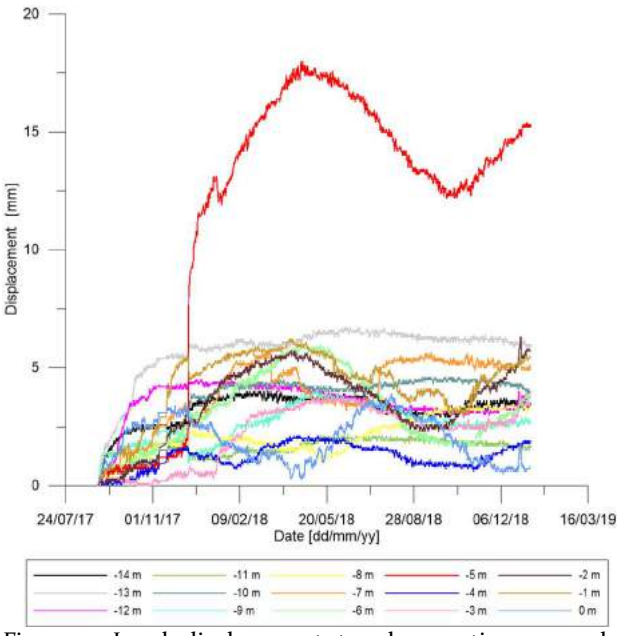

Figure 4 Local displacement trend over time, recorded by DT0080 MEMS.

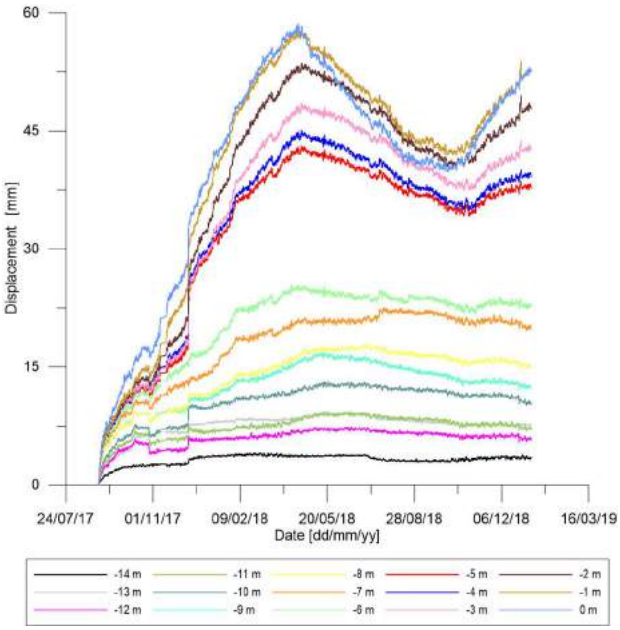

Figure 5 Cumulative displacement trend over time, recorded by DT0080 MEMS.

The multi-parametric nature of the instrument, together with the high sampling data acquisition, allowed to correlate different physical quantities in order to assess cause-effect relationships. An example can be observed in Fig. 6 representing the water level variation recorded by the piezometer and the local displacement trend at 5 and 10 metres of depth. It is possible to note how the sudden increasing of water level triggered the movements starting from December 2017. The following peaks did not display any further impulsive displacements, a behaviour that could be related to a more stable configuration of the wall due to maintenance works. This representation underlines the importance of an automated tools in the detection of cause-effect relationships and efficacy control of works related to geotechnical field.

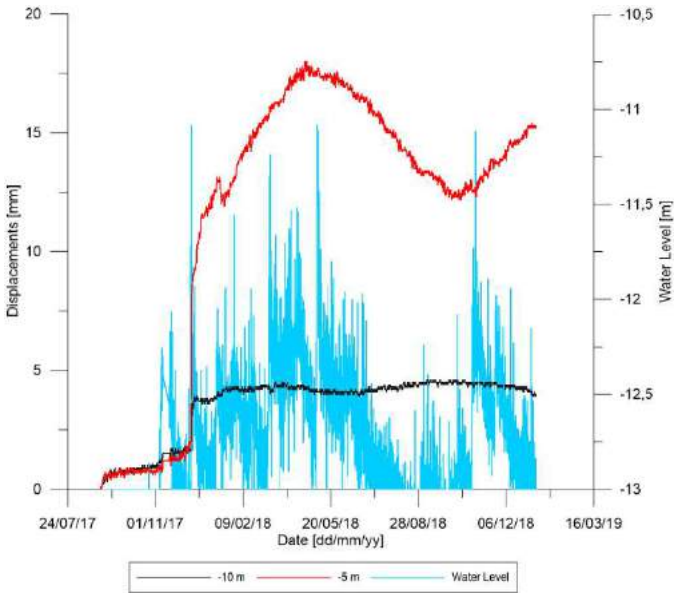

Figure 6 Water level variation measured by Piezo Link installed on DT0080, together with local displacements recorded at -5 m and -10 m.

DT0081

DT0081 Vertical Array is the downstream inclinometer, located in close proximity to the retaining wall face. As in the case of DT0080, the device started to record the day after its installation. As can be observed in Fig. 7 and Fig. 8, respectively reporting local and cumulative displacements at the end of the monitoring activity, data are quite different compared to DT0080. It is possible to observe two main movements at -5 m and -14 m instead of a single sliding surface. In particular, the movement detected at a depth of 14 metres indicates a critical condition in a theoretically stable area, with a local displacement of 12.6 mm.

This behaviour can be observed in Fig. 9 and Fig. 10, respectively representing local and cumulative displacement trends over time for the whole monitoring period of DT0081 automatic inclinometer. These data clearly underline a rapid event that took place between 5 and 6 July 2018 and involved the lower part of the retaining wall, resulting in 18.6 mm of displacement recorded at a depth of 14 metres. Another major event started at the beginning of December 2018 at the same depth, as can be observed in Fig. 9, and continued until the end of monitoring activities on January 2019. During this time interval, the inclinometer experienced a local displacement equal to 12.5 mm.

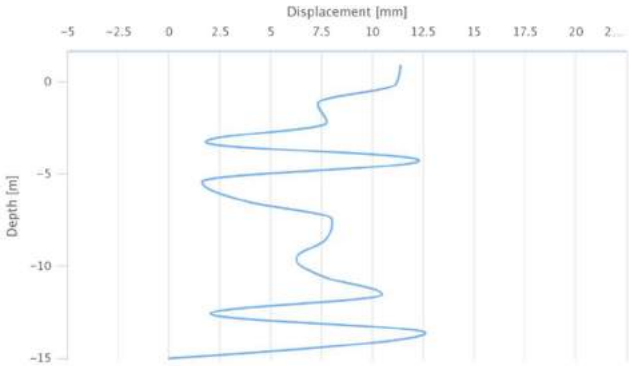

Figure 7 Local displacement recorded by DT0081 MEMS at the end of the monitoring activity (January 8th, 2019).

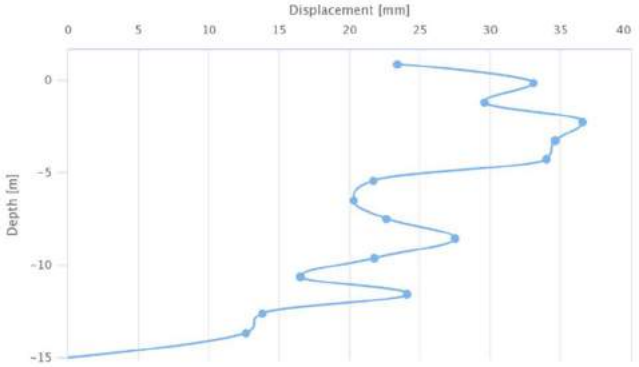

Figure 8 Cumulative displacement recorded by DT0081 MEMS at the end of the monitoring activity (January 8th, 2019).

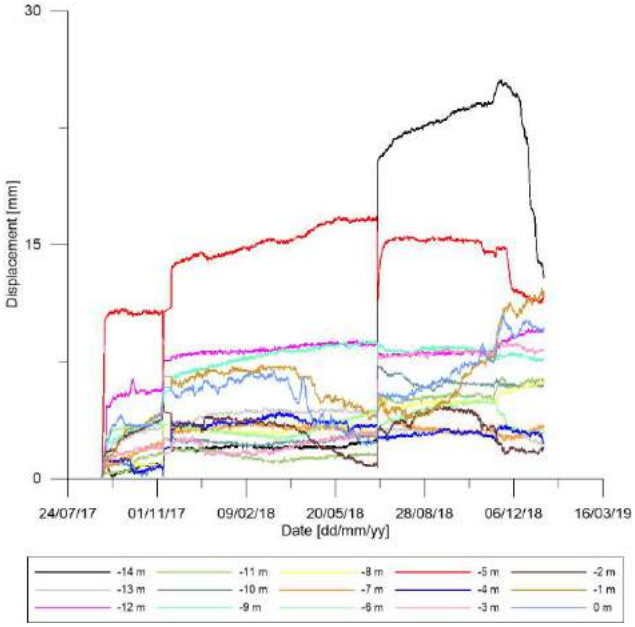

Figure 9 Local displacement trend over time, recorded by DT0081 MEMS.

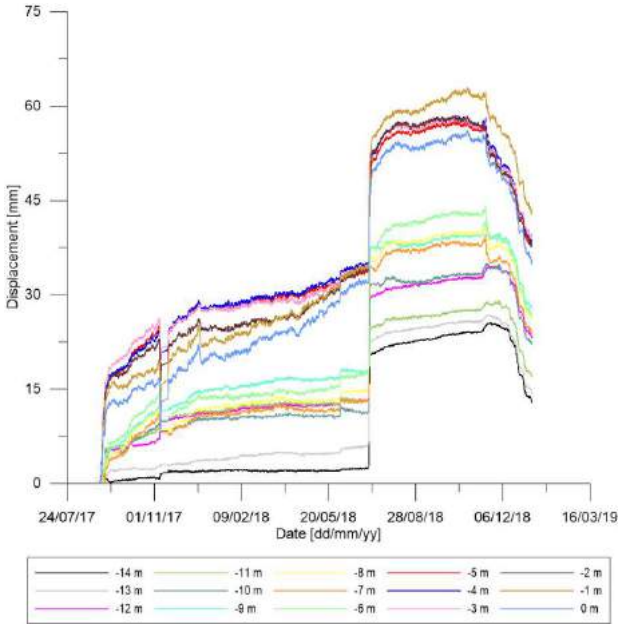

Figure 10 Cumulative displacement over time, recorded by DTo081 MEMS.

Similarly to what happened for the DTo080 inclinometer, displacement data measured by the DTo081 instrumentation never activated the alert threshold that was set at the beginning of the monitoring activity. The reason can probably be identified in the extremely rapid development of the recorded event, which took place in a time interval close to a single day.

The analysis of water level records (Fig. 11) highlights a different behaviour compared to data coming from DTo080. In particular, the piezometer displays a series of substantial variations in different time periods, probably influenced by the presence of the retaining wall. It is possible to note how these variations influence the displacement measures. However it doesn't seem to exists a direct correlation between the intensities of the water level fluctuation and movements recorded by the inclinometer. For example, the increasing of water level recorded on November 2017 caused a smaller displacement if compared to the July 2018 event, which happened in correspondence of a secondary peak of the water level variation.

Fig. 12 reports temperature data measured by Therm Link. It is possible to observe the day-night cycle and seasonal variations of this parameter, ranging from a maximum of 39.8°C in summer to a minimum of -6.5° C at the end of February 2018. In particular, the increase in temperature observed from May 2018 seems to match the relaxation process identified by DTo080 (Fig. 4 and Fig. 5). However, no evidence of direct correlations with retaining wall movements emerges from the comparison with displacement recorded by DTo081 in the upper part of the structure.

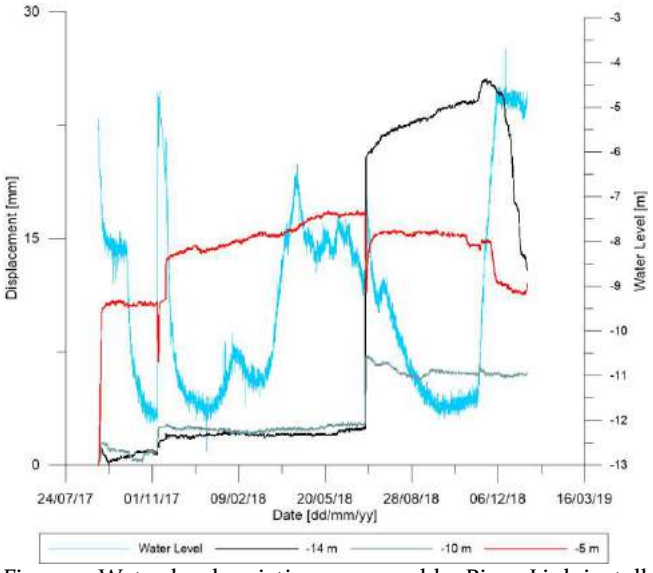

Figure 11 Water level variation measured by Piezo Link installed on DTo081, together with local displacements recorded at -5 m, -10 m and -14 m.

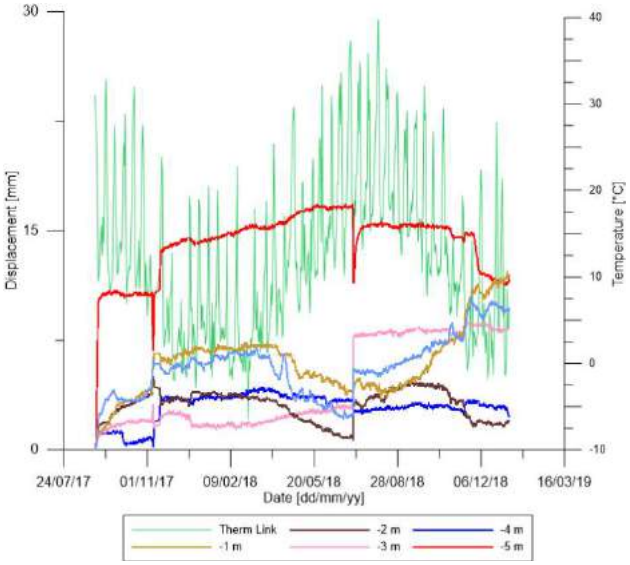

Figure 12 Temperature variation recorded by Therm Link, together with displacements measured by DTo081 in the upper part of the wall

Taking into account the considerations exposed for the piezometer results, the presence of two different tilt sensors within a single Link played a major role for the analysis and validation of data concerning the July 2018 event. In fact, since the area interested by the displacement was supposed to be stable and the other inclinometer did not record any movement at that depth, some doubts could arise about the data reliability. Tilt Link HR 3D V sensors are extremely useful and innovative for these reasons, because they provide a double independent information at the same depth. Comparing local displacements data recorded by MEMS and electrolytic sensor at -14 metres, it is possible to find matching similar behaviour for the time period of interest with slight differences related to the sensibility of sensors (Fig. 13). Both sensors highlighted a sudden movement,

which started on July 5th, 2018 at about 10 AM and ended at about 7 AM on the following day, with a difference of 1.7 mm between the two measures.

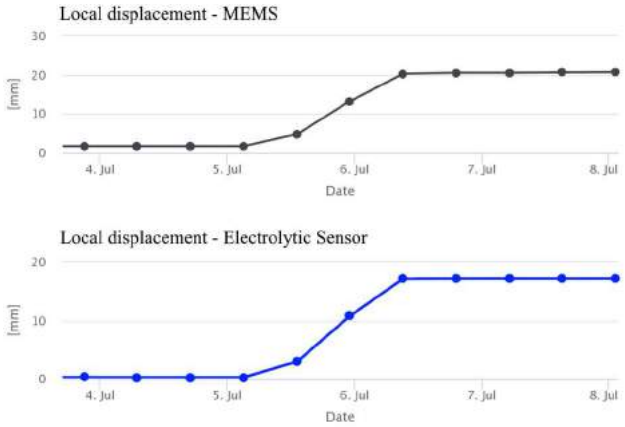

Figure 13 Local displacement trends between 4 and 8 July 2018, recorded by MEMS and electrolytic sensor at -14 m of depth.

Conclusions

This paper focuses on the monitoring activity of a reinforced earth retaining wall, performed through the application of an innovative and multi-parametric system. Consisting of two 15-metre MUMS automatic inclinometers, called Vertical Arrays, the installed system allowed to study the evolution of the structure, recording data concerning displacements, temperatures, pore pressure, and water level thanks to the different sensors installed along the same Array at different depths. MUMS technology exploits IoT principles, featuring a fully automatic process of data acquisition and elaboration, a remotely controllable data logger, and an interactive web-based platform for results visualization and analysis. This new approach could be named as "Internet of Natural Hazards" (IoNH), representing the application of IoT features to the natural hazard and risk management field.

During the monitoring activity, which lasted a total of 17 months, the MUMS instrumentation allowed to outline the structure conditions with improved results compared to traditional devices. The high sampling frequency and the automated acquisition process provided an exhaustive description of the retaining wall behaviour, identifying several time periods where unexpected displacements were observed.

In particular, the DT0080 Array evidenced a major movement at a depth of 5 metres, developing between December 2017 and May 2018 and reaching a local displacement value equal to 56 mm. Data recorded by the piezometer integrated in the same Array showed a good correlation with displacement values, indicating a cause-effect relationship between water level variation and displacement increase.

On the other hand, the DT0081 inclinometer placed in close proximity to the wall recorded a sudden movement near the structure base, resulting in a displacement of 18.6 mm in a supposedly stable area. For this reason, this outcome could have been interpreted as an instrumental error, considering also the lack of clear connections with piezometric measures. However, the integration of two independent tilt sensors (i.e. MEMS and electrolytic cell) within a single node gave the possibility of a comparison between displacement data at the same depth. The satisfying correspondence arisen from this test confirmed the validity of the measure, thus underlining the importance of a redundant system for data validation and control.

Monitoring data acquired by both automatic inclinometers ultimately evidenced a series of critical conditions in the structure stability. These results, together with previous evaluations, led to the demolition of the retaining wall on January 2019 for safety reasons. However, it should be noted that the alert threshold was never reached during the monitoring activity, due to the rapid development of recorded events. This case study underlines the importance related to the assessment of different alert thresholds, in order to be able to identify both impulsive events and long-term displacements of the monitored object.

References

Baily E, McCabe BA, Goggins J, Kieran P (2014) Real time monitoring and performance of retaining structures. In: Proceedings of Civil Engineering Research in Ireland (CERI 2014), Belfast, pp. 229-234

Benjamim CVS, Bueno BS, Zornberg JG (2007) Field monitoring evaluation of geotextile-reinforced soil-retaining walls. Geosynthetic International, 2007, 14, No. 2 pp. 100-118

Carrubba P, Moraci N, Montanelli F (1999) Instrumented soil reinforced retaining wall: analysis of measurements. In: Proceedings of Geosynthetics '99, Boston, Mass., April 1999. Industrial Fabrics Association International, Roseville, Minn., pp. 921-934.

Koerner RM, Koerner GR (2011) Recommended layout of instrumentation to monitor potential movement of MSE walls, berms and slopes. GRI White Paper #19, Geosynthetic Institute, Folsom, PA

Lienhart W, Monsberger CM, Kalenjuk S, Woschitz H (2018) High resolution monitoring of retaining walls with distributed fibre optic sensors and mobile mapping system. 7th Asia-Pacific Workshop on Structural Health Monitoring, November 12-15, 2018 Hong Kong SAR, P.R. China

Rainieri C, Dey A, Fabbrocino G, Santucci de Magistris F (2010) Monitoring and modeling of flexible retaining wall. In: Proceedings of the 3rd Asia-Pacific Workshop on Structural Health Monitoring, January 2010

Segalini A, Carini C (2013) Underground landslide displacement monitoring: a new MMES based device. In: Landslide Science and Practice, Volume 2: Early Warning, Instrumentation and Monitoring; Margottini C, Canuti P, Sassa K, Eds; Springer: Berlin/Heidelberg, Germany, 2013

Segalini A, Chiapponi L, Pastarini B, Carini C (2014) Automated inclinometer monitoring based on Micro Electro-Mechanical System technology: Applications and verification. In: Landslide Science for Safer Geoenvironment; Sassa K, Canuti P, Yin Y, Eds; Springer: Cham, Switzerland, 2014; pp 595-600

Stirling DM, Chandler JH, Clark JS (1992) Monitoring of one of Europe's largest retaining walls using oblique aerial photography. International Archives of Photogrammetry and Remote Sensing, 29(5): 701-708

doi.org/ 10.35123/ReSyLAB_2019_6

Validation and proposal of new rainfall thresholds for shallow landslide prediction in Posavsko hills, Eastern Slovenia

Galena Jordanova[(1)], Timotej Verbovšek[(2)], Mateja Jemec Auflič[(3)]

1) University of Ljubljana, Faculty of Natural Sciences and Engineering, Department of Geology, Ljubljana, Aškerčeva 12; galena.jordanova@ntf.uni-lj.si

2) University of Ljubljana, Faculty of Natural Sciences and Engineering, Department of Geology, Ljubljana, Aškerčeva 12; timotej.verbovsek@ntf.uni-lj.si

3) Geological Survey of Slovenia, Ljubljana, Dimičeva 14; mateja.jemec-auflic@geo-zs.si

Abstract This paper presents validation of the current thresholds of the Slovenian early warning system MASPREM for shallow landslide prediction, and proposal of new thresholds for the area of Posavsko hills in eastern Slovenia. Rainfall thresholds are one of the main components of the early warning systems for landslide occurrence. To achieve a sufficient forecasting of landslide occurrence it is important to study the rainfall events that caused slope instability in the past. In this study we focused on research of the rainfall patterns of 7 major rainfall events that triggered more than 180 landslides in the area of Posavsko hills. The main goal was to set new rainfall thresholds for the area of Posavsko hills using empirical method. We studied the effect of antecedent rainfall, as well as the mean intensity and peak intensity of the rainfall events. The impact of lithology on shallow landslides was also studied. We concluded, that lithology has a big impact on landslide occurrences and that the current thresholds are set rather high, leading to missed alarms for many major rainfall events. Therefore, we propose new, lower thresholds for the lithological units of sediments and clastic sedimentary rocks of different age in the studied area. The new thresholds will be used for improvements of the system MASPREM.

Keywords landslides, rainfall, early warning system, Posavsko hills, Eastern Slovenia

Introduction

Landslides are amongst the biggest threats to the safety of residents and can cause huge damage to the infrastructure. One way to avoid any serious consequences of slope mass movements is to use an early warning system (Komac et al. 2013). Landslides in Slovenia are mainly triggered by rainfall and related phenomena (short intense rainstorms, long-term rains, snow, snow melt etc.), therefore, the rainfall thresholds for landslide occurrence are the main component of the Slovenian early warning system for rainfall-induced shallow landslides - MASPREM. Beside the thresholds, the early warning system is consisted of 2 more compounds: (i) landslide susceptibility map (LSM) and (ii) precipitation forecast – ALADIN and/or INCA models (Jemec Auflič et al. 2016).

The MASPREM system was validated during the project MASPREM 3 (Šinigoj et al. 2018). The results offered an insight of how successfully the system predicted landslide occurrence. The system currently runs with 5 different test models and in the best case the system issued alarm correctly in 53%. (Šinigoj et al. 2018; Jemec Auflič & Šinigoj 2019). During the validation process, we concluded, that some areas in Slovenia are better predicted (e.g. the western part), while some areas have higher number of missed alarms (the eastern part). The western part of Slovenia is a lot more humid than the eastern and the thresholds are more often exceeded, therefore the percentage of correct predictions (true positives, see below) for the western part is much higher than the one for the eastern part of the country, which holds more false negatives. Eastern Slovenia is a lot more susceptible to shallow landslides than the west because of the geological setting, appropriately steep hillsides and eluvium thickness.

For the purpose of upgrading and improving the early warning system, a validation of the models for Eastern Slovenia was performed. The region of Posavsko hills was chosen as a subject of study, based on the results of the validation of the thresholds for the whole country.

From the beginning of the system MASPREM in September 2013 till May 2018, numerous rainfall events that caused many landslides in Posavsko hills have been registered. 7 rainfall events stand out, as they triggered around 180 shallow landslides and during most of the events the thresholds were not exceeded.

Study area

Posavsko hills are a pre-alpine region, stretching from the Ljubljana basin on the west to the river Sotla on the east, and it lies on the north and south side of the river Sava. In comparison with the other hilly areas in Slovenia, Posavsko hills are lower in altitude and less humid (Gams 1998).

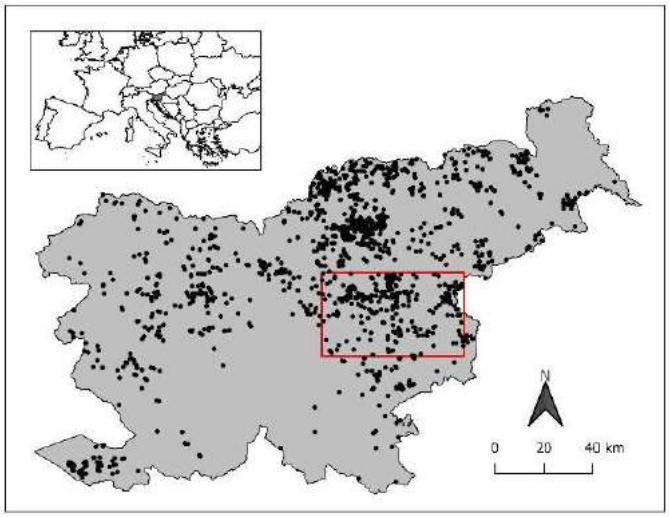

Figure 1 Map of Slovenia with recorded landslide occurrences. Studied area is marked with red rectangle.

Posavsko hills are generally divided into different lithological belts, that extend in the direction W-E and consist mainly of clastic sedimentary rocks, unbound sediments and carbonates. The oldest rocks, that occur in this area are Permo-Carboniferous shales, sandstones and conglomerates, followed by Mesozoic deep- and shallow-marine carbonate rocks (mainly Triassic and Jurassic limestones and dolomites as well as Cretaceous flysch and other deep-marine rocks), and Tertiary sediments of the Pannonian Basin. Triassic and Paleogenic volcanoclastic rocks (tuffs) also occur in some small areas (Gams 1998; Bavec 2013).

Posavsko hills are in geological terms generally known as Sava folds. They are situated in the triangle between the Periadriatic tectonic zone, Idrija tectonic zone and Mid-Hungarian tectonic zone. The W-E oriented folds are the result of tensions in N-S direction (Placer 1999). Therefore, in this area we can expect less stable rock masses and more unstable tectonically deformed rocks and alluvium.

Rainfall events

In November 2013 two major rainfall events took place; the first event lasted 3 days between 9 and 11 November. The rain gauges measured 100 mm of rain during the event. The other rainfall event happened between 19 and 27 November, when the rain gauges recorded 90 to 110 mm of rain.

The year 2014 was an above average rainy year. The yearly amount of rain in most parts of Slovenia exceeded the long-term yearly average. More than 100 landslides were triggered during 4 major rainfall events: 13–15 August, 1–3 September, 9–14 September and 4–8 November. These events were short and intense; most of the rain fell in a matter of a few hours to a few days. The amount of rain ranged from 60 to 160 mm.

September 2017 was also a very rainy month. Between 14 and 20 September the rain gauges recorded from 100 to 200 mm of rain in most parts of Slovenia.

Rain gauges

In the area of Posavsko hills there are 5 rain gauges that collect daily rainfall data at 7 am for the previous 24 hours (see Fig. 2). The maximum distance between the landslide and rain gauge was set to 10 km with a circular buffer. Larger distance would not be appropriate because of the hilly relief, and shorter distance would mean a lot of landslides outside of the buffer zones. The landslides that were out of the gauges' buffer zones were excluded from the analysis.

For the purpose of hourly rainfall data analysis, we used three different rain gauges. Due to the small number of automatic gauges and the large distances between them, we used the data from the closest gauges. They collect rainfall data every 5 minutes or every half an hour, which were recalculated into hourly data.

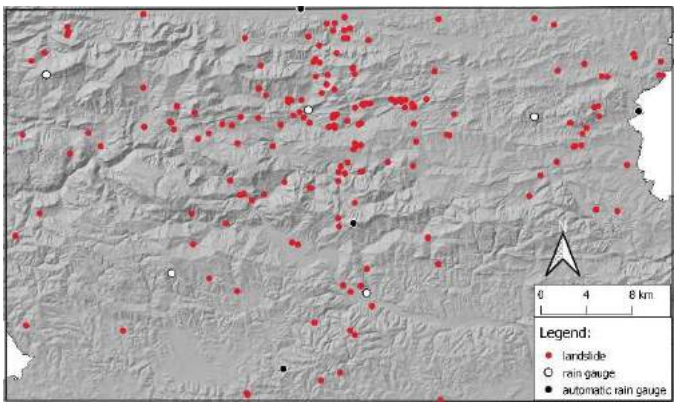

Figure 2 Posavsko hills with recorded landslide occurrences during the studied 7 major rainfall events *(red dots)* and rain gauges *(black and white dots)*.

Methodology

Validation for Eastern Slovenia

The validation of the MASPREM models was done in QGIS. It was a visual comparison of the landslide catalogue and the system's calculations of landslide occurrence probability for each day between September 2013 and May 2018. There were 4 possible outcomes:

- true positive (TP) – the system issued an alarm (higher probability of landslide occurrence) and at least 1 landslide happened;
- false positive (FP) – the system issued an alarm and no landslides occurred or were recorded;
- false negative (FN) – no alarms were issued, but at least 1 landslide happened;
- true negative (TN) – no alarms were issued, and no landslides occurred or were recorded.

The landslide catalogue consisted of information about coordinates and date of landslide trigger, as well as information about the lithological unit of the landslide

source. The results were gathered in contingency matrices and calculated by the formulas below (Tab. 1).

Five different MASPREM models, that are currently in testing phase, were validated. They differ in combination of LSM, forecast models and threshold values, as follows:

- Model 1: LSM + ALADIN precipitation forecast + thresholds 1
- Model 2: LSM + 2-day ALADIN antecedent rainfall + ALADIN forecast + thresholds 1
- Model 3: LSM + 2-day ALADIN antecedent rainfall + ALADIN forecast + thresholds 2
- Model 4: LSM + 2-day INCA antecedent rainfall + ALADIN forecast + thresholds 1
- Model 5: LSM + 2-day INCA antecedent rainfall + ALADIN forecast + thresholds 2

Thresholds 2 are empirically lowered thresholds 1 (Komac et al., 2013).

Table 1 Skill scores used for validation of the MASPREM models (Gariano et al., 2015).

Skill score	Formula	Range	Optimal value
Probability of Detection	$POD = \frac{TP}{TP + FN}$	[0,1]	1
Probability of False Detection	$POFD = \frac{FP}{FP + TN}$	[0,1]	0
Probability of False Alarms	$POFA = \frac{FP}{TP + FP}$	[0,1]	1
Hanssen & Kuipers	$HK = \left(\frac{TP}{TP + FN}\right) - \left(\frac{FP}{FP + TN}\right)$	[-1,1]	1

Rainfall data analysis

In this case study we excluded all landslides, that were triggered by snow and snow melt during the months between December and April, and focused on rainfall events during the summer and autumn months.

To determinate the effect of antecedent rainfall, we gathered daily rainfall data up to 30 days prior the landslide occurrence. We separated different rainfall events with a 48-hour dry period. Based on the cumulative antecedent rainfall, we determined the amount of rainfall needed to trigger landslides on different lithological units. With this analysis we also determined the duration of the rainfall events, that caused landslides.

With the hourly rainfall data, we analysed the temporal rainfall patterns of the events. The mean intensity analysis indicated the minimum rainfall quantity for landslide occurrences at different duration of rainfall events. The peak intensity was done for a comparison of the rainfall patterns between the different events.

Results and discussion

Validation of MASPREM models for Eastern Slovenia

The validation resulted with the probability of landslide occurrence in the eastern part of Slovenia not being accurately predicted. In the best case, the prediction was 32% correct with the model 5 (see Tab. 2). This is most probably the consequence of thresholds set too high for the area. The weakest model, that does not take into account 2-day antecedent rainfall, was only 8% accurate. This proves, that the cumulative antecedent rainfall has important role in more accurate prediction of landslide occurrence.

Table 2 Results of the validation in percent [%].

Skill score	M1	M2	M3	M4	M5
POD	8	31	28	26	32
POFD	1	6	4	3	3
POFA	45	53	48	50	38
HK	7	26	23	23	30

The probability of false detection (POFD) is the lowest for the model 1 and the highest for model 2. The models 4 and 5 have lower probability of false detection than the models 2 and 3, because of the properties of the INCA forecasting model. The latter is more accurate than the ALADIN model due to smaller cell size of its grid (1x1 km) (Haiden et al. 2010). The ALADIN models have grids with larger cell size 4x4 km (Pristov et al. 2012).

The probability of false alarm (POFA), which is the ratio between the number of false alarms and the total number of correct forecasts (Gariano et al. 2015), is the highest for model 2 and lowest for model 5. This means, that the model 5 has the lowest probability of issuing a false alarm. The Hanssen & Kuipers skill score (HK) measures the prediction accuracy for the events with and without landslides and is linearly dependent on POD and POFD skill scores (Gariano et al. 2015). Again, the model 5 has the best result, due to the thresholds 2 and INCA model. This is a direct proof, that the upgrading of the MASPREM models is progressing.

Analysis of the rainfall patterns

The analysis of antecedent rainfall showed, that the landslides in Posavsko hills occur after 3 different periods of rain accumulation (Fig. 3). The first group occurred after short rainstorms, that lasted 1 to 3 days. The lowest amounts of rain, that triggered landslides, are between 30 and 50 mm. The second group represents landslides, that occurred after 3 to 5 days long rainfall events with amounts of rain between 90 and 150 mm. The last group of landslides occurred after a longer period of continuous rainfall, that lasted 18 days. The amount of rain, that triggered these landslides, is higher – between 230 and 350 mm.

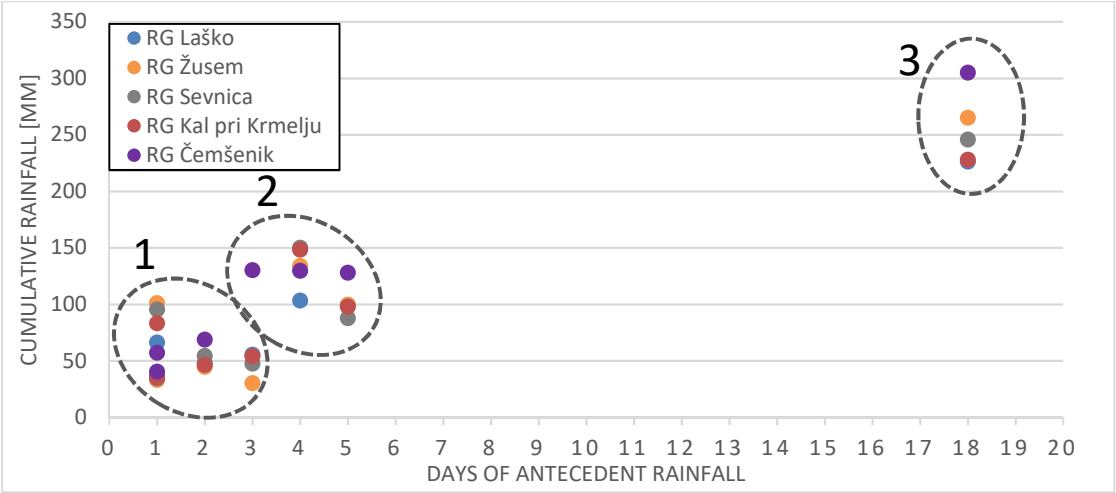

Figure 3 Landslide occurrence in 3 different groups, based on cumulative and antecedent rainfall. The different rain gauges are marked with circles of different colors.

The mean intensity of the rainfall events showed, that the landslides were triggered at similar amounts of rainfall regardless the duration of the events (Fig. 4). For the mean intensity we took hourly rainfall data on the day of the landslide occurrence. The duration of the event was determined as a continuous period of rainfall. The 7 events lasted from 7 to 30 hours continuously and the amount of rainfall varies averagely around 35 mm. The event on September 13th 2014 is an exception. It lasted 18 hours and the amount of rain reached 84.5 mm. This amount of rainfall triggered a lot of landslides on different lithological units. While we do not have accurate time frame, when the landslides were triggered (e.g. at what time during the day), we considered the time of occurrence by the end of the day. This however represents some uncertainty regarding the amount of rainfall needed for landslide occurrence, i.e. the landslides could have been triggered during the day at lower amounts of rainfall than we considered.

The peak intensity (Fig. 5) represents the rainfall patterns of the different events. Because most of the events lasted at least 18 hours, we only considered the first 18 hours of the longer lasting events. The peak intensity ranged between 2.9 and 26.4 mm h^{-1}, but the patterns of the events are mainly similar. This means that the landslides were triggered during rainfall events with similar patterns.

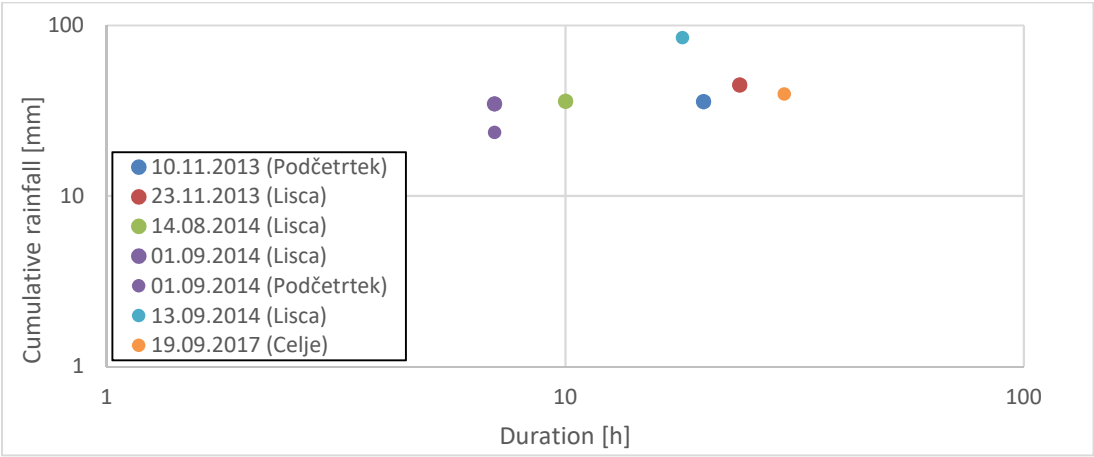

Figure 4 Mean intensity of the rainfall events. The rainfall event on September 1st 2014 is represented by two sets of data due to the different amount of rainfall, that triggered landslides near two different automatic gauges.

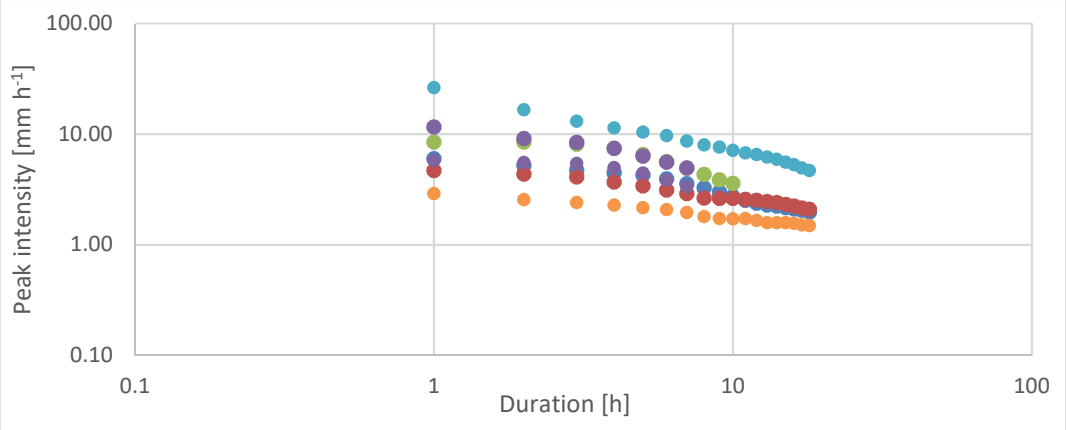

Figure 5 Rainfall patterns of the events. The event on September 1st 2014 is presented by two sets as in Fig. 4.

Conclusion

Most of the landslides (57%) occurred in marls, sands, conglomerates, clays, as well as in sandstones, marlstones, shales, tuffs, breccia and other clastic sedimentary rocks. All together more than 80% of the landslides in Posavsko hills occurred in sediments and sedimentary rocks, while less than 20% occurred in some regions of limestones and dolomites. Therefore, we conclude, that the lithology has a great impact on shallow landslide occurrence.

The thresholds for these lithological units are currently set between 70 and 100 mm. The new proposed thresholds should be lower - between 35 and 50 mm. Lowering the thresholds could result in increasing number of false alarms, therefore, we should consider these thresholds with caution.

For further improvement of the early warning system it is of great importance to research smaller areas with similar geological conditions. The validation of the MASPREM models proves, that generalization of the lithological units and their thresholds for the whole country leads to a lot of missed alarms (false negatives) for some parts of Slovenia. The generalization led to overlooking some local (geological) features that certainly have a great impact on landslide occurrences.

Furthermore, we should also stress the importance of quality landslide catalogue. Incomplete data of landslide occurrences can lead to major differences in the results, e.g. incorrect coordinates of landslides' source and incorrect dates of occurrence mean misinterpretation of the natural settings, therefore, the results would not represent the real conditions, responsible for the landslide occurrence.

Acknowledgments

This study was done in the frame of a Master's thesis (Analysis of temporal rainfall patterns for landslide occurrences in Eastern Slovenia). The authors would like to thank the Administration of the Republic of Slovenia for Civil Protection and Disaster Relief for funding MASPREM project and Agency for environment of Republic Slovenia for providing the data.

References

Bavec M (2013) Geološka karta Slovenije 1:1.000.000 [Kartografsko gradivo] = Geological map of Slovenia 1:1.000.000, Ljubljana: Geološki zavod Slovenije.

Gams I (1998) Pokrajinsko ekološka sestava Slovenije. In: Gams I, Vrišer I (eds.) Geografija Slovenije. Slovenska matica v Ljubljani. (ISBN 961-213-060-4). pp. 214-243. (in Slovene)

Gariano S L, Brunetti M T, Iovine G, Melillo M, Peruccacci S, Terranova O, Vennari C, Guzzetti F (2015) Calibration and validation of rainfall thresholds for shallow landslide forecasting in Sicily, southern Italy. Geomorphology. Vol. 228: 653–665.

Haiden T, Kann A, Wittmann C, Pistotnik G, Bica B, Gruber C (2010) The Integrated Nowcasting through Comprehensive Analysis (INCA) System and Its Validation over the Eastern Alpine Region. Weather and Forecasting. 26(2): 166–183.

Jemec Auflič M, Šinigoj J (2019) Validation of the Slovenian national landslide forecast system using contingency matrices. In: European Geosciences Union, General Assembly 2019, Vienna, Austria, 7-12 April 2019, (Geophysical research abstracts, ISSN 1607-7962, 73 Vol. 21). München: European Geosciences Union, 2019. URL: https://meetingorganizer.copernicus.org/EGU2019/EGU2019-13338.pdf [Last accessed: 25.06.2019].

Jemec Auflič M, Šinigoj J, Krivic M, Podboj M, Peternel T, Komac M (2016) Landslide prediction system for rainfall induced landslides in Slovenia (Masprem), Geologija. 59(2): 259–271.

Jordanova G (2019) Analysis of temporal rainfall patterns for landslide occurrences in eastern Slovenia (in Slovene language). Master's thesis, Faculty of Natural Sciences and Engineering, University of Ljubljana, Ljubljana, Slovenia.

Komac, M et al. (2013) Projekt: sistem zgodnjega opozarjanja za primer nevarnosti proženja zemeljskih plazov – MASPREM; DP1: Model verjetnosti pojavljanja zemeljskih plazov za območje Slovenije. Ljubljana: Geološki zavod Slovenije. 32p. (in Slovene)

Placer L (1999) Structural meaning of the Sava folds = Strukturni pomen Posavskih gub, Geologija. 41: 191-221.

Pristov N, Cedilnik J, Jerman J, Strajnar B (2012) Priprava numerične meteorološke napovedi ALADIN-SI, Vetrnica. pp. 17-23. (In Slovene)

Šinigoj J, Jemec Auflič M, Kumelj Š, Peternel T, Krivic M, Vegan J, Zakrajšek M, Prkić Požar N, Podboj M, Šinigoj M, Jordanova G (2018) Nadgradnja sistema za obveščanje in opozarjanje v primeru proženja zemeljskih plazov v RS - MASPREM 3: končno poročilo. Ljubljana: Geološki zavod Slovenije. 175p. (In Slovene)

doi.org/ 10.35123/ReSyLAB_2019_7

Continuous monitoring of the Kostanjek landslide

Martin Krkač[(1)], Sanja Bernat Gazibara[(1)], Marin Sečanj[(1)], Željko Arbanas[(2)], Snježana Mihalić Arbanas[(1)]

1) University of Zagreb, Faculty of Mining, Geology and Petroleum Engineering, Zagreb, Pierottijeva 6, +385 1 5535 896

2) University of Rijeka, Faculty of Civil Engineering, Rijeka, Croatia

Abstract Landslide movements pose a substantial risk to people and infrastructure. Sometimes, in cases of complex or large volume landslides, monitoring and prediction are the only reliable and cost-efficient methods for the mitigation of the landside risk. This paper presents six years monitoring data series observed by the Kostanjek landslide monitoring system (Zagreb, Croatia). The Kostanjek landslide monitoring system consist of multiple sensor networks for continuous observations of external triggers, hydrological properties and displacements. The presented data are continuous displacement and groundwater level data measured at the central part of the landslide, while presented precipitation data are measured at the meteorological station Zagreb-Grič. During the period 2013-2018 the Kostanjek landslide experienced multiple reactivations, with maximal displacements up to 750 mm, with the highest velocities measured in the central part of landside. All reactivations are consequences of high groundwater levels. During the monitoring period the groundwater level changed from to 19 to 10.5 m. The cumulative precipitations that caused groundwater level to rise ranged from 21 mm to 180 mm, depending on the initial groundwater level. This data shows that the amount of precipitation necessary for landslide reactivation depends on the soil moisture above the groundwater level.

Keywords landslide, monitoring, precipitation, groundwater, displacement

Introduction

Landslides present a natural hazard which causes human losses (e.g., Petley 2012), as well as significant damage to property and infrastructure around the world every year (e.g., Haque et al. 2016). Remediation measures are extensively used for reducing and even eliminating the landslide related hazard (Michoud et al., 2013). However, remediation measures are sometimes too expensive or too difficult, especially when dealing with complex or large volume landslides (Blikra, 2012). In these cases, monitoring of the slopes, prediction of landslide movements and finally the establishment of an early warning system, are practical measures for the reduction of landslide risk. Monitoring of triggering parameters is necessary to study landslide occurrence and behaviour, as well as to define thresholds and alert criteria to be employed in a LEWS (Pecoraro et al, 2019).

The example of monitoring of a large volume landslide is a Kostanjek landslide monitoring system. In the framework of the scientific Japanese-Croatian bilateral SATREPS FY2008 project 'Risk Identification and Land-Use Planning for Disaster Mitigation of Landslides and Floods in Croatia' a Kostanjek landslide monitoring system was established with the main objective of landslide mitigation though the development of an early-warning system (Mihalić Arbanas et al. 2013). Multiple sensor networks for continuous observations of landslide movements and its causes were setup in the period 2011–2014. This paper presents the Kostanjek monitoring system and the results of the continuous monitoring for the period 2013-2018.

Kostanjek landside

The Kostanjek landslide is the largest landslide in the Republic of Croatia (Fig. 1). It is a reactivated deep-seated translational landslide located in the urbanized area of the City of Zagreb (the capital and the largest city in Croatia) at the base of the southwestern slopes of Medvednica Mt. The total landslide area is approximately 1 km2. Since its activation in 1963, Kostanjek landslide has caused substantial damage to buildings and infrastructure in the residential and in industrial zones.

The landslide was caused by anthropogenic factors, mainly by excavations in a marl quarry placed in the toe part of the landslide. Despite extremely slow to slow landslide movements during 56 years, the risk in the area of the Kostanjek landslide is very high for residents and for material properties (approx. 300 single-family houses and infrastructure networks are placed on the moving landslide mass). The total displacement of the Kostanjek landslide is unknown because of poor temporal resolution of landslide movement observations and inconsistent measurements at stable geodetic points.

The sliding surface was developed in Middle Miocene (Sarmatian) laminated marls, while the displaced mass consists of Upper Miocene clayey marls with thin limestone layers (Lower Pannonian) and massive clayey marls (Upper Pannonian). The width of the displaced mass is 960 m, and the total length of the Kostanjek landslide is 1.26 km. The depth of the sliding surface is approximately 90 m according to the interpretation by Ortolan and Pleško (1992). The volume of the sliding mass is evaluated to be 32×10^6 m^3 (Stanić and Nonveiller 1996).

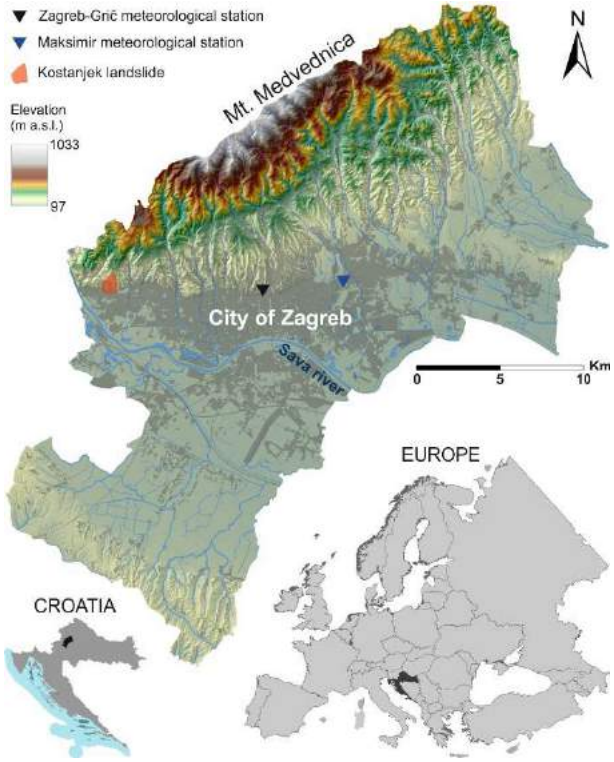

Figure 1 Location of the Kostanjek landslide and the meteorological station Zagreb-Grič.

Monitoring system

Kostanjek landslide monitoring system consist of multiple sensor networks for continuous observations of: (1) external triggers (rain gauge and accelerometers); (2) hydrological properties (pore pressure gauges and water level sensors in boreholes and domestic wells, water level sensors at outflow weirs); (3) displacement/activity (GNSS sensors, extensometers, borehole extensometers and inclinometer). The majority of monitoring equipment is installed at a central monitoring station, located in the central part of the Kostanjek landslide (Fig. 2). The following text presents the brief overview of the sensor networks (rain gauge, water level sensors and GNSS) and monitoring results for the period 2013-2018.

The external triggers, e.g. meteorological conditions relevant for the Kostanjek landslide are measured since 2011 with a 0.5 mm tipping-bucket rain gauge (NetLG-201E, Osasi Technos Inc). Due to malfunctions of the rain gauge, in December 2014, a new weather station (Davis Vantage Pro2, Davis Instruments) was installed. During the monitoring period, the meteorological conditions are also gathered from the Zagreb-Grič meteorological station of the Croatian Meteorological and Hydrological Service. Zagreb-Grič meteorological station is placed 9 km east of Kostanjek, at the southern slopes of Medvednica Mountain (Fig. 1), at the location with the similar geomorphological and hydrological conditions as Kostanjek landside (Krkač, 2015). The data from Zagreb-Grič meteorological station are available for the period from 1862.

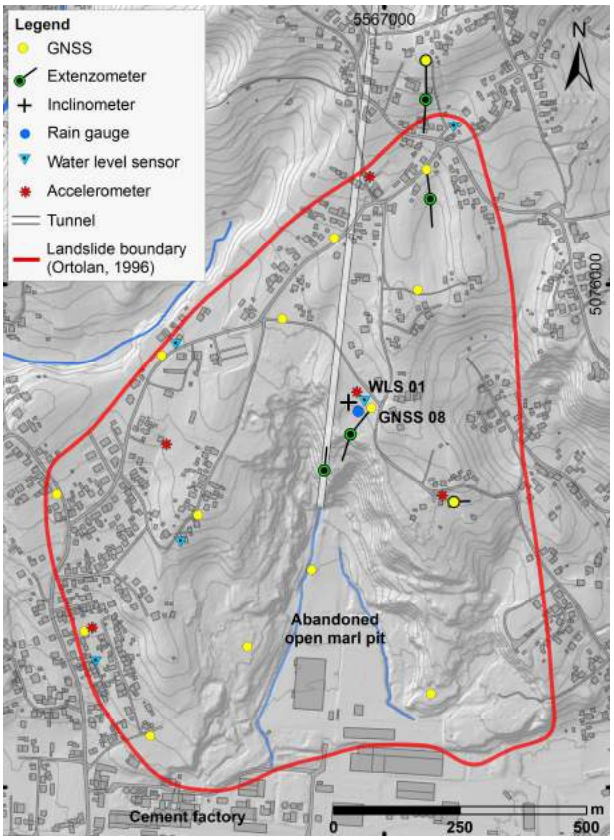

Figure 2 Locations of multiple sensor networks at the Kostanjek landslide (Krkač et al, 2017).

GWL data are continuously monitored at the five locations within the landslide, in the boreholes and domestic wells. Water level sensor (WLS-1 on Fig. 2) for measurement of hydrostatic pressures (DS-1, Osasi Technos Inc) is installed at the central part of landslide in a borehole with an accelerometer since January 2013. The sensor is installed at the depth of 40 meters. The data obtained from the water level sensor gives an average position of the water table between the top of the borehole and the depth of 35 m, whereas below this depth the borehole is sealed. Same type of sensors are installed in two domestic wells, near the northern landslide boundary, approximately 600 meters north-northeast, and in the western part of landside, approximately 400 meters southwest from WLS 1. Sensors for measurement of hydrostatic pressures (Rugged TROLL 100, In-Situ Inc) are additionally installed in two domestic wells, near the west and northwest landslide boundary. In September 2013 at the central part of landside, near WLS, three pore pressure gauges (KPB-1MPA/KPB-500KPA, Tokyo Sokki Kenkyujo Co., Ltd) are installed in the borehole, at the depths of 37.5, 50.1 and 62.8 m meters.

The Kostanjek landslide GNSS monitoring network for continuous surface displacement measurement consists of 15 double-frequency NetR9 TI-2 GNSS reference stations with Zephyr Geodetic 2 GNSS antennas (Trimble). GNSS receivers are fixed to 4 meter high poles with 1 meter deep reinforced foundations. The 16th GNSS

reference station, is a stable GNSS located approximately 7 km south of the landslide. Receivers collect raw GNSS data and deliver it in real-time (using routers) to Trimble 4D Control software (T4DC) installed on an application/data server in a data centre at Faculty of Mining, Geology and Petroleum Engineering, University of Zagreb (Fig. 1).

The precision of GNSS measurements, calculated as the root mean square error on the 24-h post-processing position (at 2σ, 95% confidence), is 3.2-4.6 mm in planimetry and 6.1-10.5 mm in altimetry (Krkač et al. 2017). The total temporal data coverage of GNSS since its installation, for most receivers, is higher than 95%.

Monitoring results

Precipitation

The climate of the City of Zagreb is continental under a mild maritime influence (Gajić-Čapka and Zaninović 2008), characterized by warm summers and cold winters. The average annual precipitation measured at the Zagreb-Grič meteorological station is 887 mm for the period 1862–2012. The maximal daily precipitations and the highest monthly precipitations (Gajić-Čapka and Zaninović 2008) occur during the summer and autumn months. The average number of days per month with precipitation is highest (an average of 12 to 14 days) from April to June and lowest (9 to 12 days) in September and October (Gajić-Čapka and Zaninović 2008).

Monthly and cumulative yearly precipitations measured at the Zagreb-Grič meteorological station for the period 2013–2018 are displayed in Fig. 3. Meteorological conditions during the first two years of the monitoring period can be considered as very wet. In 2013, the total precipitation at Zagreb-Grič meteorological station was 1,092 mm, and in 2014, it was 1,234 mm. The total yearly precipitations during the period 2015-2018 were about annual average for the City of Zagreb or slightly below (823, 854, 888 and 827 mm). The highest daily precipitation (55.2 mm) was recorded in February 2013. The maximal monthly precipitation (208 mm) was recorded in September 2014. Significant amount of precipitations during the wet periods (September to April) caused significant changes of groundwater level (GWL) and consequently landslide movement.

Groundwater level depth

The data records from water level sensors in the central part of the landslide show GWL oscillations up to 8.5 m, between depth of 19 to 10.5 m, corresponding to variation of the pore pressures at the sliding surface, in the central part of landslide, from 425 to 510 kPa. Fig. 4 shows GWL depths and pore pressures monitored at the central part of the landslide during the period 2013-2018. GWL depths and pore pressures are calculated as 24-h average daily data. The pore pressure change pattern measured with the deepest sensor shows almost identical pattern as GWL change pattern measured with WLS 1. Altogether, 21 periods of groundwater level rise occurred, during which groundwater level relatively changed from 0.19 to 5.04 m. The maximal observed groundwater level rise rate was 0.87 m/day, whereas the maximal observed groundwater level recession rate was 0.16 m/day. The average groundwater level recession rate was 0.05 m/day.

The cumulative precipitations that caused GWL rise at the central part of landslide ranged from 21 mm to 180 mm, depending on initial GWL depth. At the deeper GWLs, for example at the summer months, higher amounts of precipitation are necessary to influence GWL rise, while at the lower GWL depths, during the autumn or winter months, lower amounts of precipitation are necessary to influence GWL rise. Example for that is 91 mm precipitation during six days in August 2013, at the initial GWL depth of 18.5 m, which did not cause a groundwater level to rise. In contrast, 21 mm of precipitation during seven days in November 2014 (approximately 25 days after intensive precipitation of 125.5 mm), at the initial GWL depth of 12.5 m, caused a groundwater level rise of 0.23 m (Krkač et al., 2017). This phenomenon is related to the soil moisture conditions and different hydraulic conductivity above the groundwater level during the wet and dry periods (Krkač, 2015).

Data measured with other water level sensors, which are located near the landslide boundaries, generally shows smaller GWL depths (7.5-3 m near the main scarp and 3.5-1 m at the right landslide flank). Additionally, GWL changes near the landslide boundary are much more prone to short term and light precipitations.

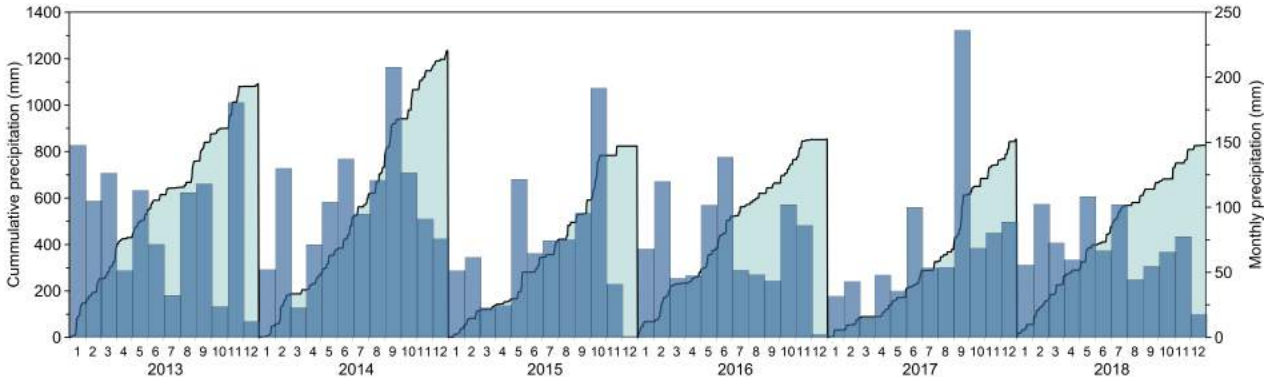

Figure 3 Cumulative and monthly precipitations measured at Zagreb-Grič meteorological station

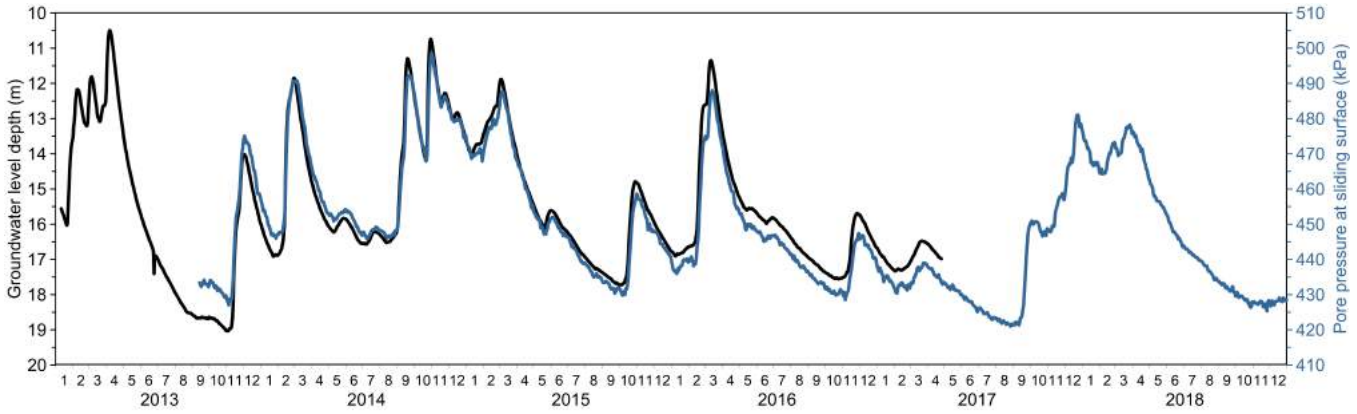

Figure 4 Groundwater level depth and pore pressure at the sliding surface measured at central part of Kostanjek landslide.

Movement

Analysis of monitoring data from all 15 permanent GNSS stations showed similar patterns of landslide movements across the entire landslide area, but with different velocities. The highest velocities were measured in the central part of the landslide, while the smallest near the landslide boundaries. The total horizontal displacements in the central part of the landslide, during the period 2012-2018, were between 550 and 750 mm, and the vertical displacements were between -120 and 400 mm. The total horizontal displacements measured near the landslide boundaries were between 70 and 500 mm, and the vertical displacements were between -200 and 70 mm. Fig. 5 presents the cumulative displacements measured at the central part of landside (GNSS 08).

From the GNSS measurements, totally seven period periods of faster movements and seven periods of slower movement can be distinguished. The patterns of faster movement are similar to patterns observed at the Utiku landslide (Massey 2014) and can be considered as reactivations in which movement occurs along a fully developed sliding surface in which the material is assumed to be at residual strength (Skempton 1985). The maximal observed velocity was 4.5 mm/day, which was reached in the first period of faster movement during the first week of April 2013. The longest period of faster movement lasted from the end of January 2013 to the end of May 2013, during which the total horizontal displacement was 168 mm. All seven periods of faster movement occurred as a consequence of groundwater level rising (Fig. 6).

Generally, greater movement velocities at the Kostanjek landslide occurred during the groundwater level rise periods that start at high initial groundwater levels (Krkač et al. 2017). Also, monitoring data display that landslide velocities at the certain GWL during the GWL rising are higher than at the same level during the GWL falling. Periods of slower movement can be described as periods of rest or suspended state of activity according to Cruden and Varnes (1996). During periods of slower movement, the landslide velocities were up to 6 mm/month.

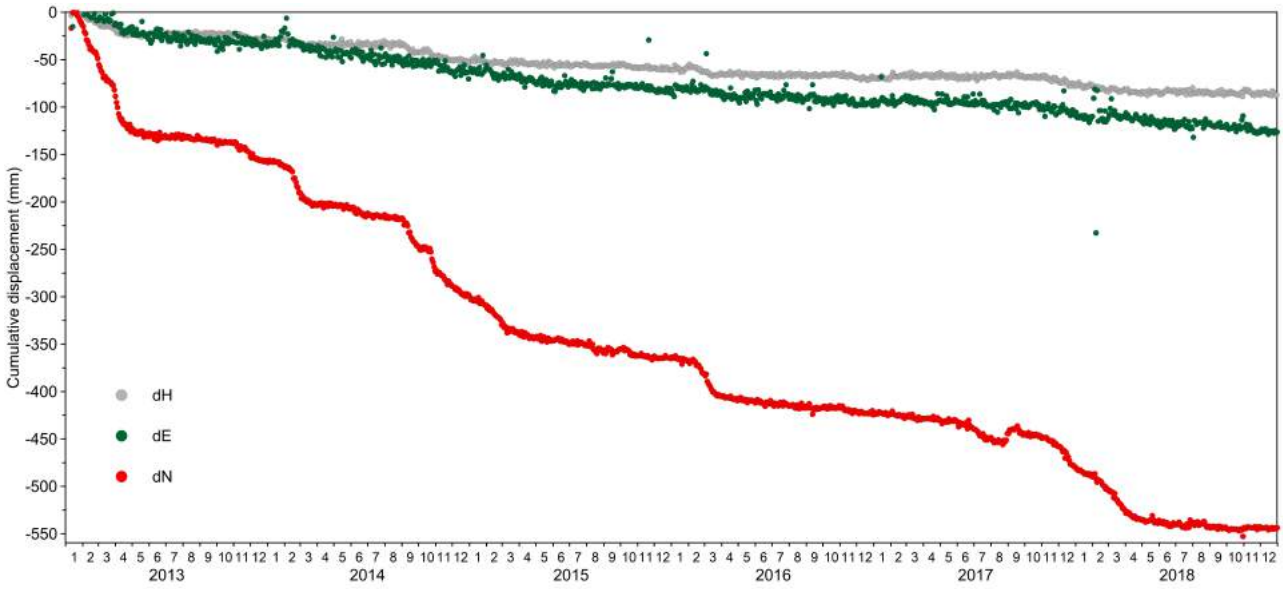

Figure 5 Cumulative displacements measured at the central part of landside (GNSS 08).

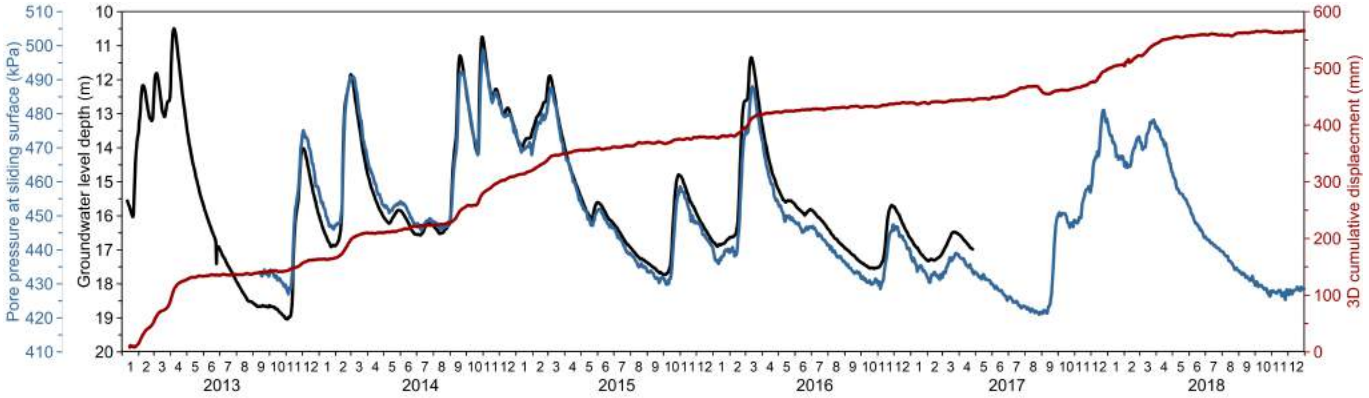

Figure 6 Cumulative 3D displacements (measured with GNSS 08), compared with groundwater level/pore pressure measured at the central part of landslide.

Conclusion

The Kostanjek landside monitoring system, with a multiple sensor networks for measurement of external triggers, hydrological properties and displacement, was set up in the period 2011–2014. During the period 2013-2018 the total cumulative displacement measured with GNSS sensor 08, at the central monitoring station, was 565 mm. From the movement pattern, totally seven periods of faster movements and seven periods of slower movement can be distinguished. The maximal observed velocity was 4.5 mm/day, which was reached in the first period of faster movement during the first week of April 2013.

Periods of faster displacement occurred as a consequence of GWL rising in the central part of landslide. The data records show GWL oscillations up to 8.5 m, between depth of 19 to 10.5 m. From the data comparison between GWL and movement, it can be concluded that the threshold value of the GWL depth, for initiation of faster landslide movement, is between 15 and 16 meters. From monitoring data, it is also visible that greater movement velocities at the Kostanjek landslide occur during the groundwater level rise periods that start at high initial groundwater levels. Additionally, lower values of landslide velocities were recorded for the same value of groundwater level during the groundwater level recession. All groundwater level rising periods occurred after periods of intensive precipitations and snowmelt.

The total yearly precipitations during the period 2013-2018 were above, and around average, for the City of Zagreb. The amount of precipitations that caused GWL to rise depends on the initial GWL. At the deeper GWLs higher amounts of precipitation are necessary to influence GWL rise, while at the lower GWL depths, lower amounts of precipitation are necessary to influence GWL rise, and consequently to initiate the landslide movement.

References

Blikra LH (2012) The Åknes rockslide, Norway. In: Landslides: Types, Mechanisms and Modeling. Clague JJ, Stead D (eds). Cambridge. 323–335.

Cruden DM, Varnes DJ (1996) Landslide types and processes. In: Landslide investigation and mitigation (Special Report / Transportation Research Board, National Research Council; 247). Turner AK, Schuster RL (eds). National Academy Press, Washington DC. 36–75.

Gajić-Čapka M, Zaninović K (2008) Climate of Croatia. In: Climate atlas of Croatia 1961-1990 and 1971-2000. Zaninović K (ed). Croatian Meteorological and Hydrological Service, Zagreb. 15-17.

Haque U, Blum P, Da Silva PF, Andersen P, Pilz J, Chalov SR, Malet J-P, Jemec Auflič M, Andres N, Poyiadji E, Lamas PC, Zhang W, Peshevski I, Pétursson HG, Kurt T, Dobrev N, García-Davalillo JC, Halkia M, Ferri S, Gaprindashvili G, Engström J, Keellings D (2016) Fatal landslides in Europe. Landslides. 13(6): 1545–1554.

Krkač M (2015) A phenomenological model of the Kostanjek landslide movement based on the landslide monitoring parameters. PhD Thesis, University of Zagreb (in Croatian).

Krkač M, Špoljarić D, Bernat S, Mihalić Arbanas S (2017) Method for prediction of landslide movements based on random forests. Landslides. 14(3): 947-960.

Massey CI, Petley DN, McSaveney MJ (2013) Patterns of movement in reactivated landslides. Engineering Geology. 159: 1-19.

Michoud C, Bazin S, Blikra LH, Derron M-H, Jaboyedoff M (2013) Experiences from site-specific landslide early warning systems. 13: 2659-2673.

Mihalić Arbanas S, Arbanas Ž, Krkač M (2013) Comprehensive Landslide Monitoring System: The Kostanjek Landslide Case Study, Croatia. In: ICL Landslide Teaching Tools. Sassa K, He B, McSaveney M, Osamu N (eds). International Consortium on Landslides, Kyoto. 158-168.

Ortolan Ž, Pleško J (1992) Repeated photogrammetric measurements at shaping geotechnical models of multi-layer landslides. Rudarsko-geološko-naftni zbornik. 4: 51-58.

Pecoraro G, Calvello M, Piciullo L (2019) Monitoring strategies for local landslide early warning systems. Landslides. 16(2): 213–231.

Petley DN (2012) Global patterns of loss of life from landslides. Geology. 40(10): 927–930.

Skempton AW (1985) Residual strength of clays in landslide, folded strata and the laboratory. Geotechnique. 35(1): 3-18.

Stanić B, Nonveiller E (1996) The Kostanjek landslide in Zagreb. Engineering Geology. 42: 269-283.

doi.org/ 10.35123/ReSyLAB_2019_8

The slope stability around an artificial lake Jablanica, with landslide sample project recovery in DonjePaprasko - Jablanica

Toni Nikolic[1-2], Azra Špago[1], Suad Špago[1], Merima Šahinagić-Isović[1], Naida Ademović[3]

1) The University of "Dzemal Bijedic" Mostar, Faculty of civil engineering, Sjeverni logor bb 88104 Mostar, +387 61 331 615

2) Federal geological survey, Sarajevo (BIH)

3) The University of Sarajevo, Faculty of Civil Engineering Sarajevo

Abstract The slope around an artificial lake becomes very sensitive to hydrology impact, and even more if geological properties are vulnerable to condition changes. Jablanica Lake is one of the biggest artificial lakes in Bosnia and Herzegovina and the coastal slope always has some impact on the water level oscillation in the lake. However, in other cases, the anthropogenic factor has more impact to trigger a landslide, like in the case of Donje Paprasko. This article elaborates on the history and solution of this specific case. After an intensive rain period landslide formation on the coast of the lake was evident and a part of the slope was cut inside the lake having a massive crash. The Civil Protection Agency of Jablanica monitored the slope instability for a few months and stated that there was no direct impact nor threat to lives or houses. Many factors may trigger landslides and all of them should be solved before a complete recovery of the slope could be done (collecting the water over the road, improper overstress of the slope by imposing additional soil, no drainage and other). This problem had to be solved urgently and the project had to be implemented as soon as possible because houses on the slope could be impacted if there was a continuation of the landslide movement.

Keywords landslide, anthropogenic factor, artificial lake, stabilization, slope stability

Introduction

Research activities regarding this problem took place and a plan for landslide recovery was made for the location of Donje Paprasko near a bridge located on the main road (M17 Mostar-Sarajevo) over Jablanica lake as indicated in Fig.1. Objects that were directly affected by this activity were located in Dobrigosce where a natural cliff is situated having coordinates:
x – 6 483111 y – 4 837 576 and z – 290.

Landslide is 15 m width and 25 m length with a depth 2-3 m depend from artificial material bring on slope. This is not tipical landslide because slide line was on contact between natural and artificial material supported by underground and surface water. Water come from the magistral road and that be obligation to evacuated from nacional road company FBIH, so that way water didn't be taken in account of sanation this slope.

Figure 1 Position of the landslide on the map (topographic map Jablanica 1:25.000)

The location of the structure is on the bedrock and behind it is a slope with an angle over 40°. A cut slope happened just five meters from the structure. As informed by the local inhabitants the movement of the slope was very fast and manifested in a loud crash that occurred in January 2018. At that time the entire artificial bank and all the threes ended inside of the lake.
The Civil Protection Agency of Jablanica followed the situation and gave instructions to the survey engineers to make a geodetic base for future activities for the recovery of the slope.

Geological data

The observed location is located inside the massive of the Lower Triassic (T_1^2) as indicated in Fig. 2.

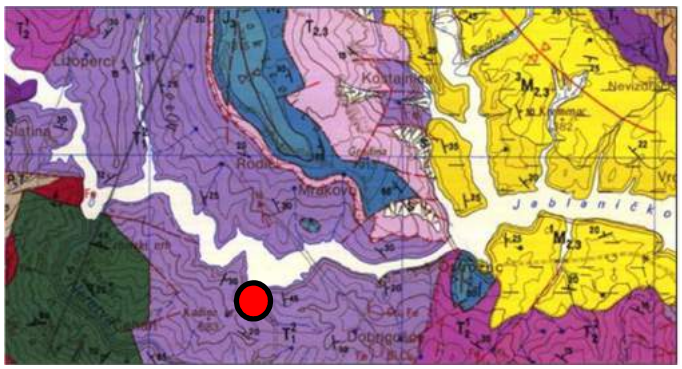

Figure 2 Position of the landslide on the map (basic geological map of Prozor 1:100.000)

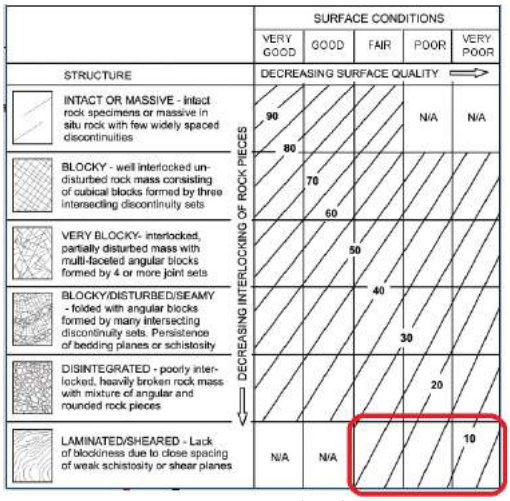

Figure 3 Gelogical Strength Index (GSI) value diagram

The basic material on this location is shale alevrites. Due to the layers and the position of cleavage a typical disintegration "brill" shape can be seen which is characteristic of atmospheric forces affecting this type of stone. Small layers of sandstone and limestone inside of the rock base of 1-2 cm thickness can be seen in the surrounding profiles. The material is very sensitive to porosity and has low geomechanical properties, however, if isolated from the atmospheric impact, it can be in a stable condition. In Fig 4. a fresh cut on the other side of the lake coast is shown. The GSI value obtained after the visual inspection of the stone on the field is shown in Fig.3. The condition of the surface layer is of very poor quality and becoming even poorer during rainfall and due to the sun impact, some disintegration of the material is evident as well (where limestone and sandstone layers are located) GSI = 5 – 30.


Figure 4 Basic rock on the lake of Jablanica coast (photo, Nikolic T. 2018.)

Field research - landslide triggers

It has been predicted that water is the main cause that triggered this landslide. No waste system was identified on the structures, meaning that all waste and surface water had gone in the lake (probably just behind the structure which was observed).


Figure 5 The current situation on the field (Nikolic T. 2018)

After the activation of the slope, the same water was directed by a pipeline to the bottom of the slope (Fig. 5).

The water going over the slope was the main problem that had to be solved. Fig.5 shows the pipe indicated by red arrows from which the water came into the slope.


Figure 6 Fracture of the concrete wall below the house (Nikolic T. 2018)

Fig 6. shows a fracture of a concrete wall below the house. Fortunately, the house remained intact with no evident damages due to the landside formation at the moment of the visual inspection of the structure. The reason for this may be seen in the fact that the structure was constructed on the bedrock (even though the landslide is just a few meters away from the house basement). The slope below the structure became so sensitive, indicating that as soon as possible, some actions should be done in order to prevent the impact of the landslide on the stability of the structure.

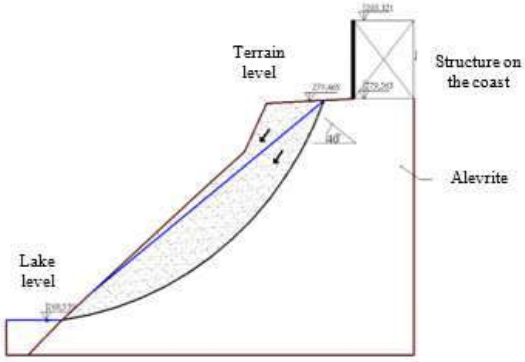

Figure 7 Landslide profile on the site

Fig.7 shows the landslide profile on the site indicating the landslide formation and the water level of the lake in the moment of conducted research. The sliding line is located on the contact of the bedrock and the artificial material, making additional pressure on the slope. The underground water level is presented by a blue line.

Over the main road M17, from the information obtained from the local inhabitants, a water spring collector is located, and the remaining water goes below the road into the slope, which is just below the observed structure. Just after the slope collapse, this system was closed. It was not possible to conclude nor to obtain any information where did this water go. According to the Federal Law on Roads drainage of water from and around the roads are under their jurisdiction. A small gulf on the coast of the lake was formed from a small stream, which becomes torrent during the raining periods (debris flow). There is no protection system from the water impact, erosion, abrasion or capillary water on the slope below the structure. It can be stated that the lake had partially triggered the activation of the landslide, especially taking into account that the fluctuations of the water levels in the lake are very frequent. During the period of the low water levels, small pieces of soil were ripped off by the water of the saturated slope, disintegrating the structure and thus leading to friction reduction. As the friction parameter is being decreased, this changes the conditions of the soil stability and as a result, a collapse of the terrain occurs.

Proposal for a temporary stabilization activity

At this moment it can be noted that the stability of the slope after the"crash" became conditionally stable. The impact of rain, waste and surface water is very important for the stability of this slope and the water should be drained in a way not to have any impact on the slope below. It is very important to remove the water from and around the structure to the recipient (lake), with special attention on the impact of the lake on the slope due to frequent variation of water levels in the lake and capillary impact of the water on the slope. Only after the water has been drained in an appropriate manner from the slope and detail conditions have been defined, permanent recovery can take place.

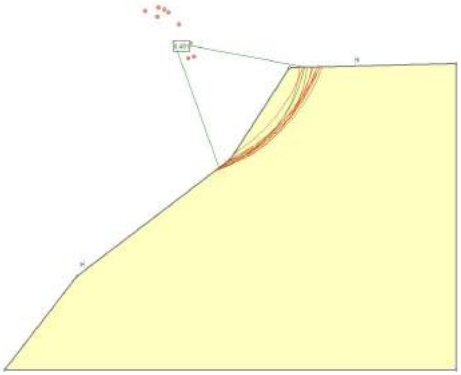

Figure 8 Local sliding simulation – Fs=0,491 (estimate with low parameter of rock: GSI = 5, m_i =2; σ_{ci} = 5 MPa, γ = 25 kN/m^3, after aggressive impact of the local condition)

The data collected on the site was used as input data for the local analysis of the slope stability. As stated before, due to the aggressive impact this type of rock lost its initial mechanical properties. Fig.8 shows a profile of the slope after local strength loss.

The first step was to isolate the slope from the atmospheric impact and make a reinforced concrete (RC) wall with a rock cover behind it (Fig. 9).

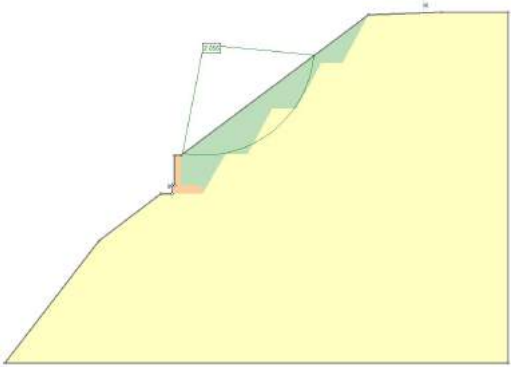

Figure 9 Slope stability check with RC wall and rock cover behind the wall (Fs =2.056)

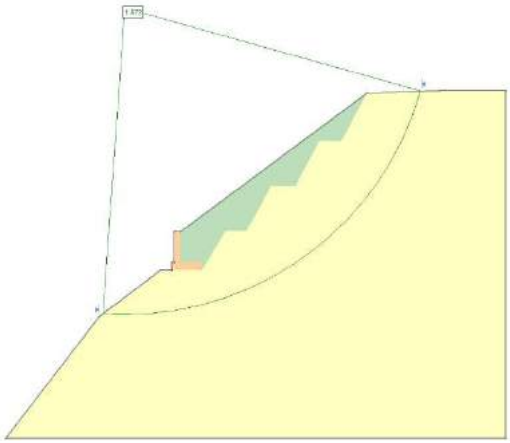

Figure 10 Slope stability check with RC wall and rock material behind the wall (Fs =1,872)

The optimal result was obtained after testing a wide and deep area with Fs=1.872.

Shear strength parameters are given in Fig. 11 used to recheck the stability of the wall by utilizing the RockLab software.

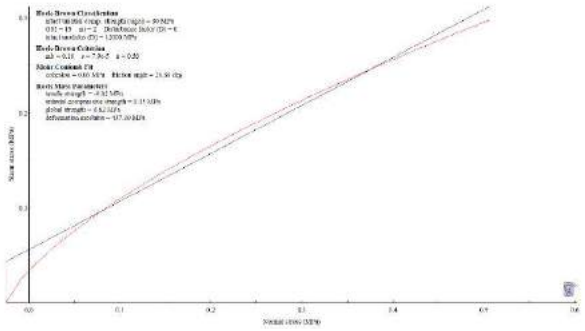

Figure 11 Data from RockLab software

After constructing the RC wall and global stability check, the stability of the wall was rechecked using a GEO5 software, respecting the provisions given in Eurocode 7. The results are presented in tables 1, 2 and 3.

Table 1 Check for overturning stability

Approach/ Design load		M_{ove} [kNm/m]	M_{res} [kNm/m]	Utilization
Approach 1	combination1	18.26	66.07	0.28
	combination 2	24.49	69.32	0.35
Approach 2		18.26	47.19	0.39
Approach 3		24.49	69.32	0.35

Table 2 Check for slip

Approach/ Design load		H_{slip}[kN/m]	H_{res}[kN/m]	Utilization
Approach 1	Combination 1	24.42	47.60	0.51
	Combination 2	33.78	39.36	0,86
Approach 2		24.42	43.27	0.56
Approach 3		33.78	39.36	0.86

Table 3 Bearing capacity of foundation soil

Approach		The maximum stress of the footing bottom [kPa]	Bearing capacity of foundation soil [kPa]
Approach 1	Combination 1	68.21	214.29
	Combination 2	64.01	
Approach 2		68.21	
Approach 3		71.04	

Conclusion

The most active problem for the stability of this slope is underground and surface water. The slope becomes unstable in a "temporary" condition. Surface water, wastewater, and other waters have a very negative impact on the slope. Before any stability measures are undertaken it is necessary to conduct a systematic draining of the slope. Wastewater should be systematically removed away from the structures. Construction of a reinforced concrete wall with rock material behind is seen as a first recommendation. In order to make a final solution of this problem a detail geological research, geodetic measurements and precise determination of the geological parameters should be done.

During the slope rehabilitation, a geotechnical engineer should be present in the field with the aim to monitor the slope situation during the cutting of the slope and if the situation requires to adapt the parameters, depending on the quality of the cut material on the site.

Acknowledgments

Authors would like to thank the municipality of Jablanica and the Faculty of Civil Engineering of the University of "Dzemal Bijedic" Mostarfor supporting this research within the project of recovery landslide in Donje Paprasko.

References

Nikolic T., Spago A., Sahinagic-Isovic M., Hajdarevic A., Cecez M., Helebic A., Spago S. (2018) Project of recovery landslide in Donje Paprasko. University "Dzemal Bijedić", Civil engineering faculty with the institute for project and testing building materials, October 2018. Mostar (BIH), 120-2-2-14/18.

Neziric O., Properties and photos from landslide DonjePaparasko in different periods of a move, (2017-2018), Civil protect agency of Jablanica Municipality.

www.finesoftware.eu/newsletter/

doi.org/ 10.35123/ReSyLAB_2019_9

Finite element modelling of a creeping landslide induced by snowmelt groundwater

Akihiko Wakai [(1)], Deepak Raj Bhat [(2)], Kenta Kotani [(3)], Soichiro Osawa[(4)]

1) Professor, Dr., Department of Environmental Engineering Science, Gunma University, Japan, wakai@gunma-u.ac.jp

2) Dr., Okuyama Boring Co., Ltd., Japan, deepakbhat@okuyama.co.jp

3) Gunma University, Japan, t181c017@gunma-u.ac.jp

4) Gunma University, Japan, t160c015@gunma-u.ac.jp

Abstract In this study, a finite element based numerical method is considered to evaluate the creeping behaviour of a creeping landslide induced by snowmelt groundwater. A novel 2D-Elasto-viscoplastic constitutive model is used to simulate the creeping behaviour owing to groundwater level fluctuations of the Tomuro landslide of Gunma, Japan as a Case study. Two new control constitutive parameters are incorporated in the numerical model for the first time to better understand the creeping behaviour of a landslide. Such control constitutive parameters are estimated based on the relation between the total factor of safety, calculated by the various Limit Equilibrium Methods and Finite Element Method, and the field monitoring displacement rate of the Tomuro landslide. In addition, the snowfall precipitation is also considered during the calculation of total factor of safety using both limit equilibrium methods and finite element method. Others required material parameters for landslide simulation are obtained from the field investigation and laboratory tests of the collected blocked samples. The simulation results of deformation pattern and shear strain pattern are also discussed to understand the creeping behaviour of the Tomuro landslide. Moreover, the predicted and measured time histories of horizontal displacement of the Tomuro landslide are compared for the validity of the proposed numerical model, and found in good agreements with each other.

Keywords Landslide, Finite element method, Elasto-viscoplasticity, Groundwater fluctuation, Creep, Snowmelt groundwater

Introduction

In these days, creeping landslides are becoming one of the major natural disasters in mountainous regions. Such landslide sites accommodate human settlement and development activities (Bhat et al. 2016, 2017). When the displacement rate of such landslides is suddenly increased and accelerated, it leads a huge mass failure which damages human life, property, nature, and environment. If a numerical approach to predict the creeping behaviour of a landslide is possible, each damage can be prevented (Bhat et al. 2016, 2017, 2018). Therefore, study of creep displacement behaviour of a landslide and associated geotechnical hazards issues seems very important. Terzaghi (1950) was most likely the first to consider the relationship between soil creep and landslides. Ter-Stepanian (1963) has introduced the threshold approach to explain soil creep in simple natural slopes by considering the zone of creep and its rate as being dependent on the groundwater level. Bhat et al. (2016, 2014) have proposed a new regression model to understand the creeping behaviour of clay soils materials at the residual-state of shear.

Groundwater level fluctuations of a landslide body may play the major role for controlling the creep displacement behaviour of a landslide (Conte et al. 2014, Picarelli et al. 2004, Ter-Stepanian (1963) therefore, groundwater level fluctuations should be incorporated during the numerical simulation and analysis of such landslides. However, most of previous numerical approach (Picarelli et al. 2004, Ter-Stepanian 1963, Yin et al. 2010) of soil creep and associated problems are focused on the laboratory creep tests (i.e., consolidation/oedometer test and triaxial test), which could not address the fluctuation of groundwater level. Based on the theoretical, experimental, and numerical models, a few researches (Bhat et al. 20114, 2016, 2018, Huvaj and Maghsoudloo 2013, Yin et al. 2010, Picarelli et al. 2004, Ter-Stepanian 1963) have tried to address these issues till 1950 to until now, but they are not fully understood, especially in relation to the displacement behaviour of a creeping landslide. Huvaj and Maghsoudloo 2013 have simulated the fluctuation of groundwater level in different phases to understand of displacement behaviour of a slow-moving landslide, but the exact value of the deformation at any required point (location) couldn't be captured perfectly. Recently, a few researchers (Savage and Chleborad [18], Ishii et al. 2012, Conte et al. 2014) have proposed a 2D-Elasto-viscoplastic constitutive model using finite element method based on the field instrumentation and monitoring results, but they are only considered the single control constitutive parameter based on the trial and error method, which could not control the displacement rate of the landslide, and also far to address the realistic field problem of the creeping behaviour of a landslide. Therefore, the main

objective of this study is to propose a novel FEM-based numerical model to address the above-mentioned problems, and to apply this model to understand the creeping behaviour of Tomuro landslide induced by snow melt water as a Case study.

Study area

Fig. 1 shows the Location of study area (Tomuro landslide) and simplified topographical map of Tomuro landslide, showing the location of sampling point, Piezometers and Extensometer. The size of Tomuro landslide has been measured approximately 135 m by 110 m. Fig. 2 shows the variation of the rainfall and snowfall precipitation. The snow has accumulated at a thickness of 2 to 73 cm on the surface of the landslide body during the period of 2014/2/8 to 2014/2/25. The maximum snowfall was recorded up to 73 cm on 2014/2/15 (Fig. 2). After the 2014/2/25, the deposited snow was starting to melt, and the groundwater level was also starting to rise. The Piezometers were installed at the location of BV-1 and VB-2 for monitoring the groundwater level of the landslide body. The results of the groundwater level fluctuations at the boreholes (BV-1, BV-2) are presented in Fig. 3.

The horizontal displacement of the landslide mass was measured using the extensometer at S-1. The variation of the displacement rate during the period of 2014/1/14 to 2015/7/6 is considered in this study. The maximum displacement rate of 9.9 mm/day was recorded on 2014/3/4, where the groundwater level was also recorded maximum at the VB-1 and VB-2. From the comparative study of groundwater level and displacement rate with various time periods, it is understood that the displacement rate depends upon the fluctuation of the groundwater level. When the groundwater level has raised, the displacement rate has been also increased and vice versa. The creep displacement of the landslide as directly related to the groundwater condition. Therefore, the fluctuation of groundwater should be considered to better understand the creeping behaviour of a landslide (Bhat et al. 2017). In this study, the groundwater fluctuation is considered for the stability analysis using the various Limit Equilibrium Methods and Finite Element Method, as well as the numerical simulation of the Tomuro landslide.

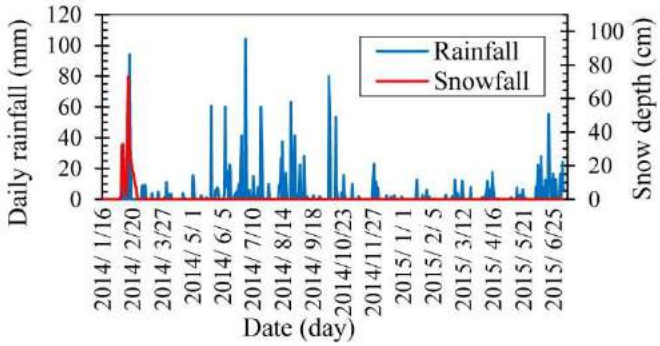

Figure 2 Variation of the rainfall and snowfall precipitation

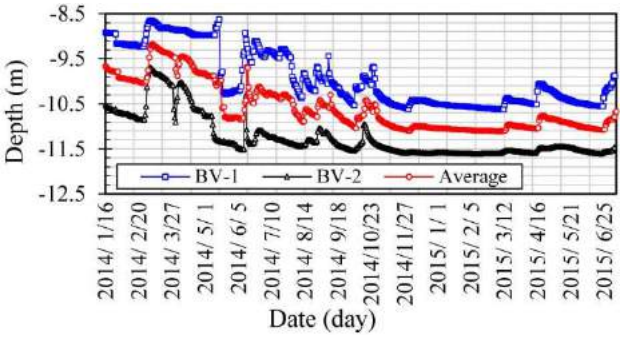

Figure 3 Groundwater level fluctuation in the boreholes

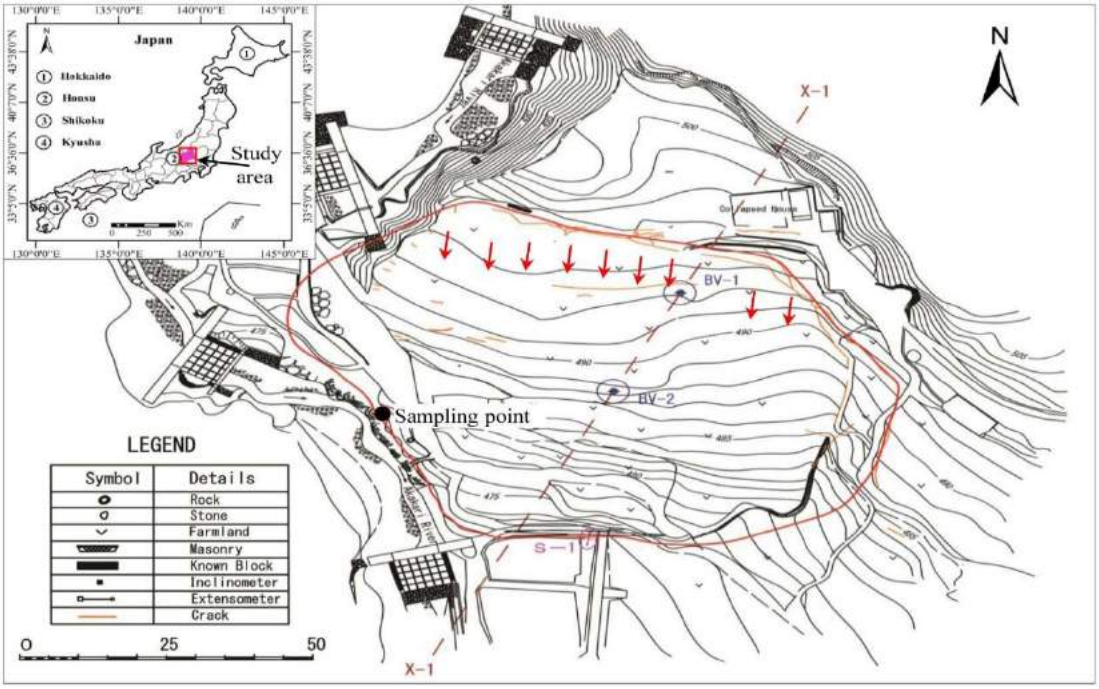

Figure 1 Location of study area (Tomuro landslide) and simplified topographical map of Tomuro landslide, showing the location of Sampling point, Piezometers and Extensometer

Proposed FEM model

In this study, we assumed that all the plastic strain components occurring at the time of yielding are viscoplastic components. Suppose, the Eq. 1 represents the flow law based on plastic potential.

$$\dot{\varepsilon}^{p} = \dot{\Lambda}\frac{\partial g}{\partial \sigma} \quad (1)$$

Where $\dot{\varepsilon}^{p}$ is a plastic strain increment per unit time,

$\dot{\Lambda}$ is a plastic multiplier, varies according to the effective stress, and g is plastic potential

Both the failure criterion (f) and the plastic potential (g) are assumed to be defined by the Mohr-Coulomb type equations as follows:

$$f = (\sigma_1 - \sigma_3) - (\sigma_1 + \sigma_3)\sin\emptyset - 2c\cos\emptyset \quad (2)$$

$$g = (\sigma_1 - \sigma_3) - (\sigma_1 + \sigma_3)\sin\psi \quad (3)$$

Where, σ_1 is maximum principal stress, σ_3 is minimum principal stress, $\emptyset$ is internal friction angle, c is cohesion, and ψ is dilatancy angle

Based on the literature survey, Vulleit and Hutter (1998) has reported that the displacement rate is inversely proportional to the total factor of safety for a landslide. Bhat et al. (2017, 2018) have also agreed with the theoretical concept of Vulleit and Hutter (1998). Following the theoretical concept of Vulleit and Hutter (1998), we have proposed a relationship between the displacement rate and local factor of safety as shown in Eq. 4.

$$\dot{\gamma}_{max} \leq \frac{\dot{\alpha}}{F_{s,local}{}^{n}} \quad (4)$$

Where, $\dot{\gamma}_{max}$ is displacement rate, $F_{s,local}$ is local factor of safety, and $\dot{\alpha}, n$ are new control constitutive parameters, which can directly control the displacement rate and local factor of safety of the sliding block/mass.

Here, the $F_{s,local}$ at each element is defined by the following Eq. 5.

$$F_{s,local} = \frac{\frac{1}{2}(\sigma_x+\sigma_y)\sin\emptyset + c.\cos\emptyset}{\sqrt{(\frac{\sigma_x+\sigma_y}{2})^2+\tau_{xy}{}^2}} \quad (5)$$

Where, σ_x , σ_y are the normal stress components, and τ_{xy} is shear stress component

It is important that each stress component includes the contribution of the viscous resistance mobilized at each element (Eq. 5). If the rigid-perfectly plastic modeling is applied to the materials, the values of the $F_{s,local}$ at all elements become consistent with the value of the total factor of safety (F_s). Here, F_s is evaluated using the slope stability analysis by the finite element method. During the calculation of F_s, the whole landslide body for each slope is assumed a single block/unit. However, during the calculation of $F_{s,local}$, the landslide block is divided into many different elements and the factor of safety for each element is evaluated separately.

Finite element modelling

For checking applicability and validation of the numerical model, the newly proposed model is applied to analysis the creeping behaviour of Tomuro landslide of Gunma, Japan. Fig. 4 shows the 2D-finite element mesh used for the analysis, which is prepared based on the geological cross-section of the slope of such landslide site. The base of the model is assumed to be fully impervious and fixed, and the lateral side (left and right) is constrained by hinged. The hydraulic head is imposed at the lateral boundaries based on the field monitoring results of groundwater fluctuation. S-1 represents the location of point (i.e., node 199), where the maximum displacement of the landslide body was measured in the field during the period of 2014/1/14 to 2015/7/6 (Fig. 4).

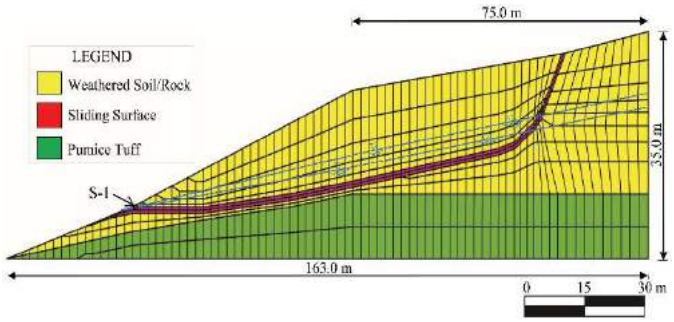

Figure 4 Finite element model of Tomuro landslide

The two new unknown control constitutive parameters ($\dot{\alpha}, n$) are estimated based on the relation between the total factor of safety and displacement rate based on the Eq. 4. Initially, the total factor of safety (Fs) is calculated using the various Limit Equilibrium Methods (LEM) based on the slices and Finite Element Method (FEM). In LEM Methods, three frequently used methods are used to calculate Fs of Tomuro Landslide of Gunma, Japan. At first, the ordinary method of Slices (Swedish Method of Slices or Fellenius 1936) is used, which is referred as Case I. Bishop's method (1955) has used to address the limitation of the ordinary method of slices, which is referred as Case II. Again, Janbu's Simplified method (1973) is also used to incorporate the drawback of the Bishop's method (1955), which is referred as Case III. Finally, the FEM Method is also used to address the drawback of the LEM, which is named as Case IV. In FEM method, Shear Strength Reduction Method (SSRM) is used to estimate the Fs of Tomuro Landslide of Gunma, Japan.

The snowfall precipitation (Fig. 2) is also considered during the calculation Fs of the landslide body. After the calculation of Fs, the relations between $\dot{\gamma}_{max}$ and Fs have been established for the Cases I to IV. After that, the general equations are obtained based on the well fitted curve between $\dot{\gamma}_{max}$ and Fs. Then, the unknown two new control constitutive parameters ($\dot{\alpha}, n$) were estimated by solving of these general equations for each Case. The other required materials parameters for the landslide simulation (Table 1) are estimated based on field and laboratory test results. The drained residual friction angle ($\emptyset_r$) of sliding surface soils is estimated by using the empirical equations developed by Stark and Hussain (2013). The summary of the material parameters for landslide simulation are summarized in Table 1.

Table 1 Material parameters for landslide simulation

Materials/ Parameters	Weathered Soil/Rock	Sliding Surface				Purnice Tuff
		Case I	Case II	Case III	Case IV	
Young's modulus, E (kN/m^2)	5000	1000				50000
Poisson's ratio, ν	0.40	0.30				0.45
Cohesion, c' (kN/m^2)	50	0				5000
Internal friction angle, φ' (deg.)	35	15.2				30
Dilatancy angle, ψ (deg.)	0	0				0
$\dot{\alpha}$ (day^-1)	-	0.00089	0.000489	0.00023	0.0011	-
n	-	53.398	46.4900	55.833	67.233	-
Unit weight, γ (kN/m^3)	24					26

Model results and discussion

Fig. 5 shows the results of deformation pattern at the end (i.e., 2015/7/6) for the Case I as a representative result. The red dot line shows the result of a maximum deformation pattern of each node at the end of the numerical simulation with compare to without the deformation (i.e., initial condition). The maximum deformation of 0.26921 m was recorded at node 199 (i.e., S-1). Similarly, the result of deformation pattern at the end is also analysed for the Cases I to IV. The maximum deformation of 0.26735 m, 0.26683 m, and 0.26921 m were obtained at the same node 199 in the Cases II, III and IV respectively. From the comparative analysis of the results of deformation pattern in the Cases I to IV, it was found that the value of the deformation at node 199 is almost the same. Moreover, the maximum deformation was occurring at the same node 199, where the maximum displacement of the landslide body was recorded during field monitoring.

Similarly, Fig. 6 show the results of the shear strain pattern at the end (i.e., 2015/7/6) for the Case I as a representative result. The maximum shear strain of 0.92647 was obtained at element 278 at the end of the numerical simulation in the Case I. Similarly, the results of the shear strain pattern at the end are also studied for the Cases I, II and IV. The maximum shear strain of 0.91059, 0.90419, and 0.93865 were found at the same element 278 in the Cases I, II and IV respectively. Based on the comparative study of the results of shear strain pattern in the Cases I to IV, it was found that the maximum shear strain has exhibited along the sliding surface of the Tomuro landslide. Moreover, the results of overall shear strain trends of each Case were found almost same. The maximum shear strain value is also almost same and occurred at the same element 278, where the maximum displacement rate of the landslide body was recorded during the field monitoring

Fig. 7 shows the comparison of predicted time histories of displacement in model and measured displacement in the field. Here, the predicted time histories of displacement were measured at the same point S-1 (i.e., node 199), where the displacement was measured in the field. Moreover, the horizontal component of the measured time histories of horizontal displacement at S-1 has slightly increased from

Figure 5 Results of deformation pattern

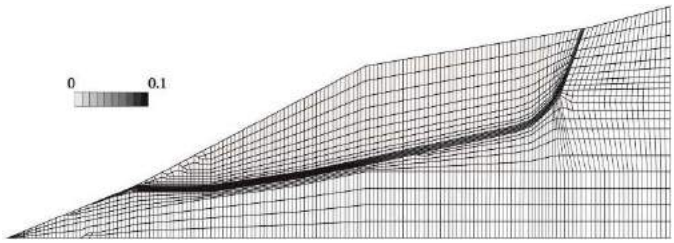

Figure 6 Results of shear strain pattern

2014/1/14 to 2014/2/14. After that, it was rapidly increased until 2014/4/29. Then, it has almost constant from 2014/4/29 to 2015/7/6. Similarly, the predicted time histories of horizontal displacement at S-1 has slightly increased from 2014/1/14 to 2014/2/17. After that, it has also rapidly increased from 2014/2/18 to 2014/5/14. Then, it has also almost constant until 2015/7/6. The maximum horizontal displacement of 0.2717 m was recorded at the end of the field monitoring. Similarly, the maximum displacement of 0.2617 m, 0.2673 m, 0.2668 m, and 0.2692 m was obtained by the numerical method in the Cases I to IV respectively. In numerical method, the results of maximum horizontal displacement at the S-1 is almost same and they are also following the similar trends as shown in Fig. 7.

Concluding remarks

A newly proposed 2D-Elasto-viscoplastic constitutive model has been used to simulate and analyse the creeping

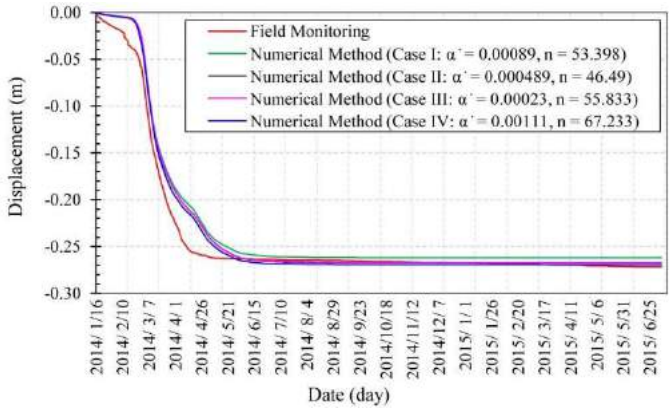

Figure 7 Comparison of predicted and measured time histories of horizontal displacement at S-1

behaviour of clayey soil along the sliding surface of a creeping landslide induced by the snowmelt groundwater. A simplified procedure has been developed for the determination of two new control constitutive parameters for numerical simulation. Such new control constitutive parameters were estimated based on the relation between the total factor of safety, calculated by the various Limit Equilibrium Methods such as Ordinary Method of Slice (Fellenius 1936) (Case I), Bishop's Method (1955) (Case II), Janbu's Simplified Method (1973) (Case III), and Finite Element Method (Shear Strength Reduction Method) (Case IV), and the field monitoring displacement rate of the Tomuro landslide. The snowfall precipitation has been also considered during the calculation of total factor of safety by the various Limit Equilibrium Methods. The simulation results of deformation pattern and shear strain pattern have been presented and discussed to understand the creeping behaviour of clay soils along the sliding surface of Tomuro landslide considering the groundwater level fluctuations by snowmelt groundwater. Finally, the results of predictedtime histories (numerical model), and measured time histories (field measurement) of horizontal displacement at S-1 has been compared, and foundin good match with each other. Therefore, it is believed that this model can be used as a standard numerical tool to understand the creeping behaviour of a landslide induced by snowmelt water in the future.

Acknowledgements

This work was supported by JSPS KAKENHI Grant Number 16F16354. The authors would also like to acknowledge Mr. Yoshihiko EGUCHI and Mr. Haruo SEKI, Nihon Survey Co., Ltd., and Yuuichi UENO, Nittoc Construction Co., Ltd. for providing the field investigation data and supporting during the field visit. The authors are grateful to Nakanojo Public Works Office and Sediment Control Division of Gunma Prefectural Government for their support.

References

Bhat DR, Wakai A, Kotani K: A comparative study of two newly developed numerical models to understand the creeping behaviour of landslides Proc of the 20th International Summer Symposium, Japan, 2018, pp 101-102.

Bhat DR, Wakai A, Kotani K: A finite element approach to understand the creeping behaviour of large-scale landslides Proc of the 19th International Summer Symposium, Japan, 2017, pp 9-10.

Bhat DR, Yatabe R: A Regression Model for Residual State Creep Failure, Proc of the 18th International Conference on Soil Mechanics and Geotechnical Engineering, USA, 2016, pp 707-711.

Bhat DR, Bhandary NP, Yatabe R: Creeping Displacement Behaviour of Clayey Soil in A New Creep Test Apparatus, Geotechnical Special Publication, ASCE, 2014, Vol 236, pp 275-285.

Conte E, Donato A, Troncone A: A finite element approach for the analysis of active slow-moving landslides, Landslides, Vol 11, No 4, 2014, pp 723-731.

Huvaj N, Maghsoudloo A: Finite Element Modeling of Displacement Behaviour of a Slow-Moving Landslide, Geo-Congress 2013, USA, 2013, pp 670-679.

Ishii Y, Ota K, Kuraoka S, Tsunaki R: Evaluation of slope stability by finite element method using observed displacement of landslide, Landslides, 2012, Vol 9, No 3, pp 335-348.

Picarelli L, Urciuoli G, Russo C: Effect of groundwater regime on the behaviour of clayey slopes, Can Geotech J, 2004, Vol 41, No 3, pp 467-484.

Stark TD, Hussain M: Drained Shear Strength Correlations for Slope Stability Analyses, J of Geotech Eng, 2013, Vol 139, No6, pp 853-862.

Ter-Stepanian G: On the long term stability of slopes, Nor Geotech Inst, 1963, Vol 52, pp 1-14.

Terzaghi K: Mechanism of landslide In application of Geology to Engineering Practice, Berkey Volume, Geological Society of America, USA, 1950, pp 83-123.

Vulleit L, Hutter K: Viscous-type sliding laws for landslides, Can Geotech J, 1988, Vol 25, No 3, pp 467-477.

Yin ZY, Chang CS, Karstunen M, Hicher PY: An anisotropic elastic-viscoplastic model for soft clays, Int J of Sol and Struc, 2010, Vol 47, pp 665-677.

doi.org/ 10.35123/ReSyLAB_2019_10

Development of landslide control measures in Japan

Hideaki Marui[(1)]

1) Em. Prof. Dr. agr., Dr. nat. techn. Hideaki Marui, Niigata University, Research Institute for Natural Hazards and Disaster Recovery,Ikarashi-Ninocho 8050, Nishi-ku, Niigata, 950-2181 JAPAN, 08marui@gmail.com

Abstract This paper aims to highlight the essential items of the development of landslide control measures in Japan. Landslides have a major socio-economic impact in Japan, as they are responsible for substantial direct and indirect social costs as well as for loss of human lives. Protection of human lives and their living environment is an important aspect of public welfare policies in Japan. The Japanese Archipelago is a part of the Circum Pacific Orogenic Zone and is geologically very fragile and unstable.The bedrock materials which comprise the mountainous and hilly terrain have been severely fractured since its formation and have developed numerous faults and fractured zones. Furthermore, the Japanese Archipelago is located within the monsoon zone and receives abundant precipitation. Landslide areas and landslide remnants are widely distributed in most of mountainous and hilly regions in Japan. Control of landslideshas a significant meaning for rural and urban populations in Japan which is strongly threatened by landslide risks. It requires an appropriate scientific understanding of landslide phenomena and risks caused by them. A lot of experts with various interdisciplinary backgrounds are fully committed to this task and have been promoting research activities in the field of landslide control more than a half century. First, actual state of landslide occurrences is reported. Then, major landslide control measures, both soft measures and hard measures, including „Hazard zoning“, „Monitoring“, „Early warning“ and „Technical counter measures“ are described.

Keywords Landslide control measures, Soft measures, Hard measures, Hazard zoning, Monitoring, Early warning, Technical counter measures.

Introduction

In Japan, the „Landslide Prevention Law“ was enacted 61 years ago, namely in 1958. This law supplies a specific legal basis for whole public works for landslide prevention and mitigation. Several years after in 1963, the Japan Landslide Society was established and has made continuous efforts to promote comprehensive scientific research on mechanism of landslides and to develop appropriate technology for mitigation of landslide disasters. Nowadays various techniques are available for comprehensive mitigation of landslide disasters, including investigation and analysis methods, planning and design of stabilization measures, as well as maintenance and administration of installed structures. The importance of so-called "soft measures" to avoid human casualities such as landslide hazard zoning and arrangement of warning and evacuation system is continuously increasing as supplements to the conventional landslide mitigation measures by so-called "hard measures" to stabilize active landslides. In the following chapters, at first background conditions, and then, actual state of landslide occurrence, investigation methods, hard and soft mitigation measures will be illustrated in due consideration of various investigation and research results over the past decades in Japan.

Geology and Geomorphology of Japanese Archipelago

The Japanese Archipelago is comprised of five main islands arcs extending approximately 3000 km in the northeast to southwest direction (Fig. 1) and encompasses a total area of about 378,000 km2. Seventy-five percent of the total area consists of mountainous and hilly terrain.

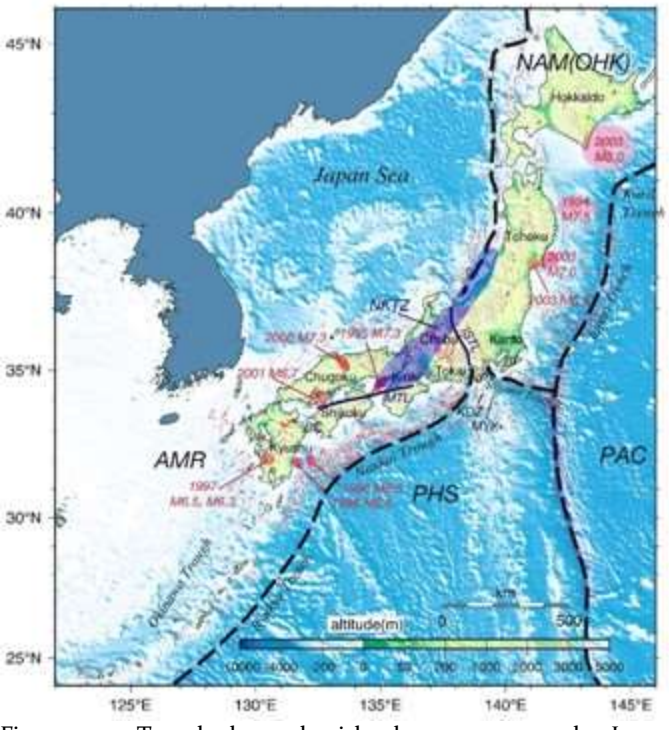

Figure 1 Trenched and island arcs around Japan (Modified after Japan Landslide Society, 1996)

The five main islands arcs are, from northeast to southwest, Kurile Arc, Northeast Honshu Arc, Izu-Mariana Arc, Southwest Honshu Arc and RyuKyu Arc. These approximately represent plate boundaries among

the North American Plate, Pacific Plate, Euracian Plate and Philippine Sea Plate. Because of interrelationship between arcs and plates, Japan is located in the area under strong crustal movements and belongs to one of the seismically most active regions. There are 86 active volacnoes in Japan. It means approximately 10% of the whole active volcanoes in the world. Furthermore, epicenters of deep-seated earthquakes around Japan are distributed along Kurile-Kamchtka Trench, Japan Trench, Izu-Ogasawara Trench, Nankai Trough and Ryukyu Trench. Landslides occur frequently in the following physiographic zones. The Inner Northeast Honshu Arc is representative landslide zone. The Northwest Kyushu Island in the Southwest Honshu Arc is a zone of high-density landslide distribution. The Outer Southwest Honshu (Shikoku Mountain) and the Central Western Honshu (Chubu Mountain) are zones represented by landslides of very slow movement and by very large-scale slope failures of rapid movement.

Figure 2 Monthly mean precipitation (after Japan Landslide Society, 1996)

Climate of Japan

The Japanese Archipelago is situated in the monsoon region of eastern Asia between North Latitude of 20°and 45°. Its southeastern side is faced to the Pacific Ocean and its northwestern side is faced to the Sea of Japan and Eurasian Continent. Its winter climate is dominated by wind and air from eastern Siberia. During the winter monsoon, the cold seasonal winds generated from the continental cold air masses move through the Sea of Japan and absorb large quantities of moisture. When the moist seasonal winds reach to Japan, the cold air masses collide into mountain ridges. As the air masses rise with increasing elevation, a large quantity of moisture is precipitated as snow. In spring, due to the low-pressure zones moving west to northeast, the cold-warm cycles are repeating and gradual warming occurs. Numerous landslides have been tiggered by the large quantity of snowmelt along the slopes facing the Sea of Japan. In June and July, Japan has a rainy season. In this period, a high-pressure mass of warm air above the Pacific Ocean moves from the south, and another high-pressure mass of cold air above the Sea of Okhotsk moves from the north. Both air masses collide with each other above the Japanese Archipelago, forming a stationary seasonal rainy front. Usually, this stationary rainy frontlasts acouple of months and intermittently brings a large quntity of rainfalls. These rainfalls often cause landslide disasters. During the summer months, Japan is under high temperature and high humidity due to the Northern Pacific High Pressure Zones that cover most of Japanese Archipelago. In autumn, typhoons are formed in the low latitude regions of the Pacific Ocean move northward and circle the western rims of the of the Northern Pacific air masses and often attack the Japanese Archipelago. These typhoons usually generate very strong winds and intensive rainfalls and cause frequently severe landslide disasters. The mean annual precipitation of Japan is ca. 1800 mm. However, at Owase in Kii Peninsula it records ca. 4000 mm and Joetsu (at the side of The Sea of Japan) it records ca. 2900 mm (of which one-half is snow). Fig. 2 shows regionally different characteristics of monthly mean precipitation.

Distribution of landslides and geotectonic structures

In the 1950th, Japan has experienced a series of severe landslide disasters. Such frequent landslide disasters lead to the enactment of the „Landslide Prevention Law“ in 1958. Under this legislation, landslide control measures have been intensively developed. The Landslide Threatened Areas administrated by the three governmental agencies are summarized in Table 1.

Table 1 Designated Landslide Threatened Areas

	Ministry of Land, Infrastructure and Transport	Ministry of Agriculture, Forestry and Fisheries		Total
		Rural Developement Bureau	Forestry Agency	
Number of area	3,329	1,868	1,725	6,922
Total area (ha)	114,023	107,061	97,927	319,011

The number of the wohle Landslide Threatened Areas amounts to 6,992 and total area of them amounts to 319,011 ha. It means that about 0.8% of the total area of Japanese territory is designated as Landslide Threatened Areas. The total expenditures of landslide mitigation measures implemented by the responsible agencies during the fiscal year of 2000 are shown in in Table 2.

Table 2 Landslide Mitigation Expenditures in Fiscal Year 2000

	Ministry of Land, Infrastructure and Transport	Ministry of Agriculture, Forestry and Fisheries	
		Rural Developement Bureau	Forestry Agency
State Subsidy	37,505	14,068	22,273
Direct spending	8,421	5,892	6,471
Total	45,926	19,960	28,744

Unit : 1 Million Yen

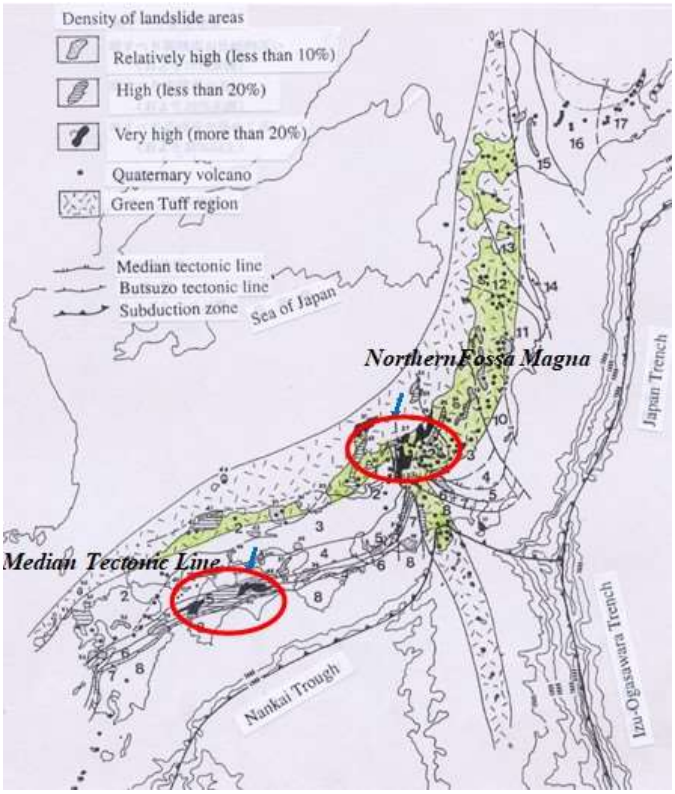

Figure 3 Distribution of landslide prone areas and geotectonic structures (Kitamura, 1992)

The distribution of landslide prone areas and related geotectonic structures are shown in Figure 3. Landslides are highly concentrated along the major tectonic lines such as in the northern Fossa Magna Region and near to the Median Tectonic Line in Shikoku Island. A typical landscape chracterized by landslides in the northern Fossa Magana Region are shown in Fig. 4. Another typical landscape characterizes by landslides along the Median Tectonic Line are shown in Fig. 5. Further, Fig. 6 shows an example of extremly high concentration of landslide areas in Matsunoyama-District in Niigata Prefecture. This area is geologically characterized by Neogene formations which consist of black mudstone or alternation of sandstone and mudstone. Soils along the sliding surface in these formations show extremely low shear strength. Twenty percent of the total landslide areas in whole Japan are concentrated in Niigata Prefecture and especially in neighbourhood of this district.

Figure 4 Landslides in Neogene formation

Figure 5 Landslides in metamorphic rock formation

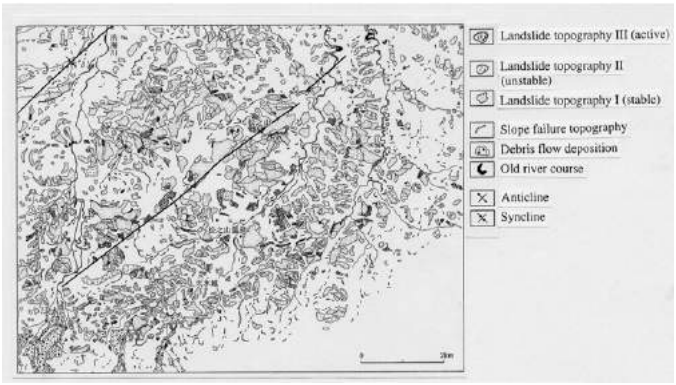

Figure 6 Distribution of landslide areas in Matsunoyama-District in Niigata Prefecture (Suzuki, 2005)

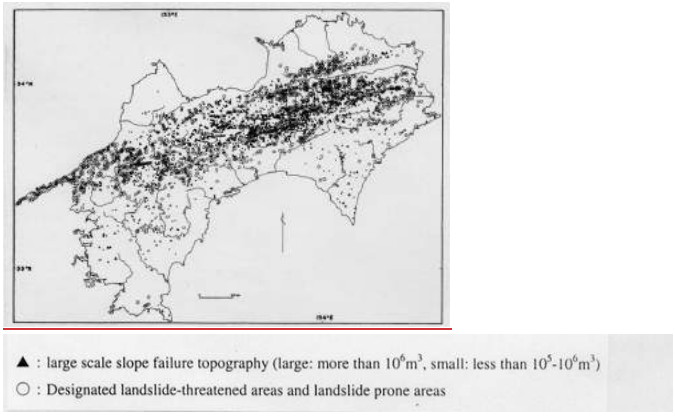

Figure 7 Distribution of large scale landslides in Shikoku Island (Terado, 1986)

Fig. 7 shows distirbution of large-scale landslide areas and landslide threatened areas in whole Shikoku Island. Landslide areas are concentrated in fractured zones which are composed of metamorphic rock formations.
There are significant differences in the shear strength characteristics of two types of landslides, namely landslides in Neogene formation and landslides in fractured metamorphic rock formation (Fig. 8). The shear resistance angles at residual state ϕ_r of landslides in Neogene formationare significantly lower than the shear resistance angles at the residual state ϕ_r of landslides in fractured metamorphic rock formation.

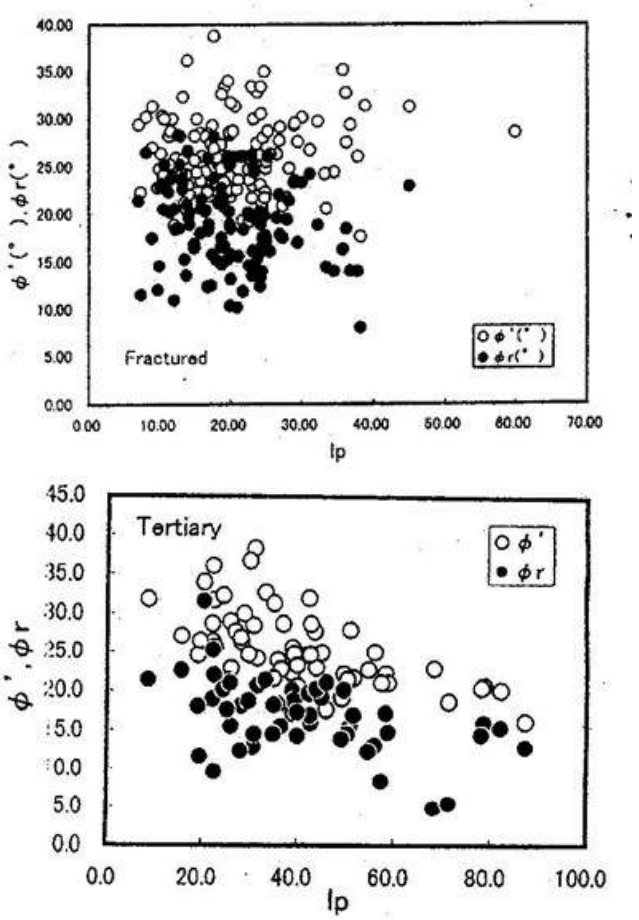

Figure 8 Relationship between peak strength ϕ' or residual strength ϕ_r and plasticity index I_p in landslides in fractured metamorphic rock formation and in landslides in Neogene formation (Yatabe et.al., 2000)

Investigation measures essential for landslide control

Various investigation measures are required for formulating an effective and appropriate landslide mitigation plan. The flow chart shown in Fig. 9 illustrates the general investigation procedures in order to understand the mechanism of landslide occurrences and to predict the movement and the resulting deformation of sliding soil mass. Preliminary investigations are carried out prior to detailed investigations and are necessary information for drafting full investigation plan.

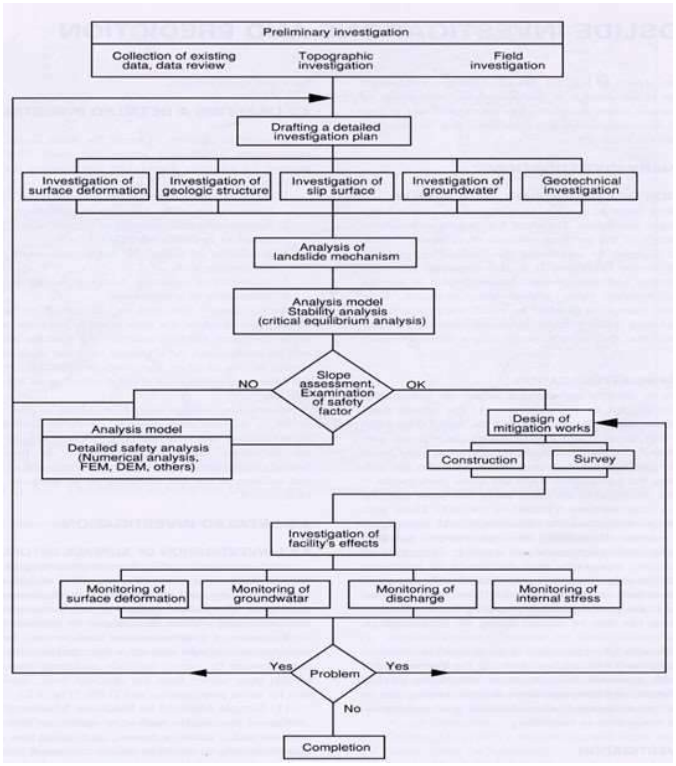

Figure 9 Flow chart for landslide investigation and analysis (Japan Landslide Society, 1996)

Preliminary investigation

As a first step, it is important to utilize existing data in order to grasp geomorphological and geological conditions, meteorological factors and history of past landslide movements. Interpretation of aerial photography is an effective tool to identify topographical changes in a target landslide area. Recently remote sensing methods using satellite images and aerial laser profiling have been highly developed. As a next step, preliminary field investigations are carried out in order to determine necessary target areas and essential items for full investigation. A draft plan of detailed investigations should be framed up to include proper examination of the following items: (1) spatial extent of the landslide area, identification of moving blocks, direction of movement, (l2) location and configuration of sliding surface, (3) characteristics of sliding soil mass, (4) possibility of subsequent movement, (5) possibility of accelerated sliding, (6) distribution of groundwater.

Investigation of surface deformation

In order to define the boundaries of landslides, activity level, direction of movement and individual moving blocks, it is necessary to investigate surface deformation. A comprehensive instrumentation used for the investigation of surface deformation includes extensometers, ground tilt meters, equipment for surveying movement like transverse surveying, grid surveying, laser surveying from opposite slope, and GPS. Surface movements are also determined by detailed aerial photographs.

Investigation of geologic structure

In most cases, investigation of geologic structure relies on exploratory borings. Geophysical exploration using seismic survey, electrical survey and radioactive survey are combined with the boring data. Geologic assessments based on the boring data obtained from the drilling site should include evaluation regarding the differentiation of moving blocks, semi-moving soil blocks and stable ground. Clays along the sliding surface generally have high moisture content and highly sticky, plastic and often associated with abration scars and slickensides. Furthermore, using the boreholes the following investigations and tests are performed: (1) Determination of sliding surface, (2) Observation of groundwater level, (3) Detection of groundwater flowing layer, (4) Tracing of groundwater flowing path, (5) Standard penetration tests, (6) Sampling of soil specimens for various soil tests.

Determination of sliding surface

The sliding surface of active landslides can be determined by measuring displacement of casing pipe according to the movement of the sliding soil mass. Depending on the requirements for surveying accuracy and magnitude of movement, appropriate instruments should be selected from the following representative instruments: (1) Pipe strain gauge, (2) Inclinometer, (3) Multi-layer movement meter.

Groundwater investigation

Investigation of the behavior of groundwater, which is essential triggering factor of sliding, is very important item, because groundwater control works as landslide mitigation measure can be effectively planned and designed on the basis of this investigation results. The investigation includes determination of groundwater level, measurement of pore water pressure, detection of groundwater flowing path, pumping test, water quality analysis, electric survey and geothermal survey.

Geotechnical investigation

In order to conduct slope stability analyses and to design appropriate control measures for mitigation of landslides, physical properties such as strength of soils along the sliding surface, location and depth of the sliding surface must be determined. The following tests are generally performed: Standard penetration tests, soil physical tests, soil mechanical tests (unconfined compression tests, tri-axial compression tests, box shear tests, ring shear tests, in-situ shear tests along the sliding surface). Furthermore, the intensity and degree of alteration of sliding surface clay are evaluated by X-ray diffraction methods.

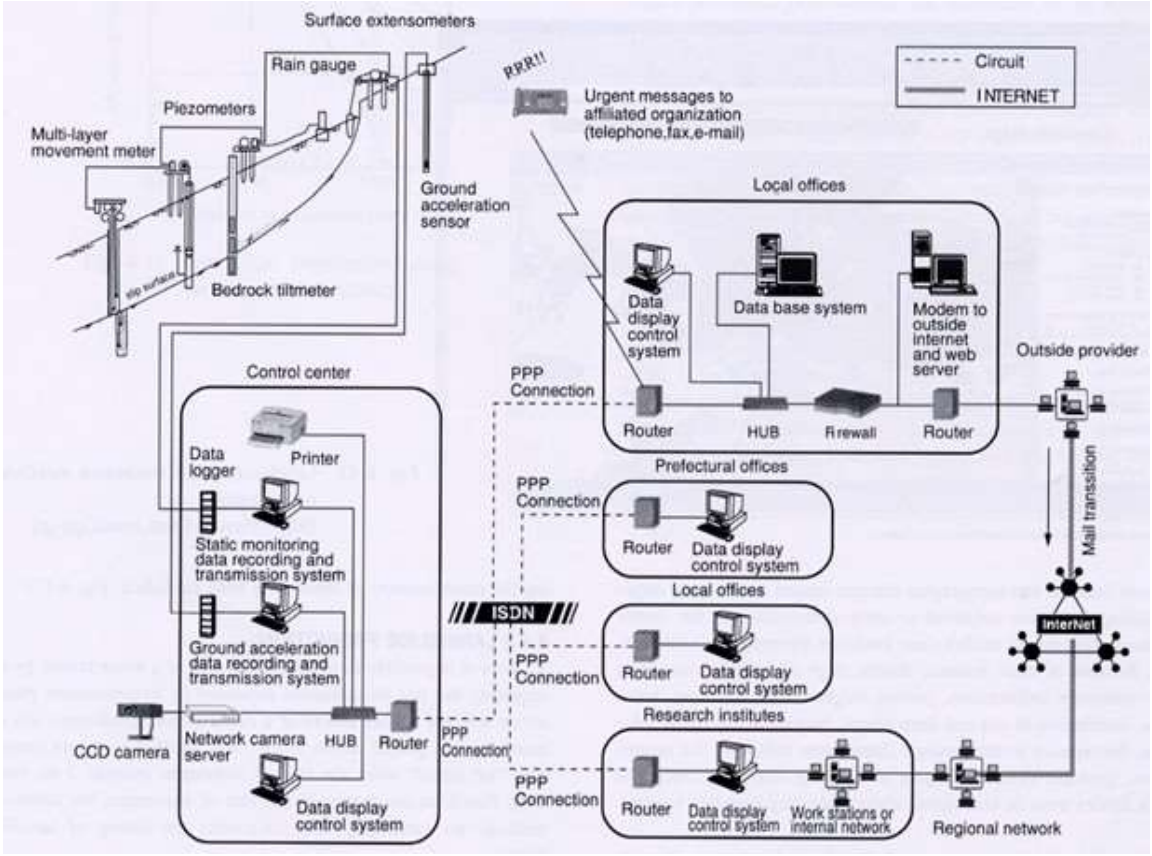

Figure 10 Automated monitoring sytem using IT technology (Japan Landslide Society, 2002)

Automated monitoring system

Recently, automated monitoring systems using data loggers and computers are being used. The instruments set up in the targetted landslide area has been designed for easy installation and weatherproof, durable, maintenance-fridendly and economical. The following points are main objectives to install automated monitoring system: (1)Surveillance of the situation of landslides, (2) Understanding of the situation of landslide deformtaion, (3) Evaluation of effectiveness of landslide mitigation measures. Fully automated systems permit remote control in real time and rapid graphic data processing and display and would provide early warning signs of sliding activity. Fig. 10 shows a schematic diagram of an automated monitoring system using IT technology.

Advanced remote sensing technology for topographic investigation

Airborne laser scanning is very useful tool for the identification of landslide in a wide area. It can identify also shallow landslides even when they are only several meters. This method is appropriate to detect geomorphological features that provide essential information in formulation of landslide inventry maps and assessng susceptibility to slope movement (Fig. 11).

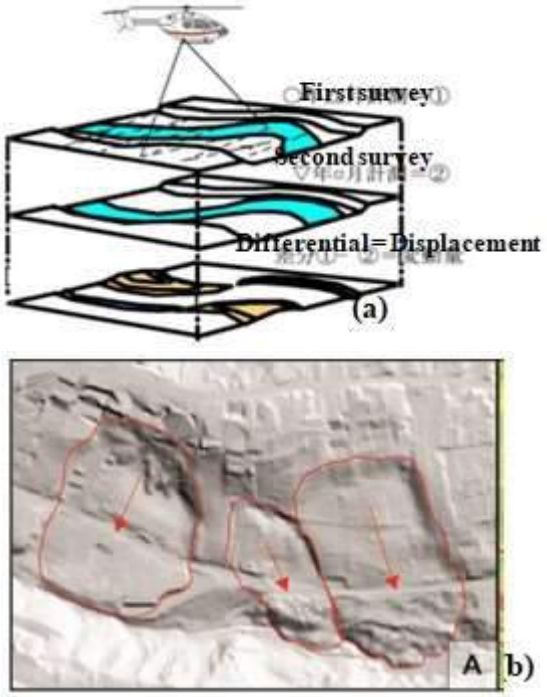

Figure 11 Airborne laser scanning (a): Schematic diagram, (b): An example on landslides in Medvednica mountain in Zagreb

Recently a method using satellite SAR(Synthetic Aperture Radar) interferometry was developed to detect ground motion. It can be useful for assessing the risk of large-scale landslide.This method is appropriate to detect spots exhibiting indices of large-scale movement in a wide area before the occurrence of landslides (Fig. 12).

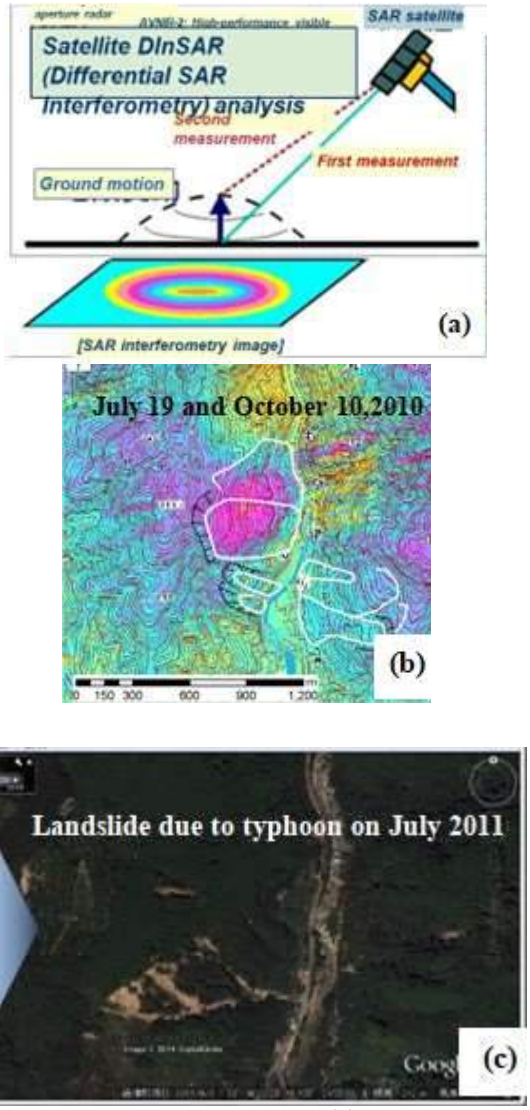

Figure 12 Satellite DInSAR analysis (a):Schematic diagram, (b):Detection in 2010, (c): Landslide in 2011 (Mizuno, 2014)

Landslide control measures

Landslide control measures are conducted in order to prevent or reduce the movement of the sliding soil mass so that the resulting damages can be minimized. For planning of effective and appropriate control measures, a clear understanding of causes and mechanism of the target landslide by necessary mitigation measures is the essential prerequisite. Landslide control measures can be classified into two major categories; namely „hard measures „ and „soft measures“. Hard measures involve construction and implementation of various engineering structures. Soft measures mean non-structural measures which involve land use restrictions and arrangements of warnig and evacuation system. The necessity of soft measures for landslide control has been increasing parallel to the intensive urban development expanding into threatened areas by landslides in recent decades. It is important not only to promote instrumentation of the auomated landslide monitoring system, but also to impose land use restrictions on inhabitants in densely populated areas.

Figure 13 Schematic representation of „hazard zoning" for three processes (Ministry of Land, Infrastructure and Transport, 2014)
Remarks: Red zone and yellow zone are designated concerning individual landslide area.
Individual landslide areas are identified on the basis of the interpretation of aerial photographs.
Red zone: Development activities are restricted. Structure of buildings is to be regulated.
Yellow zone: Risk awareness and warning and evacuation system must be arranged.

Under such circumstances a specified law to promote landslide disaster prevention in affected areas was enacted in 2000 (Act on Prevention of Sediment Disasters). The purpose of this law is to protect human lives through non-structural measures in the event of catastrophic landslides.

Hazard zoning

Hazard zoning system was introduced in Japan in 2001after the severe disasters caused by slope failures and debris flows in Hiroshima in 1999. On the basis of the law, the responsible Ministry formulated the basic guidelines (Fig. 13). Each Prefecture carried out necessary investigations based on the guidelines and mapped the areas affected by landslides, namely red and yellow zones were designated. Hazard zoning system is directly connected with warning and evacuation. It is obligatory for the prefectures to inform the public about the results of the specified hazard zoning and to make known the warning information before disastrous movement of landslides to the mayors and inhabitants of the relevant municipalities. Individual landslide areas are identified on the basis of the interpretation of aerial photographs.

Monitoring and early warning

Concerning large scale landslides, which have high potential danger to the affected areas, automated monitoring systems are installed and early warning systems are arranged using appropriate threshold values. Nowadays two methods are available in order to predict landslide occurrence time. One method was proposed by Saito in 1965 based on laboratory measurement of the strain rate during secondary creep using load-controlled triaxial tests (Fig. 14, left). Another method was proposed by Fukuzono in 1985 based on an experimental study of small-scale slope models conducted to failure under monotonically increasing load. He found that for rapid failure the logarithm of acceleration is proportional to the logarithm of velocity of the ground surface displacement (Fig. 14, right). Fig. 15 shows an example of comprehensive monitoring system for early warning in large-scale Takisaka landslide.

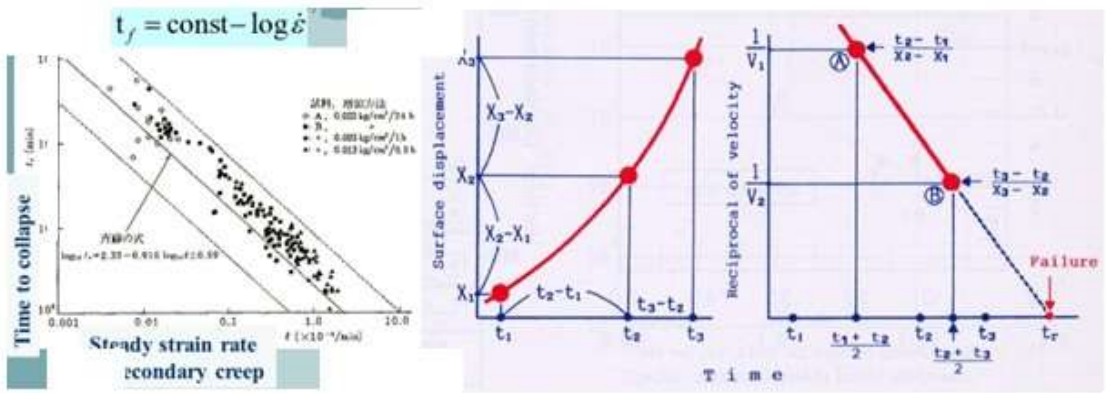

Figure 14 Left: Diagram ilustrating method by Saito; Right: Diagram ilustrating method by Fukuzono

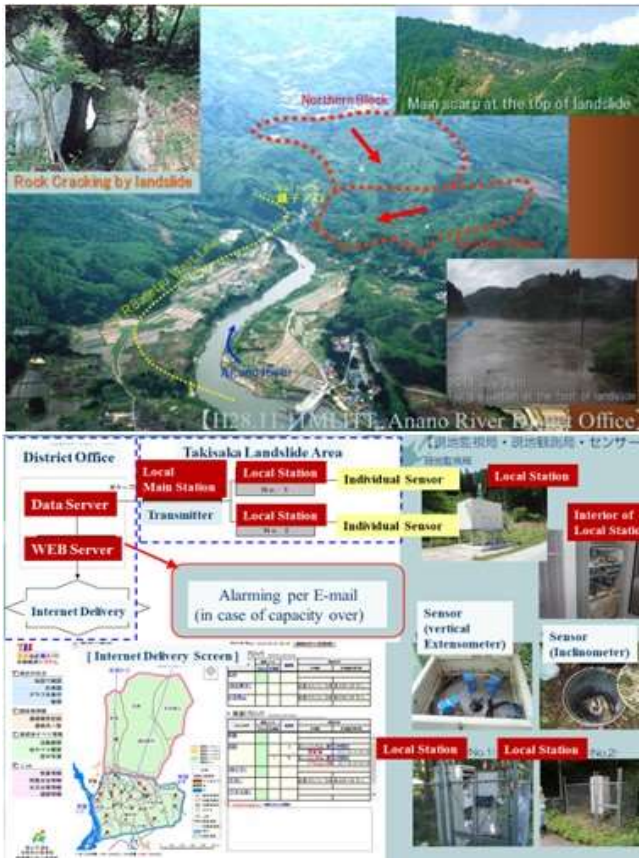

Figure 15 Monitoring system for early warning in Takisaka landslide (Agano River District Office, 2016)

Hard measures

Hard measures are classified into two types; namely „landslide control measures", and „landslide restraint measures". Landslide control measures involve modifications of the natural conditions of landslide areas such as topography, groundwater and other conditions that indirectly control the landslide movement. Landslide restraint measures, on the other hand, rely on preventing the landslide movement by directly adding a resisting force to the sliding movement. Individual measures included in both types of mitigation measures are listed in Fig. 16, and examples shown in Figs. 17 to 19.

Landslide control measures

Surface drainage control measures

These measures are implemented to control movement of landslide accompanied by infiltration of rainwater and spring flows. They include two major elements; namely drainage collection works and drainage channel works. Drainage collection works are designed to collect surface water flow by installing corrugated half pipes or lined U-ditches along the slopes and then connecting them to the drainage channels. Drainage channels were designed to remove the collected water from the landslide area quickly.

Groundwater control measures

The purpose of the groundwater control measures is to remove the groundwater in the sliding soil mass and to prevent the inflow of groundwater into the sliding soil mass from outside sources. (1) Interceptor Underground Drains and Interceptor Trench Drains: They are most useful to remove shallow groundwater up to 3 m below the ground surface. (2) Horizontal Gravity Drains: In order to remove groundwater, horizontal gravity drains with length of 30 to 50 m are installed. (3) Drainage Wells: Wells with a diameter of 3.5 to 4.0 m are excavated in areas of concentrated groundwater. A series of radially positioned horizontally gravity drains are drilled at various elevations and collect the groundwater into the drainage wells. (4) Drainage Tunnels: Tunnels which are constructed below the sliding surface in a stable bedrock formation is installed to remove collected water in the sliding soil mass by interconnecting the drainage wells.

Earth removal

This is one of the methods by which the most reliable results can be expected and generally applied to small to

medium size landslides. Except for special cases, the earth removal is focused on the head portion of the landslide areas.

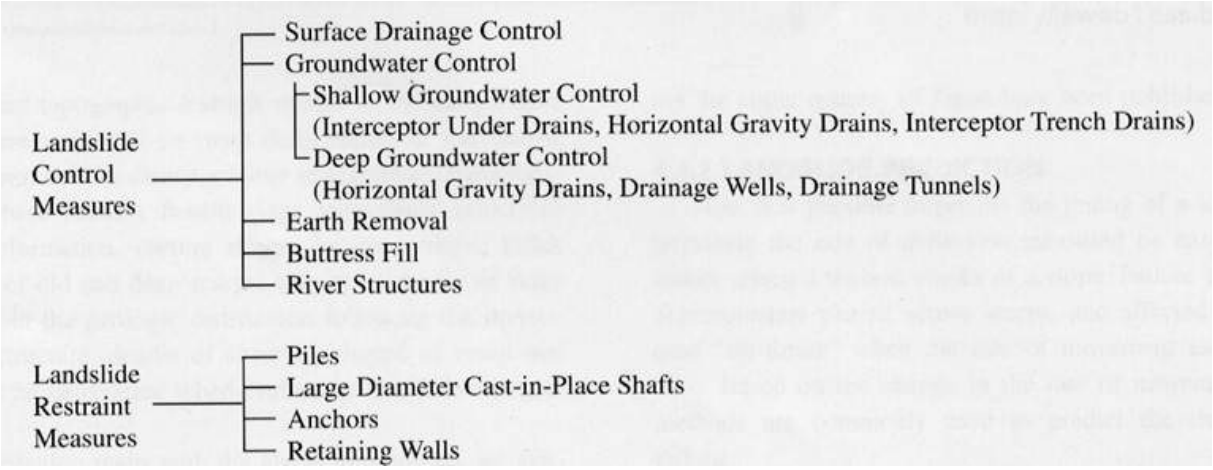

Figure 16 Various types of landslide mitigation measures

Buttress fill

This measure is placed at the lower portion of the landslide areas in order to counterweight the sliding soil mass. This method is often managed as an emergency measures. It is most effective, if the soils generated by earth removal works are used.

River structures

Degradation and channel bank erosion reduce stability of soil mass and often tend to induce landslide activity. In such cases, check dams, ground sils, revetments and other river structures can be constructed to prevent further erosion by the river water.

Figure 17 Illustration of various types of landslide mitigation measures (Agano River District Office, 2016)

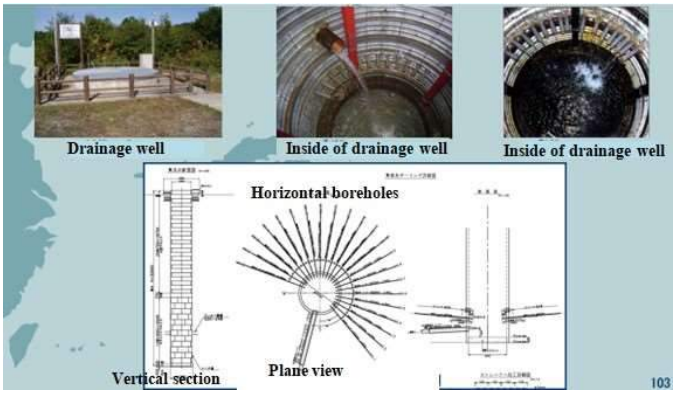

Figure 18 Illustration of drainage wells (Agano River District Office, 2016)

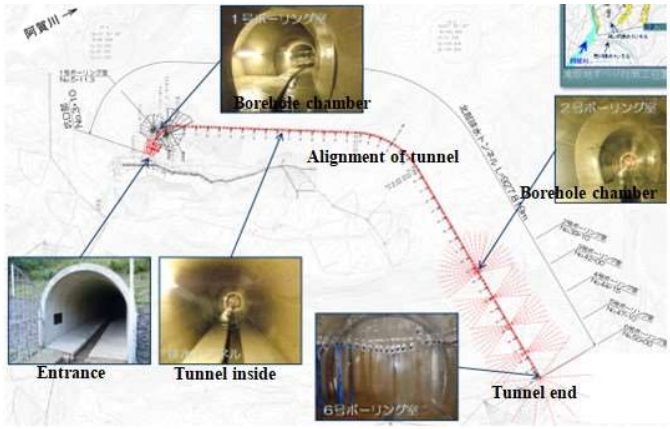

Figure 19 Illustration of a drainage tunnel installed in Takisaka landslide (Agano River District Office, 2016)

Landslide restraint measures

Piles

Piles are driven into the pre-drilled shafts in order to tie the moving landslide blocks and the stable ground together. Piles are designed to resist against shearing and bending stress and generally consist of steel pipe constructions with thick wall. The interior spaces of the pipes are filled with concrete.

Large diameter Cast-in-place shafts

Largediameter cast-in-place shafts function similar to those of piles and are also designed to tie the moving landslide block and the stable ground together. However, this measure uses shafts with much larger diameter than piles. However, this measure uses shafts with much larger diameter than piles. In order to construct a large diameter cast-in-place shaft, a vertical shaft hole with diameter of 1.5 to 6.5 m is dug and then it is filled with reinforced concrete. Compared to the piles, the large diameter cast-in-place shafts are much more resistant to bending stresses.

Anchors

Anchors utilize the tensile force of anchor bodies embedded through the sliding soil mass into stable bedrock. Anchors are connected to thrust blocks located at the ground surface. The thrust blocks are anchored with tendon members that counteract the driving forces of the sliding soil mass to restraint the sliding movement. The advantage is that large restraint forces can be obtained from tendon members with relatively small cross section.

Retaining walls

Retaining walls are installed to directly resist the thrust of sliding soil mass. This method is used to prevent small-scale landslides. It may be also applied to part of a landslide which has only small thrust, or to the base of an embankment structure. It is usually used with other methods, since it is difficult to prevent a landslide with only a retaining wall. The movement of the groundwater is active in a landslide area, therefore, flexible structure such as concrete crib, steel crib or gabion should be used.

Concluding remarks

Vulnerability for landslide disasters essentially depends on both natural and social conditions. It can be fundamentally improved by preparedness for emergency case and continuous mitigation efforts of extreme landslide events. Landslide-prone areas are extensively distributed in the entire Japanese Archipelago. Since hundreds of years ago people have been living also in landslide-prone areas. Especially in the last several decades, much more people have to settled in such areas with high vulnerability for landslide disasters because of high population density corresponding to the last fast economic growth. Therefore, mitigation of landslide

became a very important task of public welfare policy. Intensive landslide mitigation measures have been installed as public works on the legal basis of the Landslide Prevention Law. Nowadays, a comprehensive system of various landslide mitigation measures is available and proved to be practically effective so fa as for conventional type of landslide which are triggered by intensive rainfall and/or snow melt.In recent decades we have experienced remarkable disasters caused by earthquake-induced landslides. After then, intensive field studies and analyses have been carried out to clarify the mechanism of earthquake-induced landslides as well as to propose appropriate landslide control measures. As a result of such research activities on earthquake-induced landslides, certain advances have been achieved.

However, in recent decades, we are faced with a very difficult situation where we are frequently hit by extreme rainfall that far exceeds conventional assumptions, probably due to global climate change. Under such circumstances, it is feared that landslide disasters will increase in magnitude and frequency in the near future. It will be no longer possible to deal with increasing landslide risks only by hard measures, and the importance of appropriate soft measures such as further development of warning and evacuation system will increase. Further researches are essential to formulate a more accurate and sophisticated „Hazard zoning method“, and to establish an effective „Warning and evacuation system“ with more accurate timing.

References

Agano River District Office: Technical Information on Takisaka landslide, unpublished material, 2016.

FukuzonoT.: A new method for predicting the failure time of slope, Proceedings of the 4th International conference and field workshop on landslides, Tokyo, 1985, pp.145-150.

Japan Landslide Society: Landslides in Japan, 7th edition, 2012.

Japan Landslide Society: Landslides in Japan, 6th edition, 2002.

Japan Landslide Society: Landslides in Japan, 5th edition, 1996.

Kitamura S.: Landslides of Green Tuff area in Northeastern Region, Landslide Engineering, Vol.18, No.3, 1992, pp.27-35, (in Japanese).

Ministry of Land, Infrastructure and Transport: Overview of the Sediment Disaster Prevention Act, 2014, (in Japanese). www.mlit.go.jp/river/sabo/sinpoupdf/gaiyou.pdf

Mizuno M.: Application of High-Resolution SAR Satellite Images to Large Scale Landslide Disaseters, 2015, unpublished material.

Suzuki I: Geomorphology of Niigata, Daiichi-Insatsu, 2005, pp.27-35, (in Japanese).

Saito M.: Forecasting time of occurrence of a slope failure, Proceedings of the 6th international conference on soil mechanics and foundation engineering, Montreal, 1965, pp.537-541.

Terado T.: The Distribution of Landforms Caused by Large-scale Mass Movement on Shikoku Island and Their Regional Characteristics, The Memoirs of the Geological Society of Japan, No.28, Landslides, 1986, pp.221-232.

Yatabe R. et.al.: Comparison of strength of sliding surface clay between landslides in Tertiary and landslides in Fractured zone, Report of Disaster Prvention Research Insitute. Kyoto University: Study on Creeping Mechanism of Tertiary Landslides and Crystalline-Schist Landslides, 2000, pp.95-102. (in Japanese)

doi.org/ 10.35123/ReSyLAB_2019_11

Geogrid-reinforced wall as quick and flexible solution in mountainous region: Trieben landslide project, Austria

Oliver Detert [1], Hasslacher Thomas [2]

1) HUESKER Synthetic GmbH, Gescher, Germany, detert@huesker.de

2) HUESKER Synthetic GmbH, Gescher, Germany, hasslacher@huesker.com

Abstract A large-scale construction project was implemented between June 2006 and September 2008 to reroute the B114 mountainside link road between Trieben and Sunk in Austria. In addition to comprehensive drainage and anchorage measures, the works included the extensive use of extra-steep, geosynthetic-reinforced slope structures to build the route and stabilize critical slip-prone slopes. This paper presents a technically expedient and practically feasible solution for the use of geosynthetic-reinforced retaining structures on projects subject to extremely difficult geotechnical and topographical conditions. Following a description of the geotechnical situation and associated problems, the procedure for dimensioning the geogrid-reinforced structures and practical aspects of the site operations are outlined, explained and discussed.

Keywords Geotextile reinforced wall, landslide, stabilization, steep slope

Introduction

General

The approx. 48 km long B114 link road in the Austrian Province of Styria runs from the town of Trieben in the Paltental valley via the municipality of Hohentauern (Triebener Tauern pass) to Judenburg in the Murtal valley. With an estimated traffic volume of around 2,000 vehicles/24 h, including 9% heavy-goods vehicles (Lackner 2008), it constitutes an important north-south axis. Most of the southern part of the B114, which mainly runs along the Pölsbachtal valley, has a gentle gradient. The northern road section in the Tauernbachtal valley, on the other hand, covers a difference in altitude of some 570 m over a distance of 8 km. Until the 1970s, gradients of up to 21% were encountered in some places. During a first improvement project implemented at that time, the gradients were largely reduced to a maximum of 13%.

September 2008 then saw completion of a second improvement scheme on this road section, with its severe geotechnical and topographical challenges. This second scheme is described in greater detail in the following, with a particular focus on the steep geosynthetic-reinforced slopes constructed as part of the works.

Geotechnical challenge

The steeply rising section of the road to Sunk immediately outside the town of Trieben crosses an extensive geological fault zone (see Fig. 1).

Until recently, the damage caused to retaining structures, slope bridges and the pavement construction by creep movements in the slope necessitated major rehabilitation at regular intervals. Despite this, the condition of the road section continued to worsen noticeably: the pavement surfacing and lateral retaining walls exhibited substantial cracking. In places, this even led to the detachment of retaining wall facings or the destruction of rock bolts/anchor heads (see Figure 2). Apart from the risks posed by localized problem areas, even the possibility of large-scale landslips could not be completely ruled out.

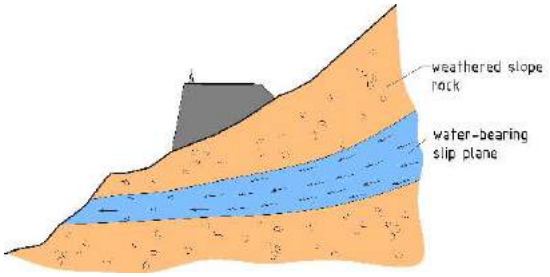

Figure 1 Schematic diagram showing geological fault zone

Given the extent of the existing damage and, above all, the anticipated scope of future damage to the road, the option of rehabilitating the existing route was rejected for both technical and financial reasons. The decision was thus taken to rebuild the affected road section.

To ensure safe operation of the road until completion of the new section, the first step entailed setting up a satellite-based system to monitor slope movement. The continuous measurement of absolute slope movement and deformation speed allowed landslip risks to be assessed and appropriate action to be taken, if necessary through complete closure of the "old" road section.

Figure 2 Damage to retaining walls along "old" route

Route Mapping

The analysis of options for rehabilitation of the affected road section started as early as 1990. The decision-making process was, however, complicated by the extremely tough geological and topographical conditions. Ultimately, the client – the local public works office of the Austrian Province of Styria – in collaboration with the appointed engineering practices Birner and Dr. Lackner from Graz – opted to reroute the road on the opposite side of the valley, more or less parallel to the existing route. This allowed continued, unobstructed use by traffic of the old B114 road between Trieben and Sunk during the construction period. In all, the new road section is approx. 2.9 km long and covers a difference in altitude of 221 m. From Trieben, the route runs along the right-hand side of the Wolfsgraben valley when viewed in the downstream direction (see Figure 3). A 70 m long bridge carries it over to the left-hand side of the Triebenbach stream after approx. 1 km. To limit the gradient to 10%, two hairpin bends are integrated further along the route. Roughly 3 km out of the town of Trieben, the road crosses back to the other side of the valley over a 40 m long bridge. After a further 500 m, it then joins the existing road near the village of Sunk.

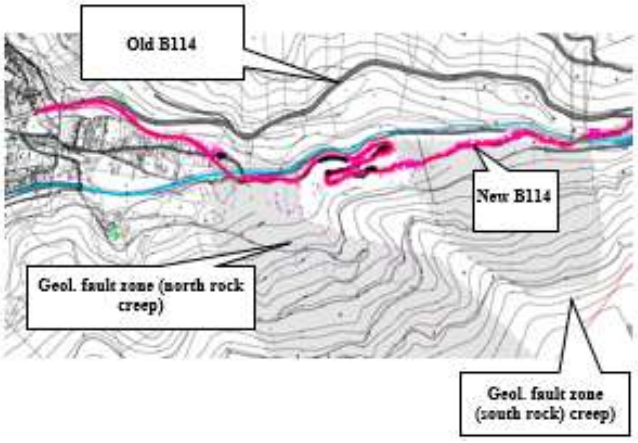

Figure 3 B 114 route between Trieben

Slope Stabilization and Retaining Structures

Given the virtually impassable terrain, dotted with steep slopes, and the fault zones on this side of the valley, the application of conventional stabilization methods using reinforced concrete, sheet piling or gravity constructions had to be rejected. After extensive analysis of the options, detailed parametric studies and careful assessment of the residual risks, a combined solution featuring geogrid-reinforced earthworks and rock bolts was adopted. The key advantage of this concept, developed by engineering practice Dr. Lackner, is the high ductility and geometrical flexibility of the resulting system. Absolute and differential displacement can be largely accommodated without damage and while maintaining structural stability and serviceability.

The geosynthetic-reinforced retaining walls, generally with a batter of 70°, reach heights of up to 28 m.

Structural Stability Calculations

Dimensioning of reinforced earthworks using iterative analytical methods

The geosynthetic-reinforced retaining walls were dimensioned in a separate process – independently of a consideration of the overall structural stability of the surrounding terrain – on the basis of iterative analytical verifications. The analysis did, however, make allowance for the sometimes steeply inclined areas of fill necessitated by the topography behind the reinforced earthworks. The structural stability of the overall slope fill was thus shown to be regulations-compliant. In general, this also led to an improvement of the overall stability of the slope in the area around the structure. Where necessary, low-level drainage or additional works to stabilize the foundation level or support deeper-seated slip surfaces were separately designed as an adjunct to the main structure. This dimensioning and verification approach had been tried out several times previously for the rehabilitation of landslip areas in unpredictable Alpine terrain using geosynthetic-reinforced soil (GRS) structures.

Figure 4 Measures to stabilize and drain slope cuttings at foundation level

The external geometry of the earthworks, as applied in the calculations, was selected with due regard for the planned route and the requirement for a body of soil of maximum homogeneity at the foundation level of the road structure.

Once the external geometry of the slope had been established, it was then possible to specify the required geometry of the cuttings. Here, the first step was to perform structural checks on external stability. As with slope/embankment verifications for standard retaining walls, only slip surfaces running outside the reinforced earthworks were considered. These verifications were performed in accordance with DIN 4084 (1981) using Bishop's method for circular slip surfaces and the vertical slice method for diverse polygonal slip surfaces. This allowed determination and verification of the cutting geometry needed or predetermined by fixed geometric points. In this particular case, the calculations had to allow for the fact that any changes arising from the iterative determination of the required reinforced earthwork dimensions automatically entailed an adaptation of the cutting geometry – thereby significantly increasing the computational effort. The definitive arrangement of the reinforcement layers was then specified and the requirements for the incorporated geosynthetic reinforcement products established. This involved further iterative analysis, likewise based on circular (i.e. "mixed") and polygonal slip surfaces, either running only inside or running inside and outside the reinforced earthworks. The length and spacing of the reinforcement layers along with the design strength of the incorporated geosynthetic products were repeatedly varied until the optimum solution was found.

Important background information on the iterative analytical design of GRS structures is set out, for example, in EBGEO 1997 ("Recommendations on soil reinforcement with geosynthetics"). Further details and recommendations, specifically regarding the impact of the terrain gradient in the backfill zone – which was particularly relevant to this project – and the allowance for slip surfaces running through the backfill zone and reinforced earthworks, are also presented in Alexiew 2005.

Numerical analysis of structural stability improvement due to retaining wall

The analytical procedure described in Section 4.1 for specification and dimensioning of the reinforced earthworks was complemented by a detailed finite element method (FEM) analysis carried out for a diploma thesis at Graz University of Technology using the commercially available Plaxis 2D V8 and Plaxis 3D Tunnel computational software. The focus here was on investigating the impact of spatial failure mechanisms and different construction stages. The numerical simulations provided confirmation of the analytical calculation results and showed how the completed works served to stabilize the slopes. Parametric studies additionally allowed estimation of the maximum projected geogrid and anchor forces together with overall settlement. The applied background conditions, material laws and computational parameters for the numerical simulations are described in Lackner 2008.

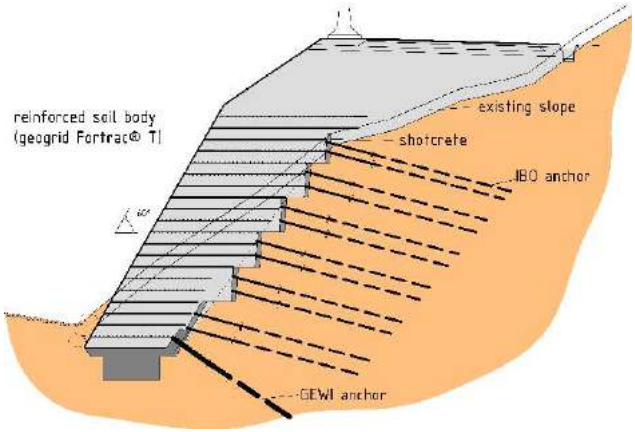

Figure 5 Schematic of standard cross-section

Construction Works

The local geological and topographical conditions posed a major challenge for the Salzburg-based contractor, Alpine Bau GmbH.

Most of the works were performed in extremely difficult, steep terrain. The haul roads had to be built with very tight widths, steep gradients and small curve radii. Every effort was therefore made to maximize efficiency in the complex process of transporting soil and materials.

The flexibility of the specified geogrid product (Fortrac®) played a key role in simplifying transportation. The geogrids were cut to size, folded and palletized at a central location on the basis of detailed placement plans. This allowed problem-free movement of the geogrids along the narrow haul roads to the work location.

Figure 6 Haul roads

In some places, slope debris had to be removed prior to construction of the GRS retaining walls. These excavations were performed in 2.0 m steps and stabilized by a reinforced, 15 cm thick shotcrete layer and IBO self-drilling hollow anchors.

As mentioned in Section 4.1, the extremely steep terrain and sometimes very low stability of the slope necessitated the minimization of excavations for the base footprint of the geosynthetic-reinforced retaining walls (see also Figure 5).

In critical sections, the only means of providing a sufficiently strong, non-displaceable foundation level for the reinforced retaining walls was by constructing 1.0 m deep, 2.50 m wide vertical concrete ribs at 4.0 m intervals. Reinforced-concrete head slabs were additionally fastened to the concrete ribs and permanently tied back with GEWI anchors. To achieve a slip-free bond between the tied-back concrete base and the footprint of the geosynthetic-reinforced retaining wall, the concrete surface was textured with a special ribbed finish and covered by a course of crushed stone prior to placement of the first geogrid layer. Given the short geogrid lengths at the base of the structure, particular attention was also given to optimizing the bond between geosynthetic product and fill material. Specification of the geogrid mesh size (70 mm x 70 mm) was thus dictated by the nature of the coarse fill material used on the project.

Preformed steel mesh angles were incorporated in the wall face as lost formwork and vegetation support layer. As these are not provided with any special corrosion-resistant coating, they cannot be viewed as being relevant to long-term structural performance. Hence, to ensure the permanent accommodation of earth pressure at the outer skin of the slope, the geogrids were wrapped back into the structure. A special fabric was also inserted inside the geogrid to protect against erosion and the washing-out of fine particles, and to provide a base for hydroseeding. Immediately upon completion, the slopes were vegetated using the hydroseeding method.

Years of experience have shown this design concept to offer a practical, reliable, durable and cost-effective solution.

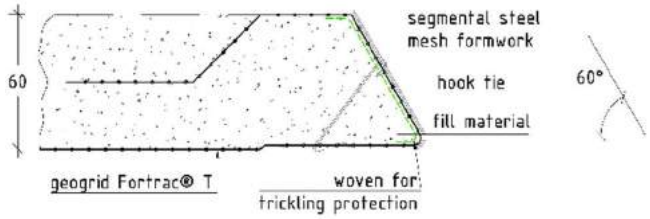

Figure 7 Schematic showing front slope design with wrap-back and vegetation

A greater bar diameter was specified for the steel mesh on this project than for normal applications. This permitted the use of relatively heavy compaction plant also at the front of the retaining structure – thus enabling the works to proceed at an adequate rate to meet the tight construction window. At the start of the works, a continuous wall inclination was achieved by preforming the steel mesh with an opening angle precisely matching the slope batter. As the works proceeded, there was a switch to steel mesh with a 90° angle, the required batter then being achieved by means of horizontal set-backs between successive layers. This further simplified the process of soil placement and compaction. Moreover, the resulting berms in the structure facilitated the infiltration of rainwater into the wall, thereby promoting the growth of vegetation on the slope. Once the steel mesh was in place, the cut-to-size geogrids were installed with the extra length allowed for the wrap-back left temporarily hanging over the mesh units.

Measurement and Monitoring

To monitor the deformation behaviour of individual structures and, in particular, of the overall slope, and to verify the effectiveness of the various stabilization measures, numerous geotechnical measurement devices were installed in the course of the works. In addition to a tightly-knit arrangement of geodetic measurement points, these specifically included inclinometers and sensors to monitor anchor forces. Analysis of the initial measurement data shows that, while the expected slope deformation continues, its magnitude has been significantly reduced. All results confirm the fitness for purpose of the described system solution comprising ductile retaining and slope systems built with geosynthetic-reinforced soil, including anchorages, in conjunction with optimized geometry and layout for slope stabilization.

Summary

The featured project testifies to the high technical, economic and ecological efficiency of geosynthetic-reinforced constructions.

The ductile material behaviour of the geosynthetic reinforcement, which is tailored to local conditions,

combined with a flexible outer skin makes this type of construction the ideal solution, even on creep-prone slopes. Not only does GRS offer favourable mechanical properties, the resulting structures can also be designed to blend harmoniously with the landscape setting. The high flexibility of the specified geogrids allows efficient and practical transportation to the work location – a major advantage, particularly on constricted sites.

The featured project is a prime illustration of the effective combination of different stabilization methods, such as GRS, anchorages, soil nailing and drainage, in difficult terrain.

The successful implementation of construction projects of this technical complexity requires in-depth experience and the commitment of all project team members to the pursuit of innovative solutions.

Figure 8 View of some of the described GRS slopes

References

Alexiew 2005: "Zur Berechnung und Ausführung geokunststoffbewehrter 'Böschungen' und 'Wände': aktuelle Kommentare und Projektbeispiele" ("On the calculation and construction of geosynthetic-reinforced 'slopes' and 'walls': recent commentaries and project examples"), contributions to 5th Austrian Geotechnical Conference (2005)

Christian Lackner 2008: "Numerische Simulation von kunststoffbewehrten Dämmen" ("Numerical simulation of geosynthetic-reinforced embankments"), diploma thesis, Institute of Soil Mechanics and Foundation Engineering, Graz University of Technology, January 2008

DIN 4084 1981: Subsoil; Calculations of terrain failure and slope failure, DIN Standards Committee Building and Civil Engineering

EBGEO 1997: "Empfehlungen für Bewehrungen aus Geokunststoffen" ("Recommendations on soil reinforcement with geosynthetics"), German Geotechnical Society

doi.org/ 10.35123/ReSyLAB_2019_12

Monitoring landslides movements by the newly developed low-cost Geodetic Integrated Monitoring System (GIMS)

Ela Šegina[(1)], Mateja Jemec Auflič[(1)], Eugenio Realini[(2)], Ismael Colomina[(3)], Michele Crosetto[(4)], Angelo Consoli[(5)], Sara Lucca[(6)], Joaquín Reyes Gonzáles[(7)]

1) Geological Survey of Slovenia, Dimičeva 14, Ljubljana, Slovenia; mateja.jemec@geo-zs.si; ela.segina@geo-zs.si
2) Geomatics Research & Development srl, Lomazzo, Italy; eugenio.realini@g-red.eu
3) GeoNumerics, S. L., Castelldefels, Spain; ismael.colomina@geonumerics.com
4) Centre Tecnològic de Telecomunicacions de Catalunya, Castelldefels, Spain; michele.crosetto@cttc.cat
5) Saphyrion Sagl, Bioggio, Switzerland; angelo.consoli@saphyrion.ch
6) Sviluppo Como - ComoNExT SpA, Lomazzo, Italy; lucca@comonext.it
7) Market Development Technology, European GNSS Agency Česká republika, joaquin.reyes@gsa.europa.eu

Abstract Geodetic Integrated Monitoring System (GIMS) units are being developed for the low-cost monitoring of ground deformations with a focus on landslides and subsidence. They are based on the complementary methods including three different monitoring techniques: GNSS, InSAR and Inertial Measurement Unit. GIMS units measure ground deformations with millimetric accuracy daily and give real-time alerts. The system is being in the process of testing on the two sites in Slovenia where different motion intensities are expected: one pilot area is located on the active landslides close to Vipava and another on a deep-seated landslide close to Koroška Bela. The present contribution will focus on the field implementation and the first testing at the first pilot area in Vipava valley. After validation, the unit will be released to the market for potential customers to use in geohazard monitoring and serve as an early-warning system. The developed GIMS unit will contribute to the detailed and timely knowledge of the landslides motion behavior, improved planning maintenance intervention and mitigation of casualties and injuries caused to the population.

Keywords landslide, monitoring, GNSS, SAR, IMU

Introduction

The growing interest in natural risk awareness implies the extended landslides monitoring and at the same time the demand for reduced equipment cost. Such needs triggered the development of the GIMS units (Geodetic Integrated Measurement System) which is a part of the EU project GIMS (https://www.gims-project.eu/).

Individual sensors have already been used as components in the different monitoring systems that were applied for the detection and measurement of landslide movements, as GNSS (Global Navigation Satelite System) (Cina et al. 2014, Biagi et al. 2016, Gümüş et al. 2019) and SAR (Synthetic Aperture Radar) (Cascini et al. 2010, Raucoules et al. 2013, Schlögel et al. 2015, Strozzi et al. 2018). IMU (Inertial Measurement Unit) sensors have mostly been used in laboratory experiments to determine their usability in measuring ground movements (Abdoun et al. 2006, Hanto et al. 2011, Ćmielewski et al. 2013, Tran et al. 2015, Kumar & Naidu 2015, Leng Ooi et al. 2016, Lo Iacon et al. 2017). Less frequently they were applied to the field to measure landslide velocity (Wang et al. 2017, Yang et al. 2017, Awaludin & Agni Dhewa 2018). Combination of different sensors has also already been applied for a similar approach (Benedetti et al. 2017, Carlà et al. 2019). The GIMS unit measure ground movements by the three complementary methods: GNSS, InSAR and IMU. Such a multidisciplinary approach promises improved accuracy and verifiability of the data. Application of the open access Copernicus and Galileo systems reduced the cost of the landslide monitoring.

Materials and methods

The GIMS unit is a stand-alone monitoring unit based on the three surveying technologies: GNSS, SAR and IMU (Fig. 1).

Figure 1 Standalone GIMS unit (Photo: E. Šegina).

GNSS

Dual frequency (Galileo E1/E5 + GPS L1/L5) EGNSS hardware, and software for geodetic monitoring have been developed to monitor temporal series of the ground movement.

InSAR

Active SAR transponder hardware has been developed to create spatial and temporal deformation maps based on the Sentinel 1-A/B data.

IMU

Inertial measurement unit software has been developed to detect fast spatial movements. Due to its implementation, the GIMS monitoring system can be used as an early-warning system.

Study area

Seven GIMS units have been installed along the Highway Vipava-Razdrto in the SW of Slovenia.

Complex Pleistocene to recent landslides in the area are related to the Mesozoic carbonates thrust over folded and tectonically fractured Tertiary siliciclastic flysch (Fig. 2). Such overthrusting has caused steep slopes and fracturing of the rocks, producing intensely weathered carbonates and large amounts of scree deposits. The combination of geological conditions and periods of intense short or prolonged rainfall (average precipitation is approximately 1,700 mm to 2,500 mm/year on the karstic plateau) has led to the formation of different types of complex landslides. Recently, carbonates have been breaking down in the form of steep fans of carbonate scree in the upper part of the valley, increasing the thickness of these sediment layers over 10 m. In the lower part, superficial deposits range from large-scale, deep-seated rotational and translational slides to shallow landslides, slumps, and sedimentary gravity flows in the form of debris or mudflows reworking the carbonate scree and flysch material.

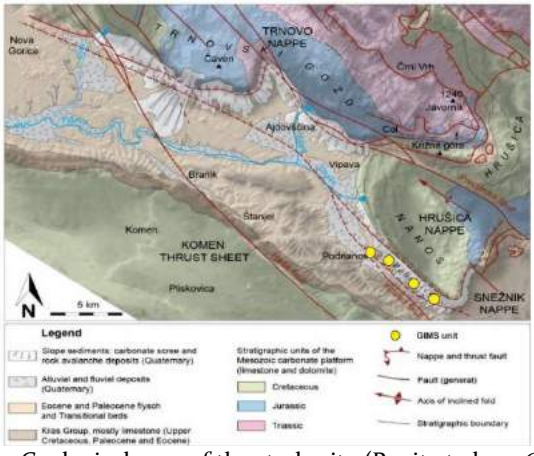

Figure 2 Geological map of the study site (Popit et al. 2016) with marked locations of GIMS units.

Preliminary measurements

Figures 3-8 show preliminary measurements performed by one of the installed GIMS unit. Note that IMU and inclinometer results still need to be processed to remove the effect of temperature. Here we report the preliminary results of only one station as an example.

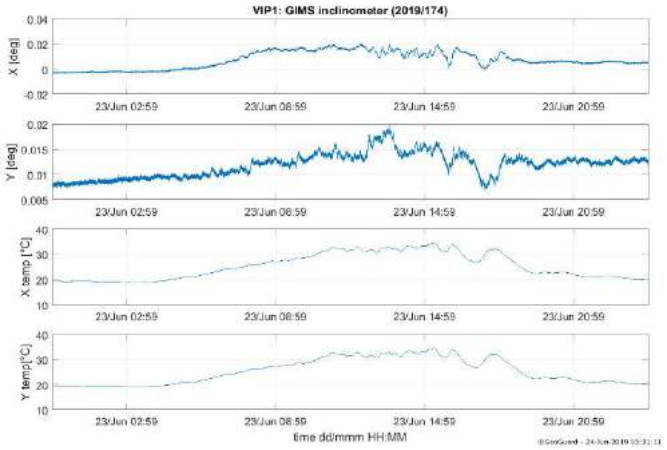

Figure 3 Inclinometer's preliminary measurements.

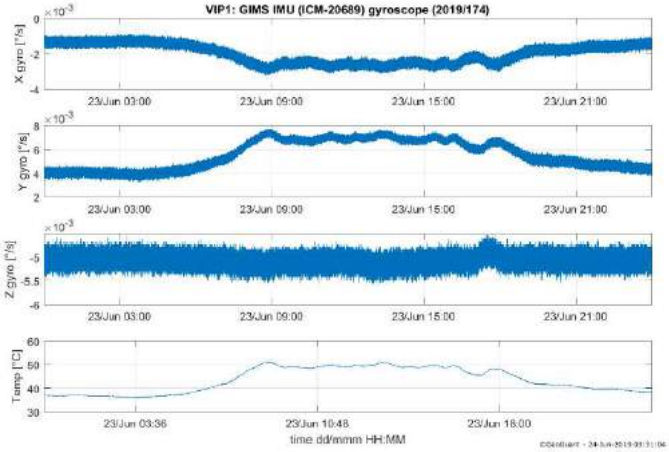

Figure 4 Gyroscope's preliminary measurements.

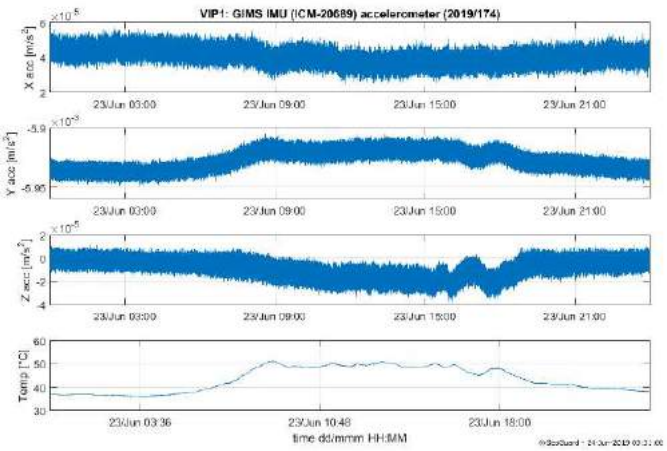

Figure 5 Accelerometer's preliminary measurements.

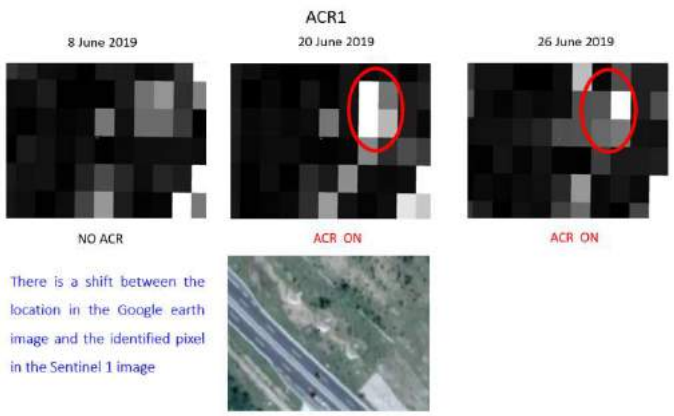

Figure 6 First compact active SAR transponders measurements.

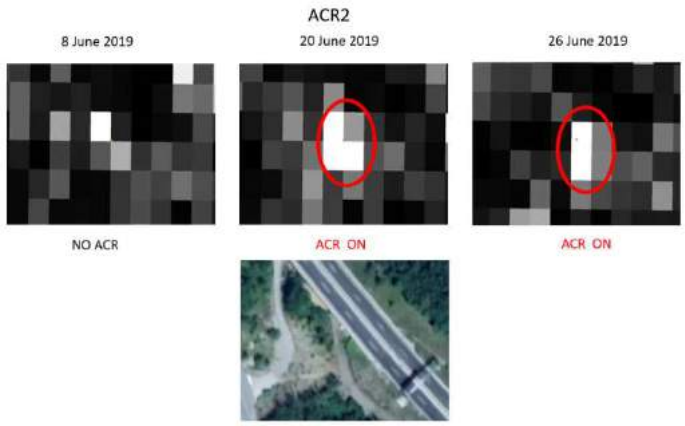

Figure 7 First compact active SAR transponders measurements.

Note that so far, only the satellite images of three passages are available for verifying their correct installation and functioning. On the bases of a preliminary check, we expect positive results, but further data are needed to confirm it.

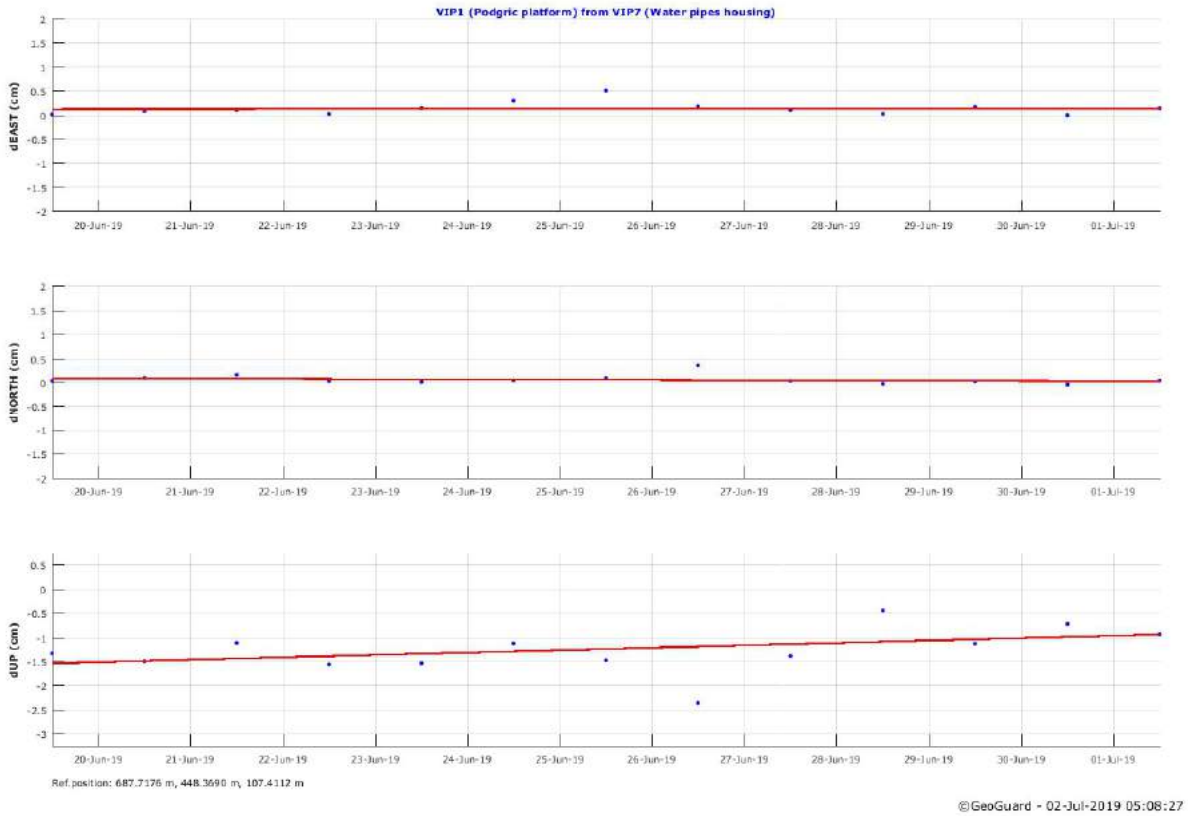

Figure 8 Preliminary results: first GNSS positioning measurements in the east, north and up components computed relatively to VIP7 (reference point).

Conclusions

Preliminary measurements have been successfully performed with the prototype GIMS units. In the next step, monitored data will be validated with the in-situ data.

Acknowledgements

The GIMS project is funded by the European GNSS Agency under the European Union's Horizon 2020 research and innovation programme under grant agreement No. 776335.

References

Abdoun T, Danisch L, Ha D (2006) Advanced sensing for real-time monitoring of geotechnical systems. Geotechnical Special Publication.

Awaludin L, Dhewa, O A (2018) Low cost sensor node device for monitoring landslides. Indonesian Journal of Electronics and Instrumentation Systems (IJEIS). 8(2): 201-210.

Benedetti E, Dermanis A Crespi M (2017) On the feasibility to integrate low-cost MEMS accelerometers and GNSS receivers. Advances in Space Research. 59: 2764-2778.

Biagi L, Grec F C, Negretti M (2016) Low-cost GNSS receivers for local monitoring: experimental simulation, and analysis of displacements. Sensors. 16: 1-16.

Cascini L, Fornaro, G, Peduto D (2010) Advanced low- and full-resolution DInSAR map generation for slow-moving landslide analysis at different scales. Engineering Geology. 112: 29-42.

Carlà T, Tofani V, Lombardi L, Raspini F, Bianchini S, Bertolo D, Thuegaz P, Casagli N (2019) Combination of GNSS, satellite InSAR, and GBInSAR remote sensing monitoring to improve the understanding of a large landslide in high alpine environment. Geomorphology. 335: 62-75.

Cina A, Piras M., Bendea H I (2014) Monitoring of landslides with mass market GPS: an alternative low cost solution. The International Archives of the Photogrammetry, Remote Sensing and Spatial Information Sciences. XL-5/W3. The Role of Geomatics in Hydrogeological Risk, 27 – 28 February 2013, Padua, Italy.

Ćmielewski B, Kontny B, Ćmielewski K (2013) Use of low-cost MEMS technology in early warning system against landslide threats. Acta Geodynamica et Geomaterialia. 10(4): 485-490.

Gümüş K, Selbesoğlu M O (2019) Evaluation of NRTK GNSS positioning methods for displacement detection by a newly designed displacement monitoring system. Measurement. 142: 131-137.

Hanto D, Widiyatmoko B, Hermanto B, Puranto P, Handoko L T (2011) Ral-time inclinometer using accelerometer MEMS.

Kumar S D, Naidu V J (2015) Landslide detection and monitoring using mems and zigbee. SSRG International Journal of Electronics and Communication Engineering (SSRG-IJECE). 2(5): 30-34.

Leng Ooi G, Siang Tan P, Lin M L, Wang, K L, Zhang Q, Wang Y H (2016) Near real-time landslide monitoring with the smart soil particles. Japanese Geotechnical Society Special Publication. 2/28: 1031-1034.

Lo Iacono F, Navarra G, Oliva M (2017) Structural monitoring of "Himera" viaduct by low-cost MEMS sensors: characterization and preliminary results. Meccanica. 52: 3211-3236.

Popit T (2016) Transport mechanisms and depositional processes of Quaternary slope deposit in Rebrnice area. Doctoral thesis. Ljubljana Univ., Ljubljana, Slovenia.

Raucoules D, de Michele M, Malet J P, Ulrich P (2013) Time-variable 3D ground displacements from high-resolution synthetic aperture radar (SAR), application to La Valette landslide (South French Alps). Remote Sensing of Environment. 139: 198-204.

Tran D T, Nghia T D, Dinh-Chinh N, Duc-Tuyen T (2015) Development of a rainfall-triggered landslide system using wireless accelerometer network. International Journal of Advancements in Computing Technology. 7(5): 14-24.

Schlögel R, Doubre C, Malet J P, Masson F (2015) Landslide deformation monitoring with ALOS/PALSAR imaginary: A D-InSAR geomorphological interpretation method. Geomorphology. 231: 314-330.

Strozzi T, Klimeš J, Frey H, Caduff R, Huggel C, Wegmüller, Rapre A C (2018) Satelite SAR interferometry for the improved assessment of the state of activity of landslides: A case study from the Cordilleras of Peru. Remote Sensing of Environment. 217: 111-125.

Wang K L, Hsieh Y M, Lin J T, His M H (2017) Sliding behavior monitoring of a deep-seated landslide with differential interferometric synthetic aperture radar, mems tiltmeter and unmanned vehicle images. 34th International Symposium on Automation and Robotics in Construction (ISARC). 1045-1051.

Yang Z, Tian H, Shao W, Lei X (2017) A multi-source early warning system of MEMS based wireless monitoring for rainfall-induced landslides. Applied Sciences 7: 1-12.

doi.org/ 10.35123/ReSyLAB_2019_13

Cyclic stress ratio of landslide deposits in Vinodol Valley, Croatia

Vedran Jagodnik[(1)], Petra Đomlija[(1)], Loren Vorić[(1)], Željko Arbanas[(1)]

1) University of Rijeka, Faculty of Civil Engineering, 51000 Rijeka, Croatia

Abstract Earthquakes are among the most significant landslide triggering factors. Earthquake induced vibrations produce small cyclic shear strains, and the resulting cyclic stresses gradually increase pore pressure. The Vinodol Valley is characterized by numerous relatively small and shallow debris slides, initiated in eluvial deposits, or along the contact between the eluvial deposits and flysch bedrock. The area of the Vinodol Valley is seismically active, which makes it susceptible to earthquake triggered landslides. In this study, three samples were collected from the landslide body of a debris slide and tested under three different cyclic stress ratios for the first time within the presented studied area. The preliminary results enabled insights into an understanding of possible earthquake impact on cyclic behaviour of soils from the eluvial deposits in the Vinodol Valley.

Keywords landslide, cyclic stress ratio, double amplitude cyclic strain, Vinodol Valley

Introduction

Earthquakes are considered to be a significant landslide triggering factor (for eg., Popescu 2002; Highland and Bobrowsky 2008; Xu et al. 2015). Small cyclic shear strains resulting from the earthquake induced vibrations produce cyclic stresses and graduate pore pressure rise. Therefore, it is highly valuable to determine cyclic behaviour of a material under the different cyclic stress ratios (CSR).

The cyclic stress ratio is defined as a ratio between cyclic shear amplitude and effective overburden stress (Kramer 1996). It is frequently used as a load parameter in stress controlled simple or triaxial tests (for eg., Seed and Lee 1966; Mohamad and Dobry 1986; Hyodo et al. 1992; Boulanger and Idriss 2004). Beside the original purpose of testing a liquefaction potential (Seed and Lee 1966), it has also been used for determination of the cyclic strength and cyclic mobilisation of a tested soil (e.g., Seed and Peacock 1971; Seed 1979; Boulanger and Idriss 2004). Cyclic stress ratio can be directly related with the ground acceleration (for eg., Kramer 1996; Idriss and Boulanger 2008).

The Vinodol Valley (64.57 km^2), Croatia, is characterized by numerous relatively small and shallow landslides, which were developed along the contact of the eluvial deposits and the flysch bedrock. For the study area, the geomorphological historical landslide inventory map was created (Đomlija, 2018), based on the visual interpretation of topographic datasets derived from the 1 m Digital Terrain Model (DTM), obtained from the airborne LiDAR (Light Detection and Ranging) data. More than 600 debris slides and debris slide-debris flows in the Vinodol Valley are identified. The most of these phenomena are located within the complex gullies (Đomlija 2018) dissected deep in the soft flysch bedrock, which are almost entirely covered by dense forest vegetation. Landslides were mainly triggered by the intense and/or prolonged rainfalls during the rainy season, which usually lasts from November to May.

The wider area of the Vinodol Valley is seismically very active (Prelogović et al. 1981), which makes it also susceptible to earthquake triggered landslides (Popescu 2002). The Valley represents a part of a regional neotectonic unit, which strikes in Dinaric direction (NW-SE) from the Klana settlement in the northwest to the Senj settlement in southeast, and with relatively high earthquake magnitudes occurring throughout in the past (Kuk and Prelogović 1998; Herak et al. 2017). The value of the maximal expected peak ground acceleration in the Vinodol Valley ranges between 0.1g and 0.26g, depending on the earthquake return period.

Even though landslides in this area were known since the historical times (eg., Rogić 1968), they are studied in detail and mapped just recently (Đomlija 2018). Knowledge about the landslide types and spatial distribution of the landslide phenomena identified in the Vinodol Valley enabled further studies on landslide-forming materials, such as the static and the cyclic soil properties. This paper presents the first and preliminary results of the cyclic properties of soil from the eluvial deposits originating from weathering of flysch bedrock, in which landslides in the Vinodol Valley are mainly being triggered. Three soil samples were collected from the landslide body of one of the debris slides located in the north-western part of the Vinodol Valley. For the purpose of this study, three stress control triaxial tests were performed under different cyclic stress ratios. The preliminary results enabled the first insights into understanding of possible earthquake impact on cyclic behaviour of soils from the eluvial deposits in the Vinodol Valley.

Study area

The Vinodol Valley (64.57 km2) is situated in the north-western coastal part of Croatia (Fig. 1a). It is characterized by complex geological conditions (Blašković 1999), and an elongated, irregular shape. The steep Valley flanks are built of Cretaceous and Paleogene carbonate

rock (limestone and dolomites) (Fig. 1b), while the inner parts and the bottom of the Valley are built of Paleogene flysch deposits, mainly composed of marls, siltstones, and sandstones in alternation. Flysch bedrock is almost entirely covered by various types of superficial deposits (Đomlija 2018). Distinctive topography is different in the three main parts of the Vinodol Valley (Đomlija 2018).: the north-western (NW), the central, and the south-eastern (SE) part. The NW and the central parts of the Vinodol Valley belong to the Dubračina River Basin, and the SE part belongs to the Suha Ričina River Basin. For the purpose of this study, soil sampling from the eluvial deposits was performed in the NW part (19.33 km2) of the Vinodol Valley (Fig. 1a), located near the Drivenik settlement. The Valley is predominantly rural, encompassing more than 50 small settlements, two county roads, and numerous local and unnamed roads and pathways.

The Vinodol Valley is seismically active (Prelogović et al. 1981). The contacts between the flysch and carbonate rock mass are mainly tectonic, with a predominantly reverse character of displacement (Blašković 1999). The active fault systems generally strike along the three main directions: (i) the longitudinal faults strike along the NW-SE direction; (ii) the transversal faults strike along the NE-SW direction; and (iii) the diagonal faults strike along the N-S direction. Earthquakes are shallow, with the depths varying between approx. 2 and 30 kilometres. The strongest earthquake that was recorded in the Vinodol Valley occurred in 1916 (Prelogović et al. 1981). The epicentre was about ten kilometres east from the Novi Vinodolski settlement, situated in the SE part of the Vinodol Valley. The earthquake hypocentre was 18 km deep, and the earthquake magnitude was M = 5.8. The earthquake triggered the rock falls along the relatively steep carbonate slopes at the Valley flanks, as well as the landslides, and cracks along the terrain surface. According to Herak et al. (2011), the maximal expected peak ground acceleration in the Vinodol Valley ranges between 0.1g and 0.26g, depending on the earthquake return period.

The eluvial deposits (Fig. 1b) in the NW part of the Vinodol Valley cover an area of 2.26 km^2. These deposits originate from weathering of soft flysch bedrock, and their composition varies along the entire study area, depending on lithological composition of a local bedrock. During the previous studies, it was determined that eluvial deposits in the Vinodol Valley are mainly composed of the low plasticity clays, high plasticity clays, low plasticity silts to clayey gravels (Pajalić et al. 2017; Đomlija 2018). In some locations eluvial deposits contain the rock fragments originating both from the carbonate and the flysch rock mass. In the NW part of the Vinodol Valley, there are identified 54 small debris slides (an average landslide area of 750 m^2) based on the visual interpretation of 1 x 1 m LiDAR imagery (Đomlija 2018). However, the debris slide from which the soil samples were taken (Fig. 1c), occurred after the airborne laser scanning was performed in March 2012 and it was identified in the field. The landslide is very small, with the total length of approx. 12 m, and the maximum width of approx. 5 meters.

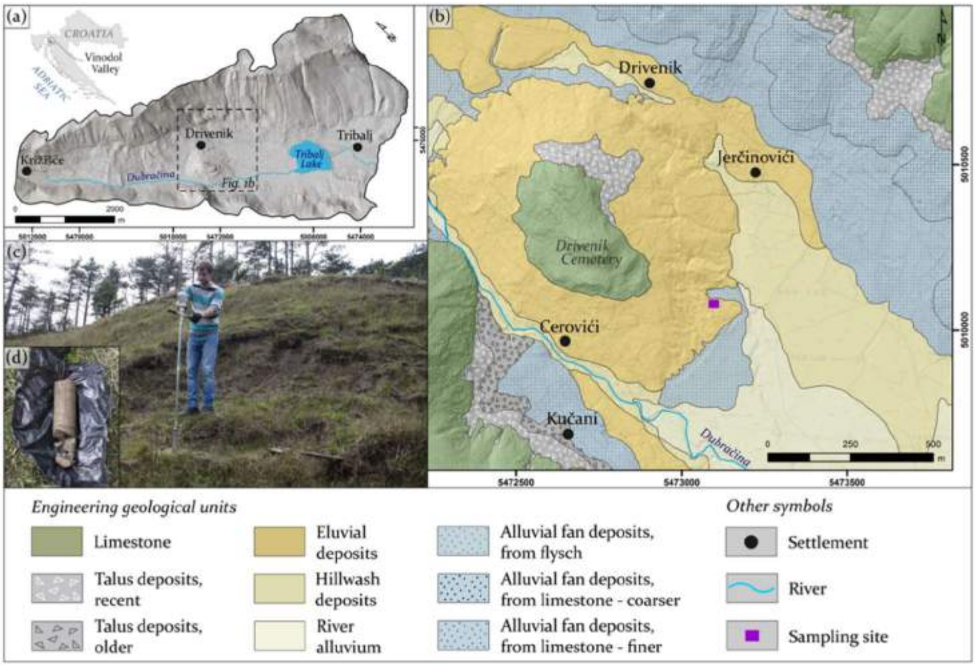

Figure 1 (a) Geographical position of the Vinodol Valley in Croatia, and the hillshade map of the northwestern part of the Valley, derived from the 1 m LiDAR DTM. (b) A detail from the Engineering geological map of the nort-western part of the Vinodol Valley (Đomlija, 2018), with the soil sampling site. Photographs (c, d) were taken during the sampling of eluvial deposits from the landslide body.

Material and methods

Soil sampling

For the purpose of this study, three soil samples were taken from the eluvial deposits in the body of a small debris slide (area of approx. 60 m2) in the NW part of the Vinodol Valley. This landslide was chosen for the study because of an easy access to its location, its small size, and an absence of the vegetation cover. Samples were taken from the landslide body by applying the manual drilling, using an Eijkelkamp sampling drill and a sampler (Fig. 1c). According to the applied sampling technique, the samples were almost undisturbed (Fig. 1d). Samples were taken from the relatively shallow depths, ranging between 0.70 and 1.50 m, above the shallow surface of rupture.

Soil classification tests

In this study, the soil classification tests were performed firstly: (i) specific gravity, (ii) grain-size distribution and (iii) Atterberg's limits. Soil classification was performed based on the ISO standards (EN/ISO 14688-2 2017). For determination of the specific gravity, ASTM standard was used (ASTM D0854 2000), by applying the boiling technique. Grain-size analysis was performed using the wet sieve analysis for the coarse-grained soil, and the hydrometer analysis for the fine-grained soil components. For the wet sieve analysis, soil sample was submerged in the solution of 2g of sodium - hexametaphosphate in 1000 ml water, for 24 hours (EN ISO 14688-1 2002). This procedure ensured breaking the cohesion bonds between the fine-grained particles, leading to easier passing of particles through the sieves. Hydrometer analysis was performed on 50 g of soil sample passing through 63 μm sieve (EN ISO 14688-1 2002). Atterberg's limits were also determined on a soil component passing through 425mm sieve. Soil was mixed with the deaired water 24 hours prior to the testing, that the soil minerals can soak in the water (ASTM D4318 2010).

Triaxial test

Cyclic tests were performed on Dynatriax triaxial system manufactured by Controls Group Ltd (Controls Group Ltd. 2017). The Dynatriax system is a closed loop triaxial system with the capability of performing dynamic cyclic triaxial test in both drained and undrained conditions. It is pneumatically based system that consists of following main components: triaxial frame (Fig.Figure 2(a)), triaxial cell (Fig.Figure 2(b)), actuator (Fig.Figure 2(c)), and control unit (Fig.Figure 2(d)). The maximum cell pressure that can be applied to the soil samples is 1 MPa. Actuator has a frequency of 10 Hz and maximum dynamic capacity of 15 kN and it is controlled through the control unit with a pneumatic air control (Fig.Figure 2(e)). The system has two linear variabile differential transformers (LVDT's) which are used for measuring vertical displacement, one outside triaxial cell and another within the actuator. The submerged load cell (Fig.Figure 2(f)) with the capacity of 25 000 N is used to measure a load on the sample. Cell and back pressure are measured with pressure transducers on the pneumatic unit (Fig.Figure 2(g)), also used for its control, while the pore water pressure transducer (Fig.Figure 2(h)) is directly connected to the main unit (Fig. 2(d)).

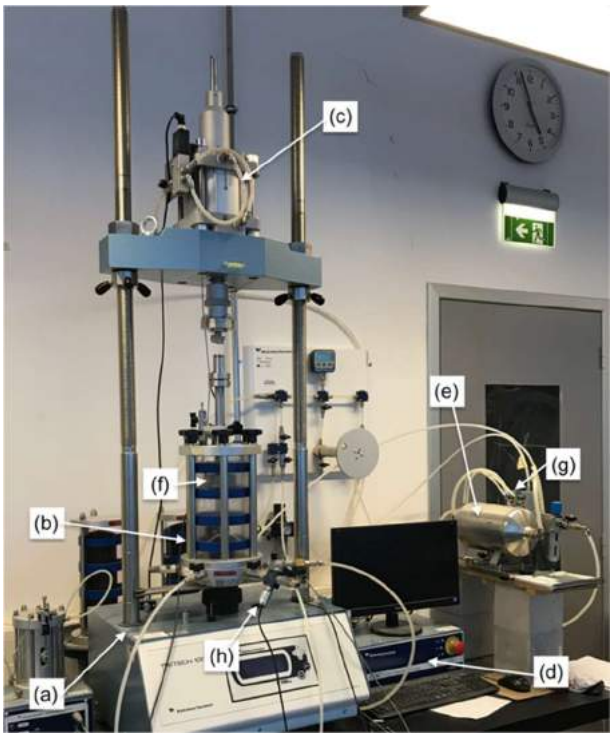

Figure 2 Dynatriax cyclic triaxial system

The soil sample is shaped into the soil specimen for cyclic triaxial testing using specially designed cutter. Cutter is pushed in the soil sampled in the field, resulting in the soil sample of 38 mm in diameter and 76 mm in height. During sample preparation, small part of soil is used to determine the initial water content. Sample is placed in triaxial cell and subjected to B -test (Lade 2016) until B value of 0.96 was reached.

Cyclic stress ratio

In geotechnical earthquake engineering, cyclic shear stress amplitude can be directly related to the ground surface acceleration (Seed and Idriss 1971). The relation between a cyclic shear stress amplitude and a ground acceleration is expressed with the equation [1].

$$\tau_{cyc} = 0.65 \frac{a_{max}}{g} \sigma_v \, r_d \qquad [1]$$

where τ_{cyc} is uniform cyclic shear stress amplitude on site, a_{max} is the maximum ground acceleration, g is the acceleration of gravity, σ_v is the total vertical stress and r_d is the stress reduction factor.

The cyclic behaviour is very often presented with cyclic strength curves, which represent the relationship between relative density, cyclic stress amplitude and cyclic numbers (Kramer 1996). There are often normalised with the effective consolidation stress, for comparable results,

thus giving the *cyclic stress ratio* (CSR). Therefore, the cyclic stress ratio in the field can be easily calculated as:

$$CSR_{field} = \frac{\tau_{cyc}}{\sigma_v'} \quad [2]$$

where σ_v' is the effective overburden stress.

Such conditions can be easily reproduced in the laboratory, changing the deviatoric cyclic stress and consolidation stress according to perform the test type (eg., triaxial cyclic test or cyclic simple shear). For the cyclic triaxial test, cyclic stress ratio can be calculated as:

$$CRS_{tx} = \frac{q}{2 \cdot \sigma_c'} \quad [3]$$

where q is the deviatoric stress as the difference in axial and radial stress and σ_c' is the effective consolidation stress.

The CSR is very affected by the type of laboratory test. Analysis performed by Seed et al. (1975) found that the relation between the field CSR and laboratory CSR measured with triaxial device is defined with equation:

$$CSR_{field} = 0.9\, c_r CSR_{tx} \quad [4]$$

where coefficient c_r represents correction factor, mostly depending on k_0 (Finn et al. 1971; Seed and Peacock 1971; Castro 1975) and varies from 0.55 to 1.15.

The main objective of this paper is to present the first and preliminary results of the cyclic properties of soil from the eluvial deposits originating from weathering of flysch bedrock. The cyclic properties will be presented by results of stress controlled cyclic triaxial test at different CSR. The test will demonstrate the behaviour of soil material under different CSR and establish different double amplitude axial cyclic deformation as well as change in pore water pressure.

Three tests were performed as presented in Tab.Table 1, at the same effective consolidation stress of 50 kPa and with varying CSR ratio. The frequency of the stress control test was constant during all three tests and it was chosen as 0.1 Hz.

Table 1 Summary of cyclic tests

CSR	Effective stress	Deviatoric stress
0.2	50	20
0.3		30
0.5		50

Results of the performed laboratory tests are presented in the following section. Special attention is given to the determination of cyclic stress ratio and the cyclic double amplitudes of relative deformation.

Results

Soil classification

Boiling technique used to determine the specific gravity of landslide material resulted in the value of 2.63. Wet sieve analysis and hydrometer analysis confirmed that the analysed soil was silty clay. The overall particle size contributions are summarised in Tab.Table 2.

Performed liquid limit and plastic limit test showed that the liquid limit is at 44% of water content and that the plastic limit is at 18% of water content resulting in plasticity index (PI), of 26%. The activity of the material is 1.35.

Table 2 Summary of cyclic tests

Gravel [%]	Sand [%]	Silt [%]	Clay [%]	LL [%]	PL [%]	PI [%]	A	ESCS symbol
1.41	20.1	59.2	19.3	46	18	26	1.35	saCl

The soil was classified according to EN ISO 146882-2 (EN/ISO 14688-2 2017). Following the classification procedure defined with standard (EN/ISO 14688-2 2017), the soil is classified as *intermediate plasticity sandy clay*.

Cyclic stress ratio

Three tests on different CSR ratio have been performed, as it is presented in Tab.Table 1. The results of cyclic stress control tests are presented in Fig.
Figure 3 and Fig. Figure 4. The variation of CSR with the number of cycles as well as variation in double amplitudes of cyclic axial deformation with respect to CRS and number of cycles are presented in Fig.
Figure 3. Different marks represent the data obtained through the cyclic triaxial test, connected with the full line, while the dashed lines are used to interpolate suggested cyclic behaviour. It is possible to notice that after the double amplitude of 0.5%, the slope of CSR with number of cycles is steeper. It is caused by the rapid loss of soil stiffens which is usually plotted as a degradation index versus a number of cycles (for eg. Vucetic and Dobry 1988). Due to the limitation in length of this paper, such results are omitted from the presentation.

Fig. Figure 4 presents the rise of pore water pressure during cyclic shearing in terms of r_u coefficient, which is often used in slope stability analysis (Bishop and Morgenstern 1960). The value of r_u is calculated as the ratio of excess pore water pressure and confining stress.

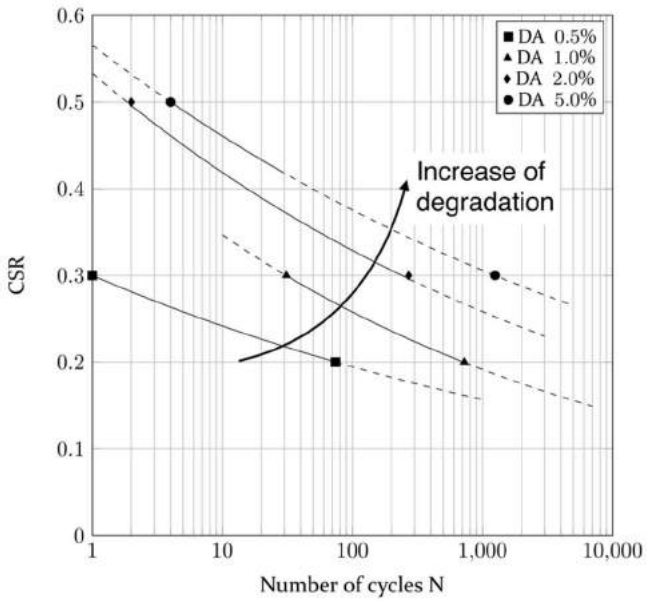

Figure 3 Variation of CSR with number of cycles with respect to double amplitude cyclic strain

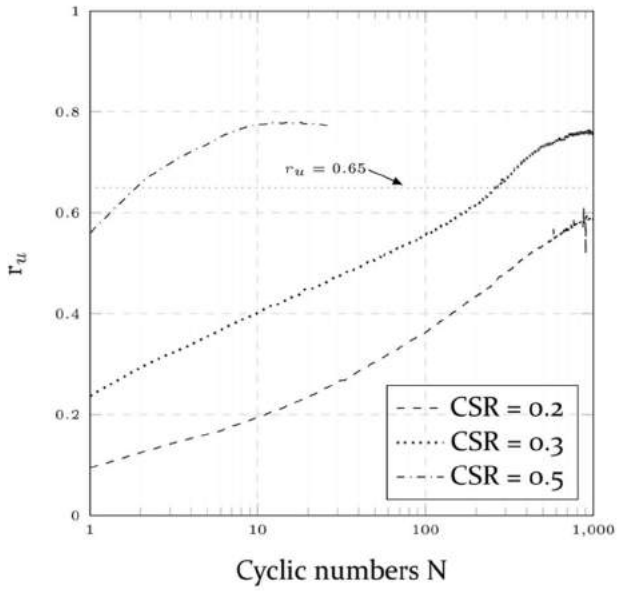

Figure 4 Change of r_u coefficient with the number of cycles

Discussions and conclusions

The first and preliminary cyclic tests of soil from the eluvial deposits originating from weathering of flysch bedrock have been performed. Along with the standard classification tests, the cyclic tests encompassed three stress control tests in order to establish basic cyclic behaviour of sliding material.

The results presented on Fig.

Figure 3 show a decrease in cyclic stress ratio with the number of cycles, no matter what the double strain amplitude is taken into account. It can be noticed that the larger the double amplitude cyclic strain impacts on steeper slope of the CRS drop. This is emphasised on the Fig.

Figure 3 where the curve representing the direction of degradation increasing. More than 70 cycles are needed for CSR = 0.2 to reach 0.5% of double amplitude cyclic axial strain, or 0.75 % of double amplitude cyclic shear strain, in comparison to CSR = 0.3, for the same double amplitude in the first cycle. In the test under CSR = 0.5, the sample reached double amplitude axial cyclic strain of 2% in the second cycle while 5% of double amplitude was reached in four cycles. Additional tests should be performed to fully capture how the 5% double amplitude changes with CSR and number of cycles N. Based on the plots in Fig.

Figure 3, the envelopes representing double amplitude axial cyclic strain are plotted. They indicate that the increase in the slope of degradation is around 0.5% of double amplitude axial cyclic strain.

The rise of excess pore water pressure with the number of cycles is plotted in Fig. Figure 4. For the CSR = 0.2 and 0.3, the slope of r_u increase is almost the same for the first 100 cycles, with very minor oscillations. The most likely reason of the concavity of the curve for CSR = 0.2 is due to Dynatriax system and the proportional, integrate and derivate error estimator. After 200 cycles a convex curvature of r_u versus number of cycles starts to form. For CSR = 0.2, the limiting stress is too small to generate sufficient excess pore pressure in material to degrade it. At CSR = 0.3 a significant increase in excess pore water pressure after 200 cycles is shown, which coincides with the r_u value of 0.65. The maximum value of r_u = 0.75 is reached at around 1000 cycles (the test was stopped at N = 1000). Sample tested at a CSR = 0.5 immediately reached the r_u value of 0.56. The nonlinear increase in r_u begun after the second cycle, which also coincided with r_u = 0.65. Within 10 cycles, sample reached the maximum value of r_u=0.77.

From results of these preliminary tests it can be concluded that the critical double amplitude cyclic axial strain is around 0.5%. Further test should be made to determine the behaviour at cyclic threshold. CSR values under 0.2 do not represent critical stress on cyclic behaviour of eluvial deposits, which are related to lower magnitudes and ground accelerations. There is a rapid increase of r_u ratio after the value of 0.58 is reached.

Based on the result of initial cyclic stress control tests it can be concluded that the degradation of fully saturated intermediate plasticity eluvial deposits starts when the double cyclic strain amplitude of 0.5% is reached. It can be achieved in only one cycle at CSR = 0.3!

The peak ground acceleration in the Vinodol Valley is expected to result the CSRs between 0.2 and 0.25. These CSR would present an issue for high frequency seismic activity with the number of cycles larger than 100. Seismic activity at lower frequencies, characteristic for the most of earthquakes in this region, would not represent a trigger for a landslide activation

Acknowledgments

The research presented in this paper was partially supported by the following projects:

- University of Rijeka uniri-tehnic-18-113 Laboratory research of static and cyclic behaviour at landslide activation
- Ministry of Science, Education and Sports of the Republic of Croatia under the project Research Infrastructure for Campus-based Laboratories at the University of Rijeka, number RC.2.2.06-0001. Project has been co-funded from the European Fund for Regional Development (ERDF).
- Croatian Science Foundation under the Project IP-2018-01-1503 Physical modelling of landslide remediation constructions behaviour under static and seismic actions (ModLandRemSS).

This support is gratefully acknowledged.

References

ASTM D0854 (2000) Standard Test Methods for Specific Gravity of Soil Solids by Water Pycnometer. Astm 2458000:1–7

ASTM D4318 (2010) Standard Test Methods for Liquid Limit, Plastic Limit, and Plasticity Index of Soils. ASTM International

Bishop AW, Morgenstern N (1960) Stability Coefficients for Earth Slopes. Géotechnique 10:129–153. doi: 10.1680/geot.1960.10.4.129

Blašković I (1999) Tectonics of Part of the Vinodol Valley Within the Model of the Continental Crust Subduction. Geol Croat 52:153–189. doi: 10.4154/GC.1999.13

Boulanger R, Idriss I (2004) Evaluating the potential for liquefaction or cyclic failure of silts and clays. Neurosci Lett 339:123–126. doi: UCD/CGM-04/01

Castro G (1975) Liquefaction and Cyclic Mobility of Saturated Sands. J. Geotech. Eng. Div. 101:551–569

Controls Group Ltd. (2017) Dynamic electromechanical triaxial systems, Controls. https://www.controls-group.com/eng/soil-mechanics-testing-equipment/dynamic-electromechanical-triaxial-systems-dynatriax-ems.php. Accessed 20 Jul 2019

Đomlija P (2018) Identification and classification of landslides and erosion phenomena using the visual interpretation of the Vinodol Valley digital elevation model (in Croatian). Faculty of Geology, Mining and Petroleum Engineering, University of Zagreb

EN/ISO 14688-2 (2017) Geotechnical investigation and testing — Identification and classification of soil — Part 2: Principles for a classification. Geneva, CH

EN ISO 14688-1 (2002) Geotechnical investigation and testing. Identification and classification of soil. Identification and description

Finn WD, Pickering DJ, Bransby PL (1971) Sand liquefaction in triaxial and simple shear tests. J Soil Mech Found Div

Herak D, Sović I, Cecić I, et al (2017) Historical seismicity of the Rijeka region (northwest External Dinarides, Croatia) - Part I: Earthquakes of 1750, 1838, and 1904 in the Bakar epicentral area. Seismol Res Lett 88:. doi: 10.1785/0220170014

Herak M, Allegretti I, Herak D, et al (2011) Map of the earthquake areas of the Republic of Croatia for Tp = 95 and Tp = 475 years(in Croatian). Državna Geod uprava (DGU), Zagreb

Highland L, Bobrowsky PT, others (2008) The landslide handbook: a guide to understanding landslides. US Geological Survey Reston

Hyodo M, Yasuhara K, Hirao K (1992) Prediction of clay behaviour in undrained and partially drained cyclic triaxial tests. Soils Found 32:117–127

Idriss IM, Boulanger RW (2008) Soil Liquefaction During Earthquakes. Earthq Eng Res Inst 136:755. doi: 10.1016/j.ajodo.2009.10.006

Kramer SL (1996) Geotechnical Earthquake Engineering. New York

Kuk V, Prelogović E (1998) Seismological and seismotectonical characteristics of NW part od Croatia. In: Mohorovičić 140. obljetnica rođenja"

Lade P V. (2016) Triaxial Testing of Soils, 1st edn. John Wiley & Sons, Ltd, London, UK

Mohamad R, Dobry R (1986) Undrained Monotonic and Cyclic Triaxial Strength of Sand. J Geotech Eng 112:941–958. doi: 10.1061/(ASCE)0733-9410(1986)112:10(941)

Pajalić S, Đomlija P, Jagodnik V, Arbanas Ž (2017) Diversity of Materials in Landslide Bodies in the Vinodol Valley, Croatia. In: Mikoš M, Vilímek V, Yin Y, Sassa K (eds) Advancing Culture of Living with Landslides. Springer International Publishing, Cham, pp 507–516

Popescu ME (2002) Landslide causal factors and landslide remediatial options. 3rd Int Conf Landslides, Slope Stab Saf Infra-Structures

Prelogović E, Blašković I, Cvijanović D, et al (1981) Seizmotectonic characteristics of the Vinodol Region (in Croatian). Geološki Vjesn 33:1–5

Rogić V (1968) Vinodol – contemporary conditions of the regional zonality relations (in Croatian). Croat Geogr Bull 30:104–125

Seed HB (1979) Soil Liquefaction and cyclic mobility for level ground during earthquakes. ASCE J Geotech Eng Div 105:201–255

Seed HB, Idriss IM (1971) Simplified procedure for evaluating soil liquefaction potential. J Soil Mech Found Div 97:1249–1273

Seed HB, Lee KL (1966) Liquefaction of Saturated Sands During Cyclic Loading. J. Soil Mech. Found. Div 1970:83–89

Seed HB, Lee KL, Chan CK (1975) Representation of Irregular Stress Time Histories by Equivalent Uniform Stress Series in Liquefaction Analyses. Earthquake Engineering Research Center, College of Engingeering, University of California

Seed HB, Peacock WH (1971) Test Procedures for Measuring Soil Liquefaction Characteristics. J Soil Mech Found Div ASCE 97:1099–1119

Vucetic M, Dobry R (1988) Degradation of Marine Clays under Cyclic Loading. J Geotech Eng 114:133–149. doi: 10.1061/(asce)0733-9410(1988)114:2(133)

doi.org/ 10.35123/ReSyLAB_2019_14

Study of slopes for Orikum-Llogara road, at Vlora County, Albania

Julian Belliu[(1)], Skender Allkja[(1)], Artila Elezi [(1)], Ardita Malaj[(1)], Klajdi Petriti[(1)]

1) A.L.T.E.A. & Geostudio 2000 ltd, Tirane-Albania, +355 68 20 74 332

Abstract Orikum-Llogara Road was built from the 1930s, but part of this road between km 7+000 up to km 13 + 500, has always had problems of slope stability. At that time there were not taken detailed geological studies and engineering measures to protect the slopes of this route, therefore after 1 or 2 years of operation, the road has slide back and the circulation has been difficult.

In 2018, it was decided to carry out a detailed geological and geotechnical study, which included: geological surveying, borings, sampling, laboratory testing and monitoring.

The purpose of this study was to decide the best variant of crossing the road, and in the most suitable area.

Reconstruction of this segment required obtaining efficient engineering measures and monitoring of slope stability, before and after taking these measures. Based on the results obtained from the inclinometers measurements, the speed of sliding motion and its depth, the designing team of the road decided to change the engineering measurements taken already.

Orikum-Llogara road segment, continues to be under monitoring and if there is seen any other movement, recalculations and more sophisticated engineering measures are a must.

More in detail, the paper will present the complete geological-engineering study with laboratory and in-situ data, carried out to explain the hazardous phenomena encountered, between km 7+000 up to km 13+500.

Keywords geological survey, laboratory testing, monitoring.

Introduction

Orikum-Himara road segment was built 80 years ago. This road has had many slope stability problems and time after times it has been repaired but not fully stabilized. In recent years, some part of the road have been completely destroyed.

Due to this fact, it has been decided to undertake a detailed study including green drilling techniques, laboratory analysis and monitoring, to verify the velocity of the movement of the landslide.

Investigations and monitoring

Geomorphology

The limestone slope above of the existing road is very steep, with average grade of the order of 80%. At the tectonic contact with the flyschoid, is the fault zone with steep subvertical cliffs with height about 45 meters. The cemented scree materials are characterized by much smoother average grades of the order of 30%.

Locally, steep cliffs also exist, which are usually the crests of very old (abandoned) landslides of the cemented screes.

The uncemented screes are characterized by very smooth grades, in general smoother than 25%. The slope grades of the flyschoid are smooth, of the order of 20-25% in areas of landslides and steeper in locations where the flyschoid is found and, in particular, in locations where there is significant presence of sandstone layers. In these locations, the average slope grades are of the order of 40%.

The river terraces are characterized by sub-horizontal morphology. Near Dukat i Ri village, where they have been eroded by the river, they form steep or even sub-vertical cliffs, with heights of the order of 15 meters.[1],[2]

Geological structure

Quaternary deposits (Q_4 pl + al)

Alluvial deposits; composed by moderately consolidated gravel, silty clay, silty sand and sand.

Quaternary deposits (Q_4 dl + el)

Colluvium deposits; represented by firm to stiff, brown to beige, silty clay, silty sand, clayey gravel.

Neogene deposits (N_2^1h; N_1^3m; N_1^3t; N_1^1b)

Represented by moderately weak, beige to grey, fractured, mudstone, sandstone and rare conglomerate.

Paleogene deposits (Pg_3^2)

Represented by moderately weak to moderately strong, mudstone and sandstone.

Limestone deposits (Cr_2, Cr_1)

These deposits are represented by moderately strong, fractured, limestone rocks. [2]

Hydrogeological condition

Upper Cretaceous limestones are karstified and thus they have very high percolation coefficient and very high permeability.

Most of the karst springs appear at the foot of the limestone slopes, at the contact surface of the limestones or the limestone screes with the much less permeable Serravalian flyschoid.

Karst springs also appear along the transverse to the river secondary fault system. Hydraulic gradient and the groundwater level inside the limestones is low. [1-4]
On table 1 are presented the underground water levels:

Table 1 Piezometer monitoring [2]

Piezometer Monitoring						
Dukat Landslide						
Date	Time	Borehole ID				
		BH-1	BH-4	BH-6	BH-10	BH-13
		Water level (m) from ground level				
01/10/2018	11:00	-3.40	-7.00	-7.30	-5.00	-7.80
04/10/2018	12:00	-3.10	-7.20	-7.43	-6.30	-7.40
24/10/2018	11:00	-3.10	-7.20	-7.60	-7.00	-7.60
26/11/2018	13:00	-2.78	-7.01	-5.40	-5.30	-6.90
04/01/2019	15:00	-2.11	-3.24	-4.53	-4.72	-5.34

Slope stability conditions, km 7+500

Factors contributing to slope instabilities

The road section of the project has been affected by several landslides and slope instabilities. [5-7]

Main factors which contribute to these phenomena are mentioned below:

1. Road section runs parallel to the overthrust of the Ionian on the Sazani zone. This overthrust has caused shearing of the Serravalian Neogene formation (flyschoid), which from an engineering geological point of view, become like flysch, but with lower compressive strength of its constituent layers (claystone / siltstone and sandstone), which are of more recent geological age.

2. The presence of the very permeable karstified limestones and dolomitic limestones above of the impermeable clayey flyschoid, with their contact being parallel to the road.

Karstic aquifer is relieved with springs appearing at the base of the limestone slopes, charging hydraulically the natural slope, which due to its composition and shearing is very prone to landslides.

3. Continuous erosion by the river, which start on the riverbanks and progress towards up-slope.

4. Loading of the natural slope, from the existing and old road embankments and other spoil materials, which have been dumped below the road in several areas.

This caused the initiation or the extension of pre-existing slope instabilities, which progressed, both towards up-slope and down-slope.

5. Flyschoid composition, consists of alterations of permeable (sandstone) and impermeable (siltstone and claystone) layers. Heterogeneity, coupled with the inclination of the natural slope, result in the appearance of artesian pressures at sandstone layers, which contribute to sliding on the weak claystone layers.

Geological field investigations included also preparing a map of the risk of sliding areas and sampling.

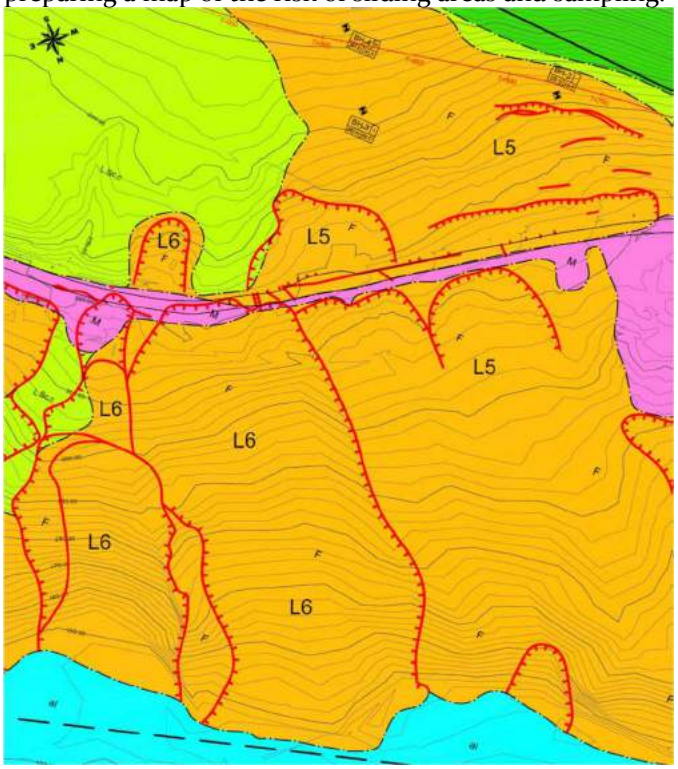

Figure 1 Geological mapping near km 7+500[2]


Figure 2 Landslide view, km 7+500[2]

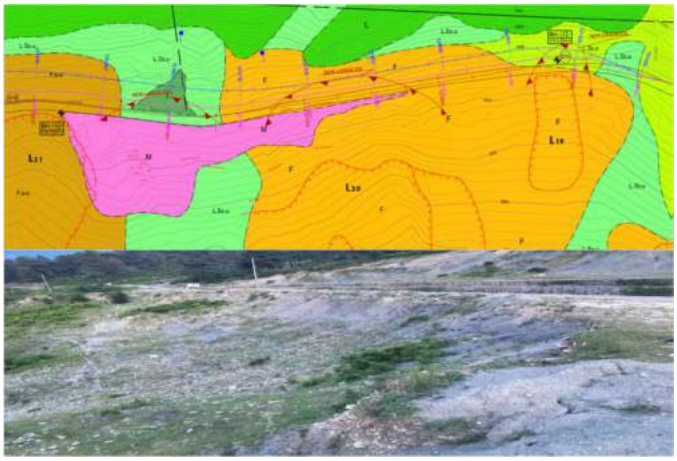

Figure 3 Landslide view, km 10+600[2]

Figure 4 Open slope near km 7+800[2]

Geotechnical investigation

On the area of unstable slopes of Orikum-Himare road, Shen Elize area the following works have been carried out: [2-4]

- 13 boreholes with depth 15.00-40.00 m,
- 2 inclinometers at BH-3 and BH-5,
- laboratory analysis

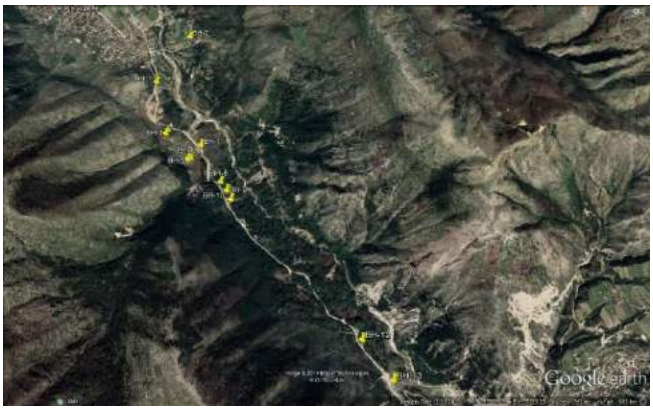

Figure 5 Location of Boreholes [2]

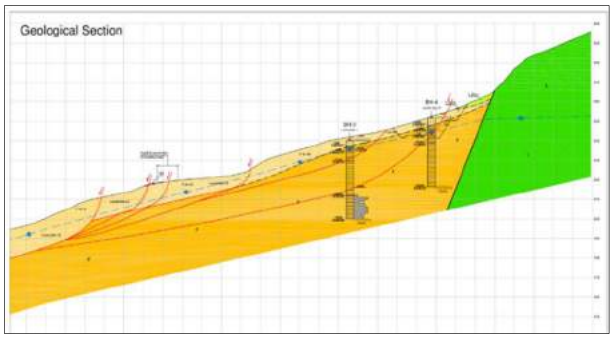

Figure 6 Geological section from borehole BH-3[2]

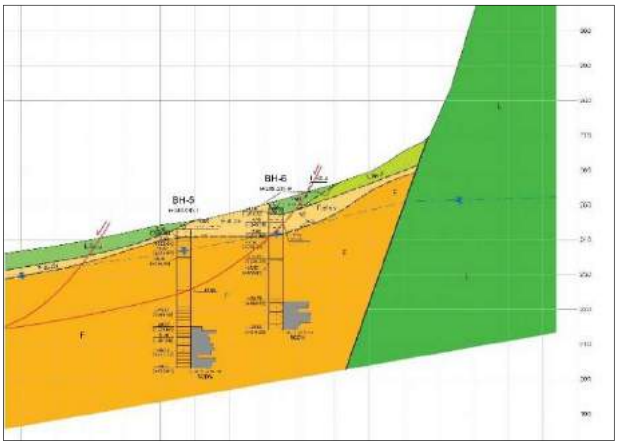

Figure 7 Geological section from borehole BH-5 [2]

In the laboratory detailed testing, are performed to obtain the necessary parameters for assessing the stability of the slopes. These testing included grain size distribution, Atterberg limits, bulk density, specific gravity, direct shear test, residual direct shear test, unconfined compressive strength test, etc...

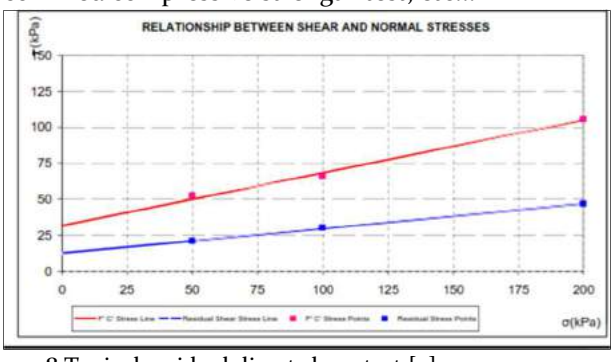

Figure 8 Typical residual direct shear test [2]

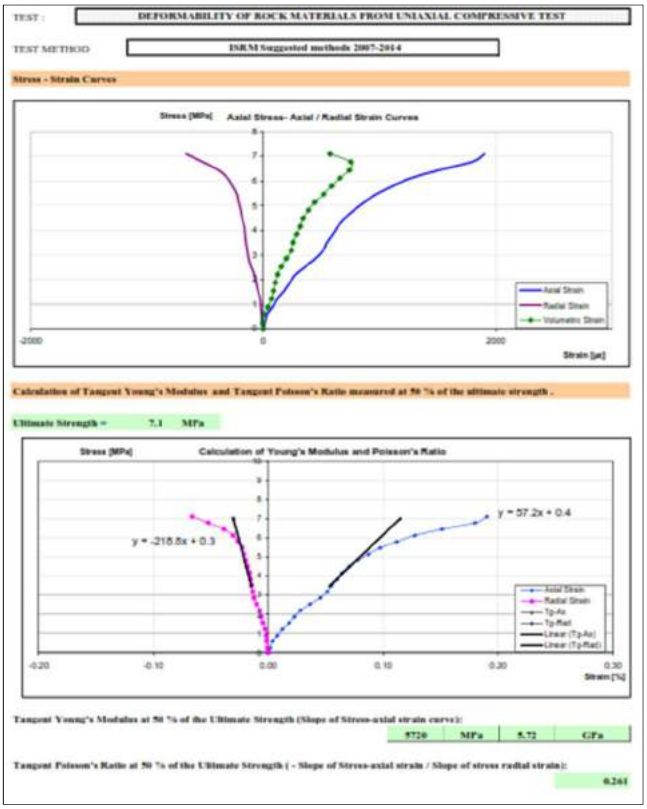

Figure 9 Typical unconfined compressive strength test[2]

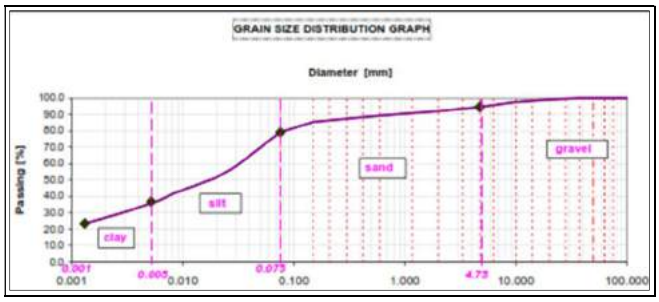

Figure 10 Grain size distribution test[2]

Monitoring of the movements of landslide

To evaluate the sliding movement velocity, we have periodically read the installed inclinometers. These inclinometer readings determined the velocity of the motion (varying depending on the hydrogeological conditions), and the maximum motion depth.

Up to the 3rd set of measurements on the 26th of November 2018, the maximum incremental displacement for BH-3 is in the order of 1mm with a rate of 0.02mm/day, while for BH-5 is in the order of 2 mm, with a rate of 0.04mm/day.

The aforementioned recorded displacements are not considered as worrying.

A 4th set of measurements was taken on the 4th of January 2019. This set of measurements has recorded an increase of the cumulative displacement from 5 mm to approximately 17mm for the inclinometer in BH-3, and from 4 mm to approximately 9mm for the inclinometer in BH-5.

The increase in the incremental displacements was from 0.5 mm to approximately 1.3 mm for the inclinometer in BH-3, and from 1 mm to approximately 5 mm for the inclinometer installed in BH-5, with the greatest values being recorded at the surface and at a depth of 16-17 m below the ground.

This increase in measurements was due to an earthquake of 4.5 magnitude that struck the region, prior to the measurement.

Following the submission of the design report on the 18th of February 2019, a 5th set of measurements was taken on the 21st of February 2019.

Based on the latest set of measurements an increase of the cumulative displacement from 17 mm to approximately 35 mm for the inclinometer in BH-3, and from 9 mm to approximately 16mm for the inclinometer in BH-5.

The increase in the incremental displacements was from 1.3 mm to approximately 3.2 mm for the inclinometer in BH-3, and from 5 mm to approximately 12 mm for the inclinometer in BH-5.

Greatest values were recorded at the surface and at a depth of approximately 26 m for BH-3 and at approximately of 16-17 m for BH-5.

The above recordings correspond to a movement rate of approximately 0.5 mm/day for the inclinometer in BH-3 and of 0.2 mm/day for the inclinometer in BH-5. It is noted that the incremental displacements for BH-3 are still considered as non-worrying.

Depth of landslide according to the measurement in 16/05/2019 for BH-3 is 26 m depth; for BH-5 is 16.00 m depth. [2-4]

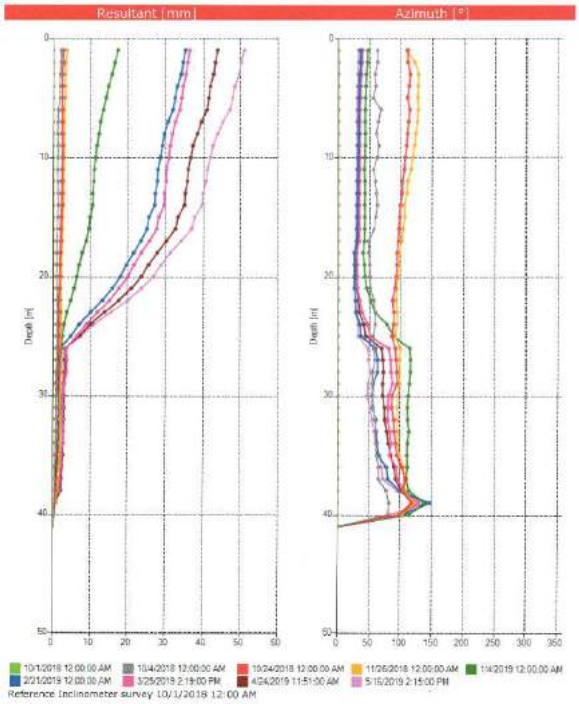

Figure 11 Inclinometer results at BH-3 from January 2018 up to May 2019[2]

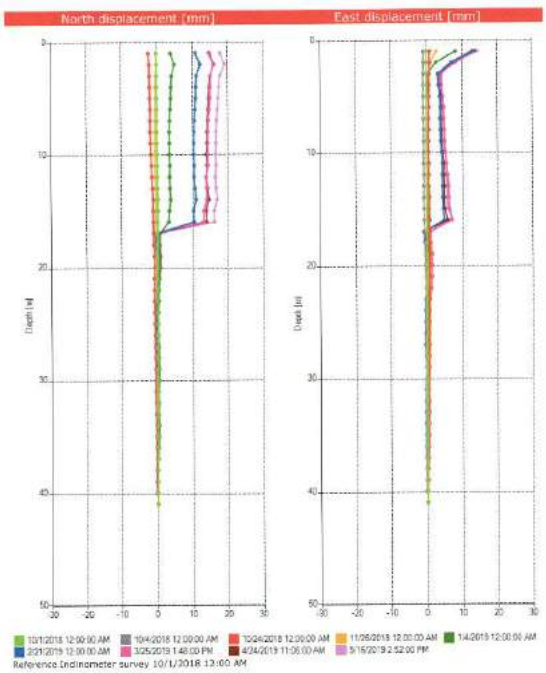

Figure 12 Inclinometer results at BH-5 from January 2018 up to May 2019[2]

The characteristics of soil and rock at the sliding area

According to field works and laboratory testing we have classified the following layers:

Layer no.1

Top soil; made ground, soft to stiff, silty clay, brown, moist, containing root plant and a little fine gravel. This layer meets the surface of the ground to a depth of 0.50 m.

We recommended removal of the layer and replacement with granular material. After that to construct the overburden layers of the road.

As most of the road is in the existing road alignment, we recommend to remove only the asphalt layers.

Layer no.2

Delluvial-elluvial deposits, represented by very stiff, silty clay, beige to light brown, moist, containing thin lenses of silty sand and pieces of flysch rock.

This layer slides in the direction of the relief downfall.

Table 2 Summary of physical-mechanical features[2]

Layer no.2	
Moisture	Wn=21.40%
Specific gravity	Gs=2.67g/cm3
Unit Weight	ɣ=1.96g/cm3
Liquid Limit	LL=39.60 %
Plastic Limit	PL=22.30%
Plastic Index	IP=17.30
Friction Angle	Φ=22.00°
Res. friction angle	Φr=8.00°
Cohesion	C'=19.00kPa
Residual Cohesion	9.00 kPa
Void Index	e=0.720
California Bearing ration	CBR=3-4%

Layer no.3

Medium dense to dense, gravel, beige to grey, moist. The gravel is medium to coarse fraction, containing breccia stone of fine, medium and coarse fraction, limestone origin.

Table 3 Summary of physical-mechanical features[2]

Layer no.3	
Moisture	Wn=13.90%
Specific gravity	Gs=2.68g/cm^3
Unit Weight	ɣ=2.06 g/cm^3
Friction Angle	Φ=30°
Cohesion	C'=15.00kPa
Void index	e=0.680
California Bearing ration	CBR=15%

Layer no.4

Eluvial deposits represented by weak to moderately weak, beige to grey, fractured mudstones and sandstone.

In some cases, this part of the basic formation, slides with overlapping formations (deluvial-eluvial deposits).

Table 4 Summary of physical-mechanical features [2]

Layer No.4	
Moisture	Wn=13.40%
Specific gravity	Gs=2.65g/cm^3
Unit Weight	ɣ=2.23 g/cm^3
Liquid Limit	LL=40.70 %
Plastic Limit	PL=21.50%
Plastic Index	IP=19.20
Friction Angle	Φ=29°
Cohesion	C'=45.00kPa
Void index	e=0.680
California Bearing ration	CBR=2-4%

Layer no.5

Weak to moderately weak, grey, mudstone and sandstone with fractures. The fractures are in dip angle 45 degree but have and small fracture in dip angle 5 degree, with undulated and slickensides surfaces.

Table 5 Summary of physical-mechanical features[2]

Layer No.5	
Moisture	Wn=9.40%
Specific gravity	Gs=2.65g/cm3
Unit Weight	ɣ=2.35 g/cm3
Friction Angle	Φ=30°
Cohesion	C'=54.00kPa
Void index	e=0.42
California Bearing ration	CBR=3-5%

Layer no.6

Moderately strong, white to grey, fractured limestone, containing small karstic caves, the fractures and cavers are filled with silty clay and are rarely empty.

Table 6 Summary of physical-mechanical features[2]

Layer No.6	
Moisture	Wn=4.50%
Specific gravity	Gs=2.66g/cm^3
Wet Unit Weight	ɣ=2.52 g/cm^3
Friction Angle	Φ=36°
Cohesion	C'=13.20kPa
Void index	e=0.16
California Bearing ration	CBR=80-100%

Engineering measures for slope stabilization

Based on the data obtained from field and laboratory testing for stabilization of the road from km 7+100 up to km 11+000, we have recommended the passage of the road in the upper quotas where the slope is more stable.

Stabilization of the road in the existing axis requires costly engineering measures, which doubtfully can stabilize the slope for a long time period.

Highway crossing will be accompanied by additional engineering measures such as: [2], [3], [7]

a) Use of canals to collate the surface waters
b) Regulation and protection of the road embankment
c) Removal of soils created by excavation outside the road area
d) Planting of the slope below the road with acacia trees, which will affect the stability of the slope
e) Effective engineering measures to reduce the erosion from the river Izvor,
f) Continuous monitoring during usage phase of the road and if recurrence of sliding it is noticed towards road direction, engineering measures should be taken to stabilize the slope

Conclusions

In the area where the new road from km 7+100 up to km 11+000 passes, quaternary deposits and rock deposits are encountered.[3],[6]

Main geotechnical risks linked to the study area are:

- some active landslides
- a relatively small landslide, (landslide L4) which requires complete stabilization
- overall stability of the road cuts, particularly in the flyschoid formation
- potential rock falls in an area where there is a proximity of steep and high limestone slopes
- potential rock falls in road cuts excavated in cemented screes and limestones, the mitigation of which requires the systematic application of suitable techniques to control the blasting damage,
- surficial weathering and erosion of the road cuts excavated in the flyschoid and in uncemented screes, which requires the systematic application of suitable erosion control measures.

At km 7 + 100 to km 11 + 000 we have encountered many active landslides.

From inclinometer measurements resulted that the movement rates are approximately 0.5 mm / day for the inclinometer in BH-3 and of 0.2 mm / day for the inclinometer in BH-5.

Effective engineering measures should be taken according to the current geological and geotechnical study.

After taking these engineering measures, the road will be monitored and, in case that there will be soil movement, additional engineering measures are a must.

Acknowledgments

The work presented here represents a collaborative effort between the authors and numerous colleagues from "A.L.T.E.A & Geostudio 2000" ltd.

References

Detailed geological report for the transmission line OH L 110 kW from Babica up to Saranda. A.L.T.E.A & Geostudio 2000, 2014

Geological & geotechnical reports for road Orikum-Shen Eliza Bridge. A.L.T.E.A & Geostudio 2000, 2018- 2019.

Geological reports prepared for landslide area at Shushica river valley. A.L.T.E.A & Geostudio 2000, 2009-2016.

Geological study for road from Vlora up to Saranda. A.L.T.E.A & Geostudio 2000, 2000-2005

Geological Hazards, Fred G. Bell. Teylor & Francis, 2006

Rock Slope Engineering Civil and Mining, Duncan C.W, Christopher W.M. Taylor & Francis, 2009

The Slope Stability, 2nd Edition, Bromhead E.N. Teylor & Francis, 2006

doi.org/ 10.35123/ReSyLAB_2019_15

Landslide types identified along carbonate cliffs using LiDAR-based DTM imagery – examples from the Vinodol Valley, Croatia

Petra Đomlija[(1)], Vedran Jagodnik [(1)], Željko Arbanas[(1)], Snježana Mihalić Arbanas[(2)]

1) University of Rijeka, Faculty of Civil Engineering, Rijeka, 51000

2) University of Zagreb, Faculty of Mining, Geology and Petroleum Engineering, Zagreb, 10000

Abstract This paper presents possibilities for landslide identification and mapping along the carbonate cliffs, on the basis of the visual interpretation of high resolution (HR) airborne LiDAR (Light Detection and Ranging) imagery. The study was performed for the carbonate cliffs (2.12 km²) located in the Vinodol Valley, Croatia. An airborne bare-earth LiDAR Digital Terrain Model of 1 m resolution was created for the study area in March 2012. Seven different topographic datasets were derived from DTM and were visually interpreted for topographic signatures specific for landslides. Totally 118 chutes are identified along the cliffs, representing the areas for rock fall initiation. Also, 25 rock irregular slides, and two rock slope deformations were identified directly from the LiDAR imagery. For several identified accumulations of rock material is considered that they represent accumulations of rock avalanches.

Keywords rock fall, rock topple, chute, rock irregular slide, rock slope deformation, rock avalanche, Vinodol Valley, LiDAR

Introduction

Very steep to almost vertical slopes where a bedrock is exposed are commonly related to rock falls and rock topples, as the predominant landslide types controlled by discontinuities in a rock mass (Cruden and Varnes 1996). Identification of an individual landslide phenomenon, especially of a relatively small one, directly from remote sensing imagery is difficult or sometimes impossible (e.g., Soeters and van Westen 1996). Still, falls and topples can be indirectly identified, based on the recognition of the cliff free face, chutes formed along the cliff, and talus deposits accumulated at the foot slope. By contrast, some other landslide types that may occur along the steep rocky slopes such as the rock irregular slide, form distinct topographic features which enable their direct identification on the remote sensing imagery. Specific morphologic characteristics of talus deposits can indicate the certain landslide type such as rock avalanche.

This paper presents different possibilities for identification and mapping of landslides occurring along the carbonate cliffs based on visual interpretation of high resolution (HR) shaded digital elevation model completed from airborne LiDAR data (Light Detection and Ranging). Seven types of LiDAR topographic datasets were derived from the 1 m Digital Terrain Model (DTM) of the Vinodol Valley in Croatia, available from March 2012. Carbonate cliffs are formed along the entire north-eastern border of the central and the south-eastern parts of the Vinodol Valley, in the total area of 2.12 km2. Five types of landslides classified according to the updated Varnes classification of landslide types (Hungr et al. 2014), were identified along the carbonate cliffs in the Vinodol Valley. Procedures of landslide identification and mapping are presented and briefly discussed for the representative examples of different landslide types.

Study area

The Vinodol Valley (64.57 km²) is situated in the NW coastal part of the Republic of Croatia (Fig. 1a). The area is predominantly rural, with more than 50 settlements connected by relatively dense road network. The valley has an elongated shape, with the length of approx. 22 km, and the maximum width of approx. 4 km. The topography of the Valley is divided into three parts (Đomlija 2018): the north-western (NW), the central, and the south-eastern (SE) part. The NW and the central parts of the Valley belong to the Dubračina River Basin, while the SE part belongs to the Suha Ričina River Basin. The prevailing elevations range from 100 to 200 m a.s.l., and maximum elevation reaches more than 900 m a.s.l. (Fig. 1b).

Valley flanks are composed of carbonate rocks, while the lower parts and the bottom of the valley are composed of flysch bedrock in a synclinal position (Blašković 1999). Flysch is mainly composed of marls, siltstones and sandstones, and is mostly covered by Quaternary soils formed by geomorphological processes active both in the carbonate and flysch rock mass (Đomlija 2018). The NE carbonate slopes of the Vinodol Valley are composed of Upper Cretaceous limestone and dolomites, and Palaeogene foraminiferal limestone (Blašković 1999). In the area between the Antovo and Novi Vinodolski settlements these carbonate slopes have the form of almost vertical cliffs (Fig. 1b), which were formed by destruction of the Cretaceous-Palaeogene anticline crest overturned in the SW direction. Cliffs are in a reverse tectonic contact with Palaeogene flysch deposits. This thrust contact is almost entirely covered by the Quaternary talus deposits.

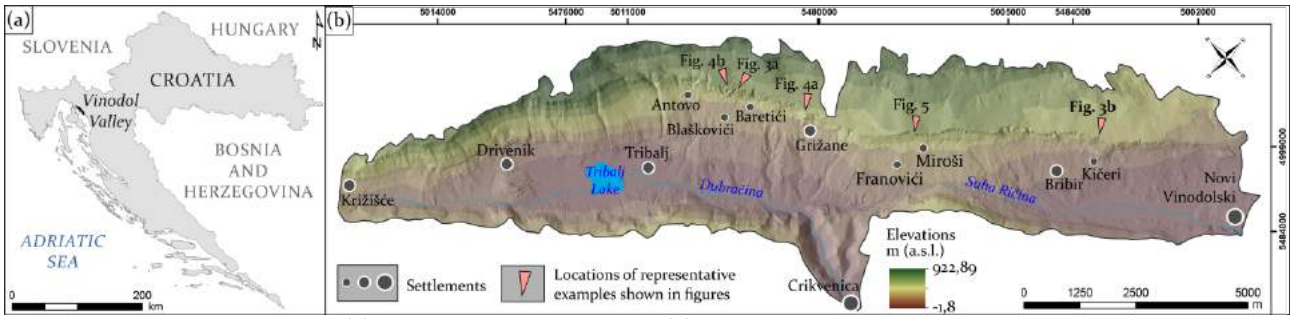

Figure 1 (a) Geographical location; and (b) relief map of the Vinodol Valley.

Carbonate cliffs represent a geomorphological unit identified in the Vinodol Valley (Đomlija 2018). The total area of cliffs is 2.12 km². Elevations range from 248 to 638 m a.s.l. in the central part, and from 90 to 555 m a.s.l. in the SE part of the Valley. Maximum slope angle is 88°. Carbonate cliffs are the highest in the area between the Antovo of Grižane settlements (Fig. 1b) in the central part of the Vinodol Valley, with the approximate hight of 200 m. The bedrock is exposed along almost the entire area of the cliffs, with sporadical vegetation, mainly transitional woodland schrubs.

Materials and method

LiDAR data

The airborne LiDAR data used in this study were acquired in March 2012, using multi-return LiDAR system (Đomlija 2018). The last returns were acquired with the density of 4.03 points per m2, with an average point distance of 0.498 m. These data were used for calculation of the 1 m bare-earth DTM. The average accuracy of the altitude data is 30 cm. Seven types of topographic datasets were derived from DTM using the standard Spatial Analyst tools in ArcGIS 10.0 software (Tab. 1) and were used for identification and mapping of landslide types along the carbonate cliffs. The hillshade maps were created using the azimuth angles of 315° and 45°, and the sun angles of 45° and 30° and then were additionally overlapped, in order to obtain the optimal shaded relief for each part of the study area (Van Den Eeckhaut et al. 2005). Contour line map was created with 1-m contour interval. Topographic roughness map was calculated according to Slope Variability Method (e.g. Popit and Verbovšek, 2013; Popit et al., 2016).

Table 1 Topographic datasets used in this study, with ArcGIS tools used for derivation from the 1 m bare-earth LiDAR DTM.

Topographic dataset (DTM image)	ArcGIS 10.0 Spatial Analyst tool used for calculation	
Hillshade map	Surface	Hillshade
Slope map		Slope
Contour line map		Contour
Aspect map		Aspect
Profile curvature		Curvature
Planform curvature		Curvature
Topographic roughness	Neighborhood	Focal Statistics
	Map Algebra	*Raster Calculator*

Visual interpretation of DTM imagery

DTM imagery were visually interpreted, singularly and in combinations, for topographic features specific for landslide phenomena that occur along steep to vertical rock slopes. These features included (Cruden and Varnes 1996; Soeters and van Westen 1996; Hungr et al. 2014): (i) distinct free face associated with (ii) talus cones and talus slopes; (iii) chutes; (iv) large concave scars; (v) tension cracks; and (vi) flow-like depositional forms of rock blocks and olistoliths accumulated at a considerable distance from the source area.

During the landslide mapping, zones of landslide accumulation were delineated first, with polygons depicting the recent talus deposits, the older talus deposits, and the accumulations of limestone olistoliths and boulders. Subsequently, a precise delineation of topographic features specific for landslides along the cliffs was performed, using polygons depicting the zones of landslide depletion. Mapping was performed in a large scale, mainly ranging between 1:100 and 1:300. Portions of individual landslide features were separately manually delineated using different DTM maps depending on their visibility on each map. Such separately drawn lines of landslide feature boundaries were subsequently merged into a unique polygon using the *ArcGIS 10.0* tools.

Landslides are classified according to the updated Varnes classification of landslide types (Hungr et al. 2014). The type of movement was determined according to the shape and size of a delineated polygon, while the material was identified based on the knowledge of geological conditions in the study area (Blašković 1999).

The visual interpretation of DTM imagery completed from airborne LiDAR data was simultaneous with the visual analysis of orthophotos, in order to check the morphological forms that were identified on DTM maps as talus deposits, as well with the field investigations, in order to identify certain landslide phenomena in the field. Almost all the accessible terrain portions situated below the cliffs, as well as at the opposite carbonate slopes overlooking the cliffs, were extensively walked by the numerous local and unnamed roads and pathways passing through the Valley.

Results

Five types of landslides (Hungr et al. 2014) are identified along carbonate cliffs in the Vinodol Valley, based on the

visual interpretation of HR DTM imagery completed from LiDAR data. These are: (a) rock fall; (b) rock topple; (c) rock irregular slide; (d) rock slope deformation; and (e) rock avalanche. Definitions of landslide types are given in Table 2.

Table 2 Definitions of landslide types (Hungr et al., 2014) identified along the carbonate cliffs in the Vinodol Valley.

Landslide type	Definition (Hungr et al. 2014)
Rock fall	Detachment, fall, rolling and bouncing of rock fragments, with little dynamic interaction between moving fragments.
Rock topple	Forward rotation and overturning of rock columns or plates, separated by steeply dipping joints.
Rock irregular slide	Sliding of a rock mass on an irregular rupture surface consisting of a number of randomly oriented joints, separated by segments of intact rock.
Rock avalanche	Extremely rapid, massive, flow-like movement of fragmented rock from a large rock slide or fall.
Rock slope deformation	Deep-seated slow to extremely slow deformation of slope, with development of cracks or faults, without a well-defined rupture surface.

Rock falls and rock topples

Rock falls and rock topples were first identified in the field along almost the entire cliff face, by numerous scars of recent landslide phenomena (Fig.2a). It is assumed that most of these scars are from rock falls, especially along the hypsometrically higher portions of cliffs. Many overhanging blocks were also identified, along the cliff face, and within chutes (Fig. 2b and 2c). Numerous potentially unstable blocks were identified along the cliffs, as well as the detached blocks (Fig. 2d).

Individual rock falls and rock topples cannot be identified on DTM maps directly. Therefore, these landslide types were indirectly mapped, with polygons depicting: (i) the cliff face, as the source area for the rock fall and rock topple phenomena; and (ii) the chutes, formed at specific place where rock falls occurred more frequently. The precise delineation of chutes (Fig. 3) was performed first, based on the visual interpretation of mainly the aspect map, since this map best reflects the V-shaped chute form, coupled with the contour line map and planform curvature map. The boundary between the cliff face and the karstic plateau located above the cliffs was delineated using the slope map (Fig. 3) mainly, from the abrupt changes of slope angle between these geomorphological units (Đomlija 2018), and the contour line map. The boundary between the cliff face and recent talus deposits was delineated using the topographic roughness map, given that this map most clearly reflects textural differences between the rough cliffs face and the smoothed recent talus deposits.

There are 118 chutes identified along the carbonate cliffs, with the total area of 0.36 km² (Đomlija 2018). The total area of the cliff face is 1.54 km². The smallest chute has an area of 125 m², and the largest chute has an area of 29,831 m². However, 75 % of all identified chutes have an area less or equal to 3,634 m². Most of the chutes have simple shape, defined by the two opposite steep sides and a central line, along which the descending debris is funnelled. Certain larger chutes are more complex, consisting of mainly two to three channel branches. In the central part of the Vinodol Valley, chutes are generally larger and are mainly formed along the entire cliff's height, with recent talus cones identified at the mouth (Fig. 3a). Chutes identified in the SE part of the Valley are smaller and are mainly formed along the hypsometrically higher cliff portions (Fig. 3b).

Rock irregular slides

Rock irregular slides were possible to identify directly on DTM maps (Fig. 4). Landslides were mapped with polygons depicting the zones of depletion. Such zones were recognized by a relatively large and concave scar with, in the most cases, visible landslide crown and flanks (purple and yellow arrows in Fig. 4). For certain landslides it was also possible to assume the portions of talus that represent the zones of accumulation (white arrow in Fig. 4a). The precise delineation of rock irregular slides was performed primarily based on interpretation of the profile curvature map (Fig. 4a), and the topographic roughness map, coupled with the contour line map.

There are 25 rock irregular slides identified along the cliffs in the Vinodol Valley. The area of the smallest landslide is 927 m², and the area of the largest landslide is 11,827 m². About 75 % of all identified landslides have an area that is less or equal to 6,096 m² (Đomlija 2018).

Rock slope deformations

Two phenomena identified along the cliffs are assumed to represent the rock slope deformation (Đomlija 2018). Both phenomena are actually formed above the cliffs at the area of the karstic plateau, such as in the example presented in Fig. 4b. In both cases, the main and only recognition features are the tension cracks, which were easily recognized already on the hillshade map. The length of the tension crack presented in Fig. 4b (blue arrows) is 136 meters. The beginning of a visible part of the crack is at the top of one of the largest complex chutes (21,851 m2) identified in the study area, and it strikes eastward along the karstic plateau. Based on the recognition of features visible on DTM imagery, it was possible to delineate the rock slope deformations only in portions of the karstic plateau which are surrounded by the tension crack and the upper cliff boundary. Such procedure was performed based on the visual interpretation of the slope map mainly (Fig. 4b), coupled with using of the profile curvature map.

Figure 2 Rock falls and rock topples identified along carbonate cliffs in the Vinodol Valley: (a) scars of recent rock falls; (b, c) chutes with overhanging blocks, rock fall scars, and associated recent talus deposits; and (d) potentially unstable an detached blocks.

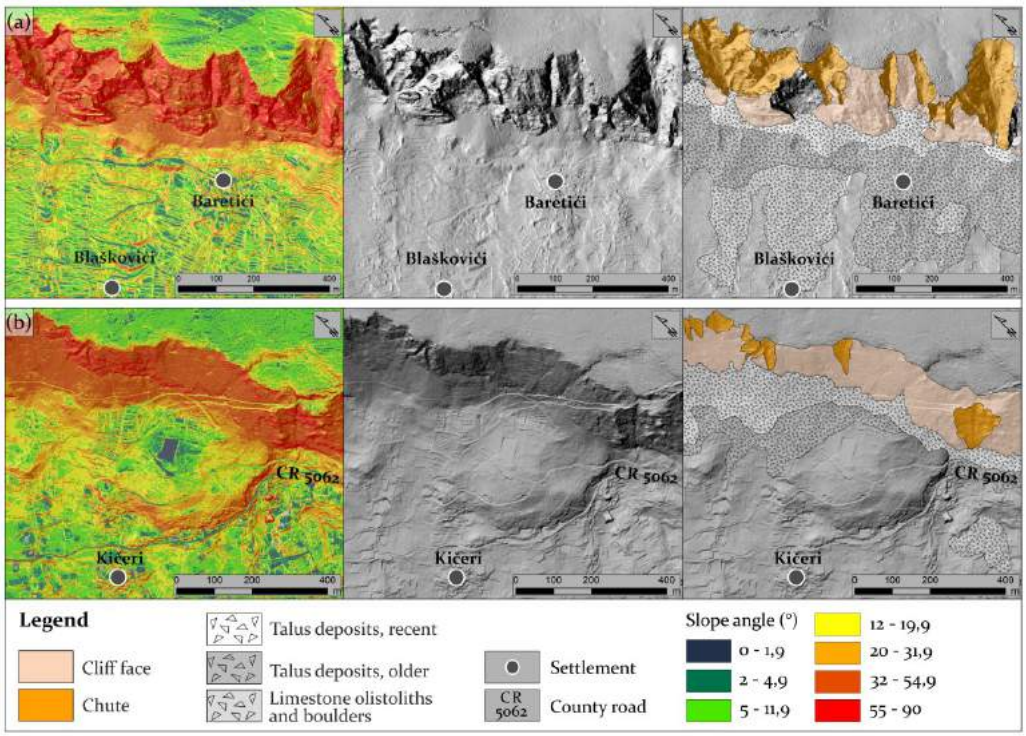

Figure 3 Examples of the rock fall and rock topple topography presented on (from left to right) the slope map, the hillshade map without, and with delineated landslide polygons, identified in: (a) the central part; and (b) in the SE part of the Vindol Valley.

Rock avalanches

The topographic features of talus deposits on DTM imagery, such as the elongated shape, the rough texture, and the topographic location of accumulated material, indicate that a certain amount of fragmented rock was transported down the slope in the form of an avalanche. A representative example of the assumed rock avalanche is presented on Fig. 5. The elongated sedimentary body (47,306 m²) that has reached the maximum distance of 366 m away from the cliffs was first identified on the hillshade map (Fig. 5b). During the field investigations, it was found that it is mainly composed of limestone boulders and olistoliths (Fig. 5c). Its rough texture is clearly visible on the topographic roughness map (Fig.

5a), and a flow-like appearance was clearly expressed on the profile curvature map. Surface roughness was identified as the most appropriate method and can be an indispensable tool for geomorphological mapping of fossil landslide (Popit, 2016). However, no topographic signatures could be with certainty identified along the cliffs, as the unambiguous source area for an assumed avalanche phenomenon. In the presented case, it is possible that the sedimentary body is actually composed of the two smaller, elongated accumulations of rock material, which may originate from a rock irregular slide phenomenon, and a large rock fall (Đomlija 2018).

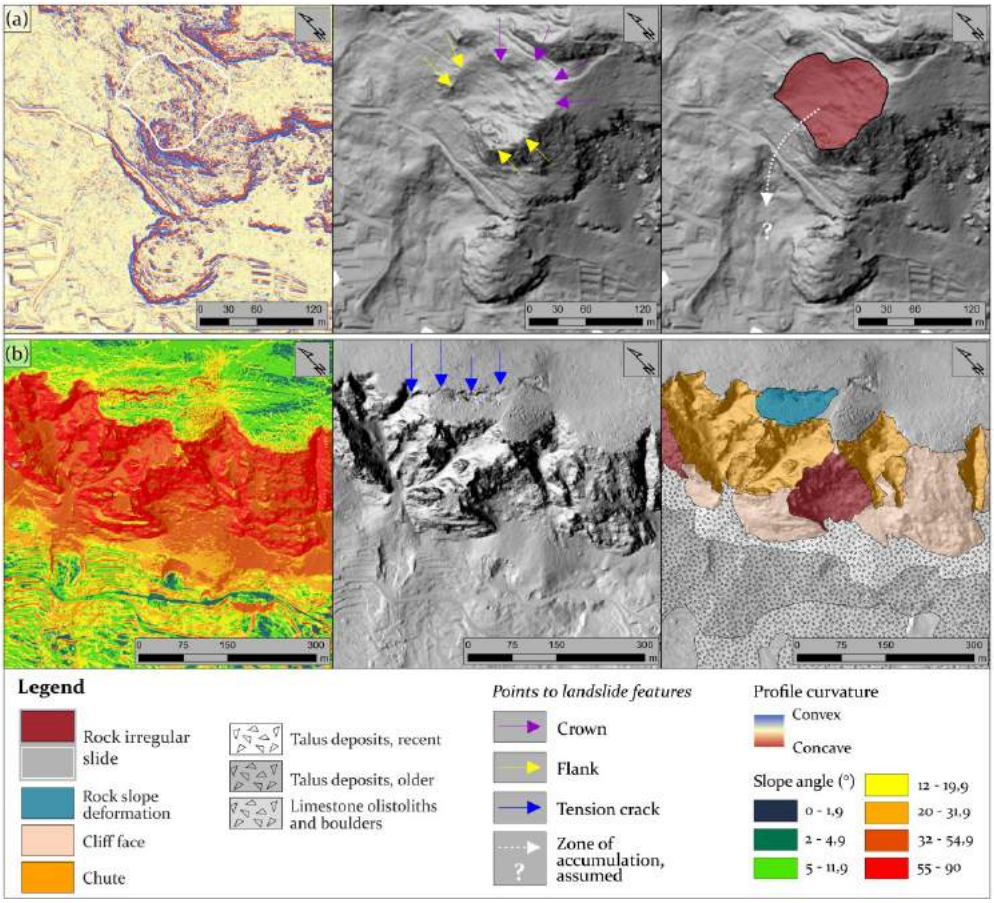

Figure 4 Examples of the: (a) rock irregular slide; and (b) rock slope deformation topography, shown on (from left to right in (a)) the profile curvature map, the hillshade map without, and with delineated landslide polygon, and on (from left to right in (b)) the slope map, the hillshade map without, and with delineate landslide polygons.

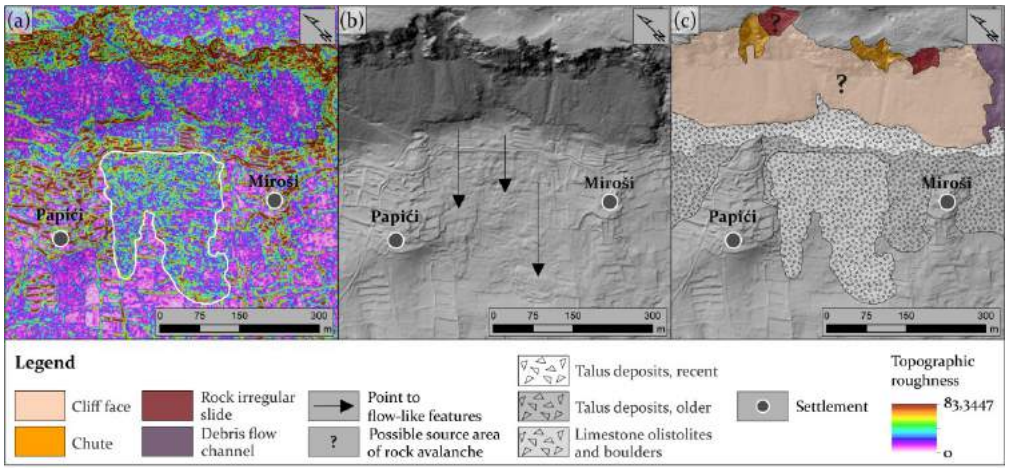

Figure 5 Example of the rock avalanche topography presented on (from left to right) the topographic roughness map, the hillshade map without, and with delineated landslide polygons, identified in the SE part of the Vinodol Valley.

Discussion and conclusions

Five types of landslides (Hungr et al. 2014) were identified along the carbonate cliffs (2.12 km2) in the Vinodol Valley, based on the visual interpretation of seven LiDAR 1 x 1 m topographic derivatives: (a) rock fall; (b) rock topple; (c) rock irregular slide; (d) rock slope deformation; and (e) rock avalanche. Based on the recognition of landslide feature topography, it was possible to directly identify only the rock irregular slides on DTM imagery. Totally 25 rock irregular slides were identified along the cliffs, according to relatively large and concave scars. All phenomena were delineated with polygons depicting only the zone of depletion (Fig. 4 and 5c). Further, it was also possible to identify the rock slope deformations directly on DTM maps, according to tension cracks formed along the karstic plateau located above the cliffs (Fig. 4b). However, these phenomena were possible to delineate only for the portions of the karstic plateau surrounded by tension cracks and the upper cliff boundary; so, their real extent remains unknown. On the other hand, direct identification of individual rock falls and rock topples on DTM imagery was not possible. These landslides were first identified in the field, where it was found that rock falls prevail. The subsequent landslide mapping on DTM imagery was performed indirectly, by delineating the cliff face, and chutes, representing the areas of rock fall and rock topple initiation. Topographic features related to rock falls and rock topples cover 90 % (1.9 km2) of the carbonate cliffs in the Vinodol Valley. Therefore, these landslides are considered to be predominant landslide type within investigated environment. Although talus deposits generally point to rock falls and rock topples (e.g., Soeters and van Westen 1996), it was difficult to identify their portions that represent the individual zones of accumulation, due to the cumulative effect of recent and historical geomorphological processes along the carbonate cliffs. However, distinct morphologic characteristics of talus deposits, and limestone olistoliths and boulders, such as the elongated shape and the rough texture, were indicative for identification of individual rock avalanches.

According to the adopted landslide mapping procedure, the geographical accuracy of results is considered to be high. However, the thematic certainty of information can potentially be reduced for a certain number of landslides, particularly for rock falls and rock topples, because it does not necessary mean that landslide phenomena occur along the entire delineated areas. There is also a possibility for relatively small topographic signatures identified as chutes that originate from a large rock wedge slide (Hungr et al. 2014). Also, certain morphological features identified as rock irregular slides could potentially be the traces of landslides initiated by some other type of motion. The remote sensing results could theoretically be improved and complemented with field data, for example with points collected at locations of identified rock falls. However, it remains difficult to accurately locate all these points on the ground, because that data collection in the field is spatially restricted by the cliff height and steep slopes. This study determined that the visual interpretation of HR DTM imagery is fully applicable method for performing the geomorphic characterization of cliff topography related to landslide phenomena. Although this method did not allow the direct identification and mapping of individual rock falls and rock topples, it is still very useful for limiting the areas where these types of landslides occurred, as well as for identification of the zones of landslide accumulation and determination of their extent, spatial distribution and volume estimation.

Acknowledgments

The results have been obtained in the frame of the Croatian-Japanese bilateral project Risk Identification and Land-Use Planning for Disaster Mitigation of Landslides and Floods in Croatia, funded by Japan Agency for Science and Technology (JST) and Japan International Cooperation Agency (JICA) through the Science and Technology Research Partnership for Sustainable Development (SATREPS) Program, and in the frame of scientific project Research of Rockfall Processes and Rockfall Hazard Assessment (uniri-tehnic-18-276) supported by University of Rijeka.

References

Blašković I (1999) Tectonics of part of the Vinodol Valley within the model of the continental crust subduction. Geologia Croatica. 52(2): 153-189.

Cruden D M, Varnes D J, (1996) Landslide types and processes. Turner, A K, Schuster, R L (eds.): Landslides, Investigation and Mitigation. Transportation Research Board, Special Report 247, Washington D.C., USA (ISBN 0-309-06151-2). 36–75.

Đomlija P, (2018) Identification and classification of landslides and erosion phenomena using the visual interpretation of the Vinodol Valley digital elevation model (in Croatian). Dissertation. University of Zagreb, Faculty of Mining, Geology and Petroleum Engineering.

Hungr O, Leroueil S, Picarelli L (2014) The Varnes classification of landslide types, an update. Landslides. 11: 167-194.

Popit T, Verbovšek, T (2013) Analysis of surface roughness in the Sveta Magdalena paleo-landslide in the Rebrnice area. RMZ – Materials and Geoenvironment. 60:197-204.

Popit, T, Supej, B, Kokalj, Ž, Verbovšek, T (2016) Comparison of methods for geomorphometric analysis of surface roughness in the Vipava valley. Geodetski vestnik, 60/2, 227-240.

Selby M J (1993) Hillslope materials and processes. Oxford University Press, Oxford (ISBN 0-19-874183-9). 320-355.

Soeters R, van Westen C J, (1996) Slope instability recognition, analysis, and zonation. Turner, A K, Schuster, R L (eds.): Landslides, Investigation and Mitigation. Transportation Research Board, Special Report 247, Washington D.C., USA (ISBN 0-309-06151-2). 129-177.

Van Den Eeckhaut M, Poesen J, Verstraeten G, Vanacker V, Moeyersons J, Nyssen J, van Beek L P H (2005) The effectiveness of hillshade maps and expert knowledge in mapping old deep – seated landslides. Geomorphology. 67: 351-363.

doi.org/ 10.35123/ReSyLAB_2019_16

Landslide hazard forecasting combining rainfall thresholds and susceptibility maps: from scientific to operational issues

Samuele Segoni[(1)], Ascanio Rosi[(1)], Veronica Tofani[(1)], Filippo Catani[(1)], Nicola Casagli[(1)]

1) University of Florence, Department of Earth Science, Firenze, Via La Pira 4, samuele.segoni@unifi.it

Abstract Operational landslide forecasting and early warning at regional scale is a very difficult task and statistical methods are the most used in this field. Landslide susceptibility maps are based on the analysis of predisposing factors to assess the spatial probability of landslide occurrence. Rainfall thresholds provide a straightforward correlation, valid on a wide area, between landslide occurrence and triggering factors (usually a couple of rainfall parameters, such as rainfall duration and intensity). While susceptibility maps are static instruments that can be used for spatial prediction, rainfall thresholds can be used for temporal prediction with a coarse spatial resolution (usually a mosaic of very wide alert zones). Rainfall thresholds and susceptibility maps can be conveniently combined into dynamic hazard matrixes to obtain spatio-temporal forecasts of landslide hazards; however, this technique is largely unexplored, and many issues need to be investigated. In this work, we describe a possible implementation of this technique into a prototype early warning system at sub-regional scale in a test site located in Northern Tuscany (Italy). We focus on the issue of the spatio-temporal aggregation of the outputs of the system, exploring a new option to find a balance between the scientific soundness and the cogent needs of end-users like mayors, local administrators and civil protection personnel.

Keywords Landslide, hazard, forecasting, early warning, rainfall threshold, susceptibility.

Introduction

Landslides are responsible for casualties and economic damages worldwide (Froude and Petley, 2018); therefore, establishing methods to forecast landslides and setting up early warning systems are cogent needs for scientists and administrators (Stähli et al., 2015; Chae et al., 2017; Piciullo et al., 2018).

A spatio-temporal forecasting of landslides can be accomplished using distributed physically based models, but due to the difficulty of getting reliable sets of distributed input data (Tofani et al., 2017), their application over large areas is still limited to few case studies, mainly presented as prototypes (Mercogliano et al., 2013; Canli et al., 2018).

Regarding regional scale applications, rainfall thresholds are the most used methods worldwide to establish early warnings (Guzzetti et al., 2007; Baum and Godt, 2010; Piciullo et al., 2018; Segoni et al., 2018a): they need only a few parameters to be defined and to be operated, and they can provide the temporal forecasting of landslide occurrences with good detail. However, their spatial resolution is very limited as the territorial units over which alarms are issued, typically have an extension of several hundreds of square kilometres (Segoni et al., 2018a).

Susceptibility maps, on the contrary, rely on the analysis of predisposing factors to assess the spatial probability of landslide occurrence (for a review, see e.g. Reichenbach et al., 2018). Thus, they can have a fine spatial resolution, but they do not carry any temporal information.

Rainfall threshold and susceptibility maps can be jointly used to estimate space and time of landslide initiation (Hong et al., 2007; Miller et al., 2009; Kirschbaum et al., 2012) or they can be combined into hazard matrixes to obtain more complex levels of landslide hazard forecasts (Segoni et al., 2015a and 2018b; Jemec Auflič et al., 2016; Tiranti et al., 2018; Wei et al., 2018).

In this paper, we combine rainfall thresholds and a susceptibility map to build a dynamic hazard matrix; moreover, we investigate the possibility of using municipalities as intermediate territorial units for landslide hazard warnings at regional scale, trying to find a compromise between scientific soundness and need for an easy interpretation and use in the complex operational chain of Italian civil protection, where landslide hazards and related warnings need to be properly understood and managed also by non-trained personnel.

Material and methods

Study area and administrative framework

The study area is located in Italy and encompasses three provinces (Lucca, Prato and Pistoia) of the Tuscany Region. It includes alluvial plains, hills, and mountains belonging to the Apennine fold and thrust belt, with a complex geological setting. The main bedrock lithologies are flyshs (mainly to the North and East) and, in the western sector, carbonatic rocks and phyllitic–schists (see e.g. Segoni et al., 2018b for further details).

According to Civil Protection organization, in each Italian Region a Functional Centre is in charge of monitoring and forecasting meteorological and hydro-geological hazards (including landslides), issuing alert

states (according to a 4-levels standardized code) in large subdivisions of the region called "alert zones" (AZ). Warnings are addressed to all the mayors of each municipality included in the alert zone deemed critical. According to Italian laws, mayors are the main local Civil Protection authorities and when alerted, they are expected to take all necessary countermeasures included in the Civil Protection Plan which had been previously studied, discussed and approved for each municipality.

The study area is divided into 5 alert zones and encompasses 72 municipalities.

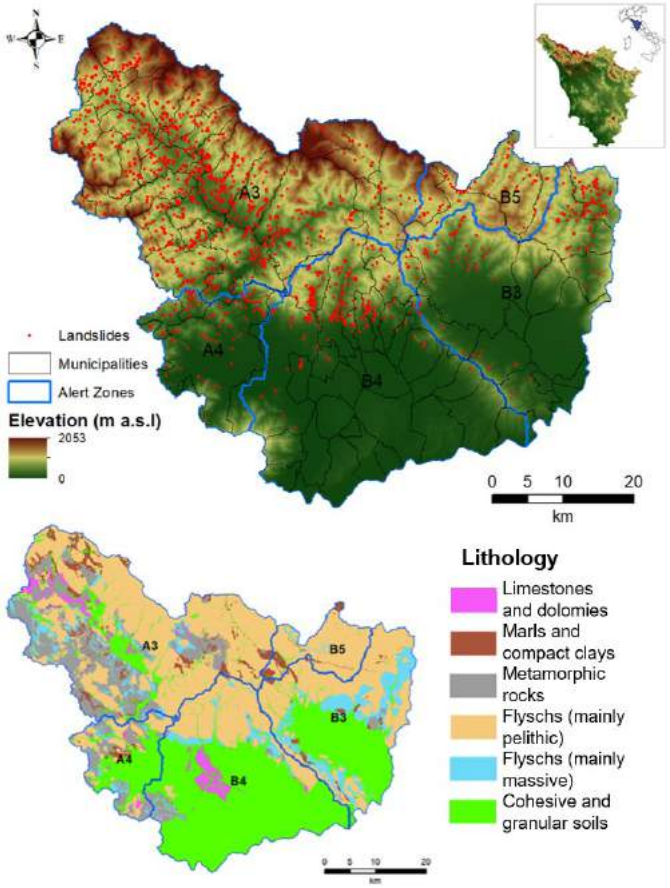

Figure 1 Test site

Basic data: rainfall thresholds and susceptibility map

In this work, we make use of a set of thresholds purposely calibrated on each alert zone (Segoni et al., 2018b). The thresholds are based on rainfall intensity and duration: this is a very popular combination of parameters since the work of Caine (1980), moreover previous studies demonstrated that in this area this approach performs better than others, based e.g. on cumulative rainfall (Lagomarsino et al., 2015). The thresholds were defined according to a robust and objective statistical approach (Segoni et al., 2014) and were further calibrated according to an extended dataset (Rosi et al., 2015). In each AZ a pair of thresholds definines three rainfall rates (R1, R2, R3) associated to increasing probability of landslide occurrence (Segoni et al., 2018b): for R1 the rainfall rate is below both thresholds (safest rainfall condition), in R3 the rainfall rate is above both thresholds (most hazardous rainfall condition) and in R2 the rainfall rate is intermediate between the two thresholds.

Concerning landslide susceptibility, we use a recent map of the area (Segoni et al., 2016), obtained by means of a software implementing the random forest treebagger algorithm (Lagomarsino et al., 2017). The map expresses the spatial probability of occurrence of landslides in a 100m sized grid of square pixels. The classification of these values into classes is original part of this work and constitutes the key step of the calibration procedure of the hazard matrix.

Susceptibility classification

The pixel resolution of the susceptibility map is not the optimal spatial unit for hazard management in our case of study: the hazards levels would be scattered across the territory, resulting in a difficult interpretation and management for mayors and non-trained personnel. Therefore, a more straightforward information is needed, and pixel outputs need to be aggregated into a synthetic output.

In this work, the susceptibility values were aggregated using administrative boundaries as the main spatial unit. As a start, each of the 72 municipalities was considered as a spatial unit. All municipalities with the territory across two alert zones were split accordingly. Moreover, for a better match with spatial distribution of typical susceptibility values, municipalities with territory pertaining to very different geomorphological settings (e.g. mountains, hills or alluvial plains), were subdivided into distinct spatial units, for a total number of 86 units at the sub-municipality level. Each unit was then characterized with a mean susceptibility value using the original data at 100m pixel resolution.

Dynamic hazard matrix

The objective of this step of the procedure is to build a dynamic matrix in which static susceptibility classes at the sub-municipality level (S1, S2, S3) are combined with dynamic rainfall rates measured (or forecasted) at the alert zone level (R1, R2, R3), to provide a dynamic output corresponding to the hazard levels expected (Fig. 2).

As suggested by Segoni et al. (2018), the effectiveness of this matrix can be maximized by a calibration procedure aimed at identifying the susceptibility values that define the susceptibility classes leading to the desired level of correct predictions/missed alarms ratio in the hazard matrix. Moreover, the calibration could be used to characterize each hazard class in terms of forecasting uncertainties or in terms of expected damage scenarios. In this study, the procedure of calibration was carried out using a landslide database composed by 1721 landslides for which the day and location of occurrence was known. The sources of information were mainly an automated search engine of

internet news (Battistini et al., 2013) and admisitrative reports (Rosi et al., 2015).

Susceptibility	Rainfall rate R1	Rainfall rate R2	Rainfall rate R3
S1	Ho	H1	H2
S2	H1	H2	H3
S3	H2	H3	H4

Figure 2 Hazard matrix combining rainfall rates and susceptibility levels into hazard classes

Each landslide was associated to the rainfall rate registered by the threshold system during the day of its occurrence and to the susceptibility value of the spatial unit where it is located. After that, it was possible to simulate the hazard classes that would have been associated to each landslide if the dynamic matrix was active at that time.

Defining the break values between the susceptibility classes is a crucial step of the methodology that influences the quality and the interpretation of the results. In this work, we adopted a two-steps procedure that maximises the correct predictions, which is a modified version of the one proposed by Segoni et al. (2018b):

1. S1-S2 break value is adjusted to have no landslides in the Ho class (misses);
2. S2-S3 break value is adjusted to get the lowest possible number of landslides in H1 class (tolerated misses), and possibly more than 95% landslides in the higher hazard classes (hits);

This procedure was applied separately for each alert zone, because each of them has peculiar physical characteristics that would reflect into different break values. Table 1 shows the optimal susceptibility values selected.

Table 1 Optimal set of mean susceptibility values for the definition of the susceptibility classes.

Alert zone	S1-S2 limit	S2-S3 limit
A3	1.55	3.20
A4	3.00	3.75
B3	3.00	3.95
B4	1.75	3.00
B5	2.15	3.35

Results and discussion

Municipality aggregation of spatial hazard

As a result of the abovementioned procedure, the 86 spatial units were classified according to three susceptibility levels, as shown in Fig. 3. S3 and S2 classes are distributed across the hilly and mountainous sectors of the study area, while S1 units are mainly located in the flat alluvial plain and, to a lesser extent, also in some hilly and mountainous areas.

This map provides an overview of the relative spatial probability of each municipality to be affected by landslides during a rainfall event.

This static dataset that can be combined with the dynamic information of the rainfall rate registered (or expected, in case of rainfall forecasts) in each alert zone. Depending on the observed combination of susceptibility level and rainfall rate, the spatial units will be associated to distinct hazard levels (as per the hazard matrix presented in Tab. 1). The result is a dynamic map that is updated whenever a rainfall rate changes over at least one alert zone. For the sake of simplicity, we call this spatial aggregation of the outputs "municipality aggregation".

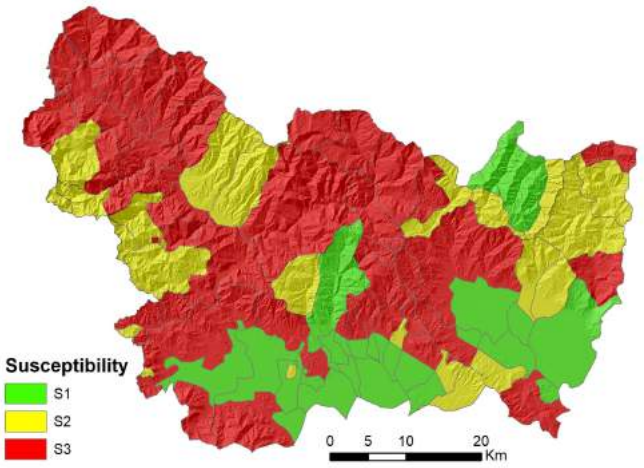

Figure 3 Classification of the sub-municipality units in S1, S2, and S3 categories, according to their mean susceptibility

Validation

The results were validated against an independent landslide dataset spanning from 01/01/2017 to 31/08/2018, obtained with an automated search engine on internet news (Battistini et al., 2017). The outputs of the proposed version of the warning system were compared to the landslide dataset and it was possible to verify the state of the system during the days when landslides occurred.

According to this validation procedure, in case of operational employ of the proposed version of the warning system, 15 landslides would have interested a sub-municipality unit alerted at the H4 level, 14 at H3, 10 at H2, none at H1 or Ho. This outcome is in line with the hazard matrix calibration (no landslides in Ho class, as few as possible landslides in H1 class and more than 95%

landslides in the other classes). More importantly, this result is obtained with a spatial resolution much finer than the original version of the warning system, as further discussed in the subsequent section.

Possible use

Usually, regional scale landslide warning systems use large alert zones as the spatial unit for monitoring the landslide hazard and for issuing the alerts (Lagomarsino et al., 2013; Segoni et al., 2015b; Rosi et al., 2016; Devoli et al., 2018; Krøgli et al., 2018; Tiranti et al., 2018). This spatial resolution is too coarse for mayors (which are in charge of taking countermeasures in their municipalities): if hazards are spatially localized, all the majors of a given AZ are alerted, while only a few of them will be actually experiencing relevant impacts. For them, the AZ warning would be a precious aid in risk management, but for all the other municipalities, a false alarm could be perceived, even if the hazard prediction is correct at the alert zone level.

Segoni et al. (2018b) combined rainfall thresholds and susceptibility maps to increase the spatial resolution of the warning system up to the pixel scale. However, this improvement has the drawback of providing an output that is very complicated to understand for mayors, as it carries a very fine spatial detail that is difficult to properly address in the operative response.

We believe that the approach proposed in this paper is a good trade-off between these two situations. From a scientific point of view and concerning spatial resolution, municipalities undoubtedly represent an improvement with respect to alert zones. As instance, in the study area the average extension of every municipality is about 36 km², while the area of the alert zones ranges from 252 to 1163 km². At the same time, municipalities are better than small pixels concerning operational issues such as emergency response and activation of countermeasures by the mayors. This is shown also by Fig. 4, where a typical situation is depicted, and the three aforementioned methods are visually compared: the traditional alert zone output provides a very coarse spatial resolution (Fig. 4a), and the pixel detail proposed by Segoni et al. (2018b) is too complicated to be understood and used by mayors (Fig. 4b). The output resolution proposed in this work (municipality) (Fig. 4c), proposes a spatial aggregation in which a scientific assessment is provided with a spatial aggregation perfectly matching the administrative level in charge of emergency response, thus easing a straightforward operational application.

Conclusion

We combined rainfall thresholds and a landslide susceptibility map to obtain a prototype version of a regional scale landslide warning system using municipalities as a basic spatial unit. The combination between the static input provided by the susceptibility map and the dynamic input provided by the rainfall thresholds is obtained by means of a hazard matrix that combines three susceptibility classes and three rainfall rates into four possible hazard levels.

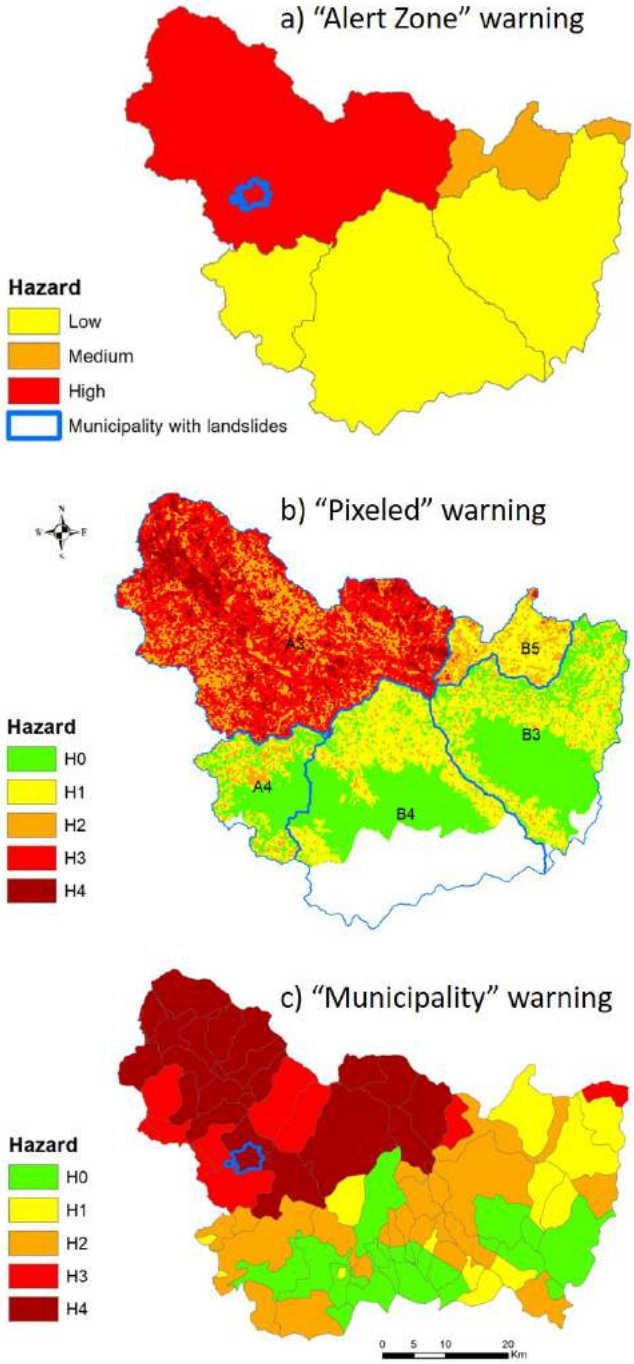

Figure 4 Representation of different output aggregations of the warning system for the day 28-12-2017 (validation period): a) is the original configuration providing warnings at the alert zone level; b) is the output proposed by Segoni et al. (2018ba), which is based on 100m x 100m pixels; c) sub-municipalities aggregation proposed in this work

The susceptibility values were aggregated at the municipality level and reclassified in three classes. The choice of the susceptibility values to break the

susceptibility classes was the result of an optimization procedure calibrated with 1721 landslides, for which time and location of occurrence was known with good approximation. The optimization procedure was carried out during the calibration of the hazard matrix and allows for linking the hazard classes to the desired level of statistical confidence in the results.

A validation procedure provided encouraging results. In particular, the approach of using municipalities as spatial units for the warning system brought two advantages: first, it increased the spatial resolution with respect to the original version of the warning system; second, it perfectly matched the administrative level that is most involved during the emergency response procedures, since mayors are the main local authorities of civil protection according to Italian regulation.

References

Battistini A, Segoni S, Manzo G, Catani F, Casagli N (2013) Web data mining for automatic inventory of geohazards at national scale. Applied Geography. 43:147-158.

Battistini A, Rosi A, Segoni S, Lagomarsino D, Catani F, Casagli N (2017) Validation of landslide hazard models using a semantic engine on online news. Applied geography. 82: 59-65.

Baum R L, Godt J W (2010) Early warning of rainfall-induced shallow landslides and debris flows in the USA. Landslides. 7(3): 259-272.

Caine N (1980) The rainfall intensity-duration control of shallow landslides and debris flows. Geografiska annaler: series A, physical geography. 62(1-2): 23-27.

Canli E, Mergili M, Thiebes B, Glade T (2018) Probabilistic landslide ensemble prediction systems: lessons to be learned from hydrology. Natural Hazards and Earth System Sciences. 18(8): 2183-2202.

Chae B G, Park H J, Catani F, Simoni A, Berti M (2017) Landslide prediction, monitoring and early warning: a concise review of state-of-the-art. Geosciences Journal. 21(6): 1033-1070.

Devoli G, Tiranti D, Cremonini R, Sund M, Boje S (2018) Comparison of landslide forecasting services in Piedmont (Italy) and Norway, illustrated by events in late spring 2013. Natural Hazards Earth System Sciences. 18(5): 1351-2018.

Froude M J, Petley D (2018) Global fatal landslide occurrence from 2004 to 2016. Natural Hazards and Earth System Sciences. 18: 2161-2181.

Guzzetti F, Peruccacci S, Rossi M, Stark CP (2007) Rainfall thresholds for the initiation of landslides in central and southern Europe. Meteorog Atmos Phys. 98:239–267.

Hong Y, Adler R F, Huffman G (2007) An experimental global prediction system for rainfall-triggered landslides using satellite remote sensing and geospatial datasets. IEEE Transactions on Geoscience and Remote Sensing. 45(6). 1671-1680.

Jemec Auflič M, Šinigoj J, Krivic M, Podboj M, Peternel T, Komac M (2016) Landslide prediction system for rainfall induced landslides in Slovenia (Masprem). Geologija. 59(2): 259-271.

Kirschbaum D B, Adler R, Hong Y, Kumar S, Peters-Lidard C, Lerner-Lam A (2012). Advances in landslide nowcasting: evaluation of a global and regional modeling approach. Environmental Earth Sciences. 66(6): 1683-1696.

Krøgli I K, Devoli G, Colleuille H, Boje S, Sund M, Engen I K (2018) The Norwegian forecasting and warning service for rainfall- and snowmelt-induced landslides. Nat Hazards Earth Syst Sci. 18: 1427-1450.

Lagomarsino D, Segoni S, Fanti R, Catani F (2013) Updating and tuning a regional-scale landslide early warning system. Landslides. 10: 91-97.

Lagomarsino D, Segoni S, Rosi A, Rossi G, Battistini A, Catani F, Casagli N (2015) Quantitative comparison between two different methodologies to define rainfall thresholds for landslide forecasting. Natural Hazards and Earth System Sciences. 15(10): 2413-2423.

Lagomarsino D, Tofani V, Segoni S, Catani F, Casagli N (2017) A tool for classification and regression using random forest methodology: applications to landslide susceptibility mapping and soil thickness modeling. Environmental Modeling & Assessment. 22(3): 201-214.

Mercogliano P, Segoni S, Rossi G, Sikorsky B, Tofani V, Schiano P, Catani F, Casagli N (2013) Brief communication: A prototype forecasting chain for rainfall induced shallow landslides. Nat. Hazards Earth Syst. Sci. 13: 771-777.

Miller S, Brewer T, Harris N (2009) Rainfall thresholding and susceptibility assessment of rainfall-induced landslides: application to landslide management in St Thomas, Jamaica. Bulletin of Engineering Geology and the Environment. 68(4): 539.

Piciullo L, Calvello M, Cepeda J (2018) Territorial early warning systems for rainfall-induced landslides. Earth-science reviews. 179: 228-247.

Reichenbach P, Rossi M, Malamud B, Mihir M, Guzzetti F (2018) A review of statistically-based landslide susceptibility models. Earth-science reviews. 180: 60-91.

Rosi A, Lagomarsino D, Rossi G, Segoni S, Battistini A, Casagli N (2015) Updating EWS rainfall thresholds for the triggering of landslides. Natural Hazards. 78(1): 297-308.

Rosi A, Peternel T, Jemec-Auflič M, Komac M, Segoni S, Casagli N (2016) Rainfall thresholds for rainfall-induced landslides in Slovenia. Landslides. 13(6): 1571-1577.

Segoni S, Rossi G, Rosi A, Catani F (2014) Landslides triggered by rainfall: A semi-automated procedure to define consistent intensity–duration thresholds. Computers & Geosciences: 63: 123-131.

Segoni S, Lagomarsino D, Fanti R, Moretti S, Casagli N (2015a) Integration of rainfall thresholds and susceptibility maps in the Emilia Romagna (Italy) regional-scale landslide warning system. Landslides. 12:773–785.

Segoni S, Battistini A, Rossi G, Rosi A, Lagomarsino D, Catani F, Moretti S, Casagli N (2015b) Technical note: an operational landslide early warning system at regional scale based on space–time-variable rainfall thresholds. Nat Hazards Earth Syst Sci 15:853–861. https://doi.org/10.5194/nhess-15-853-2015

Segoni S, Tofani V, Lagomarsino D, Moretti S (2016) Landslide susceptibility of the Prato–Pistoia–Lucca provinces, Tuscany, Italy. Journal of Maps. 12(sup1): 401-406.

Segoni S, Piciullo L, Gariano S L (2018a) A review of the recent literature on rainfall thresh-olds for landslide occurrence. Landslides. 15:1483–1501

Segoni S, Tofani V, Rosi A, Catani F, Casagli N (2018b) Combination of rainfall thresholds and susceptibility maps for dynamic landslide hazard assessment at regional scale. Front Earth Sci 6:85. https://doi.org/10.3389/feart.2018.00085

Stähli M, Sättele M, Huggel C, McArdell B W, Lehmann P, Van Herwijnen A, Berne A, Schleiss M, Ferrari A, Kos A, Or D, Springman S M (2015) Monitoring and prediction in early warning systems for rapid mass movements. Nat Hazards Earth Syst Sci. 15: 905-917.

Tiranti D, Nicolò G, Gaeta A R (2018) Shallow landslides predisposing and triggering factors in developing a regional early warning system. Landslides. https://doi.org/10.1007/s10346-018-1096-8

Tofani V, Bicocchi G, Rossi G et al. (2017) Soil characterization for shallow landslides modeling: a case study in the Northern Apennines (Central Italy). Landslides. 14:755-770.

Wei L W, Huang C M, Chen H, Lee C T, Chi C C, Chiu C L (2018) Adopting the I_3–R_{24} rainfall index and landslide susceptibility for the establishment of an early warning model for rainfall-induced shallow landslides. Nat. Hazards Earth Syst. Sci. 18:1717-1733.

doi.org/ 10.35123/ReSyLAB_2019_17

Development of physical model of landslide remedial constructions' behavior

Željko Arbanas[(1)], Sara Pajalić[(1)], Vedran Jagodnik[(1)], Josip Peranić[(1)], Martina Vivoda Prodan[(1)], Petra Đomlija[(1)], Sanja Dugonjić Jovančević[(1)], Nina Čeh[(1)]

1) University of Rijeka, Faculty of Civil Engineering, Rijeka, Croatia, Radmile Matejčić 3, spajalic@uniri.hr

Abstract Physical modelling of landslides using scaled landslide models behavior began at the end of 1980s when behavior of flow slides and liquefaction of sliding materials were investigated in a scaled physical model (so called flume or flume test). The main purpose of landslide physical modelling in the last 25 years was research of initiation, motion and accumulation of fast flow like landslides caused by infiltration of water in a slope. Existing studies of landslide remedial constructions' behavior using physical modelling are very rare. In October 2018, at the Faculty of Civil Engineering, University of Rijeka, started a four-year research Project Physical modelling of landslide remediation constructions' behavior under static and seismic actions, funded by the Croatian Science Foundation. The main Project aim is modelling of landslide remedial constructions' behavior in physical models of scaled landslides in static (rainfall triggered landslides) and seismic conditions (earthquake triggered landslides). Static landslide triggering conditions will be reached by artificial rainfall using a rainfall simulator, while the seismic landslide triggering conditions will be induced by a pair of shaking platforms. Landslide movements will be observed with an innovative photogrammetric equipment and complex sensor network with ability to measure displacements, pore pressures and force pressures within a landslide body as well as at an applied remedial construction. Several different remediation constructions are planned to be embedded and their behavior tested in the small scale model: retaining walls, pile walls, buttressing and drainage systems. All measured data and results will be imported in 3D numerical model for stress-strain analysis. Results from both physical and numerical modelling will provide better insight into behavior of landslide remedial constructions in engineering practice. In this paper the development of the physical model platform will be described as well as some observations about conditions that should be reached during the small scale modelling research.

Keywords physical modelling, landslides, rainfall, earthquake, remediation

Introduction

Landslides are one of the most important geohazards that threaten vulnerable human settlements in mountains, cities, along river banks, coasts and islands. Due to climate change we are witnesses of an increase in the frequency and/or intensity of heavy rainfall, as well as shift of locations and periodicity of rainfall, which significantly increase landslide risk in landslide prone areas. Urban expansion due to population growth, development of coastal and mountain areas, construction of roads and railways increase exposure to the landslide hazard. Strong earthquakes are the second triggering factor for numerus rapid and long runout landslides in seismically active areas.

Risk reduction by human intervention is manifested through urban planning, building codes, land use, risk assessment, early warning systems, and most of all, substantial educational and awareness-raising efforts by relevant parties. According to Petley (2012), landslides cause human causalities and substantial economic damages every year all around the World. Croatia is also affected by landslide occurrences (Mihalić Arbanas et al. 2017) and some parts of Croatia were hit by massive landslide occurrences that caused significant damages (Bernat et al. 2014).

Scientists and professionals dealing with landslide risk reduction, continually develop the landslide science in different directions such as landslide identification, mapping and investigation; landslide susceptibility, hazard and risk assessment; soil and rock testing; landslide modelling and simulation; landslide monitoring, and landslide mitigation and remediation. For a long time landslide modelling was based on numerical modelling only. Development of numerical methods started from the simple 2D limit equilibrium method (LEM) and, with advancement of computer power, progressed to the 3D limit equilibrium method (LEM) and more advanced finite element method (FEM) in landslide analysis (Duncan 1996).

Physical modelling of landslides using scaled landslide models behavior began at the end of 1980s at the James Cook University in Australia where in a scaled physical model (also known as flume or flume test) behavior of flow slides and liquefaction of sliding materials were investigated (Eckersley 1990). The main purpose of landslide physical modelling in the last 25 years was research of initiation, motion and accumulation of fast flow like landslides caused by infiltration of water in a slope (Wang and Sassa 2001).

The established models and research can be divided into two main groups related to the main landslide triggering factors: rainfall and earthquakes. The main problem in small scale landslide modelling is test conducting at 1.0g that requires very precise scaling of soil parameters. This deficiency was successfully overcome in centrifuge modelling (e. g. Take et al. 2004) but this type of testing was limited by very small landslide model dimensions that would be useful in modelling of real landslides and modelling of landslide remedial constructions.

A four-year research Project Physical modelling of landslide remediation constructions' behavior under static and seismic actions, funded by the Croatian Science Foundation, started in October 2018 at the Faculty of Civil Engineering, University of Rijeka. The main Project aim is modelling behavior of landslide remedial constructions in physical models of scaled landslides in static and seismic conditions.

Physical model

Because of differences in main triggering factors as landslide causes, physical model will be designed for two different actions - one model for static actions (Fig. 1) and one for seismic actions (Fig. 2). Methodology of the Project research consist of the following phases: i) design, construction and testing of the platform for a landslide model; ii) installation of the measuring equipment; iii) construction of slope model; iv) testing a model in static and seismic conditions (with and without remediation measures); v) analysis of measured data and comparison with results of numerical simulations; vi) calibration of equipment and improvement of the model; and lastly vii) reiteration of the same phases of testing. Approximate layout dimensions of the model platform are 1.5x2.0m and a depth of soil slope till 0.50m. The platform will have possibility to adjust slope angle and different depths of built-in slope material.

Static model

Physical model of a scaled landslide under static actions, where the landslide triggering factor is rainfall, was designed to enable initiation of a landslide caused by controlled artificial rainfall and equipped with adequate photogrammetric equipment and complex sensor network with ability to measure displacements, pore pressures and soil pressures within a landslide body (Fig. 1).

An important issue in physical models to simulate landslide initiation and motion caused by rainfall infiltration is full controlled intensities of artificial rainfall and there are many researches related to simulation of artificial rainfall using developed sprinkler systems used in landslides and soil erosion studies (e.g. Iserloh et al. 2012; Lora et al. 2013).

Although it would possible to use some of developed rainfall simulators (Iserloh et al. 2012; Lora et al. 2013); there is necessity for developing of rainfall simulator that will be adjusted to the rainfall intensities characteristic for precipitation events in Croatia. Construction of rainfall simulator will include ordinary elements usually used for watering plants and will have the ability to control intensity, flow, uniformity of wetting and time of rainfall simulation. Rainfall simulator will consist of system of sprinklers with different types of nozzles.

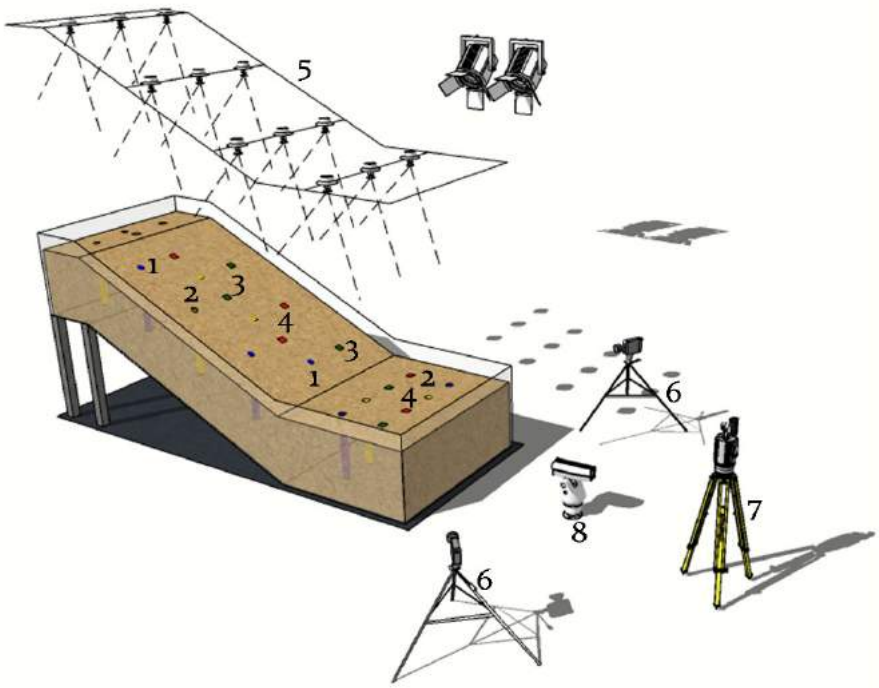

Figure 1 Physical model for static actions: 1-tensiometers, 2-pore pressure transducers, 3-strain gauges, 4-accelerometers, 5-rainfall simulator (sprinkler system), 6-high speed cameras, 7-terrestrial laser scanner, 8-infrared camera

Nozzles number, placement and height will be variable depending on the required rainfall intensity and type of soil material that will be built-in in the testing model. The supply of the system should be controlled by flow meters to enable uniform precipitations over the whole model. Before the use, the rainfall simulator should be tested and calibrated in different regimes to enable adequate simulation of real precipitations applied to the model.

Dynamic model

Physical model of a scaled landslide under seismic actions, where the landslide triggering factor is an earthquake, was designed to enable initiation of a landslide triggered by shaking caused by artificial earthquake or to control possible landslide occurrence caused by a historical landslide with registered accelerogram from earthquake database. (Fig. 2). Although the number of earthquake triggered landslides in Croatia is relatively low, according to the seismicity of some parts of Croatia including the wider area of the City of Rijeka, earthquakes could be a landslide triggering factors in the future. A list of most important historical earthquakes in the Rijeka Region (Herak et al. 2017, 2018) is listed in Tab. 1. The most significant earthquake triggered landslide in Croatia is the Grohovo Landslide triggered by the Rijeka Earthquake 1750, with the epicentre in the immediate vicinity of the City of Rijeka (Arbanas et al. 2014).

Table 1 List of the most significant historical earthquakes in the Rijeka Region (modified according to Herak et al. 2017, 2018). The intensity and damage are described according to Medvedev-Sponheuer-Karnikov (MSK) scale.

Locality	Year	I_{max} by MSK	MSK 64 Scale
Rijeka	1750	VIII	Damaging
Krk	1838	VII	Very strong
Klana	1870	VIII	Damaging
Krasica	1904	VI - VII	Strong to very strong

The most of existing researches, that studied landslide initiation and motion caused by an earthquake, used shaking tables that induce vibration corresponding with natural or artificial earthquake seismograms and accelerograms. The main goal of these studies was determination of seismic slope behavior or seismic response and failure of slope material (e.g. Wang and Lin, 2011; Fan et al. 2016).

Seismic impulses will be induced by a pair of shaking platforms (Quanser STI-II biaxial shaking platforms) commonly used for structures testing under cyclic loading in the Laboratory of structures at the Faculty of Civil Engineering University of Rijeka. The dynamic model platform is designed according to the limitations that arise from shaking tables' characteristics (dimensions and mass of testing object). During the testing, the pair of shaking platforms will be synchronized for joint dynamic action (shaking) in direction of the model slope.

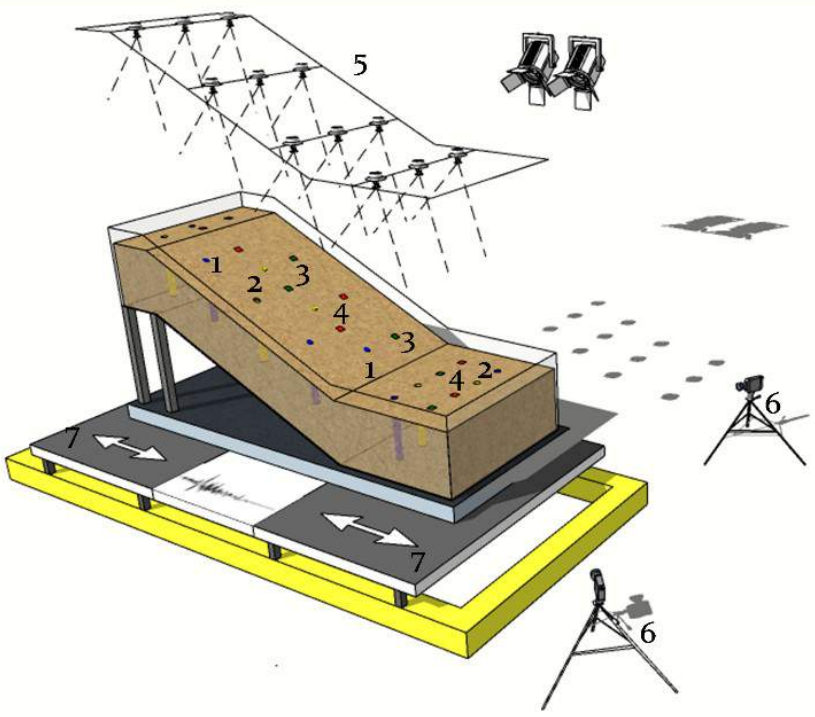

Figure 2 Physical model for seismic actions: 1-tensiometers, 2-pore pressure transducers, 3-strain gauges, 4-accelerometers, 5-rainfall simulator (sprinkler system), 6-high speed cameras, 7-biaxial shaking tables

Measuring equipment

The selection of the measuring techniques and equipment in the physical model follows the practice of monitoring systems established on real landslides. In that sense, the sensor systems used in physical models can be divided in geotechnical monitoring systems and geodetic monitoring systems (Mihalić Arbanas and Arbanas 2015).

Geodetic monitoring will be based on innovative photogrammetric equipment for multi-temporal landslide analysis (Zanuta et al. 2006) from stereo image sequences obtained by pair of high speed cameras (Feng et al. 2016). As an additional tool, an infrared camera will be used for thermal analysis by infrared tomography (IRT) that enables determination of zones in a slope where the landslide process causes changes in moisture, stress and temperature in zones of shearing, tension or raising pressures. IRT will be used in combination with terrestrial laser scanner (TLS) which makes it more efficient (Frodella et al. 2017). TLS survey will enable determination of reached 3D landslide surface or high resolution digital model of a landslide model after sliding very precisely.

Geotechnical monitoring will be consisted of a complex network of miniature sensors equivalent to those used in geotechnical monitoring in the field (Wieczorek and Snyder 2009). Built-in sensors will have ability to measure displacements, pore pressures, soil pressures and contact forces through the soil profile in the model and at an applied remedial construction. The sensors intended to be used and their purposes are listed in Tab. 2. All sensors used in the model will be connected to data loggers for continuous data collection during the test.

Table 2 Measuring equipment in the model.

Sensor number	Measuring equipment	Measurement
1	Tensiometers	Suction
2	Pore pressure transducers	Pore water pressure
3	Strain gauges	Strain
4	Accelerometers	Acceleration
5	Rainfall simulator	Rainfall intensity

Materials and remediation

It was planned to include three main landslide models and their testing in static and dynamic conditions without and with applied remediation measures. The first model will be the simplest one and the model complexity will rise through the upcoming phases and steps of research. The basic model will use sandy soil because of relatively simple behavior of infiltration process and failure triggering and it will be fast and easy to reach the critical stability state. During the establishment of the slope model the scaling procedure will be tested and defined. Model will serve its main purpose to test the functionality of the designed platform models, embedded equipment and planned testing procedures. In the next phases of the Project, more complex soil materials will be built in the models, ranging from silty to clayey soil. These soil materials will have an increase in shear strength in unsaturated conditions while through infiltration they will lose shear strength due to reduction in suction and rise of pore pressures until the slope failure. The soil materials used for slope models will be

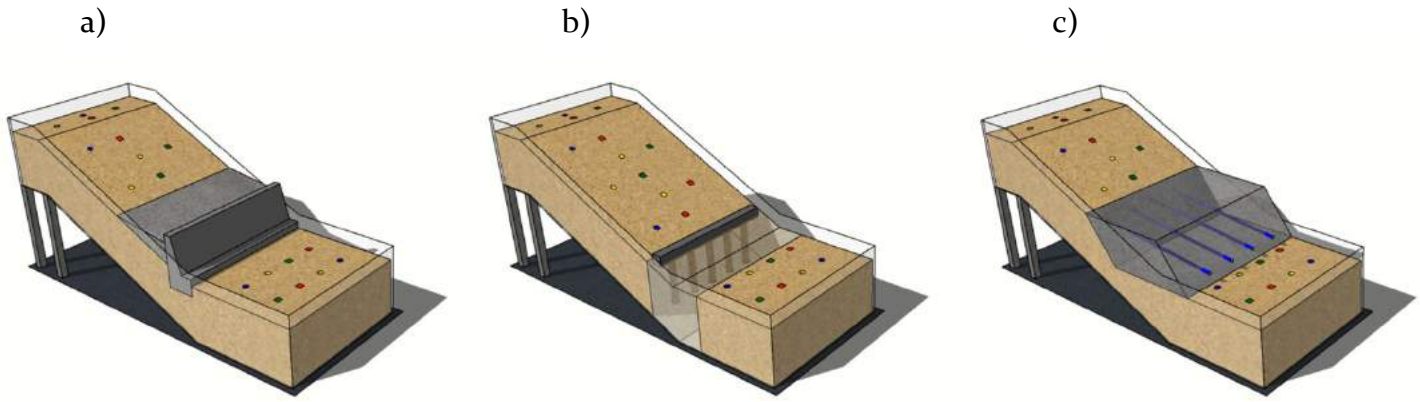

Figure 3 Physical model with different remediation constructions – a) retaining wall; b) pile wall; c) buttressing with drainage systems.

local materials taken from recent or significant landslides in Croatia (Arbanas et al. 2017).

The simplest slope model will be tested under different rainfall intensities, different slope inclinations and simple dynamic loads (vibration). After the model functionality confirmation, several different small scale remediation constructions will be embedded and their behavior will be tested in the model: retaining walls in the foot of the slope, pile walls, buttressing construction in combination with drainage systems etc. (Fig. 3). The impact of different retaining wall dimensions, pile raster and bored drain raster on slope stability in the model will be analyzed. The models with remediation constructions will be tested under the same conditions applied to slope: rainfall and simple dynamic loads, both separately and together.

Conclusion

Physical modelling of landslides using scaled landslide models behavior began at the end of 1980s. The main purpose of landslide physical modelling in the past was research of initiation, motion and accumulation of fast flow like landslides caused by infiltration of water in a slope. The studied models and research were divided into two main groups related to the main landslide triggering factors: rainfall and earthquakes. The research Project Physical modelling of landslide remediation constructions' behavior under static and seismic actions, funded by the Croatian Science Foundation, started at the Faculty of Civil Engineering, University of Rijeka in October 2018 with the main aim to modelling behavior of landslide remedial constructions in physical models of scaled landslides in static and seismic conditions.

Physical model of a scaled landslide under static actions, means it was designed to enable initiation of a landslide caused by controlled artificial rainfall using sprinkler system and equipped with adequate photogrammetric equipment and complex sensor network with ability to measure displacements, pore pressures and soil pressures within a landslide body.

Physical model of a scaled landslide under seismic actions, was designed to enable initiation of a landslide triggered by shaking caused by artificial earthquake or to control possible landslide occurrence caused by a historical landslide with registered accelerogram from earthquake database. Seismic conditions impulses will be induced by a pair of shaking platforms commonly used for structures testing under cyclic loading.

The selection of the measuring techniques and equipment in the physical model follows the practice of monitoring systems established on real landslides. In that sense and the sensor systems used in physical models can be divided in geotechnical monitoring systems and geodetic monitoring systems. Geodetic monitoring system will be based on innovative photogrammetric equipment for multi-temporal landslide analysis from stereo image sequences obtained by pair of high speed cameras supported by an infrared camera for infrared tomography (IRT), as well as terrestrial laser scanner (TLS). Geotechnical monitoring system will be consisted of a complex network of miniature sensors that will have ability to measure displacements, pore pressures, soil pressures and contact forces etc. through the soil profile in the model.

Different types of soil will be used in modeling: from sandy to clayey soil material with completely different behavior in conditions of heavy precipitations and earthquakes. Several different small scale remediation constructions are planned to be tested in the model: retaining walls, pile walls, buttressing construction in combination with drainage systems, in both static and seismic conditions and their combination.

On the basis of photogrammetric measurement 3D model of scaled physical model will be established using software for processing digital photos and 3D point clouds obtained from high speed cameras, IRT and TLS. The 3D models, with and without remediation constructions, will be imported into 3D numerical software for stress-strain analysis and analysis of run out paths. Data measured by sensor network installed in the landslide body will be used to calibrate the 3D numerical model. All data measured with equipment from physical model and results from numerical simulations will be combined and analyzed.

Combining modelling results from the physical model and numerical simulations will ensure much better insight into the behavior of landslide remedial constructions and their interaction with soil. Research results would represent the possibility to change remedial constructions design approach in modern engineering practice.

Acknowledgments

The research presented in this paper was supported by Croatian Science Foundation under the Project IP-2018-01-1503 Physical modelling of landslide remediation constructions behavior under static and seismic actions (ModLandRemSS). This support is gratefully acknowledged.

References

Arbanas Ž, Mihalić Arbanas S, Vivoda M, Peranić J, Dugonjić Jovančević S, Jagodnik V (2014) Identification, monitoring and simulation of landslides in the Rječina River Valley, Croatia. Proceedings of the SATREPS Workshop on Landslide Risk Assessment Technology, 29-30 July 2014. Hanoi, Vietnam. pp. 200-213.

Arbanas Ž, Mihalić Arbanas S, Vivoda Prodan M, Peranić J, Sečanj M, Bernat Gazibara S, Krkač M (2017) Preliminary investigations and numerical simulations of landslide reactivation. Proceedings of World Landslide Forum 4, Advancing Culture of Living with Landslides, Vol. 2: Advances in Landslide Science. Mikoš M, Tiwari B, Yin Y, Sassa K (eds). Springer, Cham. pp. 649-657.

Bernat S, Mihalić Arbanas S, Krkač M (2014a) Landslides triggered in the continental part of Croatia by extreme precipitation in 2013. Proceedings of the XII IAEG Congress, Engineering Geology for Society and Territory, Vol. 2, Landslide Processes, 15-19 September 2014. Springer, Heidelberg. pp. 1599-1603.

Duncan J M (1996) State of the art: limit equilibrium and finite-element analysis of slopes. Journal of Geotechnical Engineering. 122(7): 577-596.

Eckersley J D (1990) Instrumented laboratory flowslides. Geotechnique. 40(3): 489-502.

Fan G, Zhang J, Wu J Yan K (2016) Dynamic response and dynamic failure mode of a weak intercalated rock slope using a shaking table. Rock Mechanics and Rock Engineering. 49(8). 3243-3256.

Feng T, Mi H, Scaioni M, Qiao G, Lu P, Wang W, Tong X, Li R (2016) Measurement of Surface Changes in a Scaled-Down Landslide Model Using High-Speed Stereo Image Sequences. Photogrammetric Engineering and Remote Sensing 82(7): 547-557.

Frodella W, Gigli G, Morelli S, Lombardi L, Casagli N (2017) Landslide Mapping and Characterization through Infrared Thermography (IRT): Suggestions for a Methodological Approach from Some Case Studies. Remote Sensing. 9(12): 1-25.

Herak D, Sović I, Cecić I, Živčić M, Dasović I, Herak M (2017) Historical Seismicity of the Rijeka Region (Northwest External Dinarides, Croatia) – Part I: Earthquakes of 1750, 1838 and 1904 in the Bakar Epicentral Area. Seismological Research Letters. 88(3): 904-915.

Herak M, Živčić M, Sović I, Cecić I, Dasović I, Stipčević J, Herak D (2018) Historical Seismicity of the Rijeka Region (Northwest External Dinarides, Croatia) – Part II: The Klana Earthquakes of 1870. Seismological Research Letters. 89(4): 1524-1536.

Iserloh T, Fister W, Seeger M, Willger H, Ries J B (2012) A small portable rainfall simulator for reproducible experiments on soil erosion. Soil and Tillage Research. 124: 131-137.

Lora M, Camporese M, Saladin P (2016) Design and performance of a nozzle-type rainfall simulator for landslide triggering experiments. Catena. 140: 77-89.

Mihalić Arbanas S, Arbanas Ž (2015) Landslides - A guide to researching landslide phenomena and processes. In Handbook of Research on Advancements in Environmental Engineering. Gaurina-Međimurac N (ed). IGI Global, Hershey, 474-510.

Mihalić Arbanas S, Sečanj M, Bernat Gazibara S, Krkač M, Begić H, Džindo A, Zekan S, Arbanas Ž (2017) Landslides in the Dinarides and Pannonian Basin – from the largest historical and recent landslides in Croatia to catastrophic landslides caused by Cyclone Tamara (2014) in Bosnia and Herzegovina. Landslides. 14(6): 1861–1876.

Petley, D (2012) Global patterns of loss of life from landslides. Geology. 40(10): 927-930.

Take W A, Bolton M D, Wong P C P, Yeung F J (2004) Evaluation of landslide triggering mechanisms in model fill slopes. Landslides 1: 17-184.

Wang G, Sassa K (2001) Factors affecting rainfall-induced flowslides in laboratory flume tests. Geotechnique. 51(7): 587-599.

Wang K, Lin M (2011) Initiation and displacement of landslide induced by earthquake – a study of shaking table model slope test. Engineering Geology. 122(1-2): 106-114.

Wieczorek G F, Snyder J B (2009) Monitoring slope movements. Geological Monitoring, Young R and Norby L (eds). Boulder, Colorado, Geological Society of America, pp 245–271.

Zanuta A, Baldi P, Bitelli G, Cardinalli M, Carrara A (2006) Qualitative and quantitative photogrammetric techniques for multi-temporal landslide analysis. Annals of Geophysics. 49(4/5): 1067-1080.

doi.org/ 10.35123/ReSyLAB_2019_18

Strength reduction curve of soils from eluvial deposits in Vinodol Valley, Croatia

Vedran Jagodnik[(1)], Petra Đomlija[(1)], Katarina Oštrić[(1)], Željko Arbanas[(1)]

1) University of Rijeka, Faculty of Civil Engineering, Rijeka, Radmile Matejčić 3

Abstract Earthquakes are one among the most significant landslide triggering factors. Small strains induced by earthquake vibrations can result in strength reduction even at the lower level of stress. For such purpose, strength reduction curve is frequently established for material of interest. In combination with soil damping, strength curves can be used for various numerical simulations involving both static and dynamic simulation of landslide behaviour. There are numerous relatively small and shallow debris slides in the Vinodol Valley, initiated in the eluvial deposits originating from the weathering of flysch bedrock. The area of the Vinodol Valley is seismically active, which makes it susceptible to earthquake triggered landslides. In this study, eluvial deposits were tested on small strain behaviour. Two samples were collected from the landslide body of a debris slide. The preliminary results enable the first insights into an understanding of strength reduction and damping of soil from the eluvial deposits in the Vinodol Valley. The established G/G_{max} vs. γ_c and λ vs. γ_c curves can be used as an input parameter for numerical analysis of slopes under seismic loading

Keywords eluvial deposits, Vinodol Valley, small strain, resonant column, torsional shear

Introduction

The area of the Vinodol Valley, Croatia, is characterised by numerous, relatively small and shallow landslides, mainly initiated within eluvial deposits originating from the flysch bedrock and activated by heavy rainfalls. The Vinodol Valley is also seismically active area where the earthquakes with significant magnitude occurred in the past. The maximum shear modulus of soil G_{max} is one of the most important parameters that determine both the static and cyclic soil behaviour. The ratio of secant shear modulus, G_s, and maximum shear modulus, G_{max}, in combination of plasticity index (PI) can give a valuable insight of soil shear strength reduction due to static or cyclic loading. The soil strength reduction at small strains plays a significant role in the cyclic behaviour of soils. Earthquake induced cyclic shear strains can lead to pore water pressure rise and accumulation of the plastic cyclic shear strains, which leads to the strength reduction and, ultimately, to the failure. Because of that facts, it is of great significance to determine the appropriate value of G_{max}. G_{max} can be mainly determined in two ways: (i) field measurements using geophysical methods, and (ii) laboratory test methods (using resonant column device or bender elements test). The paper presents preliminary results of laboratory tests on samples taken from eluvial deposits in the Vinodol Valley at small strains. The tests were performed using resonant column device and, as the result, the shear strength reduction curves for the tested samples were determined. The results obtained from such tests can represent a valuable input data for advanced static and dynamic numerical analysis and simulations of landslides. There are numerous computer software's that uses G/G_{max} and damping as an input parameter (based on the constitutive model), such as for example Plaxis (Brinkgreve 2006), Geostudio (Krahn 2004), FLAC (Cundall 2011) and DEEPSOIL (Hashash et al. 2016).

Study area

The Vinodol Valley (64.57 km2) is situated in the north-western coastal part of Croatia (Fig. 1a). The Valley has an elongated, irregular shape and it stretches in the north-western to south-eastern direction (Fig. 1a). The steep Valley flanks are built of Cretaceous and Paleogene carbonate rock (limestone, and dolomites) (Fig. 1b), while the inner parts and the bottom of the Valley are built of Paleogene flysch deposits, composed mainly of marls, siltstones, and sandstones in alternation (Blašković 1999) Flysch bedrock is mostly covered by various types of superficial deposits (Đomlija 2018). Based on the general morphological and geological conditions, the topography of the Vinodol Valley can be generally divided into three main parts (Đomlija 2018): the north-western (NW), the central, and the south-eastern (SE) part. The NW and the central parts of the Vinodol Valley belong to the Dubračina River Basin, and the SE part belongs to the Suha Ričina River Basin. For the purpose of this study, the soil sampling from the eluvial deposits was performed near the Drivenik settlement, located in the NW part (19.33 km2) of the Vinodol Valley (Fig. 1a).

The Vinodol Valley is seismically active (Prelogović et al. 1981). The contacts between the flysch and carbonate rock masses are mainly tectonic, with the predominantly reverse character of displacement (Blašković 1999). The active fault systems generally strike along the three main directions: (i) the longitudinal faults strike along the NW-SE direction; (ii) the transversal faults strike along the NE-SW direction; and (iii) the diagonal faults strike along the N-S direction. Earthquakes occurred in the Valley were shallow, with the depths ranging between 2 and 30

kilometres. The strongest earthquake in the Vinodol Valley was recorded in 1916 (Prelogović et al. 1981). The epicentre was about ten kilometres east from the Novi Vinodolski settlement, situated in the SE part of the Vinodol Valley. The earthquake hypocentre was 18 km deep, and the earthquake magnitude was M = 5.8. The earthquake triggered the rock falls along the relatively steep carbonate slopes at the Valley flanks, as well as landslides and cracks at the terrain surface. According to Herak et al. (2011), the maximal expected peak ground acceleration in the Vinodol Valley ranges between 0.10g and 0.26g, depending on the earthquake return period.

The eluvial deposits (Fig. 1b) cover an area of 2.26 km² in the NW part of the Vinodol Valley (Đomlija, 2018). These deposits originate from weathering of soft flysch bedrock, and their composition varies along the entire study area, depending on lithological composition of a local bedrock. Previous studies showed that eluvial deposits in the Vinodol Valley are mainly composed of the low plasticity clays, high plasticity clays, low plasticity silts to clayey gravels (Pajalić et al. 2017; Đomlija 2018). Based on the visual interpretation of 1 x 1 m LiDAR imagery, there are 54 small debris slides identified in the NW part of the Vinodol Valley, with an average landslide area of 750 m² (Đomlija 2018). However, the debris slide from which the soil samples were taken in this study (Fig. 1c) occurred after the airborne laser scanning was performed in March 2012, and the landslide phenomenon was identified in the field. The landslide is very small, with the total length of approx. 12 m, and the maximum width of approx. 5 meters.

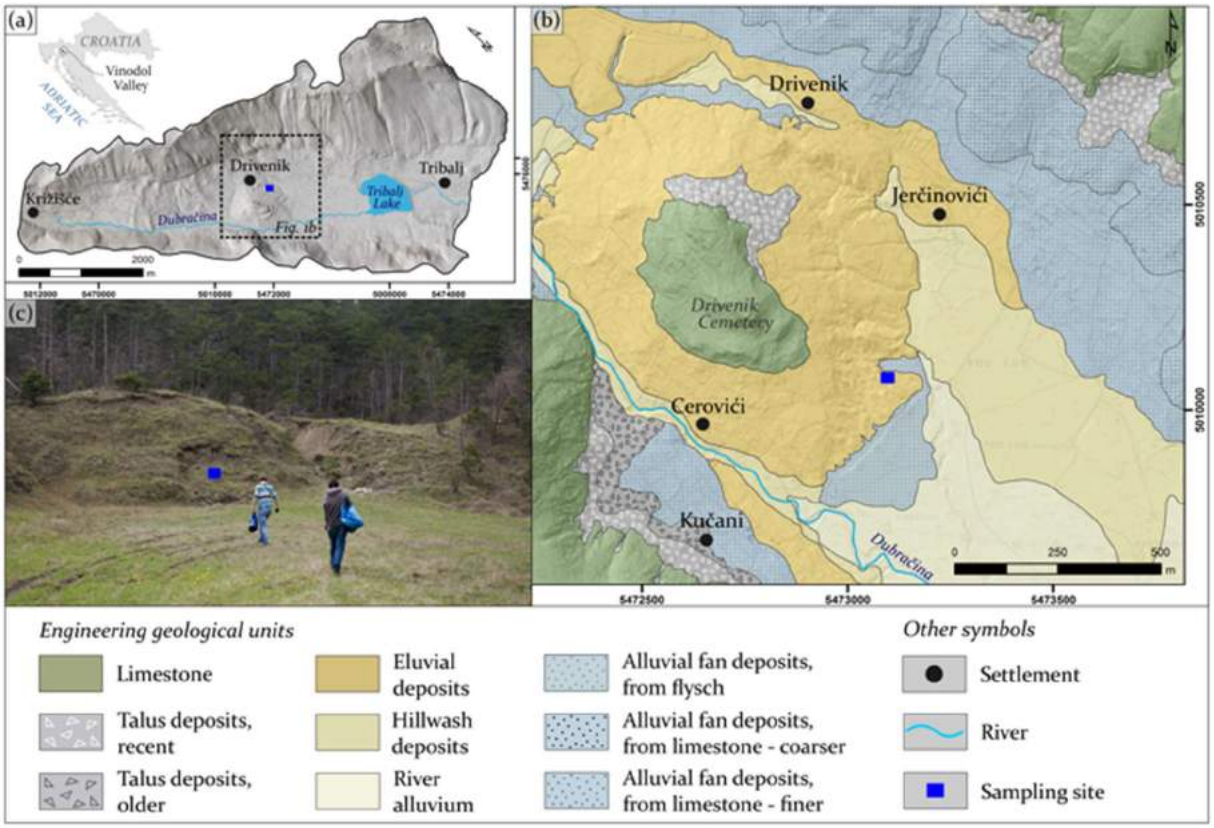

Figure 1 (a) Geographical position of the Vinodol Valley in Croatia, and the hillshade map of the northwestern part of the Valley, derived from the 1 m LiDAR DTM. (b) A detail from the Engineering geological map of the nort-western part of the Vinodol Valley (Đomlija, 2018), with the soil sampling site. Photo (c) was taken during the sampling of eluvial deposits from the landslide body.

Material and methods

Soil sampling

Two soil samples were taken from the eluvial deposits in the body of a small debris slide (area of approx. 60 m²) in the NW part of the Vinodol Valley (Fig. 1(c)). This landslide was chosen for the study because of an easy access to its location, its small size, and an absence of the vegetation cover. Eijkelkamp sampling drill and sampler was used and two samples were taken from the landslide body. The sampling process ensured minimal sample disturbance.

Soil classification tests

Soil was tested and classified according to the ISO standards (EN/ISO 14688-2 2017). Physical – mechanical properties tested are: (i) specific gravity, (ii) grain-size distribution and (iii) Atterberg limits. ASTM standard (ASTM D854-14 2014) was used for the specific gravity test while the ISO standard was used for gran-size distribution and Atterberg's limits (EN ISO 14688-1 2002). Full grain-size distribution was performed, meaning both mechanical and hydrometer analysis.

For better comparison of the obtained resonant column and torsional shear tests with the results from

literature, Atterberg limits were also determined according to the ASTM standard (ASTM D4318 2010).

Resonant column and torsional shear test

In the basic theory of vibrations, the velocity of shear wave can be related to the shear modulus and soil density (e.g. Yoshimi et al. 1978; Prakash 1981; Kramer 1996; Verruijt 2009). The resonant frequency of the sample can be correlated to the wave velocity and polar moments of measuring system and soil sample. The governing equation of the use of resonant frequency in soil dynamics is define with:

$$G = \frac{4\pi^2 h^2 \rho}{\beta^2} f_r^2 \quad [1]$$

where h is the sample height, ρ is the sample density, β presents the ratio between polar moments of system and soil, and f_r is the resonant frequency.

For very small resonant frequencies (and very small shear wave velocities), the resulting shear modulus represents maximum shear modulus of soil (eg. Hardin and Richart 1963; Hardin and Drnevich 1972; Lanzo et al. 1997). Behaviour of soil is referred to this, initial shear modulus. Many researchers have tried to define the empirical equation for the G_{max} for sand (eg. Saxena and Reddy 1989) and clay (e.g. Hardin and Black 1968; Hardin and Drnevich 1972; Hardin 1978).

According to the ASTM standard (ASTM D4015-15 2015), the resonant column test is classified as non-destructive test if the shear strains are less than 0.01% enabling that several tests can be performed on the same sample if the shear deformations are under mentioned limit.

The load moment is applied to the active end of the sample (upper end; Device Type 1 according to ASTM standard (ASTM D4015-15 2015)). The resonant column (RC) test is based on the relation between the dynamic shear modulus and the resonant frequency of the material, f_r . In a standard RC test, the frequency is gradually increased at certain intervals and the resonant frequency is the one at which the sample response amplitude is maximal.

In this research, the authors used resonant column device manufactured by Wykeham Farrance (Controls-Group 2019), which ensure conducting of both resonant column and torsional shear test. For the purpose of this research, resonant column chirp test is used. RC Chirp combines basic two stages of the standard resonant column test, that is, wider spectre of frequency and narrow spectre of frequency, which makes it faster to complete the resonance test (Cavallari 2014). The free oscillations are induced by applying a small torque excitation on the active end of the sample (top of the sample) and let it vibrate while measuring its vibrating frequency. RC Chirp allows testing at frequencies of 10Hz to 300Hz at minimal deformations of 10^{-6} to 10^{-4} (Cavallari 2016; Controls-Group 2019). RC Chirp uses a so called linear modulation where frequency increases within the limits set by the user (Cavallari 2014).

In the torsional shear test, the sample is subjected to torsion with sinusoidal oscillation at small frequencies (up to 2Hz). The torsion load is applied in the same way as in the resonant column test, but with defined torsional relative deformation, defined with the test amplitude. Additional test parameters are the amplitude of torsional excitation and number of load cycles. The torque value is calculated on the basis of the calibration coefficients and the voltage that flows through the coils of electromotor, positioned at the top end of resonant column device (Cavallari 2014). According to ASTM norm (ASTM D4015-15 2015) the average value of the tangential stress component is 0.8 τ_{max}. The maximal torsional stress τ_{max} is calculated using the equation [2]:

$$\tau_{max} = \frac{T R}{J} \quad [2]$$

where T is the moment torque, R is the sample radius and J is the torsional constant.

Damping of soil is usually described as an area of a cyclic curve. This assumption is valid for cyclic loading of soil. In resonant column test, the damping is calculated based on a complex relation between the active end inertia, specimen rotational inertia, frequency of resonant apparatus and resonant frequency (ASTM D4015-15 2015). The equation used for calculating a soil damping is incorporated in the Dynator computer software. The equation corresponding to the computation of soil damping will be omitted due to a limitation in length of this paper

In general, and for the purpose of torsional shear test, the soil damping can be calculated as:

$$\lambda = \frac{1}{4\pi} \frac{w_d}{w_s} \quad [3]$$

where w_d represents the area of cyclic curve, and the w_s represents the area of the triangle (Fig. Figure 2).

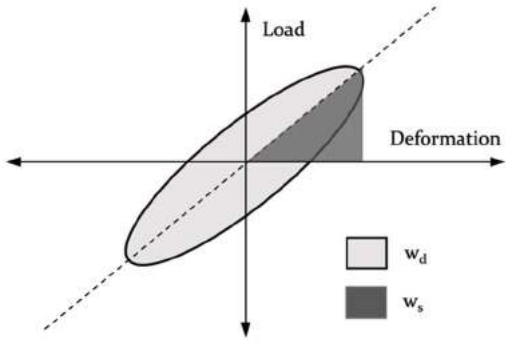

Figure 2 Area of cyclic loop

The resonant column/torsional shear system consists of several main components. The system is computer operated through the *Dynator* computer software and main control unit (Fig.2a). Maximal capacity of the cell pressure and pressure transducers (pore water and back pressure) is 1000 kPa. A sample is placed in triaxial cell

(Fig.2b) and a torque force on the sample for both types of the tests is induced with the system of coils (Fig.2c) while the response is measured with the pair of proximity transducers (Fig.2d). The vertical displacement of the sample can be measured with the LVDT (Fig.2d). Sample is placed on pedestal (Fig.2e) and then covered with the top loading cap (Fig.2f). The top cap has the bottom surface scarred in order to achieve better grip with a sample. Back pressure in a sample can be measured using the back-pressure transducer (Fig.2g), while the pore water pressure transducer is positioned on the opposite side. The volume control device (Fig.2h) is connected to the main control unit where the data are collected.

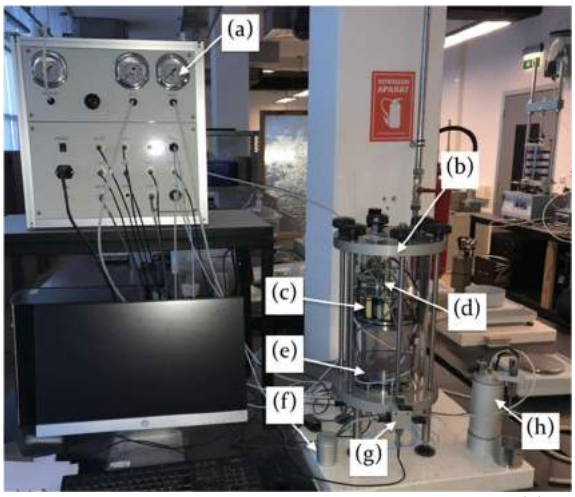

Figure 3 Resonant column/Torsional shear system: (a) main control unit, (b) triaxial cell, (c) coils with electromagnet, (d) LVDT's, (e) sample pedestal, (f) loading cap, (g) back-pressure transducer and (h)volume control.

Specimens' preparation

For the purpose of this first and initial tests, two samples were collected and prepared. The samples were collected in the field using Eijkelkamp sampling drill and sampler, making them almost undisturbed (Fig.Figure 1c). Small parts of soil samples were expected to determine in situ moisture content. The samples were protected with paraffin wax to preserve natural water content. The sampled soil is then shaped into a soil specimen for cyclic triaxial testing using specially designed cutter. Cutter is pushed in the soil samples resulting in the soil specimens of 50 mm in diameter and 100 mm in height. During the specimens' preparation, a small part of soil is used to determine the initial water content.

Resonant column test and torsional shear test

The two prepared specimens were tested on two different test types. One specimen is used for resonant column test, while the other is used for torsional shear test. Test types and test parameters are summarised in Tab.Table 1. Te specimens are saturated before the consolidation stage. The B value of pore pressure coefficient was 0.96. The effective consolidation stress was 50 kPa, simulating the approximate effective stress at the sampling site.

The specimens are subjected to different amplitudes of excitation presented in Tab Table 1. For the resonant column chirp test, amplitudes in the range form 0.001 V to 0.016 V were applied on the top of the specimen, resulting in the resonant frequency for the applied excitation. The duration of excitation in RC Chirp test was 10 seconds.

Excitation amplitudes of torsional shear test are summarised in Tab Table 1. Values varies from 0.1 V to 2.5 V. Frequency of performed test was 0.1 Hz. Shear modulus and damping at the specific torsional excitation are calculated as an average value of 5 cycles.

Table 1 Summary of small strain cyclic tests

Test type	Effective stress	Amplitude (V)
Resonant column	50	0.001; 0.002; 0.005; 0.01; 0.02; 0.04; 0.08; 0.016
Torsional shear		0.1; 0.25; 0.5; 1.0; 1.5; 2.0; 2.5

Results

Soil classification

Based on the laboratory tests performed on the sampled soil, basic physical mechanical properties were determined (Tab. 2). Specific gravity of landslide material determined with the boiling technique resulted in the value of 2.63. Combining wet sieve analysis and hydrometer analysis resulted a grain-size distribution for both coarse grain and fine grain particles. Liquid and plastic limit test showed the water content of 44% for liquid limit and 18% for plastic limit and resulting plasticity index of 26 (%).

The soil was classified according to EN ISO 14688-2 (EN/ISO 14688-2 2017). Following the classification procedure defined with standard (EN/ISO 14688-2 2017), the soil is classified as *intermediate plasticity sandy clay*.

Table 2 Summary of soil classification tests

Grain-size Distribution	Gravel [%]	1.41
	Sand [%]	20.1
	Silt [%]	59.2
	Clay [%]	19.3
Soil Plasticity	LL [%]	46
	PL [%]	18
	PI [%]	26

Stress reduction curve and damping

Initial tests on sandy specimens from eluvial deposit were performed at small strain shear deformations. The response of soil at such small strains results in the values

of shear module very close to the value of G_{max}. For the purpose of these tests the first value of the shear modulus obtained form RC Chirp tests was used as the G_{max} value (value obtained for the excitation value of 0.001 V). The latter obtained shear modulus from both resonant column and torsional shear test were referenced to the initial value. The result of these two tests are presented in Fig Figure **4**. The dashed lines represent the values of shear strength reduction curves for plasticity index of 15% and 30%, respectively, commonly used in geotechnical earthquake engineering (e.g. Vucetic and Dobry 1991; Kramer 1996). The results of strength reduction obtained from resonant column test are plotted with circular markers while the torsional stress results are presented with triangles.

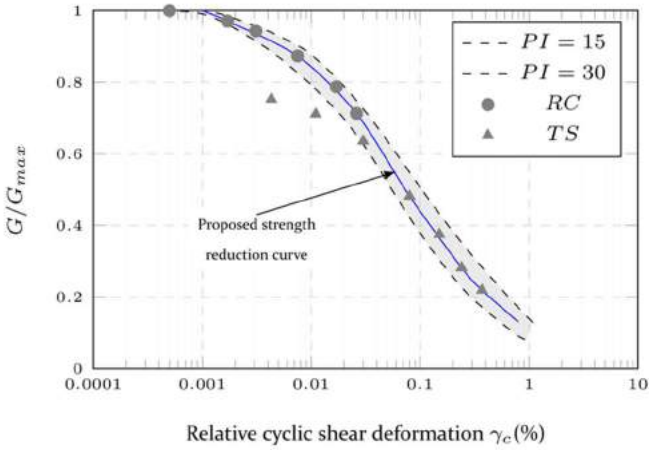

Figure 4 $\boldsymbol{G/G_{max}}$ reduction curve of soil from eluvial deposit in the Vinodol Valley

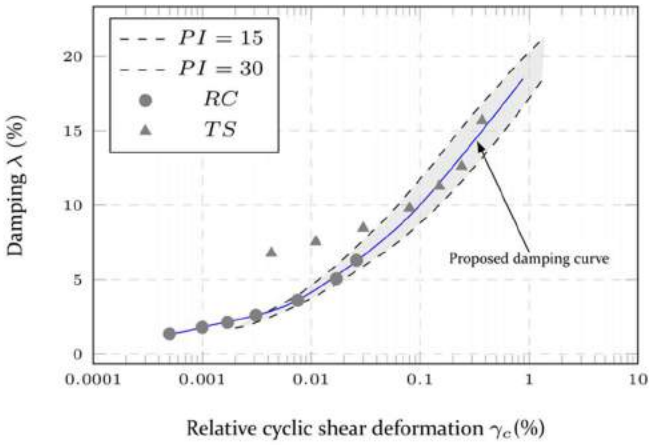

Figure 5 Damping of soil from eluvial deposit in the Vinodol Valley

Fig. 5 presents the variation of soil damping related to shear strain. The results obtained in resonant column test are plotted as a circular marker while the results of torsional test are plotted as triangle markers. The results of both resonant and torsional test are compared with the variation of damping and shear strain for plasticity index of 15 and 30, taken from the literature (Vucetic and Dobry 1991). Shaded zone represents the variation of plasticity index from 15 to 30.

Blue lines on Fig. 4 and Fig. 5 represents the proposed approximation curves for G/G_{max} reduction and soil damping, respectively. Those two proposed curves are plotted on Fig. 6 and can be used for geotechnical calculations.

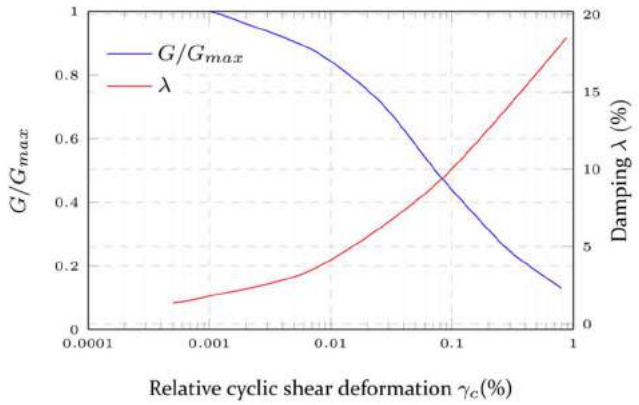

Figure 6 Proposed $\boldsymbol{G/G_{max}}$ and damping curve for soil from eluvial deposit in the Vinodol Valley

Discussion and conclusions

The first and preliminary cyclic tests of soil from eluvial deposits originating from weathering of flysch bedrock have been performed. Along with the standard classification tests, the small strain tests encompassed test using resonant column device and torsional shear in order to establish basic cyclic properties of sliding material were conducted.

The results presented in Fig. 4. are similar to other research performed on small strain deformations (eg. Vucetic and Dobry 1991; Kramer 1996; Towhata 2008). The results performed in resonant column test are ranging from approximately 0.00045% to the 0.025 % of a shear strain deformation. The reduction of a strength in this range in around 30%, meaning that even a small cyclic shear strain can result in a notable reduction. The values of shear modulus obtained in torsional shear test show some discrepancies for smaller values of shear strain. This can be caused due to a torsional cap and the possibility of slippage at smaller strain.

The result of conducted tests on resonant column gave the insight of soil damping for the values of shear strain smaller than 0.002%. The results plotted in Fig.5 coincide very good with the results from the literature (eg. Vucetic and Dobry 1991; Kramer 1996; Towhata 2008). Torsional shear test resulted in a somewhat higher values of damping for smaller values of shear strains from 0.004% to 0.03%, approximately. At the value of shear strain of 0.1% the damping of tested soil is in a range documented in literature (eg. Vucetic and Dobry 1991).

From results of these preliminary tests it can be concluded that the behaviour of soils from eluvial deposits in the Vinodol Valley at small strains are in good

agreement with the results for similar soils presented in literature (eg. Vucetic and Dobry 1991; Kramer 1996; Towhata 2008). Based on the presented results, proposed strength reduction curve and soil damping curve for soils from eluvial deposits originating from weathering of flysch bedrock are obtained. Such curves can be used in both static and dynamic numerical modelling and simulations of landslide initiation and run out.

Acknowledgments

The research presented in this paper was partially supported by the following projects:

- University of Rijeka uniri-tehnic-18-113 Laboratory research of static and cyclic behaviour at landslide activation;
- Ministry of Science, Education and Sports of the Republic of Croatia under the project Research Infrastructure for Campus-based Laboratories at the University of Rijeka, number RC.2.2.06-0001. Project has been co-funded from the European Fund for Regional Development (ERDF);
- Croatian Science Foundation under the Project IP-2018-01-1503 Physical modelling of landslide remediation constructions behaviour under static and seismic actions (ModLandRemSS).

This support is gratefully acknowledged.

References

ASTM D4015-15 (2015) Standard test methods for Modulus and damping of soils by fixed-base resonant column devices. ASTM International

ASTM D4318 (2010) Standard Test Methods for Liquid Limit, Plastic Limit, and Plasticity Index of Soils. ASTM International

ASTM D854-14 (2014) Standard Test Methods for Specific Gravity of Soil Solids by Water Pycnometer

Blašković I (1999) Tectonics of Part of the Vinodol Valley Within the Model of the Continental Crust Subduction. Geol Croat 52:153–189. doi: 10.4154/GC.1999.13

Brinkgreve RBJ (2006) Plaxis: Finite Element Code for Soil and Rock Analyses: 2D-Version 8.5:(User's Guide)

Cavallari A (2014) Soil testing using a Chirp RC. In: 20th IMEKO TC4 Symposium on Measurements of Electrical Quantities: Research on Electrical and Electronic Measurement for the Economic Upturn, Together with 18th TC4 International Workshop on ADC and DCA Modeling and Testing, IWADC 2014. pp 195–199

Cavallari A (2016) Resonant column testing challenges. In: 1st IMEKO TC4 International Workshop on Metrology for Geotechnics, MetroGeotechnics 2016. pp 149–156

Controls-Group (2019) Resonant column, Soil mechanics testing equipment, Controls. https://www.controls-group.com/eng/soil-mechanics-testing-equipment/resonant-column.php. Accessed 23 Jul 2019

Cundall PA (2011) FLAC Manual: A Computer Program for Fast Lagrangian Analysis of Continua. Itasca Consult Gr Inc

Đomlija P (2018) Identification and classification of landslides and erosion phenomena using the visual interpretation of the Vinodol Valley digital elevation model (in Croatian). Faculty of Geology, Mining and Petroleum Engineering, University of Zagreb

EN/ISO 14688-2 (2017) Geotechnical investigation and testing — Identification and classification of soil — Part 2: Principles for a classification. Geneva, CH

EN ISO 14688-1 (2002) Geotechnical investigation and testing. Identification and classification of soil. Identification and description. Geneva, CH

Hardin BO (1978) The nature of stress-strain behavior for soils. In: From Volume I of Earthquake Engineering and Soil Dynamics--Proceedings of the ASCE Geotechnical Engineering Division Specialty Conference, June 19-21, 1978, Pasadena, California. Sponsored by Geotechnical Engineering Division of ASCE

Hardin BO, Black WL (1968) Vibration Modulus of Normally Consolidated Clay. J Soil Mech Found Div 94:353–369

Hardin BO, Drnevich VP (1972) Shear Modulus and Damping in Soils: Design Equations and Curves. J Soil Mech Found Div 98:

Hardin BO, Richart JFE (1963) Elastic wave velocities in granular soils. ASCE Proc J Soil Mech Found Div

Hashash YMA, Musgrove MI, Harmon JA, et al (2016) DEEPSOIL 6.1, user manual. Urbana, IL, Board Trust Univ Illinois Urbana-Champaign

Herak M, Allegretti I, Herak D, et al (2011) Map of the earthquake areas of the Republic of Croatia for Tp = 95 and Tp = 475 years(in Croatian). Državna Geod uprava (DGU), Zagreb

Krahn J (2004) Dynamic Modeling with QUAKE / W. Alberta

Kramer SL (1996) Geotechnical Earthquake Engineering, 1st edn. New York

Lanzo G, Vucetic M, Doroudian M (1997) Reduction of shear modulus at small strains in simple shear. J Geotech Geoenvironmental Eng 123:1035–1042

Pajalić S, Đomlija P, Jagodnik V, Arbanas Ž (2017) Diversity of Materials in Landslide Bodies in the Vinodol Valley, Croatia. In: Mikoš M, Vilímek V, Yin Y, Sassa K (eds) Advancing Culture of Living with Landslides. Springer International Publishing, Cham, pp 507–516

Prakash S (1981) Soil Dynamics prakash, 1 st. McGraw-Hill, New York

Prelogović E, Blašković I, Cvijanović D, et al (1981) Seizmotectonic characteristics of the Vinodol Region (in Croatian). Geološki Vjesn 33:1–5

Saxena SK, Reddy KR (1989) Dynamic moduli and damping ratios for Monterey No.0 sand by resonant column tests. Soils Found 29:37–51. doi: 10.3208/sandf1972.29.2_37

Towhata I (2008) Geotechnical Earthquake Engineering. Springer Berlin Heidelberg

Verruijt A (2009) An Introduction to Soil Dynamics. Springer Netherlands

Vucetic M, Dobry R (1991) Effect of Soil Plasticity on Cyclic Response. J. Geotech. Eng. 117:89–107

Yoshimi Y, Richart FE, Prakash S (1978) Soil dynamics and its application to foundation engineering. State-of-the-art report: Proc 9th International Conference on Soil Mechanics and Foundation Engineering, Tokyo, 1977, V2, P605--650. In: International Journal of Rock Mechanics and Mining Sciences & Geomechanics Abstracts. p A28

doi.org/ 10.35123/ReSyLAB_2019_19

Categorization of sloping terrain on soil stability - Nova Gradiška example

Tomislav Novosel[(1)], Željko Miklin[(1)], Željko Sokolić[(2)]

1) Croatian Geological Survey, Sachsova 2, P.O.Box 268, HR-10000 Zagreb, tel: +385 (1) 6160 888

2) Geotehnički studio Ltd. Zagreb, Nikole Pavića 11, 10090 Zagreb – HR, tel: +385 (1) 3879 141

Abstract Every day we witness the damage to the structures built on slopes caused by slope instability. Many of these structures have been constructed in accordance with the existing legislation governing urban planning and construction issues. When the damage arises, the claim for compensation is referred to the authorities responsible for issuing construction and operating permits. In the desire to avoid similar situation in the future, some cities and municipalities have decided to minimize these problems.

For the area of the city of Nova Gradiška, located on a sloped terrain, four categories of the terrain were defined on the maps scale 1:5000, for which the degree of stability and, accordingly, the conditions for construction were determined.

The authors consider that this and similar approach to regulating conditions for design and construction on conditionally stable terrain in the future , the damage caused by soil instability should be reduced to a much smaller extent than what is present today.

Keywords slope instability, categories of terrain, damage caused

Introduction

In the northern part of the Republic of Croatia the damages and consequences of landslide activities are the increasing problem of the cities, municipalities and counties, as well as of the state. The intensive conversion of the natural areas in the agrarian and construction view, in the last 50 to 100 years, brought to great changes in the stage of the soil resistance concerning destabilization. Forest clearance, and the increasing soil surfaces covered by vineyards and plough-lands, excavations and filling up the greater soil surfaces on slopes, construction of roads and other line infrastructural objects, residential and farm buildings, waterworks, with parallel non construction for water acceptance and water drainage, had the consequence of new states of the slope stabilities. Gravitational and hydrodynamic forces have been changed on the slopes. In the geological media characterized by bedding, by mechanical properties and the material properties of permeability, the security factors concerning destabilization have constantly been decreased. On increasing surfaces, they fall on the somewhat greater values or at the value Fs=1, which activates the process of creeping (velocities of movements up to 300 mm per year) and sliding (movements with the velocity of several mm per day - to 300 km per second).

The competent government bodies failed in the past in prevention the terrain destabilization and in the prevention the damages caused by these phenomena.

The legal regulations prescribe well the way of preparation, construction and maintaining of buildings. The project of each building should have the geotechnical survey as the base. By accepting the geotechnical survey the designer overtakes the responsibility for stability and mechanical resistance of the building. During the construction, the investor should follow the technical correctness of building through the technical supervision. For serious geotechnical buildings, the study of the technical revision of the designed solution has been required.

In the phase of using and maintaining the building, the investor is obliged to secure the stability and mechanical resistance of the objects and surrounding terrain. The construction is done after getting the building permit. After construction finishing the technical inspection and the operating permit have to be obtained. The water law is very clear concerning the part of obligations of the participants in the construction connected to the insurance of the conditions of technically correct acceptance and water drainage, which is particularly important for the constructions built on the slopes.

The practice shows that in most cases, that which is legally proscribed, has not been applied in reality. The construction designs have been made without the geotechnical surveys. The project solutions do not comprise the solutions connected to the acceptance and water drainage. Great number of buildings has been constructed without the construction permit and it is rare that the object has the operating permit as well. The performed legalisation of the illegal constructed objects presents the additional burden for the competent governing bodies. With the mentioned legalisation the obligation of the damage settlement of numerous constructions built on the unstable slopes is accepted.

Because of the mentioned reasons the competent governing bodies are faced today with the need of solving the increasing number of cases in which the instability of

the terrain has caused the damage on the legally constructed objects. The amounts of these damages greatly exceed the budget possibilities.

The competent authorities have different approach in solving these problems. In practice, the solving of problems connected with the activation of the terrain destabilisation happen after the terrain displacements.

In recent times in some territories the approach to solve these problems has been changed. There are several examples how the cities solve such problems, from the city of Zagreb, to the city of Slavonski Brod, the city of Ivanić Grad and the city of Nova Gradiška.

For a long time the city of Zagreb has no easy accessible areas suitable for building, so the building take place on the unstable terrains or potentially unstable ones. Before construction such areas have to be treated for this purpose by solving the instability issues. The city of Zagreb has come furthest in solving these problems. The detailed engineering geological maps (DEGM) in the scale of 1:5000 of the unstable areas, the hydrogeological maps, the engineering geological cross sections (in order to get the third dimension of the geological structure), the ground slope maps, have been made. The data bases for the landslides have been made (in Access) and all the maps are presented in the unique GIS project, on the interactive map of the city of Zagreb. The "Preliminary simplified map of sliding hazard" has been made. The seismic and geological micro zoning according to euro code 8 is in the elaboration phase, for which the seismic refraction measurements, MASW measurements, trembling measurements and down hole investigations in deep boreholes have been done. All these works are in accordance with the geotechnical investigation works. These investigation works and other works of that kind are very expensive and profitable only when the value of planned constructions is high. But there are considerably cheaper works, adjusted to the needs of the cities, which can ensure the development and decrease the costs connected with the negative influence of the potentially unstable terrain, or already destabilized ones.

Investigation methods in smaller cities

Two examples have been presented how the cities have come up to solving of problems of conditionally stable and unstable slopes, with the aim to decrease the costs connected with these problems. The city of Slavonski Brod has a series of similarities with Podsljemenska zona of the city of Zagreb. New geological maps (scale 1:5000) for the city of Slavonski Brod, that is for Brodsko Brdo (Miklin, Ž., Podolszki, L., Martinčević, J., 2012), have been made as well as the engineering geological maps (scale: 1:5000) with the presentation of landslides and dredging. The landslide registry with the data base opened for filling is made and the whole project has been given in GIS with the possibility of the interactive map elaboration. Representative sample sediments have been used as the verification of the mapped sediments and the basic indicators of the mechanical characteristics of the material on the slopes have been performed by IN-SITU tests with the usage of pocket penetrometers and cone vanes. In the initially phase of the project the landslides and the unstable slopes - the IV category, have been mapped. The detailed categorisation of slopes according to the stability criterion has not been foreseen. That will be the task of the second phase of the investigation works (it would be necessary to do the investigation drillings and expensive investigations). For the objects which will be on the boundaries of two categories it is necessary to adapt stronger criterion, that is they will have to be put in higher (worse) category. The basic geological maps have been made here and only the landslides have been mapped (the contours of instabilities on the terrain have been made), the cadastre sheets have been filled in Access and the representative soil samples are processed within Excel table together with the basic laboratory tests that have been made.

Methodology applied for the city of Ivanić Grad is based on the terrain categorization without spending considerable amount of money. The first step in the work is the visual terrain overview performed by engineering geologist and geotechnical engineer which is based on the evaluation and experience of the experts. The geologist confirms the existing geological maps, maps the landslides (unstable slopes) and forecasts the depth of the sliding plane. For more efficient tracking of the state on the terrain the data base in Access is filled which will be complemented after each further investigation work to gain better knowledge about the terrain. On the base of the experience and available geological data the geotechnical engineer hypothesizes which construction works could be used to stabilize the slope. He proposes the preliminary technical design for remediation of the destabilized slopes, composes the forecast cost estimate of works and with the usage of designers costs of single works he forecasts the total cost of all the remediation works as well as the duration of the works.

Such estimations have mostly led to the conclusion that the costs of the terrain remediation are far greater than the market value of the terrain and objects on the slope. For example, on one slope there are four old cottages with the value of 200.000 kn and the maximal value of the vineyards and the abandoned farmland is up to 150.00 kn that is the total value of 350.000 kn. The evaluation of the finances necessary for terrain stabilization rises up to the value of 1.683.000 kn.

In the following table the presentation of the forecast costs of the works to stabilize 5 unstable slopes is given.

In the following table the presentation of the forecast costs of the works to stabilize 5 unstable slopes is given.

Table 1 Forecast costs of geotechnical works, documentation making and remediation works on the processed terrain. Total remediation costs are given in kuna.

Landsl.	Geotechnical	Design	Remediation	Total (kn)
1	118.590	50.000	1.517.500	1.686.090
2	59.070	25.000	490.960	575.030
3	128.260	52.000	2.320.046	2.500.306
4	115.210	48.000	919.945	1.083.155
5	82.930	37.000	385.710	505.640
TOTAL				6.350.224

The forecast sums were far higher than the ones which the local community possessed, so instead of complete slope remediation works, the measures of state improvements were suggested by performing some activities in which the potentials of the city could be included. The measures which have to be undertaken by the inhabitants of the houses on slopes, and which are connected to the acceptance and drainage of waters on their plots have been determined. The cooperation with the local municipally firm (final processing of water drainage from roads) has to be established as well as the cooperation with the volunteer fire company (which has to pump out water from the wells on slopes, etc. (Miklin, Ž., Podolszki, L., Ofak, J 2016). By establishing the mentioned way of behaviour with smaller investments the determined improvements connected with slope activities have been achieved.

What's more the city government got very valuable documents for making the activity plans for ensuring the properties and inhabitants security.

This model is based on the terrain survey and on rough estimation of costs for particular works, without the investigation drilling and laboratory investigations. The basic idea is to lean on the help of the inhabitants, city firms and associations.

The investigation results in the area of the city of Nova Gradiška

Before the beginning of works the data about the investigations in the area of the city of Nova Gradiška were collected. Geological, geotechnical and the old mining maps were placed in space and compared with recent data. The terrain is mapped on the chosen area which was of interest to city government. In the area of the city of Nova Gradiška the terrain has been categorized in four categories.

With the aim of better and uniform acquaintance with the sediments the 6 sites were chosen in order to complete the data base. The shallow terrain sounding has been performed by Geotechnical boreholes with the depth of 2.5 m. Two undisturbed samples were taken from each borehole. Total of 15 meters was drilled and 12 samples were taken for the laboratory testing. Collecting the necessary data for evaluation of the slope stability enabled the making of the final product: maps of geotechnical terrain categorization from the view of stability.

Instabilities on the investigated area are limited to landslides, falls and in smaller degree to dredging and erosion. "Cadastre of landslide and unstable slopes" has been made and the end user, the city of Nova Gradiška, has got the cadastre in Access form.

Collected data were registered in the data base and the landslide contours were presented on the engineering geological map, in the scale of 1:5000 (Figure 2). The basic activity stages of particular landslides according to (WP/WLI, 1993) and according to: A suggested method for describing the activity of landslides (Bulletin no.47 Paris 1993) were taken into consideration. Since it is an urban area, where the landslides have different investigation stages, the classification of landslides according to the bulletin 47 from 1993 has been applied. This classification is connected with the graphic marks taken over from "Public Review Draft – Digital cartographic standard for Geologic map Symbolisation", April 2000 (PRD-DCsGms).

The landslides are presented on the map in red colour (the active ones), the creeping is marked with violet colour and smaller instabilities are presented by light violet colour.

According to the slope categorization model after stability which is applied in the city of Zagreb, four categories of the terrain stability are abstracted. The first category (I category) has not been found in the area of the city of Nova Gradiška. The whole area of Nova Gradiška is covered mainly with the categories II and III. The IV category of landslides and unstable slopes is marked by red lines on the engineering geological map. The categories of stability on the engineering geological map (modelled after the city of Zagreb – official gazette of the city of Zagreb) of the terrain are:

Category I – Stable terrains are the areas stable in natural conditions and in the condition of construction. Special geotechnical conditions are not necessary. In the design phase the conditions of construction foundations are determined based on geotechnical investigation works;

Category II – Conditionally stable slopes are the areas stable in natural conditions. During the building construction, these slopes can become unstable caused by careless work. Based on geotechnical investigations special geotechnical conditions will be determined. Special geotechnical conditions, as a rule, are the building conditions on slopes and condition of building foundation;

Category III - Conditionally unstable slopes are the areas in which the natural conditions exist, which disturb the stability of the slopes or make difficulties in any other way and temporarily disable the usage of the terrain for building. There are no visible signs of instability. Building on such areas is possible when the causes which temporarily disable or make the building difficult are removed, which is achieved by preventive measurements

for terrain remediation. The volume and type of preventive measurements for the terrain remediation will be determined after the detailed geotechnical investigation. Based on the detailed geotechnical investigations special geotechnical conditions will be determined;

Category IV – Unstable slopes are the landslide areas with the existence of failure planes or zones along which the shear strength parameters are on residual values (active and old sliding or registered failure zones in slopes of the tectonic origin). The detailed geotechnical investigations will determine the conditions for previous remediation of the terrain which can comprise complex remediation measures (drainage, filling, retaining structures and similar). The terrain remediation can be performed so that the planned buildings make the part of the remediation measures so that the conditions of the terrain remediation contain special geotechnical conditions for building. With the geological structure and categorization of the terrain the landslides and erosions in the field have been described.

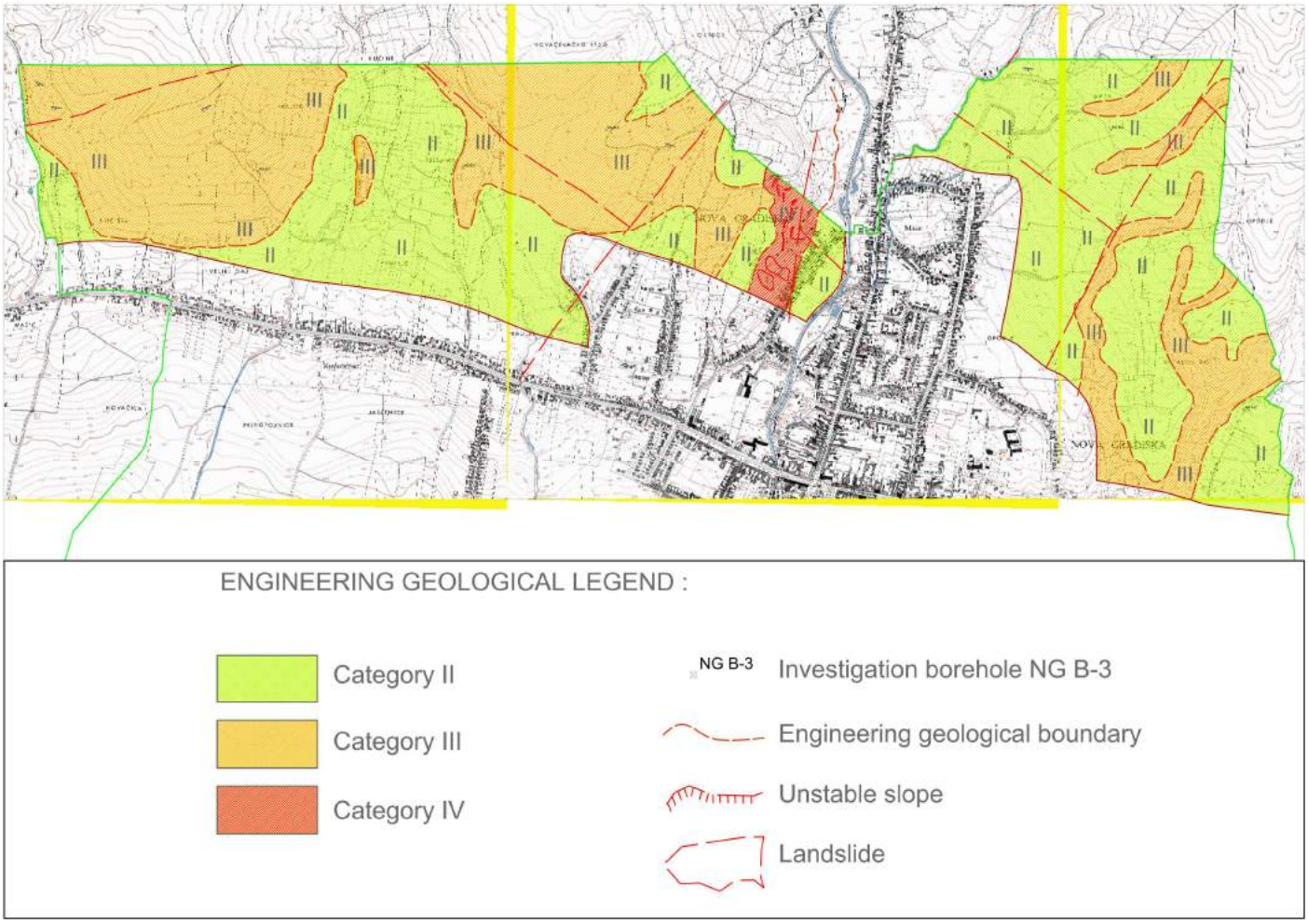

Figure 1 Categorized area of the city of Nova Gradiška (Literatura)

Conclusions

The financial means which the authorities possess are not high enough as those necessary for the remediation of the landslides and unstable slopes.

Struggle with problems connected to the landslides has to be divided in two parts. The inhabitants living in the objects which are damaged so much that their security and life is endangered have to be relocated and accommodated. In other buildings which have the certain reserve in security factors concerning the stability disturbance and the loss of the mechanical resistance of the bearing capacities of the construction elements, the optimal approach in finding the solutions for stopping the soil movement process has to be chosen. Secondly: to elaborate the professional documents on which base the building of objects on slopes has to be performed.

In undertaking the measures for state improvements the approach to activities for decreasing the negative influence on slope stability stage has to be applied. First of all, the measures by which the state connected to correct acceptance and drainage of waters on slopes will be improved. By observing the activities of unstable slopes the positive effect of the undertaken activities has to be determined. When these measures are not enough, the additional stabilization measures have to be added. These activities comprise the available potentials of the

local community, the owners of buildings, communal services, fire departments and similar. Where the remediation works have to be performed all the owners of the objects on unstable slopes, owners of roads, waterworks, sewage system, electro installations and others have to be incorporated into the financing of works.

The future constructions have to be undertaken in accordance with the regulations of the geotechnical documents, engineering geological maps and the maps of the terrain categorization on stability. These documents should be made for all the sites which are on the slopes. Except that it is obligatory to keep up with law and technical regulations concerning the building. No object can be built without geotechnical elaboration. The design solutions should be revised by professionals, the building should be performed under the professional supervision and in the phase of object usage the security measures for terrain stabilization have to be undertaken as well as the maintaining of the stability and mechanical resistance of the building. One should keep up to the legal regulations of waters concerning the acceptance and the drainage of waters. The majority of the mentioned has already been incorporated into legal regulations. The geotechnical cadastre has to be established which will collect and file all the geotechnical data collected by investigation works.

References

Miklin Ž., Podolszki L., Martinčević, J. (2012): Geological and engineering-geological investigations in Brodsko Brdo area – expanded Edition. 4. Internacionalni naučno–stručni skup Građevinarstvo – nauka i praksa. Zbornik radova 2079- 2085 , 3-7 Mart 2012. Žabljak, Crna Gora.

Miklin, Ž., Sokolić, Ž., Podolszki, L., Ofak, J. (2016): Prognoza tehničko financijskih pokazatelja za nestabilne padine, korištenjem postojećih podataka i prospekcije terena. 7 savjetovanje Hrvatskog geotehničkog društva s međunarodnim sudjelovanjem. 7th conference of Croatian Geotehnical Society whit international participation. 161-167. Varaždin 10-12. 11.2016. Hrvatska.

Miklin, Ž., Novosel, T., Sokolić, Ž. Šoban, S. (2018). Geološka i inženjerskogeološka istraživanja područja padinskog dijela urbanizirane zone Nove Gradiške; 1:5000. Br. 57/18, arhiv HGI

Službeni glasnik Grada Zagreba, godina XLVI, broj 8, od 17. svibnja 2001. godine

doi.org/ 10.35123/ReSyLAB_2019_20

Preliminary testing of clay activity from landslide deposits in Dubračina River Basin, Croatia

Petra Đomlija[(1)], Marijana Prša [(1)], Vedran Jagodnik[(1)], Željko Arbanas[(1)]

1) University of Rijeka, Faculty of Civil Engineering, 51000 Rijeka, Radmile Matejčić 3

Abstract This paper presents the preliminary results of clay activity testing from landslide deposits located in the Dubračina River Basin (43.52 km²), Croatia. Numerous small shallow landslides were identified in the study area, based on the visual interpretation of high-resolution airborne LiDAR (Light Detection and Ranging) imagery. The main landslide types in the Dubračina River Basin are debris slides and debris slide-debris flows. Most of the landslide phenomena are located within complex gullies formed in the flysch bedrock. Samples of colluvial deposits from nine debris slides were tested to determine clay activity, with the main aim of establishing a potential relationship between sliding processes and activity of present clay minerals. Results of this preliminary study indicate that inactive and normally active clay minerals (i.e., kaolinite and illite) prevail in the colluvial deposits of the investigated landslides, while in only one soil sample the more active clay minerals (i.e., montmorillonite) have been found. Although the activity of clays cannot be directly related to the landslides triggering, it can be a relative indicator for identification of slope material more susceptible to sliding. The soils with lower activity generally have lower values of cohesion and can retain less quantity of infiltration water before a loss of the strength. According to these facts, soils with lower activity have consequently lower shear strength and are more sensitive to transition in weaker consistency caused by water content increasing. Those facts are very important for shallow landslide occurrences and knowing of activity of clays in a slope can be a valuable data in landslide susceptibility determination in the Dubračina River Basin.

Keywords debris slide, landslide deposits, clay activity, clay minerals, Dubračina River Basin, Vinodol Valley

Introduction

The Dubračina River Basin (43.22 km2) is located in the Vinodol Valley, in north-western coastal part of the Republic of Croatia. The inner Basin area is composed of the flysch rock mass (Blašković 1999) mostly covered by various types of superficial deposits (Đomlija 2018), and is surrounded by the carbonate rock mass located in the Basin flanks. More than 600 hundred of relatively small and shallow debris slides and debris slide-debris flows (Hungr et al. 2014) were identified in the Vinodol Valley, based on the visual interpretation of high-resolution LiDAR (Light Detection and Ranging) imagery (Đomlija 2018). Most of these landslides (i.e., more than 500 phenomena) are identified in the Dubračina River Basin, encompassing the north-western and the central part of the Vinodol Valley, and are located within the relatively large and deep gullies dissected in the soft flysch bedrock. Gullies are mostly morphologically complex (Đomlija 2018) and are almost entirely covered by dense forests.

During the previous studies in the Vinodol Valley, the soil classification properties of landslide-forming materials were investigated by Pajalić et al. (2017), and Đomlija (2018). Soil samples were taken both from the individual active and dormant landslide bodies, and from the superficial deposits at locations without pronounced slope instabilities. According to the results of these studies, soils range from the high plasticity clays (ClH) to the gravely clays (clGr), according to the applied European Soil Classification System (ESCS) scheme (Kovačević and Jurić-Kaćunić 2014). All landslide-forming materials correspond to a debris material, according to the updated Varnes classification of landslide types (Hungr et al. 2014). Toševski (2018) previously analysed the correlation between the clay activity and the swelling behaviour of the soils in the Dubračina River Basin, based on the testing of 21 soil samples. In that study, totally 18 samples were determined as inactive clays (i.e., kaolinite), and three samples were determined as normal clays (i.e., illite). Activities (A) for the inactive clays ranged from A = 0.40 to A = 0.74, and for normal clays ranged from A = 0.86 to A = 0.99 (Toševski 2018).

In this study, the preliminary testing of soil activity from landslide deposits in the Dubračina River Basin was performed, with the main aim to establish a potential relationship between the sliding processes and the activity of clay minerals (Prša 2018). Soil samples from landslide colluvial deposits were collected from nine debris slides. Two debris slides are located in the north-western part, and seven debris slides are located in the central part of the Vinodol Valley. Eight debris slides are located within complex gullies, and one debris slide is located in the urbanized area in the north-western part of the Vinodol Valley.

Study area

The Dubračina River Basin is a part of the Vinodol Valley, situated in the north-western coastal part of

Croatia (Fig. 1a). The Valley (64.57 km²) has complex geological and morphological conditions (Blašković 1999), and an elongated shape, with a length of approx. 22 km. Due to the specific topography, the Vinodol Valley can be divided into three main parts (Đomlija 2018): the north-western (NW), the central, and the south-eastern (SE) part. The NW and the central parts of the Vinodol Valley belong to the Dubračina River Basin (43.22 km²), while the SE part belongs to the Suha Ričina River Basin (21,35 km²). The area is predominantly rural, with more than 50 small settlements connected by relatively dense road network.

The prevailing elevations range from 100 to 200 m a.s.l., and the prevailing slope angles range between 5° and 20°. The Valley flanks are composed of Cretaceous and Paleogene carbonate rocks (limestone, and dolomites), while the lower parts and the bottom of the Valley are composed of flysch bedrock (marls, siltstones and sandstones in alternation), in a synclinal position (Blašković 1999).

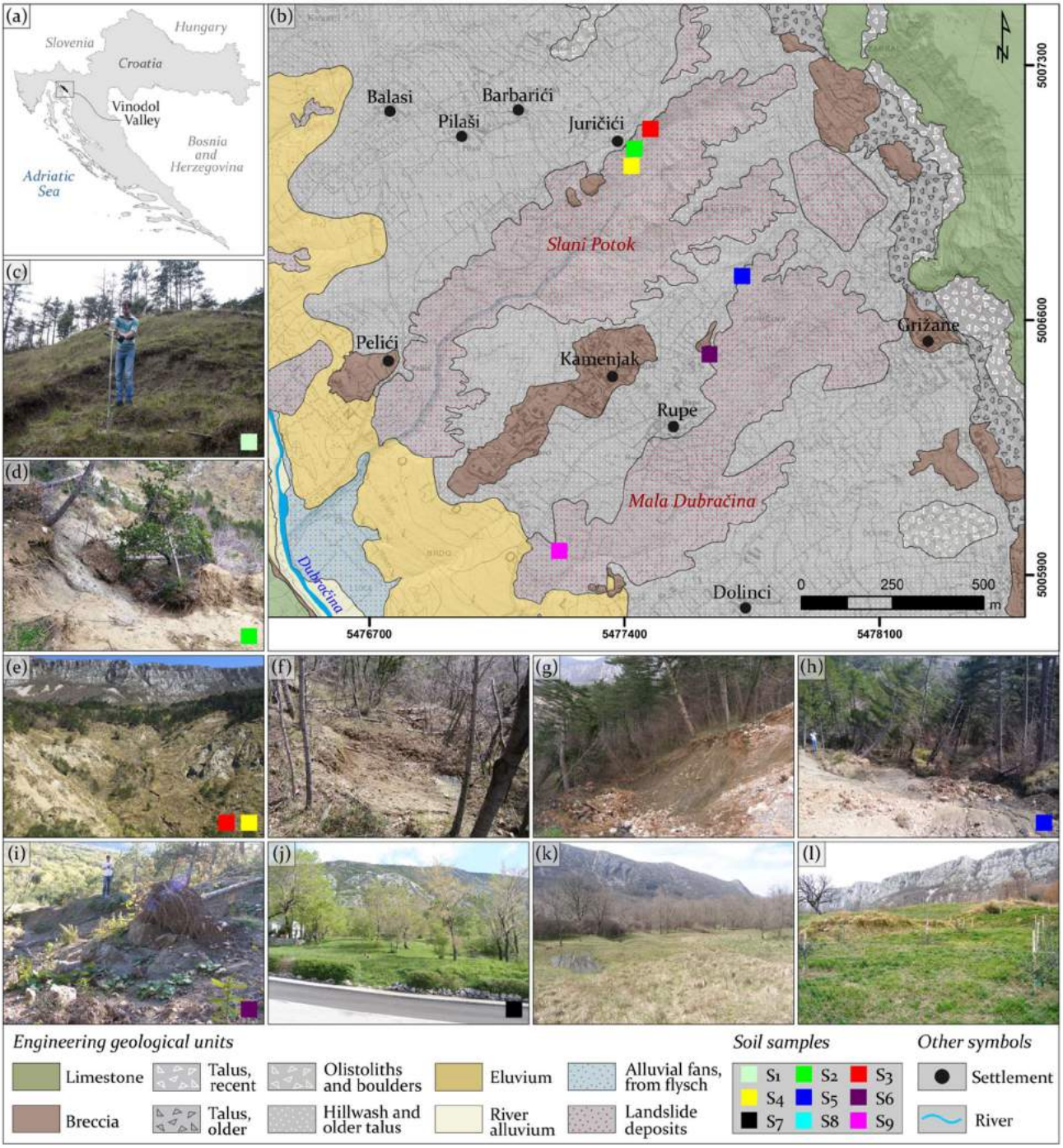

Figure 1 (a) The geographical location of the Vinodol Valley; (b) a detail from the Engineering geological map of the central part of the Vinodol Valley (Đomlija, 2018). Locations of individual soil sampling sites are also presented. Photographs of debris slides located in the nortwestern part (c), and in the central part (from (d) to (l)) of the Vinodol Valley. Investigated debris slides are labelled, according to the soil samples labels.

In the Dubračina River Basin, the NE carbonate slopes have a form of almost vertical cliffs, (Fig. 1b), which are in a reverse tectonic contact with the Palaeogene flysch deposits.This tectonic contact is almost entirely covered by the older talus, and the recent talus deposits (Fig. 1a). Individual limestone boulders were transported to the hypsometrically lower portions of the cliff's foothills, probably as a result of larger rock falls (Đomlija, 2018). Flysch outcrops are rare, because the bedrock is mostly covered by Quaternary superficial deposits (Đomlija 2018), formed by geomorphological processes active both in the carbonate and the flysch rock mass (Đomlija et al. 2017).

Flysch slopes in the central part of the Vinodol Valley are mostly covered by the hillwash and older talus deposits (Fig. 1b), mainly composed of high plasticity clays to gravely clays (Pajalić et al. 2017), and mixed with the limestone and flysch rock fragments. These soils vary in thicknesses and engineering geological properties along the study area, due to the gravitational transport and mixing of fragments. Breccias have a patchy occurrence along the flysch slopes, and individual sedimentary bodies are characterized by variations in sizes and shapes.

Flysch slopes have been dissected by several relatively large and deep gullies, such as the Slani Potok, and the Mala Dubračina gullies located in the central part of the Vinodol Valley (Fig. 1b). In the Dubračina River Basin, more than 500 debris slides and debris slide-debris flows (Hungr et al. 2014) are identified within the gullies (Đomlija 2018). Details of individual investigated debris slides located within gullies are presented in Fig. 1c to 1i. These landslides are relatively small and shallow, with an estimated volume in a range between $<10^3$ and 10^5, and estimated depth in a range between one and several (approx. 5) meters. Most of the landslides are activated along the gully channel margins, and they extend to the gully channel bottom. Landslides are mainly of successive distribution. Thus, the landslide deposits (i.e., zones of accumulations) occupy almost the entire area of gully channels and, therefore, landslide deposits are identified as a separate engineering geological unit of the Vinodol Valley (Đomlija 2018). The area of this unit is 1.03 km^2 in the Dubračina River Basin (Fig. 1b). Certain amount of single, mainly suspended and dormant landslides (Fig. 1j to 1l) are located at the flysch slopes outside the gully channels, even in the urbanized areas. These landslides are generally larger, with volumes greater than 10^5 m^3, and estimated depths of several meters.

Material and methods

Soil sampling procedure

For the preliminary testing of clay activity from landslide deposits in the study area, samples were taken from the colluvial deposits of nine debris slides. Two samples were collected in the NW part, and seven samples were collected in the central part of the Vinodol Valley. Locations of six soil samples collected in the central part of the Vinodol Valley are presented in Fig. 1b. Sampling locations were selected based on the accessibility to the landslide bodies. However, selection of the sampling sites was limited by morphological and land-use conditions of the studied area, given that most of debris slides are located within complex gullies covered by dense forests. Eight samples (S2 to S9) were taken by applying the rectangular soil block sampling technique using the sampling box, and one sample (S1) was taken by applying the manual drilling using an auger and a sampler. All samples were taken from the subsurface depths. Depths of the samples taken using the sampling box ranged from 0.50 and 1.00 m, while the depth of the sample taken using the auger and sampler was 1.50 m.

Laboratory testing methods

Two type of laboratory tests were performed on soil samples taken from landslide deposits, according to the British Standards (BS 13377-2 2010): (1) particle-size analysis; and (2) Atterberg's limits. The testing was performed in the Geotechnical laboratory of the Faculty of Civil Engineering, University of Rijeka.

The particle-size analysis was performed by sieve analysis for the coarse-grained, and by hydrometer analysis for the fine-grained soil samples components. All soils were sieved by applying the wet sieving method (Fig. 2a). A series of sieves were in range from 20 mm and 0.063 mm. Preparation of samples started 24 hours prior the wet sieve analysis. Samples were initially soaked in a solution of water and sodium hetamethaphosphate, and then shacked in the sieve shaker according to the used standard. Sieves were left to drain, and samples were dried in the dryer on 105 °C for 24 hours. The dried soil material masses retained on the sieves were weighted and recorded. The hydrometer analysis relates the terminal velocity of the grains in suspension, their density, and the density of the fluid (Holtz et al. 2011). Based on this test, the grain diameter can be calculated from the distance and the time of fall. The hydrometer also determines the density of the suspension, and this provides the calculation of the percentage of particles of a certain equivalent particle diameter at a given time. From the results of the hydrometer analysis, the percentage of clay fraction in whole tested sample was calculated for each sample.

Liquid-limit (LL) tests were performed using the Casagrande liquid-limit device (Fig. 2c). Each sample was prepared 24 hours prior the test (BS 1377-2 2010). After performing the liquid-limit tests, plastic-limit (PL) tests were performed (Fig. 2d), and the plasticity index (PI) was calculated for each sample. Finally, the activity of clays was determined for each sample, as the ratio of the plasticity index (PI) and the percentage of clay particle size (Skempton 1953), providing a good correlation between the activity and the type of clay minerals (Holtz et al. 2011).

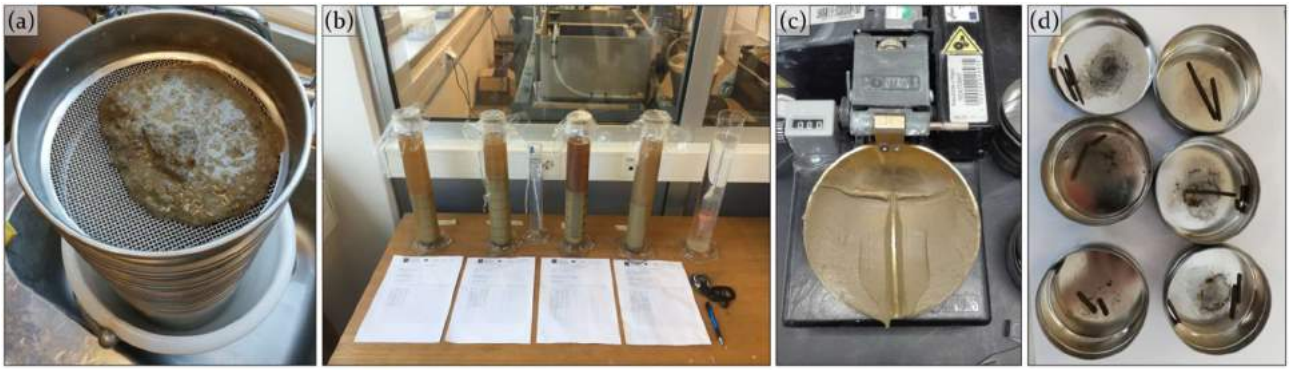

Figure 2 Soil samples during the laboratory testing methods: (a) the wet sample prepared for the wet sieve analysis; (b) the fine-grained soil sample components during the hydrometer analysis; (c) the sample prepared for the liquid-limit test; and (d) the samples after the plastic-limit test.

Results

Particle size distribution and Atterberg's limits

Results of the particle-size analysis are displayed in the ternary plot presented in Fig. 3. Silt fraction prevails in most of the tested soil samples, with percentages in range between 50.89 % (S8) and 77.13 % (S6). Five samples (S2, S3, S4, S5, and S9) have the similar percentage of silt size particles, that is approximately 60 % (i.e., 57.73 % for S9, and 64.22 % for S2).

The percentage of the coarse-grained soil sample component is the highest for the sample S7 (Fig. 3). This sample contains almost the equal amount of gravel (19.78 %) and sand (18.62 %) size particles (Prša 2018). Sample S8 contains 15.18 % of coarse-grained particles, with the 13.33 % of sand, and 1.85 % of gravel size particles. Other tested soil samples contain less than 10 % of coarse-grained component (Fig.3), with the sand size particles prevailing in samples S1, S3, S4, S5, S6, and S9 (Prša 2018).

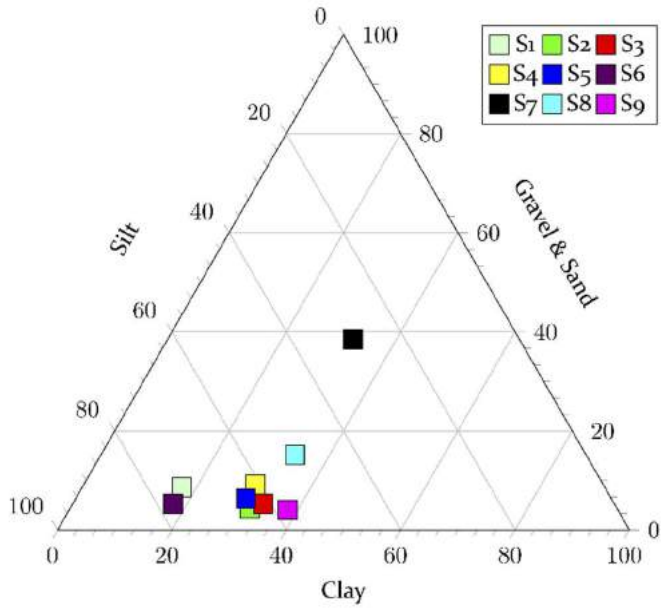

Figure 3 Particle size distribution in soil samples from landslide deposits in the Dubračina River Basin.

The amount of clay size particles in tested soils ranges between 17.46 % (S1) and 38.17 % (S9). For most of the tested samples (i.e., S2, S3, S4, S5, S7, and S8), the clay fraction is approximately 32 % (min. of 29.80 % for the sample S5, and max. of 33.93 % for the sample S8).

All tested soil samples are displayed above the A-line in the plasticity chart (Fig. 4). Six samples (S1, S3, S4, S5, S7, and S9) are displayed in a domain of intermediate plasticity clay (ClI according to the ESCS Scheme), with samples S4 and S5 having the same LL and PI values. Two samples (S2, and S8) are high plasticity clays (ClH), and one sample (S6) is low plasticity clay (ClL).

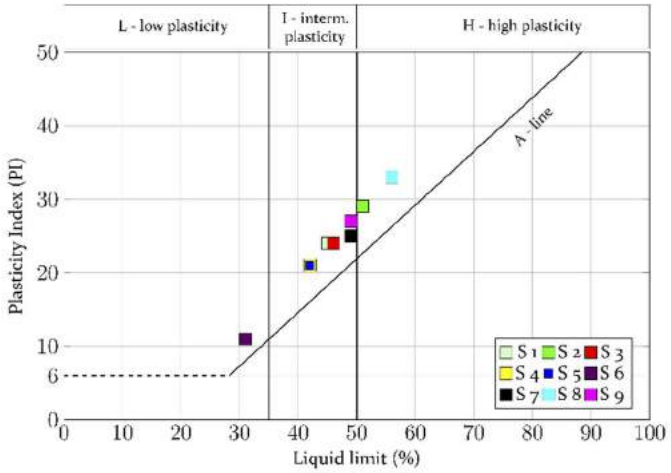

Figure 4 Plasticity chart of soil samples from landslide deposits in the Dubračina River Basin.

Clay activity

Results of the preliminary testing of clay activity from landslide deposits are presented in Fig. 5. According to this study, inactive clays (i.e., kaolinite) prevail in tested soil samples. Namely, five samples (i.e., S3, S4, S5, S6, and S9) have an activity that is in range between A = 0.70 (S4, and S5) and A = 0.72 (SS3). These activity values are around the lower boundary of the activity values for normal clays. Three samples (S2, S7, and S8) have normal clay minerals (i.e., illite), with activities that are in range between A = 0.92 (S2) and A = 1.07 (S7). The most active clay minerals (i.e., montmorillonite) have been found in one tested soil sample (S1), with the activity of A = 1.37.

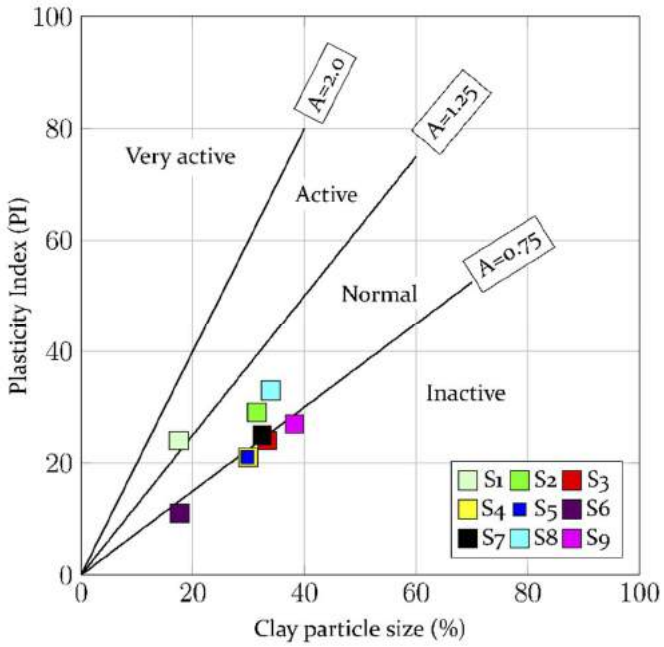

Figure 5 Activity of clay minerals in soil samples from landslide deposits in the Dubračina River Basin.

Discussion and conclusions

The preliminary results of conducted tests on only nine samples taken from landslide deposits in the Dubračina River Basin showed that the tested soil materials have similar basic geotechnical properties as the soil materials from landslides activated in the wider area within the flysch domain (Maček et al. 2017): the soil materials are mostly inorganic clays of intermediate plasticity (ClI) to high plasticity (ClH), with prevailing inactive and normal clay minerals. Soil activity pointed on the presence of particular clay minerals (kaolinite and illite, in this case), but it cannot substitute the complete mineralogical analysis that is, however, time consuming, more expensive and requires more sophisticated laboratory equipment in a case of these soil types (Vivoda Prodan et al. 2017).

Although the activity of clays cannot be directly related to the landslide triggering factors, it can be a relative indicator for identification of slope material more susceptible to sliding. Activity of clays can be related to soil strength parameters (Skempton 1953), and especially to residual friction angle (Collotta et al. 1989) that is important for landslide triggering and run-out analysis. The soils with lower activity generally have lower values of cohesion and can retain less quantity of infiltration water before a loss of the strength. According to these facts, soils with lower activity have consequently lower shear strength and are more sensitive to transition into a weaker consistency caused by increasing of the water content. A fall down from peak to residual value of friction angle is relatively small in inactive and normal clays (Collotta et al. 1989; Polidori 2009). That can be explained by analyzing a type of shearing: the soils with the clay content that is lower than 25% behave much like sand and silt and are characterized by rolling shear, while the residual strength of soils with more than 50% of clay fraction is controlled by sliding friction of the platy clay minerals (i.e., sliding shear). When the amount of clay fraction lies between 25% and 50%, there is a transitional shear involving both rolling and sliding mechanisms in different part of a shear zone (Skempton 1985; Polidori 2009). The amount of clay fraction in tested soils ranges between 17.46 % (S1) and 38.17 % (S9), thus classifying the shear mechanism in rolling and transitional shear, with the corresponding consequence that landslides formed in this type of soil material have a relatively short run-out.

Previous discussion is related to the tested soils that contain almost inactive and normal clay minerals. However, it is well known that landslide in some other parts of the Dubračina River Basin are formed in soils with more active clay minerals and higher content of clay fraction (Aljinović et al. 2010; Jurak et al. 2005; Vivoda Prodan et al. 2017). Consequently, the sliding shear mechanism with significant fall down of the shear strength from peak to residual value, and consequently a longer run–out, prevail in these soils. There are also present some other processes, such as the cation exchange, that can significantly impact on geotechnical properties of clays.

These facts are very important for landslide occurrences in the Vinodol Valley. Knowing the activity of clays in a slope can indicate the rainfall threshold, the potential landslide type, as well as the landslide run-out. All these data are necessary in landslide susceptibility, hazard and risk assessment in the Dubračina River Basin, as well as in the entire area of the Vinodol Valley.

Acknowledgments

We acknowledge the project Research Infrastructure Development at the University of Rijeka Campus (RC.2.2.06-0001) co-financed by the European Regional Development Fund (EFRR) and the Ministry of Science, Education and Sports of the Republic of Croatia.

References

Aljinović D, Jurak V, Mileusnić M, Slovenec D, Presečki F (2010) The origin and composition of flysch deposits as an attribute to the excessive erosion of the Slani Potok valley (''Salty Creek''). Geologia Croatica. 63(3): 313–322.

Blašković I (1999) Tectonics of part of the Vinodol Valley within the model of the continental crust subduction. Geologia Croatica. 52(2): 153-189.

BS 1377-2 (2010) Methods of test for soils for civil engineering purposes. Classification tests.

Collotta T, Cantoni R, Pavesi U, Ruberl E, Moretti P C (1989) A correlation between residual friction angle, gradation and the index properties of cohesive soils. Géotechnique. 39(2): 343–346.

Đomlija P, Bočić N, Mihalić Arbanas S (2017) Identification of geomorphological units and hazardous processes in the Vinodol Valley. Abolmasov B, Marjanović M, Đurić U (eds.): Proceedings of the 2nd Regional Symposium on Landslides in the Adriatic-Balkan Region. University of Belgrade, Faculty of Mining and Geology, Belgrade. 109-116.

Đomlija P (2018) Identification and classification of landslides and erosion phenomena using the visual interpretation of the Vinodol Valley digital elevation model (in Croatian). Dissertation. University of Zagreb, Faculty of Mining, Geology and Petroleum Engineering.

Holtz RD, Kovacs WD, Sheahan TC (2011) An introduction to geotechnical engineering. Pearson, Upper Saddle River, USA (ISBN 978-0-13-031721-6).

Hungr O, Leroueil S, Picarelli L (2014) The Varnes classification of landslide types, an update. Landslides. 11: 167-194.

Jurak V, Slovenec D, Mileusnić M (2005) Excessive flysch erosion—Slani Potok. Excursion guidebook of the 3rd Croatian geological congress. Opatija, Croatia. 51–55.

Kovačević MS, Jurić-Kaćunić D (2014) European soil classification system for engineering purposes. Građevinar. 66(09): 801-810.

Maček M, Petkovšek A, Arbanas Ž, Mikoš M (2017) Geotechnical aspects of landslides in flysch in Slovenia and Croatia. Abolmasov B, Marjanović M, Đurić U (eds.): Proceedings of the 2nd Regional Symposium on Landslides in the Adriatic-Balkan Region. University of Belgrade, Faculty of Mining and Geology, Belgrade. 25-31.

Pajalić S, Đomlija P, Jagodnik V, Arbanas Ž (2017) Diversity of Materials in Landslide Bodies in the Vinodol Valley, Croatia. Mikoš M, Vilímek V, Yin Y, Sassa K (eds.): Advancing Culture of Living with Landslides, Volume 5. Springer, Berlin (ISBN 978-3-319-53483-1). 507-516.

Polidori E (2009) Reappraisal of the activity of clays. Activity chart. Soils and foundations, 49(3), 431–441. doi:10.3208/sandf.49.431

Prša M (2018) Testing the clay activity of the colluvial deposits of the Dubračina River Basin (in Croatian). BSc thesis. University of Rijeka, Faculty of Civil Engineering.

Skempton AW (1953) The Colloidal Activity of Clays. Proceedings of the 3rd International Conference on Soil Mechanics and Foundation Engineering, Volume 1. 57-61.

Skempton AW (1985) Residual strength of clays in landslides, folded strata and the laboratory. Geotechnique. 35(1): 3-18.

Toševski A (2018) Susceptibility of the Dubracina River Basin to the superficial geodynamical processes (in Croatian). Dissertation. University of Zagreb, Faculty of Mining, Geology and Petroleum Engineering.

Vivoda Prodan M, Mileusnić M, Mihalić Arbanas S, Arbanas Ž (2017) Influence of weathering processes on the shear strength of siltstones from a flysch rock mass along the northern Adriatic coast of Croatia. Bulletin of Engineering Geology and the Environment. 76(2), 695–711. doi:10.1007/s10064-016-0881-7

doi.org/ 10.35123/ReSyLAB_2019_21

Case study of collapsed landslide in Asenovgrad, Bulgaria

Andrety Totsev[1],

1) University of architecture, civil engineering and geodesy, Department of Geotechnics, Sofia

Abstract The article presents a landslide near the town of Asenovgrad in Bulgaria, which caused damages to the road. A design was prepared to strengthen the slope, but because of some problems the slope collapsed again. Additional geological survey was made, being subject to a new project. This article presents the stabilization of the second landslide occurrence. The study presents the analysis which has been carried out comparing the results of Eurocode 7 and the Regulation for design concerning landslide areas which has been in force in Bulgaria before the introduction of Eurocode 7. The study covers an analysis of the bearing capacity of anchors in case of an earthquake.

Keywords landslide, pile, anchors,

Introduction

In 2015, as a result of an execessive soil moisture along the slope caused by rainwater infiltration, a landslide was activated, which led to destroying part of the road situated above the aquapark together with damages caused by the lower parts of the landslide to the newly built facilities (Photos 1 and 2). Some colleagues have been engaged in design and execution of a stabilization structure and restoration of the roadway. In the summer of 2015, a pile-anchore strengthening works (Photos 3 and 4) were performed in the area of the roadway failure (above and below the road line) and the body of the road was restored. Subsequently, a new local landsliding occurred below the area of the stabilization structure (Photo 4). At this point, the owners of the aquapark contacted the author of the present study to express their concern about the ongoing movement of the earth masses in the direction of their property, in spite of the accomplished strengthening works. A new design had been developed and implemented concerning stabilization (anchored system with bored piles and pile cap) in the foot of the landslide. To drain the lithological varieties in the area of the sliding surface and to improve its loading properties, drainage wells with a depth of 10.00 m have been drilled right behind the stabilization structure.

The observation conducted until 2019 (almost 4 years after the second stabilization), show that the landslide is stabilized and no movements have been observed. This article presents a solution for stabilization of the landslide, along with some comments on Regulation 12 (Bulgarian norms for stabilization of landslides) and Eurocode 7 [1, 4]. In addition, a solution is presented for determining the bearing capacity of anchors in seismic conditions.

Photo 1 a) Satellite image of the landslide. b) Displacement of the road. c) Local stabilization of the road. d) Slide after the execution of the primary stabilization.

Engineering-geology conditions on site

The geological survey shows that the area of construction consists of quaternary and paleogene deposits. The quaternary layer is represented by gravel filling. Under the gravel there is yellow-brown clay, compacted with separate gravel fills. The paleogene layer is represented by light to dark brown sandstone clays. In the area of the investigated landslide the following lithological varieties are revealed: LITHOLOGICAL TYPE №1 - Backfilling - part of the pavement of the adjacent road. It is composed of large gravel stones and boulders with sandy filling. LITHOLOGICAL TYPE №2 - Quaternary clay with gravel fills. This variety is found immediately under lithological type 1. It is established in all boreholes. LITHOLOGICAL TYPE №3 – Visually, it consists of quaternary clay to be defined as yellowish-brown, with admixtures of gravel. This variety is located under lithological type 2. An increased content of gravel has been established in this lithological variety - up to 30% compared to lithological type 2 and higher water content compared to lithological type 2. LITHOLOGICAL TYPE 4 – Sandy clay, light brown to dark brown with limestone particles, in some areas with gravel stones. It is found in all test pits.

Soil assessment parameters which have been used for slope stability calculations are shown in Table 1. 1 (according to Regulation 12) and in Table 2 (according to Eurocode 7). Lithological type 1 due to its relatively small thickness (0,20 cm) was not taken into account in the calculations performed.

Table 1 Values of the calculation parameters according to Regulation 12

Layer	Dry unit weight γ_d [kN/m^3]	Angel of int. friction φ_d [°]	Cohesion c_d [kPa]
Lit. type 2	20.80	16.28	11.80
Lit. type 3	19.53	10.60	0
Lit. type 4	20.80	19.83	9.25

Table 2 Values of the calculation parameters according to Eurocode 7

Layer	Dry unit weight γ_d [kN/m^3]	Angel of int. friction φ_d [°]	Cohesion c_d [kPa]
Lit. type 2	20.80	15.36	15.10
Lit. type 3	19.53	10.11	0
Lit. type 4	20.80	18.72	11.84

Underground water in the area of the investigated site has been identified at different levels in all test pits. Underground water is accumulated by rainwater infiltration, by the surrounding slopes and in some places the water is supplied by leakages from the water supply network. The seasonal fluctuation of the water level for this area varies. For the purpose of calculation, it is accepted that the groundwater level is about 4.50 m below the ground level.

Normative documents

The regulation for design of landslides that has been valid in Bulgaria prior to the introduction of Eurocode is "Regulation 12 for the design of geo-protection structures, buildings and facilities in landslide areas". Following the introduction of Eurocode 7 [1,4], a special interpretation of the norms has been adopted in Bulgaria, with some of the approval authorities demanding the basic checks related to the stability calculations of the landslide, calculation checks of piles, pile caps and reinforcement walls, as well as design of anchors, to be carried out in accordance with Eurocode 7 (EC7), as well as to be in compliacne with the requirements of Regulation 12 (R12). The design solution presented in this case study ensures the stability of the landslide according to the requirements of the Bulgarian norms and the Eurocode. Here are some of the more significant differences between R12 and EC7:

Partial factors between characteristic and calculation values of soil parameters.

The values of the soil stability parameters are calculated with different factors according to R12 and EC7. According to the national annex to EC7, Bulgaria adheres to DA2, for all cases except for the slope stability check of the slopes where the coefficients for DA3 are in force. Below are shown the correction coefficiants for

$tg\phi_d = \frac{tg\phi_{ch}}{\gamma_{\phi'}}$; $c_d = \frac{c_{ch}}{\gamma_{c'}}$;$\gamma_d = \frac{\gamma_{ch}}{\gamma_\gamma}$,

as follows:

Regulation 12 $\gamma_g = 1{,}0$; $\gamma_c = 1{,}6$; $\gamma_\phi = 1{,}2$;
EC7 - GEO - DA3 $\gamma_\gamma = 1{,}0$; $\gamma_c{}' = 1{,}25$; $\gamma_\phi{}' = 1{,}25$.
EC7 - STR - DA2 $\gamma_\gamma = 1{,}0$; $\gamma_c{}' = 1{,},0$; $\gamma_\phi{}' = 1{,}0$.

Calculation methods

For the purposes of conduction a stability analysis, EC7 allows the surfaces of failure to have a variety of shapes (flat, cylindrical, and free form), explicitly stating that resistance can be verified by the Finite Element Method, which allows use of the popular in the practice method of „ϕ, c - reduction“. The stability analysis according to R12 is carried out by checking the sliding on a circular-cylindrical or other slip surface. Here, EC7 and R12 do not differ, and given the delayed entry into practice of the "ϕ, c - reduction" method, it is not specifically mentioned in R12, but there is a certain freedom in the interpretation referring to a stability factor for "other methods". A significant difference is observed in the assessment of the stability of the adopted calculation methods. A comparison between the minimum acceptable factor of safety, representing the ratio of holding to sliding resistance, for landslides I and II category, according to R12 and EC7, is shown in Table 3.

Table 3 Minimum acceptable factors of safety

Normative document	Fellenius		Bishop/ „ϕ, c - reduction“	
	Basic combination of loads	Seismic combination	Basic combination of loads	Seismic combination
Regulation 12	1,20	1,10	1,25	1,15
Eurocode 7	1,00	1,00	1,00	1,00

Typically, the designers in Bulgaria together with the slope stability analysis use also the subgrade reaction method (SRM) for determining the shear strength of a structure (pile caps, piles and anchors). In the table 4 are shown the partial coefficients according to R12 and DA2 at STR ultimate limit states:

Table 4 Partial factors on actions or the effects of actions

Actions	Limit state	
	Regulation 12	STR (DA2)
Permanent unfavourable	1,00	1,35
Permanent favourable	1,00	1,00
Variable unfavourable	1,00	1,50
Variable favourable	0	0

Seismic forces

According to BDS EN 1998-5 (Eurocode 8), the calculation seismic inertial forces FH and FV acting on the soil mass in the pseudostatic analysis in the DA3 stability analysis are determined by:

$F_H = 0{,}5 \cdot \alpha \cdot S \cdot W$

$F_V = 0{,}5 \cdot F_H$ at $a_{vg}/a_g > 0{,}6$ $\quad F_V = 0{,}33 \cdot F_H$ at $a_{vg}/a_g \leq 0{,}6$.

According to BDS EN 1998-5, for determination of the earth pressure load for determination of the STR ultimate limit state, the formulas of Mononobe и Okabe have been used:

$E = \frac{1}{2}\gamma(1 \pm k_v)K_{AE}H^2$.

In addition, according to BDS EN 1990 NA (National Annex to Eurocode 0), the partial coefficients for impact on seismic computational situations are assumed to be equal to 1,0. The value of the coefficient ψ2 for obtaining the quasi-constant value of the variable impact, which reduces the load on the road from vehicles, is taken according to table NA.A1.1 and varies in the range 0,3-0,6.

According to Regulation 12, in the investigation of the resistance in seismic areas, shall be also included the inertial forces of the soil masses over the possible sliding surface. When using the Method of slices, the moment of inertial forces of the soil mass relative to the centre of rotation is determined by the formula:

$M_{\Pi} = R_{\Pi} \cdot K_C \cdot \sum_{i=1}^{n} G_i h_i$,

where Kc is the seismic coefficient, RП is the coefficient of subgrade reaction that is considered to be 0,4-0,5 for landslides.

According to Annex 4 of R12, in some cases the seismic component of the landslide pressure can be determined by the formula:

$E_S = C \cdot R_{\Pi} \cdot K_C \cdot G$, where the coefficient of significance C=0,75-1,50 depending on the category of the landslide; RП is the coefficient of subgrade reaction and is accepted to be 0,5.

Retaining structure

The reinforcement has been executed with an anchors and bored piles with pile caps with framed action (Figure 1) at the foot of the landslide. The reinforced concrete wall, taking up the load from a certain area of the landslide body and transmitting the forces on the piles and anchors, has been executed with a thickness of 0.80 m. It is also a retaining support wall that transmits the pressure in the anchors and the pile caps for the pile reinforcement. Piles are bored cast-in-place concrete piles, with a round cross-section D600, with a distance between axes of 1.50 m.

a.

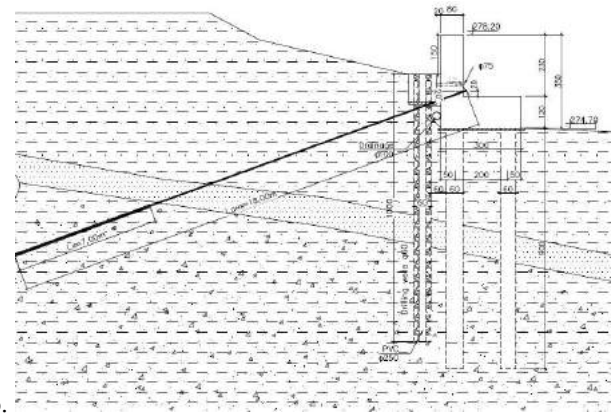

b.

Fig. 1 Retaining structure a. plane view; b. section view

The piles are installed in two parallel rows, joined with a pile cap. The layout is of quincunx double-row piles. The length of the piles is 9.00 m. There are passive single bar anchors. The designers have preferred to execute IBO

R32N anchors (tension load of 230 kN / ultimate load of 280 kN). Water well drilling wells - for drainage of the lithological varieties in the area of the failure surface and improving its strength properties, have been executed immediately behind the retaining wall - 5 pcs. water drilling wells with a diameter of 60 cm and a depth of 10.00 m.

Stability analysis of the landslide in Assenovgrad

The terrain has been separated into sections and studied by the method of the circular-cylindrical sliding surface and by a specified sliding surface. Additionally, calculations were performed with Tower on the sub-grade reaction method. The calculations were conducted with the specialized geotechnical program "Slope". The results are obtained by various calculation methods. The most reliable method in this case study is the Bishop method which is part of the national regulatory framework. Tests have been executed in compliance with the minimum allowed safety factors according to R12 concerning basic and seismic combinations of loads which are 1,25 and 1,15 respectively.

Table 5 Coefficients of stability using retaining structures acc. Regulation 12.

Slope condition	Basic combination		Seismic combination	
	Circular-cylindrical slip surface (Bishop)	Specific slip surface (Jambu)	Circular-cylindrical slip surface (Bishop)	Specific slip surface (Jambu)
Slope with natural water content	1,92	1,99	1,17	1,16

Table 6. Coefficients of stability using retaining structures acc. Eurocode 7 (Fs ≥ 1).

Slope condition	Basic combination		Seismic combination	
	Circular-cylindrical slip surface (Bishop)	Specific slip surface (Jambu)	Circular-cylindrical slip surface (Bishop)	Specific slip surface (Jambu)
Slope with natural water content	1,89	2,01	1,15	1,13

Additionally, the terrain was modeled and investigated using the circular-cylindrical slip surface method in accordance with the Eurocode 7 DA 3 method. The safety factor for the most unfavourable sliding surface (the minimum value) Fs should fulfill the condition Fs ≥ 1. Summarized results for the obtained coefficients are given in table 5 (according to Regulation 12) and in table 6 (according to Eurocode 7). Sample solutions are shown in Fig. 2 and Fig. 3.

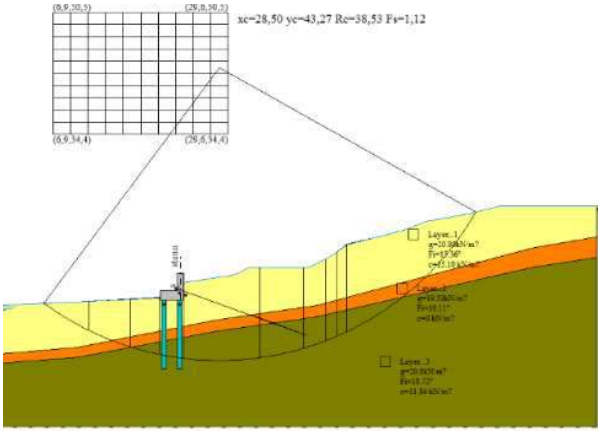

Figure 2 Analisys as per the circular-cylindrical slip surface method of Bishop for local and global stability

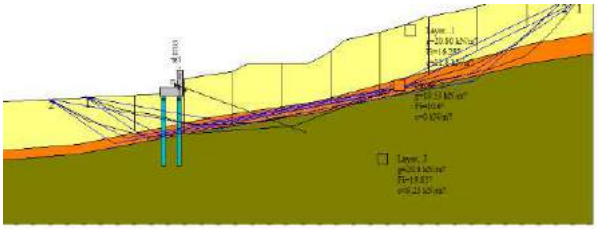

Figure 3 Analisys as per the specific slip surface method of Jambu

Calculation and construction of the reinforcement structure

In order to ensure stability during exploitation a stabilization reinforcement has been implemented. According to Regulation 12, considering the accepted values of the soil parameters, the force of the landslide pressure can be determined by the formula:

$$E_{cв} = m(\phi)\frac{\gamma \cdot h^2}{2} cos^2\,\phi - 2 \cdot c \cdot h \cdot cos\,\phi$$

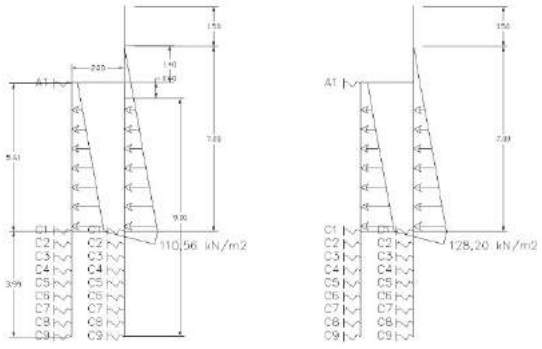

Figure 4 Calculations scheme for: a. basic combination of loads; б. particular combination of loads

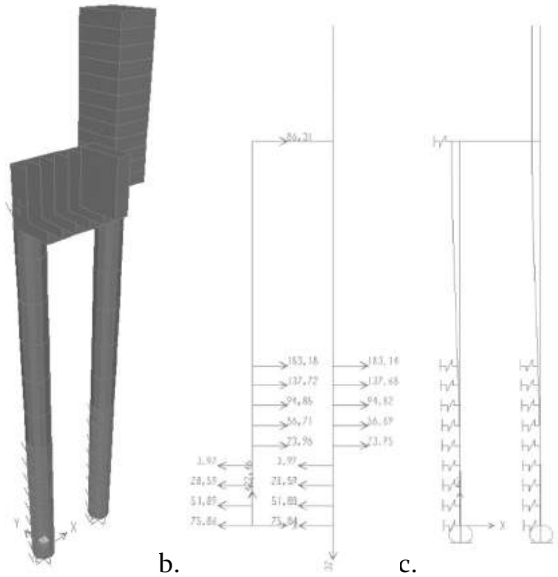

a. b. c.

Figure 5 Solution as per 3PM of Tower (basic combination of loads): a. model; b. Reactions in the springs; c. Deformation scheme δmax=5,05 cm < xrp = 10 cm according to Regulation 12.

Thus, for the landslide pressure has been obtained the following result Els = 386.95 kN. The inertial seismic force of the earth mass above the sliding surface is ES = 61.80 kN. Given the accepted distance between the piles of 1,50 m in row or 0,75 m for static calculations as a frame structure, the following pile loads are taken: Els,p = 386,95 * 0,75 = 290,22 kN and Es,p = 61.80 * 0.75 = 46.35 kN. Two load combinations have been analysed: the basic load combination – activated sliding pressure; a seismic load combination - the sliding pressure and the inertial seismic force act. The coefficient for horizontal load of earth base according to R12 is changed following a linear pattern Cx=Cxz=0 + k*z. In accordance with Regulation 12, the clear distance between piles bo ≤ bкр: bкр = 5,14*c*D/qсв = 0,925 m > 0,75 m. A scheme of calculation has been adopted using a triangular pattern of the loads in compliance with the requirements of Regulation 12, as shown in Fig. 4.

The used calculation scheme was implemented with the Tower program. The results obtained for the basic combination are shown in Fig. 5.

Calculation of anchors

Basic combination

Prior to the introduction of Eurocode 7 in Bulgaria there were no established rules for design of anchors. However, Regulation 12 provides some guidelines, such as: anchors are designed with a slope to the horizon of 10-300; minimum length of the anchor bond is 4.00 m, in the solid layers below the sliding surface; design tension for the anchors should be 50 to 60% of their computational load, etc. In the specialized studies there are numerous formulas and tables for determining the anchor bearing capacity and the results may vary by more than 100%. Eurocode 7 and Regulation 12 enable the designer to choose how to determine the anchor's bearing capacity.

According to calculations made in compliance with EC7, the computation value Ra,d of the ultimate bearing capacity of the anchor shall satisfy the condition Pd ≤ Ra,d where Pd is the calculation of the design strenght in the anchor; Ra,d = Ra,k /γa, where γa,t (for temporary anchors) = γa,p (for permanent anchors) = 1,10. Pd = 86,31 kN - for a basic load combination. Pd = 100,13 kN - for a seismic load combination. Soil parameters in the anchor bond area: γk = 20,80 kN/m3, ϕk' = 19,830, ck' = 9,25 kN/m2. Calculated value of the anchor strenght Pd = PG,k.γ; PG,k = 86.31 kN; Pd = 1.35. 86.31 = 116.51 kN; γG = 1.35. The accepted dimensions of the anchor are free length Lo = 11.00 m and bond length Lk = 7.00 m. The bearing capacity is determined by several methods:

Ostermeyer graphics

Acording to "Ostermeyer" the characteristic value of the bearing capacity of the anchor is Ra,k = 250-360, accepted to be 250 kN (calculated as per the Ostermayer graphics for high plasticity clays).

Ra,d =Ra,k /γa = 250/1,1 = 227,27 kN.

Pd = 116,51 kN ≤ Ra,d = 227,27 kN

Methos of Bowles (Bowles 1997)

Lk = 7,00 m, Dk = 0,15 m и km = 1,0

Ra,k = km.π.d.Lk.(0,75γ.z.tgφк + ck) = 195,25 kN

Ra,d =Ra,k /γa = 195,25/1,10 = 177,51 kN.

Pd =116,51 ≤ Ra,d = 177,51 kN

Method according to DIN 4128

qs = 50 kPa

Ra,k = π.d.lk.qs,k = 164,85 kN

Ra,d =Ra,k /γa = 195,25/1,10 = 149,86 kN.

Pd =116,51 ≤ Ra,d = 149,86 kN

Seismic combination

The problem of determining the bearing capacity of anchors during earthquakes has not been yet solved. In the specialized books there are some guidelines for determining the reduction. One possible solution is using the Russian building codes (SNiPs) 2.02.03-85 [5] for the design of pile foundations in seismic conditions. Correction coefficients are introduced in order to be used in multiplication with friction and peak resistance. In anchors, peak resistance is absent, but the principle of skin friction is acting in a similar way and therefore it is possible to determine the bearing capacity of anchors in seismic conditions with the coefficient of reduction of ambient friction in piles (refer to table 5).

In 2014 the author of the case study together with Dr. Eng. I.Markov [2,3] developed a shake table for determining the bearing capacity of anchors in seismic conditions. More than one hundred and fifty anchor tests were run in the setup shown in Figure 6. The device consists of a steel structure with a volume of 1m³ soil (sand). On the soil media is exerted overburden pressure by a hydraulic jack, which reproduces the effect corresponding to different soil depths. The anchor force is

exerted by loading systems. The device is isolated from the building by vibration isolators. The device is designed to test the anchors in terms of static and dynamic conditions and the scope of testing is: ground acceleration – (0÷0.4)g; displacement of the device – (2÷3) cm; frequency – (2÷12) Hz; overburden pressure – up to 4m soil layers; anchor force up to 10 kN.

Table 5 Correction coefficients γeq2 for reducing the friction in determining the bearing capacity of piles in seismic conditions [34].

Intensity of earthquakes as per MKSK scale	Dense to medium dense sands		Clays with a parameter of consistency Ic		
	Slightly damp to damp	saturated	Ic ≤ 0,25	0,25<Ic ≤ 1,00	Ic>1,00
VII	0,95	0,90	0,95	0,85	0,75
VIII	0,85	0,80	0,90	0,80	0,70
IX	0,75	0,70	0,85	0,70	0,60

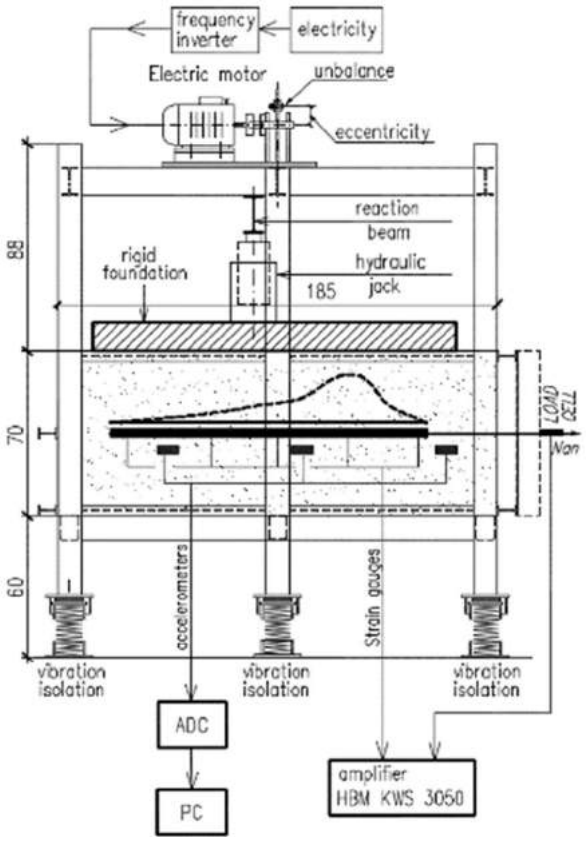

Figure 6 Model for testing anchors

After analyzing results from the models, the following conclusions were made, about sand with different water content:

- acceleration equal to 0.09 g there is 0-5% reduction of the anchor bearing capacity
- acceleration equal to 0.18g there is 5-15% reduction of the anchor bearing capacity
- acceleration equal to 0.28g there is 20-35% reduction of the anchor bearing capacity.

As a result of the analysis, it is accepted that the bearing capacity according to Markov&Totsev [2,3] should be reduced with 20-35% and according to SNiP – with 30%. The accepted value is 30%.

Conclusion

The article has been aimed to present a practical solution for stabilization of a landslide in Bulgaria, in compliance with the current norms. The presented dependence on the anchor strength reduction is one possible, though simple solution to the problem. An importance of the exact position of the strengthening structure was shown.

Photo 5 The landslide, the retaining wall and the aquapark

References

Design guidelines according to EC7, Ilov G., , 2011

Eurocode 7 Geotechnical design

Young Geotechnical Engineers Conference (EYGEC), Durham, UK, Markov I., Totsev A. Influence of dynamic load on the ground anchors bearing capacity,Proceedings of the 24th European 2015

12th international symposium on landslides, Napoli, Italy Markov I., Totsev A Expiremental and Experimental and Numerical Modeling of Anchors Under Seismic Conditions, ,2016

SNiP 2.02.03-85

doi.org/ 10.35123/ReSyLAB_2019_22

Significance of landslide susceptibility maps in creation of spatial planning documentation

Kenan Mandžić[(1)], Nedreta Kikanović[(2)], Adnan Ibrahimović[(3)]

1) University of Tuzla, Faculty of Mining, Geology and Civil Engineering, Univerzitetska 2, Tuzla, Bosnia and Herzegovina, +38735320557, kenan.mandzic@untz.ba,

2) Tuzla city administration, Department for Geodetic and Property Affairs, ZAVNOBIH-a 11, Tuzla, Bosnia and Herzegovna nedreta.k@gmail.com

3) University of Tuzla, Faculty of Mining, Geology and Civil Engineering, Univerzitetska 2, Tuzla, Bosnia and Herzegovina, adnan.ibrahimovic@untz.ba

Abstract Social development of an area implies the development of infrastructure systems. Construction of infrastructure systems has faced a multitude of obstacles, among which the landslide processes are one of the most significant problems. The success of the realization of the development of any particular area, including the development of the necessary infrastructure systems, is based on the quality design of the spatial plan, which must consider the aggravating circumstances of these landslide processes. Therefore, one of the fundamental bases for the creation of a quality spatial plan is a previously created landslide susceptibility map of the area.

This article presents the advantages of using landslide susceptibility maps, as an inevitable base for creation of the spatial plans.

Keywords: landslides, spatial planning, landslide susceptibility maps

Introduction

Social and economic development has increased the need for new infrastructure systems and the adaptation of existing ones, which leads to new engineering challenges for professionals in various fields. Adequacy, in the sense of exploitation and safety, of new infrastructure systems also implies systematics in their planning, realization and further development.

As one of the aggravating circumstances in the process of planning infrastructure systems, in general, are processes that lead to movement of soil and rock mass. Among them, as the most common, is the phenomenon of the occurrence of new and further development of current landslides. These processes directly or indirectly jeopardize infrastructure systems, whose risks range from disrupting their functionality, through their complete physical destruction to fatal cases for users of these systems (Ibrahimović A., Mandžić K., 2013). In addition, we should not underestimate the influence of climate change, which is increasing the number of occurrences classified as the landslide triggers (intensive rainstorms, extreme change of temperature and fast snow melt) and has made the situation even more complex.

It is obvious that, given all the facts presented above, there is a need for an assessment of the landslide susceptibility for areas planned for urbanization, which would improve the quality of the planning processes. First of all, we have in mind the planning processes in the preparation of spatial plans at different levels. The assessment of the landslide susceptibility is interpreted through the creation of landslide susceptibility maps and it should be one of the basis of the required quality for the creation of spatial plans, but also the basis for further activities and processes in designing of the infrastructure systems.

There is a different approach (methodology) in creating landslide susceptibility maps, which leads to different results and accuracy of maps, so it is necessary first to determine the methodology for creation of these maps in different scale. Because landslide susceptibility maps are not used in spatial planning in Bosnia and Herzegovina, it is necessary to find the way to implement that methodology in legal regulations. For the purpose of developing an adequate methodology for creating landslide susceptibility maps, Faculty of Mining, Geology and Civil Engineering in Tuzla together with partners (Croatian Geological Institute Zagreb, Institute for Geological Research from Podgorica and Development Agency Žepče) have launched the "safEarth" project (HR-BA-ME59), as a part of the IPA-CBC IPA Croatia-Bosnia and Herzegovina-Montenegro 2014-2020 program, which has been implemented from June 1, 2017. The main goal of the project is to define the influence of certain input parameters (factors) on the accuracy of the created landslide susceptibility maps. Based on this results, methodology for creating landslide susceptibility maps in small (1:100000) and large (1:25000) scale will be defined and implemented in current legal regulation. One of the project goals is to emphasize the importance of the landslide susceptibility maps in spatial planning (Mandžić K., Ibrahimović A., Babajić E., Kikanović N., 2016-2019).

Landslide susceptibility maps

The first official application of landslide zoning dates from the 1970's and was based on a qualitative approach, while quantitative approaches were developed at the end of the 1980's. (Corominas et all., 2014)

The main causes of the landslide occurrence can be identified and the majority of them can be mapped, which make it possible to assess the degree of landslide risk. (Varnes & IAEG, 1984).

The assessment of the degree of landslides risks starts with the landslide zoning that allows the creation of appropriate maps, which provide different relevant data on the occurrences and their assessment. The landslide zoning is done with the purpose of creating maps that can be divided into four basic types. The results of landslide zoning of particular area, or data obtained in this process, are interpreted by creating the four basic map types:

• Landslide inventory–database of already occurred landslide events;

• Landslide susceptibility map - spatially defined areas of varying degree of susceptibility to the landslide occurrences;

• Landslide hazard map – spatial definition of specific sites and conditions under which the landslide phenomenon can be realized, with an estimation of the probability of the occurrence of this event and its magnitude;

• Landslide risk map – spatial distribution of qualitative and quantitative consequences (damage) of the possible landslides. (Corominas et all., 2014; Chacon at all., 2006).

Many landslides are found in densely populated areas and directly threaten people and property. Given the high degree of danger in such circumstances, the first step is to identify and classify areas that are susceptible to landslide, which requires the creation of the landslide susceptibility maps (LSM). This is recognized as one of the bases for further process of risk management and prevention.

Landslide susceptibility maps represent the spatial probability of landslide occurrence. They are made in different scales, depending primarily on the purpose and size of the research area, as well as on the scale and details of available input data.

Depending on the scale, creating of landslide susceptibility map is done by using an experiential (heuristic) approach that allows estimation of susceptibility without the use of landslide inventory or a scientific (scholastic) approach that quantitatively defines the influence of parameters, such as terrain characteristics, on the spatial probability of landslide.

To create a landslide susceptibility map in the scale of 1: 100 000, heuristic approach can be assessed as an optimal approach. (Fell at all., 2008; Cascini, 2008).

Adequate zoning of the terrain can estimate the degree of susceptibility to landslides, which is the first step towards the final goal - determining the zone of increased danger and defining the risks on a large area surface. These activities enable us to plan reducing the level of dangers to humans and property in the occurrence of a landslide. Therefore, it can be said that landslide susceptibility maps are only the first, but necessary step in a systematic landslide risk management.

Creating landslide susceptibility maps (LSM) is an important step in the process of creating spatial plans. Namely, defining the areas where there is the possibility of landslide occurrence is the basis of rational land management, with emphasis on the obligation to build infrastructure facilities that meet the criterion of exploitation safety. Zones that are susceptible to landslide occurrences are classified in accordance with the probability degree of landslide occurrence in a given area, but it is not possible to predict at what point a landslide will be activated (they do not define the possibility of the occurrence in the function of time). However, the very fact that suggests a certain degree slope material susceptibility to the landslide appearance is important information for spatial planners as an influencing factor on spatial planning. (Mandžić K., Ibrahimović A., Babajić E., Kikanović N., 2016-2019).

Consequently, creating a landslide susceptibility maps provides a better approach to defining areas that are currently or potentially most vulnerable.

Proper defining of these areas provides an improved approach to the creation of other documents such as: spatial plans, environmental impact studies, engineering geology and geotechnical studies, design projects for large infrastructure facilities, in the field of construction, geology, mining, agriculture, forestry, water management and many more, with the following aims:

- planning, designing and implementing measures to reduce the number and size of anthropologically initiated landslides,

- reduction of damage to property and avoidance of human casualties, both during the construction of facilities and during their exploitation and

- reducing the cost of landslide rehabilitation.

Existing methods of creating landslide susceptibility maps on a small scale (1 : 100 000) involve analysis of different input data, but they are often reduced to three basic data sets in the form of factor maps. These are the geological factors (lithological characteristics of an area), geomorphological factors (terrain slope) and terrain/soil cover (Castellanos Abella & Van Westen, 2007; Hervás i dr., 2010; Lima i dr., 2017; Nadim i dr., 2006).

With the change in the scale, or with the creation of a larger (1:25000 or 1:5000) scale map, other influencing factors may be added depending on the type of material (soil or rock), soil or rock type, etc.

In rock material, influencing factors can also include the type of rock per genesis, discontinuity, decay, rock material alteration, which affect the possibility and mechanisms of loss of rock masses from the slopes. (Mandžić. E., 2001).

The soil can also include the thickness of the genetic cover, the mineral and granulometric composition of the soil, the physical-mechanical characteristics, and changes of these characteristics with different water content, water permeability changes, etc.

After defining the influencing factors, GIS technology enables us to perform several iterative procedures on the basis of which the relevant conclusions for the creation of the landslide susceptibility maps are made. Babajić, E., Kikanović, N., Mandžić, K., Ibrahimović, A., Hodžić, S. (2018). The following can be defined as basic steps in the creation of the landslide susceptibility map at the small scale of 1: 100000:

1. Creation of a reclassified map of the terrain slopes - can be derived from a digital elevation model (DEM) obtained on the basis of the topographic map of the scale 1: 25000 and the size of the network cell of 20 x 20 m.

2. Creation of a reclassified map of engineering geological units - made from the basic geological maps at scale 1: 100000 that are used for defining engineering geological units and the units are separated on the basis of engineering and geological features.

3. Creation of a reclassified map of the land cover – it is based on the map of the land cover that is based on the European database on bio-physical land use CORINE Land Cover (CLC), made according to CORINE standards that define the output scale of 1: 100000, a minimum mapping area of 25 ha and the minimum polygon width of 100 m. The CLC nomenclature includes 5 level 1 classes, 15 level 2 classes and 44 level 3 classes of land use. For the purpose of drawing a landslide susceptibility map, the level 3 of the CLC nomenclature was used.

4. Overlapping of reclassified maps - all listed factors are classified, i.e. classified into several groups of similar characteristics. Each determined class is associated with an appropriate number of points that quantify the class impact on the landslide occurrence. The highest number of points is awarded to the class that represent the most unfavorable factor features regarding the landslide susceptibility, and the smallest number to class that represent the least unfavorable factor. The influence of each individual factor on the final landslide susceptibility is defined by the weight factors. The total number of points of each cell obtained as described is a relative landslide susceptibility of the area of 20 x 20 m. However, such a representation is too complex for the defined scale, so for the final presentation of the landslide susceptibility map at scale of 1: 100000 additional points were added, according to their ranges, to define low, medium, high and very high landslide susceptibility areas.

The working version of a small-scale landslide susceptibility map for the municipality of Žepče, is given in the following figure (Figure 1). (Babajić, E., Kikanović, N., Mandžić, K., Ibrahimović, A., Hodžić, S. 2018)

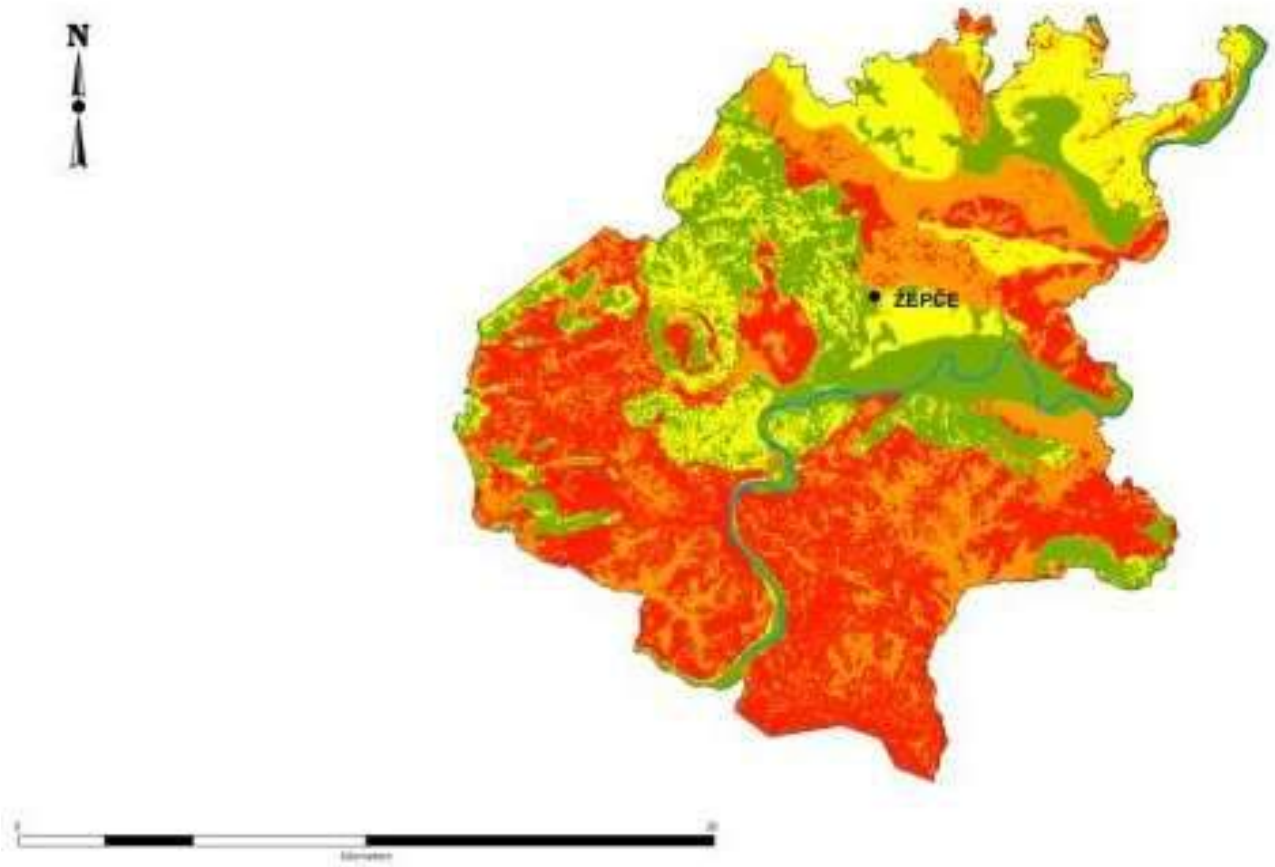

Figure 1 Landslide susceptibility map of the municipality of Žepče (blue color-Water surfaces, green-low susceptibility to landslides, yellow-medium susceptibility to landslides, orange- high susceptibility to landslides, red- very high susceptibility to landslides)

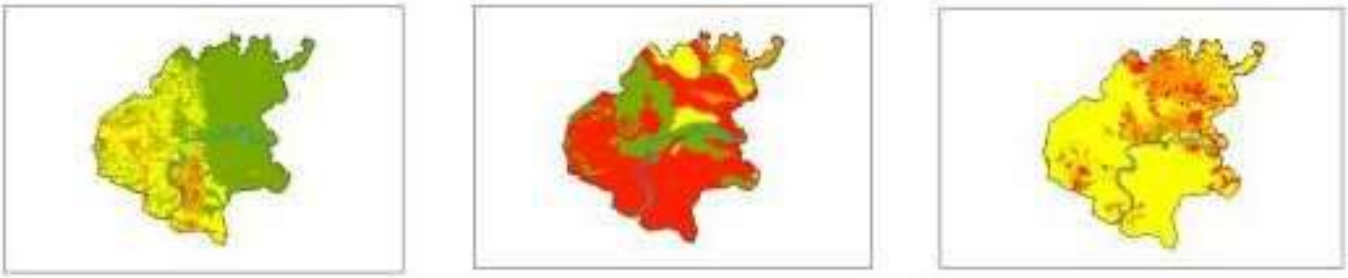

Figure 2 Reclassified maps for derivation of final map (from the left - reclassified map of terrain slope, reclassified map of engineering geological units, reclassified map of terrain cover)

Due to the significant number of landslides in the region of Bosnia and Herzegovina and their impact on the overall quality of life of its population, it can be concluded that landslide susceptibility maps are the necessary bases for spatial planning and designing, and before realization of any larger investment by individuals, the local community, private companies, as well as other major investments and ventures, particularly those of great social importance.

The concept of spatial planning in the Federation of Bosnia and Herzegovina and its disadvantages

Spatial planning, as the cornerstone of development of any area, represents a complex, demanding and sensitive multidisciplinary category.

The primary goal of each spatial planning is to enable rational use and resourceful management of physical resources to protect and improve the quality of space in order to achieve economic and social development and create better conditions for a humans and a quality life of the population.

In space or on the ground, there are macro-and micro-spatial entities and they are determined by a social decision about what type of spatial planning design will be applied. There are plans of higher and plans of lower order. Plans of higher order are done for macro-spatial entities, and plans of lower order are used for micro-spatial entities. Macro-spatial entities are defined as areas of municipalities, cities, cantons, states or interstate specific areas for which spatial plans are developed, which may be developmental plans of general character or developmental plans for spatial arrangement of special areas or areas with a special purpose. On the other hand, the spatial planning of the micro-spatial entities is done by urban (master) plans, regulatory plans and urban planning projects, and they cover areas of cities, settlements, parts of settlements or land complexes used for a particular purpose.

The spatial plan, as the plan of a higher order, consists of two phases:

1. Phase 1 - Design of a SPATIAL BASIS with a proposed spatial development concept

2. Phase 2 - Design of a SPATIAL PLAN as a final document (pre-draft, draft, proposal) (Bogunović S., 1984).

In the space basis, the state of the space is followed through the structure of the thematic areas. Each thematic area has the people responsible for a thematic area. Those people are responsible for the accuracy and credibility of the data. According to the Regulation on the Uniform Methodology for Drafting of Planning Documents of the Federation of Bosnia and Herzegovina (Official Gazette of the Federation of Bosnia and Herzegovina, 63/04; 50/07; 84/10) the thematic areas are:

- Geodetic-topographic-map base;
- Spatial plan of the Federation of Bosnia and Herzegovina and other documents from the jurisdiction of the:

Federation of Bosnia and Herzegovina;

- Spatial plans of cantons or municipalities;
- Natural resources with their qualitative and quantitative characteristics, etc.;
- Population;
- Infrastructure systems;
- Constructional and natural heritage and specially protected areas;
- Endangering the environment;
- Areas with possible dangers of the consequences of natural and man-made disasters;
- Personnel and legal entities involved in the field of spatial planning;
- Economy;
- Social activities;
- Tourism;
- Utilities;
- Other data relevant to the planning and maintenance of a single information system.

Considering that all buildings have been constructed in or on the terrain, the behavior of the slopes in the process of the building construction is one of the important input indicators for the analysis of areas predicted for construction in the spatial planning. For this reason, the thematic area "Natural resources with qualitative and quantitative characteristics", as well as the thematic “area with the danger of the consequences of natural and man-made disasters” are a very important part of the spatial plan design.

Thematic area of natural resources with qualitative and quantitative characteristics etc., as well as the thematic area where there is a risk of the consequences of natural and man-made disasters require analysis of the geological characteristics of the terrain (basic morphological form of the relief, lithological and stratigraphic structure of the terrain, structural and tectonic features of the terrain, hydrogeological and hydrographic characteristics, engineering geological characteristics of the terrain, seismological characteristics of the terrain, ect). However, the experience of spatial planners for these thematic areas shows the lack of adequate and quality data base, as input data, for an overall spatial analysis, which makes it difficult for planners to make decisions when determining the purpose and conditions for land use.

The study "Natural Conditions and Resources" is a document that should be done prior to the preparation of spatial plan because, with its contents, it represents the basis not only for the preparation of the plan but also for other specialist studies. However, very often this study is not done, and if it is done, the field of the spatial defining of natural and geotechnical risks is not assessed in the right way. Namely, within the scope of this field, an overview of existing available geological, engineering, geological, hydrogeological, seismological and other maps are shown without giving a timely analysis of the interactions between individual parameters and their overlapping. Because of this, planners do not get good input in this aspect that is necessary for analyzing the existing situation within the spatial development concept proposal.

Defining a clear methodology for drawing up landslide susceptibility maps and incorporating this methodology into legal regulation would greatly facilitate the work of the personnel in charge of the thematic area "Natural conditions and resources" and thus help spatial planners, but also define spatial plans with significantly reduced impact of landslides as unfavorable processes.

Importance of application of landslide susceptibility maps in spatial planning

In order to work on the prevention of the impact of landslide processes on facilities planned for construction according to spatial plans, it is necessary to have as many influencing factors as possible on the durability and usability of the objects themselves when making spatial plans. Landslide processes, which occur more and more frequently in Bosnia and Herzegovina, have a significant influence on the durability and usability of facilities built in a given area. When spatial plans are being developed in Bosnia and Herzegovina, spatial planners are faced with the problem of defining areas outside the zone affected by the landslide process, in the aspect of safety and convenience of building specific facilities. The current practice in creating spatial planning documentation has shown, in most cases, the shortcomings in this part. Namely, only basic geological maps of the scale 1: 100000 are used, and, in rare cases, the engineering geological maps of the scale 1: 25000 are created and the existing landslides are mapped as a basis for creating maps of specific area by degree of stability. These maps of specific area classify area, by degree of stability, into one of the three categories: stable, conditionally stable and unstable. This classification is based on the engineering geological survey and collection of field data. These maps do not give the detail data about conditionally stable areas (for example, how susceptible is the area on landslide occurrence).

Therefore, in spatial planning, areas outside the zones affected by some of the landslide processes, due to the lack of adequate data, are usually considered stable and various facilities are planned to be built on them. For spatial planners to carry out an adequate assessment of the state of spatial planning and to provide possible spatial development directions for the thematic area of natural conditions and resources, it is necessary to have a high-quality foundation, among other things, of the landslide susceptibility of the entire area.

By creating a landslide susceptibility map, input data is provided to spatial planners for the entire area for which a creation of the spatial plan is planned, and the zones that are not currently affected by the landslide processes are covered, which in the future have a certain spatial probability of the occurrence of the landslides processes, as well as the probability of endangering people and material goods. Red color, which are used to mark areas with very high landslide susceptibility, does not necessarily mean that this particular area has an active a landslide process, but that it is the area with the highest degree of probability of occurrence of landslide processes, which represent a type of warning when designing a spatial plan. Also, areas in green color do not mean that there is no possibility of landslide occurrence, but that there is little chance of landslides in this area. To put it simple, the landslide susceptibility zones represent differences in the likelihood of a landslide occurrence in a given area, having in mind that it is not possible to predict when the landslide will be activated (this is defined by hazard maps).

The landslide susceptibility analysis at the regional level (1:100000) clearly defines areas with high susceptibility of landslides and allows the focus for a detailed local research and creation of urban and regulation plans for areas of interest (1:25000 or 1:5000). Also, this analysis allows spatial planners to adapt the type of facilities to terrain conditions while planning additional research works. In this way, significant savings of the financial resources necessary for building objects are achieved (detailed research, adaptation of construction method, etc.). These maps are the basis for the creation of the hazard and risk maps, as well as the maps of vulnerable areas, which can also be used while creating spatial plans.

Only a systematic approach to the definition of landslide susceptibility in creation of the spatial plans can significantly reduce risk associated with the occurrence of landslides.

Conclusion

As landslides represent a limiting factor for the use of existing facilities, as well as for the design and construction of new facilities, it is necessary to use a landslide susceptibility map as a basis in creation of the spatial plans.

By examining the problem of landslide susceptibility of a terrain, the economic and technical aspects are commonly emphasized, thru cost estimate and type of construction, possible preventive measures etc. However, they are only a part of the range of problems that represent potential limiting factors in spatial planning of a normal organization and functioning of the city/region as a living organism subject to a daily change.

Landslide susceptibility maps enable spatial planners to determine the probability of the landslide occurrence in a given area when determining the purpose of the land use, primarily construction land and infrastructure corridors, going from a more general to a more detailed spatial view, to provide the probability of the landslide occurrence in a given area, and, thereby, to make the right decisions when determining land use. Although a landslide susceptibility map does not predict when exactly landslides will occur, it provides adequate input data where there is a more or less probability of a landslide occurrence.

Thus, the zones of high and very high landslide susceptibility shown on the map (Figure 1) does not have to mean that there is a landslide there or that nothing can be built on that terrain, but directs spatial planners to define the type and purpose of individual objects in a particular area. In the areas of high and very high landslide susceptibility the Decision on Spatial Planning Documentation requires a detailed engineering, geological and geotechnical research as a prerequisite for doing any constructional interventions in that area.

The assessment of landslide susceptibility of a terrain should first be carried out at the regional level (1:100 000) and then, after analyzing the obtained results, define areas at the local level with the highest risk of landslides occurrence (1:25000 or 1:5000).

The creation of these maps, using a clearly defined methodology, should be part of the legal framework related to the preparation of spatial plans, both at regional and local levels. That is, the significance of landslide susceptibility maps points out to the necessity of adopting legislative documents which will clearly define or oblige the thematic fieldworkers, for study natural resources with qualitative and quantitative characteristics and areas with risks of the occurrence of natural and man-made disasters, to create and apply these maps in the spatial planning process.

Such approach to designing and using landslide susceptibility maps in spatial planning enables significant savings in defining ways of building objects in certain areas, and reduces the risk of potential damage caused by the activation of landslides.

Therefore, necessary activities at the level of the Federation of Bosnia and Herzegovina should be carried out in order to amend the by-laws, in particular the Regulation on the content and the holders of a single information system, methodology for data collection and processing, and unique forms on which the records are kept (Official Gazette of the Federation of Bosnia and Herzegovina, 33/07 and 84/10) and the Regulation on the uniform methodology for drafting the planning documents of the Federation of Bosnia and Herzegovina (Official Gazette of the Federation of Bosnia and Herzegovina, 63/04; 50/07; 84/10), which will oblige the creators of thematic maps to do them according to the appropriate methodology that is used for creating landslide susceptibility maps.

References

Bogunović S., (1984): Metodološke osnove za izradu prostornih planova, Institut za arhitekturu, urbanizam i prostorno planiranje Arhitektonskog fakulteta u Sarajevu, Sarajevo.

Burrough P.A, i McDonnell R.A., (2006): Principi geografskih informacionih sistema, Građevinski fakultet Univerziteta u Beogradu, Beograd.

Babajić, E., Kikanović, N., Mandžić, K., Ibrahimović, A., Hodžić, S. (2018): Radne upute za izradu karte podložnosti na klizanje. Project:Transnational advanced management of land use risk through landslide susceptibility maps design. Interreg IPA-CBC. HR-BA-MNE 59. RGGF Tuzla, pp 1-19.

Babajić, E., Kikanović, N., Mandžić, K., Ibrahimović, A., Hodžić, S. (2018): Tumač za kartu podložnosti na klizanje za općinu Žepče. Project:Transnational advanced management of land use risk through landslide susceptibility maps design. Interreg IPA-CBC. HR-BA-MNE 59. RGGF Tuzla, pp 1-22.

Babajić, E.(2018), Kikanović, N., Mandžić, K., Ibrahimović, A., Hodžić, S. : Methodology of landslide susceptibility maps creation in small scale on municipality Prozor-Rama example, Journal of Faculty of Mining, Geology and Civil Engineering Tuzla ISSN: UDK: Vol. 2013/1, pp. 01-08.

Castellanos Abella, E.A. & Van Westen, C.J., (2007): Generation of landslide risk index map for Cuba using spatial multi-criteria evaluation. Landslides, 4: 311-325.

Cascini, L. (2008): Applicability of landslide susceptibility and hazard zoning at different scales. Engineering geology, 102: 164-177.

Corominas, J., Van Westen, C.J., Frattini, P., Cascini, L., Malet, J.P., Fotopoulou, S., Catani, F., Van Den Eeckhaut, M., Mavrouli, O., Agliardi, F., Pitilakis, K., Winter, M.G., Pastor, M., Ferlisi, S., Tofani, V., Hervas, J., Smith, J.T. (2014)): Recommendations for the quantitative analysis of landslide risk. Bulletin of Engineering Geology and the Environment, 73 (2): 209-263.

Chacon, J., Irigaray, C., Fernandez, T., Hamdouni, R.E. (2006): Engineering geology maps: landslides and geographical information systems. Bulletin of Engineering Geology and the Environment, 65 (4): 341-411.

Fell, R., Corominas, J., Bonnard, C., Cascini, L., Leroi, E., Savage, W.Z. on behalf of the JTC-1 Joint Technical Committee on Landslides and Engineered Slopes (2008): Guidelines for landslide

susceptibility, hazard and risk zoning for land use planning. Engineering Geology, 102: 85-98.

Hervás, J., Günther, A., Reichenbach, P., Malet, J.-P., Van Den Eeckhaut, M., (2010): Harmonised approaches for landslide susceptibility mapping in Europe. Proceeding of the International Conference Mountain Risks: Bringing Science to Society. CERG, 501-505.

Ibrahimović A., Mandžić K.,(2013): Sanacija klizišta, Tuzla BiH, d.o.o. Mikroštampa.

Lima, P., Steger, S., Glade, T., Tilch, N., Schwarz, L., Kociu, A., (2017): Landslide Susceptibility Mapping at National Scale: A First Attempt for Austria. Mikos, M., Tiwari, B., Yin, Y., Sassa, K. (eds.): Advancing Culture of Living with Landslides. WLF 2017, 943-951.

Mandžić. E., (2001): Hazard i risk. Autorized lectures. Faculty of Mining, Geology and civil Engineernig, University of Tuzla. Marinović-Uzelac A., (2001): Prostorno planiranje, "Dom i svijet", Zagreb.

Mandžić K., Ibrahimović A., Babajić E., Kikanović N., (2016-2019): Project "Transnational advanced management of land use risk through landslide susceptibility maps design". Interreg IPA-CBC. HR-BA-MNE 59, Faculty of Mining, Geology and Civil Engineering

(Official Gazette of the Federation of Bosnia and Herzegovina, 33/07 and 84/10)

(Official Gazette of the Federation of Bosnia and Herzegovina, 63/04; 50/07; 84/10),

Varnes, D.J. & IAEG Commission on Landslides and Other Mass Movements on Slopes (1984): Landslides hazard zonation: a review of principles and practice, UNESCO, Paris-France.

doi.org/ 10.35123/ReSyLAB_2019_23

The impact of the choice of the form of the retaining structure on the cost of restoration of the landslide

Zijad Ferhatbegović[(1)], Ismet Gušić [(2)]

1) The University of the Tuzla, Faculty of mining, geology, and civil engineering, Tuzla, Univerzitetska 2, +387 35 320580

2) The University of the Tuzla, Faculty of mining, geology, and civil engineering, Tuzla, Univerzitetska 2, +387 35 320580

Abstract This paper analyzes the cost of repairing landslide in Jukići, municipality of Sapna, using three forms of the support structure. Based on geological surveys on the terrain, a geomechanical study was carried out on the subject site. After the elaboration of the geomechanical elaborate, it was proposed to repair the landslide with supporting constructions and drainage on two locations.

The retaining structures are designed in three variants, namely: gravitational walls, reinforced-concrete walls supported on the strip footing and walls leaned on counterforts. A proposal for rehabilitation for all three forms of the retaining structure with the static calculation of the walls and the designs of the reinforcement was carried out, taking into account the geological profiles, the depth of the supporting soil and the characteristics of the soil below and behind the retaining structures. Based on the completed remediation plans, the volume of works and calculations for each variant of the retaining structure were made. Also, for each variant, an analysis of the cost of rehabilitation was performed. The results of the performed analysis were used to select the most favorable variant, to make conclusions and recommendations to future designers.

Keywords landslide, slope rehabilitation, the form of retaining structure, worksheet, calculation of works, costs

Introduction

In May 2014, a landslide was activated in the village of Jukići, the municipality of Sapna, where the local road, the residential building of Suvad Jukić, and potentially several more buildings. During the activation of the landslide, there was damage to the local road that was temporarily rehabilitated by put wooden piles and stone. Part of the retaining wall near the house of Suvad Jukic was damaged due to the slipping of the terrain, which affects the stability and security of the entire facility. To prevent further wetting and falling apart of the earth, preventive measures were taken in the form of covering the soil in front of the house with nylon and putting wooden piles. Since the slipping of the ground broke pipes, as a temporary solution, drainage pipes were placed next to the house to regulate gutter waters. To drain water from the body of the landslide, an open drainage channel was dug in the direction of slipping the terrain. Putting wooden piles near the house and under the road, covering the land with nylon and making an open drainage channel largely stabilized the further slipping(Fig.3-Fig 8)

Geomorphological and engineering-geological characteristics of the terrain

The slope of the surrounding area of the subject location has an exposition towards the east, and the inclination of the slope is 10° (Fig.1) The site is located in the part of the terrain that builds up the upper Miocene sediments (M_3^1) represented by clay, sandstones, marls and subordinate limestones (Fig.2). The dip of sediments is towards the northeast at an angle from 20 to 35 degrees.

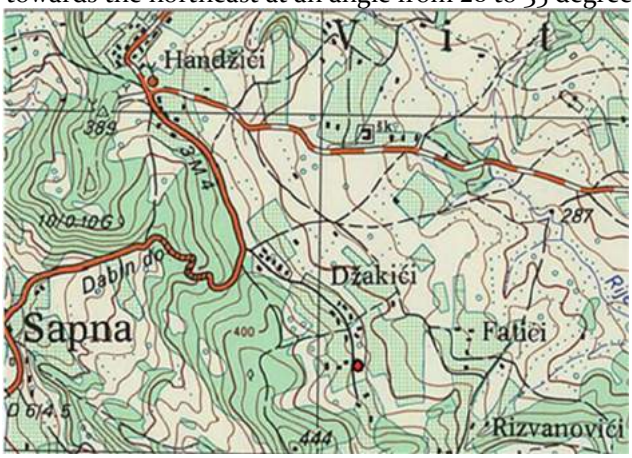

Figure 1.Situation of landslide-topographic map Stari Teočak scale 1:25000

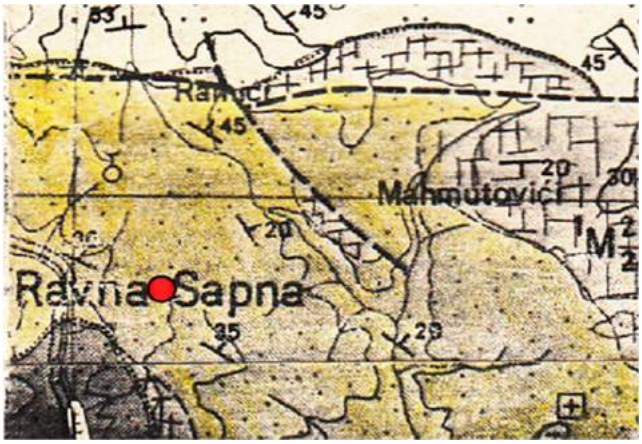

Figure 2 Basic geological map of the list Zvornik scale 1:100000

To remedy the landslide, detailed engineering-geological and geomechanical tests were carried out.

Based on the results, a landslide remediation project was done. In total, four exploratory boreholes marked B-1 to B-4 were drilled with taking samples that were processed laboratory to obtain the necessary parameters for the calculation. Along with the drilling, the standard penetration test was carried out. At the indicated location the level of the underground water wasn`t registered, while the groundwater level was registered only in the borehole B-4 at a depth of 3.0 m and after 24 hours and the groundwater level at a depth of 3.30 m. On the treated site the geological substrate is made of gray layered marls with dip to the northeast with an angle of 20-35°. In geomechanical boreholes, gray marls were drilled in a well B-2 at a depth of 4.2 m and B-4 at a depth of 4.4 m. On this location, two different types of genetic covers are separated in eluvial-diluvial (ed) and colluvial covers, which are represented by sandy-dusty to marl clay. The thickness of the covers is up to 4.5 meters.

Figure 3 The landslide scar

Figure 4 Damaged local road

Figure 5 Dumped the retaining wall next to the house

Figure 6 Wooden piles

Figure 7 New plastic pipes instead of crumpled

Figure 8 Temporary road repair

In engineering and geological view, the slope with the landslide is unstable since close to this landslide has emerged several new landslides that threaten to endanger several residential buildings. For these reasons, it was necessary to approach as soon as possible the repair of landslides to prevent its further spread and thus the vulnerability of other structures down the slope. In the investigated site there was developed a shallow landslide with a sliding surface at a depth of 2.2 m Fig 9-Fig 10).

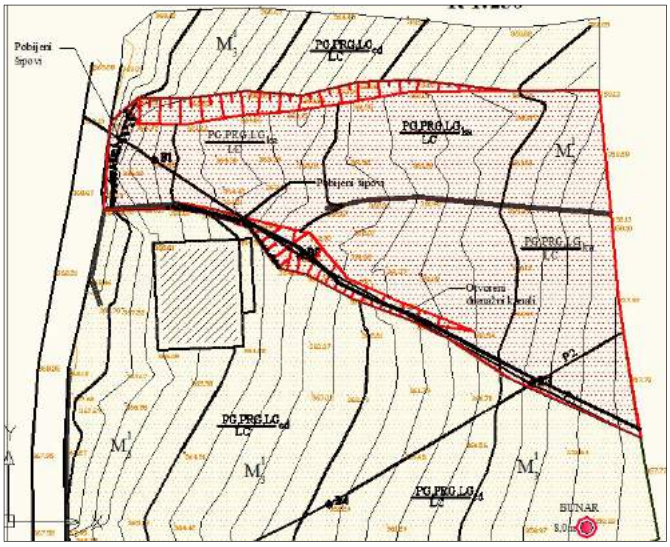

Figure 9 Map with the borders of landslide

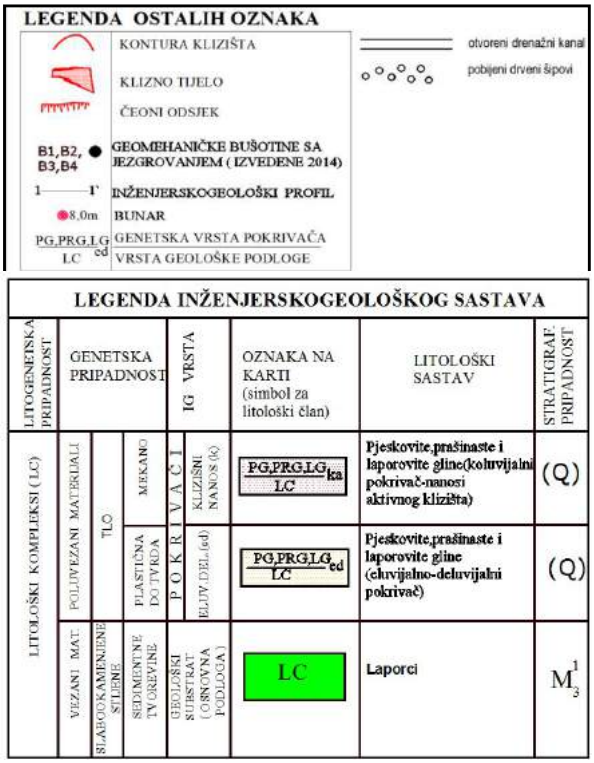

Figure 10 The Legend of engineering-geological composition

Morphometric characteristics of the complete landslide:

- landslide length 49.86 m (geodetic footage)
- the width of the landslide in the front part of 11.39m
- the width of landslides in the central part of 22.61m
- the width in the foot part 34,0 m
- the height of the forehead scar 2.0-3.0m
- the surface of landslide 1014 m2
- depth of sliding 2,2 m
- the volume of landslide 2230.8 m3
- level of head of landslide 368,60 m
- level of the foot of landslide 357.78 m
- the inclination of slope 10°

According to the structure of the natural slope and the sliding, this slope is defined as landslides created in lithologically heterogeneous and anisotropic environments, and according to the surface and volume of the sliding body are defined as small landslides.

According to the position on the slope, it is classified as medium-slope landslides. The sliding body is in the form of a tongue or glacier. This landslide belongs to landslides where the sliding action is carried out in the hypsometric higher parts of the terrain (near water divide) and the slipping is successively moved to the lower parts of the terrain. Depending on the depth of the slope, it is defined as a shallow landslide with a sliding surface at 2,2m depth. The main causes of land sliding: overburdening from precipitation, the inclination of the slope, and lithological composition.

Description of the basic concept of the solution

Based on the determined general properties of landslides in the geomechanical elaborate such as (size,

volume, type of landslide), causes and mechanism of moving of earth masses from the engineering and geological aspect, proposed sanitary measures are consisted of: making two retaining structures and drainage systems above retaining structures and a drainage system in the form of fish bones to collect and take off surface and groundwater.

Since a part of the existing sewerage is broken due to the sliding of the terrain, a new network of sewer pipes has been installed at the top and bottom of the landslide which is immersed in the existing sewer pipes diameter of 100 mm.

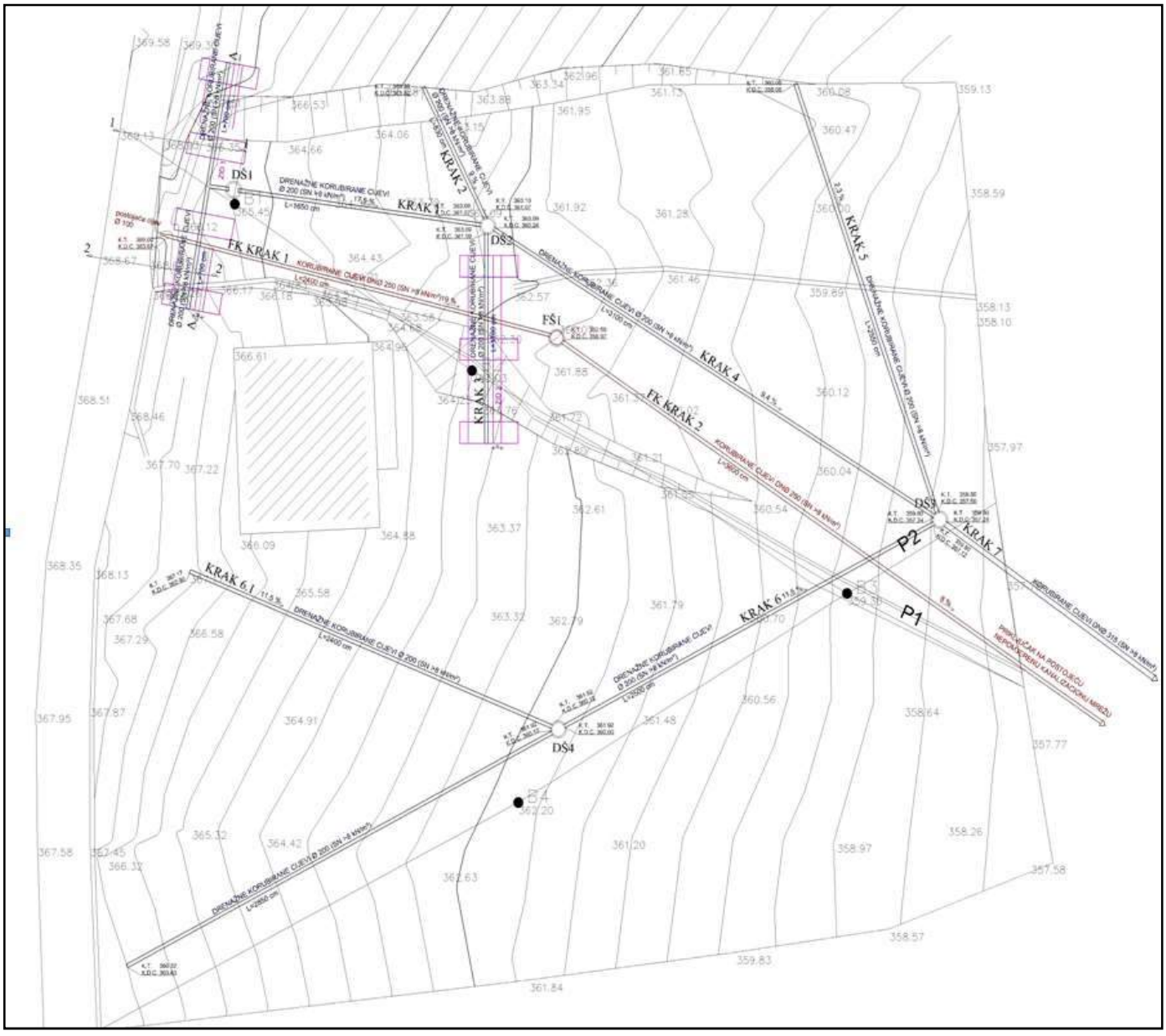

Figure 11 Making drainage

Drainage system

The drainage system consists of drainage tubes with a diameter of Ø250 mm of SN-8 quality, which is putting behind the retaining wall (Fig 11). In the drainage trenches, over drainage pipes are placed a layer with a big stone material wrapped in geotextile. The drainage trench is excavated until it reaches 30 cm in water-impermeable natural material. The excavation of the drainage channel should be done from lower to a higher level (for easier grading), with the excavation being carried out at every 5 m lengths and then the channel is filled with drainage filling, after which the excavation is extended. The bottom of the excavation must be done by hand with a proper longitudinal inclination. At the bottom of the excavation put a geotextile (200g / m2), after that plastic drainage pipes and drainage stone material which should be wrapped by a geotextile.

Retaining structures

For the restoration of landslides, three variants of the retaining structure for each of the two retaining walls were made. The subject of this paper is the choice of variant

solutions of the retaining structure, while the drainage system and sewerage are the same for each form of retaining the structure and they are not studied in this paper. During designing the retaining structure, the stability of the existing facility and road communication was taken into account.

Three variants are recommended:
- gravity retaining wall,
- the reinforced - concrete retaining wall on the strip footing
- the reinforced-concrete retaining wall on counterforts

For each variant of the retaining wall, static calculations, retaining wall designs, a cross-section through the retaining wall, work plan for each variant of the retaining wall were made. Based on the measurements of the works for each supporting wall, a pre-calculation of the works was carried out to construct each of the variants, taking into account that the unit prices of materials, labor, and mechanization for each variant are the same. In this paper, it was given only the recapitulation of works for each variant.

Gravity retaining wall

The gravity wall is made of unreinforced concrete of class C30 / 37 (MB30). The static budget was calculated, as well as the volume of the works and the estimate of the works for both retaining walls.

Recapitulation of the volume of the works and the estimate of the works for the gravitational shape of the retaining wall is given below:

Total of earthworks for the support structure.....14395,00 KM

Total of concrete works for support structure.....35656,00 KM

Total of earth and concrete works.....50051,00 KM

The reinforced concrete retaining wall on the strip footing

The reinforced concrete support wall is made of reinforced concrete of class C30 / 37 (MB30). The static calculation was made and reinforcement design was made. Depending on the dimensions and the position of the retaining wall, the volume of the works and the cost of the works for both supporting walls were made. Recapitulation of the volume of the works and the cost of the works is given in the attachment.

Recapitulation of the volume of the works and estimate of the works for the reinforced concrete retaining wall on the strip footing is given below:

Total of earthworks for the retaining structure.....8645,00 KM

Total of concrete works for retaining structure.....39645,00 KM

Total of earth and concrete works.....48290,00 KM

Retaining wall on counterforts

Two retaining walls on the counterforts have been designed (Fig 12). The task of the retaining wall is to with its weight to counter the slip of the soil behind the wall. The retaining walls are carried out from the bottom of the road and below the house. The disposition of the walls is given on the situation. The wall is hight from 4,15m to 4,90m and thick 0,5m which lies on the counterforts 120cm wide, 3.5m long and 2m deep. To prevent adverse effects of water pressure, drainage has been envisaged. Behind the wall, it is necessary filling the stone material, gravel or road metal in layers of 50cm. The density of this material should be Ms 35MPa.

For this retaining wall is foreseen concrete of class C30 / 37 (MB30), ribbed reinforcement S500S as reinforcement grid MA 500/550. The weight of the retaining wall and counterfort is provided a satisfactory coefficient of tumble safety, Fs = 1.502, and the sliding coefficient Fk = 1.62. A convenient voltage condition was also achieved in the contact of the counterfort with soil, where the voltage of pressure occurs throughout the length. Embedding of the counterfort must be made to the depth at which the supporting layer of soil is located. The static calculation of the AB wall on the counterfort was carried out to dimension the wall or adopt the required reinforcement. The calculation was carried out on the 3D model with the software package TOWER 3 D Model builder 6 based on the finite elements so that the wall was realistically modeled by shell elements. It was done a special calculation of reinforcement between wall and counterfort.

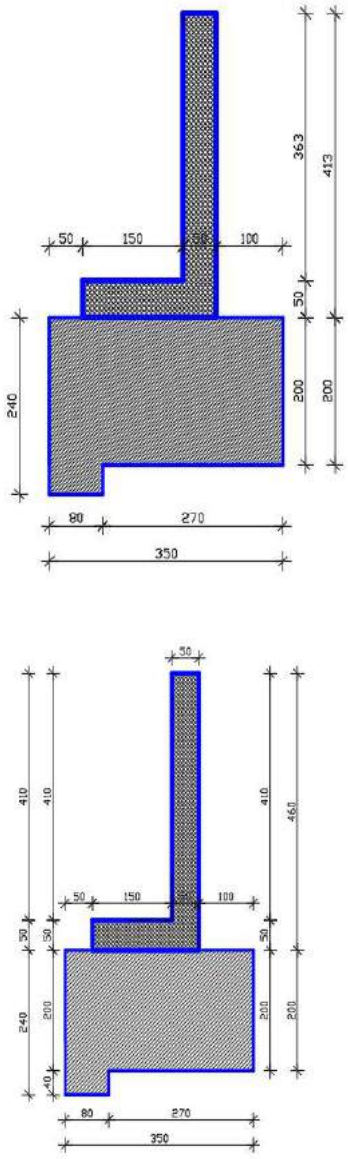

Figure 12 Retaining wall on counterforts

Recapitulation of the volume of the works and estimate of the works for the shape of retaining wall on counterfort :
Total of earthworks for the retaining structure……4483,00 KM
Total of concrete works for retaining structure……40302,00 KM
Total of earth and concrete works……44785,90 KM

According to the volume of works for each variant, it was analyzed obtained results.

Analysis of the results obtained

From the recapitulation of the volume of the works and estimate of the works, the total cost of the supporting structure for all three forms of supporting structure was taken as follows:
-Prices of works of retaining structure for the gravitational shape of the retaining wall = 50 051,00 KM
-Prices of works of retaining structure for the shape of the reinforced concrete retaining wall on the strip footing = 48 290,00 KM
-Prices of works of retaining structure for the shape of the reinforced concrete retaining wall on the counterforts=44785,90 KM

From the recapitulation of the volume of works and estimate of works for all three forms of retaining wall, it can be seen that the most expensive are works with the gravitational wall form and the cheapest works with retaining wall on the counterfort.

The selected factor of the retaining structure is only one of the factors in selecting a structure that can be and does not have to be decisive. In addition to this factor, we have a free profile factor from the outside of the retaining structure as and soil characteristics and the groundwater level.

Conclusion

Based on the previous analysis and experience of the authors of this work on landslide rehabilitation, the following conclusions were reached:
-If the foundation soil in a landslide at a depth of 6 meters, the best way to solve the landslide repair is with the retaining structure on the counterfort.
- Increasing the depth of the foundation soil increases the economics of the supporting structure on the counterforts.
-During designing deep landslides where the depth of the foundation soil is greater than 6 m, remediation of landslide should be done with retaining walls on the counterforts.
- In the case when they are not sure that the most favorable version of the retaining structure on counterforts is recommended to designers to make multiple variants of choice and choose the one that is most economical for approximately the same safety factors.
- When choosing the shape of a retaining structure, it should not go to reducing the price because of the safety factors

References

Čačković I., 2005: Stabilnost kosina i potporne konstrukcije.Univerzitet u Tuzli, 1- 401Tuzla. ISBN 9958-628-11-2.
Ferhatbegović Z., Gušić I., 2015: Elaborat o inženjerskoj prospekciji klizišta na području općin Sapna (I faza).
Ferhatbegović Z., Gušić I., 2015: Elaborat o geomehaničkim ispitivanjim tla za sanaciju klizišta u Jukićima-općina Sapna
Redžepović R., Ferhatbegović Z.,2014 : Živjeti na klizištu. Transkulturna psihosocijalna obrazovna fondacija-TPO fondacija, Sarajevo. ISBN 978-9958-9990-7-9
Redžepović R., Ferhatbegović Z.,2001 : Kako živjeti na klizištu.Specijalno izdanje Zavoda za geologiju, Sarajevo. ISBN 9958-9351-1-2
Suljić N., 2010: Potporne konstrukcije. Univerzitet u Tuzli, 1-246, Tuzla.ISBN 978-9958-628-15-3.
Vrabac S., Pašić-Škripić D., Ferhatbegović Z., 2005 : Geologija za građevinare. Univerzitet u Tuzli, 1-222, Tuzla. ISBN 9958-609-41-X

doi.org/ 10.35123/ReSyLAB_2019_24

The remediation of the landslide ``Lisovići` near Srebrenik

Zijad Ferhatbegović [1], Jusuf Husić [2]

1) The University of the Tuzla, Faculty of mining, geology, and civil engineering, Tuzla, Univerzitetska 2, +387 35 320580

2) The Institute for Protection, Ecology, and Education d .o.o. Tuzla

Abstract At the time of major natural disasters that hit the Canton of Tuzla in May 2014, a large number of landslides activated in the Srebrenik municipality. In the local community of Lisovici, 22 active landslides have been registered. One of the bigger landslides covered the area of approximately 4 ha, 230 m in width, 250 m in length with head scarp at 390 m, and a foot at 333 m. On the basis of available data, activated landslides caused damage to the environment and facilities in the form of destruction of asphalt road communications along the ridge in the length of about 100m, a macadam road in the distance of 100m in the middle of the landslide, agricultural land about 3ha, fruit trees, other trees and dug wells for water supply Also, about ten buildings were damaged, asphalt road communication in the length of about approximately 150 meters, and macadam road communication in the range of about 150 meters. Due to the activation of the landslide, ten residential buildings and about ten auxiliary facilities were endangered. As an interim measure, the remediation of the landslide in the upper part of the slope with stone embankment was performed, which also serves as stability for road communication and, on the other hand, as drainage. Detailed engineering and geological research were carried out, made an engineering-geological map and primary project of landslide rehabilitation with the purpose to solve permanent landslide remediation. Based on the collected data during the investigation works as well as the detailed enginering-geological mapping, the slope remediation will be done by the construction of a drainage system in the fishbone shape inside the landslide body. At the bottom of the slope, water will be collected into the water tank.

Keywords landslide, drainage system, slope, fishbone shape

Introduction

The slope of the surrounding area of the subject location has an exposition towards the southwest. The inclination of the slope is 19 °. According to the inclination, it belongs to the middle steep slopes with an inclination of 15-35 degrees, and according to the shape, it is the concave-convex slope. Due to the presence of water, it belongs to highly scattered slopes with occurrences of springs and a branched network of occasional and constant watercourses. Based on the basic geological map of the Tuzla 1: 100000 sheet, the wider surroundings of the site belong to the Upper Miocene sediments (M31) - represented by ceratites limestones, marl clays, marls, and sandstones less frequently conglomerates. There is the frequent alteration of marls and sandstones in the field (Fig.1.) The orientation of the sediments is north-northeast, which is favorable from the aspect of stability because they are opposite of the slope inclination. The measured elements of dip and strike of the layer are Eds = 10/60 and Eds = 20/50. At this location during exploratory drilling, groundwater levels were measured and monitored in exploration boreholes.

Figure 1 Marls and sandstones in alternation

On the slope during the rainfall, surface currents form ditches.

Figure 2 Sediment erosion on the slope

The landslide appeared on an eroded slope (Fig. 2.) where the rock mass is intensively degraded, which significantly interferes with and changes the composition, condition, and properties of the substrate present. Based on the registered large number of wells, it can be said that the slope is heavily saturated with water. In terms of stability (a division of slopes by degree of stability), this is an unstable slope where can expect the appearance of debris, rockfalls, and massive landslides. The hillside with activated landslip covers an area of 8.2 ha. According to the shape of the sliding body, the

landslides are tongue-like or glacial-shaped, stretched down the slope, with their length several times larger than the width. According to the position on the hillside, they are peak (located near the watershed). They are detrusive landslides where the activation of the sliding operation is carried out in the hypsometric higher parts of the terrain (near the watershed) and then the slipping is successively shifted towards the erosion base (a division of landslides according to the place of initiation of the sliding process). The causes of the sliding are the slope of the terrain, lithological composition, the presence of a large number of shallow wells that are abundant, unresolved drainage of surface water from the roads and heavy rainfall. Numerous landslide scars have been registered below the road at the top of the slope (Fig. 3.). In the upper part of the slope as a temporary remediation measure, a rock embankment has been used to stabilize road communication which on the other hand, serves as surface drainage (Fig. 4.).

Figure 3 Landslide scar

Figure 4 Rock embankment

Methods

The exploration of the landslide was carried out by engineering-geological exploratory works, geological mapping, and laboratory sample testing. On the basis of the investigations carried out, an opinion was given on the soil properties and the method of slope drainage. To define the geological, engineering-geological, and geomechanical characteristics of the terrain, ten exploratory boreholes were drilled. The B-1 well was drilled to 3.30 m, B-2 to 6.0 m; B-3 to 4.3 m; B-4 to 4.0 m; B-5 to 3.5 m, B-6 to 3.3 m, B-7 to 3.6 m, B-8 to 4.0 m, B-9 to 3.3 m B-10 to 2, 30 m. Based on exploratory drilling it was found that the terrain was made of humus, sandy-dusty clays, marl clays of different colors (yellow-brown, gray, light brown). These sediments form eluvial-diluvial and colluvial deposits while marls, sandstones, and conglomerates represent the substrate. The sediments of the substrate present the marls that dip at depths of 2.40 to 4.0 meters and the sandstones at a depth of 3.80 m. Also, it was analyzed by the depth and groundwater levels in 22 dug wells in the field (Fig.5). To determine the geomechanical properties of the soil from the exploratory wells, samples of the material for the

laboratory testing were taken. Laboratory testing includes determination of cohesion, internal friction angle, compressibility modulus, sample volume, plasticity index, consistency index, etc.

Figure 5 Registered dug wells on the landslide

Results

The display of engineering-geological characteristics was given through the composition, structure, and properties of rocks and individual parts of the terrain, as well as exogenous-geological phenomena and processes. The Engineering Geological Map was made based on the adopted Guidelines for making OIGK SFRJ 1: 100 000 (second amended and supplemented edition - 1988) and the IAEG (International Association for Engineering Geology) guidelines. According to the instructions, all the rocks were classified into two major engineering-geological groups: a group of rocks and soil belonging to the geological substrate, and another group where the ground and mixture of land from the stones classified as a group of blankets lying through the structures of the geological substrate.

Geological substrate (bedrock)

Layered marls, sandstones and rare conglomerates that stratigraphically belong to the Upper Miocene sediments (M31) present a geological substrate at the site location (Fig. 6) Marls were drilled in all boreholes except borehole B-8. In this borehole, sandstones were drilled. Marls are also found in the landslide bodies where they shift with the sandstone.

Figure 6 Layered marls and sandstones

Conglomerates were registered at the beginning of the ridge where the graveyard is located (Fig. 7).

Figure 7 Conglomerates on the top of the ridge

Based on their characteristics, marls, sandstones, and conglomerates belong to well-petrified rocks. The characteristic feature of these rocks is physical and mechanical decomposition building on thick eluvial-diluvial and slip surface covers. From the hydrogeological point of view, they are hydrogeological isolators that they have the function of water-impermeable rocks while decomposed sandstones have the role of hydrogeological collectors. According to the rock category (GN 200), these rocks are classified in category V.

Genetic types of surface covers

The surface covers differ in their lithological and granulometric composition, place of origin, thickness, degree of stability, degree of saturated rocks as their general physical and mechanical characteristics. Two types of surface covers are represented:

a) Colluvial cover

B) Eluvial-diluvial cover

Colluvial cover

The colluvial cover belongs to a group of covers that were created by moving the material on the slope. In essence, these deposits are parts of the **eluvial-diluvial** covers that gravitate from higher to lower parts of the hillside. The accumulation of this material on a specific part of the slope forms a blanket with poor geotechnical properties. In the structure of deposits, there are colorful clay, clay dusty-sandy, marl clay with the debris of bedrock. Its thickness is variable and ranges up to 4 m. Sediments that build the colluvial cover are characterized by soft and plastic consistency. Based on the experiment of standard dynamic penetration, the clays are **easy**, **medium, and hard consistency**. According to the GN-200, these materials belong to category II and III.

Eluvial-diluvial cover

The eluvial-diluvial cover presents the decomposition down the slope. In the investigated area, this cover is located on separate ridge forms between the parts of slopes affected by the sliding process. The eluvial- diluvial cover is represented by gray and yellow dusty and marl clay. Materials that build this cover have subcapilarry porosity. These covers have satisfactory geotechnical properties and build conditionally stable to stable terrain. According to the category of rock to dig GN-200, these covers belong to class III.

During the exploratory drilling that lasted from 04.06. until 06.06.2018, water occurrence in the B-2 well was recorded at a depth of 2.20 m from the surface of the ground, B-6 at a depth of 2.0 m and B-8 to 3.6 m, while in other boreholes were not registered the occurrence of groundwater although all are inside the landslides bodies. A large number of dug wells in the field were noticed near houses that undoubtedly prove that the slope is very seductive (Fig. 8).

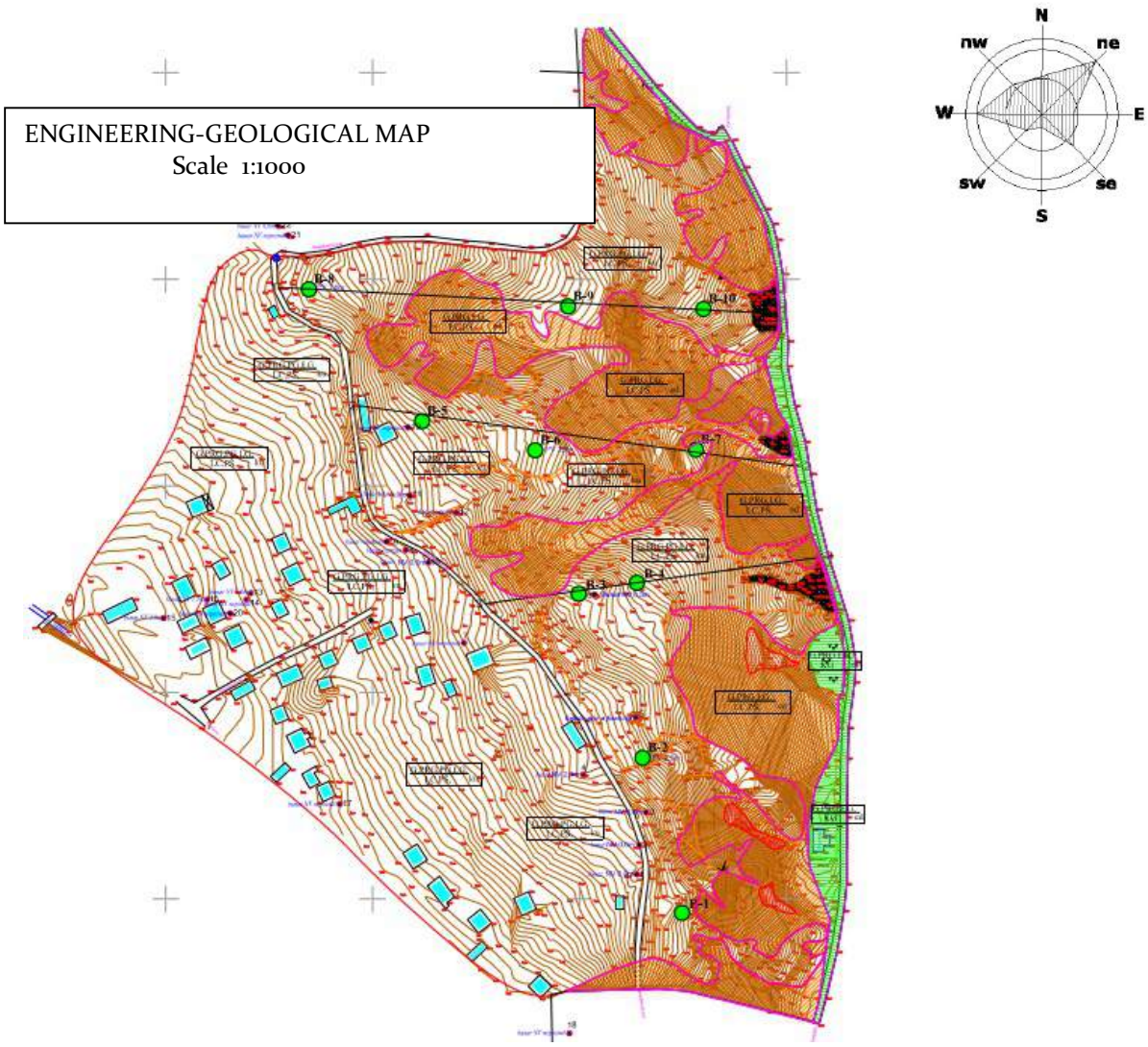

Figure 8 Engineering geological map of landslide Lisovići

Landslide remediation

In May 2014, one of the bigger landslides was registered in the local community of Lisovici, which covered the area of approximately 4 ha, 230 m in width, 250 m in length with head scarp at 390 m, and a foot at 333 m. On that occasion, ten buildings, asphalt and macadam road communications were damaged, and ten housing and auxiliary facilities were endangered. As a temporary measure of remediation, in the upper part of the slope, where road communication has been interrupted, a rock embankment has been used which has stabilized road communication and on the other hand, served as surface drainage. Based on the established general properties of landslides (size, volume, type of landslides), causes and mechanism of movement of the earth masses, a remediation project was made, consisting of making drainage system "Y" (fish bones) in the body of the landslide. Based on the project, the drainage system consists of two main drainage: Š - Š1, 127.9 mi Š9 - Š10, 148.2 m long, seven secondary drainage: Š and Š3, 103 m long, Š2-Š5, length 191.8 m, Š4-Š6, length 133.2m, Š2-Š7, length 155.7, Š7-Š8 length, Š9-Š11, length 53.9m and Š9-Š12, length 84.6m (Tab.1) . Collected water from the shafts Š1 and Š10 should take to the water tank. The excavation for the drainage trenches will be carried out to a minimum depth of up to 25 - 50 cm in water-resistant natural material. The bottom of the hole will be done manually with the correct longitudinal inclination. At the bottom of the excavation, should install a geotextile (weighing 300 mg) to rise along the sides of the trench, and at the height of approximately 100-150 cm depending on the depth, below the top of the channel, so that it can be closed over the inserted pebble filter. By placing geotextile, the passage of clay particles from the dam will be prevented, and at the same time, better drainage is possible. A flexible PVC drainage pipe diameter ø 30 cm will be put in the main drainage while in secondary will be put drainage pipe diameter ø20 cm — the gravel set over and around the pipe. The remaining part of the drainage up to 50 cm under the terrain should be filled with broken stone. The shafts should be done from pre-assembled concrete pipes with a diameter of ø100 cm. Shafts can be cover with a reinforced concrete cover diameter d = 100 cm (Fig.9).

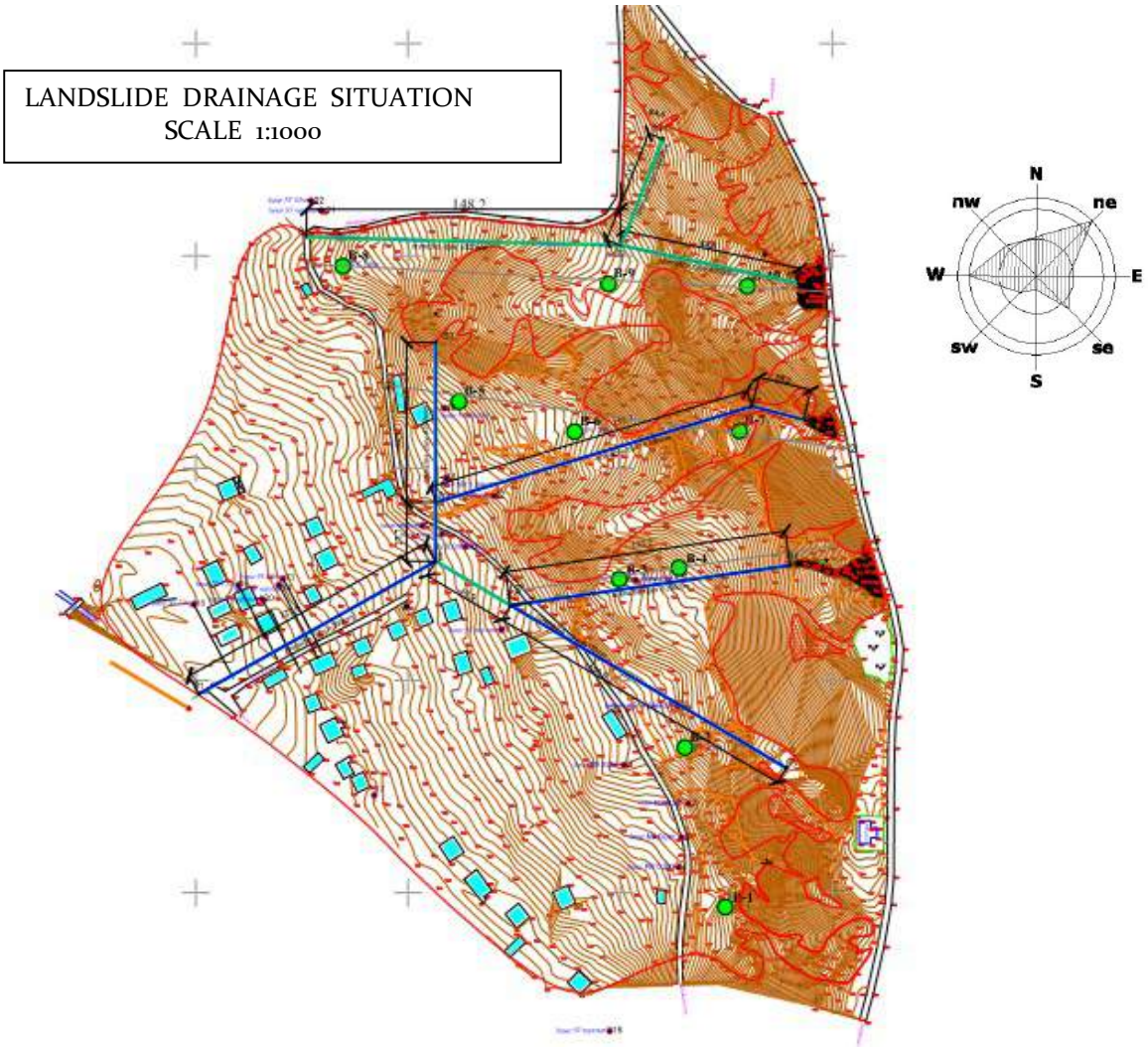

Figure 9 Remediation measures

The landslide rehabilitation should be carried out in stages to reduce the risk of slope movement on the slope and endanger the stability of the objects below the landslide. Phases of remediation measures are presented in Tab.1.

Table 1 Phases of remediation measures

Phases of remediation	
I	Making main drainage Š-Š1
II	Making Drainage Š-Š3 and Š-Š5
III	Making Drainage Š2-Š7, Š7-Š8
IV	Making Drainage Š4-Š6
V	Making Drainage Š9-Š10
VI	Drainage production Š9-Š11 and Š11-Š12

Conclusions

At the time of major elemental disasters hit by the Tuzla Canton in May 2014, in the local community Lisovići has activated a massive landslide with a surface area of 4 hectares. On that occasion, ten buildings, asphalt and macadam road communications were damaged, and ten housing and auxiliary facilities endangered. As a temporary measure of remediation, in the upper part of the slope, where road communication has been interrupted, a rock embankment has been used which has stabilized road communication and on the other hand, served as surface drainage. Taking into account the general characteristics of landslides, it was done the remediation project. The remediation project consists of making a drainage system in the form of a fishbone in the landslide body.

References

Čačković I., 2005: Stabilnost kosina i potporne konstrukcije.Univerzitet u Tuzli, 1- 401Tuzla. ISBN 9958-628-11-2.

Ferhatbegović Z., Husić J., 2019: Elaborat o geomehaničkim ispitivanjima tla za sanacije klizišta „Lisovići“ u mjestu Lisovići u općini Srebrenik.

Redžepović R., Ferhatbegović Z.,2014 : Živjeti na klizištu. Transkulturna psihosocijalna obrazovna fondacija-TPO fondacija, Sarajevo. ISBN 978-9958-9990-7-9

Redžepović R., Ferhatbegović Z.,2001 : Kako živjeti na klizištu.Specijalno izdanje Zavoda za geologiju, Sarajevo. ISBN 9958-9351-1-2

Suljić N., 2010: Potporne konstrukcije. Univerzitet u Tuzli, 1-246, Tuzla.ISBN 978-9958-628-15-3.

Vrabac S., Pašić-Škripić D., Ferhatbegović Z., 2005 : Geologija za građevinare. Univerzitet u Tuzli, 1-222, Tuzla. ISBN 9958-609-41-X

doi.org/ 10.35123/ReSyLAB_2019_25

Prediction of groundwater level fluctuation in landslide area using genetic algorithm

Yoshinori Ito[(1)], Hideaki Marui[(2)],Kousei Yamabe[(1)],Wataru Sagara[(3)]

1) Kowa Co.,Ltd. ,6-1,Shinkocho,Chuo,Niigata,Japan

2) Professor Emeritus Niigata University ,8050,Ikarashininocho,Nishi,Niigata,Japan

3) Sabo & Landslide technical center ,2-7-5,Hirakawacho,Chiyoda,Tokyo,Japan

Abstract It is generally recognized that landslides occur frequently during periods of snowmelts and intensive rainfalls. An increase of groundwater level due to snowmelt and intensive rainfall is considered to be one of the most essential triggering factors of landslides. Therefore, it is important to predict groundwater level fluctuation with sufficient precision to design appropriate countermeasures for landslide stabilization and further to evaluate effectivity of them. Although there are many research papers related with the effect of groundwater level fluctuation on landslide mechanism, there are still only few research papers to predict groundwater level fluctuation with sufficient precision. In order to find out more precise prediction method, the authors have developed a physical model using genetic algorithm for prediction of the groundwater level fluctuations in landslide areas in snowy regions. The authors examined the validity of the method through comparison between actually observed field data and estimated values by the prediction method. On the one hand, groundwater level fluctuations were observed in the specific landslide area throughout the two consecutive years. On the other hand, the groundwater level fluctuations were estimated by the model that displays response relationship between groundwater level and rainfall or snowmelt. The analysis parameters in this model were determined using genetic algorithm. The result of comparison between the observed data and the estimated values showed good coincidence with sufficient precision. Especially concerning the periods of high groundwater levels, the difference between the observed data and the estimated values was sufficiently small. It is clarified that the proposed method using genetic algorithm can predict groundwater fluctuation with sufficient precision if continuous observation data of groundwater level is obtained. The proposed method uses continuous observation data of groundwater level exclusively. Therefore, there are no need of laboratory experiments and in-situ tests which are essential in other methods with physical model. The authors think that the proposed method could be suitable and effective method. However, in order to confirm the validity of the method, further case analyses in various landslide areas should be continued.

Keywords landslide, groundwater level fluctuation, genetic algorithm

Introduction

Landslide is the phenomenon that generally comes into action by the influence of groundwater. It is common understanding that landslides occur mostly during periods of snowmelts and intensive rainfalls. An increase of groundwater level due to snowmelt and intensive rainfall is considered to be one of the most essential triggering factors of landslides (Marui, 2003). It is important to predict groundwater level fluctuation with sufficient precision to design appropriate countermeasures for landslide stabilization and further to evaluate effectivity of them.

There are many methods to predict groundwater level fluctuation. The typical methods are statistical analysis method and numerical analysis method and so on. The statistical analysis methods is favorable as it can carry out data analysis even with the limited data. However, the statistical analysis method do not consider the topographical feature of the area, distribution of the geological formations, landslide ruptures and cracks conditions and so on. Therefore, the outcome of the statistcal analysis is evaluated to be different to the outcome of the physical analysis which considers the ground conditions. In order to get more reliable analysis result, it is necessary to use physical model.

On the other hand, numerical analysis method based on physical model is the method, in which essential physical conditions like mass conservation equation, flow rates, hydraulic head and so on are taken into account to predict groundwater fluctuation. The numerical analysis method requires laboratory experiments and in-situ tests. It takes enough time to get the data of laboratory experiments and in-situ tests. As mentioned above, there are some disadvantages in the both methods.

In order to predict groundwater fluctuation with sufficient precision, a physical model using genetic algorithm is introduced by Yoshimatsu(2012). The non-linear relationship equation of rainfall quantity and groundwater level are simply expressed by the predicted groundwater level with the application of physical model. The special characteristics of this method is that it accounts the parameters of physical model using genetic algorithm. With the application of genetic algorithm, it is expected that the predicted value is highly precise and can be got more quickly.

Analysis method

Composition of equation

Groundwater level increases due to the infiltration of rain and snowmelt water into the ground. Conversely, groundwater level decreases during small amount of rainfall and continuation of drought. The authors think that groundwater level fluctuation is not a function of one dimensional curve as of straight line, it shows the behaviour of the combination of exponential and logarithmic functions. This study is basically focused on the behaviour of groundwater level fluctuation. Groundwater level is predicted with the use of calculation system using genetic algorithm and associated parameters.

Primarily, Enokida (1992) proposed an equation to predict the fluctuation of groundwater level. Later, Yoshimatsu (2010, 2012) improved the equation proposed by Enokida to predict groundwater fluctuation more precisely. These equations are composed of equation 1 to 5 as follows.

$$\Psi=\beta \sum_{n=1}^{\infty} \alpha^{n-1}(R_{-(To+\Delta t(n-1-d))} - R_o) \quad [1]$$

$$L\Psi=\log(\gamma\Psi)= \log(\gamma\beta \sum_{n=1}^{\infty} \alpha^{n-1}(R_{-(To+\Delta t(n-1-d))} - R_o) \quad [2]$$

$$h=L\Psi \quad \text{if} \quad L\Psi>Gw \quad [3]$$

$$h=L\Psi \quad \text{if} \quad L\Psi<Gw$$

$$Gw=LowWaterLevel+(1-\phi)\times(highWaterLevel-LowWaterLevel) \quad [4]$$

$$R=mt+\frac{1}{80}pt \quad (t>o) \quad [5]$$

Here,

α : Coefficient of residual effect of antecedent rainfall
β : Coefficient of groundwater level fluctuation
R : Ineffective rainfall amount including snowmelt
γ : Weighted coefficient of logarithmic transformation
ϕ : Coefficient of discriminant between exponential function and logarithmic function
d : Days of response lag
m : Coefficient of convergence from snowmelt to rainfall amount
To : Initial delay time
n : Maximum number of retrospective day
h : Groundwater level
Gw : Groundwater level for equation[3]
p : Rainfall amount
t : Temperature

Equation 1 and 2 are the equations to calculate the value of groundwater level fluctuation. If rainfall is low and drouth continues, the groundwater level decreases exponentially. Conversely, groundwater level increases logarithmically in the case of intensive rainfall. Thus, equations 1 and 2 represents the non-linear behaviour of the groundwater level fluctuations.

Even if the same amount of rainfall is occured, groundwater level fluctuation differs between high groundwater level state and low groundwater level state. Under such circumstances, the groundwater level fluctuation can be calculated using equation 1 or equation 2. Therefore, it is necessary to select the appropriate equation between equation 1 and equation 2. The most appropriate and necessary one equation is selected. The determination is carried out using equation 3 and 4.

In order to estimate the amount of snowmelt water, many researches have been carried out calculations using different methods and techniques. Some of them are based on energy balance and accumulated temperature. This research used equation 5 which belongs to the accumulated temperature method and is widely used to estimate the amount of snowmelt water in Japan.

The parameters of α, β, R, γ, ϕ , *d*, and *m* are essential to set in the equations 1 to 5 as mentioned above. The parameters are determined using genetic algorithm.

Genetic Algorithm

Genetic algorithm was first proposed by John Henry Holland in 1975. The genetic algorithm imitates the concept of the genetic change that organisms adapt to their environment and is a method to find solution. In nature, the individual with the high degree of adaptation to the environment survives. Those survived individuals form next generation, sometimes causing mutations. In this study too, the parameters which greatly influence the prediction of groundwater fluctuations are selected on the basis of the most adaptive and fittest value using genetic algorithm. This is the prediction method which responds to groundwater level most appropriately with respect to rainfall and snowmelt. The method can solve the optimization problem accurately in a short time.

Fig.1 shows the flow diagram of analysis, and it is commented as ① to ⑥:

① : Initial stage data is generated artificially. At this time, a parameter of α and β, etc. is expressed as genetic information which consists of bit line of “o(zero)” and “1(one)”.
② : Groundwater level fluctuation is calculated using parameters which are set at an initial stage. The results of calculation are placed in order on coefficient of correlation between observation data and calculation data.
③ : High adaptability parameters should be kept. Other parameters should be eliminated. It is a process of Selection.
④ : The decreased numbers of individual pairs due to elimination process are fulfilled by individual pairs of the high degree. Thus obtained genetic information is used to multiply the best individual. It is a process of crossover.

⑤ : Genetic recombination by a random number is carried out in the fixed percentage. It is a process of Mutation

⑥ : The process of ③-⑤ are repeated over several generations to determine the most adaptable parameter.

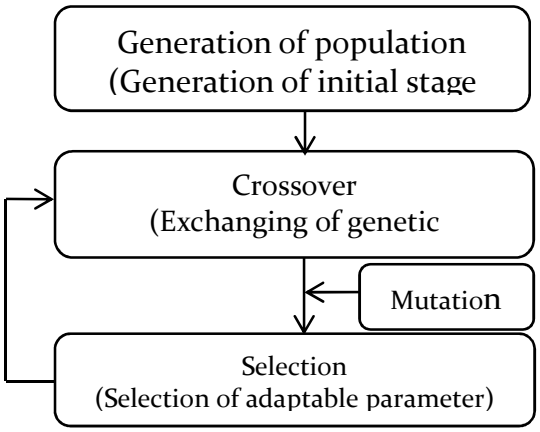

Figure 1 Flow chart of Genetic Algorithm Analysis

The analysis was carried out setting the iteration process for 500 to 1200 generations and the mutation ranging from 5 to 30%.

The outline of the landslide site

The target landslide is located in such a region which it receives approximately 2 to 3 meters of snowfall annually. Tab.1 represents outline of the landslide site and Fig.2 represents the location of the borehole for groundwater observation.

Table 1 Outline of the landslide

Items	Outline
Name of landslide Block	Block-A
Borehole name	Obs.-1
Length of landslide	350 m approximately
Width of landslide	180 m approximately
Max. Sliding surface depth of the landslide	36.4 m (assessed from borehole investigation)
Geological information	Alteration of sandstone and mudstone layers, Neogene
Landslide mass properties	Cohesive(clayey) soils and highly fractured mudstones

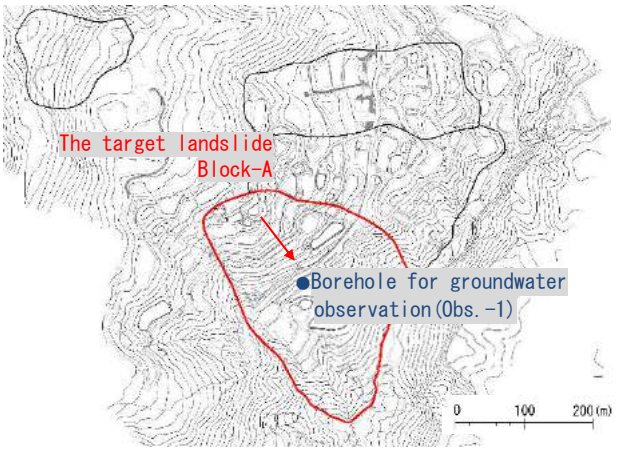

Figure 2 Location of borehole for groundwater observation

Fig.3 shows the schematic view of the observation hole. The pipes used in groundwater level observation holes are non perforated from surface upto GL-1m depth and are perforated below GL-1m. The observation frequency was once a day.

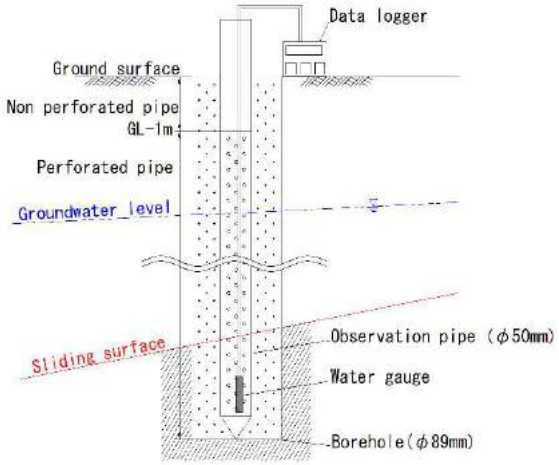

Figure 3 Schematic view of the observation hole

Regarding the meteorological data, daily rainfall amount, temperature, snow depth were taken from the meteorological station located about 500 m far from landslide site.

Prediction of groundwater level fluctuation

Fig.4 shows groundwater level fluctuation pattern obtained from groundwater observation data and the meteorological data like rainfall amount and snow depth. It is confirmed that groundwater level increases approximately 1 to 2 m from GL-7 m. The increased groundwater level is attributed to the snowmelt than the rainfall.

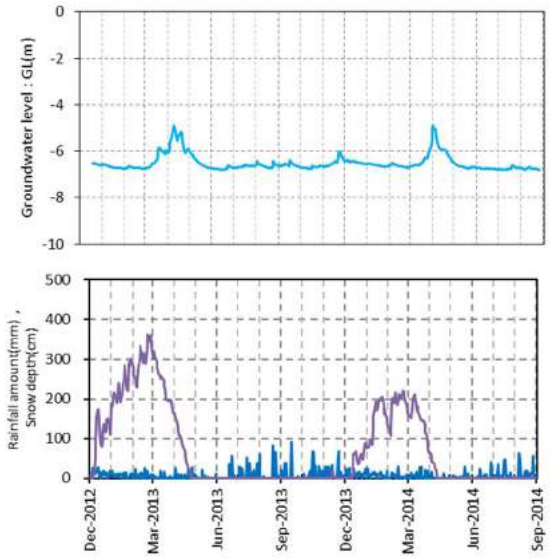

Figure 4 Observation data of groundwater level (Obs.-1), rainfall amount and snow depth

The authors performed learning analysis using genetic algorithm and built the prediction model of groundwater level fluctuation. At that time , the authors analyzed the first month exclusively in observation data with consideration of the influence of antecedent rainfall. Tab.2 shows the values of parameters in Obs.-1.

Table 2 Parameters obtained using Genetic Algorithm

Items	Value
α: Coefficient of residual effect of antecedent rainfall	0.83578
β: Coefficient of groundwater level fluctuation	0.00391
R: Ineffective rainfall amount including snowmelt	94.8
γ: Weighted coefficient of logarithmic transformation	0.0156
ϕ: Coefficient of discriminant between exponential function and logarithmic function	0.9320
d : Days of response lag	2
m : Coefficient of convergence from snowmelt to rainfall amount	5.5

Using the parameters as mentioned in the Tab.2, the calculated value of groundwater level is shown in the Fig.5.

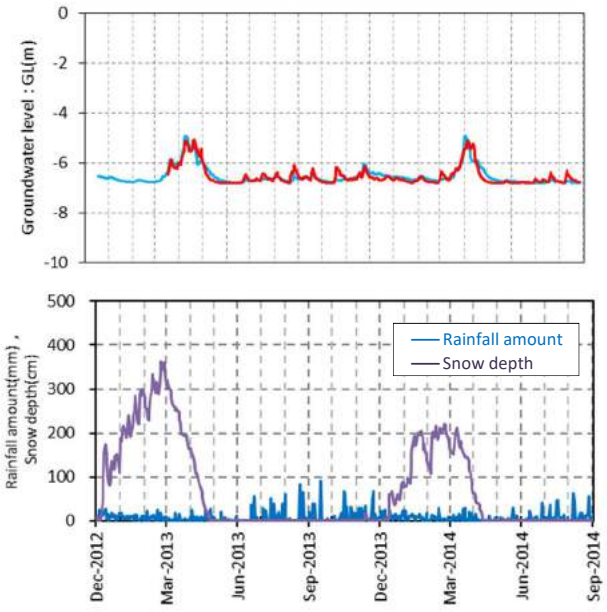

Figure 5 Calculated result

Fig.5 shows the fluctuation curve of calculation data which is attributed by the rainfall and snowmelt. This reflects the response of the real situation of groundwater level in the observation hole. It is obtained that the coefficient of correlation is 0.90 between the observation data and the calculation data.

The highest groundwater level is important in order to design appropriate countermeasures for landslide stabilization and further to evaluate effectivity of them. Therefore, the authors confirmed the difference between the observation data and the calculation data at the state of highest groundwater level. In the observation, the groundwater level tends to rise in the snowmelt period rather than rainfall period. Therefore, Fig.6 and Fig.7 show the comparison of data during the snowmelt period in 2013 and 2014.

In Fig.6, increasing of groundwater level is recognized with decreasing the snowdepth from the end of March to the end of April. The observed groundwater level recorded the highest groundwater level GL-4.90 m below ground surface on 9th April. On the otherhand, the calculated groundwater level on 10th April showed GL-5.09 m below ground surface. The difference between observed groundwater level and calcurated groundwater level is only 0.19 m.

In Fig.7, the observed groundwater level recorded the highest groundwater level GL-4.90 m on 2nd April and the calculated groundwater level showed the highest groundwater level GL-5.12 m below ground surface on 5th April. The difference between the observed groundwater level and the calculated groundwater level is only 0.22 m.

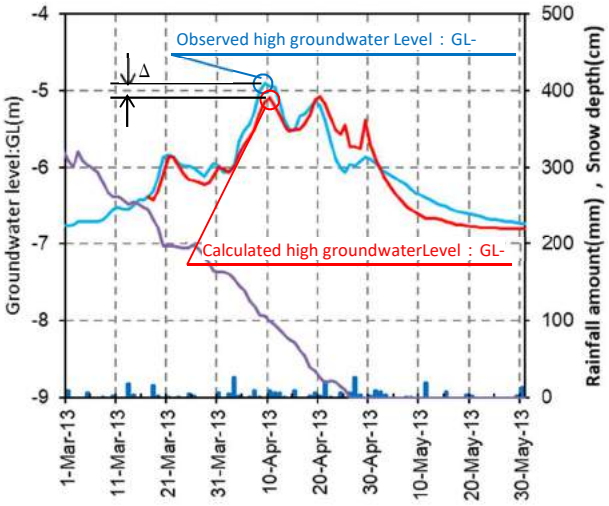

Figure 6 The observed groundwater level fluctuation and the calculated groundwater level fluctuation during snowmelt period in 2013

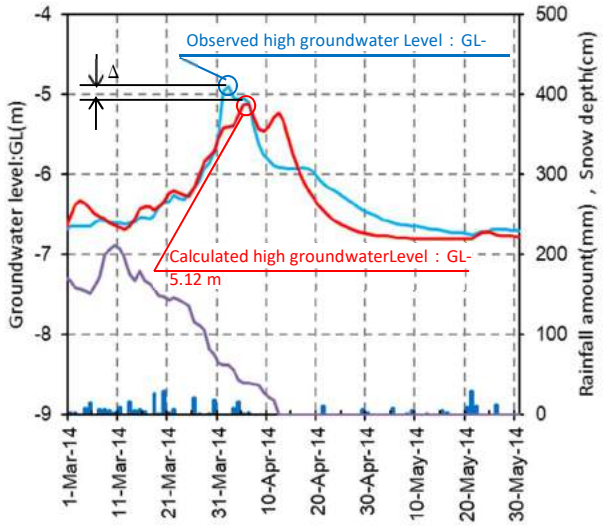

Figure 7 The observed groundwater level fluctuation and the calculated groundwater level fluctuation during snowmelt period in 2014

Conclusion

The authors reported a case analysis which can predict groundwater level fluctuation using genetic algorithm. Following output can be summarized:

An effective prediction model was proposed, in which the coefficient of correlation between the observed data and the calculation data shows high value of 0.90.

Difference between the observed groundwater level and the calculated groundwater level in the period of highest groundwater level was examined. As a result, the groundwater level difference ranged only from 0.19 to 0.22 m.

It is clarified that the proposed method using genetic algorithm can predict groundwater fluctuation with sufficient precision if continuous observation data of groundwater level is obtained. The proposed method uses continuous observation data of groundwater level exclusively. Therefore, there are no need of laboratory experiments and in-situ tests which are essential in other methods with physical model. The authors think that the proposed method should be suitable and effective method. However, in order to confirm the validity of the method, it is necessary to carry out further case analyses in various landslide areas.

References

Hideaki MARUI, (2003), Slope Movement Disasters Caused by Snow Melting in Alpine countries, Ann. Rep. of Res. Inst. For Hazards in Snowy Areas, Niigata Univ., No.25

Hiroyuki YOSHIMATSU, Masanobu OTSUKA, Keiji MIKAI, Nobuaki KATO,(2010),An estimation of ground water fluctuation of landslide area and effect evaluation of drainage prevention work by using sparse measured data, J. of the Landslide Soc.,Vol.47,No.2

Hiroyuki YOSHIMATSU, Wataru SAGARA, Takami KANNO,(2012),Prediction of long term fluction in ground water level of landslide in a snowy district, J. of the Landslide Soc.,Vol.49,No.3

Yoshinori ITO, Wataru SAGARA, RyousukeTSUNAKI, Kousei YAMABE, Hideaki MARUI, (2018), Predicting the groundwater level fluctution in landslide areas by means of genetic algorithm, J. of the Landslide Soc., Vol.55, No.3

doi.org/ 10.35123/ReSyLAB_2019_26

Site investigation for linear structures and landslide in D400 highway (Antalya-Turkey)

Ertugrul Akca [(1)], Yasemin Leventeli [(2)]

1) Department of Geological Engineering, Akdeniz University, Antalya, Turkey

2) Department of Geological Engineering, Akdeniz University, Antalya, Turkey

Abstract The world is a living organism that keeps going to its precession. The natural events like earthquake, volcanic eruption and landslide are evidence of this motion. These events are defined as "natural" in areas where there is no loss of life and also property, but if there is any loss they are named as "disaster". It is a fact that if the human could understand the language of nature and act according to science; these natural events will not turn into a disaster. For this reason; geological, hydrogeological, engineering geological and geotechnical models of the region must be accurately identified when selecting the site for engineering projects. Landslides are common problems in both residential and transportation projects. Many factors predict potential landslides such as topography, geology, vegetation and water condition. A proper geotechnical investigation before construction could protect nature; save time and money and no loss of life will happen.

A landslide has occurred on the D400 road which provides transportation between Antalya and Kumluca on February 28, 2018. Fortunately; there was no loss of life, there have been taken precautions and transitions have been blocked. The landslide starts from neritic limestones and ends in the old colluvium material. Triassic aged claystone, sandstone, siltstone, limestones and Cretaceous aged ophioliticmelange are observed at the bottom. The main aim was to understand the mechanism of the landslide. Therefore, besides the topographical characteristics of the region; the engineering and geotechnical properties of the lithological units and the water condition were examined. The landslide analysis was performed by the GEO5 software program, using the obtained engineering and geotechnical parameters. The determination of engineering geological and geotechnical properties is very important in site selection for engineering structure. The engineering and geotechnical research procedure performed in the stability analysis is explained through Candır formation, in this study.

Keywords Site investigation, Engineering geology, Geotechnics, Landslide, Antalya.

Introduction

Selection of proper alignment for the linear engineering structures like motorway-railway-pipeline and water canal, has many advantages -at least 60%- in terms of timing, environment, safety-security and cost (Leventeli and Yilmazer, 2005). Besides that, the relations between discontinuity, water and clay should be considered. Because, generally, these trinity plays an important role in the stability problems.

Nowadays, due to the rapid developing urbanization, appropriate settlement areas and transportation routes connecting these regions are gradually growing. Therefore, the building of the structures has also increased in all kinds of topographic and ground conditions. The mass movements, in both residential and transportation projects on mountain and hill slopes at risk of slipping, cause loss of life and property in our country and also in the world.In order to evaluate the stability problems for projects on slopes and also to avoid any further ones, the rock/soil parameters that cause instability is extremely important and should be investigated well.

A mass movement occurred in Yenbey crossing of Kemer - Kumluca D-400 Highway, on 26 February 2018 (Figure 1). Stability analysis studies were performed using the GEO5 (2019) / Slope Stability software program. In this study, the engineering and geotechnical properties of the Candır formation, which is widely distributed in the region, were determined to be used in the stability analysis.

Engineering geological and geotechnical properties of candir formation

Antalya nappes are divided into Tahtalıdag, Çataltepe, Alakırçay and Tekirova ophiolite nappes as stratigraphically and structurally in the study area (Senel et al. 1992; 1996). The following units were found in the landslide area: Candır (TRaç), Tekedağı (JKt), Kırkdirek (Kkm) and talus (Qym). The Candır formation (TRac), named by Kalafatçıoğlu (1973), shows a widespread at the lower elevations of the road route (Akca and Leventeli, 2019), (Figure 2).

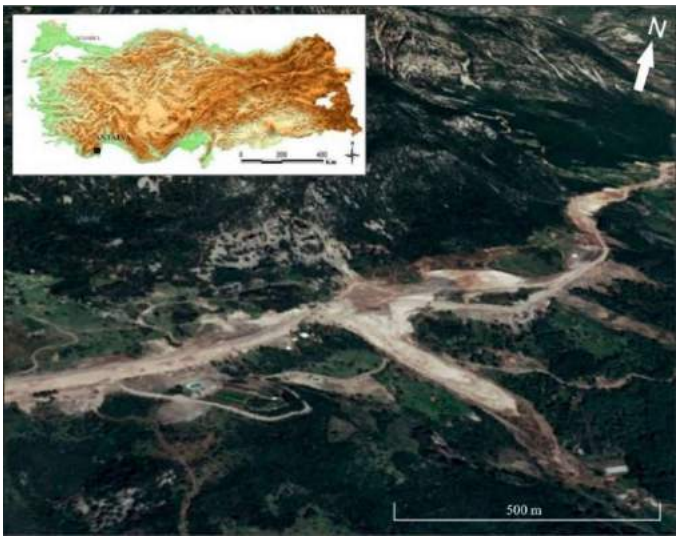

Figure 1 The location map of the landslide (Google Earth view).

Figure 2 Triassic aged Candır formation (TRac) including claystone and siltstone.

Candır formation has been evaluated in two parts according to the degree of decomposition during the analysis; as weathered (TRac-W5) and unweathered (TRac) levels (Yuksel Project, 2018). The weathered levels (TRac-W5) vary in thicknesses ranging from 3.20 to 8.80 meters in the exploration boreholes and include radiolarite and claystone / siltstone units. Radiolarite has reddish coffee - greenish coffee-brown color; brittle - less hard, weak - very weak strength and it is very - completely weathered in general. The unit is generally fragmented and partly brecciated. Discontinuities cannot be observed due to intense weathering; but the observable discontinuities are open, bright and slippery with 10°-45°dips. Claystone/siltstone units are generally gray-greenish gray, brittle - less hard, weak - very weak strength, very - completely weathered. Greenish gray, hard, resistant sandstone blocks up to 5-30 cm are observed in the unit. The unit has a brecciated appearance in places. Discontinuities with 15°-90° dips are open, rough and clay-filled; with 45°-60°dips are closed and 1-5 mm calcite filled. The results of the laboratory tests performed on the undisturbed soil samples obtained from the SPT (Standard Penetration Test) carried out in the weathered levels (TRaç) are presented in Table 1.

Table 1 SPT and laboratory test results of weathered levels of Candir formation (TRaç-W5).

SPT (N)	28 ≤ SPT (N) ≤ R
Water content (Wn)	% 9.9 ≤ Wn ≤ % 18.9
Liquid limit (LL)	% NP ≤ LL ≤ % 64.8
Plasticity Index (PI)	NP ≤ PI ≤ 36.5
Remaining on sieve 4 (+4)	% 5.5 ≤ + 4 ≤ % 47.7
Passing through sieve 200 (–	% 16.9 ≤ – 200 ≤ % 66.2
Soil Classification (USCS)	CH, CL/CH, GM, GC, GP –

Candır Formation (TRaç) includes radiolarite, intercalated claystone – limestone, claystone/siltstone, and claystone units. In general, the radiolarite unit is reddish-brown, yellowish-brown, brown, slightly hard – hard, brittle, moderate weak and weathered in places. Discontinuities in radiolarite unit have two dips: 10°-90° which are open, matte, rough and closed; 45°-90° which are irregular and closed, 1-10 mm calcite filled and sometimes filled with clay. Claystone unit of intercalated claystone – limestone is dark gray - greenish gray-reddish brown, slightly hard - moderately hard, brittle, very weak - moderately weak strength sometimes, moderately - completely weathered in places. Limestone unit intercalated claystone – limestone is generally light gray-beige-white color, hard-mediumhard, medium strength, occasionally moderately weak strength, slightly-occasionally moderately weathered. The intercalation of these units is observed generally as 5-40 cm limestone and 5-30 cm claystone. Discontinuities in this unit are bright, lubricous, rough, clay-filled with 10°-90°dips; the ones have10°-45°dips are closed and 1-20 mm calcite filled. The claystone/siltstone unit is gray, greenish gray, reddish-brown, slightly hard to brittle, weak-very weak strength and partly very weathered. Sandy limestone blocks around 5-30 cm thick and hard sandstone blocks up to 10-50 cm thick are observed within the unit. Discontinuities with 20°-80° dips are bright, lubricous, rough, clay-filled and closed; discontinuities with 20°-80° dips are generally closed but 1-5 mm calcite and clay - silt filled in places. The claystone unit is generally gray-colored, brittle, very weak strength and completely weathered. There are hard limestone blocks up to 10 cm in size in places, in the unit. The unit is extremely folded, kneaded and sometimes brecciated; it is shale-looking. Observable discontinuities are bright, lubricous, clay-filled and have 20°-45°dips.Total Core Recovery (TCR), Rock QualityDesignation (RQD),Point Load Strength Index (Is50), Uniaxial Compressive Strength (qu) and Unit Volume Weight (γ) values of Candır formation (TRac) are given in Table 2.

Table 2 The results of laboratory experiments for Candır formation (TRac).

Total Core Recovery (TCR)	% 16 ≤ TCR ≤ % 100
Rock QualityDesignation (RQD)	% 0 ≤ RQD ≤ % 73
Point Load Strength Index (Is_{50})	0.25 MPa ≤ $Is_{(50)}$ ≤ 6.86
Uniaxial Compressive Strength (qu)	1.3 MPa ≤ qu ≤ 64.4 MPa
Unit Volume Weight (γ)	2.16 gr / cm^3 ≤ γ ≤ 2.68 gr

The geological strength index (GSI) has been calculated for rock units using discontinuity Surface Condition Rating (SCR) and Structure Rating (SR) scores were determined from the field studies. In these evaluations, the number of volumetric joints was calculated using Jv = discontinuity set number / discontinuity interval (in meters) equation. It was calculated as 2 / (1/10) = 20 for the very-completely weathered (TRac-W5) and unweathered levels (TRac) of the Candır formation. After that, the Structure Rating (SR) value has been determined as 28 from the graph (Figure 3). In this case, the GSI value was determined as 24 and 34, respectively.

Then, the strength parameters obtained through the RocLab (Rocscience, 2009) software program are given in Table 3; the obtained normal stress-shear strength graphs are also given in Figure 4.

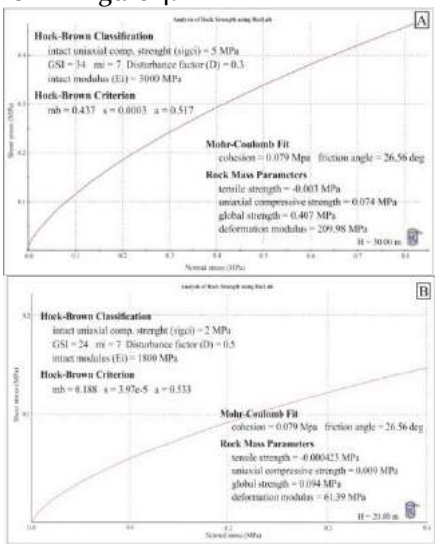

Figure 4 Normal stress-Shear strength graphics
a) for TRaçfrm; b) for TRaç-W5 frm(Sonmez and Ulusay, 2002).

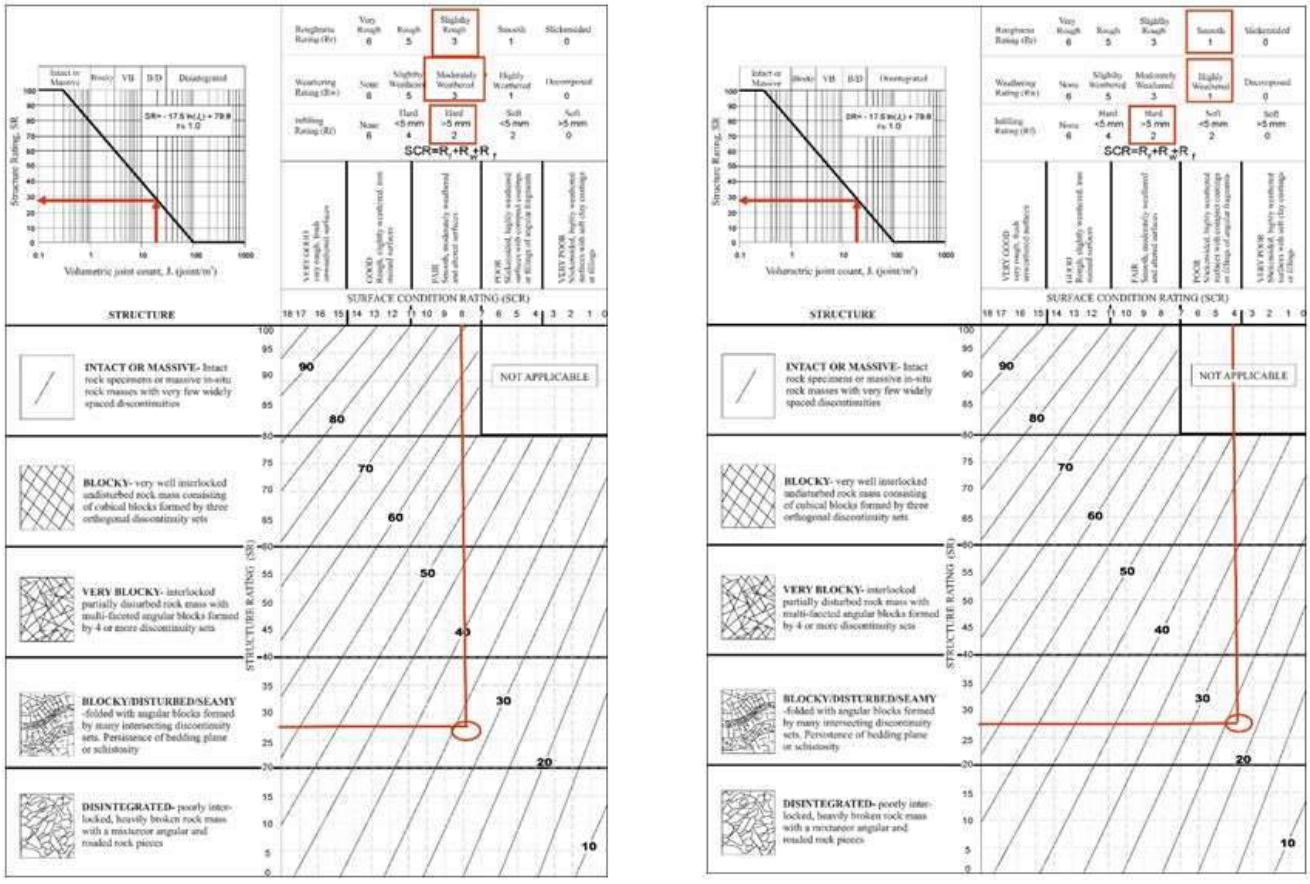

Figure 3 GSI chart for Candır formation's weathered (TRac-W5)and unweathered(TRac) levels,(Sönmez and Ulusay 2002; Yuksel Project 2018).

Table 3 Geotechnical parameters of the geological formations (Yuksel Project, 2018).

Geological Formations	Uniaxial Compressive Strength (MPa)	Material Constant (mi)	Intact Modulus (MPa)	Disturbance Factor (df)	Cohesion (kPa)	Internal Friction Angle (°)
TRaç-W5	2	7	1800	0,5	26	17,12
TRaç	5	7	3000	0,3	79	26,56

The hydrogeological properties of the lithological units in the region are described based onYilmazer et al. (1999) and hydraulic conductivity (K, m/s) of Candırformation was determined around 10^{-8}.

Conclusion

A particular survey should be done in site investigations for large-scaled engineering structures such as highway, railway and dam.In addition to topographic, geological, hydrogeological studies; engineering geology and geotechnical studies are also important. The right determination of main engineering and geotechnical parameters of both soils and rocks will provide benefits in terms of time and money to the project.These parameters, which are determined by field, laboratory and office studies, are very important in the site investigation for engineering structures and precautions to be taken in case of potential problems like instability.On 26 February 2018, in the landslide area, which occurred on the 75th kilometer of Kemer-Kumluca D-400 highway, the following units were observed; Candır (TRaç), Tekedağı (JKt), Kırkdirek (Kkm) and talus (Qym). In this study, the engineering geological, geotechnical properties and hydraulic conductivity of Candır (TRaç) formation, which is widespread in the field, are given.The laboratory tests have been performed on the undisturbed soil samples obtained from the SPT like sieve analysis, water content and Atterberg limits. Besides that, rock index parameters, like TCR-RQD-Is50-qu and γ, have been also determined. All studies and experiences have shown that "Precaution is much more professional approach than reclamation". So, it is possible to carry out these studies and researches during route selection and to take caution before landslide.

Acknowledgements

This project is supported by the Scientific Research Projects Coordination Unit of Akdeniz University. The authors would like to thank the 13th Regional Directorate of Highways and Yuksel Project for their support.

References

Akca, E. and Leventeli, Y. (2019). Study of the landslide on highway between Antalya and Fınıke. International Symposium on Advanced Engineering Technologies, 2-4 May, Kahramanmaras, Turkey, 1446-1450.

GEO5 (2019). Geotechnical Software GEO5 for Windows, Spring Update Version, Czech Republic.

Kalafatçıoğlu, A. (1973). Geology of the western part of the Gulf of Antalya. Bulletin of the Mineral Researchand Exploration, 81: 82-131.

Leventeli, Y. and Yilmazer. (2005). Geological and geotechnical database for motorways. Geosound, 46, 191-208. (In Turkish)

ROCSCIENCE, (2009). RocLab Software Version:1.007. www.rocscience.com, RocscienceInc. Toronto Canada.

Sonmez, H. and Ulusay, R. (2002). A discussion on the Hoek-Brown failure criterion and suggested modifications to the criterion verified by slope stability case studies. Yerbilimleri,Bulletin of Earth Sciences Application and Research Centre of Hacettepe University,26(1):77-99.

Senel, M., Dalkilic, H., Gedik, I., Serdaroglu, M., Bolukbasi, S., Metin, S., Esenturk, K., Bilgin, A. Z., Uğuz, M. F., Korucu, M., Ozgul, N. (1992). Geology of the areas between Egirdir-Yenisar-Bademli-GedizveGeriş-Koprulu (Isparta-Antalya). TPAO Report, No:3132, MTA Report No:9390 (unpublished), Ankara. (in Turkish)

Senel, M., Gedik, I., Dalkilic, H., Serdaroglu, M., Bilgin, A. Z., Uguz, M. F., Bolukbasi, A.S., Korucu, M., Ozgul, N. (1996). Stratigraphy of the autochthonous and allacton units in the east of the Isparta bend (Western Taurus).Bulletin of the Mineral Researchand Exploration, 118, 111-160. (In Turkish)

Yilmazer, I., Yilmazer, O., Ozkok, D., Gokcekus, H. (1999). Introduction to geotechnical design. Bilisim Pres., Ankara, 210 p. (In Turkish)

Yuksel Project (2018). Landslide modeling and design geotechnical project report between Km: 74 + 500-74 + 720 and 74 + 100 (unpublished), Ankara.

doi.org/ 10.35123/ReSyLAB_2019_27

Influence of DEM resolution on numerical modelling of debris flows in RAMMS - Selanac case study

Jelka Krušić[(1)], Biljana Abolmasov[(1)], Mileva Samardžić-Petrović[(2)]

1) University of Belgrade, Faculty of Mining and Geology, Belgrade, Đušina 7, +381 11 3219225

2) University of Belgrade, Faculty of Civil Engineering, Belgrade, Bul. Kralja Aleksandra 73, +381 11 3218538

Abstract Debris flows induced by intensive rainfall represent very hazardous phenomena in many parts of the World. Methods for prediction of runout distance of flow like mass movements are different and depending on the input data, rheology, and available or appropriate numerical solution. However, sometimes it is not easy to obtain pre event and post event high-resolution data in the rural or mountainous area. Thus, the topology of terrain is the most important input parameter for the every real case study modelling,. This paper presents results of continuum mechanics-based models tested in RAMMS:DEBRIS FLOW® with different resolution of input data on the Selanac debris flow in Western Serbia.

Keywords debris flow, modelling, RAMMS, DEM

Introduction

Debris flows are one of the most dangerous and unpredictable landslide types. In modelling of flow type landslides, there are few approaches nowadays that should be considered: mathematical, constitutive (rheological) and finally numerical approach. Generally, numerical approaches are divided into two goups: empirical-statistical (Rickenmann, 1999, Legros, 2002), while others are based on physical-deterministic (dynamical) approaches (Savage and Hutter, 1989; Hungr, 1995; Iverson, 1997; Takahashi, 2007; Wu, 2015). Many empirical-statistical methods for runout prediction require only a few input parameters and they are relatively easy to use. In contrast, dynamical models are independent from local conditions, since such models implement physical principles, like the conservation of mass, momentum and energy of bulk mixtures (Rickenmann, 2005).

In this paper, results of RAMMS debris-flow dynamical method are tested, based on Voellmy (1955) approach, which was specially designed for snow avalanches (Bartelt, 2015; Christen et al., 2007; 2010a; 2010b). Nevertheless, it is also suitable for modelling of other processes such as rock avalanches and debris flows (Schraml, 2015; Sosio, 2007; Frank, 2017). As input, three quantities must be specified to perform a numerical calculation: (1) a digital elevation model (DEM), (2) source zone area and (3) model friction parameters. Pre-event DEM resolution characterizes the natural terrain surface geometry and it is therefore the most important input parameter. Resolution of DEM defines at the same time precision of curvature, and finally precision of initial parameters and deposition zones.

The Selanac debris flow was triggered after extreme precipitation of about 230 mm over a period of 72 h in May 2014.TheSelanac is a complex debris flow, with large depth in source zone (30m), and length of about 1.5km. First results were made using30x30m DEM as input, and another with much more precise 5x5m DEM. New UAV scanning of post event topology was obtained in 2017 and additionally had helped in defining precise dimension of release, erosion and deposition zones for better models. Better resolution affected a lot in results about deposition depth, but also on choosing right frictional parameter in rheological model.

Method

One of well used rheological model is Voellmy method (Voellmy, 1955) firstly used in snow avalanche models, which means that is basically one-phase. It is assumed that the initiation mass starts to move as a plug defining shear stress in different points of transportation path.

RAMMS DBF software is FVM (Finite Volume Method) based software for modelling of debris flows. RAMMS was developed in 2005 by the Swiss Federal Institute for Forest, Snow and Landscape Research (WSL, Birmensdorf) and the Swiss Federal Institute for Snow and Avalanche Research (SLF, Davos).

The mass balance equation incorporates the field variables flow height H (x, y,t) and flow velocity U (x, y,t) and is given by:

$$Q(x,y,t)\dot{} = \partial tH + \partial x\,(H\,Ux) + \partial y\,(H\,Uy) \quad (1)$$

where Q(x, y,t) ˙ describes the mass production source term, and Ux and Uy represent the depth-averaged velocities in horizontal directions x and y (Christen et al., 2010 Frank et al 2017). The depth-averaged momentum balance equations account for the conservation of momentum in two directions x and y:

$$Sgx - Sfx = \partial t\,(H\,Ux) + \partial x\,(cxH\,Ux^2 + g_z k_a \frac{H^2}{2}) + \partial y\,(H\,UxUy) \quad (2)$$

$$Sgy - Sfy = \partial t\,(H\,Uy) + \partial x\,(H\,UxUy) + \partial y\,(c_y H\,Uy^2 + g_z k_a \frac{H^2}{2}) \quad (3)$$

where the earth pressure coefficient ka=p is normally set to 1 when running the standard Voellmy–Salm friction approach, cx and cy represent topographical coefficients determined from the digital elevation model, Sg is the effective gravitational acceleration, and Sf is the frictional deceleration indirections x and y (Christen et al., 2010b).

The frictional deceleration Sf of the flow is determined using the Voellmy friction relation (Salm et al., 1990; Salm, 1993) and specifies the dry-Coulomb term (friction coefficient / scaling with the normal stress and the viscous or turbulent friction (coefficient/ depending on the flow velocity U (Christen et al.,2010a, 2012; Bartelt et al., 2013):

$$S_f = \mu\rho g H \cos\varphi + \frac{\rho g u^2}{\xi} \quad (4)$$

where ρ is the mass density, g is the gravitational acceleration, φ is the slope angle, and Hgcos φ is the normal stress on the overflowed surface. The tangent of the effective internal friction angle of the flow material can be defined for the resistance of the solid phase (the term containing / which extensively controls deceleration behaviour of a more slowly moving flow. The resistance of the viscous or turbulent fluid phase (the term including / prevails for a more quickly moving flow (Bartelt et al., 2013).

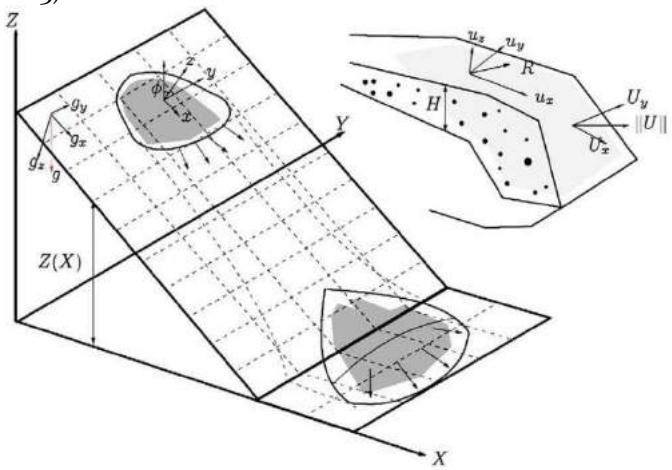

Figure 1 The topography Z(X, Y) is given in the Cartesian framework, X and Y being the horizontal coordinates. The surface induces a local coordinate system x, y, z (Christen et al., 2010a) .

It is discretized such that its projection onto the X, Y plane results in a structured mesh (from Christen et al., 2010a)(Fig. 1).

Case study

Selanac debris flow was triggered after extreme rainfall event in May 2014. Continuous precipitation for 45 days affected triggering of many new landslides across the Western Serbia. Most of new occurrences were defined as granular flows, which were not so typical landslide type for this area. The nearest meteorological station Loznica registered maximum of 230 mm of rain for 72 hours. Huge amount of material started to move as a block during the night of May, 15th 2014, which is visible on the main scarp 30m high. Material further transported as a flow throw two predisposed gullies with occasional flows. Geographical position of tested area is shown on Fig.1.

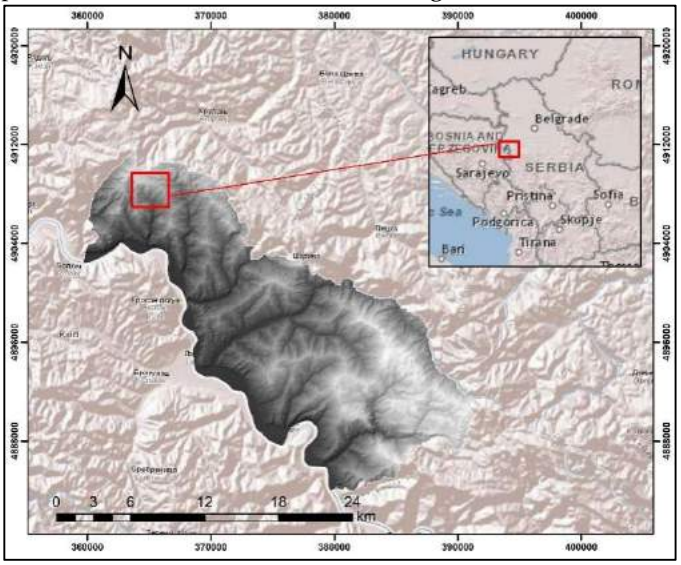

Figure 2 Geographical position of the Selanac case study

Geological settings are very complex ;initiation zone belongs to Jurassic ophiolites, while transportation and deposition area belongs to tectonic contact of Triassic limestones and magmatic rocks with Palaeozoic metamorphic rocks. Debris flow material is highly heterogeneous in lithological composition, as well as grain size distribution (up to m^3boulders) (Fig. 3).

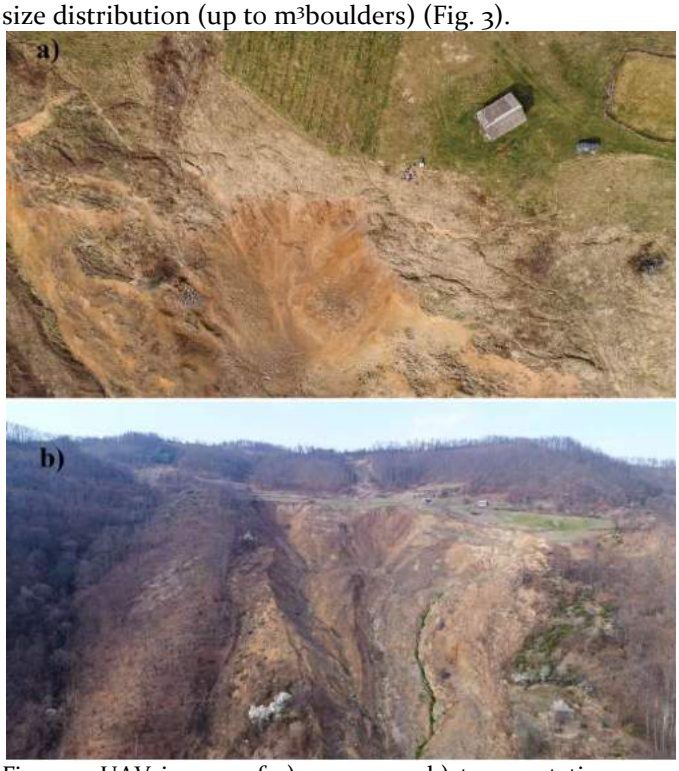

Figure 3 UAV images of a) soure area b) transportation zone (April 2017)

Erosion

The erosion algorithm in the RAMMS model, is defined using the maximum potential erosion depth e_m and a specific erosion rate. The erosion algorithm predicts the maximum potential depth of erosion e_m as a function of the computed basal shear stress in each grid cell:

$$em = 0 \; for \; \tau < \tau c \tag{5}$$

$$em = \frac{dz}{d\tau} (\tau - \tau c) \; for \; \tau \geq \tau c \tag{6}$$

The potential erosion depth (per kPa) dz/dt controls the rate of vertical erosion (in the z-direction) as a linear function of channel-bed shear stress.

Even the estimated erosion is very high in some parts (in average 12m), here will be shown results according to transported initiated mass, since first results was made without erosion calculation. Precision of topology finally affected precision in calculated eroded material, which is quite deep in this case.

Input Data

RAMMS uses DEM (Digital Elevation Model) as a basic data for defining simple geometry of model. Some researchers suggested 5x5m resolution as an optimal, explaining that even using smaller resolution gave quite similar results. New updated version of RAMMS gives opportunity to use friendly models of the terrain with better resolution, as a standard model. More precision in defining source area, erosion depth and deposition (Fig. 4) were provided after scanning of surface topology with resolution 5x5min April 2017.Those input data were used for testing numerical model and results were compared with previously obtained 30x30mresolution topology input data and results (Krušić et al, 2018). The influence of topology resolution data on erosion/deposition model was also tested.

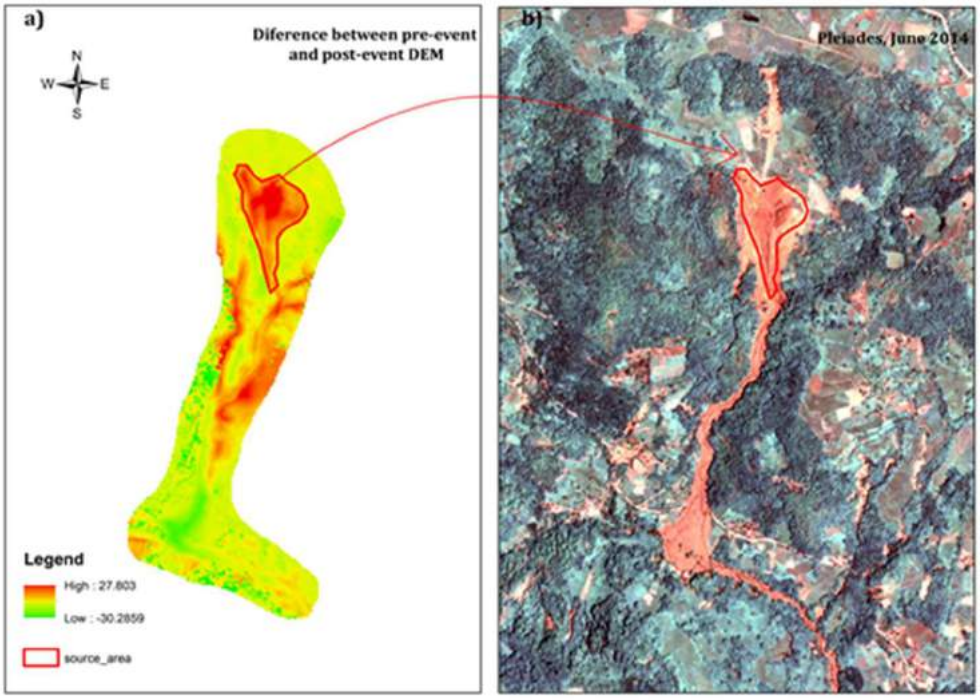

Figure 4 a) Calculation of deference in topography before and after the activation of the debris flow, b) Pleiades image after the event and position of defined release area

Source area was defined as a block within average depth of 15 m. In previous results we considered much more averaged depth which resulted in large amount of initial material. Other possibility was to define input hydrograph, much more suitable for observed processes and measured flow heights.

Results

In both cases, we used post event DEM as a comparison for deposition depth and total deposition volume.

Using 30x30m DEM, as a best result gave back calculated μ=0.05 and ξ=500 m/s^{2}best fitted resistance parameters. Enlarge of frictional parameter gave much more amount of material in deposition zone which is not estimated. Using this parameters, estimated material was reached, but with a less deposition height (Fig. 5).

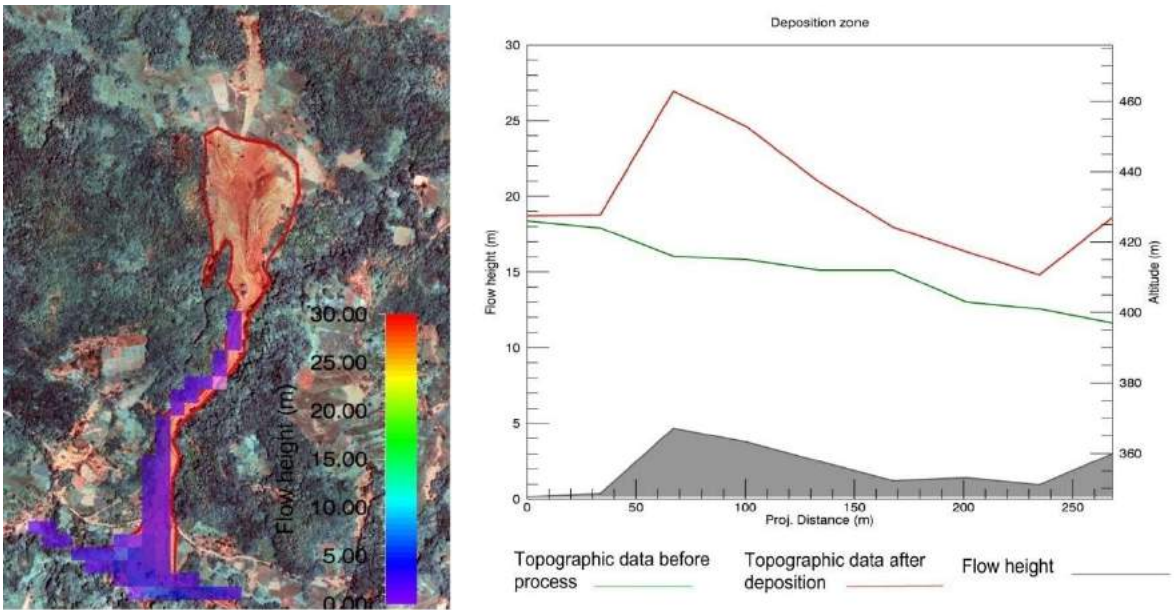

Figure 5 Final model with 30x30m DEM as input a) ξ =500 m/s²,μ=0.05 b) deposited material depth≈5m

In other case, almost the same volume was reached in deposition zone but with much greater deposition height. The best fitted parameters that were chosen are μ=0.11 and ξ=500 m/s² (Fig 6).In both cases, there are a lot of outflow materials, since material was transported further throw valley of Selanacka river. This is something that would be interesting to include in future in modelling as an affect. By now we compared only amount of estimated volume.

Results show fewer amounts of deposited volume then volume that flow out of calculation domain. Including calculation of eroded material will change volumetric of deposited zone. Even if comparison of two epochs DEM gave as a result not so much difference in volume, estimated depth with ERT investigation is more (max 20m) and we can consider that transported material outflow of calculation domain its small part of initiated mass.

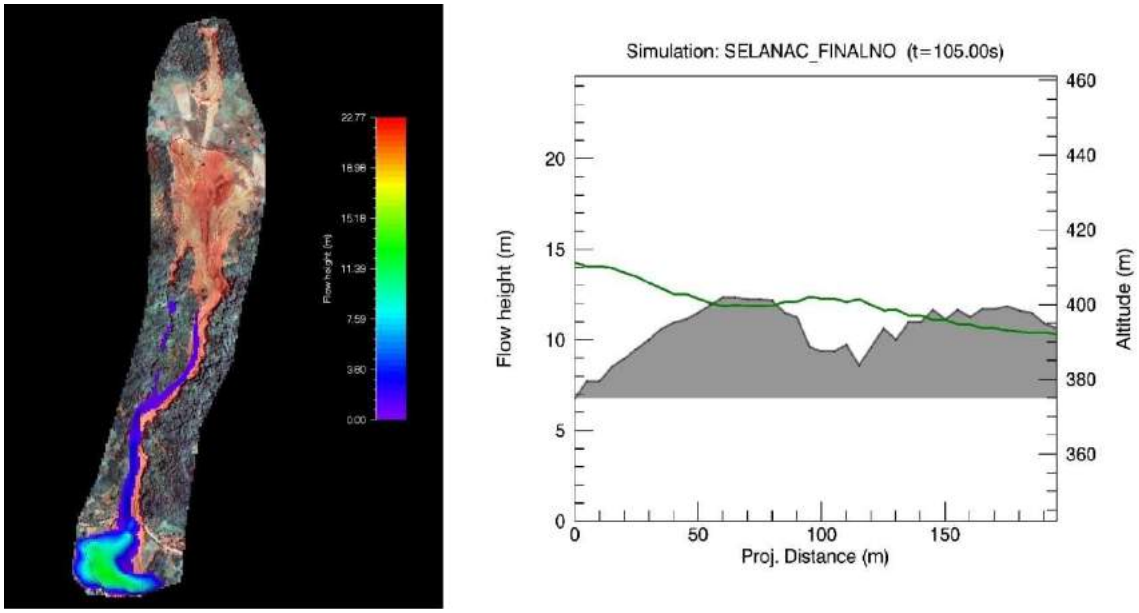

Figure 6 Final model with 5x5m DEM as input a) ξ =500 m/s²,μ=0.11 b) deposited material depth≈14m

Conclusion

According to estimated depth in deposited zone, ERT investigation supposed 20 m in deepest part, and comparison of two epoch DEM ≈15m. Numerical model with better resolution of DEM give better precision. However, if we compare behaving of the flow and spatially deposited material, previous modelling gave quite reasonable results. Also the results of flowing material in

both cases are quite similar ≈125.000 m³, while estimated volume was about 121. 000 m³. However, this prediction we can't consider as good assumption since mainly total critical mass and eroded material were stopped in deposited area, and drained water was transported further with torrential flow which also made instabilities in the Selanačka river valley. Generally it is necessary for further research to testing model with influence of the torrential flood on the deposition zone in the same time as Selanac debris flow. Also it is supposed that using some type of 2-phase numerical models potentially could provide more accurate results.

References

Bartelt P, Buehler Y, Christen M, Deubelbeiss Y, Graf C, McArdell B W (2013) RAMMS–rapid mass movement simulation, A modelling system for debris flows in research and practice, user manual v1.5, debris flow, Institute for Snow and Avalanche Research SLF, pp 126.

Christen M, Bartelt P, Kowalski J (2010b) Back calculation of the In den Arelen avalanche with RAMMS: Interpretation of model results. Annals of Glaciology 51(54): 161-168.

Christen M, Bartelt P, Kowalski J, Stoffel L (2007) Calculation of dense snow avalanches in three-dimensional terrain with the numerical simulation program RAMMS. Differential Equations.vol. Proceeding, pp. 709-716.

Christen M, Kowalski J, Bartelt P (2010a) RAMMS: Numerical simulation of dense snow avalanches in three-dimensional terrain. Cold Regions Science and Technology, 63, 1–14.

Frank F, Mc Ardell BW, Oggier N, Baer P, Christen M, Vieli A (2017) Debris flow modeling at Meretschibach and Bondasca catchment, Switzerland: sensitivity testing of field-data-based entrainment model. Natural Hazards and Earth System Sciences 17: 801-815.

Hungr O (1995) A model for the runout analysis of rapid flow slides, debris flows, and avalanches. Canadian Geotechnical Journal 32 (4):610-623.

Iverson RM (1997) The physics of debris flows. Reviews of Geophysics 35 (3): 245-296.

Jakob M, Hungr O (2005) Debris-flow hazards and related phenomena. Blondel, P. Springer Praxis Book in Geophysical Sciences, Chichester, UK .1723 p.

Krušić, J., Andrejev, K.,Andrejev, K., Abolmasov, B, Marjanović, M.(2017) Preliminary results of the Selanac debris flow modelling in RAMMS - a case study., Proceeding of the 3rd Regional Symposium on Landslides in the Adriatic-Balkan Region, Ljubljana 2017, 1, pp. 95 - 100, 978-961-6498-58-6, Ljubljana, Slovenia, 11. - 13. Oct, 2017

Rickenmann D (1999) Empirical relationships for debris flows. Natural Hazards 19: 47-77.

Savage SB, Hutter K (1989) The motion of a finite mass of granular material down a rough incline. Journal of Fluid Mechanics 199 (1): 177-215.

Schraml K, Thomschitz B, Mcardell BW, Graf C, Kaitna R (2015) Modeling debris-flow runout patterns on two alpine fans with different dynamic simulation models. Natural Hazards and Earth System Sciences 15 (7):1483-1492.

Sosio R, Crosta GB, Hungr O (2008) Complete dynamic modeling calibration for the Thurwieser rock avalanche (Italian Central Alps). Engineering Geology 100 (1-2): 11-26.

Takahashi T (2007) Debris Flow: Mechanics, Prediction and Countermeasures. Annual Review of Fluid Mechanics 13 (1): 57-77.

Voellmy A (1955) Über die Zerstörungskraft von Lawinen. Schweizerische Bauzeitung 73: 212–285

Wu W (2015) Recent advances in modeling landslides and debris flows. Springer Series in Geomechanics and Geoengineering, Published by Springer-Verlag

doi.org/ 10.35123/ReSyLAB_2019_28

Remediation measures on a deep-seated slow-moving landslide

Martina Vivoda Prodan[(1)], Martin Krkač[(2)], Snježana Mihalić Arbanas[(2)], Željko Arbanas[(1)]

1) University of Rijeka, Faculty of Civil Engineering, Radmile Matejčić № 3, 51 000 Rijeka, Croatia

2) University of Zagreb, Faculty of Mining, Geology and Petroleum Engineering, Pierottijeva № 6, 10 000 Zagreb, Croatia

Abstract The Špičunak Landslide is a deep-seated slow-moving landslide causing damages on the pavement of the state road D3 near the Lokve settlement in the Gorski Kotar region, Croatia, during the last 50 years. The landslide was formed at the contact of Permian shales and Jurrasic limestone and dolomites. The length of the landslide is 70 m, the width is 85 m and the depth of sliding surface is 20 m. Due to deformations on the state and local road as well as on the embankment stone lining between them, it was necessary to perform remediation measures. Field investigations were executed as well as monitoring of displacement and ground water level. Based on the results of field investigations, the remedial measures were designed to stop further sliding and to increase general stability of the slope. The complex remedial measures design includes pile wall anchored in the head with pre-stressed geotechnical anchors positioned below the state road, concrete grid construction and self-drilling bolts on the embankment stone linings, in combination with bored and trench drains below the road construction and in the landslide foot. The stability back analysis as well as stability analysis for the designed remediation measures were carried out. Monitoring of the landslide during and after remediation using piezometers and inclinometers is also included in design. This paper presents the case study of the Špičunak Landslide, results of stability analysis and designed measures that will be used in landslide remediation planned to be conducted during the autumn 2019.

Keywords landslide, engineering geological investigations, stability analysis, remediation, pile wall, anchors, drainage, monitoring

Introduction

Areas built in shales, sandstones, siltstones and marls such as the Gorski Kotar region, are susceptible to instability processes (Mihalić Arbanas et al. 2017). On the Špičunak Landslide (Fig 1), located in the Gorski Kotar region, there are visible signs of slope movement and threat for communities and infrastructure for a long period but, unfortunately, no documentation of geotechnical field investigation or remedial works was found.

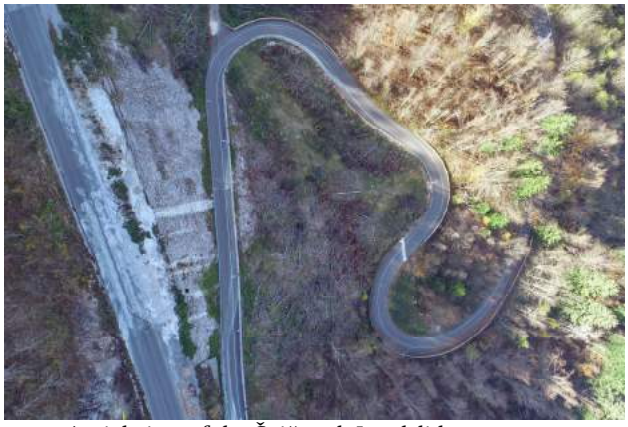

Figure 1 Aerial view of the Špičunak Landslide.

The deformations on the state road D3 pavement construction were continuously re-established, while the cracks and deformations of the stone lining at the embankment among the state road, as well as subsidence of the local road in the middle part of the landslide were observed (Fig 2).

Figure 2 Evidences of the landslide movements: a) main tension crack on the state road D3, b) subsidence of the local road towards the Lokve Lake.

The field investigations were conducted to establish geotechnical model as a base for remediation measures design. Back stability analysis to determine the average strength parameters of the soil at the sliding surface was conducted. The complex remedial measures design includes lowering of groundwater level using bored drains as well as increasing resistance forces using pile wall with pre-stressed geotechnical anchors and buttressing in the lower part of the landslide. Stability analysis confirmed effectiveness of every applied stage of designed remediation measures. A proper monitoring of the landslide during and after remediation was proposed.

This paper presents, instability features description, engineering-geological model, as well as slope stability analysis and designed remediation measures of the Špičunak Landslide, Croatia.

Investigation of the Špičunak Landslide

Field investigation

The Špičunak Landslide is located in Gorski Kotar, a hilly area of the NW Dinarides. Two main lithostratigraphic units in the study area are Permian clastic and Jurassic carbonate rocks. The tectonic setting of the area is characterised by numerous faults, frequent vertical and horizontal alteration of different lithological types, different bedding orientations and various degrees of weathering (Savić and Dozet, 1984).

Geotechnical investigations (Fig. 3) conducted to determine engineering geological units, the landslide model, included a detailed engineering geological mapping, borehole drilling, laboratory testing of disturbed soil and rock mass samples, inclinometer and piezometer measurements as well as geophysical surveying. Nine investigation boreholes, B-1 to B-9, of depth from 13 to 25 m were drilled, 182 m of length in total. In three boreholes, B-5, B-8 and B-10, inclinometer casings were installed immediately after drilling to measure displacements and indicate sliding surface position. Measured displacements indicated sliding surface position that coincides with the contact of moderately weathered layer of shales and sandstones, as it is shown in Figure 4. Piezometer casings in borehole B-2, B-4, B-7 and B-9, were installed to enable measuring of ground water level. Representative soil and rock samples were taken and tested in the Geotechnical laboratory. Geophysical survey using geoelectric tomography and seismic refraction techniques was conducted to determine depth of deposits and assess the dynamic parameters of materials.

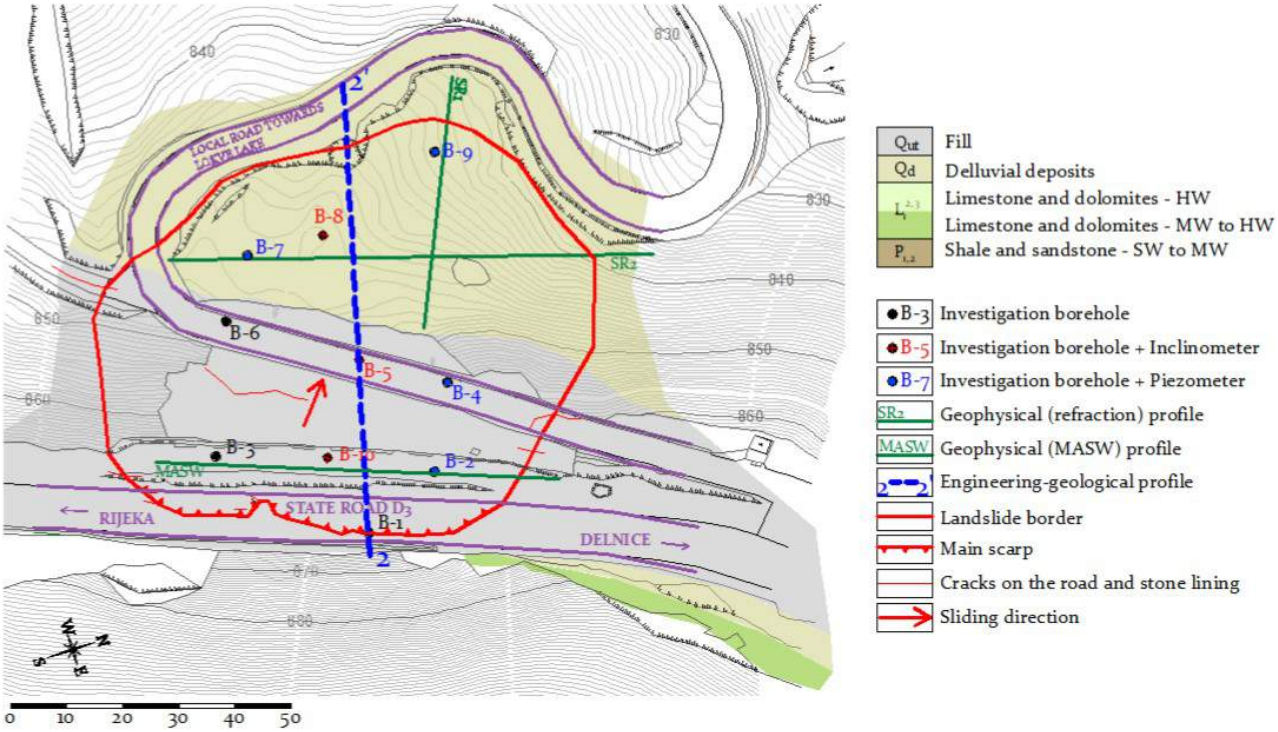

Figure 3 Engineering-geological map of the Špičunak Landslide

Engineering-geological model

From the results of field mapping and borehole determination, the landslide features were interpreted. Visible parts of landslide were landslide crown that involve a pavement of the state road, head of the landslide approximately 1 m below the crown, right flank and the zone of deformation on the stone lining at the embankment of the state road, while the foot of the landside and the left flank were not expressed and are interpreted from overall data. The total length of

landslide is 70 m, the width is 85 m and the depth of sliding surface is approximately 20 m. Activity state, according to Cruden and Varnes (1996), can be considered as active, while the style is single, very slow moving. The estimated landslide volume is 0.1 x 10^6 m^3. According to Hungr et al. (2014), landslide is classified as rock rotational slide.

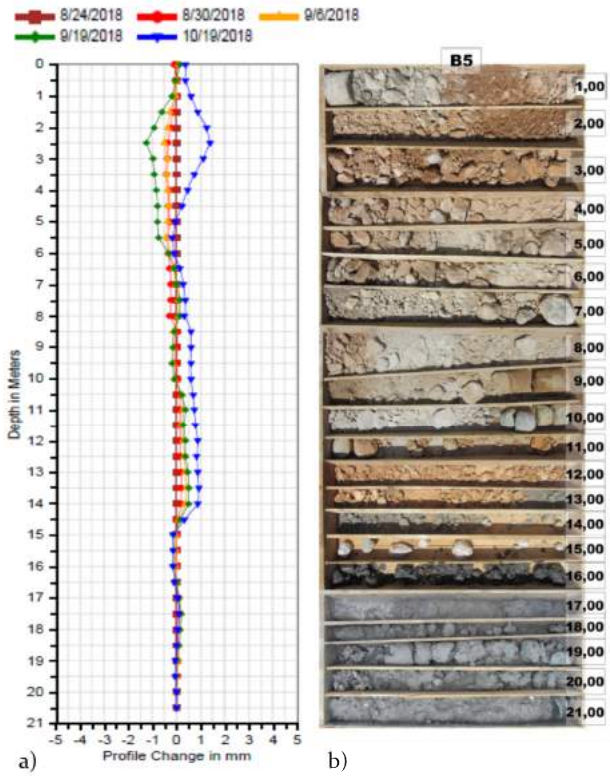

Figure 4 Borehole B-5 a) measured displacements in inclinometer, b) photography of the borehole core.

Based on results of the determination of borehole cores, the geological cross-section consists of four main engineering geological units: Permian clastic rocks, which can be considered as a bedrock and Jurassic carbonates, delluvial deposits and artificial fill, which are partly incorporated in displaced mass. Spatial distribution of engineering geological units are presented in the Figures 3 and 5.

Permian clastic rocks, identified at the bottom of all boreholes, form the underlying deposits of the study area. This unit is represented by vertical alteration of shales and sandstones (>1 to 20 cm thick layers), characterised by dark grey to grey colour, slightly to moderately fractured, and slightly to moderately weathered. The strength of intact rock generally varies between moderately soft to hard.

Jurassic (Lias) carbonates are represented vertical and horizontal alterations of limestone and dolomites, characterised by light grey to brownish grey colour, moderately to intensely, occasionally very intensely, fractured and moderately to intensely weathered. The strength of intact rock varies between moderately hard to hard.

Permian clastic and Jurassic carbonate rocks are covered with superficial deposits, composed of delluvial deposits and artificial fill. Delluvial deposits are composed of coarse grained and fine grained mixtures. Coarse grained material consists of limestone and dolomite cobbles, angular to subangular, up to 20 cm in size. Fines are composed of low to medium plasticity, yellowish brown soil. Artificial fill is a mixture of limestone and dolomite grains, angular to subangular, originating form Jurassic carbonate outcrops excavated during road construction.

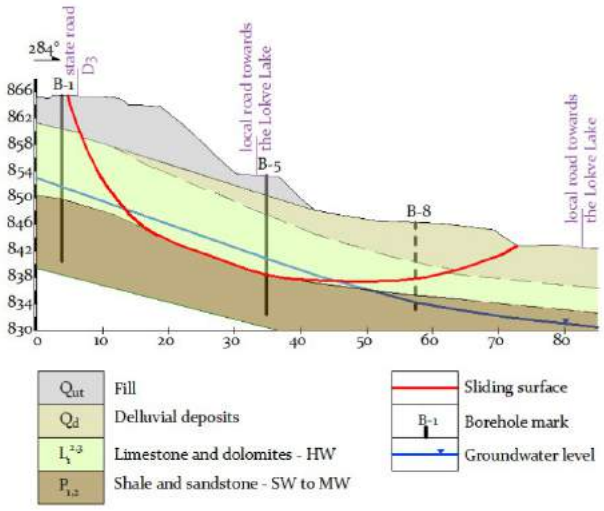

Figure 5 Engineering-geological cross-section 2-2'.

Designed remedial measures

The success of any applied landslide remedial measure largely depends on a degree to which the specific soil and groundwater conditions were correctly recognized in the investigation phase and afterwards applied in the design. Any applied landslide remedial measure must involve reduction in the driving forces or/and an increase in the available resisting forces. IUGS WG/L (Popescu, 2001; Mihalić Arbanas and Arbanas, 2015) arranged landslide remedial measures in four practical groups, namely: modification of slope geometry, drainage, retaining structures and internal slope reinforcement. Drainage is the most widely and the least costly measure used in a landslide remediation while a modification of slope geometry is the second most used method (Hutchinson 1977). Structural techniques can be extremely valuable but many times over-expensive related to non-structural measures.

The complex remedial measures design of the Špičunak Landslide included: (i) increasing of shear resistance and (ii) reducing the pore pressures at the sliding surface. Designed landslide remedial measures and position of the monitoring equipment on the representative cross section are shown in Figure 6.

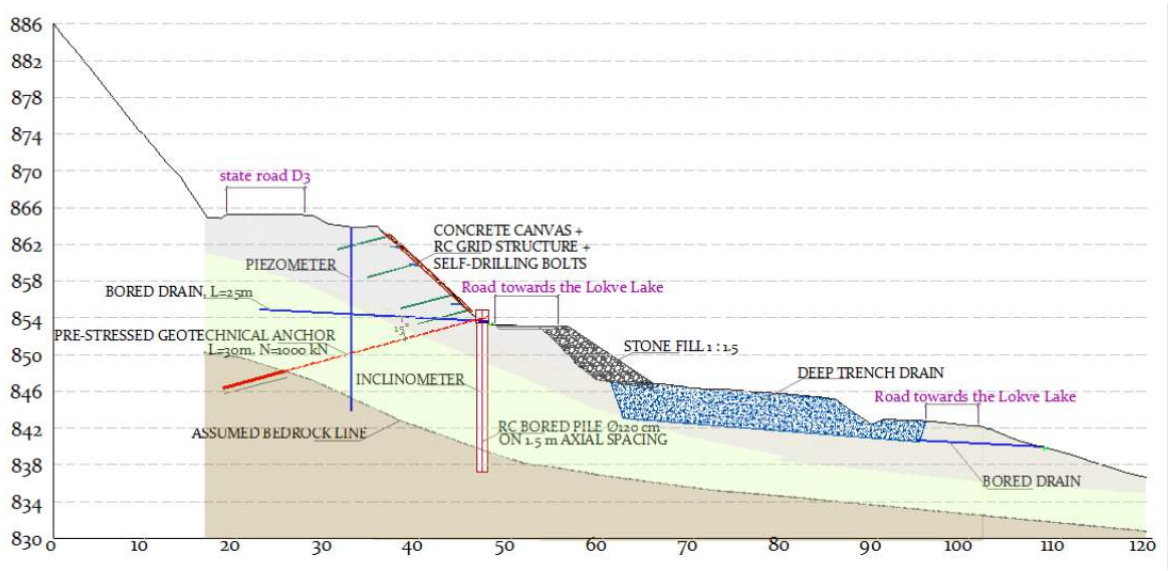

Figure 6 Representative cross section with remedial measures and monitoring equipment.

Reduction of pore pressure at the sliding surface causes increasing of effective normal stresses and shear strength of a soil. Lowering of groundwater level in the landslide foot was designed by 4 deep trench drains parallel to the slope spreading. The designed trenches are 4.0 m deep and 1.0 m wide, filled with coarse granular fill. Water from the trench is collected in the bored drain to flow it below the road construction. Additionally, bored drains through the state road D3 embankment were designed. 13 drains, 25.0 m long, will be bored on the distance of 6.0 m to collect the ground water in the upper part of the landslide body. Surface drainage to divert water from the landslide area was assumed using surface ditches, Fig 6.

Increasing of shear resistance on the sliding surface was designed with several measures that included (i) stone fill along the road towards the Lokve Lake and (ii) the pile wall anchored in the head with pre-stressed geotechnical anchors along the toe of the state road D3 embankment. Stone fill was designed 3.0 m wide and with a slope of 1 : 1.5, to increase the active forces in the lower part of the landslide and enlarge area for further construction works. Proposed reinforced concrete pile wall consisted of 50 bored piles, 120 mm in diameter, on 1.50 m axial spacing, bored minimally 2.0 m in the shale and sandstone bedrock. An average pile length is 18.5 meters. Piles were bounded with reinforced head beam, 1.40 x 1.40 m in cross-section and 74.90 m of total length. Pre-stressed geotechnical anchors were designed through the head beam, on 4.50 m spacing. Anchors are designed 30.0 m long with 7.0 m bonding length and bearing capacity of 1000 kN.

During the sliding, the embankment stone lining of the state road D3 was significantly deformed and its reinforcement was needed. Design included coverage of the lining area with 5 mm thick concrete canvas below the concrete grid construction retained with short self-drilling bolts.

Remedial works construction will start in autumn 2019 and should follow designed construction plan: (1) groundwater level decreasing by trench and boring drains installation in the landslide foot; (2) stone fill construction along the local road; (3) pile wall construction; (4) head beam construction along the pile wall; (5) pre-stressed geotechnical anchor installation through head beam; (6) embankment stone lining reinforcement with concrete canvas, concrete grid construction and self-drilling bolts; and (7) boring drains installation through the head beam.

Monitoring of the landslide during remediation works and exploitation using piezometers and inclinometers was included in design to check success of the designed measures. Installation of 6 piezometers and 4 vertical inclinometers in the bored piles was defined and 6 measurements are predicted in following intervals: (0) before beginning of construction works; (1st) after pre-stressed geotechnical anchor installation; (2nd) after concrete grid construction; (3rd) after bored drain construction; (4th) at the end of remedial works; (5th) one month after the end of remedial works.

Slope stability analysis

To confirm efficiency of designed remedial measures, 2D limit equilibrium slope stability analyses were carried out. Slope stability back analysis were conducted to determine the average material strength parameters and enable slope stability analysis with designed remedial measures. Slope stability analysis were performed using Rocscience software, program package Slide2, version 2018 8.024 (Slide 2, 2018) according to the Bishop's method (Bishop, 1955).

Back analysis

Back analysis is an effective method to determine the average material shear strength by varying parameters c' and ϕ' until the factor of safety reaches approximately value of 1.0. Model and result of back analysis on representative engineering geological cross section is presented in Figure 7. Critical sliding surface with the minimal factor of safety corresponds to position of sliding surface confirmed in the field and based on results of inclinometer measurements.

Mohr-Coulomb strength parameters obtained in back analysis are presented in Table 1. Layer above shale and sandstone bedrock was modelled as a weak layer with low residual shear strength properties that correspond to highly weathered bedrock.

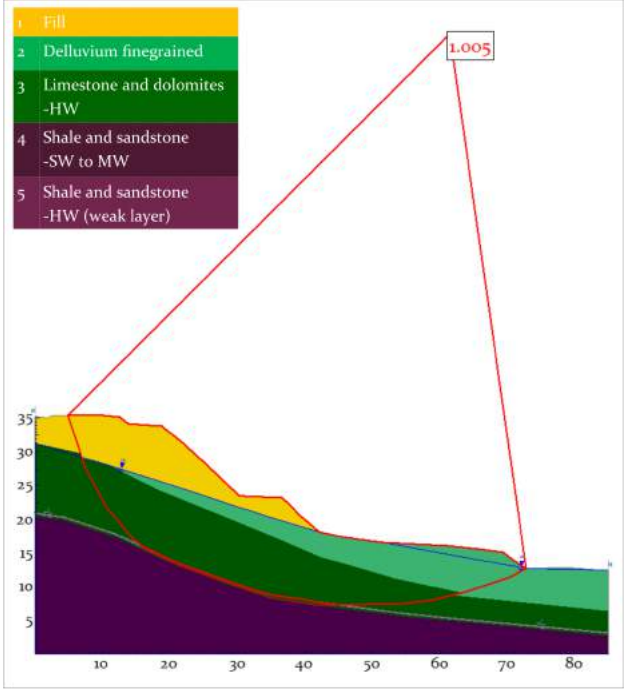

Figure 7 Slope stability back analysis on representative engineering geological cross section.

Table 1 Mohr-Coulomb geotechnical parameters of geotechnical units obtained from back analysis.

n°	Description	Unit weight	Mohr-Coulomb geotechnical parameters	
		γ [kN/m³]	cohesion c [kPa]	friction angle ϕ [°]
1	Fill	20	0	35
2	Delluvium finegrained	21	1	23
3	Limestone and dolomites-HW	24	5	26
4	Shale and sandstone-SW to MW	24	50	36
5	Shale and sandstone-HW (weak layer)	24	0	18

Slope stability analysis with remedial measures

Slope stability analysis of the landslide with applied remedial measures (Fig 8) used average material shear strength parameters. They were performed according to the designed phases of remedial measure applications: (i) lowering of ground water level with bored and trench drains below the road construction towards the Lokve Lake, (ii) stabilizing rock fill embankment construction along the lower part of the landslide, and (iii) pile wall anchored in the head with pre-stressed geotechnical anchors positioned in the toe of the state road D3 embankment.

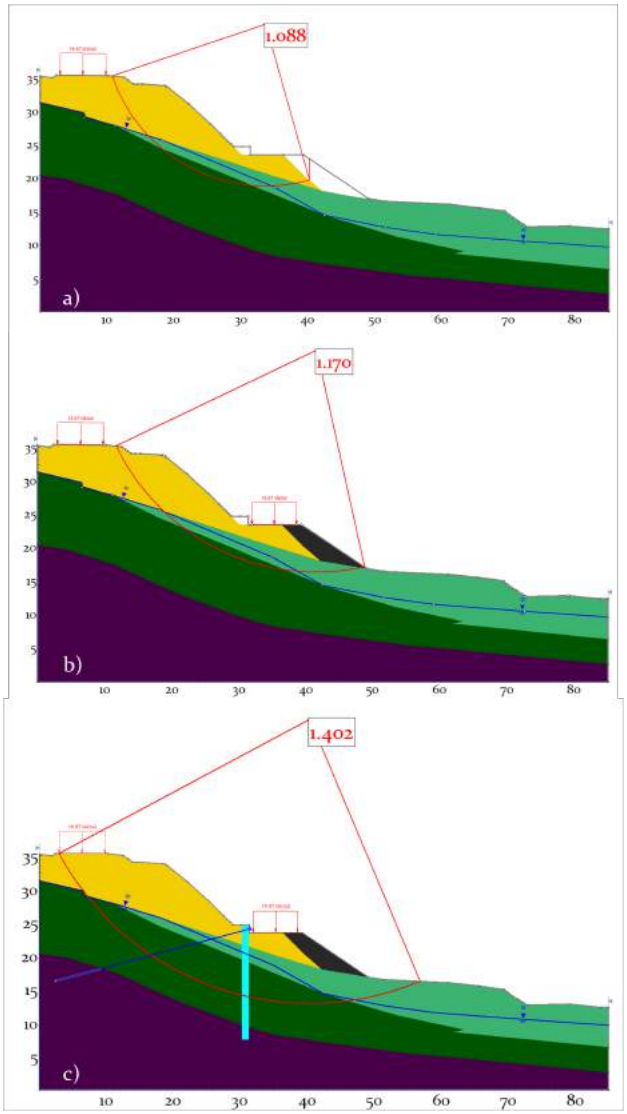

Figure 8 Results of slope stability analysis with factor of safety after remedial measures in phases: a) drains instalation, b) rock fill embankment construction, c) pile wall and geotechnical anchor instalation, on representative engineering geological cross section.

Reached factors of safety after each phase of applied remedial measures are presented in Figure 8, where an increase of stability after each remediation phase is significant: from initially FoS=1.088, to FoS=1.170 after

second phase and satisfying FoS=1.402 after completing of remedial measures. In the final phase of remediation, forces acting on the pile wall for the critical sliding surface were obtained, and the bending moment of 1320 kNm acting on each pile was calculated as critical bending moment for reinforcement analysis.

Conclusions

This paper presents the case study of investigation and remedial measures design applied to the Špičunak Landslide, a deep-seated, slow-moving landslide in the Gorski Kotar region, Croatia. Evidences of the landslide activity through the past years were visible thorough the subsidence and cracks causing damage of the road in last decades, pointed on necessary of the landslide remediation. Field investigations, slope stability analysis and designed remediation measures were described in detail. Lowering of groundwater table in combination with structural measures including anchored pile wall and buttressing in the lower part of the landslide were designed as effective remediation measures applied to mentioned landslide. Designed measures are based on conducted stability analysis where an overall factor of safety larger than 1.4 was gained, raising during application of particular remedial measures according to designed remediation plan.

References

Bishop, A W (1955) The Use of the Slip Circle in the Stability Analysis of Slopes. Geotechnique, Vol. 5, pp 7 - 17.

Cruden D M, Varnes D J (1996) Landslide type and processes. Landslides: Investigation and Mitigation. Turner A K and Schuster R L (eds). National Academy Press, Washington, D.C. Special report 247, pp. 36-75.

Hungr O, Lerouei S, Picarelli L (2014) The Varnes classification of landslide types, an update. Landslides 11 (2), pp. 167-194. doi 10.1007/s10346-013-0436-y

Hutchinson J N (1977) The assesment of the effectivness of corrective measures in relation to geological conditions and types of slope movement, Bulletin IAEG, 16: pp. 131-155. doi 10.1007/BF02591469

Mihalić Arbanas S, Arbanas Ž (2015) Landslides - A guide to researching landslide phenomena and processes. In Handbook of Research on Advancements in Environmental Engineering. Gaurina-Međimurac N (ed). IGI Global, Hershey, 474-510.

Mihalić Arbanas S, Sečanj M, Bernat Gazibara S, Krkač M, Begić H, Džindo A, Zekan S, Arbanas Ž (2017) Landslides in the Dinarides and Pannonian Basin – from the largest historical and recent landslides in Croatia to catastrophic landslides caused by Cyclone Tamara (2014) in Bosnia and Herzegovina. Landslides. 14(6): 1861–1876.

Popescu M E (2001) A suggested method for reporting landslide remedial measures. Bull Eng Geol Env. 60 (1): pp. 69-74 . doi 10.1007/s100640000084

Savić D, Dozet S (1984) Basic geological map SFRJ 1:100.000. Sheet Delnice L33–90. Geological institute Zagreb, Geological institute Ljubljana, Federal geological institute Beograd (in Croatian).

Slide2 (2018) Tutorials of Slide 2018, 2D limit equilibrium analysis of slope stability, Version 2018 8.024. Rocscience, Toronto, Canada.

doi.org/ 10.35123/ReSyLAB_2019_29

Landslide hazard analysis in national-scale for landslide risk assessment in Croatia

Sanja Bernat Gazibara[(1)], Ksenija Cindrić Kalin[(2)], Marko Erak[(1)], Martin Krkač[(1)], Marin Sečanj[(1)], Petra Đomlija[(3)], Željko Arbanas[(3)], Snježana Mihalić Arbanas[(1)]

1) University of Zagreb, Faculty of Mining, Geology and Petroleum Engineering, Zagreb, Pierottijeva 6
2) Croatian Meteorological and Hydrological Service, Zagreb, Grič 3
3) University of Rijeka, Faculty of Civil Engineering, Rijeka, Radmile Matejčić 3

Abstract The objective of this study is preliminary national-scale assessment of the landslide hazard in Croatia using qualitative approach. Landslide risk analysis was done in the frame of Disaster Risk Assessment for the Republic of Croatia during 2018. Landslide risk assessment was carried out by the scientists from Croatian Landslide Group. As final result of conducted landslide risk assessment, landslides were recognised as the second natural risk in Croatia. Landslide hazard analysis included characterisation of the landslides and the corresponding frequency of multiple-occurrence regional landslide events (MORLE). The effects of controlling factors on landslide susceptibility was estimated using knowledge-driven method based on overlay of two landslide predictor maps, lithology and slope inclination. The analysis showed that approximately 20% of the area of the Republic of Croatia is potentially prone to sliding. MORLE records and precipitation triggering events were analysed to investigate the temporal probability of landslide hazard. Frequency of MORLE was conducted for two scenarios, the worst possible scenario based on landslide events in winter 2012/2013 and the most probable scenario based on landslide events in February 2018. Frequency analysis of precipitation triggering events showed that the most probable MORLE be expected once every 15 to 20 years and the worst possible MORLE once every 100 years.

Keywords landslides, susceptibility mapping, MORLE, landslide risk assessment, Croatia.

Introduction

The Sendai Framework for Disaster Risk Reduction 2015-2030 is voluntary, non-binding agreement which recognizes that the State has the primary role to reduce disaster risk but that responsibility should be shared with other stakeholders including local government, the private sector and other stakeholders. One of priorities for action in Sendai Framework is understanding disaster risk in all its dimensions of vulnerability, capacity, exposure of persons and assets, hazard characteristics and the environment. Based on this develop, periodically update and disseminate, as appropriate, location-based disaster risk information, including risk maps, to decision makers, the general public and communities at risk of exposure to disaster in an appropriate format by using, as applicable, geospatial information technology. The most known framework for landslide risk assessment and management was developed by Fell et al. (2008a,b). Main steps in landslide risk management process are risk analysis and risk assessment. Landslide risk analysis includes hazard analysis and consequence analyses. The subject of this paper is landslide hazard analysis (Fig. 1) in national scale for Republic of Croatia, which involves characterisation of the landslides (classification, size, mechanics, location), and the corresponding frequency (annual probability) of occurrence (Fig. 1). Main data layers required for landslide susceptibility, hazard and risk assessment can be subdivided into four groups: landslide inventory data, environmental factors, triggering factors and elements at risk (Van Westen et al., 2005). Type and purpose of landslide zoning is determined by the end users, but main factor are availability of potential input data. Landslide zoning maps at national (<1:250,000) and regional (1:250,000–1:25,000) scales do not allow the mapping of individual small slope failures. As a consequence, landslides have to be treated collectively, and neither runout nor intensity–frequency analyses can be performed at these scales (Corominas et al., 2013). Zoning maps at national scale are created to give a general overview of problem areas for an entire country and can be used to inform national policy makers and the general public (Soeters and van Westen, 1996). Most common hazard descriptor for landslide hazard assessment in national and regional scale is number of landslides per administrative unit or square kilometre per year (Corominas et al., 2013).

First landslide susceptibility map of Croatia was performed by Podolzski et al. (2015) based on heuristic approach which was similar to method applied for the Classified European Landslide Susceptibility Map v1.0, *ELSUS1000* (Gunther et al., 2013) The mapping approach includes climate-physiographic regionalisation and landslide susceptibility modelling. Landslide susceptibility was analysed based on spatial multi-criteria evaluation model using slope angle, lithology and land cover, which are considered as the main conditioning factors for all types of landslides at this scale. The derived landslide susceptibility map is represented in four classes, as a 1 km raster data set. As a result, the obtained landslide

susceptibility map, 72% of the Croatia show low landslide susceptibility. Moderate, high and very high susceptible zones make up 15% (8,489.1 km²), 8% (4,527.5 km²) and 4% (2,263.7 km²)of the total area, respectively. The lack of conducted analysis is that different landslide mechanisms (slides and rock falls) were analysed simultaneously and landslide susceptibility assessment requires a multi-hazard approach, as different types of landslides may occur, each with different characteristics and causal factors, and with different spatial, temporal and size probabilities (Corominas et al., 2013). Mihalić Arbanas et al. (2016) identified landslide prone areas in Croatia and BIH with hazardous processes that require a systematic approach, starting with regional landslide hazard mapping using remote sensing techniques. Based on bedrock lithology and relief types of the main geotectonic units in Croatia it was concluded that approximately 20% of Croatia or 12,000 km² can be described as landslide-prone areas.

The first landslide risk analysis in national scale was done in the frame of Disaster Risk Assessment for the Republic of Croatia during 2018 and the coordinator was Croatian National Platform for Disaster Risk Reduction, CNPDRR. Landslide risk calculation was carried out by the scientists from Croatian Landslide Group, which members are scientists from University of Rijeka, Faculty of Civil Engineering and University of Zagreb, Faculty of Mining, Geology and Petroleum Engineering.

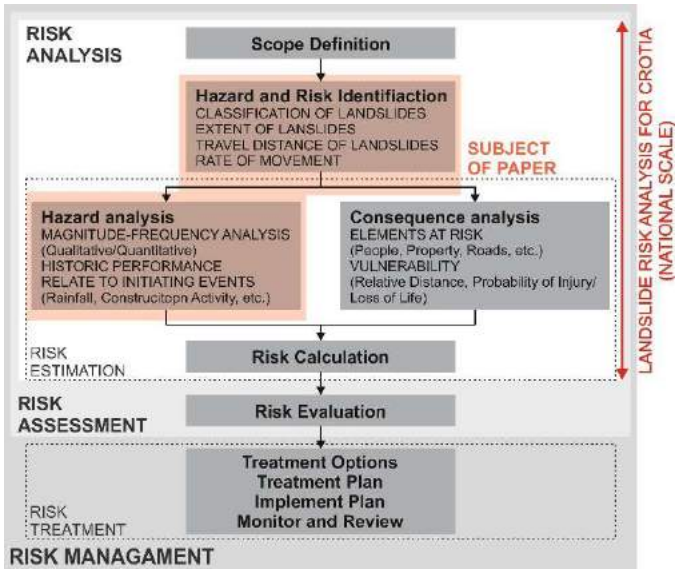

Figure 1 Framework for landslide risk assessment and management developed by Fell et al. (2008a,b) and scope of research described in this study.

Geological framework and landslides in Croatia

According to Mihalić Arbanas et al. (2016), most of the landslide-prone areas in Croatia belong to hills and lowlands composed of (i) Neogene clastic rocks (marlstones), carbonate rocks and soils in the Pannonian Basin (approximately 6000 km2), and in the tectonic unit of the High Karst (approximately 160 km2), the Pre-Karst and Bosnian Flysch Unit (approximately 130 km2), the Western Vardar Ophiolitic Unit (approximately 100 km2), and the Sava Zone (approximately 35 km2); (ii) Plio-Quaternary soils in the Pannonian Basin (approximately 2300 km2); (iii) Paleogene association of clastic rocks (flysch-type rocks) in tectonic units of undeformed part of the Adriatic Plate (approximately 450 km2), the High Karst Unit (approximately 400 km2), the Dalmatian Zone (approximately 330 km2), the Western Vardar Ophiolitic Unit (approximately 80 km2), and the Sava Zone (approximately 80 km2); and (iv) Paleozoic and Precambrian igneous and metamorphic rocks in the Pannonian Basin (approximately 380 km2); (v) Paleozoic rhythmic alteration of clastic rocks in the Pre-Karst and Bosnian Flysch Unit (approximately 300 km2); and (vi) Paleozoic alteration of clastic and metamorphic rocks in the Pannonian Basin (approximately 250 km2). Low-altitude mountains with landslide-prone areas in Croatia are only present in (i) Paleozoic rhythmic alteration of clastic rocks in tectonic unit of High Karst (approximately 270 km2); (ii) Paleozoic alteration of clastic and metamorphic rocks in the Pannonian Basin (approximately 220 km2); (iii) Paleozoic and Precambrian igneous and metamorphic rocks in the Pannonian Basin (approximately 190 km2); and (iv) Paleogene flysch-type rocks in tectonic unit of Dalmatian Zone (20 km2) and the Western Vardar Ophiolitic Unit (approximately 10 km2). In the following text is presented a brief description of selected areas of geotectonic units particularly prone to landslides: "Gray Istria," the Rječina River Valley, the Internal Dinarides, and the Pannonian Basin.

The western part of Croatia is the Istrian Peninsula (or Istria), which belongs to an undeformed part of the Adriatic Plate (Schmid et al. 2008).The most landslide-prone areas in Istria are related to "White Istria" represented with Paleogene carbonate and clastic rocks located in the NE and E part of the peninsula and "Gray Istria", the area of Eocene flysch basin located in the central part of Istria. Paleogene siliciclastic deposits (Bergant et al. 2003) are prone to weathering (Vivoda Prodan and Arbanas 2016) and to active geomorphological processes, which have been forming landslides and erosion phenomena. The most frequent landslides are small and shallow and tend to develop at contacts between transported and residual soil or residual soils and fresh siliciclastic rocks. Flysch-type rocks and underlying "Globigerina marls" of the Istrian flysch basin are prone to weathering and erosion by superficial water. More intensive weathering and selective erosion of less-durable marls compared with sandstones enable development of deeper weathering profiles with up to 10 m of weathered rock mass (Vivoda Prodan 2016). Sliding is most often along contacts between weathered and fresh flysch-type rock, especially at places of concentrated flows of superficial water (e.g., near roads), which typically cause small and shallow landslides (Dugonjić and Arbanas 2012, Dugonjić Jovančević 2013). Moreover, stratification of flysch-type deposits also enables development of

translational block slides, such as the Brus Landslide (Arbanas et al. 2010, Mihalić et al. 2011, Arbanas et al. 2013).

Most of the External Dinarides belongs to the High Karst Unit, which is primarily comprised of Mesozoic and Paleogene shallow marine carbonate platform deposits (e.g., limestone, dolomites, conglomerates, and breccia), whereas in certain parts, they are overlaid with Eocene-Oligocene flysch-like rocks (Vlahović et al. 2005). In carbonate rocks, the most important process is chemical weathering and formation of karst, which forms steep and sharp slopes with relatively thin superficial deposit originating from weathering. The most frequent landslide type in carbonate rocks is rockfalls on artificial slopes, e.g., cuts along transportation routes. Deep-seated landslides are limited to areas of geological contact of carbonate and flysch-type rocks. The area with the highest density of landslides is the Rječina River Valley near the city of Rijeka (Arbanas et al. 2014) and in the Vinodol Valley (Toševski 2018, Đomlija 2018). The erosive power of the Rječina River in the bottom of the slope was a preparatory factor for historical landslide processes, together with earthquakes (Vivoda et al. 2012) and heavy rainfall (Oštrić et al. 2011; Mihalić Arbanas et al. 2017b) as triggering factors. Slopes undercut by the Rječina River are the most hazardous slopes in the flysch-type deposits in Croatia, which was evidenced by the deadly landslide that buried the Grohovo Village in 1885 (Anon. 2011). Currently, there are often landslide reactivations in the form of shallow-to-moderately deep landslides endangering county roads and the Valići Dam (Mihalić Arbanas et al. 2017b).

The steep flanks of the Vinodol Valley are built of Upper Cretaceous and Paleogene carbonate rocks (Blašković, 1999), while the lower parts and the bottom of the Valley are built of Paleogene flysch rock mass, mainly composed of marls, siltstones and sandstones in alteration. Older and recent talus deposits have been accumulated at the foot of the limestone cliffs, as a result of different types of mass movements, predominantly of rock falls, rock topples, and irregular rock slides (Đomlija, 2018). The flysch bedrock is mostly covered by various types of superficial deposits formed by geomorphological processes active both in the carbonate and flysch rock mass (Đomlija et al., 2014). Flysch slopes have been dissected by several relatively large and deep gullies, such as Slani Potok, Mala Dubračina and Kučina. Within these gullies, the landslide deposits have been formed as a result of sliding processes. Landslide deposits represent zones of acculumation of numerous landslides identified and mapped withing the gullies (Đomlija, 2018;), composed of weathered flysch bedrock, which represents a material lying at the contact of soil and rock (Pajalić et al., 2018). According to Đomlija et al. (2019) debris slides are the most abundant landslide type identified in the Slani Potok gully, including the smallest landslide (65 m^2), and the largest landslide (10,563 m^2).

In the Pannonian Basin, approximately 42% of the area is comprised of lowlands and hills, and only approximately 2% is comprised of low-altitude mountains (Panagos et al., 2012). The plains belong to the fluvial floodplains of the Sava River, Drava River, and Danube River. Numerous lower mountains and hills (Kalnik, Moslavačka Gora, Papuk, Psunj, Krndija and Dilj Mts) existed as uplifted paleorelief through entire Neogene. Consequently, they are mainly composed of Mesozoic carbonate rocks, sporadically clastics and volcanoclastics and Paleozoic clastic rocks, sporadically carbonates, and metamorphic rocks. The lowlands are composed of Plio-Quaternary and Neogene sediments (i.e., soils and soft rock-hard soils, mainly marls). Landslides are common phenomena due to geomorphological, geological, and climatic settings and several anthropogenic factors, such as inadequate slope design, changes in land cover or slope gradients, and improper drainage of storm water. The main triggering factors are rainfall and snowmelt because most of the reported landslides in this area occurred during the months of intense precipitations (Bernat Gazibara et al. 2017b,c). The most frequent landslides are very small-to-moderately small (< 10^5 m^3) and superficial-to-moderately shallow (< 20 m) landslides (Bernat Gazibara et al. 2017b). In spite of their small volume, soil slides cause significant damage to buildings, infrastructure, and crops because of the high landslide density. For example, Bernat Gazibara et al. (2019) identified 702 landslides within the 21 km^2 area of Zagreb. Development of large and deep-seated landslides in the area of the Pannonian Basin is only possible as a consequence of improper extremely large slope cuts associated with mining activities, such as the Kostanjek landslide in the City of Zagreb (Mihalić Arbanas et al. 2017a) and the Torine landslide (Grošić et al. 2014) near Našice.

Preliminary landslide susceptibility analysis

The landslide hazard identification for the territory of the Republic of Croatia was carried out by a preliminary analysis of the spatial landslide susceptibility. Landslide risk analysis in national scale was done only for sliding processes and other sliding mechanisms (fall, topple and flow) where not analysed in this study. Input data used for landslide susceptibility analysis are basic geological map in scale of 1:300,000 and slope map derived from DEM 30 x 30 m. Geomorphological classification of slope inclination (IGU, 1968) has been used in order to define dominant geomorphological processes in each inclination category (Tab. 1). According to the Commission on Geomorphological Survey and Mapping (IGU, 1968), the slopes are classified into six categories base on their gradient (0-2°, 2-5°, 5-12°, 12-32°, 32-55° and >55°). Landslides are dominant geomorphological process on slopes of 5-55° (Tab. 1) and these areas can be considered as landslide-prone areas, or landslides can be based on the landslide preconditioning causal factors. Based on geologic map in scale 1:300,000 and expert landslide knowledge, landslide-prone lithological units have been identified.

Table 1 Geomorphological classification of slopes (IGU, 1968).

Inclination (°)	Features of geomorphologic shapes and processes
< 2	Plain. Mass movements are not evident. Soil wash intensity is minimal.
2 - 5	Mildly inclined terrain. Soil wash is weak. Soil wash and creep can be significant
5 - 12	Inclined terrain. Relatively strong soil wash and mass movement. Accented soil creep and downhill flow of material. Terrain is compromised by slope processes.
12 - 32	Significant inclination. Soil wash is intensive. Very strong slope processes. Terrain significantly compromised by soil wash and mass movement.
32 – 55	Very steep terrain. Material removal is dominant. Material is accumulated only sporadically (a thin layer). Slopes are rocky and mostly barren.
> 55	Cliffs, escarpments. Dispersal and collapsing are dominant.

Based on two predominating casual factors, lithological units where sliding can be occur and slopes inclination of 5-55°, resulting preliminary landslide susceptibility map of the Republic of Croatia was derived (Fig. 2). The spatial distribution of landslide-prone areas shows that the highest frequency of geomorphological and geological conditions for landslide occurrence is present in the continental part of the Croatia, i.e, in the Pannonian Basin. Given the relative proportion of landslide-prone areas in relation to the area of the county, the largest proportion is in the Krapina-Zagorje County, where 57.8% of the area is susceptible to sliding. Landslide assessment for all Croatian counties is given in (Fig. 2), presented from larger proportions of slide-prone areas to smaller ones. In addition to the relative proportions, the size of the landslide-prone area is relevant for the assessment of the total landslide susceptibility by county. The largest area where landslides can occur is in the Sisak-Moslavina County, which is 806.4 km². For comparison, county with the smallest landslide-prone area is in Vukovar-Srijem County and it is approximately 14.8 km². Based on performed landslide susceptibility analysis, approximately 20% of the territory of the Republic of Croatia is prone to sliding with respect to geological (rock/soil type) and geomorphological conditions (slope inclination).

Landslide risk assessment was conducted for two scenarios of multiple-occurrence regional landslide events (MORLE), the worst possible (Scenario 1) and the most probable scenario (Scenario 2). The analysed scenarios were defined based on two landslide events: landslides occurred in winter 2012/2013; and landslides occurred in February 2018.

The expected number of landslides for the worst possible MORLE scenario (Scenario 1) was estimated based on the number of landslides activated during January to April 2013. Information regarding the (re)activation of landslides in the winter period of 2012/2013 was received from citizens who informed City administration responsible for landslide remediation or civil protection throughout that time period. Evidences of examined landslides are recorded in the City offices only in the form of lists with the data about landslide locations and the date of activation. Finally, more than 900 (re)activated landslides was recorded in NW Croatia, and the largest number of activated landslides was in the Krapina-Zagorje County, 521 landslides in total (Bernat et al., 2014a; Bernat et al., 2014b). The Krapina-Zagorje County was selected due to completeness of conducted landslide data. Based on the total number of landslides activated in winter period 2012/2013, the average landslides density per unit of landslide-prone area was estimated, which is 0.733 landslides/km² for MORLE scenario 1 (the worst possible MORLE).

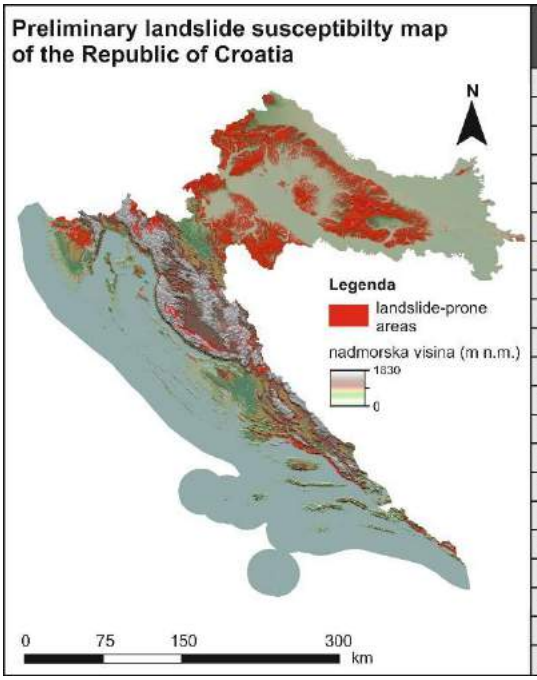

No.	COUNTY	COUNTY AREA	LANDSLIDE-PRONE AREA		EXPECTED NO. OF LANDSLIDES	
			(km²)	(%)	Scenario 1	Scenario 2
1	KRAPINA-ZAGORJE	1230,6	710.7	57.8%	521	263
2	VARAŽDIN	1261,4	398.6	31.6%	292	147
3	CITY OF ZAGREB	640,4	143.3	22.4%	105	53
4	ZAGREB	3062,4	578.6	18.9%	424	214
5	SISAK-MOSLAVINA	4468,0	806.4	18.1%	591	298
6	POŽEGA-SLAVONIJA	1823,4	258.4	14.2%	189	96
7	KARLOVAC	3622,9	498.4	13.8%	365	184
8	KOPRIVNICA-KRIŽEVCI	1748,4	238.5	13.6%	175	88
9	BJELOVAR-BILOGORA	2640,3	356.1	13.5%	261	132
10	ISTRA	6488,2	311.1	11.1%	228	115
11	MEĐIMURJE	729,8	71.5	9.8%	52	26
12	BROD-POSAVINA	2029,4	130.8	6.4%	96	48
13	PRIMORJE-GORSKI	7841,2	217.2	6.1%	159	80
14	VIROVITICA-PODRAVINA	2024,1	116.6	5.8%	85	43
15	SPLIT-DALMATIA	13555,2	225.3	5.0%	165	83
16	DUBROVNIK-NERETVA	9264,5	71.6	4.0%	52	26
17	ŠIBENIK-KNIN	5669,7	66.5	2.2%	49	25
18	OSJEK-BARANJA	4156,3	92.1	2.2%	68	34
19	LIKA-SENJ	6003,0	94.4	1.8%	69	35
20	ZADAR	7539,1	53.4	1.6%	41	21
21	VUKOVAR-SRIJEM	2452,7	14.8	0.6%	11	5

Figure 2 Preliminary landslide susceptibility map of the Republic of Croatia with proportions of landslide-prone areas and expected number of landslides based on Scenario 1 – the worst possible MORLE scenario and Scenario 2 - the most probable MORLE scenario.

The expected number of landslides for the most probable MORLE scenario (Scenario 2) was estimated based on the number of landslides activated in February 2018. Landslide event inventory was compiled by scientist from University of Zagreb, Faculty of Mining, Geology and Petroleum Engineering based on information from *Google Alerts* (monitoring specific keywords such as landslide, sliding, etc.) and technical reports. Based on the total number of landslides activated in the Krapina-Zagorje County, the average density of 0.37 landslides per unit of landslide-prone area were estimated to be activated during the most probable MORLE scenario (Scenario 2). From the average landslide density per unit of landslide-prone area activated during two MORLE scenarios, the expected number of landslides for all 21 counties in the Republic of Croatia was determined (Fig. 2).

Frequency analysis of triggering events

The Standardized Precipitation Index (SPI) is a widely used index to characterize meteorological drought on a range of timescales (McKee et al., 1993). On short timescales, the SPI is closely related to soil moisture, while at longer timescales, the SPI can be related to groundwater and reservoir storage. The SPI can be compared across regions with markedly different climates. It quantifies observed precipitation as a standardized departure from a selected probability distribution function that models the raw precipitation data. The raw precipitation data are typically fitted to a gamma or a Pearson Type III distribution, and then transformed to a normal distribution. The SPI values can be interpreted as the number of standard deviations by which the observed anomaly deviates from the long-term mean. For the operational community, the SPI has been recognized as the standard index that should be available worldwide for quantifying and reporting meteorological drought, but it is also used for monitoring and assessing rainfall at national meteorological services, including at the Croatian Meteorological and Hydrological Service. The SPI values were defined for differing periods of 10- to 100-days, using daily input data for climatological series from 1981. to 2010.

The most probable MORLE scenario

In March 2018, the Sisak-Moslavina County and Varaždin County experienced very wet weather conditions, 1.5 <SPI <1.99 (DHMZ, 2018). The cumulative precipitation from the 1st to the 20th March 2018, at the Sisak and Varaždin meteorological stations (Fig. 3), was extremely high for the period. In addition, the 3-month and 6-month cumulative precipitation (SPI-3 and SPI-6), from the beginning of January 2018/October 2017 to the end of March 2018, were extremely high at Sisak meteorological stations, while at Varaždin meteorological station SPI3 and SPI6 indicate prevailing rainy weather. On 13 March 2018, extreme precipitation conditions triggered more than 50 landslides in the Sisak-Moslavina County. Therefore, climatological analysis of the 20-, 40- and 100- cumulative day precipitation before landslide activation was conducted based on data from the Sisak meteorological station. The preliminary analysis selected 20-, 40- and 100-day cumulative precipitation as critical, because for those SPI values a certain threshold indicates a potentially damaging landslide occurring. Results of the 20-days cumulative precipitation prior to landslide activation indicates wet weather conditions and for the 40- and 100- days cumulative precipitation a prior activation indicates extremely wet weather conditions. Additionally, cumulative precipitations for 40- and 100- days prior to landslide activation (177.2 and 362.6 mm) represents the second largest measured value for the first half of March since 1961, while the 20- day cumulative precipitation (69.7 mm) is the 5th cumulative precipitation value after the maximum measured in 2016 (107.4 mm). Frequency analysis of triggering the most probable MORLE shows that the 100-day cumulative precipitation prior to the landslide activation on 13 March 2018 can be expected once every 15 years in Zagreb and once every 22 years in Varaždin.

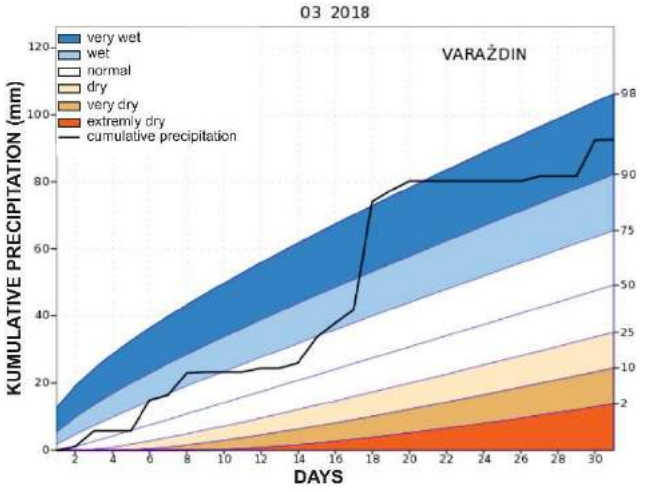

Figure 3 Cumulative daily precipitation (mm) on Varaždin meteorological station for March 2018 and the series of theoretical percentile curves (2., 10., 25., 50., 75., 90. i 98.) for period 1961 - 2000 (www.meteo.hr).

The worst possible MORLE scenario

During March 2013, the territory of Croatia experienced very wet weather conditions (1.5 <SPI <1.99), while in the NW part of Croatia prevailed extremely wet weather conditions (SPI ≥ 2). Further, the cumulative precipitations for 3-month (January-March 2013) and 6-month (October 2012.-March 2012) period prior to MORLE were extremely high (DHMZ, 2013). Climatological analysis of the 20-, 40- and 100-day cumulative precipitation before landslide activation on 30 March 2013 was conducted based on data from the Varaždin and Zagreb-Grič meteorological station. Results of the 20-days cumulative precipitation on both meteorological stations

prior to landslide activation indicates wet weather conditions (76.8 – 87.1 mm), 40- days cumulative precipitation indicates very wet weather conditions (151.3-152.4 mm) while the 100- days cumulative precipitation extremely wet weather conditions (344.4–365.4 mm). Additionally, cumulative precipitations for 100- days prior to landslide activation represents the largest measured amount on Zagreb-Grič and Varaždin meteorological station since 1961. Cumulative precipitations for 40- days prior to landslide activation represents the largest measured value on Zagreb-Grič meteorological station and the second largest measured value on Varaždin meteorological station, while the 20- day cumulative precipitation is the second largest measured value on Varaždin meteorological station and third on Zagreb-Grič meteorological station. Frequency analysis of triggering the worst possible MORLE shows that the extremely high 100-day cumulative precipitation with wet and very wet 20- and 40- day cumulative precipitation prior to the landslide activation on 30 March 2013 can be expected once every 98 years in Varaždin and once every 130 years in Zagreb.

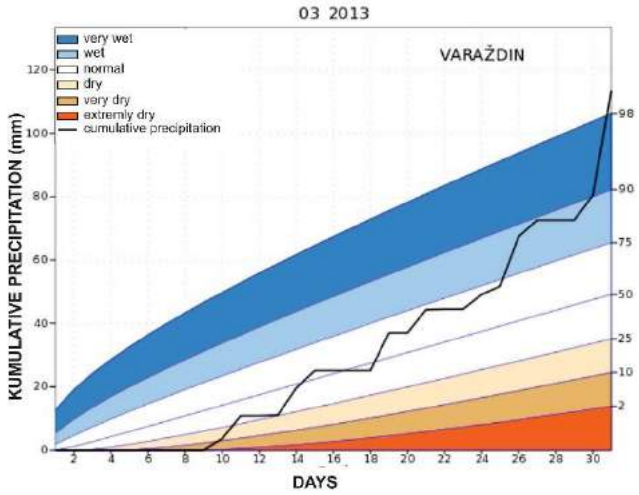

Figure 4 Cumulative daily precipitation (mm) on Varaždin meteorological station for March 2013 and the series of theoretical percentile curves (2., 10., 25., 50., 75., 90. i 98.) for period 1961 - 2000 (www.meteo.hr).

Discussion and conclusion

Landslide hazard analysis for Republic of Croatia included preliminary landslide susceptibility analysis using qualitative approach, calculation of expected noumber of landslides based on two MORLE events (winter 2012/2013 and March 2018) and frequency analysis of triggering events. The preliminary landslide susceptibility analysis showed that approximately 20% of the area of the Republic of Croatia is potentially prone to sliding. Particularly landslide prone areas in Croatia are lowlands and hills in the Pannonian Basin, the hills of the Istrian Peninsula and isolated narrow valleys in the Dinarides, such as Rječina River Valley and Vinodol Valley in Croatian Primorje. Furthermore, the same landslide susceptibility analysis arises that 60% of cities/municipalities (local administrative units) are endangered by Multiple Occurrence of Regional Landslide Events (MORLE) in case of the most probable MORLE event. In case of the worst possible MORLE scenario, 12 Croatian counties (area 4742,44 km2) will experience more than 100 landslide (re)activations per county.

Frequency analysis of precipitation triggering events showed that the most probable MORLE be expected once every 15 to 20 years and the worst possible MORLE once every 100 years. This analysis proved that recent most often unfavourable events of sliding are related to climate changes with a trend to increase its frequency. Understanding the relationship between landslide susceptibility, rainfall patterns and climate change are therefore crucially important in planning a proactive approach in landslide risk reduction. Also, the landslide hazard assessment is iterative process and should be up-dated periodically as new MORLE events occur.

References

Anon. (2011) Recovery of the Rječina River Channel. Croatian State Archive, Rijeka (unpublished)

Arbanas Ž, Mihalić S, Grošić M, Dugonjić S, Vivoda M (2010) Landslide Brus, translational block sliding in flysch rock mass. In: Zhao J, Labiouse V, Dudt J-P, Mathier J-P (eds) Rock mechanics in civil and environmental engineering. Taylor & Francis Group, London, pp 635–638.

Arbanas Ž, Dugonjić S, Benac Č (2013) Causes of small scale landslides in flysch deposits of Istria, Croatia. In Margottini C, Canuti P, Sassa K (eds) Landslide science and practice, Volume 1: Landslide inventory and susceptibility and hazard zoning. Springer-Verlag Berlin Heidelberg, pp 221–226.

Arbanas Ž, Mihalić Arbanas S, Vivoda M, Peranić J, Dugonjić Jovančević S, Jagodnik V (2014) Identification, monitoring and simulation of landslides in the Rječina River Valley, Croatia. In: Sassa K, Khang QD (eds) Proceedings of the SATREPS workshop on landslide risk assessment technology. International Consortium on Landslides, Kyoto, pp 200–213

Bergant S, Tišljar J, Šparica M (2003) Eocen carbonates and flysch deposits of the Pazin basin. In: Vlahović I, Tišljar J (eds) Field trip guidebook of the 22nd IAS meeting of sedimentology. Croatian Geological Survey, Zagreb, pp 57–64

Bernat S, Mihalić Arbanas S, Krkač M (2014a) Landslides triggered in the continental part of Croatia by extreme precipitation in 2013. In: Lollino G, Giordan D, Crosta G, Corominas, Azzam R, Wasowski J, Sciarra N (eds) Engineering geology for society and territory, volume 2: landslide processes. Springer, Heidelberg, pp 1599–1603

Bernat S, Mihalić Arbanas S, Krkač M (2014b) Inventory of precipitation triggered landslides in the winter of 2013 in Zagreb (Croatia, Europe). In: Sassa K, Canuti P, Yin Y (eds) Landslide science for a safer Geoenvironment, Volume 2: Methods of landslide studies. Springer-Verlag Berlin Heidelberg, pp 829–836

Bernat Gazibara S, Krkač M, Sečanj M, Begić H, Mihalić Arbanas S (2017a) Extreme rainfall events and landslide activation in Croatia and Bosnia and Herzegovina. In: Proceedings of the 3rd Regional Symposium on Landslides in the Adriatic-Balkan Region. Ljubljana, Slovenia.

Bernat Gazibara S, Krkač M, Sečanj M, Mihali ć Arbanas S, (2017b) Identification and mapping of shallow landslides in the City of Zagreb (Croatia) using the LiDAR-based terrain model. In: Mikoš

M, Tiwari B, Yin Y, Sassa K (eds) Advancing culture of living with landslides, volume 2: advances in landslide science. Springer International Publishing AG, Switzerland, Cham, pp 1093-a.

Bernat Gazibara S, Mihalić Arbanas S, Krkač M, SečanjM (2017c) Catalog of precipitation events that triggered landslides in northwestern Croatia. In: Abolmasov B, Marjanović M, Đurić U (eds) Proceedings of the 2nd Regional Symposium on landslides in the Adriatic-Balkan Region. University of Belgrade, Faculty of Mining and Geology, Belgrade, pp 103–107

Bernat Gazibara S, Krkač M, Mihalić Arbanas S (2019) Verification of historical landslide inventory maps for the Podsljeme area in the City of Zagreb using LiDAR-based landslide inventory. Rudarsko-geološko-naftni zbornik, 44: 45-58.

Blašković I (1999) Tectonics of part of the Vinodol Valley within the model of the continental crust subduction. Geologia Croatica 52(2):153–189

Corominas J, van Westen C, Frattini P, Cascini L, Malet JP, Fotopoulou, S, Catani F, Van Den Eeckhaut M, Mavrouli O, Agliardi F, Pitilakis K, Winter MG, Pastor M, Ferlisi S, Tofani V, Hervas J, Smith JT (2013): Recommendations for the quantitative analysis of landslide risk. Bulletin of Engineering Geology and the Environment. 73(2): 209– 263.

DHMZ (Meteorological and Hydrological Service) (2013) Meterological and hydrological bulletin 3/2013 (in Croatian)

DHMZ (Meteorological and Hydrological Service) (2018) Meterological and hydrological bulletin 3/2018 (in Croatian)

Dugonjić J, Arbanas Ž (2012) Recent landslides on the Istrian Peninsula, Croatia. Nat Hazards 62:1323–1338.

Dugonjić Jovančević S (2013) Landslide hazard assessment on flysch slopes. PhD Dissertation, Faculty of Civil Engineering, University of Rijeka, p 199 (in Croatian)

Đomlija P, Bernat S, Mihalić Arbanas S, Benac Č (2014) Landslide inventory in the area of Dubračina River Basin (Croatia) In: Sassa K, Canuti P, Yin Y (eds) Landslide Science for a Safer Geoenvironment, Vol. 2. Methods of Landslide Studies, Springer International Publishing, 837-842.

Đomlija P (2018) Identification and classification of landslides and erosion phenomena using the visual interpretation of the Vinodol Valley Digital Elevation Model. Dissertation. University of Zagreb, Faculty of Mining, Geology and Petroleum Engineering

Đomlija P, Jagodnik V, Arbanas Ž, Mihalić Arbanas S (2019) Landslide types in the Slani Potok gully, Croatia. Geologia Croatica (in press).

Fell R, Corominas, J, Bonnard C, Cascini L, Leroi E, Savage, WZ (on behalf of the JTC-1 Joint Technical Committee on Landslides and Engineered Slopes) (2008a) Guidelines for landslide susceptibility, hazard and risk zoning for land use planning. Engineering Geology, 102: 85–98.

Fell R, Corominas, J, Bonnard C, Cascini L, Leroi E, Savage, WZ (on behalf of the JTC-1 Joint Technical Committee on Landslides and Engineered Slopes) (2008b) Guidelines for landslide susceptibility, hazard and risk zoning for land-use planning. Engineering Geology, 102: 99–111.

Grošić M, Bernat S, Arbanas Ž, Mihali ć Arbanas S, Matjašić I, Vidović D (2014) Instabilities of open pit cut slopes: case studiy from the torine quarry in Croatia. In: Mihalić Arbanas S, Arbanas Ž (eds) Proceedings of the 1st Regional Symposium on landslides in the Adriatic-Balkan Region. Landslide and Flood Hazard Assessment. Croatian Landslide Group, Zagreb, pp 153–158

Gunther A, Van Den Eeckhaut M, Malet JP, Reichenbach P, Hervas J (2013) European landslide susceptibility map (ELSUS1000) version 1 methodology. Technical note, European soil portal, 3p

IGU, International Geographical Union (1968) The unified key to the detailed geomorphologial map of the world, 1: 25.000 – 1: 50.000. Folia geografica, series geographica-physica 2, Krakow.

McKee TB, Doeksen NJ, Kleist J (1993) The relationship of drought frequency and duration on timescales. In Proceedings of the 8th conference of applied climatology, 17-22 January, Anaheim,CA. American Meteorology Society: Boston MA: 179-184.

Mihalić S, Arbanas Ž, Krkač M, Dugonjić S (2011) Analysis of sliding hazard in wider area of Brus landslide. In: Anagnostpoulos A, Pachakis M, Tsatsamifos C (eds) Proceedings of the 15th European conference on soil mechanics & geotechnical engineering: geotechnics of hard soils—weak rocks. IOS Press, Amsterdam, pp 1377–1382

Mihalić Arbanas S, Krkač M, Bernat S (2016) Application of advanced technologies in landslide research in the area of the City of Zagreb (Croatia, Europe). Geologia Croatica, 69(2): 231–243.

Mihalić Arbanas S, Krkač M, Bernat S, Komac M, Sečanj M, Arbanas Ž (2017a) A comprehensive landslide monitoring system: the Kostanjek landslide, Croatia. In: Sassa K et al (eds) Landslide dynamics: ISDR-ICL landslide interactive teaching tools. Springer, Heidelberg, pp 1–20 (In press)

Mihalić Arbanas S, Sečanj M, Bernat Gazibara S, Krkač M, Arbanas Ž (2017b) Identification and mapping of the Valići Lake landslide (Primorsko-Goranska County, Croatia). In: Abolmasov B, Marjanović M, Đurić U (eds) Proceedings of the 2nd Regional Symposium on landslides in the Adriatic-Balkan Region. University of Belgrade, Faculty of Mining and Geology, Belgrade, pp 197–202

Oštrić M, Yamashiki Y, Takara K, Takahashi T (2011) Possible scenarios for Rjecina River catchment—on the example of Grohovo landslide. Ann Disaster Prev Res Inst 54B:1–7

Pajalić S, Đomlija P, Jagodnik V, Arbanas Ž (2017) Diversity of Materials in Landslide Bodies in the Vinodol Valley, Croatia. In Mikoš M, Vilimek V, Yin Y, Sassa K (eds) Advancing Culture of Living with Landslides, Volume 5, Springer, 507-516

Panagos P, Van Liedekerke M, Jones A, Montanarella L (2012) European soil data Centre: response to European policy support and public data requirements. Land Use Policy 29(2):329–338. https://doi.org/10.1016/j.landusepol.2011.07.003

Podolzski L, Pollak D, Gulam V, Miklin Ž (2015) Development of Landslide Susceptibility Map of Croatia. In Lollino G, Giordan D, Crosta G, Corominas, Azzam R, Wasowski J, Sciarra N (eds) Engineering geology for society and territory, volume 2: landslide processes. Springer, Heidelberg, pp 947-950

Schmid SM, Bernoulli D, Fügenschuh B, Matenco L, Schefer S, Schuster R, Tischler M, Ustaszewski K (2008) The Alpine-Carpathian-Dinaridic orogenic system: correlation and evolution of tectonic units. Swiss J Geosci 101(1):139–183.

Soeters R, van Westen CJ (1996) Slope instability Recognition, analysis and zonation. In Turner AK, Schuster RL (eds.) Landslides, investigation and mitigation (Transportation Research Board, National Research Council, Special Report ; 247) Washington D.C., USA: National Academy Press. pp. 129 - 177.

Toševski, A. (2018): Susceptibility of the Dubračina river basin to the superficial geodynamical processes. Dissertation. University of Zagreb, Faculty of Mining, Geology and Petroleum Engineering

van Westen CJ, Van Asch TWJ, Soeters R (2005) Landslide hazard and risk zonation; why is it still so difficult? Bulletin of Engineering geology and the Environment 65 (2): 167–184.

Vivoda Prodan M (2016) The influence of weathering process on residual shear strength of fine grained lithological flysch components. PhD Dissertation, Faculty of Civil Engineering, University of Rijeka, p 197 (in Croatian)

Vivoda Prodan M, Arbanas Ž (2016) Weathering influence on properties of siltstones from Istria, Croatia. Adv Mater Sci Eng 2016:1–15, Article ID 3073202.

Vivoda M, Benac Č, Žic E, Đomlija P, Dugonjić Jovančević S (2012) Geohazards in the Rječina Valley in the past and present. Hrvatske vode 20:105–116 (in Croatian)

Vlahović I, Tišljar J, Velić I, Matičec D (2005) Evolution of the Adriatic carbonate platform: Palaeogeography, main events and depositional dynamics. Palaeogeogr, Palaeoclimatol, Palaeocol 220:333–360

doi.org/ 10.35123/ReSyLAB_2019_30

Multi-level flexible debris flow barriers: case study in Peru

Corinna Wendeler [(1)], Vjekoslav Budimir [(2)], Helene Hofmann [(1)]

1) Geobrugg AG, Aachstrasse 11, 8590 Romanshorn, Switzerland

2) Geobrugg AG Predstavništvo u RH, Avenija Većeslava Holjevca 40, 10000 Zagreb, Hrvatska,

Abstract Flexible ring net system have proven to be an equivalent to classic large concrete protection measures over the last 10 years. At same safety level they have many advantages in terms of fast and easy installation, environmental impact as well as landscape protection considerations. A back analysis of the efficiency of some of the first reference projects was made. This presented the basis for a load design developed together with the Swiss Federal Institute of Forest, Snow and Landscape (WSL). Simulations calibrated and verified in 1:1 field tests have been used to develop standard systems for different load cases. These systems have been tested and certified for CE-Marking in 1:1 field tests. Debris flow barriers can be installed as a single barrier or in a row, to increase total retention volume. This contribution relates the dimensioning and installation of a multi-level debris flow barrier in Peru and its successful retention of a large event, protecting efficiently the urban area of Chosica. The project consisted of 22 barriers installed in 9 valleys, in the winter months of 2016. The barriers were dimensioned with the software DEBFLOW®. A year later, large debris flows occurred and we will focus on two barriers which retained approximately 10'000m3 of material and were filled to 95%. The barriers downstream presented enough retention capacity to cope with a potential following event. Maintenance was undertaken in January 2018, and the barriers are fully functional for the next debris flow season.

Keywords debris flow mitigation, flexible ring-nets, Peru

Introduction

The effect of "El Nino" combined with regular precipitation during the rainy season, from January to end of April, leads to recurring debris flow disasters, in Peru. Debris flows occasion great damage to infrastructure and endanger lives and livestock. In 2015 alone, eight people lost their lives in a debris flow event and led to infrastructure loss and destruction costs of over 58 million USD. Other examples are the debris flows, in 1987, coming from the San Antonio de Pedregal stream, which killed 100 people. Eleven years later, 320 got injured, two died and 200 houses were destroyed.

To prevent vulnerable areas from being affected by further debris flow disasters, different type of mitigation measures can be installed. The municipality of Chosica, in the Lugarincho-Chosica district of the province of Lima, is particularly affected by debris flow due to its geographic location. Enclosed by steep valleys incised by torrents, the municipality opted in 2016 for 22 flexible ring net barriers, distributed in nine of these surrounding valleys, installed during winter 2016. The used flexible ring net barriers are standardized flexible debris flow barriers. The barriers' dimensions were determined by the dimensioning tool DEBFLOW®.

A year after completing the flexible ring net barriers, large debris flows occurred again and the barriers successfully retained the debris material. As an example, two barriers retained approximately 10'000 m3 debris material and were filled up to 95%. Further downstream, additional barriers, installed as a multi-level system, presented enough retention capacity for a potential following event. This paper presents the acquired knowledge over 10 years' experience in developing, dimensioning and installing flexible ring net barriers against debris flows through the example of the mentioned case study in Peru. Another example of a multi-level installation is situated in the Spanish Pyrenees, in Port-Ainé. Nine so-called VX-barriers were installed in 2009, combined with extensive monitoring of the catchment basin and were successfully filled in a large debris flow event in Summer 2010, with a total volume of approx. 25'000 m3 (Luis-Fonseca et al., 2010).

Method

Debris flow standardization and developed systems

While using flexible ring nets for rockfall protection it was observed that some slides got retained. However, no dimensioning concept existed proving that flexible ring net barriers can retain large debris flows. Therefore, real-scale experiments with flexible ring nets were performed at Illgraben test site in Switzerland between 2005 and 2008 [Wendeler, 2008]. At least once a year, a middle to large debris flow naturally occurs at Illgraben which proved to be an ideal test site location. The tests showed that a single barrier can retain 1000 m3 depending on the channel geometry and that over 10'000 m3 of material can overflow the barrier without damage (Figure 1). Thus, a debris flow retention system with several flexible ring nets in a row, so-called multi-level system, can be planned and constructed. Another test site in Switzerland, in Merdenson, confirmed this theory and allowed the extension of the dimensioning concept to multi-level systems. An extensive measuring concept on and around the system led to the final dimensioning concept [Wendeler, 2008]. Based on the field test data, the flexible ring net dimensioning concept, the loading distributions,

and simulations with the finite element software FARO [Volkwein, 2004] led to the development of standardized flexible ring net barriers. These barriers are defined according to the load their surface can cope with, in kN/m2, as well as the system height.

Two types of standardized barriers were designed: VX-barrier and UX-barrier (Figure 2). The VX barrier takes loads up to 160 kN/m2 and is used for narrow channels (V-shaped valleys), with a width up to 15m, and a barrier height of up to 6m. UX-barrier are used for larger channels (U-shaped valleys), with additional posts as required, with expected loads up to 180 kN/m2 and a barrier height up to 6m [Geobrugg, 2016].

Figure 1 Flexible ring net barrier withstanding overflow in the Illgraben.

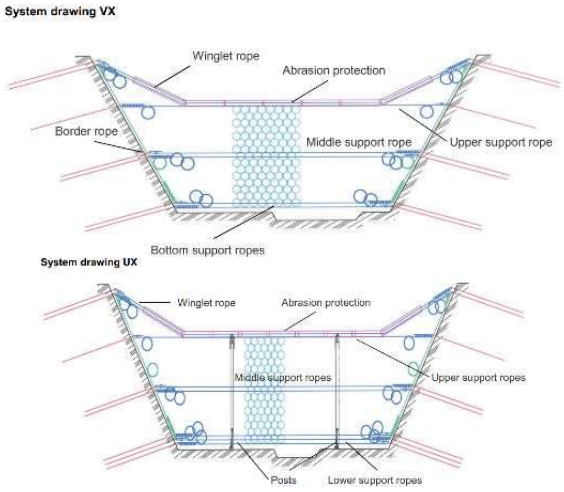

Figure 2 Top: schematic diagram of standardized VX-barrier. The main components are the flexible ring net, top, middle and bottom support ropes ring brakes, abrasion protection, winglet components, and anchoring. Below: schematic diagram of standardized UX-barrier with posts

Conformité Européenne (CE) marking

Flexible standardized debris flow barriers certification was achieved in 2017 [EAD document Nr. 340020-00-1062]. The real-scale testing served for certifying the flexible standardized debris flow barriers. The CE marking is based on a "European Assessment Document" which defines precisely the suitability, the type classification and yearly quality controls necessary to correspond to a certain standard. This states that the products with CE marking fulfil the European guidelines for product quality and field appropriateness and allows an unrestricted trade within the European Union. For further information please see: [https://ec.europa.eu/growth/single-market/ce-marking_de]. There are two main benefits CE marking brings to businesses and consumers within the European Economic Area (EEA). Firstly, businesses know that products bearing CE marking can be traded in the EEA without restrictions. Secondly, consumers enjoy the same level of health, safety, and environmental protection throughout the entire EEA. Concerning debris flow barriers, CE marking guarantees for user and client a declared performance of the net systems according to EAD Document NO 340020-00-106. The performance is declared in kN/m2 impact pressure of first debris impact.

Case Study Peru

Background and fieldwork

Peru is located in the western part of South America adjoining the Pacific and the Andes mountain range. Due to the tropical location and the large altitude range, Peru has drastically varying climatic conditions and weather phenomena such as El Niño.

Between 2003 and 2015, according to Peru's national civil defence, 4484 flood events and 1388 debris flows occurred affecting directly population, crop areas, road and productive infrastructure [ANA, 2017]. However, not all of these events are related to solely the El Niño phenomenon, short and intense precipitation combined with the presence of loose material simply leads to debris flows, with severe consequences in urbanized areas.

Since these recurring events have been recognized, several studies were realized in the last 30 years such as geological and geomorphological studies, geological hazard risk analysis, and evaluation and consequences of debris flows. Based on the knowledge obtained from these studies, the importance of mitigation measures was recognized in Peru. As already mentioned, the municipality of Chosica, was hit several times by severe debris flow events. The particular geographical setting leads to this vulnerability, Chosica being surrounded by steep dewatering slopes, covered by unconsolidated material, product of the cordillera's erosion (Figure 3). These slopes present each a sufficient large catchment area with one main dewatering direction, i.e towards the valley, where the urban area is settled. A comprehensive field analysis was conducted to stake out the barriers' best locations and to estimate the volume of potential flows. Finally, the National Water Agency (ANA) generated a tender for the installation of 22 flexible ring net barriers in nine streams to protect life and properties of more than 60'000 inhabitants (Figure 4). TDM S.A. got the work awarded and started the installation in January 2016. The dimensioning of the barriers is explained in the next section. One special application was installed in Quebrada Carossio. The barrier has a width of 60 m with 6 posts and a barrier height of 6m. Hence, it is the second largest barrier in the world and the largest in South America.

Figure 3 Steep, incised slopes overlooking Chosica's urban area and the unconsolidated material covering these slopes illustrate the debris flow potential.

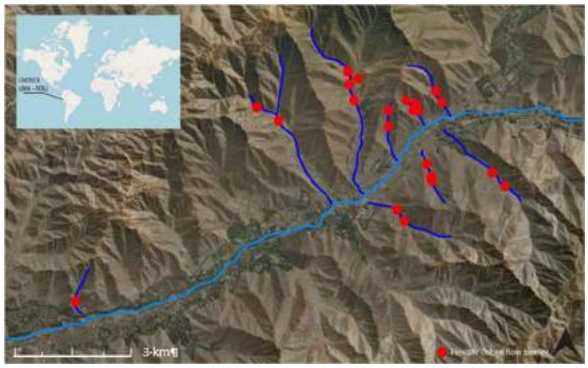

Figure 4 Case study overview in Cuenca del Rio Rimac Distrito de Lurigancho, Chosica, Peru with 22 installed flexible debris flow barriers (red dots).

Dimensioning with DEBFLOW

Flexible standardized barriers, up to a barrier height of 6m, were dimensioned with DEBFLOW, Geobrugg's official dimensioning tool for debris flow. It is freely accessible for anyone on the website1. The software is based on FARO [Volkwein, 2004] and analyses the stability of the chosen barrier system (VX/UX-barrier), calculates appearing dynamic and hydrostatic forces during the filling process and overtopping [Geobrugg, 2017]. The software is a one-page format and built up of debris flow parameters, barrier specific parameters for each selected barrier, choice of standard barrier system, proofs of maximum dynamic loading and static loading as well as of the chosen standard system. Overall retention volume of all selected barriers gets calculated, based on three load cases taking into account the type of flow, granular or muddy. Special design was undertaken for the barrier in Quebrada Carrosio, the largest flexible ring net barrier in South America, since the dimensions required from the channel geometry exceeded the standard dimensions of flexible ring net barriers.

Installation

Installation work took 2.5 months to complete and was accomplished between January and March 2016. During this time, potential debris flow streams were not activated because of no precipitation in the area. Details of installation are presented below such as scour protection of posts foundation for the UX-barriers and the special designed abrasion protection for the top support rope (see Figures 5 and 6). Depending on the hydraulic conditions and the geometry of the different streams, UX or VX barriers were installed (Figure 7 and 8), as single barrier or in a multi-level combination. The largest barrier was set up in a multi-level setting (Figure 9).

Figure 5 Scour protection around the posts for UX-barriers

Figure 6 Abrasion protection for the top support rope

Figure 7 UX- barriers with two posts in the channel bed

Figure 8 and VX barrier in a narrower channel

Figure 9 The highest barrier is the largest in South America.

Debris flow events

The first debris flows after installation happened a year later, in January 2017. Up to then, all barriers have retained debris in variable amounts. On average, their retention level has been around 4'600 m3. Subsequently, in February 2017, Peru was hit by great storms which caused even further, large, debris flow events. The flexible debris flow barriers kept fulfilling their function of retaining debris. The multi-level system was efficient since the barriers further downstream were not completely filled and still offer good retention capacity, for potential following debris flows. During the debris flow events post supports and cable supports got partially eroded. Hence, maintenance work on these elements was done. Eroded parts were rebuilt with new foundations, brakes and cables were replaced. Further, the barriers need emptying when the material is dry and stable. It can be cleaned with an excavator from behind or in certain conditions, when all safety requirements are met, from the front. Figure 10 illustrates the overall process for the barriers, from installation to filling to maintenance, ready for the next debris flow events.

Figure 10 Before (2016) and after the debris flow event (2017) and subsequent maintenance (2018) for the stream San Pedregal (above) and Carrosio (below).

Conclusion

Since the 1:1 field experiments and the publication of the design concept for flexible debris flow barriers, many projects have been successfully installed in the last ten years, the Peru case study being one of several examples worldwide. The protection system with multiple flexible ring net barriers fulfilled successfully the prevention purpose of the vulnerable area situated further downstream. After geological and hydrological studies, some fieldwork and thanks to the standardization and dimensioning with DEBFLOW, a flexible ring net barrier system composed of a total of 22 nets lead to an impressive protection concept. The CE marked barriers were rapidly installed within 2.5 months. Compared to classical protection structures, such as large concrete check dams, the flexible ring net barriers are much easier to install in the ravines, with evidently less material to be handled on the slope. Furthermore, they integrate themselves very well into the landscape, can even be installed in landscape protection zones and finally the carbon footprint is more advantageous in comparison to concrete solutions (IBU report, 2008). As observed after the first debris flow events, maintenance of the structure can be done easily and presents an overall cost-effective and elegant solution.

Acknowledgments

Thank you to Rolando Romero (Geobrugg Peru), for the material of the presentation and all his efforts in this project.

References

CE marking (2019) Retrieved from: https://ec.europa.eu/growth/single-market/ce-marking_de

European Union. (2018). Flexible kits for retaining debris flows and shallow landslides (EAD document Nr. 340020-00-1062). Retrieved from: https://ec.europa.eu/growth/sectors/construction/product-regulation/european-assessment_en

Geobrugg (2016): Ringnetzbarrieren aus hochfestem Stahldraht: Die ökonomische Lösung gegen Murgänge, Schweiz.

Geobrugg (2017): Software Manual: DEBFLOW Debris flow protection. Switzerland.

IBU Report: Kytzia S. (2008), CO2 footprint of slope stabilisation methods: the TECCO System (mesh) compared to shotcrete solution. Institute for civil and environmental engineering, Rapperswil, Switzerland.

Luis-Fonseca, R., Raïmat Quintana, C., Albalate Jimenez, J., Fernández Rodriguez, J., 2010: Protección contra corrientes de derrubios en áreas del Pirineo. Comportamiento de las barreras VX y primeros resultados de la estación de medición pionera en España. Revista de Información General de maquinaria y Obras Urbanas, N.22.

TDM S.A. (2017) ANA / Proyecto Fenomeno del Nino. Unpublished report.

Volkwein A. (2004): Numerische Simulation von flexiblen Steinschlagschutzsystemen, Dissertation ETHZ, Schweiz.

Wendeler C. (2008): Murgangrückhalt in Wildbächen – Grundlagen zu Planung und Berechnung von flexiblen Barrieren, Dissertation ETHZ, Schweiz.

Wendeler, C. (2008). DEBFLOW® [Online software]. Retrieved from: https://www.geobrugg.com/en/Welcome-to-myGeobrugg-79860.htmlintegriert

doi.org/ 10.35123/ReSyLAB_2019_31

Experimental study on squeezing-out phenomenon by landslide mass loading

Gen Furuya [1], Masatoshi Hasegawa [2], Gonghui Wang [3]

1) Associate. Professor, Ph. D., Department of Environmental and Civil Engineering, Faculty of Engineering, Toyama Prefectural University, Kurokawa 5180, Imizu-shi, Toyama 939-0398, Japan, gfuruya@ pu-toyama.ac.jp

2) Engineer, M. S., Toyama Prefectural Government Office (Former Graduate school of Engineering, Toyama Prefectural University), Shin-Sougawa 1-7, Toyama-shi, Toyama 930-8501.

3) Associate. Professor, Ph. D., Disaster Prevention Research Institute, Kyoto University, Gokasho, Uji-shi, Kyoto 611-0011, wanggh@landslide.dpri.kyoto-u.ac.jp

Abstract The schematic diagram of landslide structure by Varnes (1978) is well known in the description of landslide movement, in which the movement of landslide mass is described to be sliding along the ground surface. However, according to the field investigation on some landslides, landslide mass can result in new failure within the ground along the sliding path. The kind of failure phenomenon is called squeezing-out or squeezing (herein called squeezing-out type landslide). Nevertheless, the triggering mechanism of this kind of phenomenon has not been clarified yet. Here we report results of a series of flume tests that were performed to examine the generation mechanism of squeezing-out type landslide. In these tests, we focus on the effect of permeability of the soil layers within the ground of the accumulation zone on the resultant squeezing-out phenomenon. Our test results showed that the combination of ground layers with differing permeability can not only affect the depth of sliding surface, but also play key role on the propagation form of failures within the ground of the accumulation zone.

Keywords Propagation of failure, Pore water pressure, sand, Particle size, permeability, Flume test

Introduction

The schematic diagram of landslide structure by Varnes (1978) is well known in the description of landslide movement. Oyagi (2004) examined the components of the moving block and the deformation structure based on this schematic diagram, and pointed out the existence of a quasi-fluctuation area on the ground of the accumulation zone at the toe of landslide mass for some landslides. This suggests that the existence of an expansion (generation) of new slope or/and ground failure phenomenon associated with the loading of landslide mass. One example of such expansion is the landslide at Takarazuka Golf Course that was triggered by the 1995 Southern Hyogo Prefecture Earthquake (Figure 1), and the expansion was thought to be the result of squeezing (or squeezing-out) phenomenon (Yokoyama et al. 1995). A recent example is the slope failures (small landslides shown in Figure 2) in Atsuma Town caused by the 2018 Hokkaido Iburi Eastern Earthquake. To clarify this kind of squeezing phenomenon, we have been performing model flume tests in recent years. In this paper, we present the results of tests conducted on the model consisting of two soil layers with different permeability.

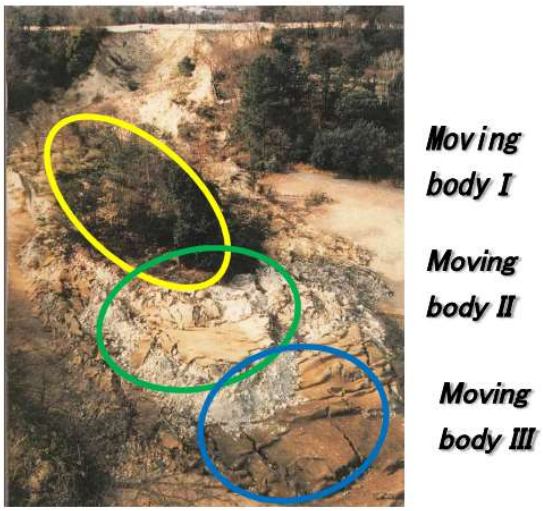

Figure 1 Squeezing-out phenomenon at the Takarazuka Golf Course landslide
(Added to photo taken by The Sankei Shimbun, referring to Yokoyama et al. 1995)

Figure 2 Squeezing-out phenomenon at Yoshino, Atsuma, Hokkaido

Flume experimantal apparatus and test procedures

Flume experimantal apparatus

Figure 3 shows the employed experimantal apparatus, which consists of a flume (180 cm long; 30 cm wide; 30 cm high) and a water tank (180.8 cm long; 33.4 cm wide; 30.4 cm high). Both the flume and water tank are made of acrylic and are transparent. Two layers of soils made of different samples were placed in the water tank to simulate the accumulation zone. It is noted that during the tests, the thickness of each soil layer 10 cm, but the up-down sequency was changed according to the test purpose.

After the soil layer was prepared, strain gauge probes for detecting the location of sliding surface were inserted vertically into the soil layer at three locations of A to C as shown in Figure 3. It is noted that in each probe (made by polypropylene sheet), strain gauges were patched at the locations with distances being 5 cm and 15 cm far from the bottom of the probe, respectively.

In addition, for clearly distiguishing the deformation with the soil layer, colored vertical belts were made by filling colored sand at an interval of 10 cm starting from the location 15 cm far from the junction point of the flume and soil layer. Pore water pressure gauges were attached to the bottom of the soil layer at locations B and C shown in Figure 3. Two video cameras were set to monitor the deformation of accumulation zone from the side and the toe parts of the water tank. Before the test, the soil layer was saturated by water injection into the water tank. The strain gauge probes ware connected to the recording system with the mediation of a bridgebox, while the pore pressure gauges ware connected directly to the recoding system. During the whole test, all the data were sampled at a frequency of 100 Hz.

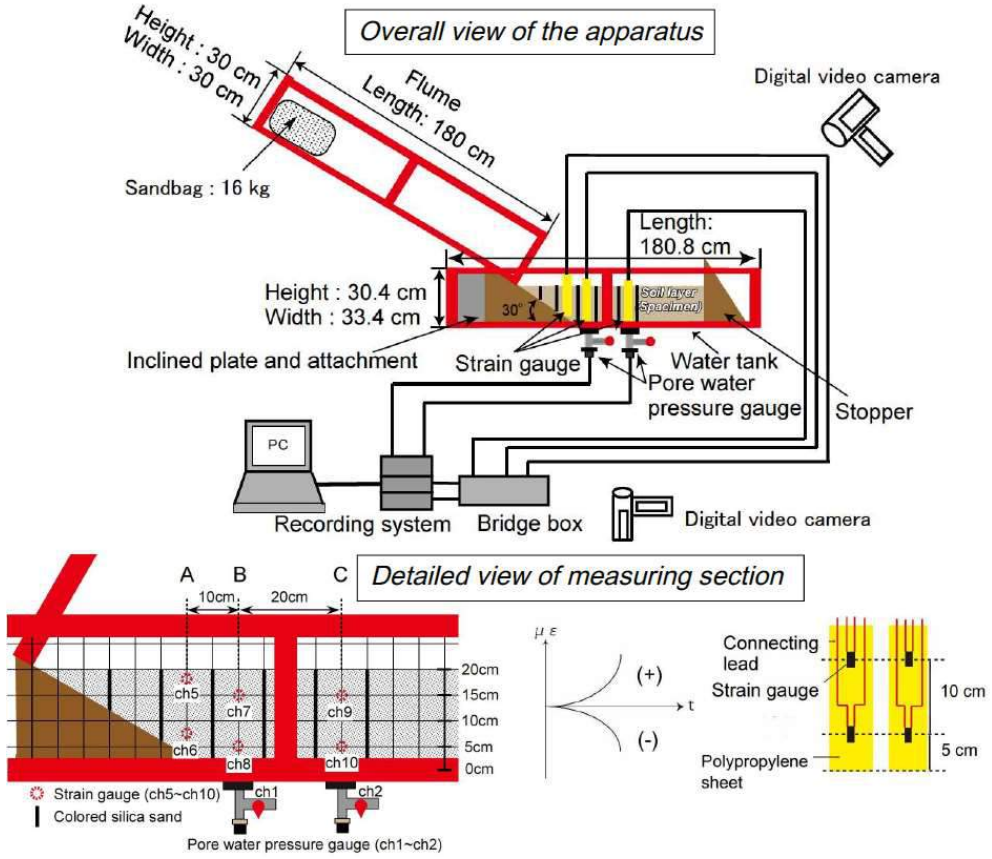

Figure 3 Schematic diagram of flume test apparatus

Test procedures

The test method is as follows. After the soil layers in the water tank had been saturated, one end of the flume far from the water tank was hoisted until the flume reached a slope of 30 °. Thereafter, a sandbag containing 16 kg of gravel was released and slide downslope from the upend of the flume to mimic the landsliding mass (see Figure 3).

In addition, three types of samples, namely, silica sand No. 6 (S6), No. 8 (S8), and gravel were used as for the construction of soil layers. The average particle sizes (D_{50}) of these sample were 0.05 mm for S8, 0.3 mm for S6, and 5.0 mm for gravel, respectively. Orders of hydraulic conductivities (k) for these sample were 10^{-6} m/s, 10^{-4} m/s, and 10^{-3} m/s, respectively. The soil layers in the water tank were prepared by different combinations of sample as shown in Table 1. We used these different combination of samples to mimic diffrenent types of stratigraphic model in accumuration zone due to the possible different history of sedimantation.

Table 1 Sample conbinations for flume test

Test No.	Sample	
	Upper layer	Lower layer
2-1	S6	S8
2-2	Gravel	S8
2-3	S8	S6
2-4	S8	Gravel

Test results

We performed tests for four soil layer cases. Table 2 summarizes the test condition, maximum depth of sliding surface (deformation depth) and Length of deformation zone in each test. Some representative measurement results are shown in Figure 4 (Test No. 2-2: Upper layer is Gravel and lower layer is S8) and Figure 5 (Test No. 2-4: Upper layer is S8 and lower layer is Gravel). Figure 4a presents a photo and the sketch at the side of water tank after loading of landslide mass, and Figure 4b plots the time series data for pore water pressure and strain. As seen in Figure 4a, a sliding surface is formed within the upper gravel layer, and another sliding surface slightly smaller than the upper layer is formed within the lower S8 layer, and the total deformation range within the accumulation zone is about 63.5 cm. In Figure 4b, it is seen that the pore water pressures vary in a sin-wave like pattern. This pattern may result from the amplification of water wave that was caused by water reflection from the

Table 2 Test results

Test No.	Sample		Number of sliding surfaces	Maximum depth of slideing surface (cm)	Length of deformation zone (cm)
	Upper layer	Lower layer			
2-1	S6	S8	2	15.7	62.3
2-2	Gravel	S8	2	16.5	63.5
2-3	S8	S6	3	9.3	66.6
2-4	S8	Gravel	3	10.1	65.1

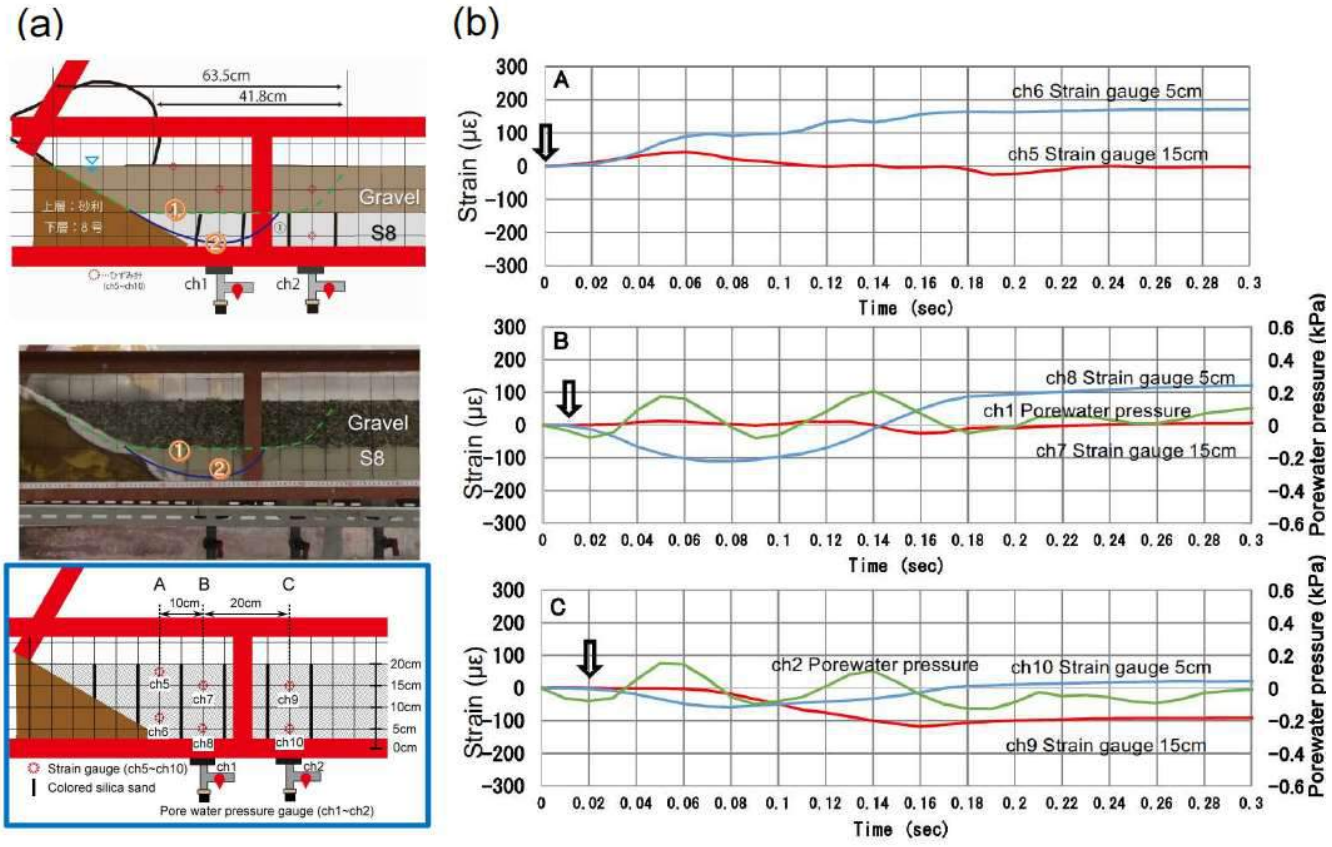

Figure 4 Result of Test No. 2-2 ((a): Photo and sketch; (b) Time serise change between starin and pore water pressure)

end of water tank wall (same phenomenon was recognized in Test 2-1). The time lags in the responses of strain gauges between section A and B, B and C are approximately 0.01 second, respectively (Outlined arrow in Figure 4b). This means that the failure was triggered by the landsliding mass was propagated within the accumulation zone. The strain gauge in ch10 shows a slight change followed by recovery during this period. This kind of slight variation followed by recovery in the strain gauge may mainly result from the elastic deformation due to the loading of landsliding mass.

For Test No. 2-4, Figure 5a presents a photo together with a sketch of the deformation within the soil layers observed from the side of water tank, and Figure 5b shows the time series data of pore water pressure and strain. From Figure 5a, it is found that the formed sliding surfaces in Test No. 2-2 are different from those in Test 2-2. In Figure 5a, there are three clear sliding surfaces within the upper layer. Detailed checking on the deformation process recorded by the video camera revealed that the primary sliding surface was formed by the loading of landsliding mass, while the second sliding surface was generated with the soil layer in front of the primary sliding surface being squeezed out, and the third sliding surface was formed soon after the formation of the second one. Finally, the range of deformation within the accumulation zone reaches 65.1 cm. In Figure 5b, the pore water pressure with negative or positive peak value (colored arrow in the figure) propagates from the section B to section C soon after the loading of landsliding mass. The strain value (open arrow) in accumulation zone also propagates forward from Section A to B, and then to C after the loading of landsliding mass. The time lag in the variation of strain values between Zone A and Zone B is 0.02 seconds, while that between Zone B and Zone C is 0.05 seconds. This result indicates that the propagation of shear failure resulting in the formation of sliding surface is slow compared to that within the soil layers in Test No. 2-2. It is noted that no sliding surface is described at the lower gravel layer in the Figure 5b, because we failed to figure out the deformation within the gravel layer through examining the movie recordings. Although the strain gauge (ch10) detected deformation, we infer that this difference between the movie recording and the strain gauge monitoring may result from the effect of side friction generated between the acrylic plate and gravel in the water tank.

Relationship between deformation depth and deformation length

Figure 6 shows the relationship between the maximum depth of sliding surface and the length of deformation zone (deformation distance) measured by movie from the side of the water tank. In this figure, ▲ is the result of the

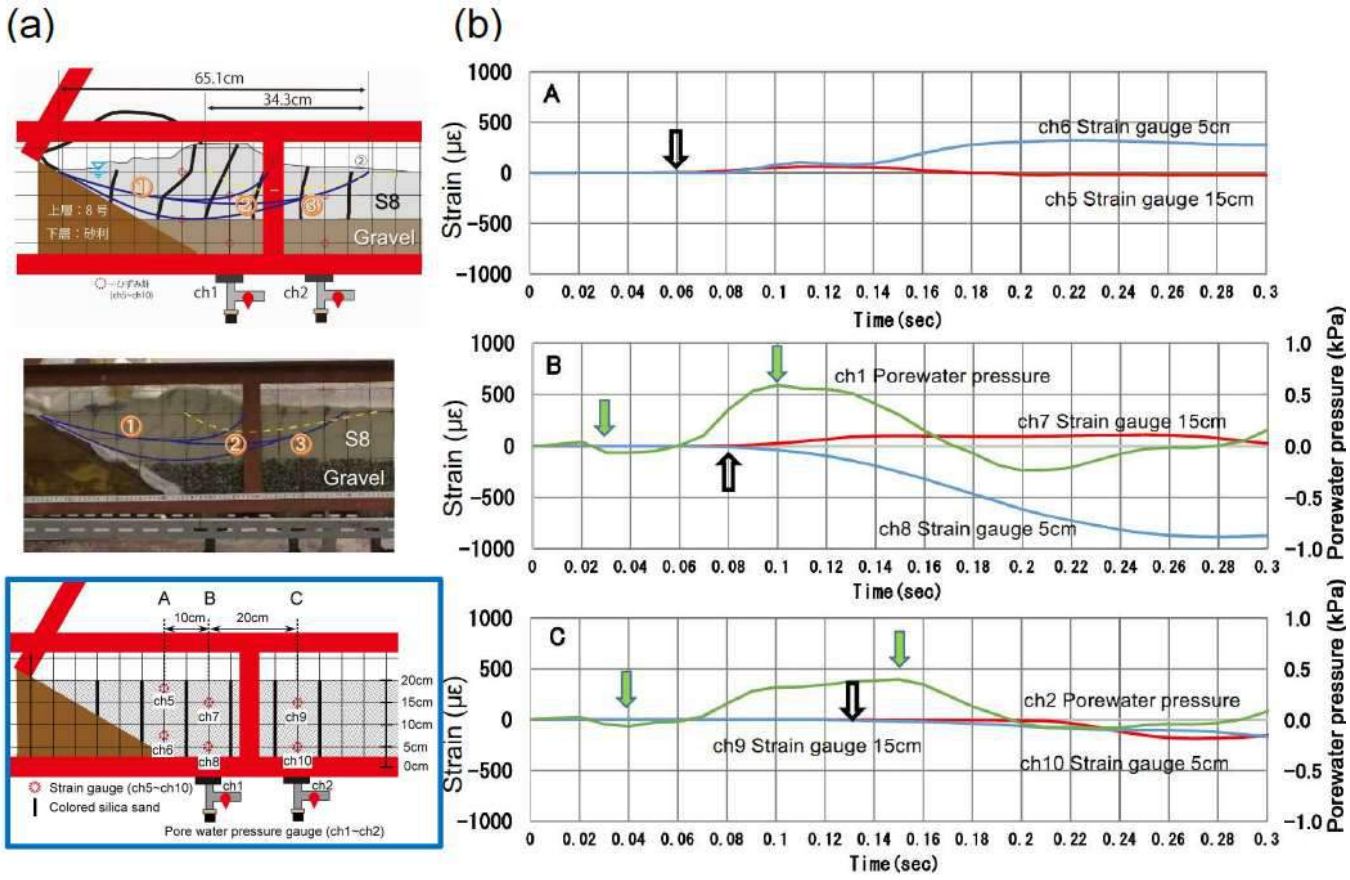

Figure 5 Result of Test No. 2-4 ((a): Photo and sketch; (b) Time serise change between starin and pore water pressure)

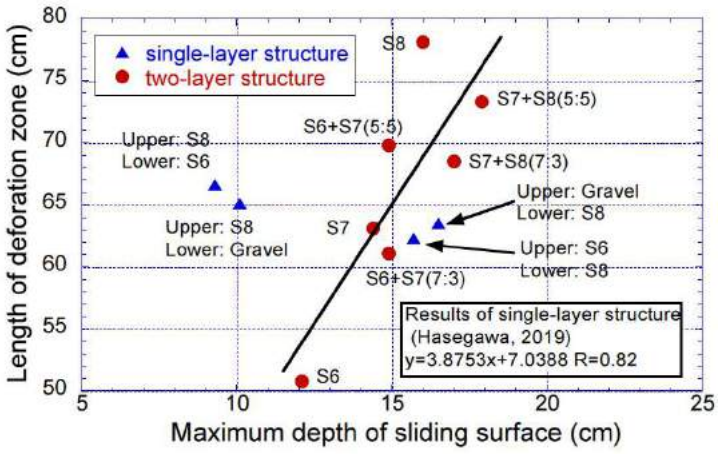

Figure 6 Relationship between Maximum depth of slideing surface amd Length of deformation zone

two-layer structure and ● is the result of the single-layer structure (Hasegawa, 2019, Furuya et al 2019). In the single-layer structure, there is a positive correlation between the depth of sliding surface and the length of deformation zone. This means that the depth of sliding surface tends to become shallow when the particle size of the samples used for the soil layer becomes large. Nevetheless, this kind of correlation is not recognized for the two-layer structure tests. When S8 (composed of small partical size) is placed as the lower layer, plots are close to the regression line as obtained from the tests on single-layer structure. However, when the samples with lager grain sizes (such as S6 and gravel) was placed as the lower layer, the sliding surface becomes shallower and the deformation zone is narrower than those in the tests on single-layer structure. This suggests that range of failure area in the accumulation zone is greatly dependent on the geotechnical properties of each soil layer and also on the sequece of the soil layers. These properties and sequence can affect the depth and range of failure due to squeezing-out phenomenon. Therefore, we infer that the natural ground resulting from different types of sedimential processes may surrfer from different types of squeezing-out phenomona, due to the different geotechnical properties of each stratum, and also due to sequence of stratum.

Conclusion

In this study, we investigated the deformation with focus on the squeezing-out phenomenon occurring on accommodation ground due to the loading of landsliding mass coming from the upper slope. Considering that a natural ground may result from the deposition of different materials at different deposition times, we composed the model ground by two soil layers, and employed different samples for different soil layer. Through releasing the sandbag from the upper slope, the loading process of landsliding mass on the model ground was simulated and the failure process with within the model ground was monitored. Our preliminary results showed that shear failure could be triggered and propagated within the model ground due to the loading of sliding mass, and properties and sequence of soil stratum forming the ground can greatly affect the depth of sliding surface and also the range of squeezing-out phenomenon. Finally, it is noted that detailed analysis on the formation within the model ground through PIV is still on going and further tests will also be performed to examine the possible effect of initial density of the model ground on the squeezing-out phenomenon.

Acknowledgements

This work was supported by JSPS KAKENHI Grant Number JP15H017972, JP16K12857, JP19H02238. We would also like to acknowledge Mr. Syun Ogawa, GIKEN incorporated, and Mr. Hiromitsu Fujimori, Takaoka city government office for experimental work on flume test.

References

Furuya,G., Hasegawa, M., Wang, G.: Deformation in sedimentary area of two-layered structure by landslide loading, Proc. 58th Annual Meeting of the Japan Landslide Society, The Japan Landslide Society, 2019, pp. 193-194 (in Japanese).

Hasegawa, M.: Propagation mechanism of failure in sedimentary layer caused by landslide mass loading, Master thesis, Graduate School of Engineering, Toyama Prefectural University, 2019, 48p (in Japanese).

Oyagi, N.: Landslide structure, Landslides Topographcal and geological recogination and terminology, The Japan Landslide Society, 2004, pp. 29-45 (in Japanese).

Varnes, D. J.: Slope Movement Types and Processes. In: Schuster, R.L. and Krizek, R.J., Eds., Landslides, Analysis and Control, Transportation Research Board, Special Report No. 176, National Academy of Sciences, 1978, pp. 11-33.

Yokoyama, S., Fujita, T., Kikuyama, K.: Slope movenment at Takarazuka Golf Course caused by the 1995 Southern Hyogo Prefecture Earthquake, Research report on landslides associated with the 1995 Southern Hyogo Prefecture Earthquake, The Japan Landslide Society, 1995, pp. 61-77 (in Japanese).

doi.org/ 10.35123/ReSyLAB_2019_32

An overview of geotechnical aspects of materials involved in slope instabilities along flysch-karst contact in Croatia

Sanja Dugonjić Jovančević[(1)], Martina Vivoda Prodan[(1)], Josip Peranić[(1)]

1) University of Rijeka, Faculty of Civil Engineering, Radmile Matejčić 3, 51000 Rijeka Croatia

Abstract The narrowed flysch zone, in the area of central Istria and Kvarner hinterland, surrounded by carbonate rock mass (limestone, dolomitic limestone) is characterized by frequent landslides. Instabilities are caused by specific position of the flysch and carbonate rock mass, specific material properties, present geomorphological, chemical and physical processes which are influencing some physical, mechanical and hydraulic properties of involved materials. Sliding surface is mostly formed on the contact of the superficial deposits and impermeable flysch bedrock. In the zones of the chemically and physically weathered flysch rock mass, during longer and continuous rainy periods, pore pressures increase, due to which gradual loss of strength and eventual failure occurs. Many researches were carried out in the mentioned research area during landslide remediation works, doctoral thesis investigations and within different research projects. This paper provides an overview of basic geotechnical properties of materials present in different locations of the investigated area, which show significant dissipation in investigated values, but also some common material characteristics, crucial for instability occurrence.

Keywords flysch, material properties, instabilities, weathering

Introduction

The key improvement toward the effective landslide risk management lies in continuous research and collaboration on international and interdisciplinary level in the field of landslide investigation. Past and present landslide evidences, the considerable understanding of present conditions, and low level of effective landslide risk management, providing high motivation for extension of existing research on the karst-flysch contact along northern Adriatic coast in Croatia (Fig 1). Existing research results are related to geotechnical properties of the flysch rock mass, their combined relations, influence of processes such as weathering on the rock mass behaviour, landslide initiation and run off modelling, landslide susceptibility, hazard and risk assessment, landslide monitoring and climate change influence on landslide appearance. One of the future research goals is to develop advanced level of understanding the materials and processes through laboratory testing and advanced modelling of landslides in this zone, giving particular attention to landslide triggering conditions.

Many instability phenomena have been recorded on flysch slopes around the karst-flysch contact in the area of central Istrian Peninsula (Arbanas et al. 2011, Mihalić et al. 2011, Dugonjić Jovančević and Arbanas 2012, Dugonjić Jovančević 2013), Rječina River Valley (Benac et al. 2005a and 2009, Benac et al. 2011, Vivoda et al. 2012, Arbanas et al. 2017), Draga Valley (Benac et al.2009, Arbanas and Dugonjić 2010), Bakarac Valley (Dugonjić et al. 2008, Dugonjić Jovančević et al. 2012) and Vinodol Valley (Benac et al. 2005b, Đomlija et al. 2014, Đomlija et al. 2017, Đomlija 2018). Mentioned area describes research range (Fig. 1), and is part of a large Adriatic flysch basin spreading from Gorizia in Italy to Albania (Marinčić 1981).

Numerous instability processes on slopes in investigated area often occur due to weathering process of flysch rock mass that causes rapid disintegration and loss of shear strength (Arbanas et al. 2013, Benac et al. 2005, Bernat et al. 2014, Dugonjić Jovančević and Arbanas 2012, Vivoda et al. 2012). When it is exposed to water and air, flysch rock mass is strongly affected by chemical weathering and decomposition, physical disintegration and as a result of these processes, the volume of the rock mass increases and residual shear strength decreases (Vivoda Prodan et al. 2017, Vivoda Prodan and Arbanas 2016). Landslide geological profile mainly consist of flysch bedrock covered by clayey colluvium and/or residual soil, sporadically containing a larger portion of rocky fragments, mostly sandstones and siltstones originating from the bedrock. Existing documentation and past research show that instabilities in the research area include mostly translational and rotational sliding, rockfalls and rarely debris flows. Landslide volumes vary between 10^2 and $>10^6$ m^3, with estimated landslide depths from 3- 20m. Distribution of the instabilities evidenced through different researches, landslide remediation works, and smaller instabilities along the roads can be seen in Fig. 1. However, the map does not present landslide inventoryThe landslide inventory map in the research area was prepared in scale 1:10 000 only for Vinodol Valley (Đomlija 2018) and includes 633 landslide phenomena. This fact, together with the indication of instabilities, shown on Fig. 1, implies on the need to perform extensive analysis and detail landslide inventory map for the whole research area.

A usual trigger of landslides in the area is raising of the groundwater caused by heavy and continuous rainfall

in a few months' period. Landslides are thus occurring mostly in the late winter and spring period (from November to May), when the number of rainy days in the three-month period is high and evapotranspiration is low. Due to relatively low permeability of the cover, the infiltration is generally slow and the runout coefficient is high (Peranić 2019, Peranić et al. 2019). The analyses of the daily, monthly and annual precipitation data have shown that the cumulative precipitation in three months (70–100 days), prior sliding, may have a great influence on water infiltration and groundwater levels rising (Dugonjić Jovančević and Arbanas 2012, 2017; Dugonjić Jovančević 2013). Material characteristics relevant for instability occurrence, investigated trough landslide remediation works, scientific research projects, student terrain investigations, doctoral thesis, etc. are presented in this paper. Laboratory testing was mostly performed in the Geotechnical laboratory, at the Civil Engineering Faculty, University of Rijeka. The aim of this research is to define some of the basic geotechnical aspect of materials involved in slope instabilities.

Grain size distribution, plasticity limits and strength parameters were tested on the flysch samples of different weathering grades: in Grey Istria (Žufić 2011, Gulam 2012, Dugonjić Jovančević 2013, Vivoda Prodan 2016, Maček et al. 2017), Rječina River Valley (Benac et al. 2014, Vivoda Prodan 2016, Peranić 2019), Vinodol Valley (Vivoda Prodan 2016, Pajalić et al 2017). Mineralogical composition in the research area has been investigated by Gulam (2012), Benac et al (2014) and Vivoda Prodan (2016). Hydraulic properties (soil-water retention curves and permeability) were investigated by Maček et al. (2017) and Peranić et al. (2018), while Peranić (2019) and Peranić and Arbanas (in press) have investigated shear strength properties in unsaturated conditions. Žufić (2011) and Vivoda Prodan (2016) and Vivoda Prodan and Arbanas (2016) investigated slaking behaviour of siltstone samples from Istria Peninsula. Some laboratory testing was performed during this research (durability characteristics and uniaxial compression strength on fresh siltstones).

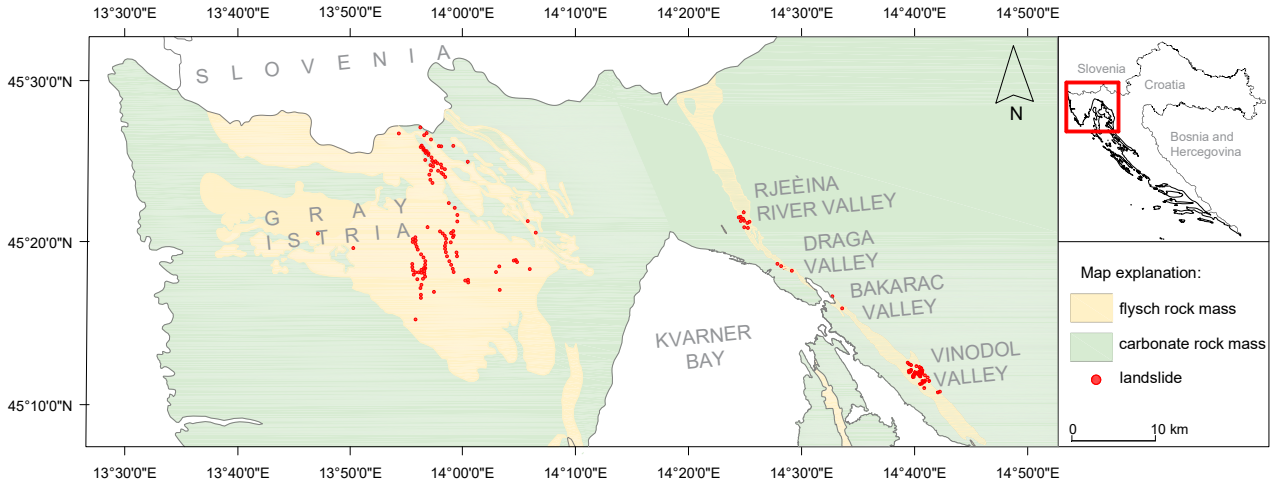

Figure 1 Study area along the coastal area of large Adriatic flysch basin

Index and strength materials properties

The study area (Fig. 1) is composed of two types of rock mass: (a) the prevailing Cretaceous and Paleogene carbonate rock mass, with karstified limestone and dolomites; and (b) Paleogene flysch rock mass. Tectonic movements from the Paleogene period, together with the after movements, have caused formation of the folding and faulting zones generally striking in the NW-SE direction. These tectonic movements caused sporadically narrowing of the flysch sediment basin in the Adriatic belt and reduced appearance of the flysch deposits on the surface, as well as rising of the surrounding karstic terrain.

The Istrian flysch basin as small part of the large Adriatic flysch basin has an approximate width of 60-90km. The upper parts of the flysch-type rocks consist of interchanges of thinly bedded marls (15–20 cm) and carbonate-siliciclastic rocks (3– 5 cm). In the lower part, there is prevailing turbidite succession of marls and carbonate-siliciclastic sandstones randomly intercalated by several thick carbonate beds of debrite origin. The geological setting of the Rječina River Valley and Vinodol Valley is similar to the general settings of the whole 100km long morphostructural unit (Ilirska Bistrica-Novi Vinodolski), which includes Cretaceous and Paleogene limestone situated at the top of the slopes, in the form of cliffs, and Paleogene siliciclastic and flysch-type rocks situated on lower slopes (Mihalić Arbanas et al. 2017). Vinodol Valley is characterized by elongated irregular shape, with a wide range of different landforms types, where karstified carbonate rocks (Đomlija et al. 2014, 2017).

Due to different weathering grades (fresh rock to residual soil) and alteration of competent and incompetent members, flysch rock mass is characterized by significant varieties of rock mass properties. Limestone and sandstone presents stronger, competent rock mass

members, inside which specific types of instabilities occur (e.g., rock falls, rock topples, rock irregular slides). Carbonate fragments, originating from the landslide occurrence in carbonate rock mass, have been mixed with the clayey soils originating from weathering of flysch, and these superficial deposits cover the flysch bedrock along the studied area in various thicknesses. Properties of the competent members and karst, however, are not of the interest for this research.

Atterberg's Limits and grain size distribution

In slope stability analyses, colluvial cover and residual soil (product of flysch rock mass weathering) are considered as materials with similar properties, forming upper layers of the geotechnical profile. It can be seen that clays of intermediate- (CI) to-high (CH) plasticity (Fig. 2) prevail in Grey Istria and Vinodol Valley, while in the Rječina River Valley low (CL) to intermediate plasticity clay (CI) prevails. Depending on the water content semisolid to plastic in consistency.

Grain size distribution analysis, including dry and wet sieving, aerometry and SediGraph methods, show that silt size particles prevail in the superficial layers (Dugonjić Jovančević 2013, Vivoda Prodan 2016, Pajalić et al. 2017, Peranić et al. 2018).

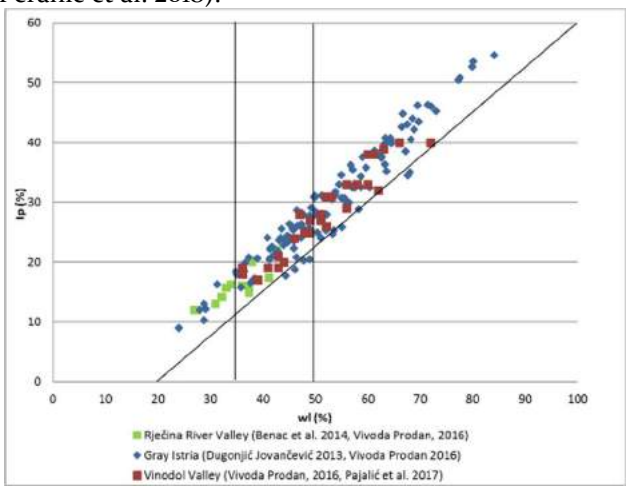

Figure 2 Plasticity chart of the colluvial cover and residual soil (product of flysch rock mass weathering).

Strength parameters

Considering the heterogeneity of materials involved in landslide occurrence in the research area, as well as their different grades of weathering (varying from soil like materials to rock), different laboratory methods were used to determine strength properties.

Mohr-Coulomb shear strength parameters were obtained from laboratory testing in direct shear and ring shear devices on the flysch surface and borehole samples (Benac et al. 2014, Vivoda Prodan 2016, Maček et al. 2017, Peranić 2019). Residual and peak shear strength parameters of flysch samples of different weathering grades show considerable variations (Table 1).

Table 1 Range of shear strength parameters of flysch samples obtained from different studies.

Research area	Test type	c'(kPa)	ϕ (°)	Source
Gray Istria	DS	3*	28*	2
	DS, RS	14-56**	20-31**	1
Rječina River Valley	DS	1-10*	24-29*	3,4
	DS, RS	4-32**	18-35**	1
Vinodol Valley	DS	5*	23*	2
		11-12**	18**	1

DS/RS – direct shear/ring shear apparatus; *- peak values **- residual values; [1] - Vivoda Prodan (2016); [2] – Maček et al. (2017); [3] – Benac et al. (2014); [4] – Peranić (2019).

To determine the uniaxial compression strength (UCS), Point Load Test (PLT) (ISRM 1985) was performed on regular and irregular samples of completely-to-moderately weathered siltstones obtained by boring. The corresponding UCS values tested in Gray Istria are researched by Vivoda Prodan (2016) 21.12-52.8 MPa; Gulam (2012) reports a wide range of UCS values 9.36-87.12 MPa; and Žufić (2011) obtained UCS 6.9-30.4 MPa. The test results of the PLT performed during this research, on irregular fresh siltstone samples from Pazin (tested 1 day after the excavation) showed that the corresponding UCS of this material ranges from 8.42 to 81.28 MPa. UCS values were also estimated using Schmidt rebound value in combination with the unit weight of flysch rock mass 25.5 kN/m^3. Testing performed in Gray Istria (Gulam 2012 and Vivoda Prodan 2016) resulted in the UCS values from 15.4 to 48 MPa. Obtaining the specimens for uniaxial compression testing in the laboratory is almost impossible (only 11 specimens were tested in Žufić (2011), and their values show considerable range of UCS value 5.3-54.03 MPa), and therefore are unreliable for engineering analyses without taking adequate precautions. In the Rječina River Valley PLT testing was performed in November 2018 and the results show UCS value ranged from 15.6 to 54MPa.

Weathering influence on durability characteristics of flysch rock mass

Weathering is the process of alteration and breakdown of rock and soil materials at or near the earth's surface by physical, chemical and biotic processes (Selby 1993). Weathering processes are particularly expressed in incompetent members, such as claystones, shales, and siltstones. The standardized slake durability index in the second cycle is not sufficient to classify the durability of weak rock masses such as siltstones (Gamble 1971, Erguler and Shakoor 2009, Miščević and Vlastelica 2011, Vivoda Prodan 2016, Vivoda Prodan and Arbanas 2016). Because greater weathering of weak rocks during testing was observed, quantification from the fragment size distribution after each of five slaking cycles and new classifications of weak rocks have been proposed by several authors (Erguler and Shakoor 2009, Cano and Tomás 2016). The slake durability index (I_{d_2}) and disintegration ratio (D_{R_2}) were determined to classify the

tested siltstone samples of different weathering grades, and the modified disintegration ratio (D_{RP_2}) was used to determine potential long term degradation of the tested samples. Highly degraded and fragmented fresh sample after each of five cycles, despite of high I_{d_2} value, is visible on Fig. 3.

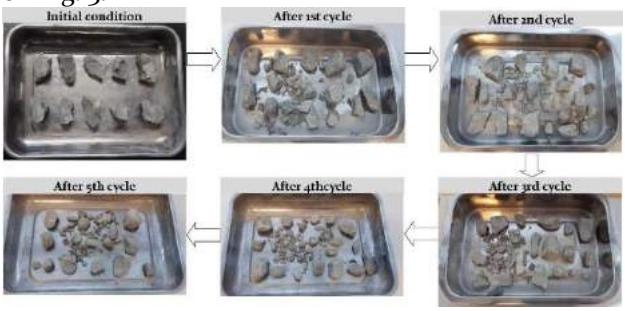

Figure 3 Highly degraded fresh siltstone from Pazin after each of five cycles of the slake durability test with I_{d_2}=86.12 % and D_{RP_2}=0.68.

Table 2 Results of the slake durability tests, including the slake durability index, disintegration ratio and modified disintegration ratio after second cycle, for siltstones of different weathering grades in the study area.

Sample	Slake durability index (I_{d2}) [%]	Disintegration ratio (D_{R2})	Modified disintegration ratio (D_{RP2})
FR Pazin*	86.12	0.68	0.31
FR (1)	88.31	0.65	0.35
MW (2)	89.69	0.60	0.40
FR (3)	97.03	0.81	0.19
MW (4)	95.39	0.79	0.21

* FR flysch sample tested during this research

Table 2 presents the slake durability index, disintegration ratio, and modified disintegration ratio after second cycle, for siltstones of different weathering grades in the study area from previous tests (Vivoda Prodan and Arbanas 2016) and a new fresh siltstone sample from Pazin tested for this research.

Hydraulic properties of the residual soil from flysch rock mass

Soil water retention curve (SWRC) relates the potential energy of a liquid phase (e.g. soil suction) with the variations in the water content of the soil. It has a crucial role when dealing with problems of rainfall infiltration process through the unsaturated part of the slope, as well as for determination of the effective stress in unsaturated soil, thus affecting the soil's shear strength. Hydraulic conductivity function (HCF) is another non-linear soil property function required when analysing the seepage process through unsaturated part of the slope.

SWRC measurement results obtained on soil samples from the Brus Landslide (Grey Istria) and Slani Potok (Vinodol Valley) were reported by Maček et al. (2017). Peranić et al. (2018) and Peranić (2019) have determined SWRC and HCF of the residual soil present at the surface of the Valići Landslide in the Rječina River Valley, which was found to play an important role for the rainfall infiltration process and time required for the slope failure (Peranić et al. 2019). Different measurement techniques (mini-tensiometers, axis-translation technique and dew-point potentiometer) and devices (suction-controlled oedometers, standard and volumetric pressure plate extractors, the HYPROP evaporation method device, and WP4-T dew point potentiometer) were successfully combined to obtain a complete SWRC of the residual soil from the Valići Landslide, both for the adsorption and desorption process. Obtained SWRC measurement results are shown in Fig. 4, while Table 3 summarizes best-fit parameters of the van Genuchten (1980) and Fredlund and Xing (1994) models obtained by a nonlinear regression analysis.

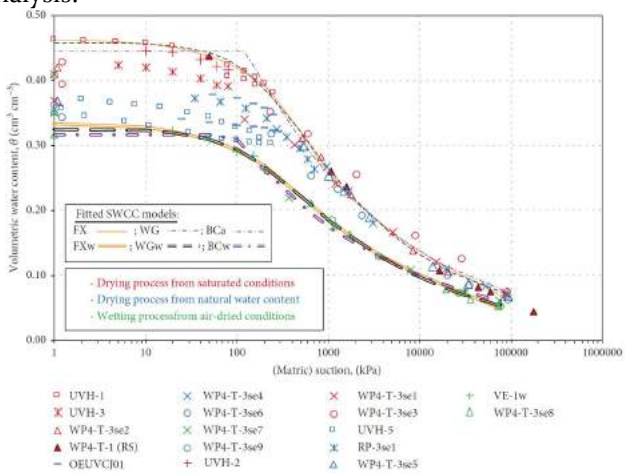

Figure 4 Measurement results and SWRC of residual soil from a flysch rock mass from the Valići Landslide (Peranić et al. 2018).

Table 1. Best fit parameters of the van Genuchten (VG) and Fredlund and Xing (F&X) models (Peranić et al. 2018).

VG	SSR(r^2)	θ_r	α	n	m
drying	0.00049	0.028	0.004	1.186	0.323
wetting	0.00021	0.011	0.005	0.973	0.348
F&X	SSR(r^2)	ψ_r	α	n	m
drying	0.00039	178	300	1.073	0.907
wetting	0.00022	254	284	0.859	1.053

The formation process of the soil covering flysch slopes in the Rječina River Valley was found to results with a complex soil structure that cannot be obtained with standard sample preparation techniques used in laboratory. Instead, undisturbed samples have to be used in order to correctly define hydraulic properties of the soil. For example, different retention properties were obtained for measurements performed on intact and remolded samples (Peranić et al. 2018), while the saturated coefficient of permeability of intact samples (k_s = 4.60E-08 m/s) was found to be around two orders of magnitude higher than was the case for completely remoulded and consolidated samples.

Discussion and Conclusions

Landslides in the research area are mostly caused by terrain condition, material properties, and present geomorphological and physical slope processes influencing the material mechanical behaviour. Presented results show significant dissipation of the investigated values, but some conclusions about the material properties correlated with the past and present instabilities can be drawn.

Clays of intermediate to high plasticity prevail in Grey Istria and Vinodol Valley, while low to intermediate plasticity clays prevail in the Rječina River Valley. Testing of the grain size distribution has shown that silt size particles prevail in the superficial layers. Further on, siltstone samples from flysch rock mass of different weathering grades investigated in this study are highly susceptible to weathering, which causes changes in the durability and geotechnical properties in a short period of time. Fresh samples disintegrate less than moderately weathered samples; therefore, fewer drying-wetting cycles are required to reach the maximum possible degradation. The standard slake durability index increases the slaking resistance of the tested siltstone samples by at least one class.

Strength parameters of flysch samples of different weathering grades show considerable variations (cohesion varies from 3-56 kPa, and friction angle is from 18-35 °). The UCS values estimated through PLT testing show a great range of values collected from different previous researches (6.9-87.12 MPa) and confirmed in testing performed during this research (8.42-81.28 MPa) in Gray Istria. Obtained UCS values in Rječina River Valley ranged from 15.6 to 54MPa. One of the limitations for correct UCS determination in the laboratory, is that cylindrical samples of the flysch rock for uniaxial compression testing are almost impossible to obtain.

Presented results highlighted the importance of the unsaturated zone existing in a flysch slope for maintaining the slope stable during prolonged periods of heavy rainfall. However, a specific position of the flysch-karst contact plays a significant role for rainfall infiltration, favouring the pore pressure rising, decrease in material strength properties and landslide triggering.

Acknowledgments

The authors would like to acknowledge the project Research Infrastructure Development at the University of Rijeka Campus (RC.2.2.06-0001) co-financed by the European Regional Development Fund (EFRR) and the Ministry of Science, Education and Sports of the Republic of Croatia, as well as support of the University in Rijeka through the projects "Analysis of the rock mass and instability phenomena along the karst-flysch contacts "(18.06.2.1.01.).

References

Arbanas Ž., Dugonjić S. (2010) Landslide Risk Increasing Caused by highway construction, International Symposium in Pacific Rim, 26 – 30th April 2010., Taipei, Taiwan, pp 333-343.

Arbanas Ž., Dugonjić S., Benac Č. (2011) Causes of small scale landslides in flysch deposits of Istria, Croatia, Proceedings of Second World Landslides Forum, Rome, 03-07th October, 2011, 221-226.

Arbanas Ž, Dugonjić S, Benac Č (2013) Causes of small scale landslides in Flysch deposits of Istria, Croatia. Landslide science and practice, volume I: landslide inventory and susceptibility and hazard zoning. Margottini C, Canuti P, Sassa K (eds). Springer, Berlin, pp 221–226.

Arbanas Ž., Mihalić Arbanas S., Vivoda Prodan M., Peranić J., Sečanj M., Bernat Gazibara S., Krkač M. (2017) Preliminary Investigations and Numerical Simulations of a Landslide Reactivation. In: Mikos M., Tiwari B., Yin Y., Sassa K. (eds) Advancing Culture of Living with Landslides. WLF 2017. Springer, Cham

Benac Č Arbanas Ž, Jurak V, Oštrić M, Ožanić N (2005a) Complex landslide in the Rječina valley (Croatia): origin and sliding mechanism. Bull Eng Geol Environ 64(4): 361–371

Benac Č., Jurak V., Oštrić M., Holjević D., Petrović G. (2005b) Appearance of exceeded erosion in the Salt creek area (Vinodol Valley). In: Velić I, Vlahović I, Biondić R (eds) Summaries of 3rd Croatian geological congress. Croatian Geological Institute, Zagreb, pp 173-174.

Benac Č., Dugonjić S., Arbanas Ž., Oštrić M., Jurak V. (2009) The Origin Of Instability Phenomena Along The Karst-Flysch Contacts, ISRM International Symposium EUROCK 2009: Rock engineering in difficult ground conditions soft rock and karst, 29 – 31th October, Cavtat, Croatia, pp 757-761.

Benac Č., Dugonjić S., Vivoda M., Oštrić M., Arbanas, Ž. (2011) A complex landslide in the Rječina Valley: results of monitoring 1998-2010, Geologia Croatica: journal of the Croatian Geological Survey and the Croatian Geological Society. 64 (2011), 3; pp 239-249.

Benac Č., Oštrić M., Dugonjić Jovančević S. (2014) Geotechnical properties in relation to grain-size and mineral composition: The Grohovo landslide case study (Croatia). Geologia Croatica : journal of the Croatian Geological Survey and the Croatian Geological Society, 67 (2014), 2; 127-136. doi:10.4154/gc.2014.09

Bernat S., Đomlija P., Mihalić Arbanas S. (2014) Slope movements and erosion phenomena in the Dubračina river basin: A geomorphological approach. Proceedings of 1st regional symposium on landslides in the Adriatic-Balkan region ''Landslide and flood hazard assessment'', 6-9 March, Zagreb, Croatia. pp 79–84.

Cano M. and Tomás R. (2016) Proposal of a new parameter for the weathering characterization of carbonate flysch-like rock masses: The Potential Degradation Index (PDI). Rock Mechanics and Rock Engineering vol. 49, no. 7: 2623–2640.

Dugonjić Jovančević, S. (2013) Landslide hazard assessment on flysxh slopes, Dissertation, Faculty of Civil Engineering, University of Rijeka. (in Croatian)

Dugonjić, S., Arbanas Ž., Benac Č. (2008) Assessment of landslide hazard on flysch slopes, 5th Conference of Slovenian geotechnics, 9th Šuklje day, 12-14th June 2008, Nova Gorica, Slovenia, pp. 263-272.

Dugonjić Jovančević S., Arbanas Ž. (2012) Recent landslides on the Istrian Peninsula, Croatia, Natural hazards. Vol.62, 3; pp 1323-1338

Dugonjić Jovančević S., Arbanas Ž., Benac Č., Mihalić Arbanas S. (2012) Landslide susceptibility analyses in flysch areas in the north-eastern part of the Adriatic coast, Risk Analysis VIII, Brebbia,

Carlos (ed.), Southampton: WIT Press, doi:10.2495/RISK120211, pp 237-248.

Dugonjić Jovančević S., Arbanas Ž. (2017) Influence of the runout potential on landslide-susceptible areas along the flysch–karst contact in Istria, Croatia. Natural hazards, 85 (2017), 3; 1347-1362. doi:10.1007/s11069-016-2640-2

Đomlija P. (2018) Identification and clasification of landslides and erosion by visual interpretation of digital elevation model of Vinodol Valley, Dissertation, Faculty of Mining, geology and petroleum; University of Zagreb (in Croatian).

Đomlija P., Bernat S., Mihalić Arbanas S., Benac Č. (2014) Landslide inventory in the area of Dubračina River Basin (Croatia), Landslide Science for a Safer Geoenvironment, Volume 2: Methods of Landslide Studies (Sassa K., Canuti P., Yin Y. eds). Switzerland: Springer International Publishing, pp 837-842.

Đomlija P., Bočić N., Mihalić Arbanas S. (2017) Identification of geomorphological units and hazardous processes in the Vinodol Valley, Proceedings of the 2nd Regional Symposium on Landslides in the Adriatic-Balkan Region (Abolmasov, B.; Marjanović, M.; Đurić, U. eds). Belgrade: University of Belgrade, Faculty of Mining and Geology, pp 109-116

Eberhardt E., Thuro K., Luginbuehl M. (2005) Slope instability mechanisms in dipping interbedded conglomerates and weathered marls—the 1999 Rufi landslide, Switzerland. Eng Geol 77(1–2): 35–56. doi: 10.1016/j.enggeo.2004.08.004

Erguler Z.A. and Shakoor A. (2009) Quantification of fragment size distribution of clay-bearing rocks after slake durability testing. Environmental & Engineering Geoscience, vol. 15, no. 2: 81- 89.

Fredlund D.G., Xing A. (1994) Equations for the soil-water characteristic curve, Canadian Geotechnical Journal, 31(4): 521–532.

Gamble J.C. (1971) Durability-plasticity classification of shales and other argillaceous rocks. Ph.D. thesis, University of Illinois.

Gulam V. (2012) Erosion of bed lands in central Istria flysch, Dissertation, University in Zagreb, Faculty of Mining-geology-petroleum, Zagreb.

ISRM (1985) Suggested Methods for Determining Point Load Strength, Int. J. Rock Mech. Min. Sci. & Geomech. Abstr. Pergamon Press, Great Britain, Vol. 22:53-60.

Maček M., Petkovšek A., Arbanas Ž., Mikoš M. (2017) Geotechnical aspects of landslides in flysch in Slovenia and Croatia. Proceedings of 2nd regional symposium on landslides in the Adriatic-Balkan region, 14-16 My, Belgrade, Serbia. pp 25–31.

Marinčić S. (1981) Eocene flysch of the Adriatic area. Geološki vjesnik 23:27–38.

Mihalić S., Krkač M., Arbanas Ž., Dugonjić S. (2011) Analysis of sliding hazard in wider area of Brus landslide, Proceedings of the 15th European conference on soil mechanics and geotechnical engineering, Athens, 12-15th September 2011, pp 1377-1382.

Mihalić Arbanas S., Sečanj M., Bernat Gazibara S., Krkač, M., Begić, H., Džindo A., Zekan S., Arbanas Ž. (2017) Landslides in the Dinarides and Pannonian Basin — from the largest historical and recent landslides in Croatia to catastrophic landslides caused by Cyclone Tamara (2014) in Bosnia and Herzegovina, Landslides, 14 (2017), 6; 1861-1876, doi:10.1007/s10346-017-0880-1.

Miščević P. and Vlastelica G. (2011) Durability characterization of marls from the region of Dalmatia, Croatia. Geotechnical and Geological Engineering, vol. 29, no. 5: 771–781.

Pajalić S., Đomlija P., Jagodnik V., Arbanas Ž. (2017) Diversity of Materials in Landslide Bodies in the Vinodol Valley, Croatia, Advancing Culture of Living with Landslides (Mikoš, M.; Vilímek, V.; Yin, Y.; Sassa, K. eds), Berlin: Springer, pp 507-516.

Peranić J. (2019) Importance of geotechnical cross-section unsaturated zone for landslide occurrence in flysch deposits, Doctoral dissertation, Faculty of civil engineering, University of Rijeka, https://urn.nsk.hr/urn:nbn:hr:157:773572

Peranić J, Arbanas Ž (accepted, in press) Impact of the wetting process on the hydro-mechanical behavior of unsaturated residual soil from flysch rock mass: preliminary results, Bulletin of Engineering Geology and the Environment. doi: 10.1007/s10064-019-01604-0

Peranić J, Arbanas Ž, Cuomo S, Maček M (2018) Soil-Water Characteristic Curve of Residual Soil from a Flysch Rock Mass, Geofluids, Article ID 6297819, 2018:15 pages. doi:10.1155/2018/6297819

Peranić J., Moscariello M., Cuomo S., Arbanas Ž. (in review) Hydro-mechanical properties of unsaturated residual soil from a flysch rock mass.

Peranić J, Arbanas Ž, Cuomo S, Maček M (2018) Soil-Water Characteristic Curve of Residual Soil from a Flysch Rock Mass, Geofluids, Article ID 6297819, 2018:15 pages. doi:10.1155/2018/6297819

Selby M.J. (1993) Hillslope materials and processes. Oxford University Press, Oxford

Van Genuchten M.T. (1980) A closed-form equation for predicting the hydraulic conductivity of unsaturated soils, Soil Science Society of America Journal, 44 (5): 892–898.

Vivoda M., Benac Č., Žic E., Đomlija P., Dugonjić Jovančević S. (2012) Geohazard in the Rječina River Valley in past and present, Hrvatske vode, Journal for water economy, 20 (2012), 81, pp 105-116. (in Croatian)

Vivoda Prodan M. (2016) The influence of weathering process on residual shear strength of fine grained lithological flysch components, Doctoral dissertation, Faculty of Civil Engineering, University of Rijeka. (in Croatian)

Vivoda Prodan M., Arbanas Ž. (2016) Weathering Influence on Properties of Siltstones from Istria, Croatia. Advances in Materials Science and Engineering. 2016 (2016), 3073202; 1-15.

Vivoda Prodan M., Mileusnić M., Mihalić Arbanas S., Arbanas Ž. (2017) Influence of weathering processes on the shear strength of siltstones from a flysch rock mass along the northern Adriatic coast of Croatia. (Bulletin of engineering geology and the environment. 76 (2017), 2; 695-711.

Žufić E. (2011) Investigation of geotechnical properties of flysch rock mass in Istria area. M.S. thesis, University of Zagreb, Croatia (in Croatian)

doi.org/ 10.35123/ReSyLAB_2019_33

Analysis of Geohazards in Road Construction

Ljubomir Palikuća[(1)], Mato Uljarević[(2)], Đorđe Raljić[(1)], Boško Miljević[(1)]

1) Integral Inženjering a.d, Department of Geomechanics, Laktaši, Omladinska 44, 78 250,

2) University of Banjaluka, Faculty of Architecture, Civil Engineering and Geodesy, Banja Luka, Vojvode Stepe Stepanovića 77/3, 78 000,

Abstract Roads, as line objects, are largely exposed to the different conditions imposed by the area through which the route is laid. One of the important parameters that influence the final definition of a road route is the analysis of geohazards in the area of route management. Reliable analysis of the hazardous phenomena of geo-materials movement in the route area will contribute to the proper decisions of the road route adoption. The failures made at this stage will manifest as a direct influence on the often significant increase in the investment value of the project. Hereby, the authors of this work have given a critical review of project approach in the implementation of the characteristic section of the road in the region, with the aim of pointing out the shortcomings in the process of planning and designing of abovementioned. A site with relatively unstable terrain has been selected for the section, where works on road construction bring geo substrates into motion with high probability.

Keywords geo hazard, roads, project approach

Introduction

The process of designing roads is characterized by a high degree of complexity and multidisciplinarity. In order to define the spatial position of these objects that are "laid" in the field, it is necessary to analyze different parameters types. The extent and type of previous analyzes will vary depending on the importance of the road and the desired level of service. The end result of all the analysis and the design process itself is the route, chosen in such a way that an acceptable solution is obtained with minimal environmental damage and minimal investment. A quality project approach at all stages of design will provide reliable bases for investment decisions with the aim of obtaining rational projects. Unfortunately, we are witnessing frequent consequences of inadequate approach during roads designing. The following is a critical analysis of the project approach on a typical example - a section of the road in the region. A section of an important Balkan road is analysed. A section of the 150 m highway, situationally shown in Figure 1, with a characteristic cross section that will be presented through the project implementation phases, with an emphasis on the project approach, was selected for analysis.

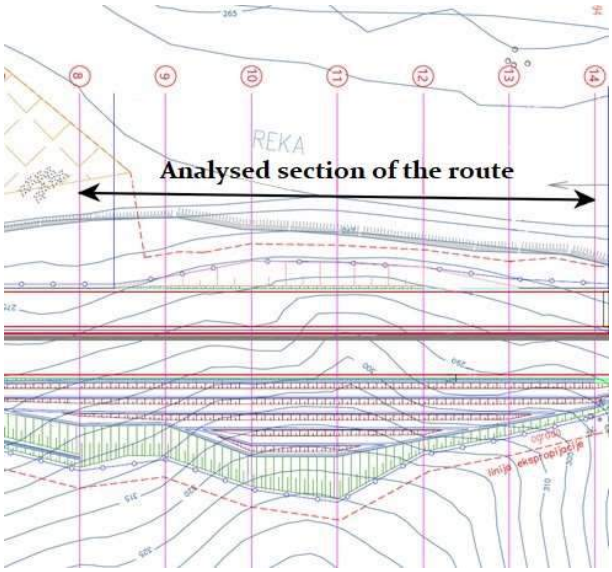

Figure 1 Analysed section of the route in the length of 150 m

Crucial question during the infrastructure facilities designing is gathering existing data at the area of the section in question. During the process of collecting and analysing available data, relevant information will be provided about the benefits as well as problems we may encounter during the implementation of a future project. The lithological type of rock mass, geological age, tectonic damage, extent of decomposition, physical - mechanical characteristics and a number of other factors need to be determined on the basis of the collection of existing documentation. The information from the previous analysis will usable in the planning of both optimal (qualitative and quantitative) exploratory works in order to provide reliable bases for the next phases of designing the project documentation of the road in question.

Project realization phases

The implementation of the project of the road in question took several years, with significant difficulties and the extension of the deadline for completion of works. Further on, as already mentioned, the analysis will be performed on one of the slopes of the road, where during the project implementation damage to the structure defined by the project occured, followed by a series of rehabilitation solutions.

Phase 1 (2010-2014)

In 2010, exploration works, which included performation of geo - exploration wells and excavations were done at the site. In the area that is the subject of analysis of this work,

4 exploratory excavations, with variables depth (1.10 m - 2.00 m) were performed. On the basis of a very limited volume of research works, values of physical - mechanical parameters of layers were adopted, and the design solution was defined, taking into account abovementioned. Table 1 lists the layer parameter values.

Table 1 The values of the parameters defined in the 2010 study are reduced by partial safety coefficients

Layer	γ (kN/m³)	φ (°)	c (kPa)
Layer 1	19.00	24.00	12.50
Layer 2	21.00	28.00	62.50
Layer 3	25.00	32.00	312.50
Layer 4	27.00	40.00	625.00

Figure 2 shows cross section 11 with the thicknesses of the layers used in the stability calculation, while Figure 3 shows the same section with the solution defined by the phase 1 project.

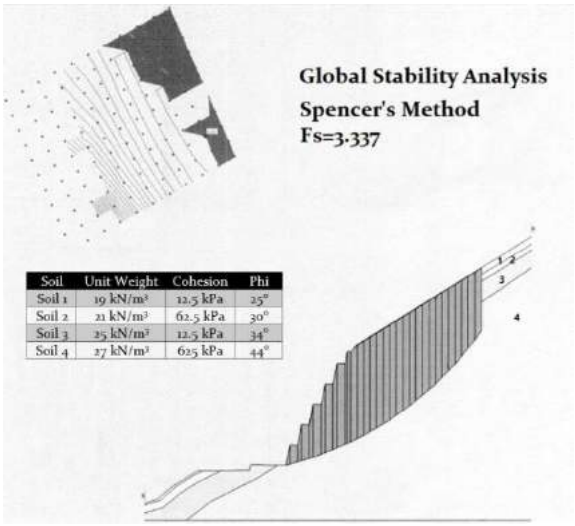

Figure 2 Cross section 11 with geological layers used in the stability calculation

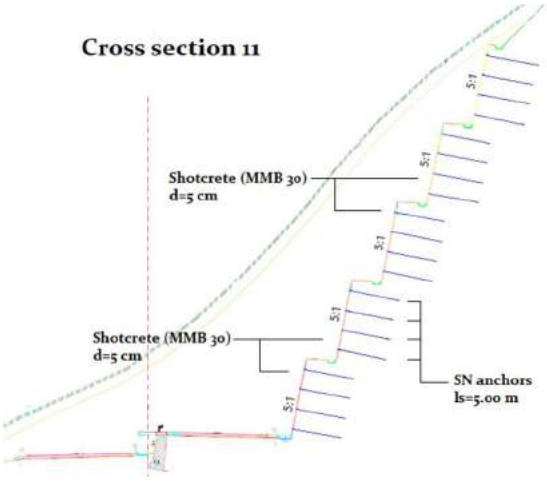

Figure 3 Transverse profile design solution 11

It is noted that the design solution in phase 1, defined on the basis of previous research, was accompanied by certain shortcomings. In the stability analysis, a rough deviation from the adopted parameters was made, all for the purpose of proof of stability and confirmation of the parameters defined during the investigation works. Layer 3 parameters are reduced multiple times to give a delusion of safety factor during the stability calculation. The adopted solution is not justified from the stability aspect, since the safety factor for the adopted geometry is Fs = 3,337, which indicates that a much smaller volume of earthwork and higher slopes inclines could be accessed.

Phase 2 (2014 - 2016)

During 2014, a significant displacement of the "cutted" slope was registered on the section in question, which caused a delay in construction, and a new design review of the slope stability and reliability of the solution defined in the first phase. During the new design phase, additional exploratory work was performed at the site, which involved the construction of 10 exploratory wells (10 - 36 m depth). Based on the mentioned investigations, the values of the layer parameters, showed in Table 2, were defined.

Table 2 Average values of parameters obtained by laboratory testing of samples (parameters marked with * - defined by back analysis, due to the impossibility of testing samples obtained by exploratory drilling).

Layer	γ_{pr} (kN/m³)	φ_{pr} (°)	c_{pr} (kPa)
Layer 1a	19.28	28.00	3.00
Layer 1b	19.18	27.00	23.00
Layer 2	18.50	21.50	8.50
Layer 3	28.50	20.00*	9.50*
Layer 4	29.50	50.00	11220.00

As the geo – exploratory drilling core provided the opportunity to test the uniaxial strength on the samples from layer 3 and layer 4, the mentioned test was performed and, in accordance with the literature recommendations, the parameters of shear strength were determined using the Hoek & Brown classification. The parameter values are showed in Table 3.

Table 3 Values of physic-mechanical parameters defined by Hoek & Brown classification

Layer	σa (MPa)	H (m)	φ (°)	c (kPa)
Layer 3	10.00	8.00	22.00	19.00
		55.00	14.00	43.00
	20.00	8.00	45.00	76.00
		55.00	34.00	170.00
Layer 4	30.00	8.00	51.00	118.00
		55.00	41.00	248.00
	50.00	8.00	59.00	353.00
		55.00	51.00	524.00

- H = 8 m (height of single berm)
- H = 55 m (the entire slope)

The parameter values determined during this phase are quite wide, as is the thickness of the established soil layers. Inspection of the project documentation revealed the absence of two wells of 30 m and 40 m depth, positioned in the zone that is the subject of analysis of this work. This is a confirmation of inadequately completed additional works, which were supposed to provide the information necessary for a good definition of both the thickness of the layers and the parameters of each layer with which the slope stability calculation is made. The geological cross sections are identical to those defined during Phase 1, which is evidence that the works performed in 2015 did not provide absolutely any additional information on the geological structure of the terrain, which was their primary purpose and task. All the work and analysis previously performed should have served as the basis for the 2016 project, which cannot be said to be the case. Since the project does not contain a global stability calculation, the parameters used in the stress and deformation analysis are given in Table 4.

Table 4 Values of physic-mechanical parameters used in the 2016 project

Layer	γ (kN/m³)	φ (°)	c (kPa)
Layer 2	22.00	27.00	15.00
Layer 3	27.00	32.00	40.00
Layer 4	28.00	49.00	100.00

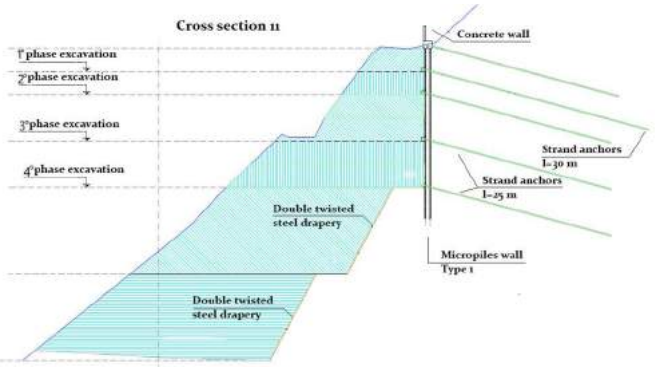

Figure 4 Transversal profile 11 with the adopted 2016 design solution

Phase 3 (2016 - 2017)

Phase 3 is basically a refined version of the 2016 project and was designed during 2017. The analysis of the project documentation and the solution revealed the use of the changed values of the physical and mechanical parameters, whose values are defined in Table 5.

Table 5 Values of physic-mechanical parameters used in the 2017 project

Layer	γ (kN/m³)	φ (°)	c (kPa)
Layer 2	20.00	30.00	30.00
Layer 3	22.00	32.00	75.00
Layer 4	24.00	36.00	100.00

The solution defined by the 2017 project was implemented in the terrain (Fig. 5). During 2018, the constructed structure was demolished on the observed section of the route. A worrying fact is that all the calculations of stability, stress and deformation were made exactly in the zone where the structural failure occurred. The realistic model proved the inaccuracy of the data used in the calculations and the inadequacy of the project approach in finding solutions.

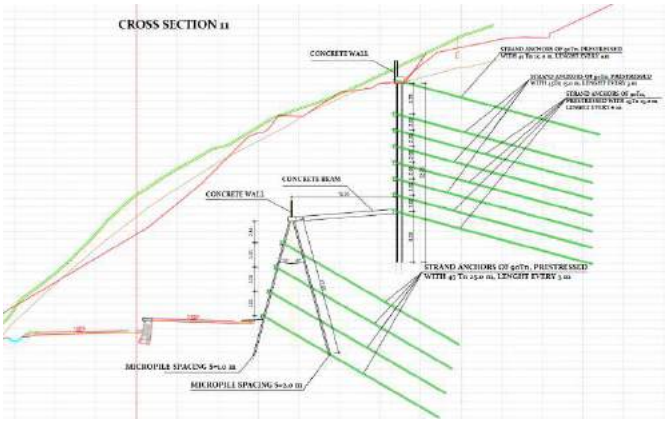

Figure 5 Cross section 11 with the adopted decision from 2017

It is necessary to point out the neglect of temperature influences in the calculation of geotechnical anchors and the consequences that such a design approach can cause. Studies have shown that by reducing the gap between anchors, the temperature influence is significantly increased compared to the geostatic one in the anchor, and it is to be expected that a reserve in the bearing capacity of the anchor for geostatic loading will not be sufficient. This can be considered as a disadvantage in the design approach when defining the solution in phase no. 3. At the moment when the displacement increment was noted, the designer's proposal was to tighten the anchors to "reduce" displacements and stabilize the structure, potentially contributing to the collapse of the structure. The temperature load, in the case of dimensioning of geotechnical anchors, is cyclical and leads to a considerable limitation of the permissible stresses in the anchors (Uljarević et al. 2019).

Phase 4 (2018 - 2019)

After the collapse of the structure and the overturn of a significant quantity of material on the route, urgent rehabilitation measures were initiated and the design solution for the stabilization of the slope in question was defined (Fig. 6). During the first half of 2018, geophysical tests were also conducted to identify potential sliding zones. Test results showed that potential sliding zones with extremely high slip tendency were spread at depths of 10 - 25 m, but additional exploratory work was done at the end of 2018 for the needs of the new project. The slope remediation and stabilization project on the section in question has undergone several changes during 2018 and 2019 and on this occasion new values of physical and

mechanical parameters are shown in the calculations shown in Table 6.

Table 6 - Values of physic-mechanical parameters used in the 2018 and 2019 project

Layer	γ (kN/m³)	φ (°)	c (kPa)
Layer 2	26.00	34.00	41.00
Layer 3	27.00	36.00	70.00
Layer 4	26.00	36.00	48.00

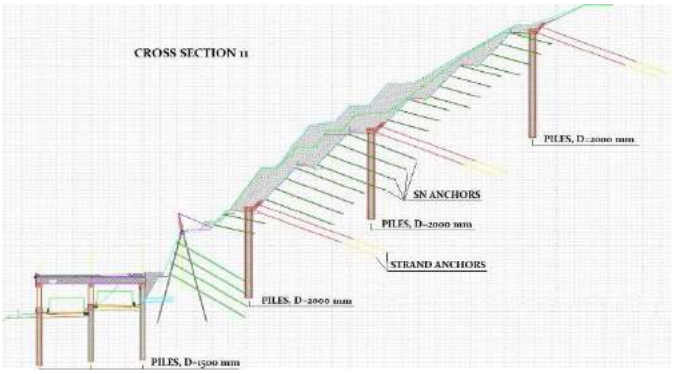

Figure 6 Transversal profile 11 with the adopted 2019 design solution.

For the sake of comparison in Table 7, the safety factors of a natural slope, excluding construction works, are presented, which are defined on the basis of the parameters obtained by exploratory works by stages. The data in the table qualitatively show the reliability of exploratory work in defining geo-technical parameters according to the above phases.

Table 7 Natural slope safety factor values by phases

Design phase	Safety factor
Phase 1 (non-technical parameters)	4.269
Phase 1 (technical parameters)	2.708
Phase 2	0.971
Phase 3	1.132
Phase 4	1.207

The data in Table 7 indicate an inadequate critical review of the results of the investigative work. Simply obtained results of exploratory works should be reviewed on a natural slope. Too high values of the factor of safety, for a given slope geometry, seem unrealistic without further testing. Likewise, the safety factor values of less than one raise the question of possible slope maintenance at a relative standstill.

Conclusion

Based on all the above information, a number of conclusions can be drawn about the consequences of an inadequate project approach in the implementation of infrastructure facilities. The collection of existing data, as well as the development of new investigative works, if needed, are one of the basic steps in the design process itself. Of great importance is the quality and scope of the investigations carried out, as they directly condition the quality of data on soil parameters. The reliability of results of analysis of potential landslides is based mostly on accuracy of input parameters, which define the soil in different conditions (Uljarević et al. 2017). Lack of exploratory work and inadequately determined soil physical and mechanical parameters will inevitably lead to the solutions discussed in this work. Overlooked in the initial design phase, deceived the designers in each successive phase and made it impossible to see the real parameters as a whole. Insufficient research has made it difficult to know the geological conditions of the site in question. The impacts of water on the slope in question were significantly neglected, both during the investigative works and during the design process, which further contributed to the adoption of poor quality and inadequate solutions. It is evident that in solving with such a complex problem from the standpoint of geomechanics and geotechnics, the process is completely reversed. During the design process, the physical - mechanical soil parameters were constantly adjusted to the design solutions, not the design solution to the physical - mechanical parameters. This fact becomes one of the key problems. Intensive bidding with parameter values and insisting on one of the project solutions led, first, to a significant extension of the project implementation time, and then to several times higher the cost of the route itself. From the realization report on the road segment in question it is clear that defining of an optimal design based on uncertain incoming parameters was less possible. Had there been adequate explorations and analysis done prior it is possible that the design solutions would have asked for a situational and height correction of the road route. It is possible that the final solution would also be optimal, but the initial solution would greatly eliminate the additional costs due to the extension of works, design delays and, ultimately, the direct loss of revenue from the early commissioning of the road.

References

GEO-SLOPE International Ltd: "Stability Modeling with SLOPE/W 2007 Version, An Engineering Methodology", Third Edition, March 2008.

G.N. Smith, I. Smith: "Elements of Soil Mechanics, Seventh Edition", Blackwell Science, UK, 1998.

Powell J.J.M. Clayton C.R.I., Field geotechnical testing, ICE Manuel of geotechnical engineering (629 - 652), Institution of Civil Engineers,2012

Uljarević M., Milovanović S., Vukomanović R., (2019) Design of geotechnical anchors on the influence of temperature, Izgradnja 73. 3-4, 132-136.

Uljarević M., Palikuća Lj., Biorac D., (2017) Realibility of Defined Geotechnical Parameters in Implementation of Geotechnical Design, Procedings of 11th International Tunneling and Underground Structures Conference, 23rd September 2017. Ljubljana, Slovenia. pp 41-47

doi.org/ 10.35123/ReSyLAB_2019_34

Current state of landslides and slopes management in the area of Srebrenik, Bosnia and Herzegovina

Maksida Zukić[(1)], Sabid Zekan[(2)], Izudin Đulović[(2)], Nedžad Ribić[(2)], Dženan Ibrahimović[(2)],

1) Municipality Srebrenik, maksida.zukic@outlook.com

2) University of Tuzla, sabid.zekan@untz.ba, izudin.dulovic@untz.ba, nedzad.ribic@untz.ba, dzenanrudarstvo@gmail.com

Abstract Landslides and floods are headmost hazard factors in the municipality of Srebrenik. They occur after heavy rainfall, especially during May and June. Floods occur in the narrow area around the Tinja river, while landslides occur in the broader area of the municipality. Thanks to the UNDP's and the assistance of the Government of Japan, landslide's cadastre was created and partial mapping of terrain's stability was performed. However, the cadastre is not sufficient to remediate 350 registered landslides. The most of the municipality's surface is mountainous area, built of weak rocks, which are susceptible to sliding. The area has the features of the potentially unstable slopes.

The Srebrenik municipality does not have financial resources required to stabilize all the landslides. Therefore, besides the landslide cadastre, management of landslides and slopes is well justified as an alternative solution. The management of landslides and slopes is not unified and there are no existing rules how and what to do. Also, there are no landslide and slope management regulations in Bosnia and Herzegovina.

This paper presents an example of landslide and slope management in Srebrenik. In addition, we are analyzing the possibility of developing Bosnian Landslides Investigation and Stabilization Methodology, (BLISM). The aim of this methodology is to achieve sustainable social communities located on the slopes in case of insufficient money available for landslides' stabilization. In Bosnia, a serious problem of the so-called illegal urbanisation, related to slopes, would be managed by the BLISM. Therefore, development and the application of methodology enable the sustainable development of the country.

Keywords: landslides, Srebrenik, slopes, methodology

Introduction

The municipality of Srebrenik covers an area of 248 km² and is located in the north-eastern part of Bosnia and Herzegovina. Urban area consists of 10% of the municipality's total area or approx. 25 km² The population density is cca 172 inhabitants/km², but in the urban areas has a concentration of 1700 inhabitants/km². However, detailed regulation plans have been drawn up only for around 3,5 km² out of a total of 25 km² of urban areas. The basis for the development of spatial and regulatory plans was a general geological map of 1:100000, which is insufficient for detailed geological-geotechnical analysis for the best urban regulation.

After heavy rainfall in 2014, a total of 350 landslides was registered manily in urban areas of the municipality. By 2019, several landslides that were a risk to human lives and infrastructure objects, were stabilized. There is no adequate monitoring applied on these landslides, only urgent stabilization measures are available if necessary.

Geological characteristics of Srebrenik area

Relief

The orography of the municipality's terrain is quite complex. The eastern and western parts of the terrain are the slopes of the Majevica and Trebovac mountains. The central part is located in the Tinja river valley. These relief characteristics are the result of geological structure and structural-tectonic relations in the area

The result of the area's lithological structure is the development of the relatively dense hydrographic network. The terrain at a higher elevation is exposed to the natural erosion and the lower terrain around the water flow to the accumulation process. Also, human activity in urban areas causes uncontrolled construction.

The average altitude is approximately 450 m. The largest part of the area belongs to the hilly - mountainous relief (65 %) and is within the altitude interval of between 300 and 500 m. Flatland areas cover up to 8 % along alluvial deposits of the Tinja river. Remaining 27 % of the municipality terrain is in the slight inclination.

Geological structure

The terrain of the municipality is characterized by a complex geological structure. The Mesozoic is formed of Jurassic ophiolite melange, discovered in the Jasenica, Zahirovići, Gornji Srebrenik, and Sladna settlements, as well as, Cretaceous sediments discovered in very small areas nearby Podpeć and Straža settlements. Cenozoic is denoted by marine and lake sediments. Marine sediments are: Paleocene-Eocene clasts and carbonates, Miocene clasts and carbonates, Pliocene clasts and quaternary clasts. The lake sediments are Lower Miocene clast series of very heterogeneous lithological composition, represented by conglomerates with different types of binders, sandstones, marls and clays.

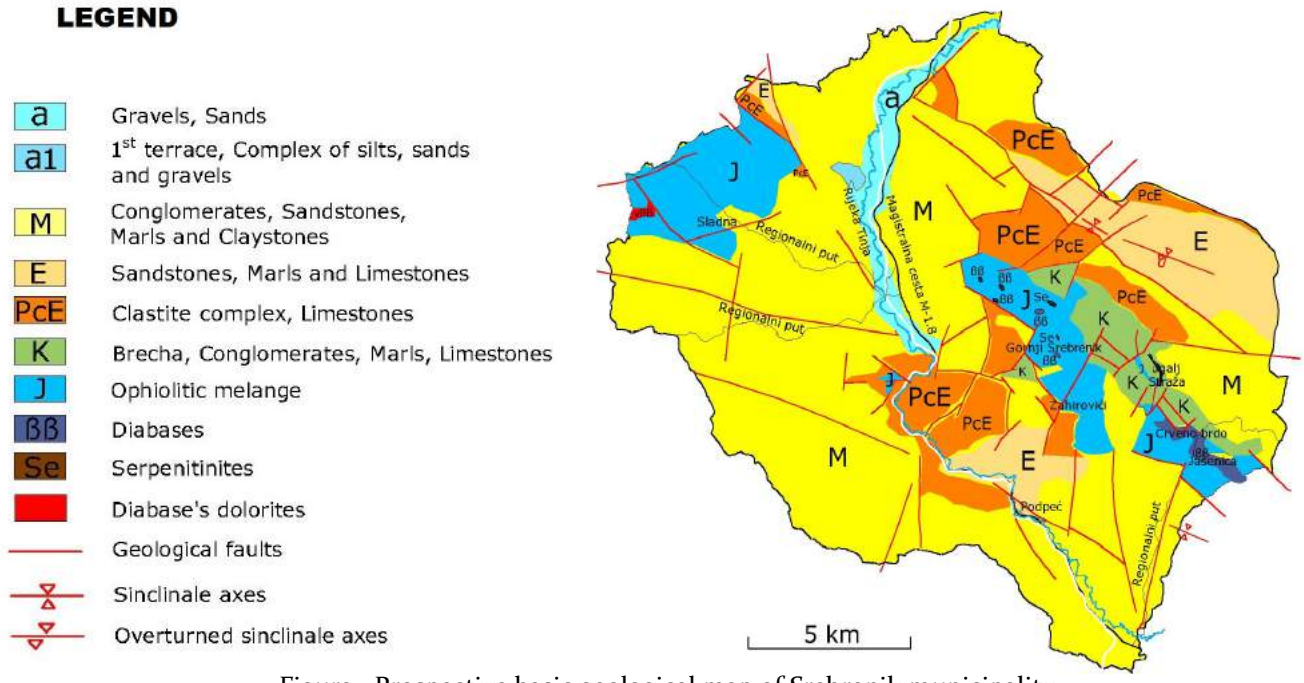

Figure 1 Prospective basic geological map of Srebrenik municipality

Engineering-geological characteristics

A complex lithological composition with frequent change of lithological units causes variable physical and mechanical properties of the rocks. As a consequence, surface decomposition processes are very diverse.

Different forms of surface erosion, such as linear, lateral, planar, are present in the IG process, resulting in different relief forms such as: bays, creeks and river valleys, etc. In general, engineering-geological process are presented by eluvial and deluvial soil sediments which cover substrate rocks. Consequences of the process are most often represented by numerous smaller to larger landslides.

Landslides are formed on slopes of varying inclination, mostly after heavy rainfall or melting of snow. Sliding depths are usual up to 10 meters. The causes of landslides are various natural and anthropogenic impacts on slopes. In general, there are landslides within the existing urban slopes due to unplanned anthropogenic activity.

Landslides cadastre and stability mapping in Srebrenik

Although, investigation and stabilization of landslides is not clearly defined by law, there are few legalities at different government levels which can be used. Landslide issues relate to multiple social activities such as urban planning, social standard, building culture, and natural phenomena. More scientific disciplines address the problem of landslides: geology, civil engineering, mining, geomorphology, geomechanics, architecture, traffic, forestry and others. In general, the scientific discipline of geotechnics has the capacity to observe landslides from the geological features of the terrain and the occurrence of landslides to remediation and monitoring. However, geotechnics is a young scientific discipline evolving together with environmental engineering disciplines. Development of urban areas and constant requirement for complex structures increase demands for building land. But, it means the more harmful impact on natural slopes and possible triggering of landslides. Due to all the circumstances, it would be difficult to define a special law for landslide treatment and terrain stability.

The term landslides denotes the movement of mass of rock, debris or earth down a slope (Mihalic 1998, Cruden 1991). Terrain stability mapping is widespread in application, and is mostly based on engineering geology. Recently, GIS technology, satellite monitoring, and powerful software that can display maps in different formats have been used to assist in mapping. Terrain stability mapping has been extended to zoning with hazard and risk assessment.

Zonation is the division of land surface into areas and the ranking of these areas according to the degrees of actual or potential hazard from landslides. (Varnes 1984)

Landslides in the territory of Srebrenik Municipality are registered with cadastral records. All important data for a landslide are entered in the cadastral sheet (Figure 2). Landslide records are based on the occurrence of landslides after extreme rainfall since May 2014. So far, 350 landslides have been registered. The total landslide area is approximately 18 ha. The sliding surface is usually shallow and up to 5.0 meters depth.


Bosna i Hercegovina

Federacija BiH

"UPRAVLJANJE RIZICIMA OD KLIZIŠTA"
- KATASTAR KLIZIŠTA -

KATASTARSKI LIST KLIZIŠTA

LIST TEČ.: A - OSNOVNI KARTON KLIZIŠTA

VRSTA POJAVE: LP

KATASTARSKI BROJ: 6H22-100 LP13

1. OPŠTI PODACI - LOKACIJA POJAVE

OPŠTINA / OPĆINA: Srebrenik

Koordinate:

Uža lokalnost: Gornji Srebrenik

x: 4 950 675 y: 6 543 020

Mjesna zajednica: Gornji Srebrenik

z: 495

PRIKAZ POJAVE

Izvod iz satelitskog snimka

Izvod iz inženjerskogeološke karte (skica klizišta)

Fotografije

Figure 2 The part of a cadastre sheet

Sliding velocity is very small with cyclic reactivation and calming. The sliding surface is in contact between the eluvial-deluvial soil and the substrate.

The sliding mass is mostly clayey, with silty-sandy content. The most often triggering is associated with extreme rainfall or decrease strength in soil due to the increase underground water level.

In Bosnia and Herzegovina, the terms: stable, potentially unstable and unstable terrain are used. Potentially unstable terrain corresponds to a non-sliding surface but there is engineering assessment for possible sliding in the future.

Figure 3 shows the stability map for the Srebrenik municipality. Registered landslides are shown on the stability map as unstable terrain. In addition, surfaces that are potentially unstable or sometimes called conditionally stable are shown. Stable and not-inventoried surfaces are the remining area shown on the map.

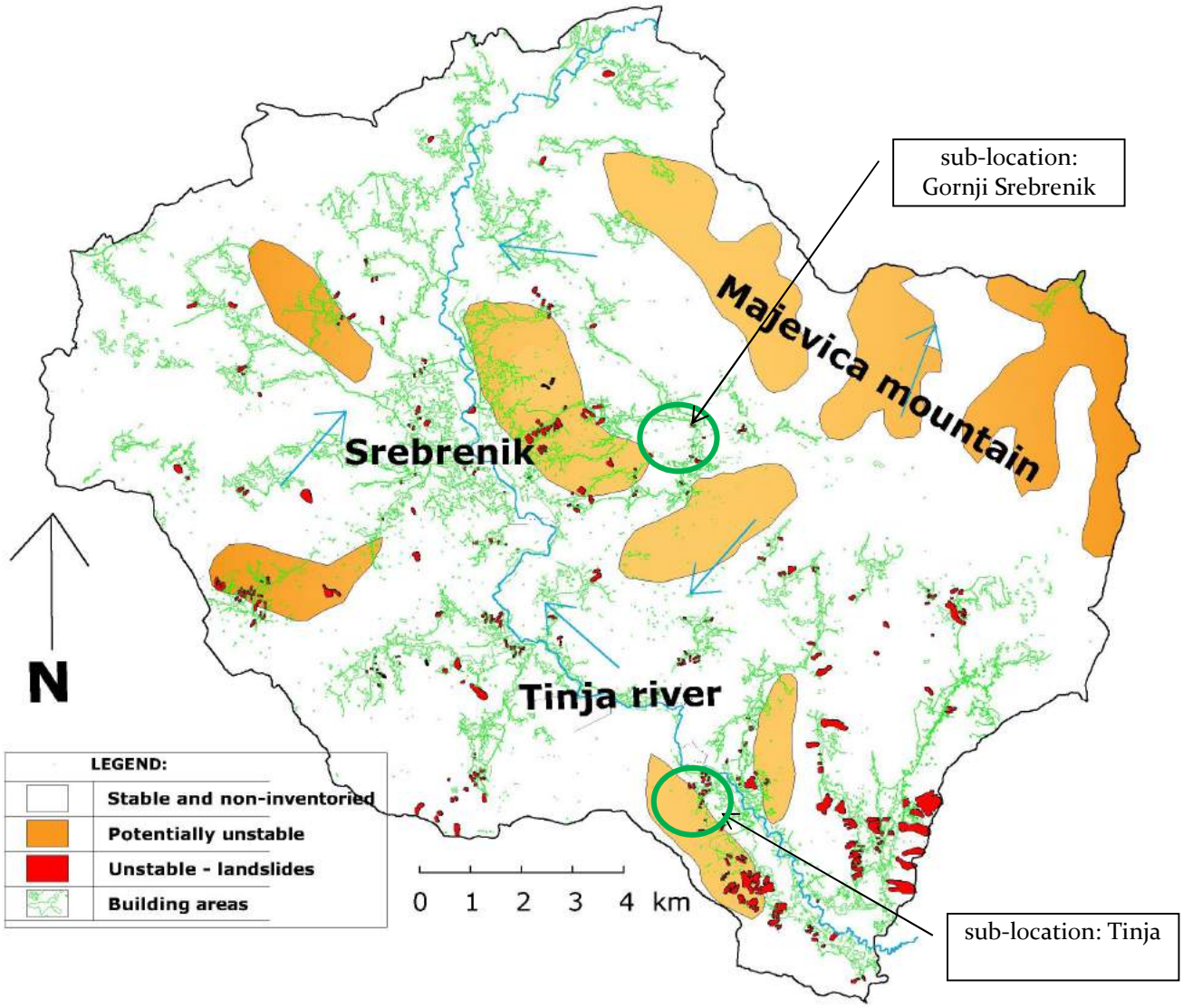

Figure 3 Stability map of Srebrenik municipality

Many methods and techniques were proposed for landslide hazard and risk mapping over the last 40 years. On the contrary, examples of landslide risk zonation are still rare because of difficulties in assessing the

probability of landslide and of the vulnerability of elements at risk (Mihalic S. 1998).

Engineering assessment of boundary between stable and potentially unstable terrain in the Srebrenik municipality is more complicated and, in general, rely on the intuition of investigator. However, there are methods for landslide hazard zonation, but implementation depends on financial and organizational capacities and is insufficient usually.

As an example of poor estimation from stable to potentially unstable and unstable terrain, the Tinja sub-location was considered, shown in Figure 4

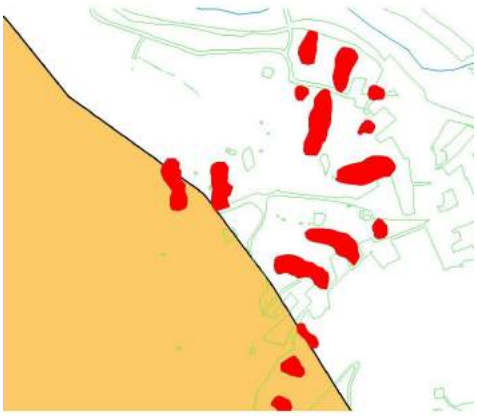

Figure 4 Sub-location of Tinja as an example of mapping mistake

In general, there are descriptive and numerical terms of stability interpretation. Descriptive ones may be for example: "landslide susceptibility", "probability of landslide occurrence", "hazard intensity - low to high" and similar. Numerical explanation most often involves "factor of safety". Also, many methods consist of rating factors to describe amount of stability.

In Figure 4, inventoried landslides are located outside the zone of potentially unstable terrain, in a zone characterized by stable terrain. There are several reasons why these mapping errors occurred. The main reason for such mistakes is the limited investigation capacity and the unsystematic approach to mapping. Landslide hazard assessments should be considered as one of stages in slope management. However, in Bosnia and Herzegovina, and due to limited capabilities, the assessment is often made superficially, which may later lead to some mistakes.

Management of slopes

After the occurrence of many landslides since 2014, the Municipality of Srebrenik has initiated more intensive activities regarding slope management and landslide stabilization. UNDP and the Government of Japan provided significant assistance. Inventory and mapping of landslides were performed along with the creation of landslide cadastres.

However, landslide mapping is not sufficient to reduce the risk of their occurrence. The current mapping state would roughly correspond to a poorly created hazard map. Risk assessment was not prepared?. Risk assessment is much more complex and requires financial investments. Risk assessment, on the other hand, is just one of the steps that provides necessary information for landslides stabilization.

Figure 4, on the Tinja sub-location, shows the phenomenon of occurrence of more landslides in urban than in non-urban areas. The hazard mapping mistakes can be made by different visual assessment in urban and non-urban locations. On the contrary, landslides occur in urban areas as a result of disordered urbanization and greater attention given to micro-locations in urban areas.

Since rigid structures don't display deformation behavior as soil, the differential displacement occurs on the place of the "soil-structure" interaction. Passive pressures and friction forces react on the outer surface of structure in compression zone. In tension zone they react towards the inner surface of structure (Zekan at all. 2018). Soil-structure interaction indicates landsliding as early as it is visible at outer surface. It menas that occurence of the active landslide is more visible close to building structure.

Risk assessment gives a more accurate picture of the vulnerability of an area. (Varnes et al 1984, Lerouiel, 1998) defined the total risk of R_T as the set of damages resulting from the occurrence of a phenomenon. It can be described by the following equation:

$$R_T = \sum_{1}^{n} H \cdot R_i \cdot V_i$$

where are:

H - hazard or the phenomenon occurence probablity within a given area and a given time period

R_i - element at a risk, potentially damaged by the pehonemenon

V_i - vulnerability of each element represented by a damage degree comprised between 0 (no loss) and 1 (total loss)

Although landslide risk mapping is relatively expensive for Bosnia and Herzegovina, this assessment could help in selecting priorities for stabilization. However, the choice of stabilization priorities is based on intuition-based engineering judgment. Engineering intuition is very important in decision making, because it is very fast and very cheap, although not as accurate as other risk and hazard assessment methods, it provides a sufficient basis for deciding how to stabilize depending on investor's financial ability. As an example, on Figure 3, the excerpt of sub-location Gornji Srebrenik is taken into consideration. It is shown that landslides are located outside the potentially unstable zone, which means that the potentially unstable zone is made with insufficient information.

In the municipality of Srebrenik, partial mapping of stability was performed with landslide records. A huge

number of landslides are located in the building areas. It can be concluded that landslide occurrence is closely related to the construction of structures. As an example, on the Figure 5, Gornji Srebrenik sub-location and the micro-location of the K-12 landslide are shown.

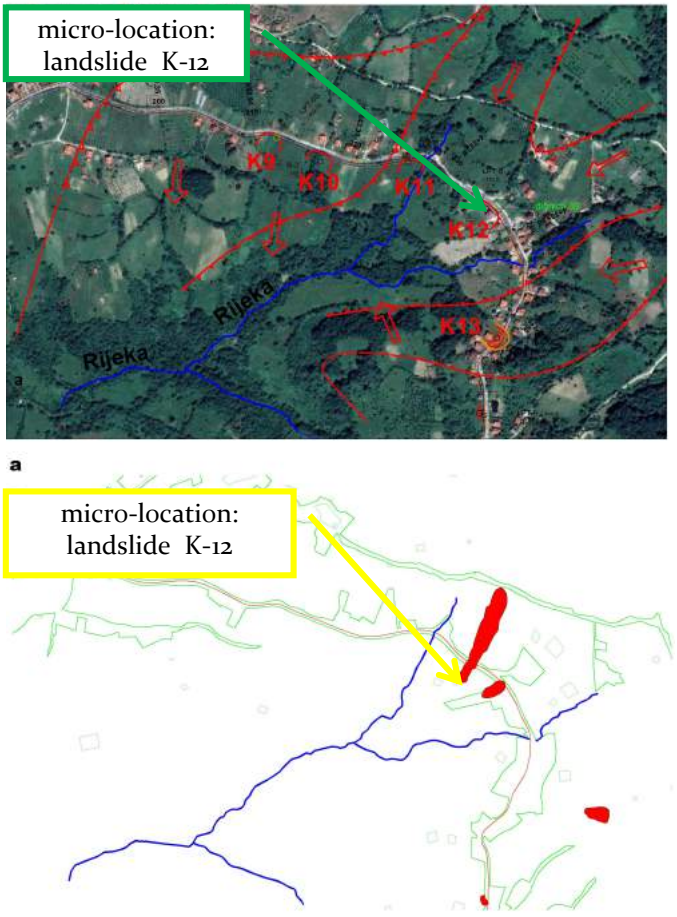

Figure 5 Sub-location Gornji Srebrenik (a – detail mapping of stability, b - except of stability map of the Srebrenik municipality)

The K-12 landslide has been identified in the stable and non-inventoried zone in relation to stability map of the Srebrenik municipality (Figure 5b). However, a huge difference in the detailed map (Figure 5a) may be seen. On detailed map of Gornji Srebrenik (Figure 5a), the stable forms were isolated, while most of the location is unstable. On the local road, 5 landslides were identified as unstable surface, because the road is interesting as infrastructure object. However, comparing two Figures (5a and 5b) to the stability map, a mistake may be noticed.

By 2019, in Srebrenik, only a few landslides, that endangered the infrastructure and housing, had been stabilized. The rest of the landslides are still uninvestigated and with no mitigation measures applied.

Although velocity of landslides has to be considered, there is no strategy for monitoring. Another behaviour of landslides is cyclical displacement or phase instability which is overlooked in Srebrenik area. While active and cyclic landslides are treated as an unstable part of the terrain, there is no clear border between stable and unstable ones. Potentially unstable terrain very often is addressed as “conditionally stable terrain”. Conditionally stable terrain is not clearly defined, except that a descriptive form of conditional stability is used. The expression of conditional stability can be understood in a wide range with the perception from absolute stability to complete instability. On the other hand, absolute stability is defined by a factor of safety. The safety factor is the ratio of resilient to active forces, but the acquisition of resilience and active forces from the field may be in a wide range. So, final numerical expression of the safety factor does not mean accurate of actual state of a landslide. It means that management of slopes is the most effective solution for Bosnian landslides and slopes.

Methodology of landslides and slopes management

Consequence analysis is, together with hazard evaluation, one of the major steps of the landslide risk assessment. However, a significant discrepancy exists between the number of published landslide hazard and landslide consequence studies. While various methodologies for regional-scale hazard assessment have been developed during the last decade, studies for estimating and visualising possible landslide consequences are still limited, and those existing are often difficult to apply in practice mainly because of lack of data on the historical damage or on landslide damage functions. (Puissant at all, 2014).

Methodologies for slope management can play a major role in reducing hazards and landslide risks. Bosnian Landslide Investigation and Stabilization Methodology (BLISM) is developing (Zekan at all 2015) and there are three segments consisted in it:

- management of slopes and urban processes,
- pre-investigative and investigative activities on unstable slopes,
- stabilization activities and monitoring.

Idea of BLISM origintaed after 2014, when thousands of landslides occured in Bosnia and Herzegovna. The methodology is in progress. In general, it needs make harmonization of the activities, recognizable by investors, researchers, designers and contractors to provide an effective system of control in slope processes, investigation and stabilization of unstable slopes in order to ensure safety of people and property with as less as possible financial expenditures.

Stabilization of landslide K-12 at Gornji Srebrenik has been shown as an example for the possibility of applying this methodology.

The original project envisaged the landslide stabilization with a retaining wall. Stabilization measures calculated by the project amounted about 93,000 KM. Based on the project design and the original research, the retaining wall provided a factor of safety of Fs> 1.5. However, it has been shown that at some projects, due to

the uncertainty in the research, the safety factor can be overestimated or underestimated. This means that the engineering calculation with the numerical safety factor is not always accurate. Due to uncertainty in the budget, either too much or too little money can be spent to stabilize the landslide.

BLISM envisages the concept of full mobilization of soil strength and gradual mobilization of a structure that will strengthen the soil. This would consume the optimal amount of money for the minimum safety required.

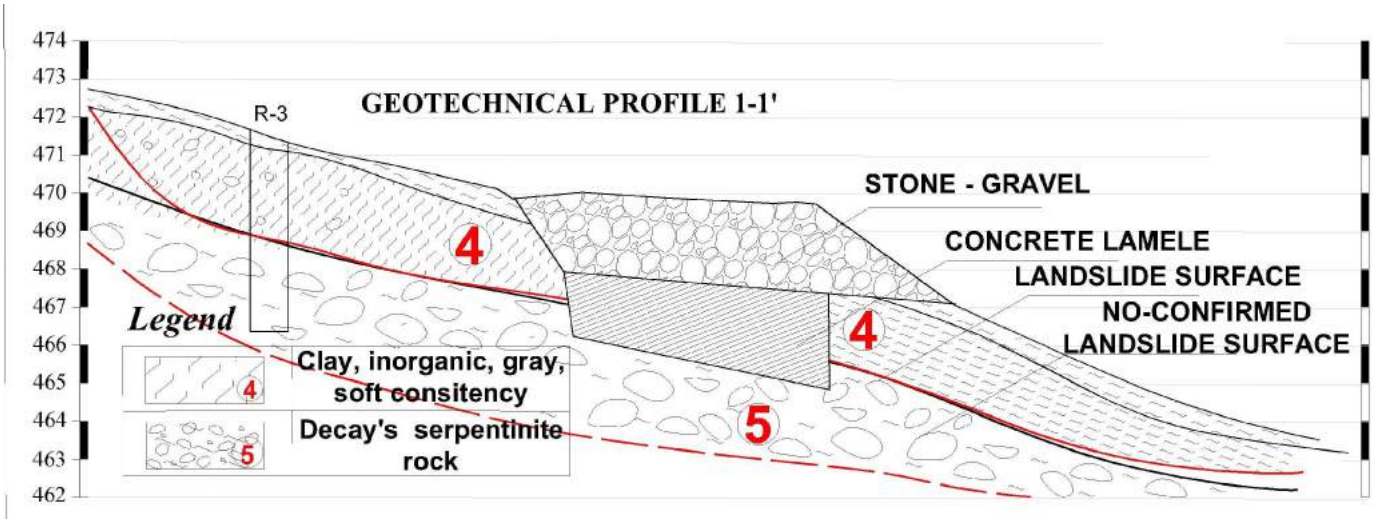

Figure 6 Concrete lamellas at K-12 landslide as a substitution for retaining wall

Figure 6 shows the application of BLISM. It was designed to install concrete lamellas instead of retaining wall. Concrete lamellas have the role of reinforcing the soil with the gradual mobilization of the structure strength on the local road to Gornji Srebrenik. The price of stabilization works was approximately 31.000 KM. The savings compared to the original project are around KM 60,000 or 70% of the original price. In the following period, monitoring will be carried out to determine that the lamellas have efficiency in the stabilization of landslides K-12, and based on this, the final conclusions can be made about the justification of the installation of such structures.

Conclusion

The Municipality of Srebrenik has made significant effort in landslide hazard mapping. Zones of unstable, potentially unstable and stable and not-inventoried terrain are shown on the stability map.

However, it has been found that the mapping process is not simple and requires much more detailed investigation to accurately define the extent of the hazard. Risk assessment, as a relatively expensive operation, was not performed. Risk assessment may be the starting point for landslide management.

Due to scarce financial resources, it is proposed to manage the slopes and landslides as an alternative solution for Srebrenik as well as for the whole of Bosnia and Herzegovina. The example of the Gornji Srebrenik location and the K-12 micro-location shows a lot of uncertainty in mapping of stability.

The management of the slopes would bring significant savings and prevent the occurrence of landslides. An example of the application of the evolving BLISM methodology is demonstrated. This methodology mobilizes maximum own soil strength with gradual structural soil reinforcement, which gives optimum use of money to control a landslide.

References

Bosnian Landslide Investigation and Stabilization Method, Zekan S., Hodžić M., Salković S., Borogovac Š., Hasić L. , (2015) Proceedings of GEO-EXPO, S. Zekan, Geotechnical Society of Bosnia and Herzegovina, Tuzla, Bosnia and Herzegovina doi.org/10.35123/GEO-EXPO_2015_12, 73-78 p

Landslide consequence analysis: a region-scale indicator-based methodology Puissant A. (2014) Landslides 11, Sassa K., Springer-Verlag, Berlin-Heidelberg, DOI 10.1007/s10346-013-0429-x, p 843-858

Landslide hazard zonation: a review of principles and practice, Varnes D.J. (1984), UNESCO, ISBN 92-3-101895-7, Paris, France,

Scales of landslide hazard and risk mapping, Mihalic S. (1998), Geotechnical hazards, B. Marić at all., Proceedings of rhe XIth Danube - Europe Conference on Soil Mechanics and Geotechnical Engineering, Poreč, Croatia, ISBN 90 54109572, p 847

Slope movements - Geotechnical characterisation, risk assessment and mitigation, Leroulei S., Locat J. (1998) Geotechnical hazards, B. Marić at all., Proceedings of rhe XIth Danube - Europe Conference on Soil Mechanics and Geotechnical Engineering, Poreč, Croatia, ISBN 90 54109572, p 95-106

Soil - Structure Interaction at the Bogatići Landslide in Bosnia and Herzegovina, Zekan S., Uljarević M., Mešić M., Baraković A. (2018). Proceedings of China-Europe Conference on Geotechnical Engineering, Wei Wu • Hai-Sui Yu, Springer Series in Geomechanics and Geoengineering, Vienna, ISSN 1866-8755, https://doi.org/10.1007/978-3-319-97115-5, p 1564

doi.org/ 10.35123/ReSyLAB_2019_35

Calculation of the slope stability considering the residual shear strength

Aniskin Aleksej[(1)], Yuriy Vynnykov[(2)], Maksym Kharchenko[(2)], Andriy Yagolnyk[(2)]

1) University North, Department of Civil Engineering, J. Križanića 31b, Varazdin, Croatia, +385923049406

2) Poltava National Technical Yuri Kondratyuk University, Educational and Research Institute of oil, gas and nature engineering, Ukraine, E-mail: vynnykov@ukr.net

Abstract The question of modeling the stability of slopes by finite element method and comparing its results with the results of standard analytical methods is considered. The need for the correct application of strength characteristics for different soil layers in the slope is indicated. It is established that the residual strength characteristics should be given to those soils that have lost their structural strength, in particular, wet loam and sandy loam. The calculations show that the factor of stability determined by the analytical method differ from the corresponding values calculated by the finite element method by 7-10%. It has been found that for slopes with complex soil layering it is important to clearly define the boundaries of soils with disturbed structure, as well as the strength characteristics according to the soil condition and the current stress-strain state.

Keywords: landslide, soil strength, cohesion, finite element method, limit equilibrium state, shearing test, residual shear strength

Introduction

The shear processes on the slopes of river valleys, associated with changes in soil properties that make up the slopes massif, when changing the groundwater regime caused by engineering and geological processes, significantly complicate the conditions for the use of these territories under construction and expose adjacent construction area to instability. These conditions require prediction of landslides on the slopes. However, in such studies, there is a need to predict slope processes depending on the change in stress-strain state of soils on the slope or changes in the properties of these soils when changing the hydrogeological regime, dynamic loads, etc. Therefore, it is actual to adequately determine the characteristics of soils to predict the possible condition of the slope [Briaud].

Slope stability failure is related with overcoming the shear resistance of the soil by shear stress acting upon some areas. For practical problems it is important to correctly determine the mechanical properties of soils and the maximum possible load on the soil mass at which slope still maintains its equilibrium and does not lose stability. The issues of determining soil strength characteristics by standard methods have already been explored in detail [Briaud].

For landslide massif, especially those composed of loess soils with the possibility of soaking, it is necessary to consider the possibility of disturbance of soil structure. As this failure results in a decrease in soil strength characteristics, they should be determined using a multiple reversal direct shear test. The characteristics obtained by this test are less values than the usual direct shear, since only the structural strength of soils is taken into account. The slope stability factors calculated from these data showed that the use of such characteristics makes it possible to estimate the stability of the slope more accurately, which is confirmed by field observations [Velykodnyy et. al.].

The finite element method (FEM) allows such calculations to be performed automatically, to take into account more factors, to discretize the calculation area more, to reduce the time spent on re-calculations taking into account changes in engineering-geological and hydrogeological conditions. Many software packages have a procedure for reducing the strength characteristics for finding critical values at which slope stability is lost, which helps to establish the actual slope stability factor [Lim et. al.]. Correct design of landslide protection structures is possible with the correct choice of the calculation scheme for the assessment of slope stability and methods for determining the mechanical characteristics of soils that most closely match the condition of the slope soils. The reliability of the slope calculation scheme also depends on the quality of geological and geodetic surveys, which should reflect the reliability of the real and potential danger of landslide development. In the modelling of stress-strain state of the slope, the question of determining the soil strength characteristics in the slope and within the potential sliding lines remains open. This is especially true for cohesive soils, the strength properties of which are due to the structural cohesion c_{st} and the colloidal bonds Σw. In particular, the question of use of the mechanical properties values obtained in laboratory tests by the method of direct shear test and by the reverse direct shear test has not been sufficiently investigated. Therefore, the task of assessing the stability of the real slope by analytical and FEM using the soil strength characteristics obtained by different methods was

chosen. By the results of comparing the theoretical data obtained with the real slope state should be determined the soil characteristics that should be used when assessing slope stability.

About the study area

A slope in the village Velikyi Pereviz, Poltava region, Ukraine is selected for stability assessment (Fig. 1). The site is located on the left bank of the river Psel with absolute elevation of the earth's surface from 125.0 to 155.0 m. Geomorphologically, the territory belongs to the slope of the Poltava loess plateau (Fig. 2). According to the results of engineering-geological surveys, it is established that loamy deposits of Quaternary formation, represented by loess and loess-like (loam) loam, are involved in the slope structure. The slope from the surface is covered with loose and deluvial deposits with a depth of about 5 m. The groundwater level was recorded only in the middle part of the slope. Groundwater was not detected on the plateau and down the slope (Fig. 3). 9 boreholes were drilled (fig. 3), 24 intact samples were taken. Selected samples for each layer were subjected to 6 experiments to determine the physical and mechanical characteristics of the soil. Also, 6 direct shear experiments and 6 reverse direct shear experiments were conducted for the contact layer were the failure plane observed (fig. 4). The deformation modulus for all layers was determined in the oedometer.

The Method of wedges

The nature of the slip surface is often determined not so much by the stress-strain state of the soil mass, but by the natural conditions and geological structure of the soil mass. The method of wedges or sliding block method [Cheng] with polygonal slip surface was used to evaluate slope stability. It is most commonly used in the following cases:

- at the base of the slope are layers or interlayers of weak soils;
- inclination of the soil layers parallel to surface of the slope;
- a stable layer of soil, on which the sliding mass slides, has straight sections.

Figure 1 General view of the study area

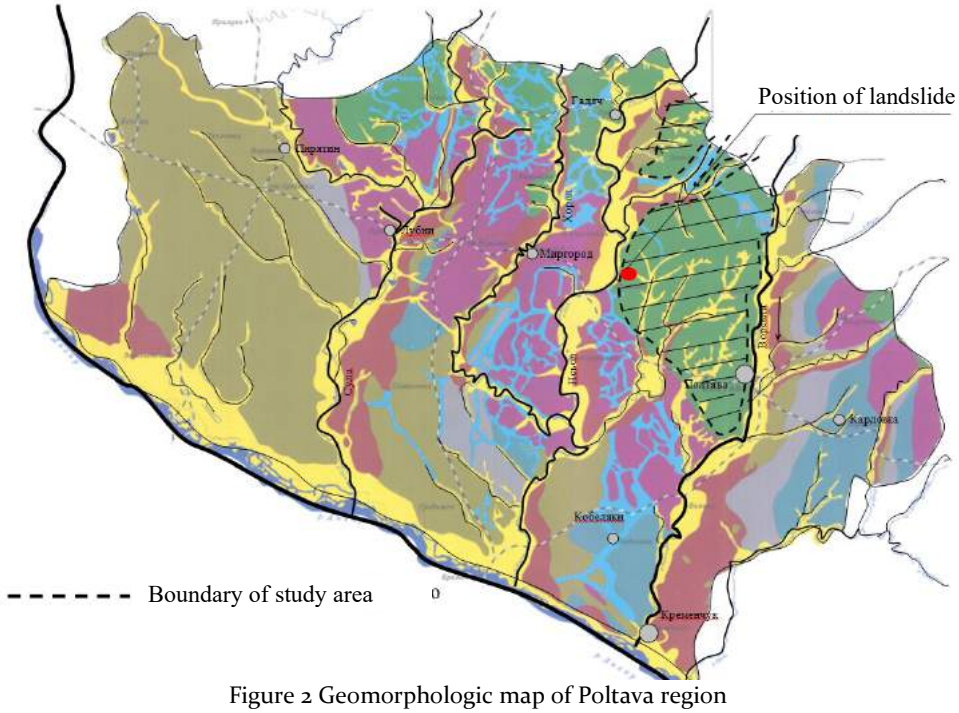

Figure 2 Geomorphologic map of Poltava region

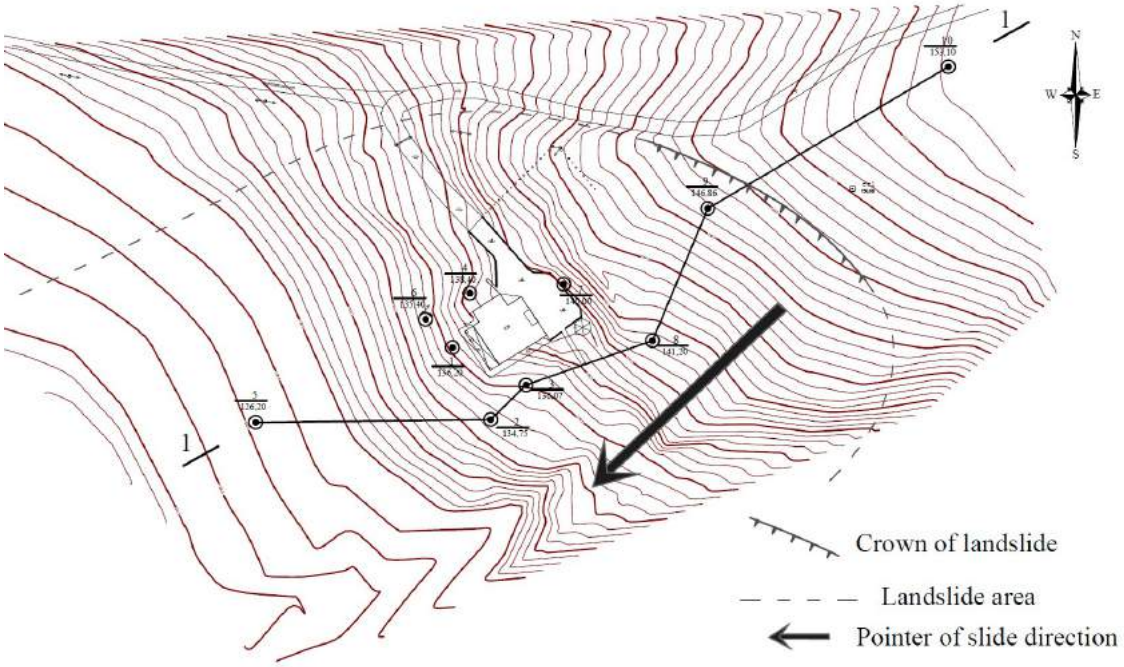

Figure 3 Top view of the study area

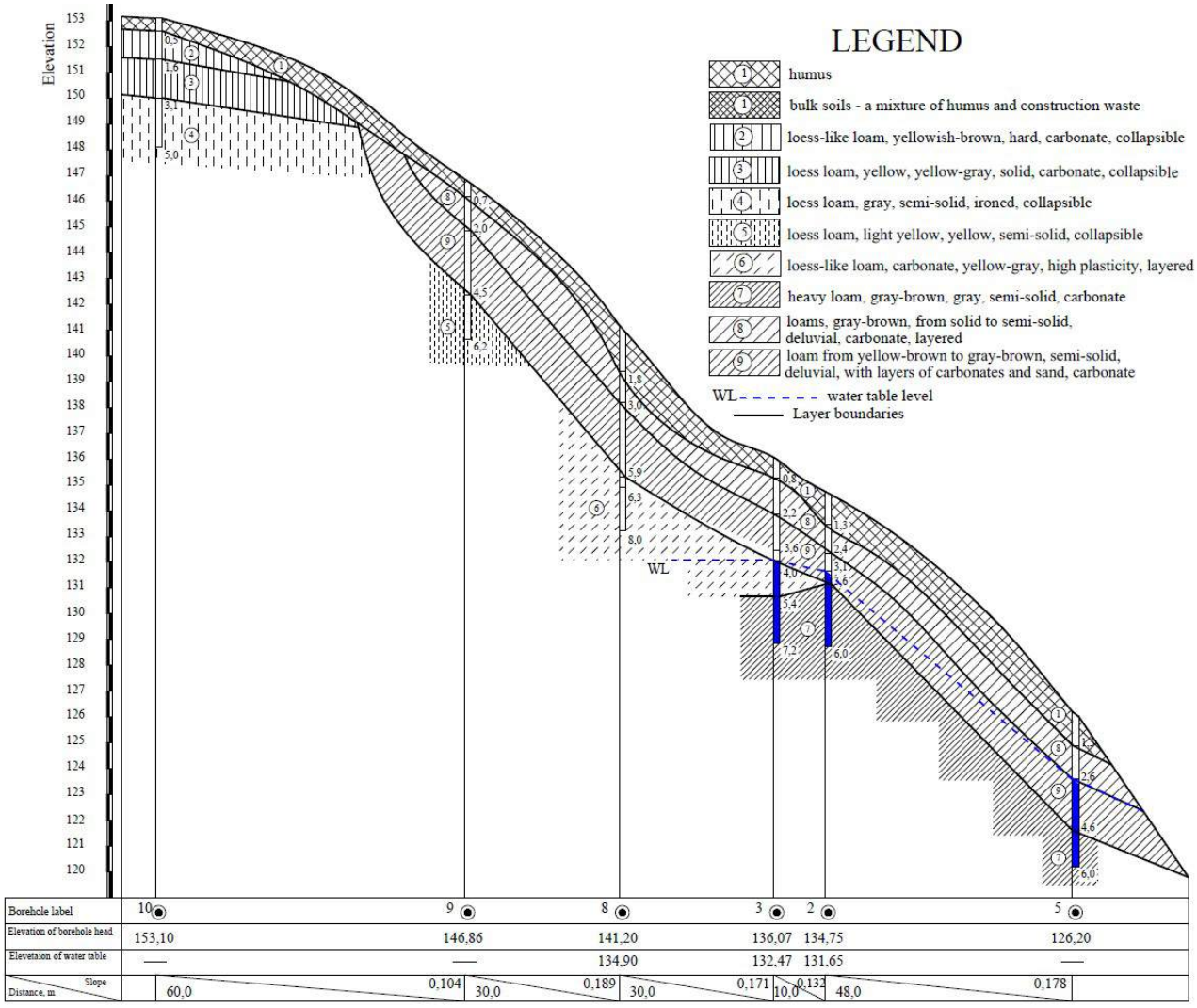

Figure 4 Engineering geological profile 1-1

For a plane problem, these slip surfaces with some approximations can be replaced in the plane of the drawing by one or another number of straight lines - slip lines (Fig. 5). Within the straight lines, blocks of soil are allocated, the weight Q and the angle of inclination α to the horizontal are calculated.

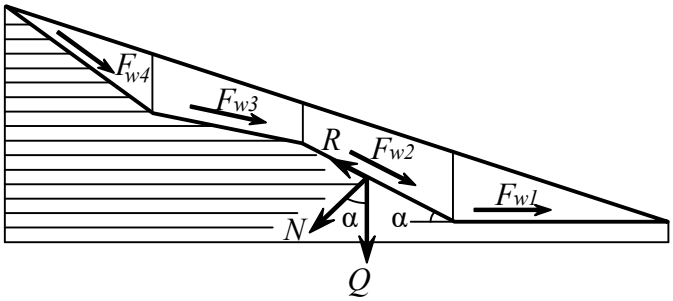

Figure 5 Scheme for calculating by the Wedge method

The shear force of the block is equal to $F = Q \cdot \sin\alpha$, and the resultant holding force is $R = Q \cdot \cos\alpha \cdot \mathrm{tg}\varphi + c_{st} \cdot \ell$, where is ℓ the block sliding length. The difference between these values will correspond to the shear pressure E. If there is a slope of the filtration flow in the soil, an additional pressure F_w will be acting [Lim et al.].

The slope safety factor k_{st} taking into account the filtration pressure is equal to:

$$k_{st} = \frac{\sum_{i=1}^{i=n} \left(Q_i \cdot \cos\alpha_i \cdot tg\varphi_i + c_{st} \cdot l_i\right)}{\sum_{i=1}^{i=n} \left(Q_i \cdot \sin\alpha_i + F_{w_i}\right)} \qquad [1]$$

The results of slope stability obtained by the Wedge method, are given in Table. 1. The distribution of wedges on study are shown on fig. 6.

The slope safety factor for the case is k_{st} = 1,326. This indicates that the slope is now in a stable condition, and the lowest additional loading, changing of soil properties, additional water saturation of the slope, excavating without a set of anti-landslide measures can lead to loss of slope stability.

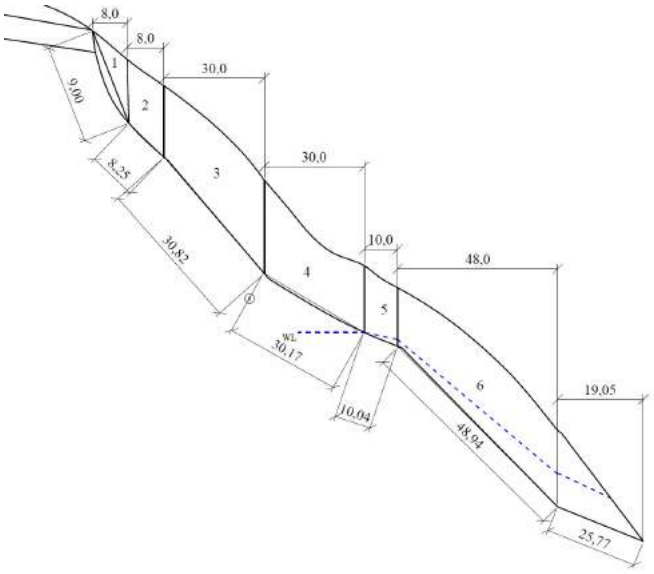

Figure 6 Distribution of the wedges in studied case

Table 1 Results of slope calculation by the Wedge method

Block No.	Eng. Geol Unit No	Block Weight, kN	α, degree	ℓ, m	Friction angle φ, deg.	Cohesion, C_{st}	Soil shear forces, kN	Shear resistance, kN	Shear pressure, kN
1	9	225,50	27,38	9,00	13	0,6	103,65	46,21	57,44
2	9	532,84	14,18	8,25	13	0,6	130,46	124,15	6,31
3	9	2683,2	13,24	30,82	13	0,6	614,22	621,19	-6,96
4	9	2583,9	6,15	30,17	13	0,6	276,67	610,90	-334,22
5	9	653,6	5,21	10,04	13	0,6	59,32	156,21	-96,89
6	9	3384,96	11,25	48,94	13	0,6	660,04	795,44	-135,39
7	9	762,32	5,9	25,77	13	0,6	78,36	190,53	-135,46
						Σ =	1923,67	2551,20	-627,53

FEM simulation

Numerical FEM simulation performed in Plaxis 8.2. software was used to estimate the soil stress-strain state on the slope. The modelling of slope soils was performed using an elastic-plastic model with the Mohr-Coulomb (MC) strength criterion. The formulation of the elastic-plastic problem assumes the following conditions:

- taken into account the manifestations of nonlinearity include plastic deformation of the shape change in a complex stress state, unobstructed deformation in tension;

- in the case of a complex stress state (shear with compression), the general deformations contain a linear (elastic) and plastic part, and the plastic component of the deformations occurs after reaching the tensile strength according to the MC condition for a flat problem:

$$\frac{1}{2}(\sigma_1 - \sigma_2) + \frac{1}{2}(\sigma_1 + \sigma_2)\sin\varphi - c \cdot \cos\varphi = 0 \quad [2]$$

Discretization of calculation area was obtained using FEM (fig. 7). The calculation was performed by the method of soil strength reduction. It is consisting in reduce of the strength characteristics by the time of limit equilibrium. In this approach, the slope safety factor is determined as the ratio of the given characteristics to their reduced values.

$$k_{st} = \frac{c + \sigma \cdot \tan\varphi}{c_r + \sigma \cdot \tan\varphi_r} \quad [3]$$

where c and φ are the initial shear strength characteristics; σ- normal component of stress; c_r and φ_r are the limit values of the shear strength characteristics.

Initial stresses from the weight of water are generated based on the groundwater level, which is introduced when the initial conditions are assigned. The initial stresses caused by gravity represent the equilibrium state of undisturbed soil or rock. To generate them, the so-called gravitational loading procedure was used.

When using this procedure, the initial stresses are zero. Then, the stresses are set by applying the soil weight on the first phase of the calculation. After generating the initial stresses, the deformations caused by them are zeroed - this stage of the stress-strain state is considered to be initial [Tschuchnigg].

The physico-mechanical properties of engineering-geological elements (EGE) adopted in the calculations are summarized in Table. 2. The calculated values of the physico-mechanical characteristics of the soils were used to determine the stability of the slopes and the design of landslide structures according to building standards were: specific gravity of the soils - the calculated values for the calculations at the first limit state; internal friction angle - calculated values for calculations at the first limit state; specific cohesion - the calculated value for the calculations for the first limit state.

The strength parameters determined by the methods of standard and reverse direct shear test were used. The calculations were performed for three options with different soil characteristics:

1) all soils within the slope with characteristics defined by the standard direct shear test;(Fig 8)

2) all soils within the slope with the parameters calculated by reverse direct shear; (Fig 9)

3) soils above the predicted sliding line (deluvial) with characteristics determined by the reverse shear, and all other (indigenous soils) with characteristics by the conventional direct shear (Fig 10)

The geometric model for the calculation was created on the basis of engineering-geological profile 1-1. Fig. 5 shows a calculation scheme with a finite element grid. The calculation was performed in two phases: 1) generation of stresses from the soil's own weight, using the gravity loading procedure “Gravity loading”; 2) Calculation of the slope stability factor ΣM_{sf} by Phi-c reduction scheme, in which it is possible to assess the stability of the slope (at the beginning of this phase the deformation caused by its soil own weight, zeroed).

The results of calculations of the three variants are shown on Fig. 6 - 8.

Table 2 Estimated values of physical and mechanical properties of soils

No. of EGE	Material Model	Specific density of soil γ, kN/m³	Specific density of saturated soil γ', kN/m3	Cohesion c, kPa		Angle of internal friction, φ		Young's modulus E, MPa	Poisson ratio, ν
				standard shear	reverse shear	standard shear	reverse shear		
1	MC	16,5	17,0	5	5	10	10	8	0,35
2	MC	16,8	18,6	18,2	7,3	20	18	5	0,35
3	MC	17,2	18,5	14,6	6,2	21	18	4	0,35
4	MC	17,4	18,5	13,5	6,0	22	20	6	0,35
5	MC	17,7	18,8	12,8	4,5	21	19	5	0,35
6	MC	18,4	18,9	16,4	5,3	19	19	7	0,35
7	MC	19,2	19,2	32,3	10,4	17	11	18	0,35
8	MC	17,5	18,7	10,2	0,3	18	16	2	0,35
9	MC	18,2	18,9	12,4	0,6	16	13	4	0,35

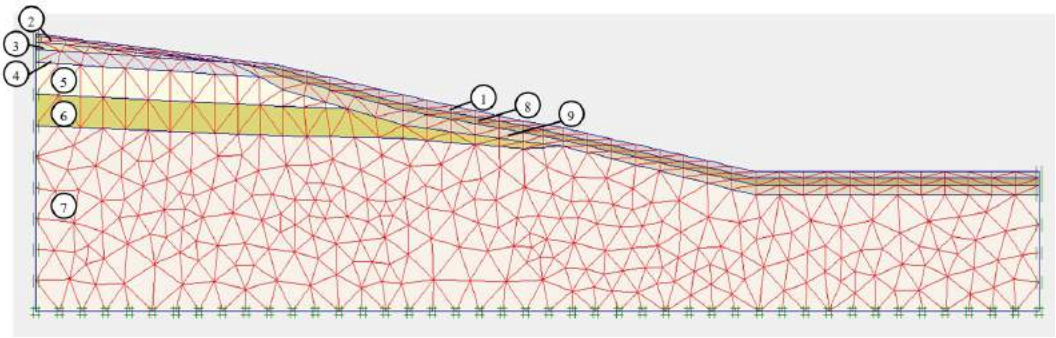

Figure 7 Numerical model with finite elements with layer lebels

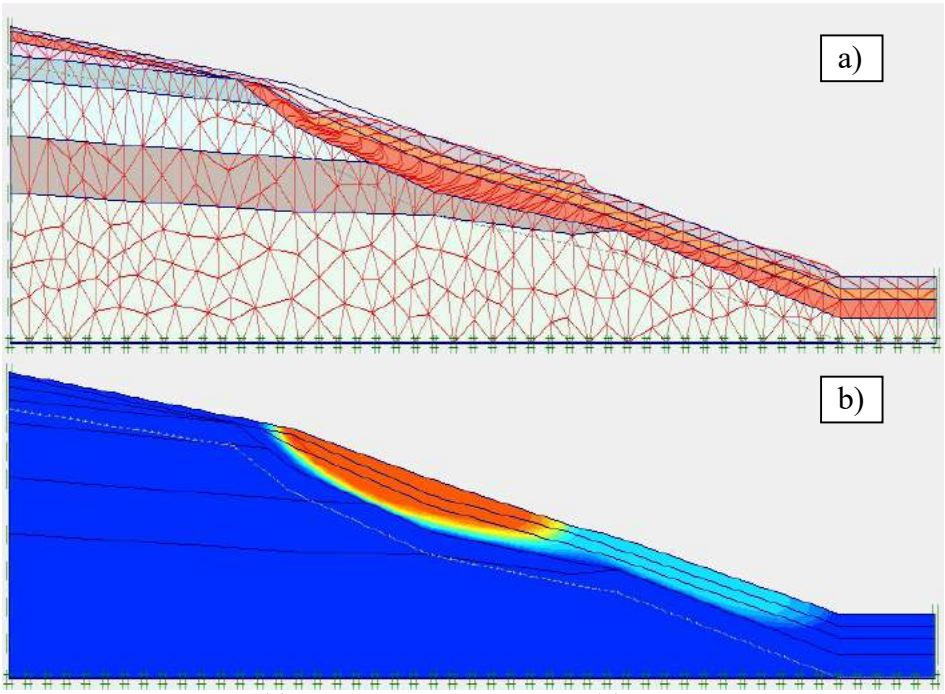

Figure 8 Deformed model (a) and isopoles of deformation (b) for the first design variant

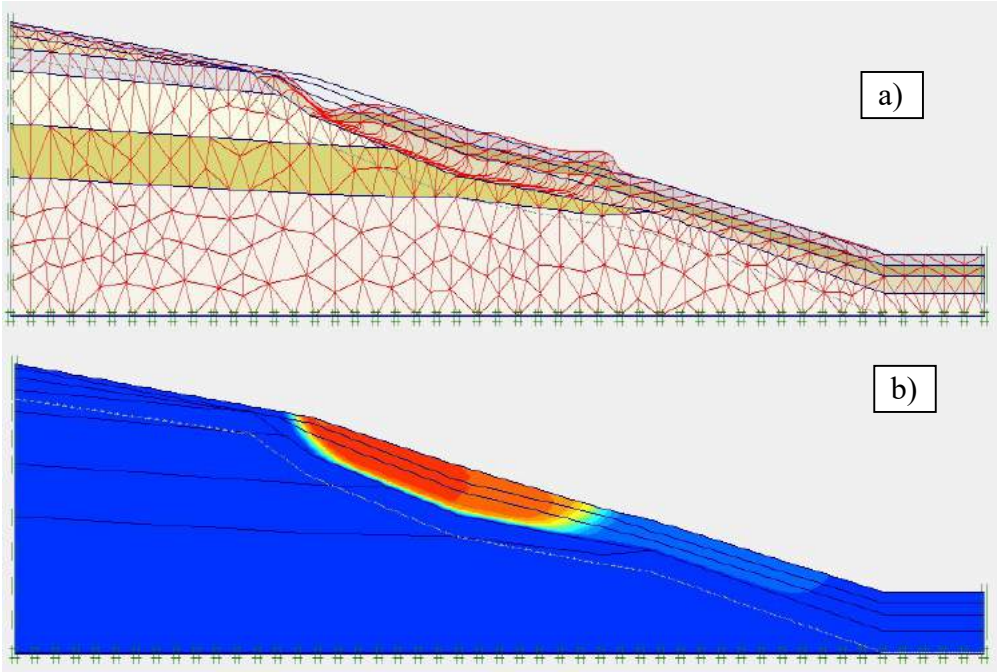

Figure 9 Deformed model (a) and isopoles of deformation (b) for the second design variant

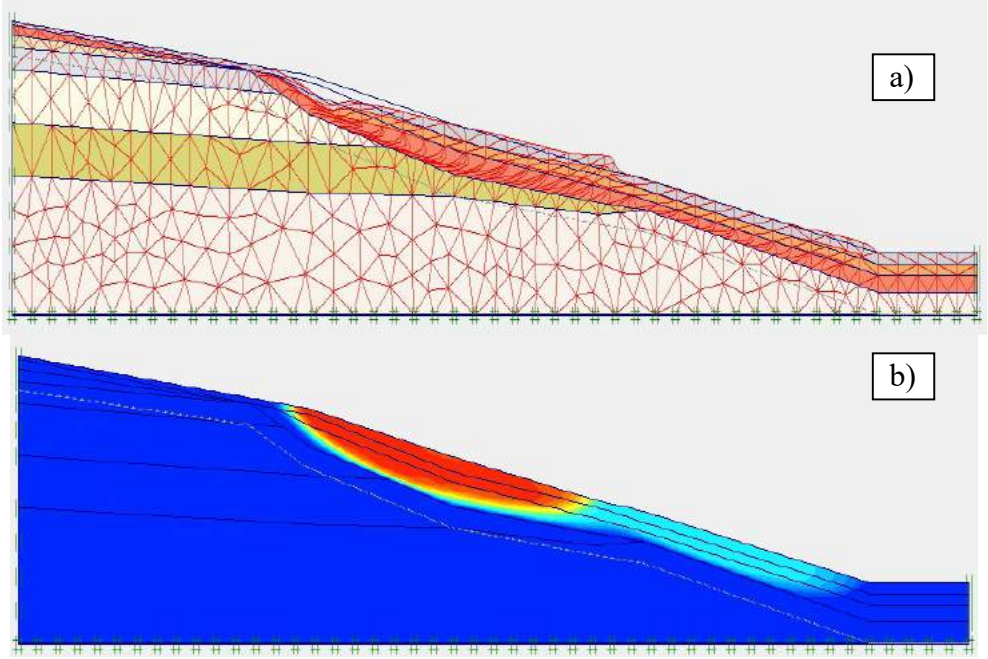

Figure 10 Deformed model (a) and d isopoles (b) of deformation for the third calculation variant

The results of numerical modelling by the FEM and the analytical wedge method are given in Table. 3.

Table 3 Comparison of calculation results by different methods

Method of slope stability assessment	Slope safety factor k_{st}
Characteristics defined by the standard method	
Method of wedges	2,456
FEM numerical modeling (Option 1)	2,697
Characteristics defined by the reverse shear	
Method of wedges	1,276
FEM numerical modeling (Option 2)	1,415
FEM numerical modeling (Option 3)	1,414

By analysis of the data obtained and its comparing with the real slope state, it can be stated that modeling using residual soil strength characteristics, when assigned to deluvial soils, yields a result that is closer to coincides with real slope processes (formation of landslide slumps, cracking, deformation of buildings and structures, "tilted trees", etc.). Other methods give too high value of slope safety factor or inadequate scheme for the slope failure development and inadequate slip surface. The difference between the analytical method and the finite element method gives a safety factor with a deviation of about 7 - 10%.

Conclusion

When performing a complex of geological engineering surveys on landslide or landslide slopes, it is mandatory to study the soil strength characteristics by methods that make it possible to determine them in conditions as close as possible to the real state of the soil massif. One of these methods is the method of residual direct shear. When drawing up the calculation scheme for the slope, it is necessary to take into account the features of geomorphological and engineering-geological structures, groundwater regime, the presence of potential sliding surfaces, etc.

When assigning strength characteristics to soils, their structure and genesis must be taken into account. For structurally unstable soils (deluvia, colluvium, loose soils, etc.), the characteristics must be determined under the most unfavorable conditions, taking into account the loss of structural strength and the formation of sliding surfaces in them. To evaluate the stability of the slope use of FEM gives reliable data of Stress-Strain state if the calculation scheme correct and values of the physical and mechanical properties of soils reliable, considering the prediction of their changes.

References

Briaud J.L. (2013) Geotechnical Engineering: Unsaturated and Saturated Soils, Wiley, (ISBN 978-0470948569), 1022 p.

Cheng Y.M. (1997) Comparison between method of slices and method of wedges in slope stability analysis, Geotechnical engineering Journal of SAGS, Vol 28, No1, Southeast asian geotechnical society, pp 71-88

Lim K.C., Li A., Lyamin M. Slope stability analysis for fill slopes using finite element limit analysis (2015), Proc. of the XVI ECSMGE Geotechnical Engineering for Infrastructure and Development 13 – 17 September 2015. Edinburgh, England, P. 1597 – 1602.

Tschuchnigg H.F. (2015) Performance of strength reduction finite element techniques for slope stability problems, Proc. of the XVI ECSMGE Geotechnical Engineering for Infrastructure and Development, 13 – 17 September 2015, Edinburgh, England, P. 1687 – 1692.

Velykodnyy YU.Y., Bida S.V., Zotsenko V.M., Lartseva I.I., Yahol'nyk A.M. (2016) Zakhyst terytoriy vid zsuviv, "Drukarnya Madryd", Kharkiv, (ISBN 978-617-7294-88-6), 160 s.

doi.org/ 10.35123/ReSyLAB_2019_36

Causes, occurrence and rehabilitation measures of landslide „Makljenovac“ near Doboj

Zlatan Talić[(1)], Dženana Haračić[(2)]

1) InfraPlan ltd. Sarajevo, Sarajevo, Džemala Bijedića No. 2, +387 61 202 432

2) Elektroprivreda BiH, ZD RMU Kakanj, +387 32 777 417

Abstract Engineering geological surveys and terrain tests at the site of the Makljenovac landslide, Doboj municipality, were carried out in December 2014. The objectiv and task of engineering-geological research and testing was to define the engineering-geological and hydro-geological conditions of the terrain, as well as to prepare the engineering-geological study and the project of rehabilitation of the Makljenovac landslide (Doboj Municipality, Bosnia and Herzegovina).

Landslide activation occurred in May of the same year, directly endangering two private houses and two local roads, one of which was completely blocked by a gravity-displaced soil mass.

The paper presents engineering geological surveys and terrain tests at landslide locations, analysis and interpretations of performed field works and obtained data, geotechnical soil modelling and corresponding calculations.

The paper also presents the concept of landslide remediation, as well as the principle of determining the optimal depth of drainage.

Keywords landslide of Makljenovac, engineering-geological investigation works, geotechnical investigation works, rehabilitation measures, reverse analysis, Plaxis.

Introduction

Landslide of Makljenovac is located in Makljenovac, Doboj Municipality, Bosnia and Herzegovina. It is located along the entity border, bordering the municipality of Usora, Federation of Bosnia and Herzegovina.

Visiting the subject site, a landslide was observed above the local asphalt road, shown in Fig. 1. Heavy rainfall caused the surface of the slope to defoliate, constant gravitational displacement of the material led to secondary shelling of the terrain with marked deformation of the terrain. The sliding process was even faster due to unfavorable slope of the terrain, which is just above the road. Sliding material covered the entire profile of the road and prevented traffic.

Figure 1 Landslide photo, a sliding mass that has been gravitationally moved along the road.

During the exploratory works, the presence of surface water was observed, and in particular the sedimentation of parts of the slope with occasional surface flow in the field above the road was observed, where a lack of mass was observed. At the hydro-geological maximum, GWL can be expected at the very surface of the terrain. Geologically, the structure of the wider area of Makljenovac is represented by small bodies of diabase and spilites, which are immersed in the ophiolite melange, Fig. 2.

This is basically a very heterogeneous complex of sedimentary and diverse magmatic rocks. The more well-exposed profiles clearly show the very chaotic arrangement of the various rock components, which make it difficult to determine the slightest regularity in sedimentation, which is and because of this complex has recently been shown as a melange.

Of the sedimentary rocks in the ophiolite melange, the most common are sandstone gravels, sandy siltstones, shale clays, and occasionally yellow iron corneas with radiolaria, which are thinly layered with layers of yellowish clay, are observed. Here and there, but very rarely, in radiolarian corneas, there are thin layers of dark gray siliceous limestone of Pelagic type and there are breccias.

Separating them separately is impossible, as they appear on a relatively small surface in a chaotic state: on heavily covered terrain.

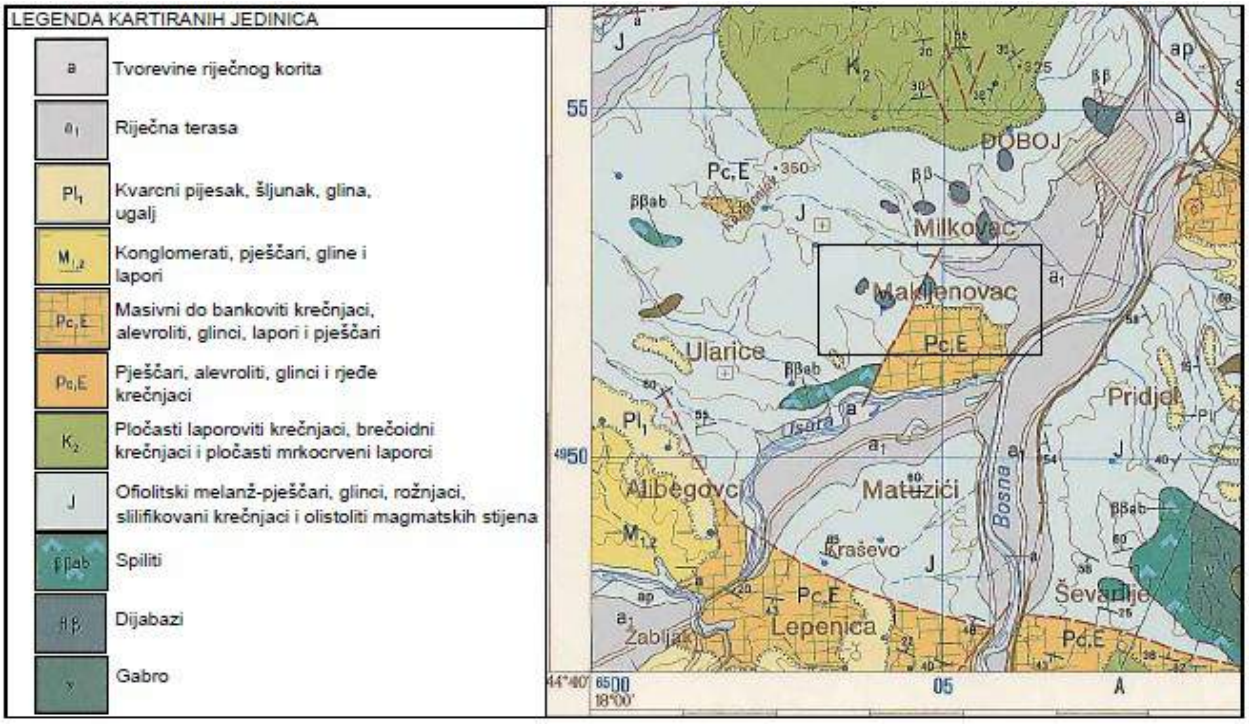

Figure 2 Geological structure of the wider area of Makljenovac, Scale 1: 100,000 (Retrieved from: OGK OGK; Doboj_L 34-109)

Engineering geological and hydro-geological works

Within the field exploration works, the following was performed: exploratory drilling, determination of material from boreholes, photographing and sampling of litho logical members, detailed engineering-geological mapping of the terrain. Laboratory testing of soil material samples was also performed.

The analysis and interpretation of the fieldwork carried out and the data obtained provided:

- Geographic and geo-morphological characteristics of the terrain;
- Geological structure of the wider study area;
- Review and analysis of the research carried out;
- Engineering geological characteristics of the terrain;
- Hydro-geological characteristics of the terrain;
- Landslide description and status of activities;
- Causes of landslides.

Detailed engineering-geological mapping was performed over a wider area than the landslide itself, as well as in the area of the entire landslide, which directly threatens the stability of the slope and structures in the immediate vicinity, in order to clearly identify its boundaries (forehead, foot, lateral contours, zones of active movements and construction of the terrain, occurrence of springs, damages in the soil, on the road and associated objects, etc. Figure 3 shows the longitudinal engineering geological and geotechnical profile of the terrain 1-1 '.accumulation material), material composition and natural

An overview of the engineering-geological and geotechnical properties, the classification and categorization of rocks and soil, and the production of engineering geological maps and profiles are given in accordance with the engineering-geological classification of rocks and soil, proposed by the International Association for Engineering Geology and the Environment of 1976 (IAEG).

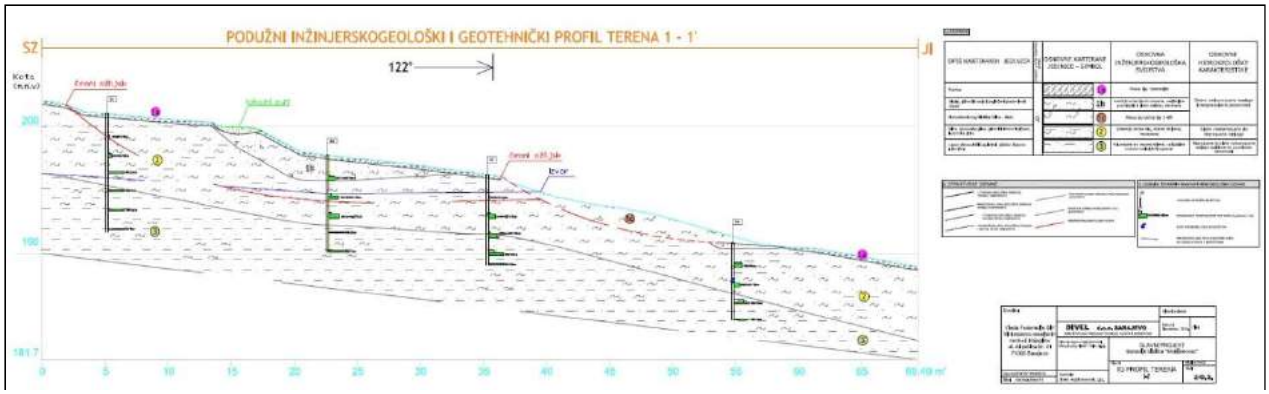

Figure 3 Longitudinal engineeringgeological and geotechnical section 1-1' Retrieved from: Elaborate, 2014)

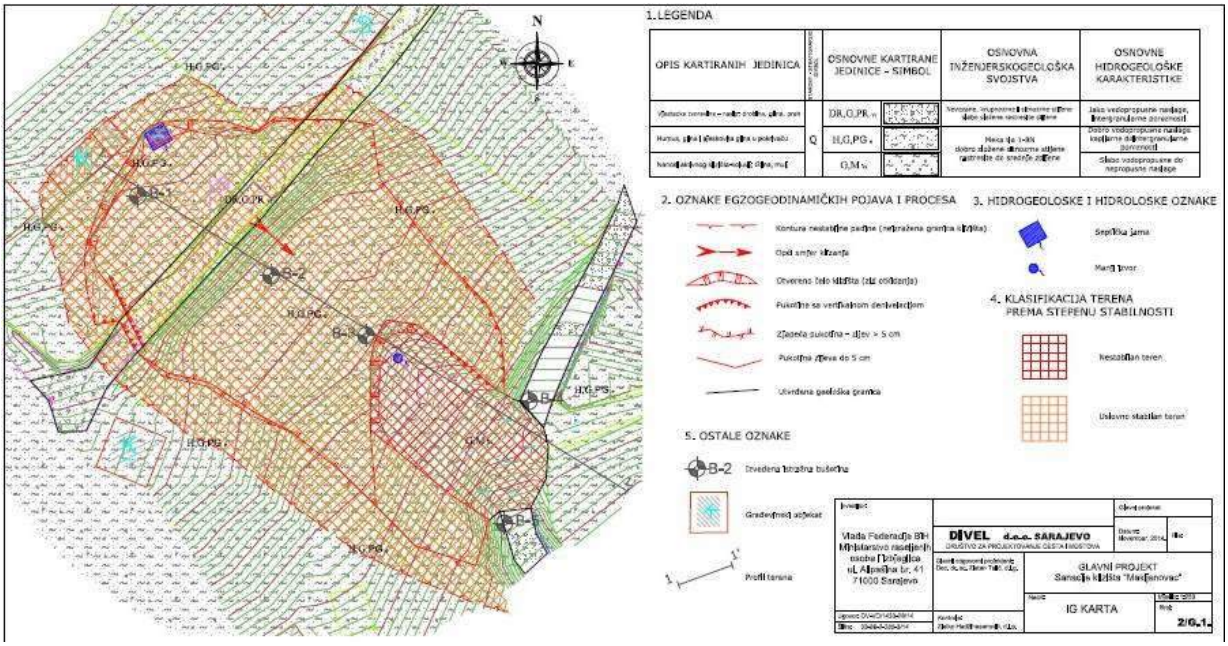

Figure 4 Engineering geological map (Retrieved from: Elaborate, 2014)

Taking these recommendations into account also the results of field investigations and tests, detailed geological mapping of the terrain, production of engineering geological maps (Figure 4) and profiles were made for the landslides of the Makljenovac landslide. Thus, the following categories were distinguished in the study area:

Cover - surface layers of soil (loose and semi-bound soil);

A weakened geological substrate (solid and soft rock).

From hydro-geological investigations GWL measurements and field hydro-geological identification of lithologic members were performed at the considered site.

The hydro-geological characteristics of the terrain in the considered locality are complex, owing primarily to the heterogeneous material composition of the subsoil (horizon 2), the different porosity structure, the variable water permeability and the slow water value of the separated lithological members.

The Makljenovac landslide is classified into landslides of medium size, measuring about 1500 m2. The landslide can be divided into two separate landslides. An internal landslide or stream whose activation triggered the activation of larger landslides. In terms of shape, the riverbed represents an elliptical type of landslide, and the larger landslide is a landslide with irregular polygonal contours reminiscent of a tongue-type landslide.

The landslide in question may be classified into shallow landslides with a slip depth of less than 5 m'. The state of landslide activity is defined as temporarily calm, because it is in the current voltage equilibrium, due to the decrease of precipitation and, consequently, the amount of PV, and the already mentioned stabilization of the central part, or the course. It should be noted that a stable course gives some stability to the entire landslide and therefore, before removing the sliding mass from the

local road, drainage and waiting for the soil to dry must be done.

The following parameters were taken to assess the urgency of landslide remediation:
Housing vulnerability;
Endangerment of public facilities;
Road and rail threats;
landslide surface;
landslide depth.

On each of the criteria, points were defined that define the landslide category by the degree of urgency of rehabilitation.

Landslide formation was preceded by a longer or shorter preparatory phase in which a gradual change in the existing primary voltage state occurred. This initial part of the process could not be observed macroscopically until the first deformations and cracks in the field occurred.

The main cause of landslides is the destructive and destabilizing effects of groundwater. Namely, the landslide period (May 2014) was preceded by large amounts of precipitation, which according to the Republic Hydro-Meteorological Institute of RS, amounted to 270 mm / m2 for Doboj, which is 3 times higher than the average for Doboj in May.

Geotechnical rehabilitation works

All performed geological, hydro-geological and geotechnical exploration works served as the basis for the development of the Main Project for the Makljenovac landslide rehabilitation, geotechnical project - mission of geotechnical engineering G21.

To determine the relevant material parameters of the GS 1 cover material in its natural state, a back analysis was carried out in the Plaxis software package, Fig. 5.

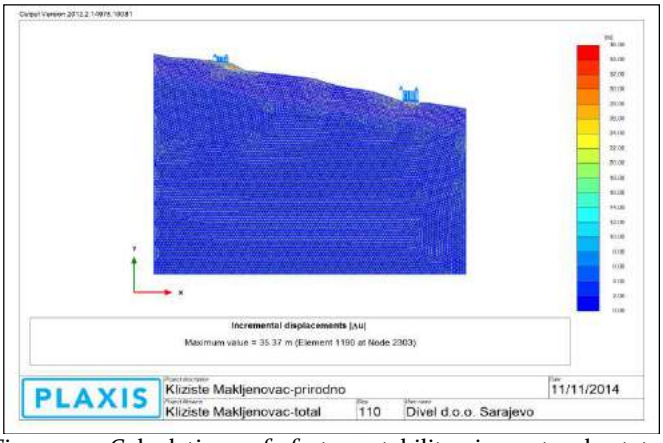

Figure 5 Calculation of factor stability in natural state Fs = 1,000. (Retrieved from: Zlatan T., Divel d.o.o. Sarajevo, 2014)

On the basis of field and laboratory research works, engineering-geological determination and classification of the core of exploration wells, as well as the results of feedback analysis, the following soil parameters have been determined for the geotechnical environments:
for cover materials - geotechnical environment GS 1

modulus of deformability Es = 8 MPa;
volume weight γ = 18 kN / m^3;
internal friction angle φ = 13°;
cohesion c = 2.5 kPa.

for degraded geological substrate materials - GS 2 geotechnical environment:

modulus of rock mass Es = 50 MPa;
volume weight γ = 20 kN / m^3;
internal friction angle φ = 30 °;
cohesion c = 11 kPa.

In the second phase of the budget, the slope stability calculation was performed after the rehabilitation measures were carried out. The budget was implemented for three different depths of burial drainage.

Table 1 Results of calculation

Drainage depth	Factor of stability
2,00 m	1,165
3,00 m	**1,298**
4,00 m	1,413

From the presented results, Table 1, it is evident that the drainage depth of 2.0 m gives an unsatisfactory safety factor Fs = 1.165 <Fs = 1.25, that is, less than the required one according to Eurocode 7. A drainage depth of 3.0 m was adopted as the optimum drainage depth, as the resulting safety factor is greater than the required Fs = 1.298> 1.250.

Fig. 6 shows the most critical sliding surface for a drainage depth of 3.0 m. The coefficient of safety Fs = 1.298 is obtained.

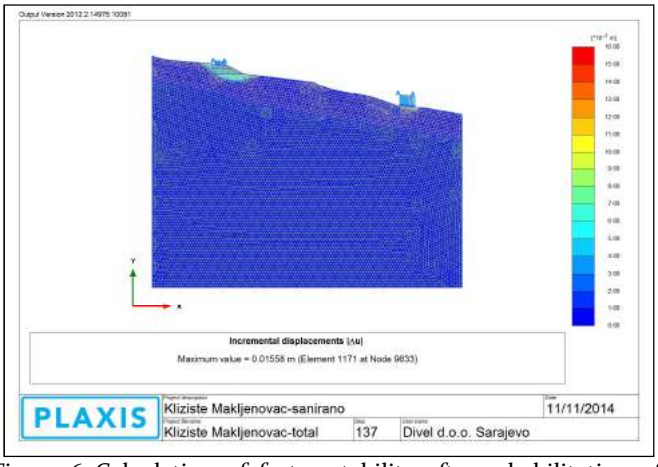

Figure 6 Calculation of factor stability after rehabilitation of landslide, Fs = 1,298. (Retrieved from: Zlatan T., Divel d.o.o. Sarajevo, 2014)

On the basis of the presented problems, as well as considering the mentioned possibilities of cheaper solutions, the following works are foreseen for landslide remediation (shown in Fig. 7):

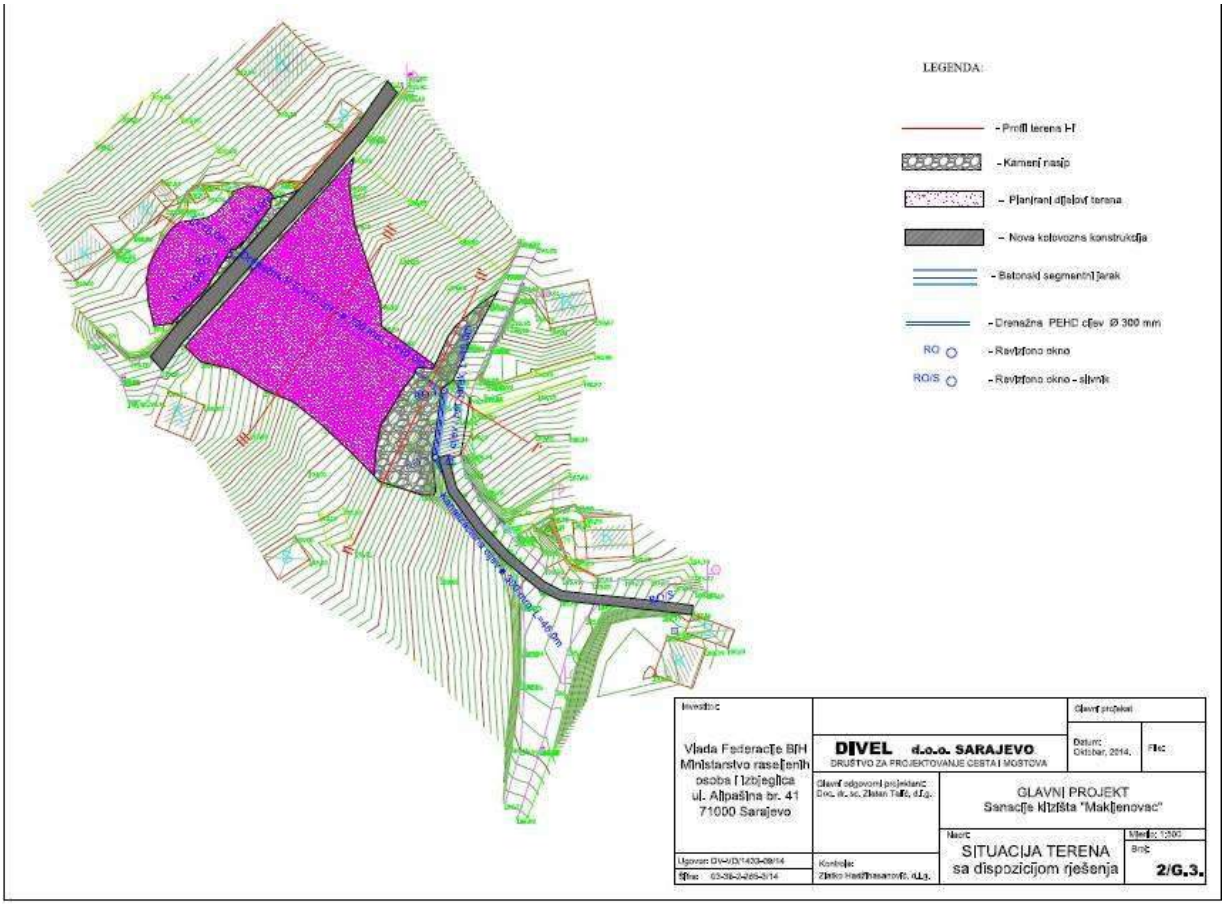

Figure 7 Geological structure of the wider area of Makljenovac, Scale 1: 100,000 (Retrieved from: Zlatan T. Divel d.o.o. Sarajevo, 2014)

In order to ensure the stability and functionality of the part of the local road that is endangered, the tarmac cover material above the road itself, which has poor geomechanical characteristics, should be removed and replaced with a counterweight that would provide both general and local stability of that part of the slope.

Construction of a drainage channel at the top of the slope, above the upper local road, into the bottom of which there are drainage pipes Ø 300 mm, which is filled up above the pipe with a filter material with a thickness of 1.0 m, a rocky embankment of variable thickness and a final layer with a thickness of 0.3 m material from the excavation.

This drainage is intended to collect all groundwater from the plateau around the houses, and above the upper local road, and conduct them to the RO2 inspection pane. Upper road hull replacements with rock material.

The counterweight would consist of a coarse-grained rock 3.00 m thick. At the bottom of the rock embankment, a drainage would be installed, consisting of a drainage pipe ∅ 300 mm protected by a filter material of the prescribed granulation in a layer of 1.00 m in height, in order to collect all surface and leachate counterweights as well as water from the upper parts of the slope, and not collected by predicted drainage. All collected water would then be taken to the nearest RO / S drainage basin. The rock material can be obtained from nearby quarries or the excavation of large-grained material from nearby excavations.

By constructing a precast concrete ditch along the edge of the lower road, which would go to the RO3 inspection pane.

On the slope above the counterweights the clay materials from the excavation should close all gaping cracks in the terrain, so that the surface waters do not penetrate through these cracks into the deeper parts of the terrain and dissolve the materials of the geological cover. Also, these materials should be covered with larger irregularities on the slope, or plan the same, so that all surface water reaches the countertops as quickly as possible and reaches the intended drainage.

References

BAS EN 1997-1: Eurokod 7 – Geotehničko projektovanje – Dio 1: Opća pravila (2008).

BAS EN 1997-1: Eurokod 7 – Geotehničko projektovanje – Dio 2: Ispitivanja tla (2008).

Laušević, M. i Jovanović, Č. (1984): Tumač za osnovnu geološku kartu lista Doboj, R – 1 : 100 000. Geoinženjering, OOUR Institut za Geologiju. Sarajevo.

Pravilnik o geotehničkim istraživanjima i ispitivanjima te organizaciji i sadržaju misija geotehničkog inženjerstva, FBiH, (2009).

Zlatan T. (2014): Glavni projekat sanacije klizišta „Makljenovac“, geotehnički projekat – misija geotehničkog inženjerstva G21, Divel d.o.o. Sarajevo.

Zubak, Ž. i Bajrić, A. (2014): Elaborat o inženjerskogeološkim karakteristikama terena na lokaciji klizišta Makljenovac. „Geosonda“ d.o.o. Zenica.

doi.org/ 10.35123/ReSyLAB_2019_37

Determination and studying rockfall hazard using process modelling in the case of rockfalls along the railway link between Renke – Zagorje (central Slovenia)

Tina Peternel [(1)], Jernej Jež [(1)], Blaž Milanič [(1)], Anže Markelj[(1)], Milan Kobal[(2)]

1) Geological Survey of Slovenia, Dimičeva ul. 14, 1000 Ljubljana, Slovenia; tina.peternel@geo-zs.si

2) University of Ljubljana, Biotechnical Faculty, Department of Forestry and Renewable Forest Resources

Abstract In Slovenia and across Europe rockfalls pose a distinct danger, especially where transportation lines (railway corridors and roads) cross river ravines that are usually steep and formed from compact rocks (limestones, sandstones, etc.). The likelihood of a rockfall increases where transportation lines cut rock slopes in the form of road and railway slope cuts. The paper focuses on the determination and study of rockfall hazards using dynamic (also known as process) modelling that is based on the simulation of process (rockfall trajectory in 3D) dynamics in the case of rockfalls along the railway in central Slovenia.

A rockfall is a slope process in which a rock mass of different rock sizes and shapes (rocks, boulders and blocks) separates or becomes detached and descends extremely quickly. Rockfalls can be caused by various trigger mechanisms, such as unfavourable topographical, geological and tectonic conditions, the strong physical and chemical weathering of rock masses, seismic activity, climatic conditions, vegetation, extreme weather conditions (winter storms, intense rainfall in combination with wind, freeze–thaw cycles, etc.) human activities, cuts and earthquakes. Such mechanisms cause changes in the balance of forces acting upon the rock mass and consequently lead to a sudden collapse of the rock mass. Since the rockfall can generate large-scale mass movements of rock material it is essential to assess and predict such hazards in the future. In order to achieve this, it is crucial to identify the key mechanics of rockfalls and to identify correlations between them and rockfall-related kinematics. In order to determine rockfall runout distance, which represents the basis of rockfall hazard and risk assessment, it is essential to determine possible rockfall pathways defined as rockfall trajectories. For this study we used probalistic process-based rockfall trajectory model RockyFor3D. RockyFor3D calculates trajectories of single individually falling rocks in three dimensions (3D). It combines physically-based, deterministic algorithms with stochastic approaches, and can be used for regional, local and slope scale rockfall simulations. Input data for the model consist of a set of 10 raster maps, which all have to have the same map extent and the same cell size. The required inputs are: digital terrain model (DTM), rock density of rockfall source area, block dimensions (height, width, length), shape of the block, slope surface roughness (values that represent 70 %, 20 % and 10 % properties of the slope), and soil type. Moreover, optionally the model can also take into account the effect of forest and rockfall protection nets in modelling the propagation area.

Keywords rockfall,

Introduction

A rockfall is a slope process in which a rock mass of different rock sizes and shapes (rocks, boulders and blocks) separates or becomes detached and descends extremely quickly (Hungr et al., 2014). Rockfalls can be caused by various trigger mechanisms, such as unfavourable topographical, geological and tectonic conditions, the strong physical and chemical weathering of rock masses, seismic activity, climatic conditions, vegetation, extreme weather conditions (winter storms, freeze–thaw activity, etc.) human activities, cuts and earthquakes (). Such mechanisms cause changes in the balance of forces acting upon the rock mass and consequently lead to a sudden collapse of the rock mass. Since the rockfall can generate large-scale mass movements of rock material it is essential to assess and go on to predict such hazards in the future. In order to achieve this objective it is crucial to identify the key mechanics of rockfalls and to identify correlations between them and rockfall-related kinematics. In order to determine rockfall runout distance, which represents the basis of rockfall hazard assessment, it is essential to determine possible rockfall pathways defined as rockfall trajectories. Rockfall trajectory depends on the geometry of the slope (height, gradient, curvature and orientation), characteristics of the detached rocks (shape, size, type of rock) and on the slope characteristics (restitution coefficient, roughness of slope, etc.) (Petje et al., 2005a; Abbruzzese et al., 2009).

The study focuses on the holistic determination and observation of rockfalls. It is based on the identification and determination of potential rockfall source areas/release points and rockfall runout distances using dynamic (process) modelling.

Rockfalls threaten communities and infrastructure in mountainous regions worldwide, and have been a particularly problematic hazard along transportation corridors. The term hazard is expressed as the probability

that particular dangerous phenomenon (in our case that would be rockfalls) of given magnitude occurs in a given area over a specified timer interval and may adversely affect human life, property or activity to the extent of causing disaster (Varnes, 1984; Fell et al., 2008). This definition includes the concepts of location (rockfall source area), frequency (i.e., its temporal recurrence) and magnitude or intensity (i.e.amount of energy involved) (Ferrari et al., 2016).

Current practices around the word show that rockfall hazard assessment and hazard mapping are essential for the rockfall risk management that is required part of preventive mitigation actions and forms (Abbruzzese et al., 2009; Volkwein et al., 2011; Ferrari et al., 2016).

The rockfalls occurrence is typical on the steep rock slopes, may involve rock fragments of different sizes giving rise to rockfalls with different degree of hazard. Rockfall hazard assessment is a very complex task because of the degree of uncertainty in the definition of the main input parameters such as the rockfall trajectory and the location of potential source areas (Losasso et al., 2017).

Exposure of Slovenia territory to rockfalls is expected, given the specific geological settings, tectonic complexity and geomorphological conditions (Komac, 2012). The rockfall susceptibility map of Slovenia in scale 1:250,000 shows that rockfall exposed areas are not related only to mountain vertical slopes but also to steep river banks, coastal cliffs and moderately steep slopes with deposits of colluvium and talus (Zorn, 2002; Zorn, 2003; Čarman et al., 2011a; Čarman et al., 2011b).

Previous researches in Slovenia were mainly focused on development of rockfall susceptibility map at national scale (1:250,000). The developed methodology was based on Chi-square analyses using linear weighted sum model approach on the basis of selected spatio-temporal factors (lithology, strata dipping, slope angle and distance to faults). The elaborated susceptibility map defines only potential rockfall source area (Čarman et al., 2011a; Čarman et al., 2011b; Zorn et al., 2012; Čarman et al., 2015).

Rockfalls could be caused by different trigger mechanisms such as extreme weather conditions (heavy rainfalls, winter storms, freeze–thaw activity, etc.); human activities cuts (changes of slope geometry) and earthquakes (Dorren, 2003). Extreme events such as strong earthquakes induced large rockfalls in Slovenia, during the event or in period after it (Mikoš et al., 2006a). The first earthquake on April 12, 1998 (Ms = 5.6) caused more than 100 failures, among them 50 rockfalls. The estimated volume of mass that could be released to the watercourses was 480,000 m3, since the 260,000 m3 of rockfall material remained on slopes (Ribičič & Vidrih, 1998; Vidrih et al., 2001; Mikoš et al., 2006a). After the earthquake of July 12, 2004 (MS = 4.9), 50 superficial slope failures including 38 rockfalls were documented (Mikoš et al., 2006a).

Two rockfalls in the Trenta valley (NW Slovenia) were further analysed using a 2-dimensional rock simulation using computer program Rockfall (Petje et al., 2005a; Petje et al., 2005b; Petje et al., 2005c; Mikoš et al., 2006b). The research showed that models were successfully calibrated using evidence ("silent witnesses") from historical rockfalls. The importance and usefulness of rockfall trajectory modelling and calculation of rockfall runout zones have been also demonstrated in the case of rockfall in Žužemberk, where rockfalls pose a significant hazard for settlement (Peternel, 2010; Čarman & Peternel, 2010).

In Slovenia and across Europe rockfalls pose a distinct danger, especially where transportation lines (railway corridors and roads) cross river ravines that are usually steep and built from compact rocks (limestones, sandstones, etc.). The likelihood of a rockfall increases where transportation lines cut rock slopes in the form of road and railway slope cuts.

With this in mind, the study focuses on rockfalls related to vertical or sub-vertical natural slopes or high manmade cut slopes along transportation lines, the railway link between Renke and Zagorje (central Slovenia). A number of rockfalls occurred in this area on the railway section over 3 km long between 10th and 11th December 2017. Rockfalls have partially damaged or completely destroyed rail tracks at several places. The railway traffic was closed for some time. The event was related to snowfall followed by rainfall and strong wind.

Methods

Study case

This paper focuses on determination and studying rockfall hazard using process modelling in the case of rockfalls along the railway link between Renke – Zagorje (central Slovenia). This area is well known by very common rockfalls along the railway link. This kind of events present direct danger transportation corridor and trains.

Recently, the largest rockfall event happened in December 2017. The location of rockfall runout distance is shown in Figure 1. Based on data collection obtained by railway authorities, the volume of rockfall boulders was somewhere in between 0.2 and 1.5 m^3.

The development of rockfall hazard assessment was based on detailed engineering geological mapping of study area and on dynamic (process) modelling of rockfall trajectories using computer simulation (Rockfor3D).

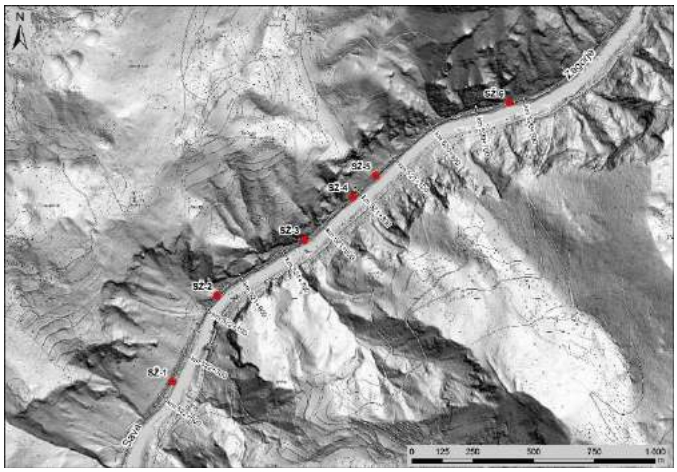

Figure 1 Map of runout distance of previous rockfall events occurred in December 2017

Detailed engineering-geological mapping

Detailed engineering-geological mapping is of key importance in determining and studying slope mass movements. Mapping included identification of recent (December 2017) rockfall evens along the railway, their magnitudes, trajectories and source areas (Fig. 2). In addition, potential source areas for future events were also detailed mapped, where location, extent, size and shape of blocks were evidenced.

Rockfall modelling

In order to model rockfall trajectory and determine rockfall runout distance, 3-dimensional dynamic modelling was applied. Because two-dimensional modelling is limited to rock motion in the vertical plane and cannot simulate lateral motion, three-dimensional modelling was applied, taking into account the entire geometry of the slope. Three-dimensional modelling was carried out the Rocyfor3D computer program (ecorisQ, Switzerland).

RockyFor3D

RockyFor3D is a probabilistic process-based rockfall trajectory model of falling blocks in three dimensions (Dorren, 2016). The model can be used for regional, local and single slope rockfall simulations. Trajectories of falling rock is simulated as 3D vector data by calculating sequences of parabolic free fall through the air and rebounds on the slope surface. The minimum input data are digital elevation model (DEM), spatial definition of the release area, rock density, size of the rock (height, width and length), shape of the rock, surface roughness and soil type (Dorren, 2016). Additionally, the RockyFor3D model enables rockfall simulation with forest and with rockfall nets. The main outputs of the model are 95% confidence level of the kinetic energy values per raster cell (kJ), 95% confidence level of the normal passage heights per raster cell (m), number of blocks passed through each raster cell, number of source cells the simulated blocks originated from per raster cell and reach probability (Dorren, 2016).

Airborne laser scanning data of Slovenia (SMARS, 2014) were used to create a rasterised digital elevation model with pixel size of 2 × 2 m. The experience of the author is that 1×1 m spatial resolution does not necessarily improve the modelling results (Dorren and Heuvelink, 2004). All potential release areas were identified during filed inspection and the volumes of all potential falling rocks and spherical rock shape were estimated. Dimensions of the rocks were calculated based on rock volume data. Rock density was set on 2600 kg/m3 (limestone). Variation of block volume was set to ± 0 % and the initial fall height was set to 0 m.

The slope surface roughness parameters were determined based on the model's tutorial and the field inspection (Dorren, 2016). Soil type on the rockfall slope corresponds to medium compact soil with small rock fragments and the following values were used for simulation: rg70 = 0.03, rg20 = 0.05, rg10 = 0.07, soil type = 3. For Sava River, the following values were used: rg70 = 100, rg20 = 100, rg10 = 100, soil type = 0. The number of simulations were set to 1000 as recommended by the authors (Dorren, 2016).

Results and discussion

Detailed engineering-geological mapping

In the frame of detailed engineering-geological mapping the following will be determined:

- the "silent witness" that reveal the past behaviour of the slope and the trajectory of past rock falls (benchmarks on the street, trees, etc.) that can be used to model the runout distance of potential rockfalls
- existing mitigation measures and their usefulness
- rockfall source areas with determination of location, extent, size and shape of rock (Figure 2).
- materials that are potential indicators of rockfall events.

Figure 2 Source area of rockfalls

Regarding the engineering-geological map of pilot area, model parameters were calibrated using data collected from "silent witnesses" such as benchmarks on the street, damaged trees, etc.) that testify to the past behaviour of the slope and the path/trajectory of past rock falls. Model parameters were used as input data for the 3-dimensional dynamic modelling of rockfall trajectories and to determine potential rockfall runout distances and, ultimately, to assess rockfalls hazards. The following parameters are required to calculate rockfall trajectories and rockfall runout distances: location of release points, the shape and geometry of rocks, possible rock sizes and their mass, mechanical properties of the slope and rocks; restitution coefficient, the land cover and geometry of the slope, and possibly crushed rocks at points of impact.

Rockfall modelling

In total, 96000 simulated falling rocks were done during simulations. Overall simulated block volumes ranges from 0.1 m^3 to 15.3 m^3, with mean value of 1.7 m^3. Maximum of the mean energy values per raster cell is 2789 kJ, while maximum energy value per raster cell equals 9123.7 kJ (Figure 3, Figure 4, Figure 5).

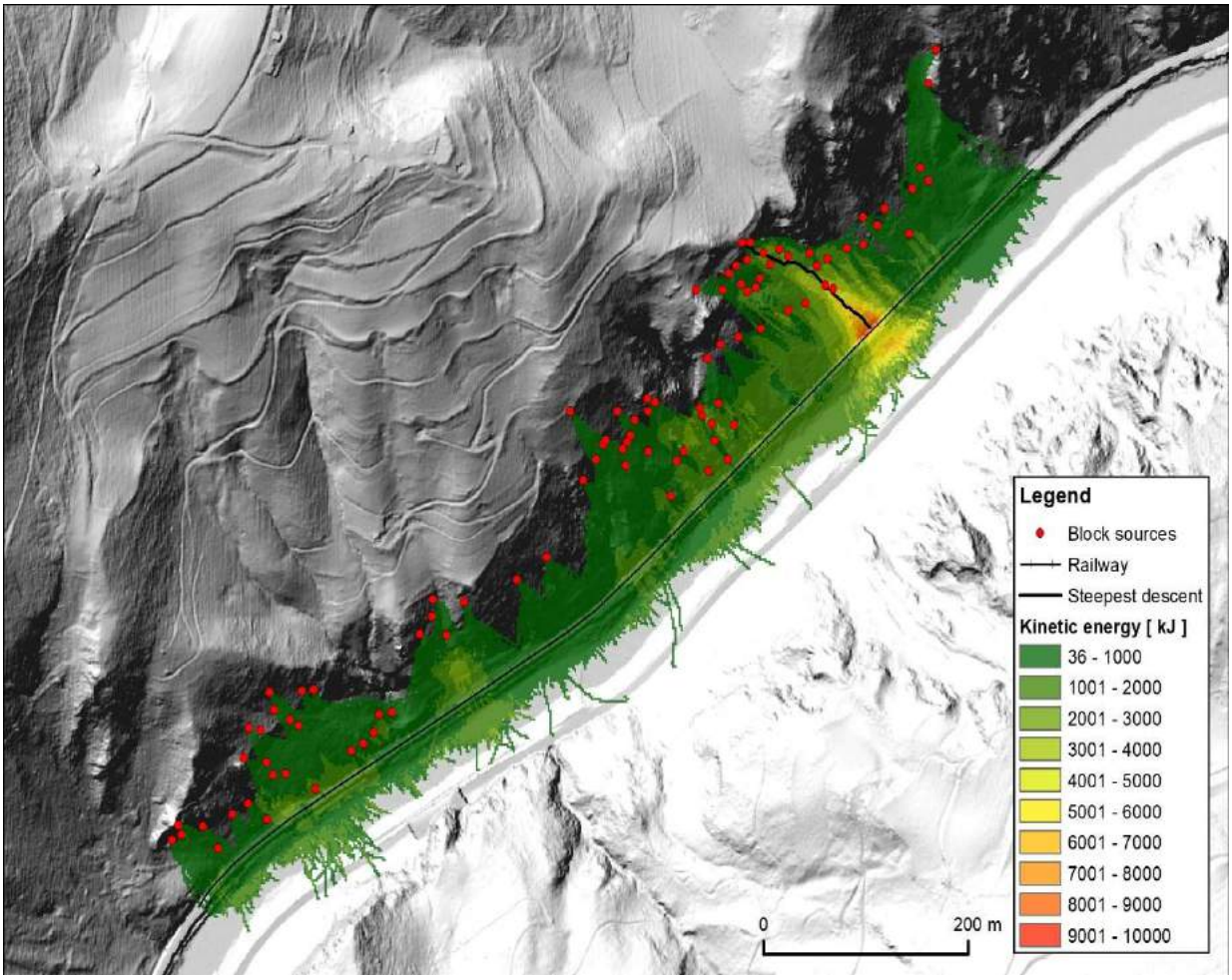

Figure 3 Kinetic energy values (95% confidence level) per raster cell for study area

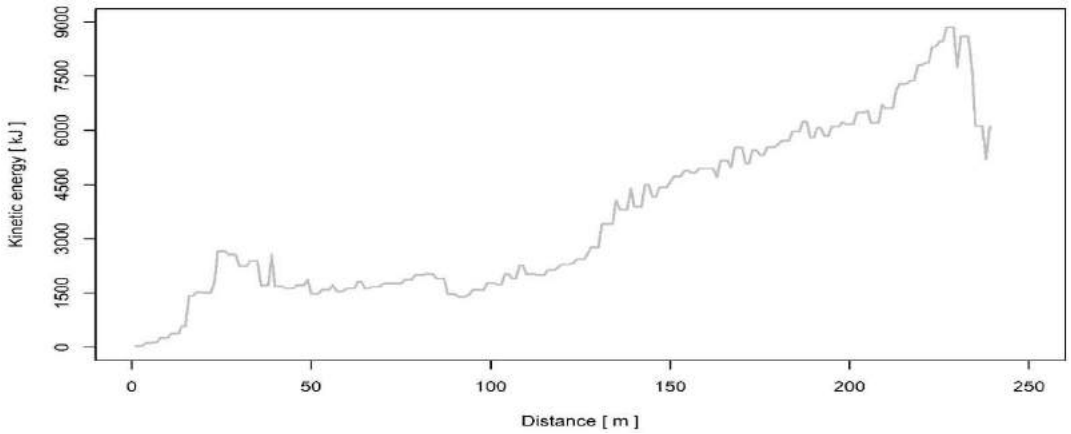

Figure 4 Increasing of kinetic energy values (95% confidence level) per raster cell along steepest descent (Figure 2) for simulated rockfall with block volume of 15 m^3

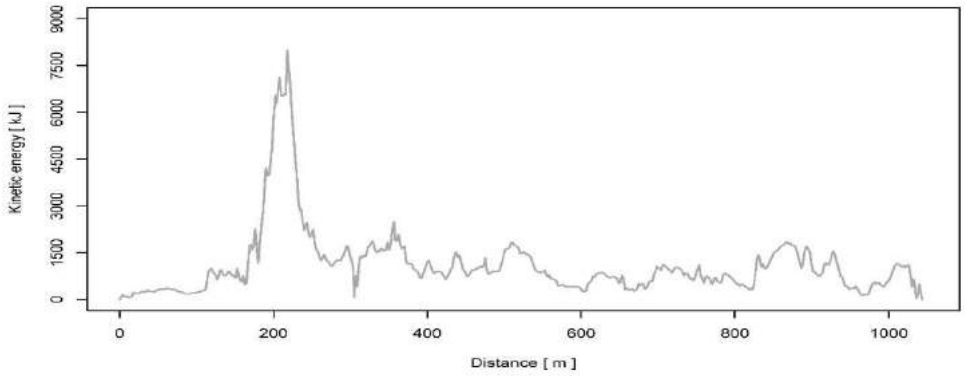

Figure 5 Variation of kinetic energy values (95% confidence level) per raster cell along railway. Maximum value is 7996 kJ

Normal passage heights (95% confidence level) per raster cell ranges from 0.9 m to 44.7 m (cliffs above railway). Mean value of normal passage heights equals 5.1 m. Along railway path normal passage heights (95% confidence level) per raster cell ranges from 0.0 m to 22.9 with mean value of 6.6 m (Figure 6 and Figure 7).

Both value, 95% CI of kinetic energy and 95% CI of normal passage heights are suggested for dimensioning rockfall hazard mitigation measures, eg. rockfall nets.

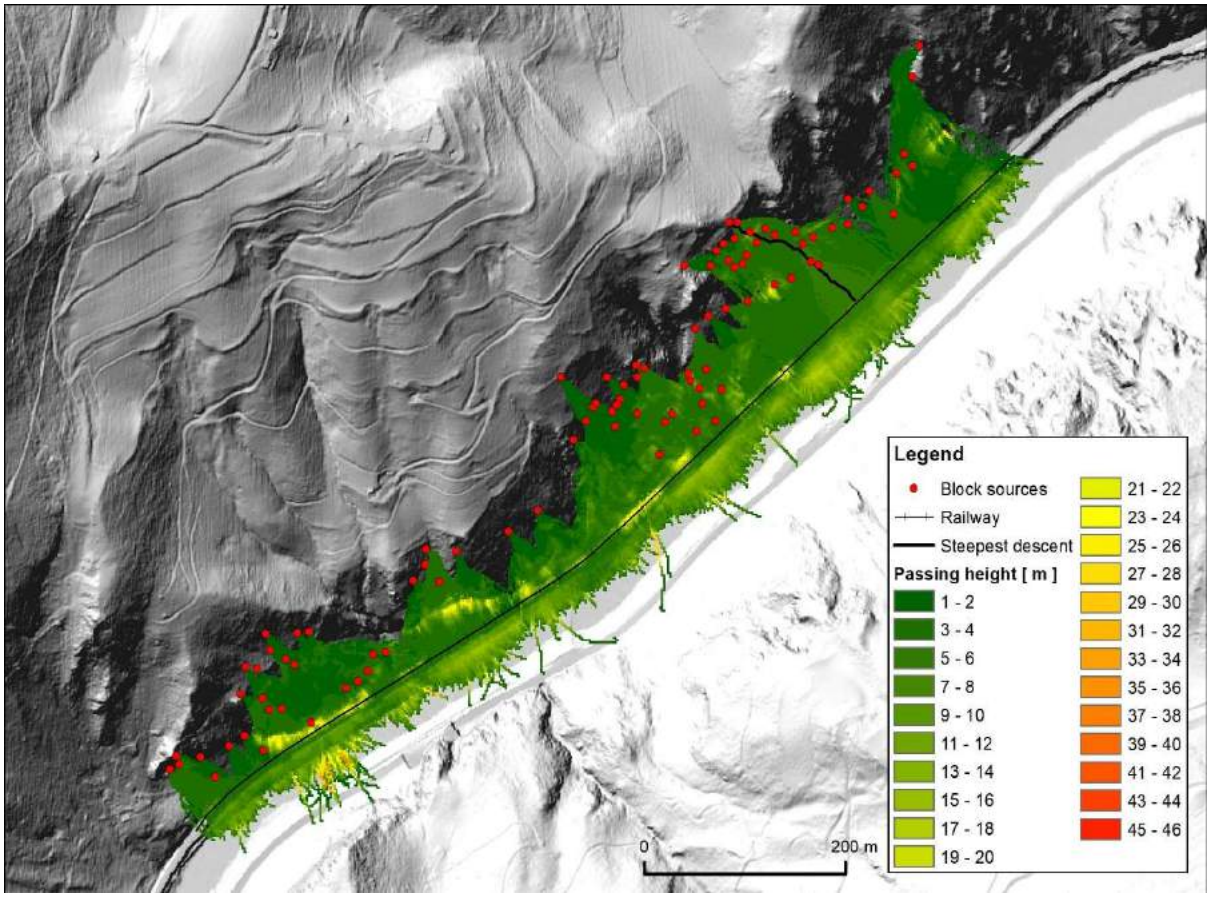

Figure 6 Normal passage heights (95% confidence level) per raster cell for study area

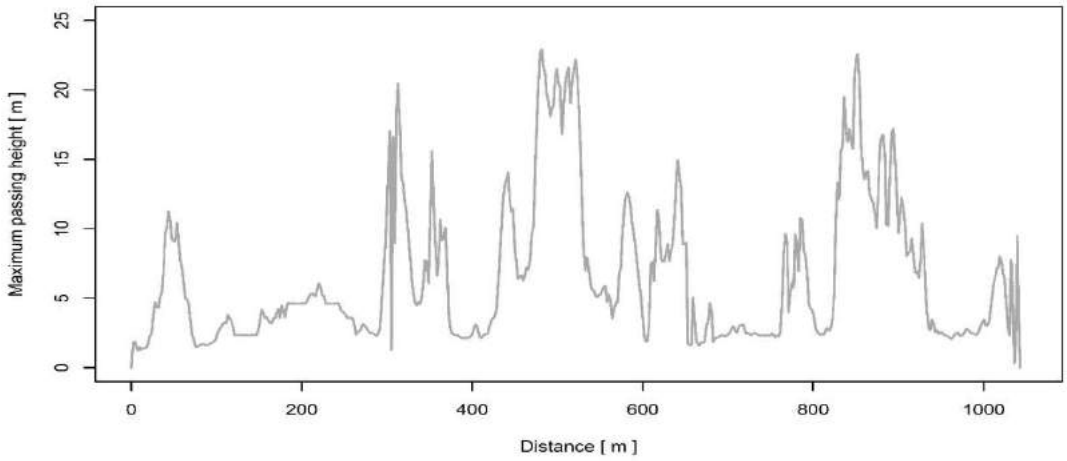

Figure 7 Variation of normal passage heights (95% confidence level) per raster cell along railway. Maximum value is 22.9 m

Conclusion

The results provide the basis for further research, which will in turn further development of effective approaches to rockfall risk management and the determination of mitigation measures and actions.

Such data will also serve to help reduce the uncertainties related to rockfall hazard zoning procedures in the future and better define the influence of certain factors on the mapping process.

References

Abbruzzese, J.M., Sauthier, C., Labiouse, V. (2009) Considerations on Swiss methodologies for rock fall hazard mapping based on trajectory modelling. Nat. Hazards Earth Syst. Sci., 9, 1095-1109.

Amato, J., Hantz, D., Guerin, A., Jaboyedoff, M., Baillet, L., Marsical, A. 2016. Influence of meteorological factors on rockfall occurrence in a middle mountain limestone cliff. Natural Hazards and Earth System Sciences, 16, 719 – 735

Bavec M., Čarman M., Durjava D., Jež J., Krivic M., Kumelj Š., Požar M., Komac M., Šinigoj J., Rižnar I., Jurkovšek B., Trajanova M., Poljak M., Celarc B., Demšar M., Milanič B., Mahne M., Otrin J., Čertalič S., Štih J., Hrvatin M. (2012) Izdelava prostorske baze podatkov in spletnega informacijskega sistema geološko pogojenih nevarnosti zaradi procesov pobočnega premikanja, poplavnih, erozijskih kart ter kart snežnih plazov – pilotni projekt. Geološki zavod Slovenije, Ljubljana (ISBN_P-II-30d/a-1/28). 40 f.

Čarman, M., Peternel, T. (2010) Skalni podori Stara gora pri Dvoru v občini Žužemberk. Geologija 53 (2), 173–180.

Čarman, M., Kumelj, Š., Komac, M., Ribičič, M. (2011a) Rockfall susceptibility map of Slovenia. In: Mölk, M. et al. (eds.) Interdisciplinary Workshop on Rock Fall Protection. Innsbruck, Austrian Service for Torrent and Avalanche Control, Geological Service, pp. 3.

Čarman, M., Kumelj, Š., Komac, M., Ribičič, M. (2011b) Pregledna karta verjetnosti pojavljanja podorov v merilu 1: 250.000. In: Rožič, B. (ed.) 20. posvetovanje slovenskih geologov, Ljubljana, Naravoslovnotehniška fakulteta, Oddelek za geologijo, str. 22-25.

Čarman, M., Bavec, M., Komec, M., Krivic, M. (2015) Rockfall susceptibility assessment at the municipal scale (Bovec municipality, Slovenia). In: Lollino, G. et al. (eds.) Engineering geology for society and territory, Landslide processes. Switzerland, Springer, str. 2017-2021.

Dorren, L.K.A. (2003) A review of rockfall mechanics and modelling approaches. Progress in Physical Geography, 27 (1), 69–87.

Fell, R., Corominas, J., Bonnard, C., Cascini, L., Leroi E., Savage, W. (2008) Guidelines for landslide suscpetibility, hazard and risk zoning for land use planining. Eng. Geol., 102, 85-98.

Ferrari, F., Giacomini, A., Thoeni, K.(2016) Qualitative Rockfall Hazard Assessment: A Comprehensive Review of Current Practices. Rock Mechanics and Rock Engineering, 49 (7), 2865-2922.

Hungr, O., Leroueil, S., Picarelli, L. (2014) The Varnes classification of landslide types, an update. Landslides 11 (2), 167–194.

Losasso, L., Jaboyedoff, M., Sdao F. (2017) Potential rock fall source areas identification and rock fall propagation in the province of Potenza territory using an empirically distributed approach. Landslides, 14 (2), 1593-1602.

Mikoš, M., Fazarinc, R., Ribičič, M. (2006a) Sediment production and delivery from recent large landslides and earthquake-induced rock falls in the Upper Soča River Valley, Slovenia. Engineering Geology, 86, 198-210.

Mikoš, M., Petje, U., Ribičič, M. (2006b) Application of a rockfall simulation program in an alpine valley in Slovenia. V: MARUI, Hideaki (ur.), MIKOŠ, Matjaž (ur.). Disaster mitigation of debris flows slope failures and landslides : proceedings of the INTERPRAEVENT international symposium : september 25-29, 2006 in Niigata, Japan, (Frontiers science series, No, 47). Universal Academy Press, Tokyo: str. 199-211.

Komac, M. (2012) Regional landslide susceptibility model using Monte Carlo approach – the case of Slovenia. Geological Quarterly 56 (1), 41-54.

Peternel, T. (2010) Ocena ogroženosti pred padanjem kamnov na območju Dvora pri Žužemberku. Diplomsko delo. Univerza v Ljubljani , NTF, Oddelek za geologijo, Ljubljana. 54 str.+priloge.

Petje, U., Mikoš, M., Majes, B. (2005a) Modeliranje gibanje skalnih podorov = Modelling of rockfall motion. Acta hydrotechnica 23/38, 19-37.

Petje, U., Mikoš, M., Ribičič, M. (2005b) Ocena nevarnosti padajočega kamenja za odsek regionalne ceste v dolini Trente. Geologija, 48 (2), 341–354.

Petje, U., Ribičič, M. & Mikoš, M. (2005c) Computer simulation of stone falls and rockfalls = Računalniško simuliranje skalnih odlomov in podorov. Acta geographica Slovenica, 45 (2), 93-120.

Rekanje, B. (2019). Vpliv meteoroloških spremenljivk na frekvenco pojavljanja padajočega kamenja v Baški grapi. Oddelek za gozdarstvo in obnovljive gozdne vire, Biotehniška fakulteta, Univerza v Ljubljani, 54 str.

Ribičič, M., Vidrih, R. (1998) Plazovi in podori kot posledica potresov. Ujma 12, 95 – 105.

Varnes, D.J. (1984) IAEG Commission on Landslides & other Mass Movements. In: Landslide hazard zonation: a review of principles and practice, 63. Paris, UNESCO Press.

Vidrih, R., Ribičič, M., Suhadolc, P. (2001) Seismogeological effects on rocks during the 12 April 1998 upper Soča Territory earthquake (NW Slovenia). Tectonophysics 330, 153-175.

Volkwein, A., Schellenberg, K., Labiouse, V., Agliardi, F., Berger, F., Bourrier, F.,Dorren, L.K.A., Gerber, W., Jaboyedoff, M. (2011) Rock fall characterisation and structura lprotection – a review. Natural Hazards and Earth System Sciences, 11, 2617-2651.

Zorn, M. (2002). Rockfalls in Slovene Alps (Podori v slovenskih Alpah). Geografski zbornik 42, 124-160.

Zorn, M. (2003). Nekateri večji skalni podori v Alpah. Ujma:17-18, 241 – 250.

Zorn, M., Komac, B., Kumelj, Š. (2012) Mass movement susceptibility maps in Slovenia: the current state. Geografski vestnik, 84 (1), 99-112.

doi.org/ 10.35123/ReSyLAB_2019_38

Remediation of the landslide of Đurđević hill clay pit in Bedekovčina, II. phase of rehabilitation

Kristijan Grabar[(1)], Matija Orešković[(2)], Ivan Cvitković[(2)]

1) SPP d.o.o., Trstenjakova 3, Varaždin,

2) Sveučilište Sjever, Trg dr. Žarka Dolinara 1, 48000 Koprivnica

Abstract In the past ten years, some observations have been made, as well as partial attempts to repair the unstable slope of a neglected clay pit on the western slopes of Djurdjević Hill. Nevertheless, the situation on the slope manifested itself with gradually increasing forms of instability, especially during the winter to spring transition when the water-soaked slope masses took on a mushy form, such as during a check-up on 8.3.2016. The remedial solution applied to the clay is based on the experiential knowledge that only with the application of flexible (self-adjusting) technical measures and interventions can optimal results be obtained in achieving slope stability, since this dictates the terrain circumstances, which give rise to the essence of the problem to be solved!

Keywords clay pit, remediation, landslide, Proctor test, embankment

Introductions

The Đurđević Hill, located northeast of Bedekovčina, is an elongated foot incision of the western slope of the Đurđević Hill. Logging into the slope of the slope had to cause destabilization of the slope at some early stage of exploitation, which prompted to take some steps 10 years ago to stabilize the slope. According to the information collected, the remediation work according to the aforementioned Report was carried out only partially, but without the expected effect. For this reason, at the beginning of 2016, it was again concluded that the rehabilitation activities were being renewed, and for this purpose, a preliminary geotechnical inspection of the clay pit at Đurđević's Hill was carried out in March of that year. From the very first impression, it could be concluded that it was devastated large-scale terrain whose surface could be estimated at least about 20 hectares.

Geodetic works

Geodetic survey was done with the unmanned aerial vehicle DJI Phantom 4 with a built-in 12 MP camera, which allows high resolution of photos in the formation of stereo pairs, using which are calculated terrain points and finally creates a terrain model, orthophoto, DMR, etc. The survey was done on 08.25.2016. between 13-15 p.m on a relatively sunny day in the presence of windy intervals. The survey covers approximately 50 ha of the surface. For orientation purposes, 9 orientation points have been set up in the national coordinate system (HTRS96 / TM) so that they evenly cover the area of operation. The landmarks are set using a Topcon GPS GNSS device with a link to the CROPOS system that provides 2-3cm real-time positioning accuracy in all three dimensions.

Figure 1 Digital orthophoto (DOF)

Geodetic survey and measurement through appropriate computer processing created a wide range of possibilities for practical use of different geodetic substrates. The elementary data of relevance to this Report are the elevation angles of the estuaries (terrains) of individual exploratory wells (a total of 14 wells in the clay pit area was constructed during the summer of 2016) as well as terrains along three rural wells (ZD1, ZD2 and ZD3), which are located along the top edge of the clay pit (ZD1) and not far behind the edge (ZD2 and ZD3).

Research tests

Exploratory drilling was mainly of a prospecting character, ie the basic purpose of the drilling was reduced to determining the depth of the indigenous soil since the condition of the entire clay pit (especially it's base) indicated the dragging of loosened, softened and extremely disturbed soil over relatively intact indigenous soil. This coating was created as an unintended consequence of the exploitation of clay pit, which is

manifested through the destabilization of the western slope of the Đurdjević Hill. Field exploratory drilling (with associated measurements and observations) was conducted during July 2016. In addition to the visual determination of the soil, attention has been focused on experiential observations regarding soil resistance to rotational drilling (for the purpose of distinguishing embedded soft surface materials from the indigenous soil). Occasionally, a standard penetration test (SPP) was conducted for the same purpose.
Groundwater was registered in two phases:

PPV = The occurrence of groundwater during drilling, i.e. the depth at which the water appeared

NPV = The groundwater level in the well after a certain amount of time that was required for the level to rise.

Through subsequent observations, only NPV could be measured if, in connection with the dry summer, there was no water in the well at all. In some wells, it was possible to clearly understand at what depth contraction (squeezing) occurs. This information was often indicative of the recent emergence of wild soil. The depth of soil is particularly carefully recorded. These, as well as all other drilling elements, are covered in the tables.

Figure 2 Basic elements of drilling

As can be seen from Figure 2, during the exploratory drilling, the SPP experiment was occasionally carried out (34 SPP trials in total) after which an attempt was made to extract a sample (Φ ca 3.2 cm) from the SPP cylinder, thus collecting samples (PUSPT) shipped to the geotechnical lab. All SPP specimens delivered to the laboratory (a total of 18 SPP specimens) were re-examined and visual observations and identification summarized. Almost all samples (except 2 samples) were tested for compressive strength (16 samples) in the laboratory, and one of the samples (B5 / 2,00-2,30) in which a considerable amount of organic matter was already observed in black was subjected to the test. To the organic matter content which confirmed that the sample contained organic matter in the amount of almost 50%. The core of B5 is shown in Figure 2.

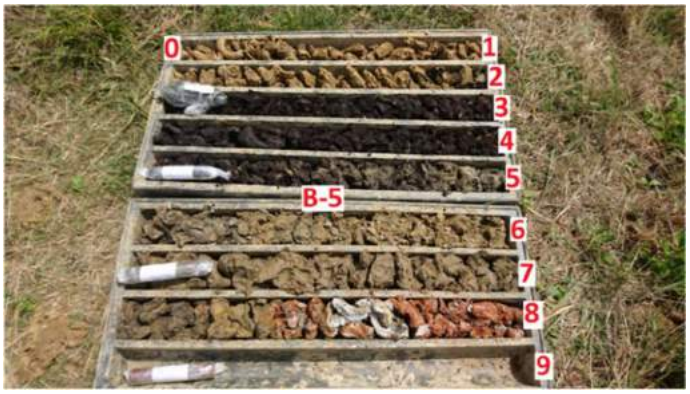

Figure 3 B5 borehole core

Should be emphasized here that the visual inspection of the samples submitted showed that it was a very heterogeneous soil mixture, which was quite in line with the expectations since these are the samples that mostly represent the deposited materials (and / or coated) over wild soil (ST) in the substrate. For all samples (18 pieces), the so-called. Current moisture (15.6≤w_0≤113.1%) and extended studies were performed on a group of six samples.

Finally, two special samples were also brought to the laboratory from the SJ-1 well and the SJ-2 well (both located within the B9, B10 and B11) boreholes for the specific purpose of being tested through the Proctor test. On the basis of the above, a total of 20 different samples was subjected to visual inspection (as well as other tests) in the geotechnical laboratory. Since the concept of remediation is conceived so that the bulk of the remediation work will be based on the displacement of earth masses provided that the installation is carried out in a technically optimal manner, large (disturbed) soil samples have been taken in the field, which have subsequently been laboratory-tested appropriately.

Two samples, which were taken from two wells, were sent to the geotechnical laboratory for testing in the Proctor experiment. This test primarily confirms (or denies) the suitability of the test material for incorporation into the embankment body (or for slope planning), and in addition, demonstrates the necessary optimum moisture at which it is possible to achieve maximum compaction of the test material with proper incorporation into the embankment body.

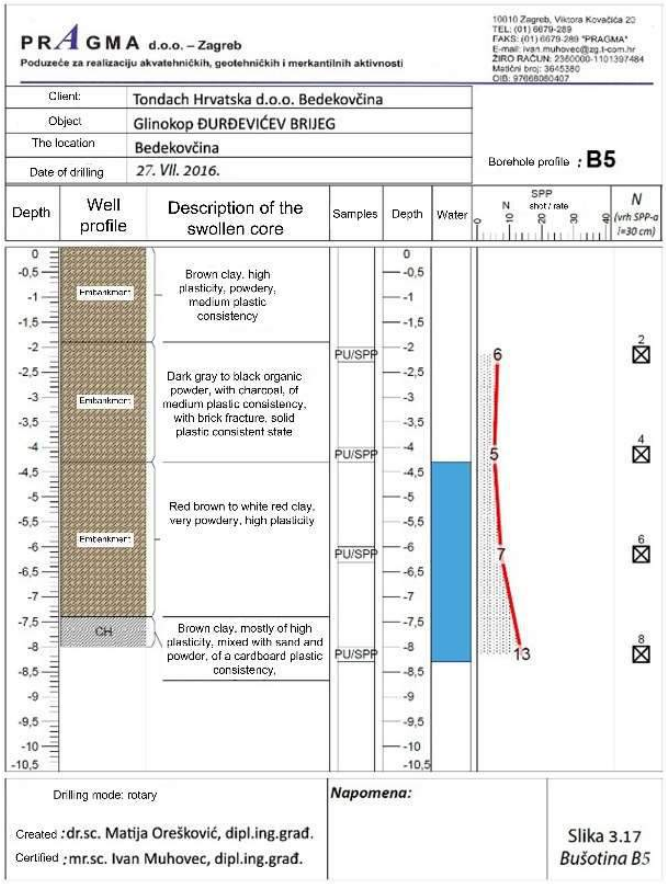

Figure 4 Drilling profile of B5

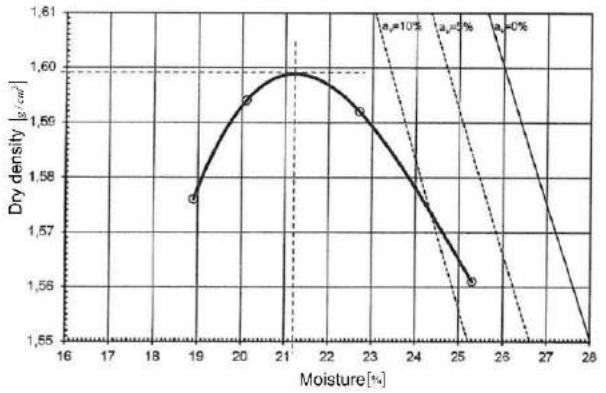

Figure 5 Results of the Proctor test for the sample from SJ-1

The test results of both samples by Proctor's experiment confirmed the suitability of fitting into the body of a controlled compacted embankment, and the optimum moisture of the material during fitting should range between 18 and 21.2%, or on average around w_{opt} = 20% (Fig 5 and 6). As the average dry density of the soil will be $1600 \leq \rho_d \leq 1700$ kg / m³. For the design of the remediation concept, all the data and results presented in this paper have a certain part, but among the most important ones should be considered the field morphology and the soil data obtained through exploratory drilling.

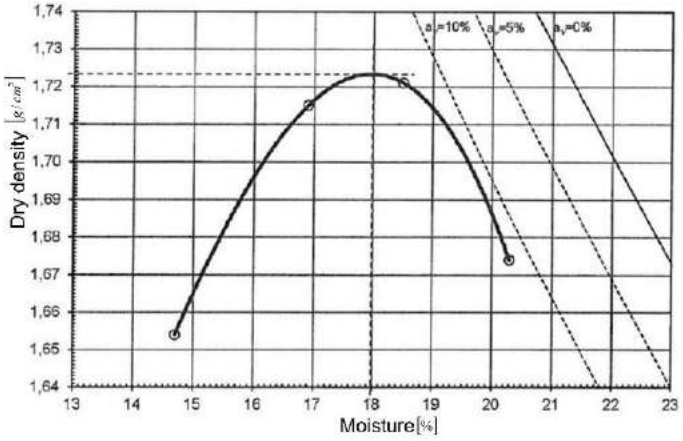

Figure 6 Results of the Proctor test for the sample from SJ-2.

The thickness of the loose cover in zone VP0 (and VP0 +) is similar to that in zones VP1 (between 5 and 5.5 m), but it is not significantly smaller in zones VP2 (4.0 m), only in zones VP3 and then in zones VP4 decreases rapidly (1.0 to 1.5 m). However, the VP3 and VP4 zones are too close to the upper edge of the landslide, so we can exclude them from considerations that focus on the route selection of the supporting foot embankment. All in all, it turns out that the route of the future supporting foot embankment (as a vital component of the remedial solution) should be placed in the zone of the height plateau VP1 where the mean depth of the ST is approximately 5.0 m and the mean height of the terrain (from the aspect of exploratory wells) is approx. 160 m n.m.

Table 1 Depths of wild soil

HEIGHT PLATE	BOREHOLE MARK	ST (m)	ST FOR THE HEIGHT PLATE		MIDDLE HEIGHT (only in relation to the well)
			CALCULATION	MEDIUM	
VPO i VPO+	B1	4,9	5,4	5,5	155 m n.m.
	B2	4,8			
	B3	6,4			
VP1	B4	0,5	5,0	5,0	160 m n.m.
	B5	7,4 (?)			
	B6	(10,1)5,5			
	B7	6,5 (?)			
VP2	B12	4,2 (KP)	4,0	4,0	170 m n.m.
	B13	3,8 (KP)			
VP3	B9	1,8(KP)	1,35	1,5	175 m n.m.
	B11	0,7 (KP)			
	B14	1,5 (KP)			
VP4	B8	1,3 (KP)	0,9	1,0	182,5 m n.m.
	B10	0,5 (KP)			

The clay slope stability check was performed through a computational model compliant with Slide 6.0 (Rockscience Inc.), which uses the limit equilibrium criterion to calculate slip factors. The Mohr-Coulomb Model (MCM) was used to describe soil behavior. The input parameters used in the program are given in the following tables.

Table 2 Input parameters for soil

INPUT ELEMENTS	LABEL	COLUVIUM, DUSTY CLAY (1)	STABLE SUBSTANCE (2)	SCREW SUPPORT BANK (3)	MEASURING UNIT
SOIL MODEL	MCM	MCM	MCM	MCM	-
DEPTH	h	1,4-4,6	>4,0	0,0- max. 5,0	m
CONDUCT OF MATERIALS	-	drained	drained	drained	-
VOLUME SOIL WEIGHT	γ	18	19	19	kN/m^3
COHESION	C_d	2	15	15	kPa
FRICTION ANGLE	ϕ_d	20	25	25	0

As a critical slope profile, the PPII-6 profile was selected for the purpose of computational stability analysis, modeled such that the characteristic geotechnical conditions (soil thinning scheme, soil materials, and their parameters and slope contour geometry) gradually followed successive chronological changes that reflected expected effect of remedial measures. The following table (table 3) can be used to track the changes in question:

Table 3 Modeled geotechnical conditions

Slope condition		Characteristic geotechnical conditions: Drain line	Characteristic geotechnical conditions: Materials within the potential glide segment	F_s
Before remediation (A) (Current condition)		The PL is close to the contour of the transverse profile, set at an elevation of the known level from the exploration wells	Flattened slope soil (colluvium): Stable lining:	1,06
After remediation	B1 By design of longitudinal drainage (UD)	PL has been lowered to the lowest point of the drain due to the installation of a longitudinal drain	Flattened slope soil (colluvium): Stable lining:	1,34
	Construction of foot supporting embankments (UD + NPN)	PL has been lowered to the lowest point of the drain due to the installation of a longitudinal drain	Flattened slope soil (colluvium): Stable lining: Foot support embankment:	1,7

A large number of potential sliding surfaces are analyzed in the safety calculation, so the analysis shows only the analysis for the most critical sliding surface.

The following are some computational analyzes relating to the following states:

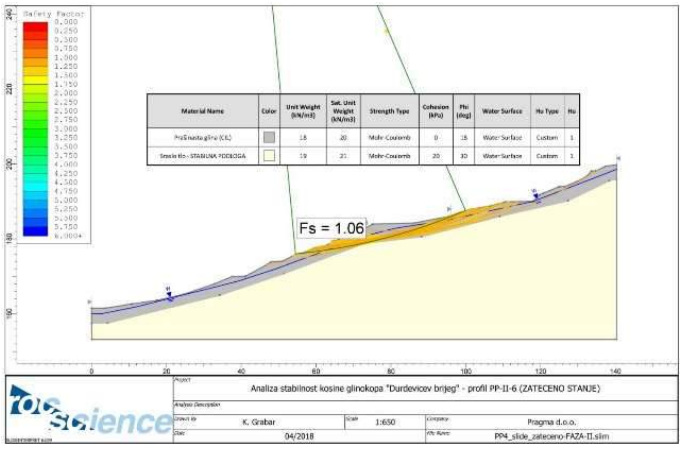

Figure 7 Current status (model A)

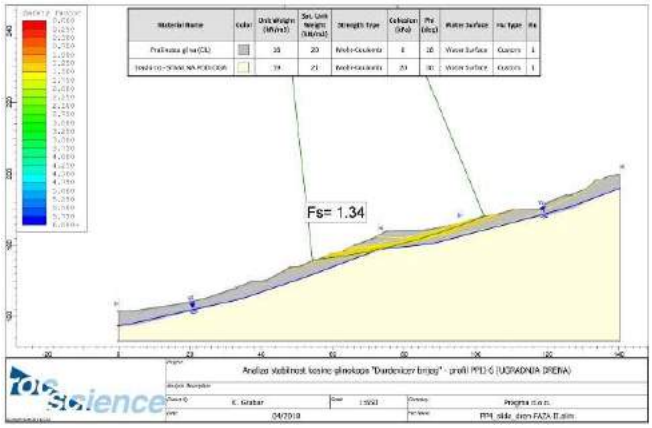

Figure 8 Drain installation (model B1)

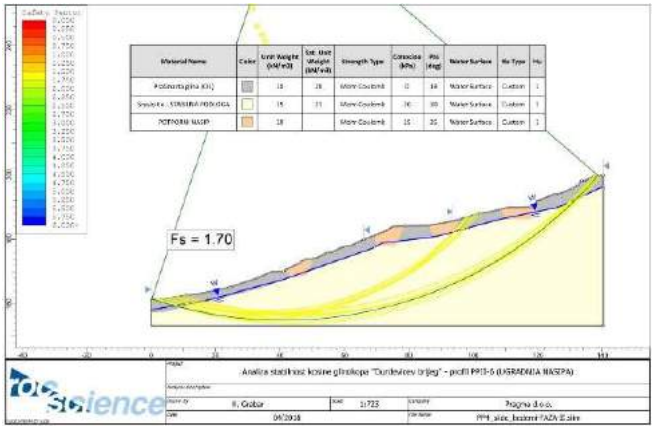

Figure 9 Construction of floor embankments, that is the embankments

Technical solution

The remediation concept consists of a series of different interventions listed below that will be meaningfully integrated into the functional unit:

- Surface water abstraction and drainage with particular emphasis on the lateral collecting ditch along the upper edge of the clay pit
- Reception and drainage of leachate, that is the establishment of a drainage system with the key role of a longitudinal drainage parallel to the aforementioned lateral ditch but performed just below the clay pit edge.
- Strictly controlled design of the foot-bearing embankment from the VP1 plateau with a buried base rate of approximately 5 to 6 m below the level of the existing terrain from the VP1 plateau.
- Formation of a neat slope with several berms between the foot embankment and the upper edge of the clay pit. The slopes must be less than 30°(Generally in the range 1: 5 to 1: 2).
- Upgrading of a unique surface water drainage system (with a particular emphasis on newly formed slopes)

and sewerage uptake and drainage all the way to the Vojsek stream.

- Applying a humus layer to the repaired slopes and planting and sowing suitable plant cover (vegetation) all over the repaired area
- Finalizing the entire area while securing subsequent access.

From the technical diagnosis set forth, a remediation concept emerged in which the essential remedial elements focus on:

Finalizing the entire area while securing subsequent access.

- Drainage of leachate and surface water from the area of an unstable slope
- Floor supportive support of the slope with emphasis on the knife belt.

The basic concept of the order in which the remediation work was carried out on the treated northern part of the slope of the Đurđević hill was comprised of twelve main activities:

1. Preliminary works
2. Surveying
3. Upper lateral canal (circumferential canal)
4. Initial earthwork on the slope
5. Main northern longitudinal drain, with simultaneous design of transverse drainage pads (drainage pads) at the positions of wet points (MP).
6. Storey supporting embankments
7. Final design of the slope
8. Split transverse channel
9. Drainage from repaired slopes
10. Planting plants
11. Maintenance of repaired slopes.
12. Postsanation oscillations

As can be seen in Figure 9, the remediation phase (north) is characterized by multi-story retaining embankments (B1,OB1,B2, B3, and B4) that are buried to a stable (load-bearing) substrate.

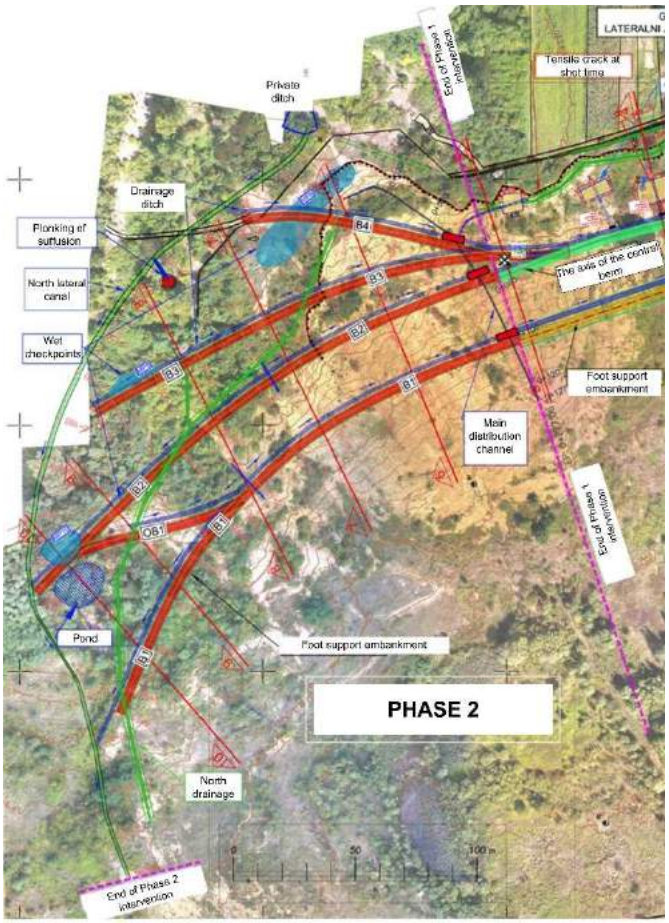

Figure 10 Situation plan II. phases of remedial actions

It is necessary to emphasize the need for the so-called stepwise slope cutting during reconstruction of slope surfaces (figure 10; figure 11).

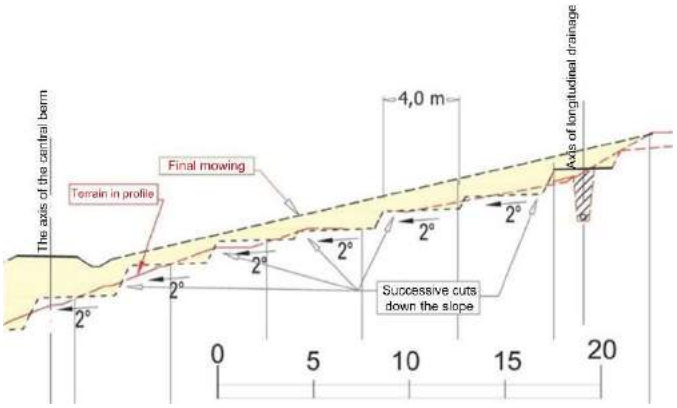

Figure 11 Successive step-by-step sloping of the slope surface (preparation for finishing the slopes) - schematic diagram

Design of underhill slopes of all embankments in a slope of 1:2, with the bottom embankment (B1) pointing with the foot of its subgrade sloping into a solidly prepared "foundation" (figure 12).

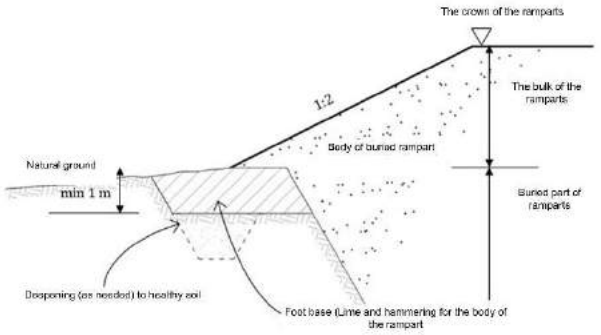

Figure 12 Schematic representation of the foot "foundation" of the hillside slope of the embankments

Control tests

During the implementation of the remediation work, great emphasis was placed on the constant implementation of control tests, primarily on the quality of the embedded material. The quality of foundation soil and embankment layers was checked for:

- Sampling
- Determination of soil moisture
- Determination of soil volume
- Determination of specific soil density
- Testing the uniaxial compressive strength of fine-grained soil
- Determination of Atterberg boundaries
- Determination of optimum moisture content
- Determination of ground resistance
- Modulus (compressibility modulus) by circular plate method
- Soil quality
- Determination of soil moisture content by sampling cylinders
- Field weight determination using the cylinder "Standard Test Method for Soil in Place by the Drive-Cylinder Method"

The required criterion for the installation of foundation and embankment materials is:

$$S_z >= 95\%, M_s > 15 \text{ MN/m}^2$$

The required amount of lime per unit area is spread over a loose layer. The spreading is done by a mechanical spreader, which ensures sufficient uniformity of spreading. Compaction was done by hedges, until they were uniformly compacted, thus mixing the binder within the bulk layer (figure 13).

The results confirmed that the depth of the trench excavation was adapted to the conditions, that is, the depth of "solid", ingrown soil, along the entire course of all supporting embankments. The results obtained indicate a favorably selected ground preparation technology, with the results of the soil modulus MS> = 15 MPa (figure 14).

Figure 13 Construction of an embankment during clay pit remediation. A sandy layer of lime is visible, which is compacted with "hedges" before installing the next layer

Figure 14 Test results of embedded material in the embankments (excerpt from the complete test table)

Conclusion

During the execution of works, in accordance with the accepted principle that only with the application of flexible (self-adjusting) technical measures and interventions can optimal results be obtained in achieving slope stability, and in the field circumstances, the design solutions have been partially modified and supplemented. Necessary adjustments were made to the project according to the current situation on the ground. In order to realize the imagined rehabilitation concept, it was necessary to make a great effort and a great deal of cooperation between all participants in the construction. Due to the very nature of the remediation, the size of the remedied area, and especially the characteristics of the soil (clay) material in the landslide and the daily changes in the appearance of the northern part (moving and sliding of the northern area around MPS), which occurred most at the turn of 2017 to 2018 and the first half of 2018 (thus changing the structure of the substrate), there was eventually an increase in the number of earthworks.

Finally, it is important to emphasize that this is a wide-scale slope of instability (in the clay pit area of the southwestern part of the Đurđević hill), which does not even theoretically allow for the unrealistic optimistic expectation that nothing else should be done after rehabilitation in the area.

On the contrary, it should be on mind that during the first few years (and on the basis of ossification and visual

observations), various additional actions will have to be carried out on the repaired clay pit, supplement and modify the existing condition. It is expected that during the first 5 years about 10% of the amount of money (spent in basic rehabilitation) will be provided for the mentioned maintenance method, which will be additionally spent on additional post-retirement measures. The maintenance cash rate will decrease substantially in the period to come.

(a) *(b)*

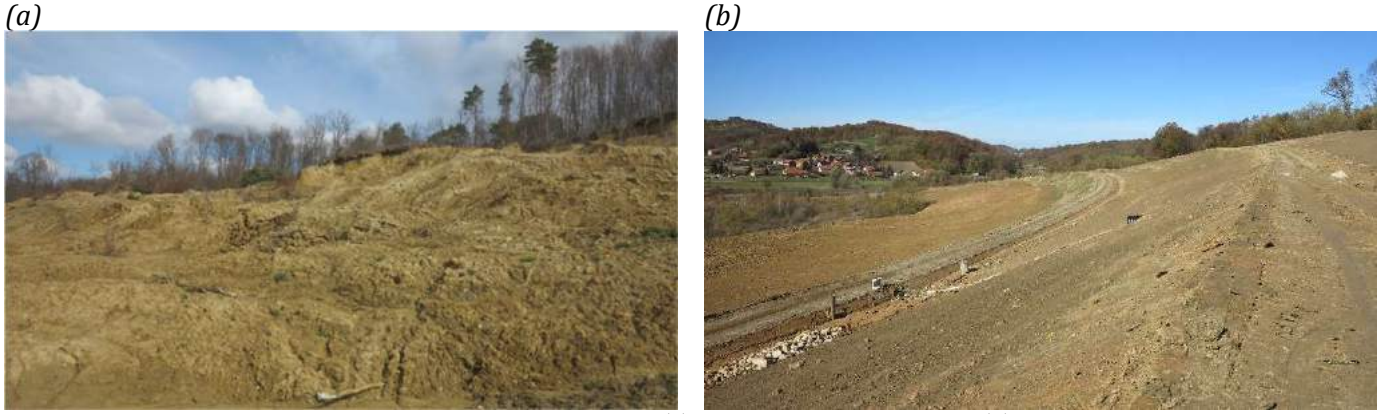

Figure 15 Comparative view of the northern part of the clay pit (a) Prior to remediation work (b) After the rehabilitation works have been carried out (Phase II) - 31.X.2018.

References

MAIN PROJECT, GEOTECHNICAL REPAIR ELABORATE for the North Clay pit Area, CONSTRUCTION PROJECT NO. TD18P01 / I., Made in: P R A G M A d. o. o. o. - Z a g r e b,

ELABORAT REPORT ON GEOTECHNICAL RESEARCH WORKS, GEOTECHNICAL ELABORAT TD18I01 Created by: PRAGMA d.o.o. – Zagreb

ELABORAT REPORT ON GEOTECHNICAL RESEARCH WORKS, GEOTECHNICAL ELABORAT TD16I07 made in: PRAGMA d.o.o. – Zagreb

Report on Design Supervision and Control Surveys (Pragma d.o.o .; study TD18I05)

Report on the ongoing testing for the purpose of internal verification and quality assurance during the execution of the remediation work (SPP d.o.o .Varaždin, on behalf of the Contractor, Tarac d.o.o. Bedekovčina - study SPP/ 2018 / 108A

doi.org/ 10.35123/ReSyLAB_2019_39

Čikla landslide in Karavanke Mts. (NW Slovenia)

Jernej Jež[(1)], Tina Peternel[(1)], Blaž Milanič[(1)], Anže Markelj[(1)], Matevž Novak[(1)], Bogomir Celarc[(1)], Mitja Janža[(1)] Mateja Jemec Auflič[(1)]

1) Geological Survey of Slovenia, Dimičeva ul. 14, 1000 Ljubljana, Slovenia; jernej.jez@geo-zs.si

Abstract The Čikla landslide, together with other surrounding landslide prone areas, poses a serious threat to the Koroška Bela settlement. A mass-flow formed from a part of a landslide body in April 2017 confirmed the serious risk that similar or larger events could appear again sometime in the future. In this respect, studies and monitoring of the landslide is crucial for risk assessment work. The studied area is situated in the Karavanke mountains in north-western Slovenia. The landslide monitoring is based on engineering geological mapping, hydrogeological investigations, geotechnical monitoring and geophysical measurements. The constant changes on the landslide surface, the open cracks, and the recorded movements in inclinometer well indicate the active landslide movements. The material is moving as a deep-seated rotational landslide, rock fall, rock avalanche, translational motion, and debris flow.

Keywords Čikla landslide, monitoring, debris flow, Karavanke Mts.

Introduction and study area

Complex and deep-seated landslides in Slovenia are most common in mountainous Alpine and pre-Alpine regions. Landslides developing from predisposed areas can reach valley sites and may constitute a serious hazard for villages and infrastructure. Within a single catchment recurrence of such events is irregular and may repeat after long periods of inactivity. One area highly prone to landslides are the the Karavanke Mts., the mountain ridge on the border of Slovenia and Austria.

Čikla landslide is located in the western part of Karavanke Mts. in north-western Slovenia, above the village of Koroška Bela (Fig. 1), at an altitude of between 1050 and 1200 meters (Lat: 46°26'16,94"; Lon: 14°07'24,73"). The debris flow in 2017 has progressed downslope to 920 m a.s.l..

The belt of tectonically fractured Younger Paleozoic rocks, mostly covered by a thick accumulations of scree and/or colluvium, appears along the entire Košuta fault zone between the Završnica valley and Planina pod Golico area at an altitude of 900 to 1300 m asl. In this zone, landslides of various types are very common. Among them, large deep-seated landslides also occur. Occasional intense or prolonged rainfall events, combined with snow melting, usually activate, re-activate or accelerate movements at landslide prone areas (Peternel et al., 2018). Previous studies in the area focused primarily on the nearby Urbas landslide (Jež et al. 2008; Komac et al. 2014; Peternel et al. 2017, 2018), which belongs to a similar general geological setting but reflects very different dynamics.

Studies of alluvial fans in the Sava valley indicated that areas high in the slopes of the Karavanke Mts. in the past have already contributed material for the formation of large sedimentary bodies in the valley. These accumulations resulted from past debris flows (Jež et al., 2008; Komac et al. 2009; Mikoš et al. 2012). The Čikla stream flows to the Bela alluvial fan which is settled by the village of Koroška Bela with some 2,200 inhabitants. The village already experienced a severe debris flow event in the 18th century, which caused the partial or complete destruction of more than 40 buildings (Lavtižar 1897; Zupan 1937).

This paper presents the results of short and medium-term landslide monitoring. The first detailed field surveys were carried out in 2017 in order to identify the potential threats to the downstream settlements and infrastructure. They included engineering geological and hydrogeological mapping, geomechanical boreholes, geophysical research, and geotechnical and hydrogeological measurements. Detailed mapping was performed with the aim to determine the spatial extent of the landslide body at the ground surface, identify all failure features on the surface and potentially active or unstable areas, and to analyse sedimentary facies of bedrock and facies of overlying sediments. A topographic base map was generated using a 1 m-grid digital elevation model (DEM) derived from LiDAR data (2014). Analyses of LiDAR and orthophoto data were performed in order to identify past sliding developments and significant morphological features. Engineering-geological mapping results at a scale of 1:1,000 served as the basis for planning other investigations. Based on measurements of hydrogeological mapping discharge locations, observation wells and in situ measurements of hydraulic conductivity were defined. Falling and constant-head tests and infiltrometer tests were performed in this framework. On a flat area in the uppermost part of the landslide two boreholes ČK-1/17 and ČK-2/17 were drilled and logged (Fig. 3). Detailed core logging provided information on the lithological composition of the

landslide body and the proximate hinterland. Absolute displacement rates were interpreted based on geotechnical monitoring using an inclinometer installed in the ČK-2/17 borehole (39 m deep), while ground water levels were measured in the Čk-1/17 borehole (40 m deep) equipped with a piezometer. Displacement profiles obtained from the inclinometers show magnitude, depth, direction and rate of ground movement. Geophysical measurements were performed behind the landslide crown cracks in the nearest vicinity of the geomechanical boreholes. According to the expected lithology and target depths, the Electrical resistivity tomography (ERT) and Seismic refraction tomography (SRT) profiles in the ENE-WSW direction were selected (Fig. 3).

Figure 1 Red dot marks the location of the studied area (map source: www.geopedia.si)

Landslide characteristics

The sliding material consists of blocky carbonate scree, sandy carbonate scree of torrential fan, dolomite boulders, and fractured shaley claystone and marlstone. The carbonate scree originates from steep slopes in the wider hinterland of the Belščica Mt. (2017 m asl.) and was accumulated over siliciclastic rocks. Sandy carbonate gravel was accumulated in the hinterland of Čikla landslide with torrential processes. Highly fractured Permian dolomite builds a vertical wall in the upper part of the landslide and structurally lies within the claystone, siltstone and sandstone of the Carboniferous age. At the contact between fine-grained clastic rocks and overlying carbonate gravel appears groundwater. The width of the current active landslide is about 105 m, the length is 140 m. The maximum depth is about 25 m. It extends over an area of approx. 8,000 m² (Fig. 2).

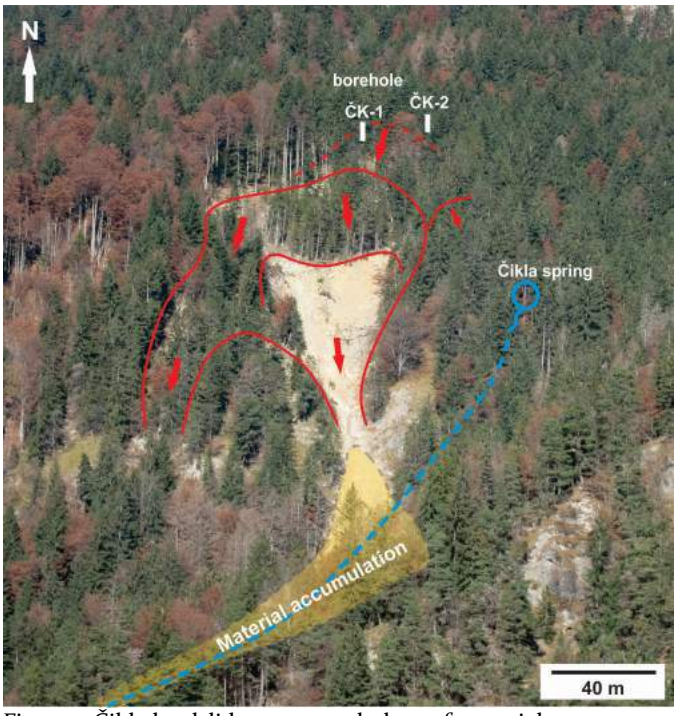

Figure 2 Čikla landslide extent and place of meterial accumulation in the Čikla stream.

Various types of mass movement processes were characteristic for the Čikla landslide. In the uppermost part the fractured dolomite wall breaks in large boulders of dimensions up to more than 10 m³. Boulders fall down into the central part of the landslide in the form of a rock-falls. Behind the dolomite wall movements in inclinometer suggest deep-seated rotational sliding. In the greater middle part of the landslide, the mixed scree material and soft clastic rocks are moving as a translational landslide (Fig. 4). This central part of the landslide is characterized by a slope gradient of more than 35°. During an intensive rainfall event in April 2017 a part of the landslide moved as a mass flow, whose material was accumulated approx. 500 m along the stream of the Čikla creek (Fig. 4). Up to 30 m thick limestone sequence in the lower part of the landslide builds solid slope scarp that supports and retains the greater part of the sliding material. Thus, the material is being transported down to the Čikla stream only through 7 m wide torrent channel.

In two boreholes ČK-1/17 and ČK-2/17 (Figs. 2 and 3) two main lithological units were recognized: Paleozoic bedded mainly siliciclastic rock successions as a base, and a cover of younger mainly coarse-grained carbonate slope sediments (Fig. 5). In addition, geophysical measurements (ERT and SRT) (Fig. 3) confirmed this structure and indicate the complex spatial distribution of the slope sediments in the hinterland. Both methods showed good contrast between the uppermost carbonate gravel and the tectonically-deformed bedrock of the clastic rocks. They indicated very thick accumulations of sandy carbonate scree NE of the landslide and local accumulations of slope clayey colluvium north and northwest of the landslide. Due to past slope processes,

gravel is locally mixed with clay and silt. Groundwater level measurements in borehole ČK-1/17 indicate rapid changes in levels, which are strongly related to precipitation (Janža et al., 2018). Amplitudes are up to 6 m.

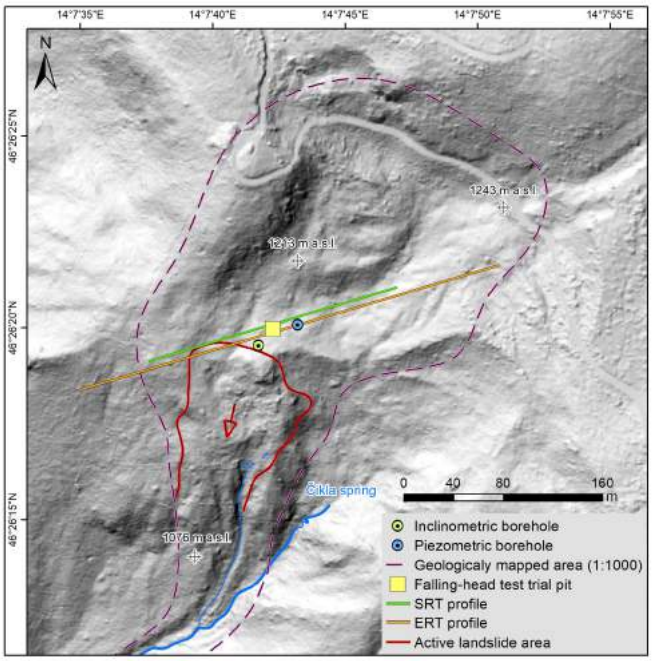

Figure 3 Map of applied methods. Inclinometric borehole = ČK-1; piezometric borehole = ČK-2.

Inclinometer shows the deepest sliding surface at approx. 23 m, while movements were evidenced also at depths of 9 and 5 metres (Fig. 5). Cumulative movement of 16 mm was measured at a depth of 23 m over a period of 18 months. As the inclinometer borehole ČK-2/17 is located behind the main landslide scarp visible on the surface, measurements indicate the deep-seated sliding and spread of the landslide towards the north.

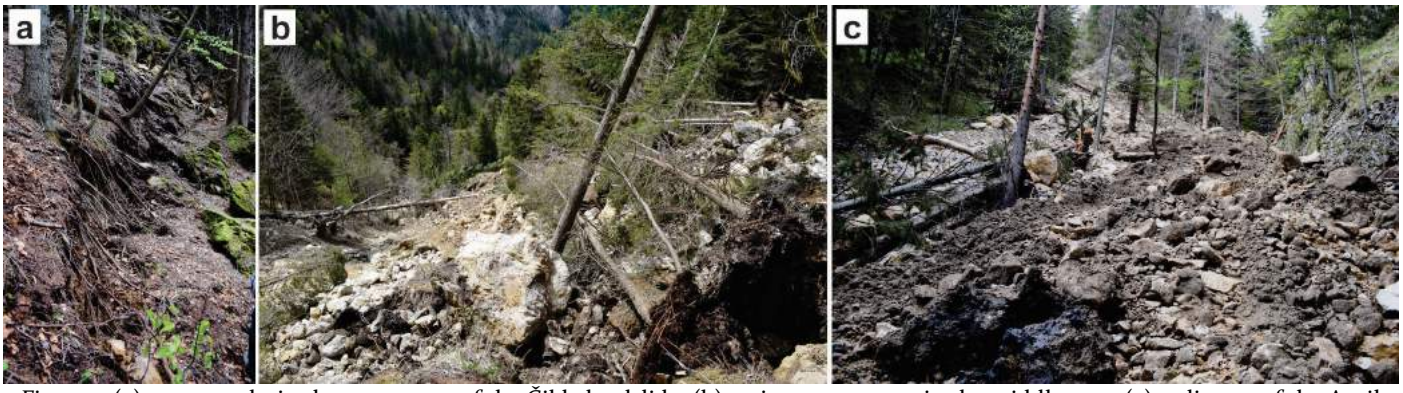

Figure 4 (a) open cracks in the upper part of the Čikla landslide; (b) active movements in the middle part; (c) sediment of the April 2017 debris flow event in the Čikla stream

Discussion

The Čikla landslide is predisposed by complex geological and hydrogeological setting and very steep terrain. The constant changes on the landslide surface, the open cracks in the hinterland, the high fluctuations of groundwater levels and the recorded movements in inclinometer wells indicate the active landslide movements. The material is moving as a deep-seated rotational landslide, rock fall, rock avalanche, and translational motion, while recent events also indicate the possibility of the occurrence of a mass flow. Deep movements detected in the hinterland (ČK-2 inclinometer) indicate the landslide can be expected to progress northwards in the future. Total sliding mass volume was calculated as 150,000 m3.

The debris flow event that developed during the heavy rainfall event of April 2017 suggests that sliding material is suitable to mobilisation as debris flow. It was composed of a mixture of fine-grained sediments, gravel and large boulders, as well as trees and roots and originated from the lower and middle part of the landslide. Debris flow flowed down at least 450 m along the Čikla stream. The event was related to approx. 220 mm of rain in less than 48 hours, with almost half of this falling within 8 hours (rainfall stations), which is not particularly extreme for this region. Events of nearly 700 mm rain in 72 hours or short-duration events bringing more than 60 mm in just 30 minutes have been recorded in recent years in the nearby pre-Alpine and Alpine region (Petkovšek et al. 2011).

Alluvial fans in the valleys due to their morphology usually appear very attractive and suitable for settlement. At the same time, planners and investors often forget or ignore the fact that these sedimentary bodies were formed during extensive torrential and/or mass flow processes in the past. The Koroška Bela alluvial fan is also just such a case. The sudden movement of large landslide masses and the transformation of the sediment-water mixture into the debris flow could pose serious threat for the settlement. Therefore, the planning of mitigation measures to protect the settlement in the future will pose a significant challenge. For this reason, an active monitoring of the landslide is planned in the future, while effective mitigation measures and possible construction works can be based on additional detailed geotechnical studies and stability analyses.

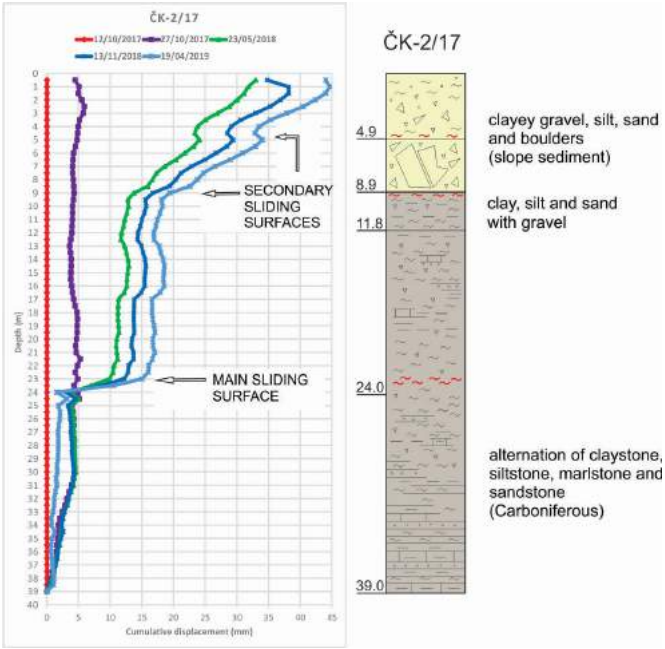

Figure **5** Borehole ČK-2/17 log (right) and results of four inclinometer measurements (campaigns from 12/10/2017 to 19/4/2019) (left)

Conclusion

Based on gathered data and interpretations the following conclusions can be drawn:

(a) Unstable areas in Karavanke Mts are predisposed by similar general geological setting, while very local hydrogeological and morphological conditions determine the exact locations of landslide occurrence.

(b) Various types of mass movement processes are characteristic for the Čikla landslide. Material can be transformed into the debris flow. A potential debris-flow event may reach the Bela alluvial fan and presents a threat to the settlement and related infrastructure.

(c) Temporal predictions of landslide dynamics pose a particular challenge. They can be simulated by using real-time monitoring data (displacement velocity, ground water level and precipitation etc.) Therefore, continuous real-time monitoring that would be part of an early warning system needs to be established.

Acknowledgments

This research was financially supported by the Slovenian Research Agency (J1-8153 project) and the Slovenian Ministry for the Environment and Spatial Planning.

References

Janža, M., Serianz, L., Šram, D., Klasinc, M. (2018) Hydrogeological investigation of landslides Urbas and Čikla above the settlement of Koroška Bela (NW Slovenia). Geologija 60/2, 191-203

Jež, J., Mikoš, M., Trajanova, M., Kumelj, Š., Budkovič, T. & Bavec, M. (2008) Koroška Bela alluvial fan - the result of the catastrophic slope events (Karavanke Mountains, NW Slovenia). Geologija. 51/2, 219-227.

Komac M, Kumelj Š, Ribičič M (2009) Debris-flow susceptibility model of Slovenia at scale 1: 250,000. Geologija 52/1, 87–104

Komac M, Holly R, Mahapatra P, Van der Marel H, Bavec M (2014) Coupling of GPS/GNSS and radar interferometric data for a 3D surface displacement monitoring of landslides. Landslides 12(2): 241-257

Lavtižar, J. (1897) Zgodovina župnij in zvonovi v dekaniji Radolica, Ljubljana

Mikoš M, Sodnik J, Podobnikar T, Fidej G, Bavec M, Celarc B, Jež J, Rak G, Papež J (2012) PARAmount—European research project on transport infrastructure safety in the Alps. In: Sassa K, Takara K, He B (eds) Proceedings IPL Symposium Kyoto, 2012: 20 January 2012, Venue: Disaster Prevention Research Institute, Kyoto University Uji, Kyoto, Japan. International Consortium on Landslides, Tokyo, pp 111–118

Peternel T, Kumelj Š, Oštir K, Komac M (2017) Monitoring the Potoška planina landslide (NW Slovenia) using UAV photogrammetry and tachymetric measurements. Landslides 14(1):395-406.

Peternel, T., Jež, J., Milanič, B., Markelj, A., Jemec Auflič, M. (2018) Engineering-geological conditions of landslides above the settlement of Koroška Bela (NW Slovenia). Geologija 61/2, 177-189

Petkovšek A, Fazarinc R, Kočevar M, Maček M, Majes B, Mikoš M (2011) The Stogovce landslide in SW Slovenia triggered during the September 2010 extreme rainfall event. Landslides 8/4, 499-506

Zupan, G. (1937) Krajevni leksikon dravske banovine. Uprava Krajevnega leksikona dravske banovine, Ljubljana

doi.org/ 10.35123/ReSyLAB_2019_40

Landslide risk management in Croatia: Current state

Snježana Mihalić Arbanas [(1)], Sanja Bernat Gazibara [(1)], Marin Sečanj [(1)], Vedran Damjanović [(1)], Davorin Oršanić [(2)], Snežana Penović [(2)], Martin Krkač [(1)], Ksenija Cindrić Kalin [(3)], Petra Đomlija [(4)], Vedran Jagodnik [(4)], Željko Arbanas [(4)]

1) University of Zagreb, Faculty of Mining, Geology and Petroleum Engineering, Pierottijeva 6, 10 000 Zagreb, Croatia

2) Ministry of Construction and Physical Planning of the Republic of Croatia, Republike Austrije 20, 10 000 Zagreb, Croatia

3) Croatian Meteorological and Hydrological Service, Grič 3, 10 000 Zagreb, Croatia

4) University of Rijeka, Faculty of Civil Engineering, Radmile Matejčić 3, 5 100 Rijeka, Croatia

Abstract The paper shortly presents concept of landslide risk management with basic definitions of activities belonging to protection and recovery. The intention of the paper is to systematize measures of the Croatian government according to risk management framework. Two groups of measures undertaken by the Croatian Ministry of Construction and Physical Planning are described: (i) national landslide risk assessment; and (2) programmes for landslide disaster recovery. It is concluded that the measures introduced by the Croatian government are in line to the agenda Sendai Framework for Disaster Risk Reduction concerning emerging risk of Multiple Occurrence Regional Landslide Events (MORLE) that is related to climate changes.

Keywords Landslide disaster, MORLE, National risk assessment, Recovery, Hrvatska Kostajnica

Introduction

Disaster risk management is an extension of the more general term "risk management" to address the specific issue of disaster risks. Disaster risk management aims to avoid, lessen or transfer the adverse effects of hazards through activities and measures for prevention, mitigation and preparedness. United Nation International Strategy for Disaster Reduction (UNISDR, 2009) defines disaster risk management as the systematic process of using administrative directives, organizations, and operational skills and capacities to implement strategies, policies and improved coping capacities in order to lessen the adverse impacts of hazards and the possibility of disaster. The same document defines disaster as a serious disruption of the functioning of a community or a society involving widespread human, material, economic or environmental losses and impacts, which exceeds the ability of the affected community of society to cope using its own resources. Disaster impact may include loss of life, injury, disease and other negative effects on human physical, mental and social well-being, together with damage to property, destruction of assets, loss of services, social and economic disruption and environmental degradation.

According to the abovementioned criteria, the Republic of Croatia has experienced disastrous Multiple Occurrence Regional Landslide Events (MORLE) in 2013 at the area of the NW Croatia (Mihalić Arbanas et al., 2013; Bernat et al., 2014a). Disaster impact consisted in a high number of affected people in terms of permanent displacement, economic cost of immediate or longer-term emergency measures, restoration of buildings, public transport system and infrastructure, property, etc., cost of disruption of economic activity, indirect cost for the economy, social cost and other direct and indirect cost, as well as social psychological impact, impact on public order and safety and other factors, such as certain environmental damage. Consequently, most of counties proclaimed a natural disaster in the spring of 2013 that was caused by extreme hydro-meteorological conditions (Bernat Gazibara et al., 2017c), unique in the last 150 years.

From the perspective of the landslide risk management in Croatia, there are two types of activities undertaken at the national level by national bodies and government. The first activity is national landslide risk assessment performed in 2018 that showed that there is very high risk from MORLE in Croatia (Croatian Platform for Disaster Risk Reduction, 2019). The second activity is related to support to people evacuated from homes destroyed by landslides. In the post-disaster period the Croatian government opened two rounds of call for financial support to people facing homelessness due to damages caused by landslide activation.

This paper lists a basic definition of the terms related to risk management according to the UNISDR (2009) terminology. It also gives a short overview of the national landslide risk assessment, methodology and main results, as well as chronology and activities of the processes of support to people affected in terms of

permanent displacement from homes. The objective of the paper is to show the current state in the landslide risk management considering MORLE in Croatia.

Risk management cycle

Figure 1 shows risk management cycle that is divided into two parts, before and after disaster occurrence. The main difference between processes before and after the disaster is that first belong to protection and latter to recovery.

Figure 1 Disaster, risk and crisis management cycle (FAO, 2004)

Here are listed definitions of the terms mitigation, prevention, preparedness, early warning system, response and recovery according to the UN terminology (UNISDR, 2009). The definition of reconstruction was taken from the newest terminology published by UN Expert Working Group on Indicators and Terminology Relating to Disaster Risk Reduction (UN, 2016).

Mitigation relates to lessening or limiting of the adverse impacts of hazards and related disasters. The adverse impacts of hazards often cannot be prevented fully but their scale or severity can be substantially lessened by various strategies and actions. Mitigation measures encompass engineering techniques and hazard-resistant construction as well as improved environmental policies and public awareness.

Prevention means outright avoidance of adverse impacts of hazards and related disasters. Disaster prevention expresses the concept and intention to completely avoid potential adverse impacts through action taken in advance. Examples include dams or embankments that eliminate flood risks, land-use regulations that do not permit any settlement in high risk zones, and seismic engineering designs that ensure the survival and function of a critical building in any likely earthquake. Very often the complete avoidance of losses is not feasible, and the task transforms to that of mitigation. Partly for this reason, the terms prevention and mitigation are sometimes used interchangeably in casual use.

Preparedness includes knowledge and capacities developed by governments, professional response and recovery organizations, communities and individuals to effectively anticipate, respond to, and recover from, the impacts of likely, imminent or current hazard events or conditions. Preparedness action is carried out within the context of disaster risk management and aims to build the capacities needed to efficiently manage all types of emergencies and achieve orderly transitions from response through to sustained recovery. Preparedness is based on a sound analysis of disaster risks and good linkages with early warning systems, and includes such activities as contingency planning, stockpiling of equipment and supplies, the development of arrangements for coordination, evacuation and public information, and associated training and field exercises. These must be supported by formal institutional, legal and budgetary capacities. The related term “readiness” describes the ability to quickly and appropriately respond when required.

Early warning system encompasses a set of capacities needed to generate and disseminate timely and meaningful warning information to enable individuals, communities and organizations threatened by a hazard to prepare and to act appropriately and in sufficient time to reduce the possibility of harm or loss. This definition encompasses the range of factors necessary to achieve effective responses to warnings. A people-centred early warning system necessarily comprises four key elements: knowledge of the risks; monitoring, analysis and forecasting of the hazards; communication or dissemination of alerts and warnings; and local capabilities to respond to the warnings received. The expression “end-to-end warning system” is also used to emphasize that warning systems need to span all steps from hazard detection through to community response.

Response implies provision of emergency services and public assistance during or immediately after a disaster in order to save lives, reduce health impacts, ensure public safety and meet the basic subsistence needs of the people affected. Disaster response is predominantly focused on immediate and short-term needs and is sometimes called “disaster relief”. The division between this response stage and the subsequent recovery stage is not clear-cut. Some response actions, such as the supply of temporary housing and water supplies, may extend well into the recovery stage.

Recovery includes restoration and improvement where appropriate, of facilities, livelihoods and living conditions of disaster-affected communities, including efforts to reduce disaster risk factors. The recovery task of rehabilitation and reconstruction begins soon after the emergency phase has ended and should be based on pre-existing strategies and policies that facilitate clear institutional responsibilities for recovery action and enable public participation. Recovery programmes, coupled with the heightened public awareness and engagement after a disaster, afford a valuable opportunity

to develop and implement disaster risk reduction measures and to apply the "build back better" principle.

Reconstruction means the medium and long term rebuilding and sustainable restoration of resilient critical infrastructures, services, housing, facilities and livelihoods required for the full functioning of a community or a society affected by a disaster, aligning with the principles of sustainable development and "build back better", to avoid or reduce future disaster risk.

Landslide risk assessment in Croatia

Landslide risk assessment in Croatia was undertaken in 2018 in the framework of the national risk assessment following recommendations from guidelines of the European Union (EC, 2010) The EU guidelines on national risk assessments and mapping do not advocate any particular risk criteria, benchmarks or standards, but do encourage transparency in this area including use of nomenclature according to the standard ISO Guide 73:2009 (ISO, 2009) and UNISDR terminology (UNISDR, 2009) as well as defined procedures of risk identification, risk analysis and risk evaluation. Risk identification is the process of finding, recognizing and describing risks. It serves as a preliminary step for the subsequent risk analysis stage. Risk analysis is the process to comprehend the nature of risk and to determine the level of risk. Risk evaluation is the process of comparing the results of risk analysis with risk criteria to determine whether the risk and/or its magnitude are acceptable or tolerable. These stages can be compared to the framework of landslide risk assessment and management developed by Fell et al. (2008a,b).

Risk identification

In the stage of risk identification, the landslide risk was recognised and described by a screening exercise covering the geographic context of the whole country (56 594 km2) during a given period of time (last 30 years). This phase has served as a preliminary step for the subsequent risk analysis stage. The methodology for risk identification was qualitative because of lack of systematic historical records necessary for application of quantitative statistical methods. Finding and recognising all likely landslide hazard and significant consequences was performed by analysing relatively frequent multiple-occurrence regional landslide events (MORLE) happened in Croatia (in 2006, 2010, 2013, 2014 and 2018). The screening was based on data about hazardous events from public sources (news from internet), scientific sources (professional and scientific papers) and governmental sources (records from local government), and the selection was based on expert opinions. Spatial and temporal extent of all MORLE was analysed based on catalogue of landslide events and catalogue of precipitation events in NW Croatia in the period from June 2006 till October 2014 (Bernat Gazibara i dr., 2017c). Identification of 85 triggering events (precipitation events) and 73 landslide events was made by temporal analysis of daily precipitation data from 19 meteorological stations in NW Croatia. The duration range of precipitation events is 1-41 days and the range of cumulative precipitation that triggers landslides is 29.5-400.5 mm. Most of the analysed precipitation events had happened during the autumn and winter period (Croatian Platform for Disaster Risk Reduction, 2019).

The outcome of the risk identification stage was a listing of two different identified risks and risk scenarios, followed by its description. "Reasonable worst case" or MORLE with the worst possible consequences was chosen as most serious credible outcomes as these pose the largest threat and are often of most concern. One more benchmark was chosen to rank a common problem that presents the most probable unfavourable MORLE. Scenario building was based on experiences from the very recent past, because hazardous MORLE from 2013 (Bernat et al., 2014a; Bernat et al., 2014b) was used as MORLE event with the worst possible consequences (Scenario 1) and hazardous MORLE event from 2018 (Bernat et al., 2019) was used as most probable unfavourable MORLE event (Scenario 2). Both scenarios were based on a coherent and internally consistent set of assumptions about key relationships between hazardous event and consequences as well as driving forces in the form of landslide susceptibility, triggering event (precipitation) and its frequency. Like any other simplification of reality, the definition of a scenario entails subjective assumptions about the number of expected landslides and geographic coverage of scenarios. Namely, risk analysis for both scenarios was performed for the area of approx. 15 800 km^2 in NW Croatia that presents union of geographic coverage experienced MORLE in 2013 and 2018.

For other parts of Croatia, MORLE events and impacts, which have so far not occurred, were also considered, assuming extreme hydrometeorological conditions (precipitation) that may happen as a consequence of climate changes and emerging landslide risk. It was essential that all information leading to the definition of scenarios was made explicit so that they can be reviewed and updated (Croatian Platform for Disaster Risk Reduction, 2019). However, the remaining uncertainties in this approach are immense (EC, 2010).

Both risk scenarios were used in the risk analysis stage, aiming to establish quantitative estimates for impacts and probabilities. A single-risk approach has been applied that determined risk from one particular type of hazard, i.e., MORLE. In most geographic areas in Croatia landslide susceptibility is not related to other hazard, e.g., floods. Coinciding hazards, also referred to as follow-on events, knock-on effects, domino effects or cascading events, are limited to very narrow areas in Croatia, such as City of Karlovac which have experienced landslides triggered by a flood in 2014.

Risk analysis

Risk analysis is the process to comprehend the nature of risk and to determine the level of risk, as it is defined by standard ISO 31000:2018 (ISO, 2018). For both risk scenario identified in the previous risk identification stage, the risk analysis process has carried out a detailed estimation of the probability of its occurrence and the severity of the potential impacts. In accordance with guidelines EC (2010), during risk analysis the geographic scope of the risk scenario and of the impacts was established, even though the precise location was left unspecified. Landslide risk analysis was based on quantitative data: (i) the assessment of the probability of two MORLEs (for Scenario 1 and Scenario 2) or hazard was based on historical frequency of triggering events, i.e., statistical analysis of precipitation records presenting the main drivers (rain), which also can help to pick up on accelerating trends, e.g., due to climate change; (ii) the assessment of the level of impact was in quantitative terms based on hazard intensity and estimated losses for few types of elements at risk. The assessment was performed to be as objective as possible, but due to lack of systematic records about historical hazards (i.e., number of landslide events) or consequences (i.e., losses), the main criteria was established based on expert opinion.

Single-risk analysis estimated the risk of a singular hazard in isolation from other hazards or risk scenarios, addressing the following subjects for MORLE from 2013 and 2018: hazard analysis; geographical analysis (location, extent); temporal analysis (frequency, duration, etc.); dimensional analysis (scale, intensity); probability of occurrence; vulnerability analysis; identification of elements and people potentially at risk (exposure); identification of impacts (physical, economic, environmental, social/political); assessment of likely impacts. An analysis of self-protection capabilities reducing exposure or vulnerability is planed to be performed in the next step of national risk assessment.

Hazard analysis

Hazard analysis encompassed: (a) analysis of spatial landslide probability, i.e., landslides susceptibility assessment resulting in zones potentially prone to landslides; (b) analysis of spatial distribution of number of expected landslides for Scenario 1 and 2; (c) temporal analysis of precipitation conditions resulting in determination of possible triggering events for Scenario 1 and 2; (d) analysis of temporal probability of occurrence of selected triggering event for Scenario 1 and 2. Hazard analyses are described in more details in the paper Bernat Gazibara et al. (2019) and here are listed only the main results important to explain and describe consequence analysis and risk estimation.

Landslide susceptibility assessment was performed in the geographic area covering eight counties in NW Croatia that had experienced MORLE in 2013 and 2018 (Krapina-Zagorje County, Varaždin County, Grad Zagreb, Zagreb County, Koprivnica-Križevci County, Međimurje County, Sisak-Moslavina County and Bjelovar-Bilogora County). The resulting landslide susceptibility map shows zones potentially prone to landslides, depicting locations of where landslides are possible in respect to lithology and relief type prone to sliding in the Pannonian Basin. The total area of landslide susceptible zones is about 3 300 km^2, or 21% of the analysed area.

Analysis of spatial distribution of the number of expected landslides for Scenario 1 and 2 was made based on estimation of the number of landslides for MORLE from 2013 and 2018. The expected number of landslides for the Scenario 1 was estimated based on the number of registered landslides activated in 2013 in Krapina-Zagorje County (Mihalić Arbanas i dr., 2013; Bernat i dr., 2014b) and the expected number of landslides for the Scenario 2 was estimated based on number of registered landslides activated in 2018. Average spatial frequencies of 0.733 and 0.37 landslides per square kilometer of landslide susceptible area were used to estimate the expected number of landslides in all eight counties for the Scenario 1 and 2. Assuming this number, it was possible to perform dimensional analysis of landslide hazard (scale, intensity) that was important for determination of extent and severity of consequences. Landslide type and size was estimated given specific geomorphological and geological settings of the analysed area in the Pannonian Basin (Mihalić Arbanas et al., 2017). Hilly areas in NW Croatia are susceptible to very small to moderate small (<10^5 m^3) superficial to moderate shallow (<20 m) landslides, mostly in soils (Bernat Gazibara i dr., 2017b). Despite small volume, landslides in soil cause significant damages on buildings, infrastructure and crops because of high landslide density. For example, Bernat Gazibara (2019) identified 702 landslides at the area of only 21 km^2 in hilly area of the City of Zagreb that are endangering people, buildings, infrastructure or environment. Main initiator of MORLE is precipitation, rain and snow (Bernat Gazibara et al., 2017a,c). Besides typical landslides, there is only one active large deep-seated landslide in NW Croatia, the Kostanjek landslide (Mihalić Arbanas et al., 2013), that needs to be treated separately because it significantly increases the intensity of landslide hazard as well as severity of consequences in one of the analysed counties, the City of Zagreb. Scientific studies of activity of the Kostanjek landslide, based on continuous monitoring in the period 2012-2018 (Krkač et al., 2019), showed that it was activated by means of accelerated displacement during MORLE in 2013 (max. velocity 4.5 mm/day) and 2018 (max. velocity 2 mm/day).

Temporal analyses of precipitation conditions were performed by estimation of precipitation conditions using Standard Precipitation Index, SPI (McKee et al., 1993) that is in common use in national meteorological services. SPI values have been calculated for both Scenarios 1 and 2 for temporal scales of 10-100 days (from date of landslide activation) at selected meteorological stations that are representative for precipitation

conditions in the analyzed period in NW Croatia. The intention was to define possible critical temporal scales of rainfall events relevant for MORLE 2013 and MORLE 2018. The resulting critical temporal scale for Scenario 1 was 100-days cumulative precipitation that was extremely high at Varaždin and Zagreb-Grič meteorological stations (344.4-365.4 mm). These values present the highest measured 100-days precipitations for the end of March in the period 1961-2018. The resulting critical temporal scale for Scenario 2 were 40 and 100 days because both cumulative precipitations (177.2 and 362.6 mm) were extremely high at Sisak meteorological stations. These values represent the second highest measured 40- and 100-days precipitations for mid of March in the period 1961-2018.

The analysis of probability of occurrence of Scenario 1 and 2 was performed by probability analysis of occurrence of triggering events identified in the previous stage. Statistical probability analysis of two selected critical precipitations was based on parameters of theoretical distributions generated from precipitation data for referent climatological sequence, i.e., for the period 1981-2010. Probability of occurrence of the Scenario 1 was estimated to once in 98 years (based on precipitation data from Varaždin station) and once in 130 years (based on precipitation data from Zagreb-Grič station). This relates to probability of extreme 100-days precipitation that has preceded activation of landslides on 30th March 2013. Similarly, probability of occurrence of the Scenario 2 was estimated to once in 15 years (based on precipitation data from Zagreb-Grič station) and once in 22 years (based on precipitation data from Varaždin station). This was derived for the extreme wet rainfall conditions during 100-days precipitation event that had preceded activation of landslides on 13th March 2018.

Consequence analysis

Consequence analysis was performed for two aforementioned scenarios of landslide hazard, for the geographic extent of all eight counties in NW Croatia. For the purpose of the national risk assessment, three types of impacts are analysed, according to requirements from guidelines (EC, 2010): human impact; economic and environmental impact; and political/social impacts. Human impacts were estimated in terms of number of affected people, and economic/environmental impacts in terms of costs/damage in Kuna. The political/social impacts were generally referred to a semi-quantitative scale comprising a number of classes, e.g. (1) limited/ insignificant, (2) minor/substantial, (3) moderate/serious, (4) significant/ very serious, (5) catastrophic/disastrous. To make the classification of such latter impacts measurable, the classes were based on objective sets of criteria established by the Croatian Platform for Disaster Risk Reduction.

The characterization of consequence scenarios was based on the expected number of elements at risk per county which was estimated from the expected number of landslides and their intensity. The analysed elements at risk were affected people, forest, agricultural land, urban land, buildings, traffic infrastructure, hospitals and schools. Cost of losses was estimated for all eight counties using specific combinations of elements at risk presenting three aforementioned types of impact. Scenario 1 was characterised by approx. 2 000 affected people and total losses of about 4 460 million Kuna related to material damages. Scenario 2 was characterised by approx. 970 affected people and total losses of about 2 310 million Kuna related to material damages.

Risk estimation

Risk estimation was performed by classification of likelihood and impact of two hazardous scenarios. The impact of the Scenario 1 presenting MORLE with the worst possible consequences was estimated to have catastrophic human impact (more than 1 500 affected people), significant economic and environmental impact (losses in range of 1 500-7 000 million Kuna); and minor or significant political/social impacts (depending on observed elements at risk). The impact of the Scenario 2 presenting the most probable unfavourable MORLE was estimated to have significant human impact (501-1 500 affected people), significant economic and environmental impact (losses in the range of 1 500-7 000 million Kuna); and limited, minor or moderate political/social impacts (depending on observed elements at risk).

Risk evaluation

Risk evaluation is the process of comparing the results of risk analysis with risk criteria to determine whether the risk and/or its magnitude is acceptable or tolerable. Risk criteria are the terms of reference against which the significance of a risk is evaluated. Risk evaluation is used to make decisions about the significance of risks whether each specific risk should be accepted or treated. Risk evaluation was performed using the risk matrix recommended by guidelines EC (2010) and the results are presented in Fig. 2. The matrix is also used as a visualisation tool for multiple risks that have been identified in the national risk assessment, to facilitate comparing the different risks.

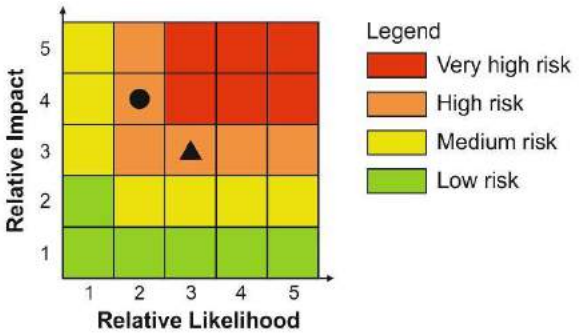

Figure 2 Results of risk evaluation in the form of risk matrix for: (a) landslide hazard with the worst possible consequences (circle); and (b) landslide hazard with the most probable unfavourable consequences (triangle).

Landslide disaster recovery in Croatia

During MORLE in 2018, one catastrophic landslide has happened in the city of Hrvatska Kostajnica in March 2018 (Podolszki et al., 2019). Sudden collapse of large moderate dip landslide completely destroyed all houses placed in the foot part of the landslide resulting in large material damage causing losses with high economic as well as environmental impact. Figure 2 presents two completely destroyed houses placed in the foot part of the landslide in Hrvatska Kostajnica that was activated on 13th March 2018.

Immediately after occurrence of the disaster, Government of the Republic of Croatia had started the recovery programme to help people in Hrvatska Kostajnica endangered by this landslide and also introduced a new follow-up recovery programme for all people endangered by landslides in Croatia. Recovery includes restoration and improvement where appropriate, of houses, livelihoods and living conditions of affected people, including efforts to reduce disaster risk factors by remedial measures. The recovery task of rehabilitation and reconstruction in Hrvatska Kostajnica began soon after the emergency phase had ended.

Figure 3 Houses destroyed by collapse of the Hrvatska Kostajnica landslide on 13th March 2018.

Recovery programme after disastrous landslide in Hrvatska Kostajnica

In March 2018, government of the Republic of Croatia proclaimed natural disaster conditions and immediately after the disastrous event in Hrvatska Kostajnica they adopted a Conclusion with recovery actions. The main decisions were related to supply of permanent housing together with removal of destroyed houses and other buildings. Governmental decision of 15th March 2018 referred to the same type of restoration or improvement, where appropriate, or removal of houses destroyed or damaged by landslides in all other parts in Croatia. The programme has been fully financed by Croatian national budget.

Systematic implementation of the Governmental Conclusion was facilitated by two Decisions: (1) *Decision About Criteria and Modes of Housing Supply for Inhabitants and Removal of Destroyed Family Houses Remnants and Other Buildings Destroyed or Damaged by Landslides in Hrvatska Kostajnica and in Other Parts of the Republic of Croatia* (of 5th July 2018); (2) *Decision About Adoption of the Program of Housing Supply for Inhabitants and Removal of Destroyed Family Houses Remnants and Other Buildings Destroyed or Damaged by Landslides in Hrvatska Kostajnica* (of 15th March 2019). The listed documents served as a basis for implementation of housing supply in joint cooperation of the Croatian Ministry of Construction and Physical Planning, Croatian Agency for Transactions and Mediation in Immovable Properties (APN) and Central State Office for Reconstruction and Housing of the Republic of Croatia. One month later, on 15th April 2019, President of the Republic of Croatia consigned new houses to owners of destroyed homes in Hrvatska Kostajnica. Duration of the whole process of improvement of livelihoods and living conditions of disaster-affected people was 13 months.

Recovery programme after MORLEs in Croatia

Just before all innovation introduced after disastrous landslide in Hrvatska Kostajnica, Ministry of Construction and Physical Planning had opened public call for co-financing landslide remediation design on 22nd February 2018 for the purpose of remediation and mitigation of landslide consequences,. Based on this call, Ministry has co-financed 37 projects dealing with execution of landslide remedial works and/or preparation of design documentation for landslide remediation, with the total value of 10 million Kuna. The maximum amount of co-financing was 80% of eligible cost or maximal 600 000 Kuna. Totally 97 local government administrations delivered 139 project proposals with a total amount of co-financing exceeding 69 million Kuna. This showed exceptional interest and need at the local level. After the administrative verification process had been completed, 129 project proposals satisfied completeness and acceptability criteria. The Committee

evaluated, ranked and suggested 37 projects for co-financing.

After the disastrous landslide in Hrvatska Kostajnica Government of the Republic of Croatia had recognized needs for recovery actions in March 2018 that resulted with new measures related to recovery and reconstruction. Amendments of the Water Management Financing Act in December 2017 created a prerequisite for permanent provision of resources for remediation of landslide consequences. This Act prescribes that the revenue from water contribution is resource for co-financing of landslide and rock fall remedial measure cost. The Act relates to unfavourable effects of erosion and flush flood processes and losses on public infrastructure caused by all types of landslides. For the purpose of landslide remediation in 2019, Croatian Water reserved 50 million Kuna and the same politics will become common practice.

Following abovementioned legislative changes, contracts about co-financing of geotechnical design documentation and landslide remedial works were signed between Croatian Water and counties, cities and municipalities on 2nd July 2019. Total value of all contracts is 54.9 million Kuna for 112 landslides and Croatian Water will co-finance 32.5 million Kuna.

On 27th July 2018 Ministry of Construction and Physical Planning had opened a new public call for the purpose of housing of all people in Croatia that are owners of houses damaged by landslides. This call was entitled: *Public call for submission of applications for realisation of the right to housing provision of inhabitants of buildings and removal of remnants of demolished family houses and other residential buildings destroyed or damaged due to landslides in the territory of the Republic of Croatia*. There were totally 75 applications for that call, including few families from Hrvatska Kostajnica. The Committee members inspected the sites of the landslides and the residential buildings of applicants, and in the fall of 2019, upon having carried out an analysis of all collected data, the adoption of the Programme of Housing Provision also to other Inhabitants of the Republic of Croatia is expected, by which an appropriate manner of housing provision to inhabitants who have followed the Public call and are eligible for housing provision shall be established.

Discussion and conclusions

In 2018 Ministry of Construction and Physical Planning undertook valuable specialised expertise for landslides, as particular types of risk in Croatia for the Croatian Platform of Risk Reduction. Based on results of landslide risk assessment, landslides are included in the national document "Disaster risk assessment of the Republic of Croatia" (Croatian Platform for Disaster Risk Reduction, 2019) that include risks which are of sufficient severity to entail involvement by national governments in the response, in particular via civil protection services. Elaboration of national landslide risk assessment was performed according to guidelines published by European Commission (2010), addressed to national authorities and other actors. The main purpose of these guidelines is to improve coherence and consistency among the risk assessments undertaken in the Member States at national level in the prevention, preparedness and planning stages and to make these risk assessments more comparable between Member States. National risk assessment and mapping, carried out in Croatia, within the broader context of disaster risk management can also become essential inputs for planning and policies in a number of areas of public and private activity. Following the development of the national risk assessment and maps, the involved authorities should seek to interface in an appropriate way with the ensuing processes of risk management, including capacity analysis and capability planning, monitoring and review, and consultation and communication of findings and results, as well as with the appropriate policy levels involved in developing building design criteria, land use planning, community disaster mitigation and response plan.

In 2018 Ministry of Construction and Physical Planning undertook few programmes of recovery to help people endangered by landslides. Based on experience from recovery actions related to the catastrophic landslide in the city of Hrvatska Kostajnica in 2018, the Ministry introduced a set of new measures with the intention to introduce new strategy and policy that facilitate clear institutional responsibilities for recovery action and enable public participation. Recovery programmes, coupled with the heightened public awareness and engagement after a disaster, afford a valuable opportunity to develop and implement disaster risk reduction measures and to apply the "build back better" principle. It can be concluded that the measures introduced by the Croatian government are in line to the agenda Sendai Framework for Disaster Risk Reduction concerning emerging risk of Multiple Occurrence Regional Landslide Events (MORLE) that is consequence of changed meteorological conditions caused by climate changes. Therefore, governmental recovery programmes is also related to measures of adaptation to climate changes within the meaning of contribution to transverse sector of risk management.

The Croatian scientist, as a stakeholder of the "Sendai Framework for Disaster Risk Reduction 2015–2030" from academic, scientific and research entities, need to increase research for regional, national and local applications on landslide hazard prediction and monitoring. The results of scientific research in the form of landslide maps and monitoring systems (Mihalić et al., 2010; Mihalić Arbanas et al., 2018; Arbanas et al., 2018; Bernat Gazibara et al., 2018; Krkač et al., 2018; Sečanj et al., 2019) are required to support action by local communities and authorities, as well as to support the interface between policy and science for scientifically based options for decision making.

References

Arbanas Ž, Udovič D, Sečanj M, Đomlija P, Mihalić Arbanas S (2018) Recent experience in rockfall hazard and risk assessment in rock mass. Proc. of the 7th Conf. of the Croatian Platform for Disaster Risk Reduction, 11th-12th October 2018. Zagreb, Croatia, pp. 222-231.

Bernat Gazibara S (2019) Methodology for landslide mapping using high resolution digital elevation model in the Podsljeme Area (City of Zagreb). PhD thesis, Faculty of Mining, Geology and Petrol. Eng. of the University of Zagreb, Zagreb, Croatia.

Bernat Gazibara S, Cindrić Kalin K, Erak M, Krkač M, Sečanj M, Đomlija P, Arbanas Ž, Mihalić Arbanas S (2019) Landslide hazard analysis in national-scale for landslide risk assessment in Croatia. Proceedings of the 4th ReSyLAB, 23rd-25th October 2019. Sarajevo, BIH, pp. 1–8.

Bernat Gazibara S, Krkač M, Sečanj M, Begić H, Mihalić Arbanas S (2017a) Extreme rainfall events and landslide activation in Croatia and Bosnia and Herzegovina. In: Proc. of the 3rd Regional Symp. on Landslides in the Adriatic-Balkan Region. Ljubljana, Slovenia.

Bernat Gazibara S, Krkač M, Sečanj M, Mihalić Arbanas S, (2017b) Identification and mapping of shallow landslides in the City of Zagreb (Croatia) using the LiDAR-based terrain model. In: Mikoš M, Tiwari B, Yin Y, Sassa K (eds) Advancing culture of living with landslides, Volume 2: Advances in landslide science. Springer International Publishing AG, Switzerland, Cham, pp 1093-a.

Bernat Gazibara S, Krkač M, Sečanj M, Mihalić Arbanas1 (2018) Landslide inventory mapping based on LIDAR data. Proc. of the 7th Conf. of the Croatian Platform for Disaster Risk Reduction, 11th-12th Oct 2018. Zagreb, Croatia, pp. 196-202.

Bernat Gazibara S, Mihalić Arbanas S, Krkač M, SečanjM (2017c) Catalog of precipitation events that triggered landslides in northwestern Croatia. In: Abolmasov B, Marjanović M, Đurić U (eds) Proc. of the 2nd Regional Symp. on landslides in the Adriatic-Balkan Region. University of Belgrade, Faculty of Mining and Geology, Belgrade, pp 103–107

Bernat S, Mihalić Arbanas S, Krkač M (2014a) Landslides triggered in the continental part of Croatia by extreme precipitation in 2013. In: Lollino G et al. (eds) Engineering Geology for Society and Territory, Volume 2: Landslide Processes. Springer, Heidelberg, pp 1599–1603.

Bernat S, Mihalić Arbanas S, Krkač M (2014b) Inventory of precipitation triggered landslides in the winter of 2013 in Zagreb (Croatia, Europe). In: Sassa K, Canuti P, Yin Y (eds) Landslide Science for a Safer Geoenvironment, Volume 2: Methods of Landslide Studies. Springer-Verlag Berlin Heidelberg, pp 829–836.

Croatian Platform for Disaster Risk Reduction Main Working Group (2019) Disaster risk assessment of the Republic of Croatia, App. 1 Scenario Development Report, Zagreb. 562p.

European Commission, EC (2010) Risk Assessment and Mapping Guidelines for Disaster Management. European Commission, Brussels. 43p.

European Commission, EC (2010) Risk Assessment and Mapping Guidelines for Disaster Management. URL: http:// https://ec.europa.eu/echo/files/about/COMM_PDF_SEC_2010_1626_F_staff_working_document_en.pdf [Last accessed: 1st Sept 2019].

FAO Subregional Office for Southern and East Africa Harare (2004) Drought impact mitigation and prevention in the Limpopo River Basin. Food and Agriculture Organization of the UN, Rome. 178p.

Fell R, Corominas, J, Bonnard C, Cascini L, Leroi E, Savage, WZ (on behalf of the JTC-1 Joint Technical Committee on Landslides and Engineered Slopes) (2008a) Guidelines for landslide susceptibility, hazard and risk zoning for land use planning. Engineering Geology, 102: 85–98.

Fell R, Corominas, J, Bonnard C, Cascini L, Leroi E, Savage, WZ (on behalf of the JTC-1 Joint Technical Committee on Landslides and Engineered Slopes) (2008b) Guidelines for landslide susceptibility, hazard and risk zoning for land-use planning. Engineering Geology, 102: 99–111.

ISO (2009) ISO GUIDE 73:2009, Risk management—Vocabulary, 17p.

ISO (2018) ISO 31000:2018, Risk management – Guidelines, 18p.

Krkač M, Bernat Gazibara, Sečanj M, Arbanas Ž, Mihalić Arbanas S (2019) Continuous monitoring of the Kostanjek landslide. Proc. of the 4th ReSyLAB, 23rd-25th October 2019. Sarajevo, BIH, pp. 1–6.

Krkač M, Bernat Gazibara S, Sečanj M, Mihalić Arbanas S (2018) Monitoring and prediction of landslide movement. Proc. of the 7th Conf. of the Croatian Platform for Disaster Risk Reduction, 11th-12th Oct 2018. Zagreb, Croatia, pp. 214-221.

McKee T B, Doeksen N J, Kleist J (1993) The relationship of drought frequency and duration on time scales. Proceedings of the 8th conference of applied climatology. Anaheim C A (ed.). American Meteorology Society, Boston MA. pp. 179-184.

Mihalić S, Arbanas Ž, Krkač M, Dugonjić S, Ferić P (2010): Landslide hazard maps and early warning systems for mitigation of landslide risk. Proc. of the 2nd Conf. of the Croatian Platform for Disaster Risk Reduction, 15 Oct 2010. Zagreb, Croatia, pp. 18-22.

Mihalić Arbanas S, Arbanas Ž, Bernat S, Krkač M, Kalinić P, Martinović K, Fabris N, Sajko J, Antolović A (2013) Management of the crisis situations caused by landslide activations. Proc. of the 5th Conf. of the Croatian Platform for Disaster Risk Reduction, 17 Oct 2013. Valbaldon, Croatia, pp. 151-164.

Mihalić Arbanas S, Bernat Gazibara S, Cindrić Kalin K, Krkač M, Sečanj M, Đomlija P, Arbanas Ž (2018) Landslide hazard and risk analysis: International and Croatian experience in last 20 years. Proc. of the 7th Conf. of the Croatian Platform for Disaster Risk Reduction, 11th-12th Oct 2018. Zagreb, Croatia, pp. 180-189.

Mihalić Arbanas S, Krkač M, Bernat Gazibara S, Komac M, Sečanj M, Arbanas Ž (2018) TXT-tool 2.385-1.1 A Comprehensive Landslide Monitoring System: The Kostanjek Landslide, Croatia // Landslide Dynamics: ISDR-ICL Landslide Interactive Teaching Tools. Vol. 1: Fundamentals, Mapping and Monitoring. Sassa K et al. (eds). Springer, Cham. pp. 449-464

Mihalić Arbanas S, Sečanj M, Bernat Gazibara S, Krkač M, Begić H, Džindo A, Zekan S, Arbanas Ž (2017) Landslides in the Dinarides and Pannonian Basin—from the largest historical and recent landslides in Croatia to catastrophic landslides caused by Cyclone Tamara (2014) in Bosnia and Herzegovina. Landslides. 14(6): 1861-1876.

Podolszki L, Parwata N S, Shimizu N, Pollak D, Vrkljan I (2019) Landslide in Hrvatska Kostajnica – collected data and analysis in progress. In: Sokolić I et al. (eds) Proc. of 8th Symp. of Croatian Geotechnical Society and ISRM Specialized Conf., 22-25 June 2009. Croatian Geotechnical Society, Zagreb. pp 323-328.

Sečanj M, Mihalić Arbanas S, Krkač M, Bernat Gazibara S, Arbanas Ž (2019) Preliminary rockfall susceptibility assessment of the rock slopes above the Town of Omiš (Croatia). In: Sokolić I et al. (eds) Proc. of the ISRM Specialised Conf. "Geotechnical challenges in karst", 11-13 April 2019. Croatian Geotechnical Society, Zagreb. pp 347-352.

UN Expert Working Group on Indicators and Terminology Relating to Disaster Risk Reduction (2016) Report of the open ended intergovernmental expert working group on indicators and terminology relating to disaster risk reduction. United Nations General Assembly, Geneva. 41p.

United Nations International Strategy for Disaster Reduction, UNISDR (2009) UNISDR Terminology on Disaster Risk Reduction. UNISDR, Geneva. 35p.

doi.org/ 10.35123/ReSyLAB_2019_41

Protection of the City of Omiš, Croatia, from rockfall threats

Željko Arbanas[(1)], Marin Sečanj[(2)], Martina Vivoda Prodan[(1)], Sanja Dugonjić Jovančević[(1)], Josip Peranić[(1)], Sanja Bernat Gazibara[(2)], Martin Krkač[(2)], Dalibor Udovič[(3)], Snježana Mihalić Arbanas[(2)]

1) University of Rijeka, Faculty of Civil Engineering, Rijeka, Radmile Matejčić 3, zeljko.arbanas@gradri.uniri.hr

2) University of Zagreb, Faculty of Mining, Geology and Petroleum Engineering, Zagreb, Croatia

3) Monterra Ltd., Rijeka, Croatia

Abstract The City of Omiš, is situated in the middle part of the Croatian Adriatic coast, at the mouth of the Cetina River in the toe of high limestone cliffs and it is very exposed to high rockfall hazards. The old center of the City of Omiš was threatened by numerous rockfalls in the past that caused significant damages at residential structures and infrastructure. During the last decades several designs of rockfall protection structures were conducted, followed by installation of protection structures from 2016 to 2018. During the final design phase in 2016, the detailed field investigation was carried out using field and remote sensing methods to identify rockfall sources as well as endangered zones of the city. Based on field investigation data, 2D and 3D numerical modelling and rockfall simulations were performed to define adequate rockfall protection structures and their locations at the slope. Installed stabilization and protection structures (protection wire fences, wire meshes reinforced by steel ropes and rockbolts, and rockfall barriers) represent the first stage of mitigation measures, while the rockfall risk originating from rockfalls sources in upper parts of the slope should be mitigated in the future. In this paper the methods of field and remote sensing investigation of the slopes, identification of rockfall sources, modelling and simulation of rockfall propagation, as well as selection of protection measures and their positions at the slope above the City of Omiš will be presented. The necessity of further mitigation measures from possible rockfalls that can detach from the upper parts of the slope will be explained based on identified rockfall sources and carried out 3D simulations of rockfall propagation.

Keywords rockfall, rockfall hazard, modelling, rockfall protection, rockfall barriers

Introduction

Rockfalls are the most frequent and dangerous rock movements in mountainous zones, generating high economic and social damages (Emmer, 2018). The danger is mainly caused by the high speed of the falling rock blocks that is very difficult for any fast response (Dorren, 20103).

Figure 1 A view at the City of Omiš and limestone slopes above the town.

The City of Omiš, Croatia, was threatened by numerous rockfall occurrences in the past that caused significant damages at residential structures and infrastructure (Arbanas et al., 2019). The old town of Omiš, is situated in the middle part of the Adriatic coast, at the mouth of the Cetina River in the toe of high limestone cliffs (Figure 1) and it is very exposed to high rockfall hazards. The rockfall events along the limestone slopes were caused by unfavorable rock mass characteristics, rock mass weathering in combination with heavy rainfalls and the man-made influences (Arbanas et al., 2012).

During the last decade more rockfalls that damaged residential houses were registered, as well as numerous rockfalls that reached roads, streets in the town and courtyards without any significant consequence. Unfortunately, there is no rockfall inventory or statistical data about the rockfall volumes, but from the documented data it was found the most usual rockfall volumes were from 0.1 to 5.0 m^3. Although all of these rockfalls can be classified as a small, the risk caused by their direct impact on residential houses and infrastructure is very high. Several blocks of a volume of 1.0 to 3.0 m^3 fallen from the cliffs hit directly in the houses and came through the roofs and construction in the past (Figure 2) without any injured

Figure 2 Fallen rock block came through the roof in the house in January 2012 (www.24sata.hr).

and human victim. These occurrences pointed on necessary rockfall hazard and risk analyses and rockfall protection measures from rockfall threats.

The administration and government of the City of Omiš started with rockfall protection measures design in 2008. In period from 2008 to 2012 several preliminary and main designs for rockfall protection measures were completed for 22 identified potentially dangerous location that included several potentially unstable blocks (source zones) at the slopes above the town as well as the zones that could be reached by rockfall mass. Based on these analyses, rockfall protection measures were designed. Two design approaches (Arbanas et al., 2012) were adopted: (i) the prevention of rockfalls by installing rock mass support systems and (ii) the reduction of rockfall mass energy and suspension of running rockfall mass using rockfall protection barriers.

Study Area

The City of Omiš is a small historical town known form Roman time and started to develop at the mouth of the Cetina River in 12 and 13 century when most of old fortress were built. The old town is located in the toe of the mountain Omiška Dinara.

The Omiška Dinara Mountain is spreading over 15 km along the Adriatic coast with the highest peak at 865 m a.s.l. It is a part of a large nappe system and it is represented as an overturned anticline striking NW–SE that is the result of compressional tectonics occurred from Cretaceous to Miocene. The core of the anticline is built of Senonian rudist limestones, while the limbs of the anticline are built of Eocene breccia, limestones and flysch (Marinčić et al. 1977).

In the wider area of the City of Omiš, geological contacts between Cretaceous and Paleogene deposits are usually along steep reverse faults, striking E–W, with the tectonic transport top to south. Complexity of the geological-structural setting, caused by faulting and folding led to the formation of numerous discontinuities in rock mass. Progressive weathering of discontinuities led to the formation of unstable rock blocks with unfavorable orientation that are prone to rock falls (Sečanj et al., 2017; 2019).

The slopes directly above the City of Omiš spread over the area of around 0.15 km2, with the highest peak at app. 300 m a.s.l. Slopes in the area are very steep, with an average dip mostly over 60°, only locally transected by natural berms in the relief. Numerous sets of discontinuities with unfavorable orientation forming potentially unstable rock blocks were determined by field mapping. Due to high fracturing, detachments of rock blocks of various dimensions were determined, which are related to possible planar, wedge and toppling instabilities (Sečanj et al., 2017; 2019).

Main Design Settings

As it was noted before, the rockfall protection measures designing started in 2008, and till 2012 the main design was completed. The main design was set up on very poor preliminary data. Therefore, it is consequently resulted with a design which ensure only partially protection of the City of Omiš from rockfall hazard.

The designing didn't precede a rockfall hazard and risk analysis that would identify rockfall potential from the slopes above the City of Omiš and necessary data for rockfall run out analysis and protection measures design such as data about potential rockfall sources, potential rockfall volumes, probable trajectories of rockfalls and, finally, possible run out areas. Old topographic maps (in scale 1:5000) were used for designing that not enabled more accurate determination of rockfall source zones and potentially unstable rock block volumes. No engineering geological survey was done and no engineering geological map was created to identify rock mass structure and rock mass characteristics. Potential unstable rock blocks on the slope were visually determined from the toe of the slope and approximately located in the maps.

Based on identified potential unstable block position and their approximate volumes, prevention or protection measures were chosen. The prevention of rockfalls by installing rock mass support systems including rock bolts and rock anchors in combination with steel ropes, steel wire fences and steel wire meshes are designed to hold the rock blocks on. To protect the building and infrastructure from running rock mass blocks, the rockfall protection barriers were designed to reduce the rockfall energy and suspense running blocks. The necessary energy absorption capacity of rockfall protection barriers was defined based on 2D rockfall analysis.

In total 22 potentially dangerous location were chosen and for each location prevention or protection measures or their combinations (Volkwein et al., 2011) were designed. The main design included 8 locations of rockfall protection barriers with energy absorption capacity of 1.000 and 2.000 kJ as well as support measure for more than 30 potentially unstable blocks at the slopes above the City of Omiš.

Final Design Settings

The final design for rockfall prevention or protection measures above the old town of the City of Omiš was carried out as the first stage of construction works. According to the Croatian Construction Law, a final design should follow the basic construction and spatial elements from the main design, and has to define implementing details of constructions. In this way, a main design limits a final design to improve and/or designed rockfall prevention or protection measures.

Despite these limitations, the final design was carried out following the modern approaches and recent techniques in rockfall hazard analysis and rockfall structural protection (e.g. Sarro et al., 2018; Volkwein et al. 2011). Modern approaches include application of remote-sensing techniques enabled to ensure digital terrain models (DTM) from three-dimensional point cloud (3DPC) of the site surface; engineering geological mapping of the rock slopes using combination of remote-sensing techniques and field mapping; rockfall hazard and risk analysis; spatial analysis of rockfall initiating, propagation and run out (Li and Lan, 2015), as well as 3D rockfall simulation to identify trajectories, kinetic energy and run out of fallen rock block as an input data in rockfall protection barriers designing (Volkwein et al., 2011; Sarro et al., 2018).

DTM was derived from three-dimensional point cloud (3DPC) of the site surface provided by terrestrial scanning by light detection and ranging (LiDAR) in combination with topography models provided by structure from motion (SfM) digital photogrammetry. Terrestrial laser scanning (TLS) was used in the toe of the slope at the parts close to buildings, where was not possible to use SfM technique from unmanned aerial vehicle (UAV). TLS enables providing a 3DPC with high precision the scanned surface (Jaboyedoff et al., 2012), but this technique was too expensive to be used for overall area. The digital photogrammetry from SfM technique using high resolution digital camera (James and Robson, 2012) mounted on an UAV (Giordan et al., 2018) provided 3DPC (Figure 3) with precision of 1:1000 (i.e., centimeter precision for 10m distances). DTMs include vegetation and existing constructions (buildings, roads, electric poles, etc.). The analysis of rockfalls requires the use of DTM and the classification of the 3DPC is a key factor to determine the surface of the terrain (Sarro et al., 2018).

Detailed engineering geological mapping was carried out on the limited parts of the rock slopes at the parts where it was possible to physically access to the slopes. Because of very steep to vertical slopes, mapping and determination of rock mass characteristics was carried out by remote sensing on a high resolution 3DPC (Riquelme et al., 2016). Analysis of high resolution 3DPC enable the main characteristics of rock mass in a slope necessary for further analyses of rockfall source and rockfall mechanism such as discontinuity orientation (Lato and Vöge, 2012; Riquelme et al., 2014), discontinuity spacing (Riquelme et al., 2015), discontinuity persistence (Riquelme et al., 2018) as well as rock block volumes (Chen et al., 2017). All these data were combined with engineering geological mapping carried out in the field.

Figure 3 3DPC provided by TLS and SfM techniques. A view at the slope (down); a layout over the middle part of the town (left up).

Based on rock mass and discontinuities characterization data, spatial kinematic analysis were conducted to identify kinematic conditions of possible planar, wedge and toppling rock mass failure in different parts of the slope. The results of these analyses expressed indicated on zones on the slope as possible rockfall sources (Sečanj et al., 2017; 2019) that, with rock block volumes determination, gave quantitative and accurate input data for rockfall simulations.

RocPro3D and RockFall software were employed to conduct the rockfall simulation. RocPro3D is a software that enables 3D simulation of rockfall trajectories, using a probabilistic approach that considers a rock block volume and form, soil properties, irregularities of slope surface and restitution coefficient. RocPro3D for simulation uses DTM developed from 3DPC. RocPro3D was used to define and check precise locations, heights and energy absorption capacity of rockfall protection barriers. More than 1.000 simulation was conducted for each of 8 location of rockfall protection barriers, Additional check was carried out using RockFall software and 2D simulations for critical points identified by 3D simulations. Both 2D and 3D simulations enabled precise defining of rockfall protection barrier positions and their heights and energy absorption capacity. Conducted simulations pointed out on the need for installation of additional rockfall protection barrier at position where rock blocks can leap over a barrier. Position of each barrier pole was precisely determined and defined in high resolution DTM and 3DPC that enabled clear positioning of protection structures in construction stage (Figures 4 and 5). Stability analyses for potentially unstable rock blocks identified in the main design were conducted that defined necessary support system for each analyzed rock block and precisely determined and defined elements of support system in high resolution DTM and 3DPC.

Figure 4 An aerial view at the rockfall protection barriers at limestone slopes above the City of Omiš (left up), a view at the rockfall protection barriers of 2000 kJ capacity at limestone slopes above the center of the City of Omiš (right up); an aerial view at the rockfall protection barrier of 2000 kJ capacity in the ravine above the City of Omiš (left down); a view at the rock mass support systems including rock bolts in combination with steel ropes and steel wire meshes at limestone slope below the Peovica Fortress (right down).

Conclusions

Construction of support systems and installation of rockfall protection barriers above the City of Omiš were completed in November 2018 according to the final design at 22 locations at the rock slopes. Conducted analyses of rockfall sources and run out areas provided by 2D and 3D rockfall simulations pointed out that the carried out protection constructions and measures will not ensure the residents and buildings in the City of Omiš from possible significant rockfall events in the future To ensure more comprehensive rockfall protection, it would be necessary to conduct a rockfall hazard and risk analysis (Arbanas et al. 2018) that would identify rockfall potential from the slopes above the City of Omiš, as well as better prediction of run out areas and associate rockfall hazard and risk. The results of this study should provide necessary data for the second stage of the rockfall protection project that will reduce the rockfall risk in the City of Omiš to an acceptable level.

Acknowledgments

This manuscript contains parts of the manuscript Arbanas et al. 2019, Rockfall Modelling and Rockfall Protection at the Slopes above the City of Omiš, Croatia presented at ISRM Specialised Conference Geotechnical Challenges in Karst, Omiš, Croatia in April 2019. The part of this research is carried out in the frame of the Project Research of Rockfall Processes and Rockfall Hazard Assessment supported by University of Rijeka, Croatia. This support is gratefully acknowledged.

References

Arbanas, Ž., Grošić, M., Udovič, D., Mihalić, S. (2012) Rockfall hazard analyses and rockfall protection along the Adriatic coast of Croatia. Journal of Civil Engineering and Architecture 6(3), pp. 344-355.

Arbanas, Ž., Udovič D., Sečanj, M., Đomlija, P., Mihalić Arbanas, S. (2018) Recent experience in rockfall hazard and risk assessment. Proc. of the 7th Conf. of the Croatian Platform for Disaster Risk Reduction, Zagreb, Croatia, pp. 222-231.

Arbanas, Ž., Vivoda Prodan, M., Dugonjić Jovančević, S., Peranić, J., Udovič, D., Bernat Gazibara, S., Krkač, M., Sečanj, M., Mihalić Arbanas, S., (2019) Rockfall Modelling and Rockfall Protection at the Slopes above the City of Omiš, Croatia. In: Sokolić I et al. (eds) Proc. of the ISRM Specialised Conf. "Geotechnical challenges in karst". Croatian Geotechnical Society, Zagreb. pp 121-126.

Chen, N., Kemeny, J., Jiang, Q., Pan, Z., (2017) Automatic extraction of blocks from 3D point clouds of fractured rock. Comput. Geosci. 109, pp. 149–161.

Dorren, L.K.A. (2003) A review of rockfall mechanics and modelling approaches. Prog. Phys. Geogr. 27, pp. 69–87.

Emmer, A. (2008) Geographies and Scientometrics of Research on Natural Hazards. Geosciences 8, pp. 382.

Francioni, M., Salvini, R., Stead, D., Coggan, J. (2018) Improvements in the integration of remote sensing and rock slope modelling. Natural hazards 90(2), pp 975–1004.

Giordan, D., Hayakawa, Y., Nex, F., Remondino, F., Tarolli, P. (2018) Review article: the use of remotely piloted aircraft systems (RPASs) for natural hazards monitoring and management. Nat. Hazards Earth Syst. Sci. 18, pp. 1079–1096,

Jaboyedoff, M.; Oppikofer, T.; Abellán, A.; Derron, M.-H.; Loye, A.; Metzger, R.; Pedrazzini, A. (2012) Use of LIDAR in landslide investigations: A review. Nat. Hazards 61, pp. 5–28.

James, M.R., Robson, S. (2012) Straightforward reconstruction of 3D surfaces and topography with a camera: Accuracy and geoscience application. J. Geophys. Res. Earth Surf 117.

Lato, M.J., Vöge, M. (2012) Automated mapping of rock discontinuities in 3D lidar and photogrammetry models. Int. J. Rock Mech. Min. Sci. 54, pp. 150–158.

Li, L., Lan, H. (2015) Probabilistic modeling of rockfall trajectories: a review. Bulletin of Engineering Geology and the Environment, 74(4), pp. 1163–1176.

Marinčić, S., Korolija, B., Mamužić, B., Magaš, N., Majcen, Ž., Brkić, M,, Benček, Đ. (1977) Osnovna geološka karta SFRJ 1:100.000. Tumač za list Omiš. Savezni geol. zavod, Beograd, pp. 21–35 (in Croatian).

Riquelme, A., Abellán, A., Tomás, R., Jaboyedoff, M. (2014) A new approach for semi-automatic rock mass joints recognition from 3D point clouds. Comput. Geosci. 68, pp. 38–52.

Riquelme, A., Abellán, A., Tomás, R. (2015) Discontinuity spacing analysis in rock masses using 3D point clouds. Eng. Geol. 195, pp. 185–195.

Riquelme, A., Tomás, R., Abellán, A. (2016) Characterization of rock slopes through slope mass rating using 3D point clouds. Int. J. Rock Mech. Min. Sci. 84, pp. 165–176.

Riquelme, A., Tomás, R., Cano, M., Pastor, J.L., Abellán, A. (2018) Automatic Mapping of Discontinuity Persistence on Rock Masses Using 3D Point Clouds. Rock Mech. Rock Eng. 51, pp. 3005–3028.

RockFall (2018) https://www.rocscience.com/software/rocfall (accessed on 15 September 2019).

RocPro3D, (2014) http://www.rocpro3d.com/rocpro3d_en.php (accessed on 15 September 2019).

Sarro, R., Riquelme, A., García-Davalillo, J.C., Mateos, R.M., Tomás, R., Pastor, J.L., Cano, M.,Herrera (2018) Rockfall Simulation Based on UAV Photogrammetry Data Obtained during an Emergency Declaration: Application at a Cultural Heritage Site. Remote Sens. 10, 1923, pp. 1-20

Sečanj, M., Mihalić Arbanas, S., Kordić, B., Krkač, M., Bernat Gazibara, S., 2017. Identification of rock prone areas on the steep slopes above the Town of Omiš, Croatia. Proceedings: of World Landslide Forum 4, Advancing Culture of Living vith Landslidees, Vol. 5 Springer International Publishing, pp. 481-488.

Sečanj M, Mihalić Arbanas S, Krkač M, Bernat Gazibara S, Arbanas Ž (2019) Preliminary rockfall susceptibility assessment of the rock slopes above the Town of Omiš (Croatia). In: Sokolić I et al. (eds) Proc. of the ISRM Specialised Conf. "Geotechnical challenges in karst". Croatian Geotechnical Society, Zagreb. pp 347-352.

Volkwein, A., Schellenberg, K., Labiouse, V., Agliardi, F., Berger, F., Bourrier, F., Dorren, L.K.A., Gerber, W., Jaboyedoff, M. (2011) Rockfall characterisation and structural protection—a review. Nat Hazards Earth Sys Sci 11, pp. 2617–2651

GEOINVEST Grupa je vodeća i najveća kompanija za realizaciju svih vrsta geotehničkih projekata u regiji, sa sjedištem u Ljubljani (Republika Slovenija) i tvrtkama u Varaždinu (Republika Hrvatska), Sarajevu (Bosna i Hercegovina) i Sremskoj Mitrovici (Republika Srbija). U sastavu GEOINVEST Grupacije je i Geostroj d.o.o. Ljubljana za proizvodnju i održavanje geotehničke opreme.


Izgradnja obilaznice oko Grada Brčko

Djelatnost firme: piloti, geotehnička sidra, mlazno injektiranje – jet grouting, poboljšanje temeljnog tla, AB dijafragme, torkretiranje, građevinske jame, geomehanička istraživanja.


Izgradnja mosta Svilaj preko rijeke Save


Izgradnja dvokolosječne pruge Beograd – Budimpešta, vijadukt Čortanovci

Temelj na kojem gradimo našu tvrtku je kvaliteta usluge, poštivanje ugovorenih rokova, fleksibilnost prema Investitorima te tržišno prihvatljive cijene.

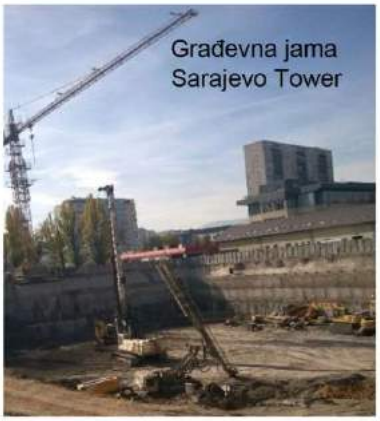
Građevna jama Sarajevo Tower


Izgradnja autoputa E-75, Caričina dolina – Vladičin Han

Geoinvest d.o.o.
Butmirska cesta 16
BIH-71000 Sarajevo

T: 00 387 33 624 710
00 387 33 624 711
00 387 33 624 717
F: 00 387 33 624 715

www.geoinvest.si, www.geoinvest.ba, www.geoinvest.hr, www.geoinvest.rs

GeoAVAS

DRUŠTVO ZA GEOLOGIJU, GEOTEHNIKU I GRAĐEVINARSTVO

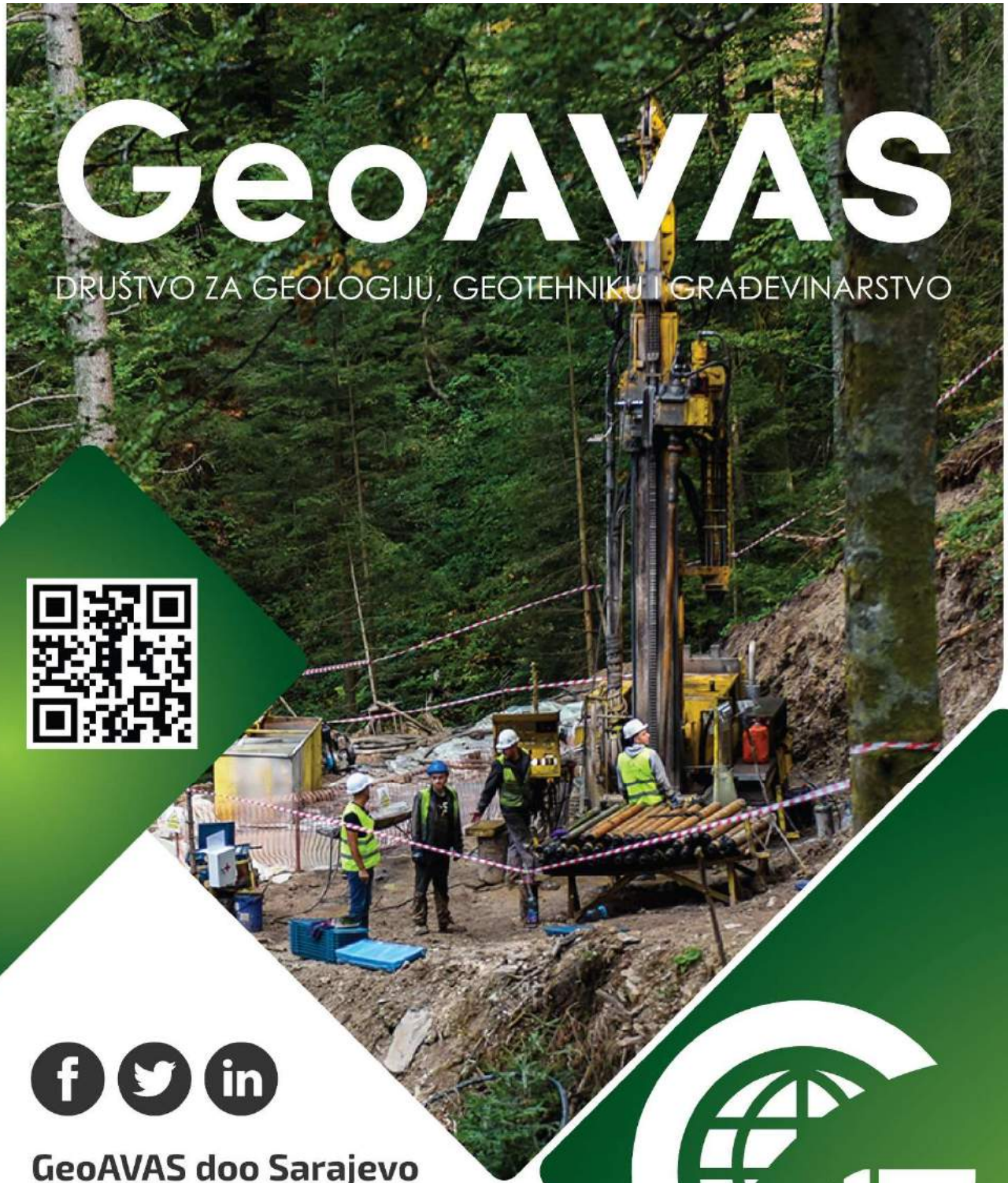

GeoAVAS doo Sarajevo

Adresa: Joze Penave 3,
71210 Ilidža, Sarajevo, Bosna i Hercegovina
Mob: +387 62 177 928
Tel: +387 33 766 160
Fax: +387 33 766 161
Web: www.geoavas.ba
E-mail: geo@geoavas.ba

ID: 4202006930006 | PDV: 202006930006 | BBI Bank račun: 141-309-53200097-28

KELLER
global strength and local focus
Building on our strengths!
We implement solutions for all your subsoil, foundation and groundwater problems. Our methods developed in-house and a wide range of modern technologies allow us to effectively solve any complex ground engineering challenge.
Ask us - we're happy to help!
www.kellergrundbau.at
Headquarters Southeast Europe
Keller Grundbau Ges.mbH
Guglgasse 15, BT 4a / 3. OG
1110 Vienna / Austria
t: +43 1 892 35 26
f: +43 1 892 37 11
e: marketing.at@keller.com
Austria • Czech Republic • Greece • Hungary • Italy • Romania • Slovakia • Switzerland • Turkey

Tensar®

THE COMPANY YOU CAN BUILD ON™

Tensar International is a worldwide leader in the manufacture and the provision of products and systems for subgrade stabilisation, pavement optimisation and soil reinforcement. Our service team provides practical and best value advice and design to support the use of Tensar products and systems in your application.

Subgrade Stabilisation Solutions

Spectra Pavement Optimisation System

TensarTech Earth Retaining Systems

Rail Trackbed Stabilisation

Asphalt Reinforcement Solutions

Embankment Foundation Systems

Tensar Project Value

€ CO_2

For further information visit
tensarinternational.com

MACCAFERRI

Engineering a Better Solution





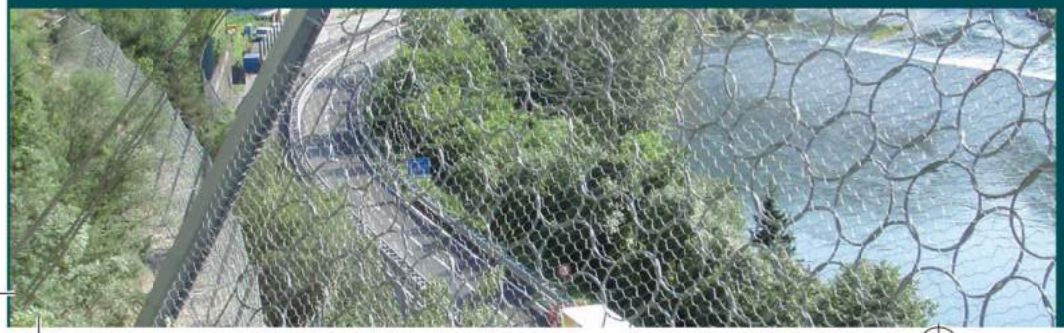

Our solutions

- *Erosion Control*
- *Retaining Walls & Soil Reinforcement*
- *Soil Stabilisation & Pavements*
- *Hydraulic Works*
- *Rockfall Protection & Snow Barriers*
- *Basal Reinforcement*
- *Safety & Noise Barriers*
- *Environment, Dewatering & Landfills*

Contact us:
Commercial & Technical office Bratislava:
Kopčianska 15, 851 01 Bratislava
Tel.: +421 2 20 24 00 56

Technical office Žilina:
Veľká Okružná 26A, 010 01 Žilina
Tel.: +421 905 703 034

info@sk.maccaferri.com

www.maccaferri.com/sk

LEISTER

MARCOM PLAST D.O.O.

NOVO U PONUDI

Twinny T7
Mašina za deponije

- Idealan za membrane 0.5 - 2.5 mm
- Motor fena bez četkica - inverter
- Digitalni displej za podešavanje parametara
- LQS - Leister sistem sa GPS prijemnikom i softverom za snimanje i praćenje parametara

Ovlašćeni distributer za Bosnu i Hercegovinu

Marcom - Plast d.o.o.
tel: +381 11 412 70 58
Novogradska 41
Beograd

www.marcom-plast.rs
office@marcom-plast.rs

Mi znamo kako.

МЈЕШОВИТИ ХОЛДИНГ
"ЕЛЕКТРОПРИВРЕДА РЕПУБЛИКЕ СРПСКЕ"
Матично предузеће, акционарско друштво Требиње

MIXED HOLDING
"POWER UTILITY OF THE REPUBLIC OF SRPSKA"
Parent Joint-stock Company Trebinje

KREŠOGEO

DRUŠTVO ZA PROJEKTOVANJE, SAVJETOVANJE I ISTRAŽIVANJE U GRAĐEVINARSTVU

INTERPROJEKT DOO
MOSTAR

Interprojekt d.o.o.
Maršala Tita 254a
88104 Mostar
Bosna i Hercegovina

email: info@interprojekt.ba
web: www.interprojekt.ba
Tel. +387 36 555 131
Fax. +387 36 555 731

FMON
Federalno ministarstvo obrazovanja i nauke

JP Autoceste FBiH

JP Elektroprivreda BiH
d.d. - Sarajevo

RUDNIK KAKANJ 1902

banovići

ISBN 978-9926-8400-0-6